

Schlumberger

Log Interpretation Charts

2013 Edition

Gen

GR

SP

Dens

Neu

NMR

RLI

RInd

REm

Rt

Lith

Por

SatOH

SatCH

Perm

Cem

Schlumberger
3750 Briarpark Drive
Houston, Texas 77042
www.slb.com

© 2013 Schlumberger. All rights reserved.

No part of this book may be reproduced, stored in a retrieval system, or transcribed in any form or by any means, electronic or mechanical, including photocopying and recording, without the prior written permission of the publisher.

While the information presented herein is believed to be accurate, it is provided “as is” without express or implied warranty.

Specifications are current at the time of printing.

13-FE-0034

ISBN-13: 978-1-937949-10-5

An asterisk (*) is used throughout this document to denote a mark of Schlumberger.

Contents

Foreword		xi
General		
Symbols Used in Log Interpretation.....	Gen-1	1
Estimation of Formation Temperature with Depth.....	Gen-2	3
Estimation of R_{mf} and R_{mc}	Gen-3	4
Equivalent NaCl Salinity of Salts.....	Gen-4	5
Concentration of NaCl Solutions.....	Gen-5	6
Resistivity of NaCl Water Solutions.....	Gen-6	8
Density of Water and Hydrogen Index of Water and Hydrocarbons.....	Gen-7	9
Density and Hydrogen Index of Natural Gas.....	Gen-8	10
Sound Velocity of Hydrocarbons.....	Gen-9	11
Gas Effect on Compressional Slowness.....	Gen-9a	12
Gas Effect on Acoustic Velocity.....	Gen-9b	13
Nuclear Magnetic Resonance Relaxation Times of Water.....	Gen-10	14
Nuclear Magnetic Resonance Relaxation Times of Hydrocarbons.....	Gen-11a	15
Nuclear Magnetic Resonance Relaxation Times of Hydrocarbons.....	Gen-11b	16
Capture Cross Section of NaCl Water Solutions.....	Gen-12	18
Capture Cross Section of NaCl Water Solutions.....	Gen-13	19
Capture Cross Section of Hydrocarbons.....	Gen-14	21
EPT* Propagation Time of NaCl Water Solutions.....	Gen-15	22
EPT Attenuation of NaCl Water Solutions.....	Gen-16	23
EPT Propagation Time–Attenuation Crossplot.....	Gen-16a	24
Gamma Ray		
Scintillation Gamma Ray—3 $\frac{1}{2}$ - and 1 $\frac{1}{8}$ -in. Tools.....	GR-1	25
Scintillation Gamma Ray—3 $\frac{1}{2}$ - and 1 $\frac{1}{8}$ -in. Tools.....	GR-2	26
Scintillation Gamma Ray—3 $\frac{1}{2}$ - and 1 $\frac{1}{8}$ -in. Tools.....	GR-3	27
SlimPulse* and E-Pulse* Gamma Ray Tools.....	GR-6	28
ImPulse* Gamma Ray—4.75-in. Tool.....	GR-7	29
PowerPulse* and TeleScope* Gamma Ray—6.75-in. Tools.....	GR-9	30
PowerPulse Gamma Ray—8.25-in. Normal-Flow Tool.....	GR-10	31
PowerPulse Gamma Ray—8.25-in. High-Flow Tool.....	GR-11	32
PowerPulse Gamma Ray—9-in. Tool.....	GR-12	33
PowerPulse Gamma Ray—9.5-in. Normal-Flow Tool.....	GR-13	34
PowerPulse Gamma Ray—9.5-in. High-Flow Tool.....	GR-14	35
geoVISION675* GVR* Gamma Ray—6.75-in. Tool.....	GR-15	36
RAB* Gamma Ray—8.25-in. Tool.....	GR-16	37
arcVISION475* Gamma Ray—4.75-in. Tool.....	GR-19	38

arcVISION675* Gamma Ray—6.75-in. Tool	GR-20	39
arcVISION825* Gamma Ray—8.25-in. Tool	GR-21	40
arcVISION900* Gamma Ray—9-in. Tool	GR-22	41
arcVISION475 Gamma Ray—4.75-in. Tool	GR-23	42
arcVISION675 Gamma Ray—6.75-in. Tool	GR-24	43
arcVISION825 Gamma Ray—8.25-in. Tool	GR-25	44
arcVISION900 Gamma Ray—9-in. Tool	GR-26	45
EcoScope* Integrated LWD Gamma Ray—6.75-in. Tool	GR-27	46
EcoScope Integrated LWD Gamma Ray—6.75-in. Tool	GR-28	47

Spontaneous Potential

R_{weq} Determination from E_{SSP}	SP-1	49
R_{weq} versus R_w and Formation Temperature	SP-2	50
R_{weq} versus R_w and Formation Temperature	SP-3	51
Bed Thickness Correction—Open Hole	SP-4	53
Bed Thickness Correction—Open Hole (Empirical)	SP-5	54
Bed Thickness Correction—Open Hole (Empirical)	SP-6	55

Density

Porosity Effect on Photoelectric Cross Section	Dens-1	56
Apparent Log Density to True Bulk Density	Dens-2	57

Neutron

Dual-Spacing Compensated Neutron Tool Charts		58
Compensated Neutron Tool	Neu-1	60
Compensated Neutron Tool	Neu-2	61
Compensated Neutron Tool	Neu-3	63
Compensated Neutron Tool	Neu-4	64
Compensated Neutron Tool	Neu-5	65
Compensated Neutron Tool	Neu-6	67
Compensated Neutron Tool	Neu-7	69
Compensated Neutron Tool	Neu-8	71
Compensated Neutron Tool	Neu-9	73
APS* Accelerator Porosity Sonde	Neu-10	75
APS Accelerator Porosity Sonde Without Environmental Corrections	Neu-11	76
CDN* Compensated Density Neutron, adnVISION* Azimuthal Density Neutron, and EcoScope* Integrated LWD Tools	Neu-30	78
adnVISION475* Azimuthal Density Neutron—4.75-in. Tool and 6-in. Borehole	Neu-31	80
adnVISION475 BIP Neutron—4.75-in. Tool and 6-in. Borehole	Neu-32	81
adnVISION475 Azimuthal Density Neutron—4.75-in. Tool and 8-in. Borehole	Neu-33	82
adnVISION475 BIP Neutron—4.75-in. Tool and 8-in. Borehole	Neu-34	83

adnVISION675* Azimuthal Density Neutron—6.75-in. Tool and 8-in. Borehole	Neu-35	84
adnVISION675 BIP Neutron—6.75-in. Tool and 8-in. Borehole	Neu-36	85
adnVISION675 Azimuthal Density Neutron—6.75-in. Tool and 10-in. Borehole	Neu-37	86
adnVISION675 BIP Neutron—6.75-in. Tool and 10-in. Borehole	Neu-38	87
adnVISION825* Azimuthal Density Neutron—8.25-in. Tool and 12.25-in. Borehole.....	Neu-39	88
CDN Compensated Density Neutron and adnVISION825s* Azimuthal Density Neutron— 8-in. Tool and 12-in. Borehole	Neu-40	89
CDN Compensated Density Neutron and adnVISION825s Azimuthal Density Neutron— 8-in. Tool and 14-in. Borehole	Neu-41	90
CDN Compensated Density Neutron and adnVISION825s Azimuthal Density Neutron— 8-in. Tool and 16-in. Borehole	Neu-42	91
EcoScope* Integrated LWD BPHI Porosity—6.75-in. Tool and 8.5-in. Borehole.....	Neu-43	93
EcoScope Integrated LWD BPHI Porosity—6.75-in. Tool and 9.5-in. Borehole.....	Neu-44	94
EcoScope Integrated LWD TNPH Porosity—6.75-in. Tool and 8.5-in. Borehole.....	Neu-45	95
EcoScope Integrated LWD TNPH Porosity—6.75-in. Tool and 9.5-in. Borehole.....	Neu-46	96
EcoScope Integrated LWD—6.75-in. Tool.....	Neu-47	98

Nuclear Magnetic Resonance

CMR* Tool.....	CMR-1	99
----------------	--------------------	----

Resistivity Laterolog

ARI* Azimuthal Resistivity Imager	RLI-1	101
High-Resolution Azimuthal Laterolog Sonde (HALS).....	RLI-2	102
High-Resolution Azimuthal Laterolog Sonde (HALS).....	RLI-3	103
High-Resolution Azimuthal Laterolog Sonde (HALS).....	RLI-4	104
High-Resolution Azimuthal Laterolog Sonde (HALS).....	RLI-5	105
High-Resolution Azimuthal Laterolog Sonde (HALS).....	RLI-6	106
High-Resolution Azimuthal Laterolog Sonde (HALS).....	RLI-7	107
High-Resolution Azimuthal Laterolog Sonde (HALS).....	RLI-8	108
High-Resolution Azimuthal Laterolog Sonde (HALS).....	RLI-9	109
HRLA* High-Resolution Laterolog Array	RLI-10	110
HRLA High-Resolution Laterolog Array.....	RLI-11	111
HRLA High-Resolution Laterolog Array.....	RLI-12	112
HRLA High-Resolution Laterolog Array.....	RLI-13	113
HRLA High-Resolution Laterolog Array.....	RLI-14	114
GeoSteering* Bit Resistivity—6.75-in. Tool	RLI-20	115
GeoSteering arcVISION675 Resistivity—6.75-in. Tool	RLI-21	116
GeoSteering Bit Resistivity in Reaming Mode—6.75-in. Tool.....	RLI-22	117
geoVISION* Resistivity Sub—6.75-in. Tool	RLI-23	118
geoVISION Resistivity Sub—8.25-in. Tool	RLI-24	119
GeoSteering Bit Resistivity—6.75-in. Tool.....	RLI-25	120

CHFR* Cased Hole Formation Resistivity Tool	RLI-50	121
CHFR Cased Hole Formation Resistivity Tool	RLI-51	122
CHFR Cased Hole Formation Resistivity Tool	RLI-52	123
Resistivity Induction		
AIT* Array Induction Imager Tool	RInd-1	125
AIT Array Induction Imager Tool.....		126
Resistivity Electromagnetic		
arcVISION475 and ImPulse 4¾-in. Array Resistivity Compensated Tools—2 MHz	REm-11	131
arcVISION475 and ImPulse 4¾-in. Array Resistivity Compensated Tools—2 MHz	REm-12	132
arcVISION475 and ImPulse 4¾-in. Array Resistivity Compensated Tools—2 MHz	REm-13	133
arcVISION475 and ImPulse 4¾-in. Array Resistivity Compensated Tools—2 MHz	REm-14	134
arcVISION675 6¾-in. Array Resistivity Compensated Tool—400 kHz	REm-15	135
arcVISION675 6¾-in. Array Resistivity Compensated Tool—400 kHz	REm-16	136
arcVISION675 6¾-in. Array Resistivity Compensated Tool—400 kHz	REm-17	137
arcVISION675 6¾-in. Array Resistivity Compensated Tool—400 kHz	REm-18	138
arcVISION675 6¾-in. Array Resistivity Compensated Tool—2 MHz.....	REm-19	139
arcVISION675 6¾-in. Array Resistivity Compensated Tool—2 MHz.....	REm-20	140
arcVISION675 6¾-in. Array Resistivity Compensated Tool—2 MHz.....	REm-21	141
arcVISION675 6¾-in. Array Resistivity Compensated Tool—2 MHz.....	REm-22	142
arcVISION825 8¼-in. Array Resistivity Compensated Tool—400 kHz.....	REm-23	143
arcVISION825 8¼-in. Array Resistivity Compensated Tool—400 kHz.....	REm-24	144
arcVISION825 8¼-in. Array Resistivity Compensated Tool—400 kHz.....	REm-25	145
arcVISION825 8¼-in. Array Resistivity Compensated Tool—400 kHz.....	REm-26	146
arcVISION825 8¼-in. Array Resistivity Compensated Tool—2 MHz.....	REm-27	147
arcVISION825 8¼-in. Array Resistivity Compensated Tool—2 MHz.....	REm-28	148
arcVISION825 8¼-in. Array Resistivity Compensated Tool—2 MHz.....	REm-29	149
arcVISION825 8¼-in. Array Resistivity Compensated Tool—2 MHz.....	REm-30	150
arcVISION900 9-in. Array Resistivity Compensated Tool—400 kHz.....	REm-31	151
arcVISION900 9-in. Array Resistivity Compensated Tool—400 kHz.....	REm-32	152
arcVISION900 9-in. Array Resistivity Compensated Tool—400 kHz.....	REm-33	153
arcVISION900 9-in. Array Resistivity Compensated Tool—400 kHz.....	REm-34	154
arcVISION900 9-in. Array Resistivity Compensated Tool—2 MHz	REm-35	155
arcVISION900 9-in. Array Resistivity Compensated Tool—2 MHz	REm-36	156
arcVISION900 9-in. Array Resistivity Compensated Tool—2 MHz	REm-37	157

arcVISION900 9-in. Array Resistivity Compensated Tool—2 MHz	REm-38	158
arcVISION675, arcVISION825, and arcVISION900 Array Resistivity Compensated Tools—400 kHz	REm-55	160
arcVISION and ImPulse Array Resistivity Compensated Tools—2 MHz	REm-56	161
arcVISION675 and ImPulse Array Resistivity Compensated Tools—2 MHz and 16-in. Spacing	REm-58	162
arcVISION675 and ImPulse Array Resistivity Compensated Tools—2 MHz and 22-in. Spacing	REm-59	163
arcVISION675 and ImPulse Array Resistivity Compensated Tools—2 MHz and 28-in. Spacing	REm-60	164
arcVISION675 and ImPulse Array Resistivity Compensated Tools—2 MHz and 34-in. Spacing	REm-61	165
arcVISION675 and ImPulse Array Resistivity Compensated Tools—2 MHz and 40-in. Spacing	REm-62	166
arcVISION675 and ImPulse Array Resistivity Compensated Tools—2 MHz with Dielectric Assumption	REm-63	167

Formation Resistivity

Resistivity Galvanic	Rt-1	168
High-Resolution Azimuthal Laterlog Sonde (HALS)	Rt-2	169
High-Resolution Azimuthal Laterlog Sonde (HALS)	Rt-3	170
geoVISION675* Resistivity	Rt-10	171
geoVISION675 Resistivity	Rt-11	172
geoVISION675 Resistivity	Rt-12	173
geoVISION675 Resistivity	Rt-13	174
geoVISION825* 8¼-in. Resistivity-at-the-Bit Tool	Rt-14	175
geoVISION825 8¼-in. Resistivity-at-the-Bit Tool	Rt-15	176
geoVISION825 8¼-in. Resistivity-at-the-Bit Tool	Rt-16	177
geoVISION825 8¼-in. Resistivity-at-the-Bit Tool	Rt-17	178
arcVISION Array Resistivity Compensated Tool—400 kHz	Rt-31	179
arcVISION and ImPulse Array Resistivity Compensated Tools—2 MHz	Rt-32	180
arcVISION Array Resistivity Compensated Tool—400 kHz	Rt-33	181
arcVISION and ImPulse Array Resistivity Compensated Tools—2 MHz	Rt-34	182
arcVISION Array Resistivity Compensated Tool—400 kHz	Rt-35	183
arcVISION and ImPulse Array Resistivity Compensated Tools—2 MHz	Rt-36	184
arcVISION675 Array Resistivity Compensated Tool—400 kHz	Rt-37	185
arcVISION675 and ImPulse Array Resistivity Compensated Tools—2 MHz	Rt-38	186
arcVISION Array Resistivity Compensated Tool—400 kHz	Rt-39	187
arcVISION and ImPulse Array Resistivity Compensated Tools—2 MHz	Rt-40	188
arcVISION Array Resistivity Compensated Tool—400 kHz in Horizontal Well	Rt-41	190
arcVISION and ImPulse Array Resistivity Compensated Tools—2 MHz in Horizontal Well	Rt-42	191

Lithology

Density and NGS* Natural Gamma Ray Spectrometry Tool.....	Lith-1	193
NGS Natural Gamma Ray Spectrometry Tool.....	Lith-2	194
Platform Express* Three-Detector Lithology Density Tool.....	Lith-3	196
Platform Express Three-Detector Lithology Density Tool.....	Lith-4	197
Density Tool.....	Lith-5	198
Density Tool.....	Lith-6	200
Environmentally Corrected Neutron Curves.....	Lith-7	202
Environmentally Corrected APS Curves.....	Lith-8	204
Bulk Density or Interval Transit Time and Apparent Total Porosity.....	Lith-9	206
Bulk Density or Interval Transit Time and Apparent Total Porosity.....	Lith-10	207
Density Tool.....	Lith-11	209
Density Tool.....	Lith-12	210

Porosity

Sonic Tool.....	Por-1	212
Sonic Tool.....	Por-2	213
Density Tool.....	Por-3	214
APS Near-to-Array (APLC) and Near-to-Far (FPLC) Logs.....	Por-4	216
Thermal Neutron Tool.....	Por-5	217
Thermal Neutron Tool—CNT-D and CNT-S 2½-in. Tools.....	Por-6	218
adnVISION475 4.75-in. Azimuthal Density Neutron Tool.....	Por-7	219
adnVISION675 6.75-in. Azimuthal Density Neutron Tool.....	Por-8	220
adnVISION825 8.25-in. Azimuthal Density Neutron Tool.....	Por-9	221
EcoScope* 6.75-in. Integrated LWD Tool, BPHI Porosity.....	Por-10	222
EcoScope 6.75-in. Integrated LWD Tool, TNPH Porosity.....	Por-10a	223
CNL* Compensated Neutron Log and Litho-Density* Tool (fresh water in invaded zone).....	Por-11	225
CNL Compensated Neutron Log and Litho-Density Tool (salt water in invaded zone).....	Por-12	226
APS and Litho-Density Tools.....	Por-13	227
APS and Litho-Density Tools (saltwater formation).....	Por-14	228
adnVISION475 4.75-in. Azimuthal Density Neutron Tool.....	Por-15	229
adnVISION675 6.75-in. Azimuthal Density Neutron Tool.....	Por-16	230
adnVISION825 8.25-in. Azimuthal Density Neutron Tool.....	Por-17	231
EcoScope 6.75-in. Integrated LWD Tool.....	Por-18	232
EcoScope 6.75-in. Integrated LWD Tool.....	Por-19	233
Sonic and Thermal Neutron Crossplot.....	Por-20	235
Sonic and Thermal Neutron Crossplot.....	Por-21	236
Density and Sonic Crossplot.....	Por-22	238
Density and Sonic Crossplot.....	Por-23	239
Density and Neutron Tool.....	Por-24	241

Density and APS Epithermal Neutron Tool.....	Por-25	243
Density, Neutron, and R_{xo} Logs	Por-26	245
Hydrocarbon Density Estimation.....	Por-27	246
Saturation		
Porosity Versus Formation Resistivity Factor.....	SatOH-1	247
Spherical and Fracture Porosity.....	SatOH-2	248
Saturation Determination.....	SatOH-3	250
Saturation Determination.....	SatOH-4	252
Graphical Determination of S_w from S_{wt} and S_{wb}	SatOH-5	253
Porosity and Gas Saturation in Empty Hole	SatOH-6	254
EPT Propagation Time	SatOH-7	255
EPT Attenuation.....	SatOH-8	256
Capture Cross Section Tool	SatCH-1	258
Capture Cross Section Tool	SatCH-2	260
RSTPro* Reservoir Saturation Tool—1.6875 in. and 2.5 in.		261
RSTPro Reservoir Saturation Tool—1.6875 in. and 2.5 in. in 6.125-in. Borehole	SatCH-3	262
RSTPro Reservoir Saturation Tool—1.6875 in. and 2.5 in. in 9.875-in. Borehole	SatCH-4	263
RSTPro Reservoir Saturation Tool—1.6875 in. and 2.5 in. in 8.125-in. Borehole with 4.5-in. Casing at 11.6 lbm/ft.....	SatCH-5	264
RSTPro Reservoir Saturation Tool—1.6875 in. and 2.5 in. in 7.875-in. Borehole with 5.5-in. Casing at 17 lbm/ft.....	SatCH-6	265
RSTPro Reservoir Saturation Tool—1.6875 in. and 2.5 in. in 8.5-in. Borehole with 7-in. Casing at 29 lbm/ft	SatCH-7	266
RSTPro Reservoir Saturation Tool—1.6875 in. and 2.5 in. in 9.875-in. Borehole with 7-in. Casing at 29 lbm/ft.....	SatCH-8	267
Permeability		
Permeability from Porosity and Water Saturation	Perm-1	269
Permeability from Porosity and Water Saturation.....	Perm-2	270
Fluid Mobility Effect on Stoneley Slowness	Perm-3	271
Cement Evaluation		
Cement Bond Log—Casing Strength.....	Cem-1	274
Appendixes		
Appendix A	Linear Grid	275
	Log-Linear Grid	276
	Water Saturation Grid for Resistivity Versus Porosity	277
Appendix B	Logging Tool Response in Sedimentary Minerals.....	279
Appendix C	Acoustic Characteristics of Common Formations and Fluids.....	281
Appendix D	Conversions	282
Appendix E	Symbols.....	285
Appendix F	Subscripts	287
Appendix G	Unit Abbreviations	290
Appendix H	References.....	292

Foreword

This edition of the Schlumberger “chartbook” presents several innovations.

First, the charts were developed to achieve two purposes:

- Correct raw measurements to account for environmental effects

Early downhole measurements were performed in rather uniform conditions (vertical wells drilled through quasi-horizontal thick beds, muds made of water with a narrow selection of additives, and limited range of hole sizes), but today wells can be highly deviated or horizontal, mud contents are diverse, and hole sizes range from 2 to 40 in. Environmental effects may be large. In addition, they compound. It is essential to correct for these effects before the measurements are used.

- Use environmentally corrected measurements for interpretation

Charts related to measurements that are no longer performed are not included in this chartbook. However, because many oil and gas companies use logs acquired years or even decades ago, the second chartbook, *Historical Log Interpretation Charts*, contains these old charts.

Why publish charts on paper in our electronic age? It is true that software may be more effective than pencil to derive results. Even more so, this chartbook cannot cope with the complex well situations that are encountered. Using software is the only way to proceed.

Thus, the chartbook has two primary functions:

- Training

The chartbook is essential for educating junior petrophysicists about the different effects on the measurements. In the interpretation process, the chartbook unveils the relationships between the different parameters.

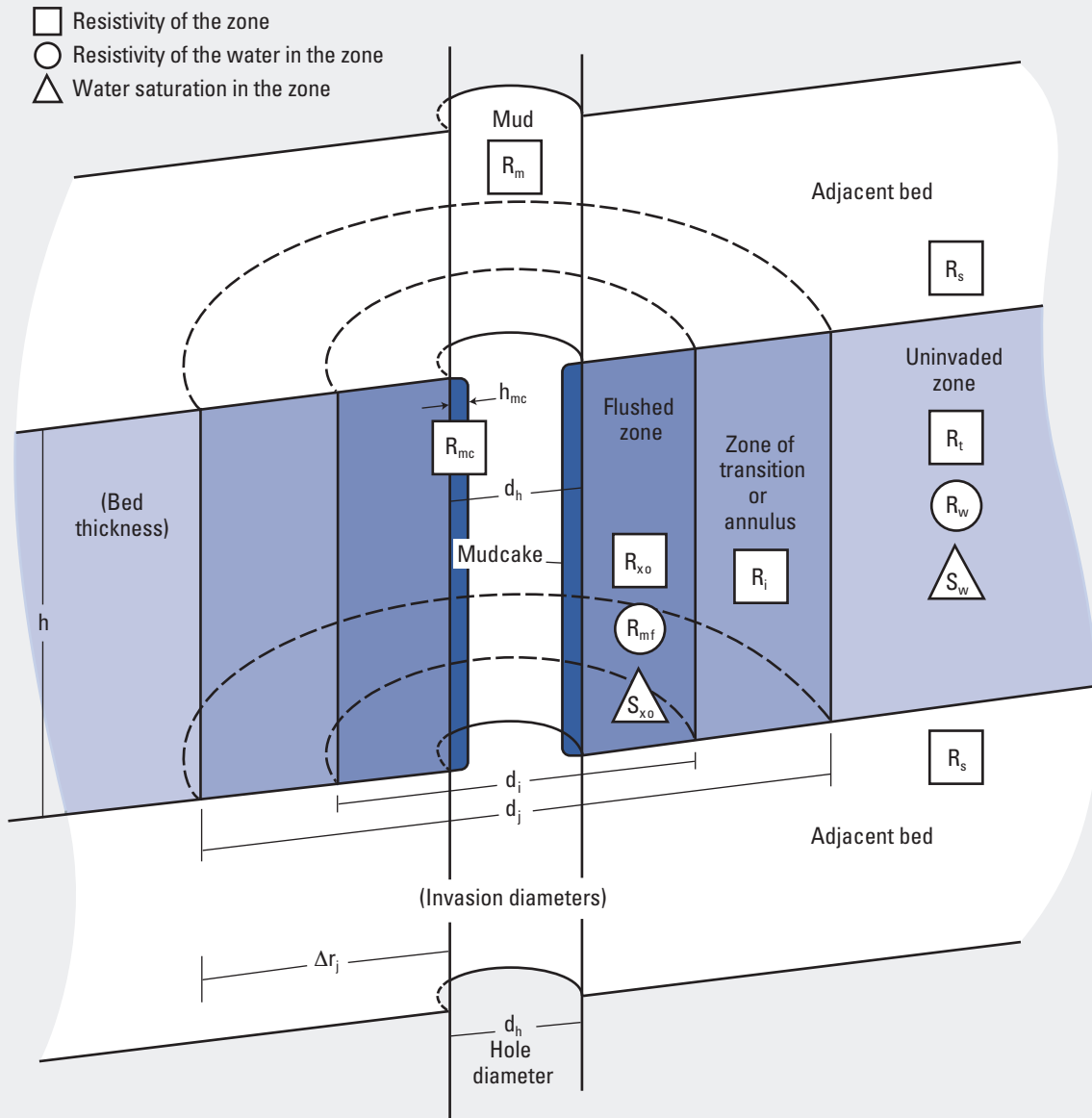
- Sensitivity analysis

A chart gives the user a graphical idea of the sensitivity of an output to the various inputs (see Chart Gen-1). The visual presentation is helpful for determining if an input parameter is critical. The user can then focus on the most sensitive inputs.

Symbols Used in Log Interpretation

Gen-1
(former Gen-3)

Gen



© Schlumberger

Purpose

This diagram presents the symbols and their descriptions and relations as used in the charts. See Appendixes D and E for identification of the symbols.

Description

The wellbore is shown traversing adjacent beds above and below the zone of interest. The symbols and descriptions provide a graphical representation of the location of the various symbols within the wellbore and formations.

Estimation of Formation Temperature with Depth

Purpose

This chart has a twofold purpose. First, a geothermal gradient can be assumed by entering the depth and a recorded temperature at that depth. Second, for an assumed geothermal gradient, if the temperature is known at one depth in the well, the temperature at another depth in the well can be determined.

Description

Depth is on the y-axis and has the shallowest at the top and the deepest at the bottom. Both feet and meters are used, on the left and right axes, respectively. Temperature is plotted on the x-axis, with Fahrenheit on the bottom and Celsius on the top of the chart. The annual mean surface temperature is also presented in Fahrenheit and Celsius.

Example

Given: Bottomhole depth = 11,000 ft and bottomhole temperature = 200°F (annual mean surface temperature = 80°F).

Find: Temperature at 8,000 ft.

Answer: The intersection of 11,000 ft on the y-axis and 200°F on the x-axis is a geothermal gradient of approximately 1.1°F/100 ft (Point A on the chart).

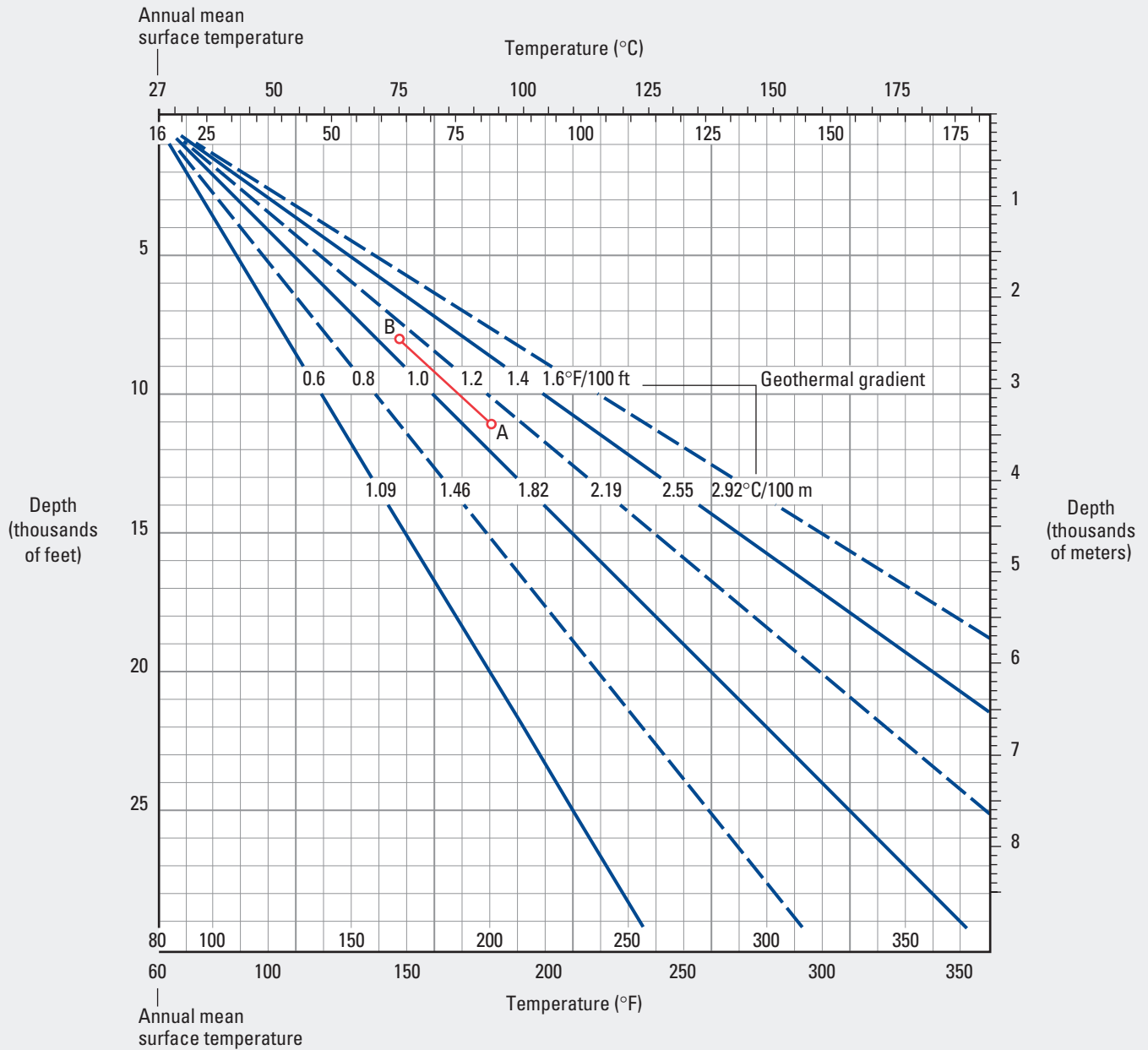
Move upward along an imaginary line parallel to the constructed gradient lines until the depth line for 8,000 ft is intersected. This is Point B, for which the temperature on the x-axis is approximately 167°F.

Estimation of Formation Temperature with Depth

Gen-2
(former Gen-6)

Gen

Temperature gradient conversions: $1^{\circ}\text{F}/100\text{ ft} = 1.823^{\circ}\text{C}/100\text{ m}$
 $1^{\circ}\text{C}/100\text{ m} = 0.5486^{\circ}\text{F}/100\text{ ft}$



Estimation of R_{mf} and R_{mc}

Fluid Properties

Gen-3
(former Gen-7)

Purpose

Direct measurements of filtrate and mudcake samples are preferred. When these are not available, the mud filtrate resistivity (R_{mf}) and mudcake resistivity (R_{mc}) can be estimated with the following methods.

Description

Method 1: Lowe and Dunlap

For freshwater muds with measured values of mud resistivity (R_m) between 0.1 and 2.0 ohm-m at 75°F [24°C] and measured values of mud density (ρ_m) (also called mud weight) in pounds per gallon:

$$\log\left(\frac{R_{mf}}{R_m}\right) = 0.396 - (0.0475 \times \rho_m).$$

Method 2: Overton and Lipson

For drilling muds with measured values of R_m between 0.1 and 10.0 ohm-m at 75°F [24°C] and the coefficient of mud (K_m) given as a function of mud weight from the table:

$$R_{mf} = K_m (R_m)^{1.07}$$

$$R_{mc} = 0.69 (R_{mf}) \left(\frac{R_m}{R_{mf}}\right)^{2.65}.$$

Mud Weight		
lbm/gal	kg/m ³	K_m
10	1,200	0.847
11	1,320	0.708
12	1,440	0.584
13	1,560	0.488
14	1,680	0.412
16	1,920	0.380
18	2,160	0.350

Example

Given: $R_m = 3.5$ ohm-m at 75°F and mud weight = 12 lbm/gal [1,440 kg/m³].

Find: Estimated values of R_{mf} and R_{mc} .

Answer: From the table, $K_m = 0.584$.

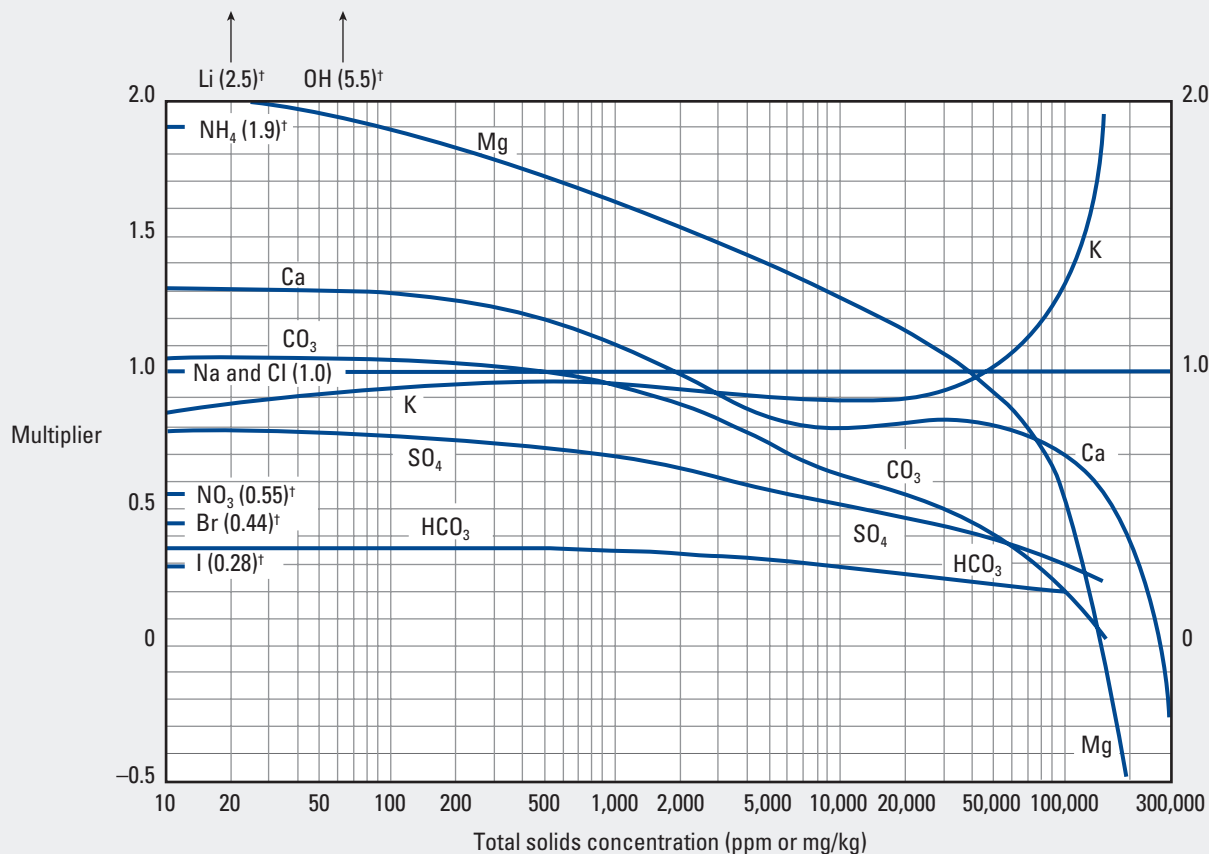
$$R_{mf} = (0.584) (3.5)^{1.07} = 2.23 \text{ ohm-m at } 75^\circ\text{F}.$$

$$R_{mc} = 0.69 (2.23) (3.5/2.23)^{2.65} = 5.07 \text{ ohm-m at } 75^\circ\text{F}.$$

Equivalent NaCl Salinity of Salts

Gen-4
(former Gen-8)

Gen



© Schlumberger

Purpose

This chart is used to approximate the parts-per-million (ppm) concentration of a sodium chloride (NaCl) solution for which the total solids concentration of the solution is known. Once the equivalent concentration of the solution is known, the resistivity of the solution for a given temperature can be estimated with Chart Gen-6.

Description

The x-axis of the semilog chart is scaled in total solids concentration and the y-axis is the weighting multiplier. The curve set represents the various multipliers for the solids typically in formation water.

Example

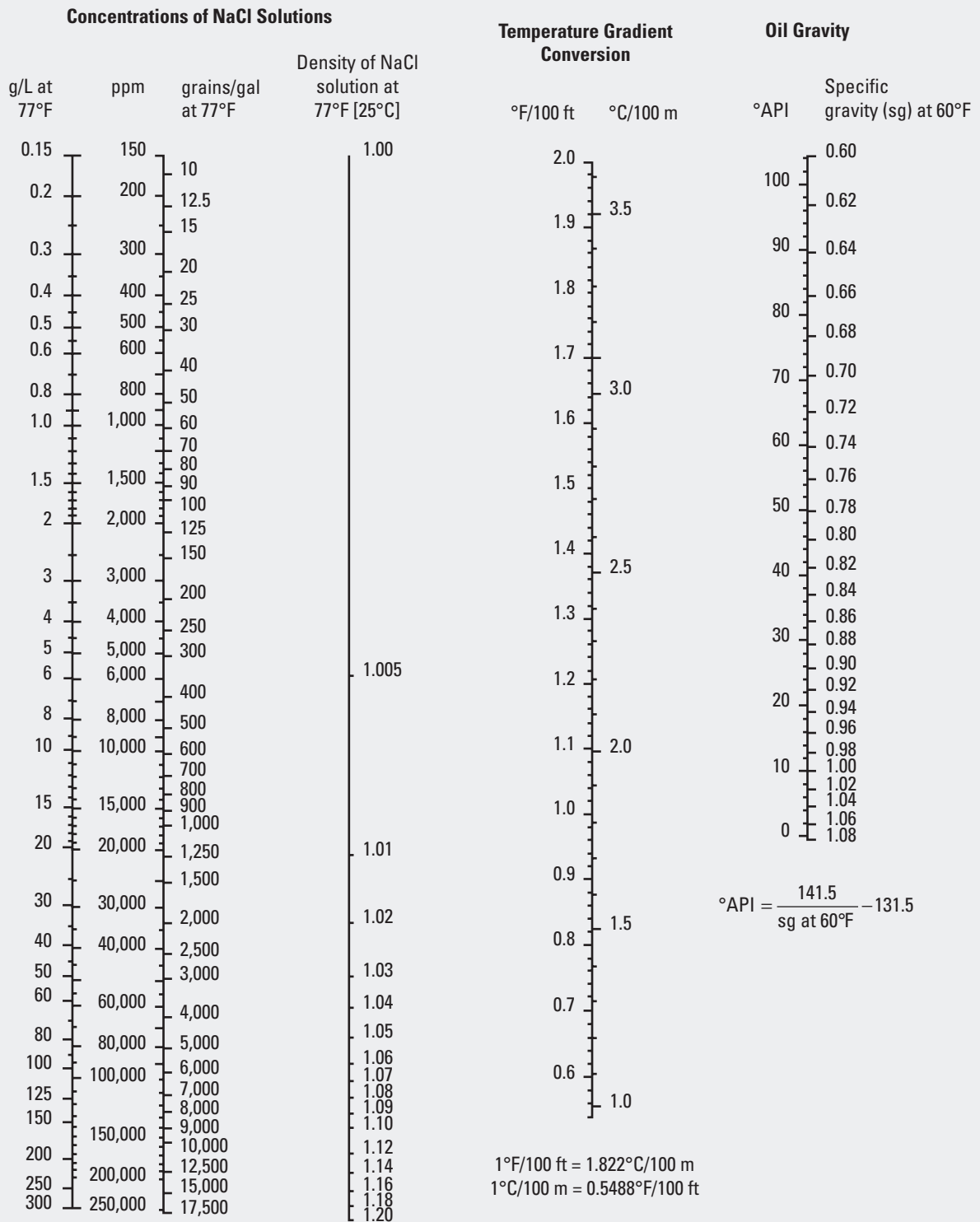
Given: Formation water sample with solids concentrations of calcium (Ca) = 460 ppm, sulfate (SO₄) = 1,400 ppm, and Na plus Cl = 19,000 ppm. Total solids concentration = 460 + 1,400 + 19,000 = 20,860 ppm.

Find: Equivalent NaCl solution in ppm.

Answer: Enter the x-axis at 20,860 ppm and read the multiplier value for each of the solids curves from the y-axis:
Ca = 0.81, SO₄ = 0.45, and NaCl = 1.0. Multiply each concentration by its multiplier:
 $(460 \times 0.81) + (1,400 \times 0.45) + (19,000 \times 1.0) = 20,000$ ppm.

Concentration of NaCl Solutions

Gen



Resistivity of NaCl Water Solutions

Purpose

This chart has a twofold purpose. The first is to determine the resistivity of an equivalent NaCl concentration (from Chart Gen-4) at a specific temperature. The second is to provide a transition of resistivity at a specific temperature to another temperature. The solution resistivity value and temperature at which the value was determined are used to approximate the NaCl ppm concentration.

Description

The two-cycle log scale on the x-axis presents two temperature scales for Fahrenheit and Celsius. Resistivity values are on the left four-cycle log scale y-axis. The NaCl concentration in ppm and grains/gal at 75°F [24°C] is on the right y-axis. The conversion approximation equation for the temperature (T) effect on the resistivity (R) value at the top of the chart is valid only for the temperature range of 68° to 212°F [20° to 100°C].

Example One

Given: NaCl equivalent concentration = 20,000 ppm.
Temperature of concentration = 75°F.

Find: Resistivity of the solution.

Answer: Enter the ppm concentration on the y-axis and the temperature on the x-axis to locate their point of intersection on the chart. The value of this point on the left y-axis is 0.3 ohm-m at 75°F.

Example Two

Given: Solution resistivity = 0.3 ohm-m at 75°F.

Find: Solution resistivity at 200°F [93°C].

Answer 1: Enter 0.3 ohm-m and 75°F and find their intersection on the 20,000-ppm concentration line. Follow the line to the right to intersect the 200°F vertical line (interpolate between existing lines if necessary). The resistivity value for this point on the left y-axis is 0.115 ohm-m.

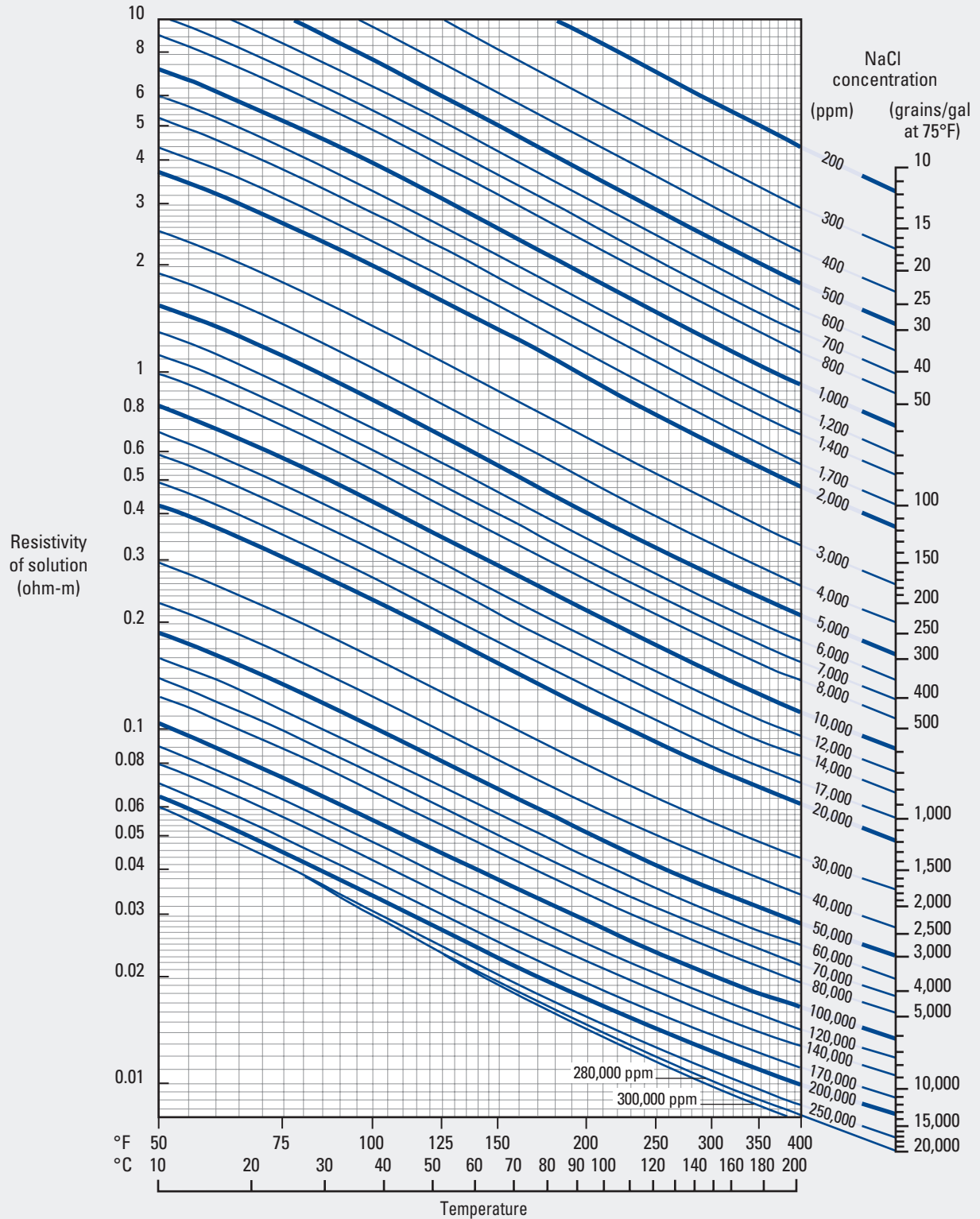
Answer 2: Resistivity at 200°F = resistivity at 75°F $\times [(75 + 6.77)/(200 + 6.77)] = 0.3 \times (81.77/206.77) = 0.1186$ ohm-m.

Resistivity of NaCl Water Solutions

Gen-6
(former Gen-9)

Gen

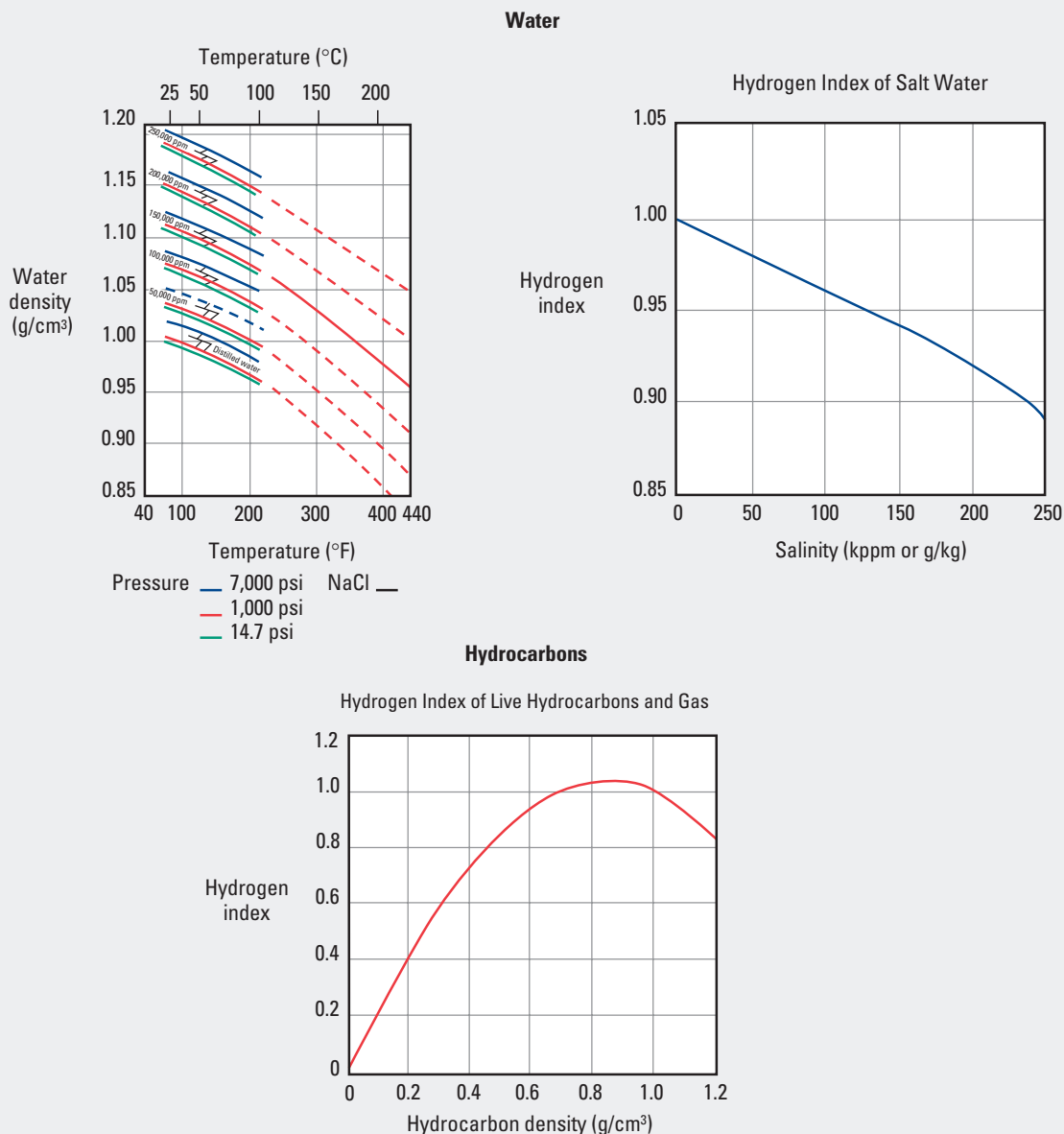
Conversion approximated by $R_2 = R_1 [(T_1 + 6.77)/(T_2 + 6.77)]^{1.04}$ or $R_2 = R_1 [(T_1 + 21.5)/(T_2 + 21.5)]^{1.04}$



Density of Water and Hydrogen Index of Water and Hydrocarbons

Gen-7

Gen

**Purpose**

These charts are for determination of the density (g/cm^3) and hydrogen index of water for known values of temperature, pressure, and salinity of the water. From a known hydrocarbon density of oil, a determination of the hydrogen index of the oil can be obtained.

Description: Density of Water

To obtain the density of the water, enter the desired temperature ($^{\circ}\text{F}$ at the bottom x-axis or $^{\circ}\text{C}$ at the top) and intersect the pressure and salinity in the chart. From that point read the density on the y-axis.

Example: Density of Water

Given: Temperature = 200°F [93°C], pressure = 7,000 psi, and salinity = 250,000 ppm.

Answer: Density of water = $1.15 \text{ g}/\text{cm}^3$.

Example: Hydrogen Index of Salt Water

Given: Salinity of saltwater = 125,000 ppm.

Answer: Hydrogen index = 0.95.

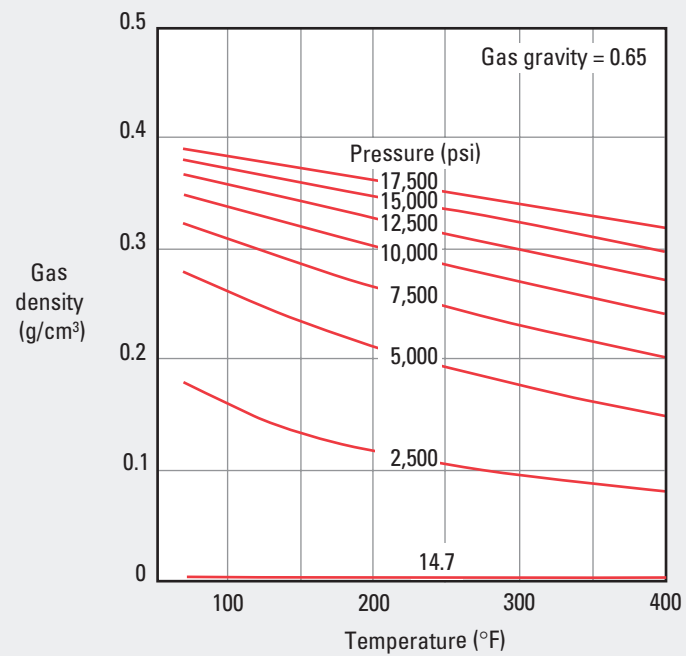
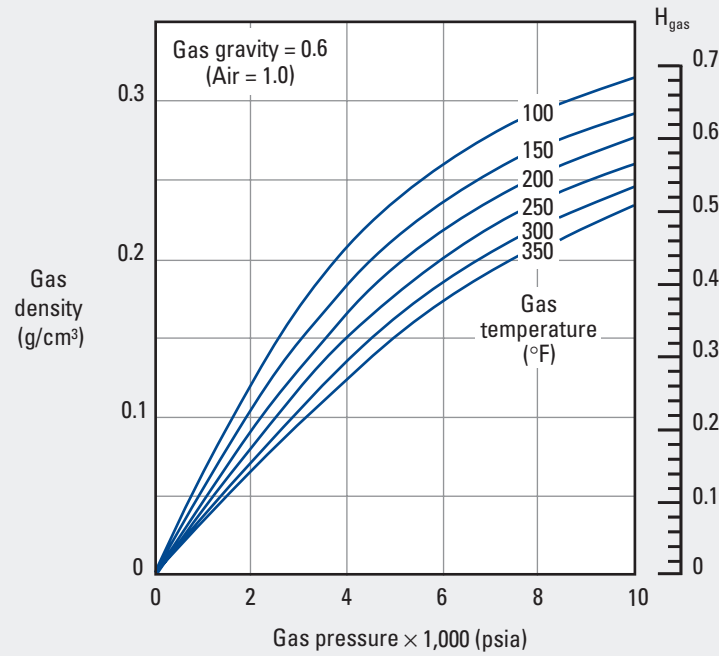
Example: Hydrogen Index of Hydrocarbons

Given: Oil density = $0.60 \text{ g}/\text{cm}^3$.

Answer: Hydrocarbon index = approximately 0.91.

Density and Hydrogen Index of Natural Gas

Gen



© Schlumberger

Purpose

This chart can be used to determine more than one characteristic of natural gas under different conditions. The characteristics are gas density (ρ_g), gas pressure, and hydrogen index (H_{gas}).

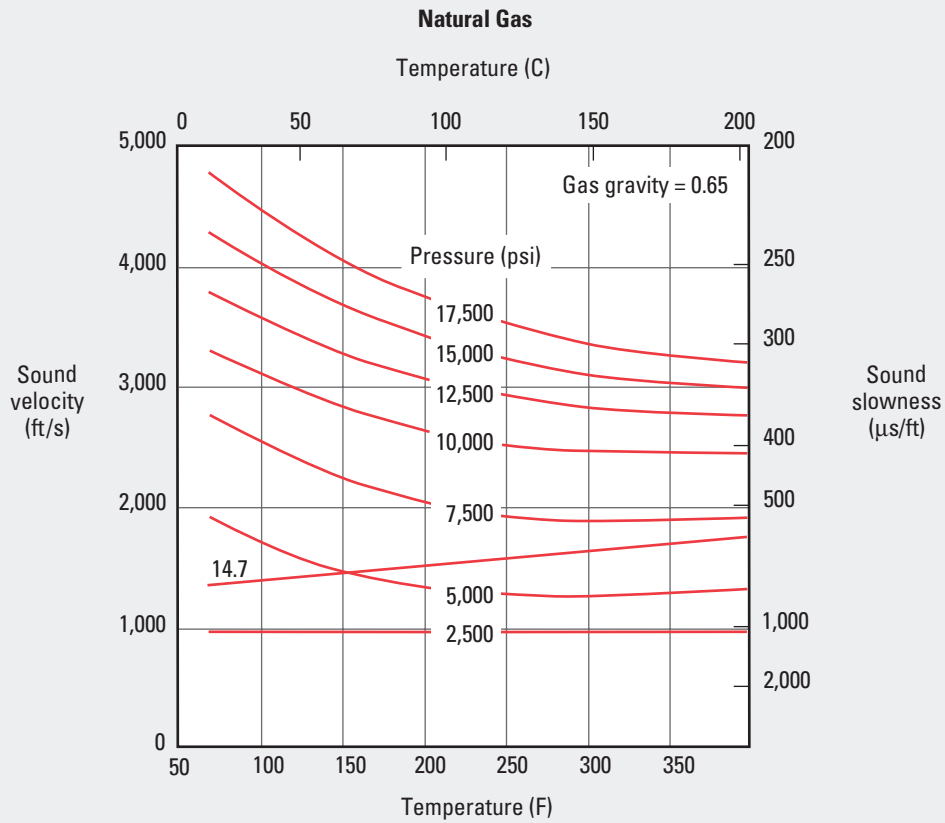
Description

For known values of gas density, pressure, and temperature, the value of H_{gas} can be determined. If only the gas pressure and temperature are known, then the gas density and H_{gas} can be determined. If the gas density and temperature are known, then the gas pressure and H_{gas} can be determined.

Example

- Given: Gas density = 0.2 g/cm³ and temperature = 200°F.
- Find: Gas pressure and hydrogen index.
- Answer: Gas pressure = approximately 5,200 psi and H_{gas} = 0.44.

Sound Velocity of Hydrocarbons



© Schlumberger

Purpose

This chart is used to determine the sound velocity (ft/s) and sound slowness (μs/ft) of gas in the formation. These values are helpful in sonic and seismic interpretations.

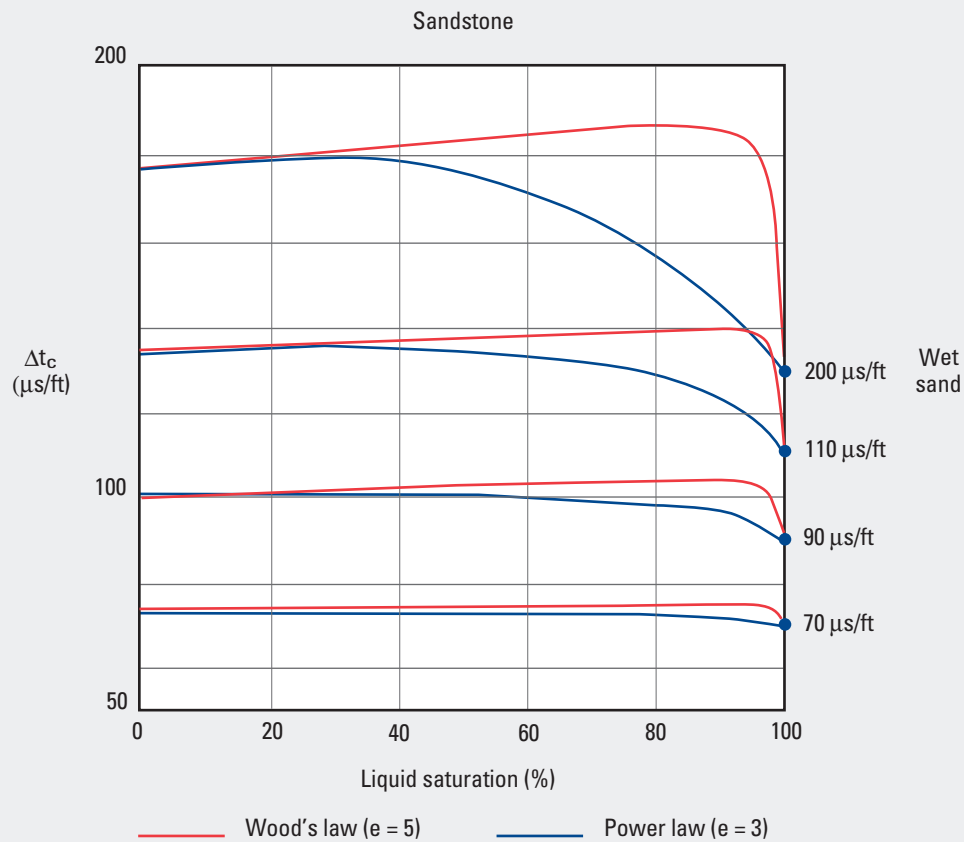
Description

Enter the chart with the temperature (Celsius along the top x-axis and Fahrenheit along the bottom) to intersect the formation pore pressure.

Gas Effect on Compressional Slowness

Gen-9a

Gen



© Schlumberger

Purpose

This chart illustrates the effect that gas in the formation has on the slowness time of sound from the sonic tool to anticipate the slowness of a formation that contains gas and liquid.

Description

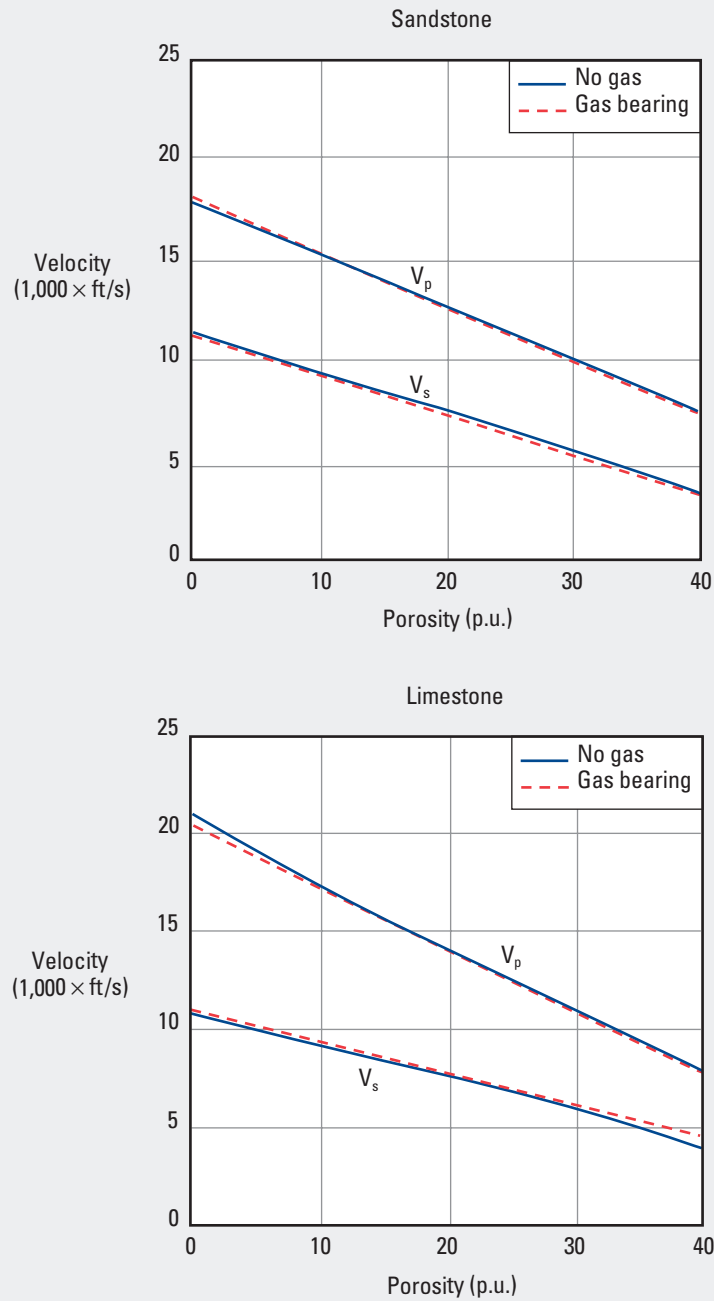
Enter the chart with the compressional slowness time (Δt_c) from the sonic log on the y-axis and the liquid saturation of the formation on the x-axis. The curves are used to determine the gas effect on the basis of which correlation (Wood's law or Power law) is applied. The slowing effect begins sooner for the Power law correlation. The Wood's law correlation slightly increases Δt_c values as the formation liquid saturation increases whereas the Power law correlation decreases Δt_c values from about 20% liquid saturation.

Gas Effect on Acoustic Velocity

Sandstone and Limestone

Gen-9b

Gen



© Schlumberger

Purpose

This chart is used to determine porosity from the compressional wave or shear wave velocity (V_p and V_s , respectively).

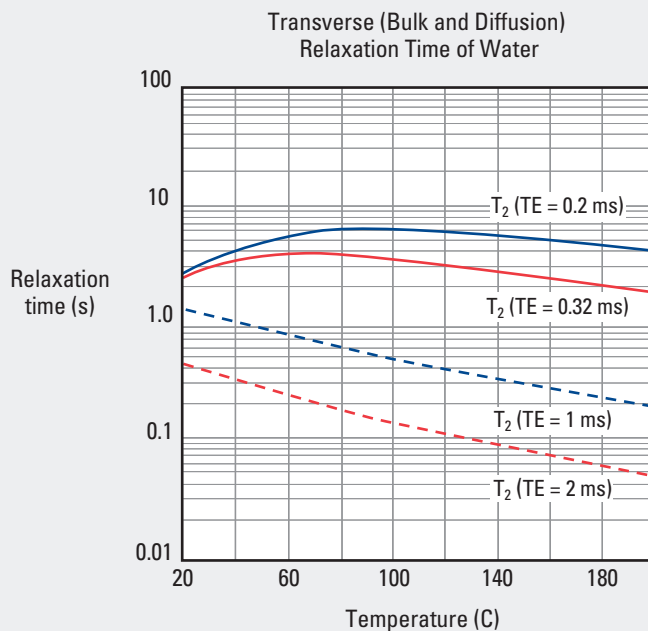
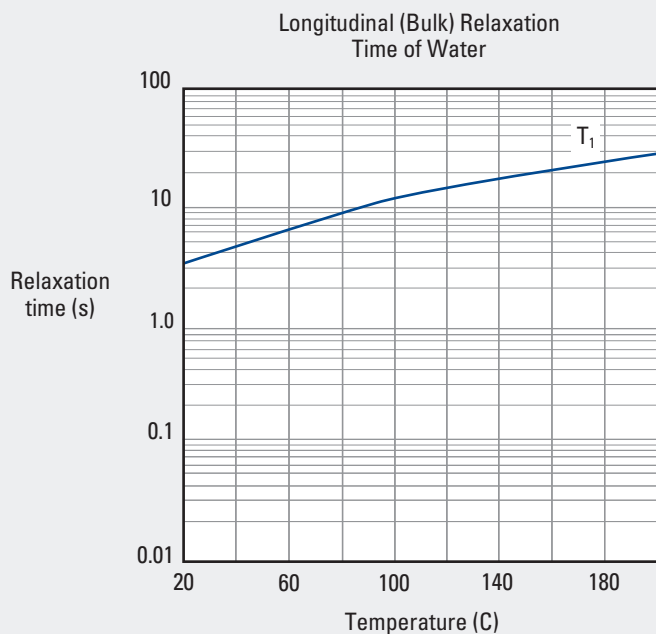
Description

Enter V_p or V_s on the y-axis to intersect the appropriate curve. Read the porosity for the sandstone or limestone formation on the x-axis.

Nuclear Magnetic Resonance Relaxation Times of Water

Gen-10

Gen



© Schlumberger

Purpose*Longitudinal (Bulk) Relaxation Time of Pure Water*

This chart provides an approximation of the bulk relaxation time (T_1) of pure water depending on the temperature of the water.

Transverse (Bulk and Diffusion) Relaxation Time of Water in the Formation

Determining the bulk and diffusion relaxation time (T_2) from this chart requires knowledge of both the formation temperature and the echo spacing (TE) used to acquire the data. These data are presented graphically on the log and are the basis of the water or hydrocarbon interpretation of the zone of interest.

Description*Longitudinal Relaxation Time*

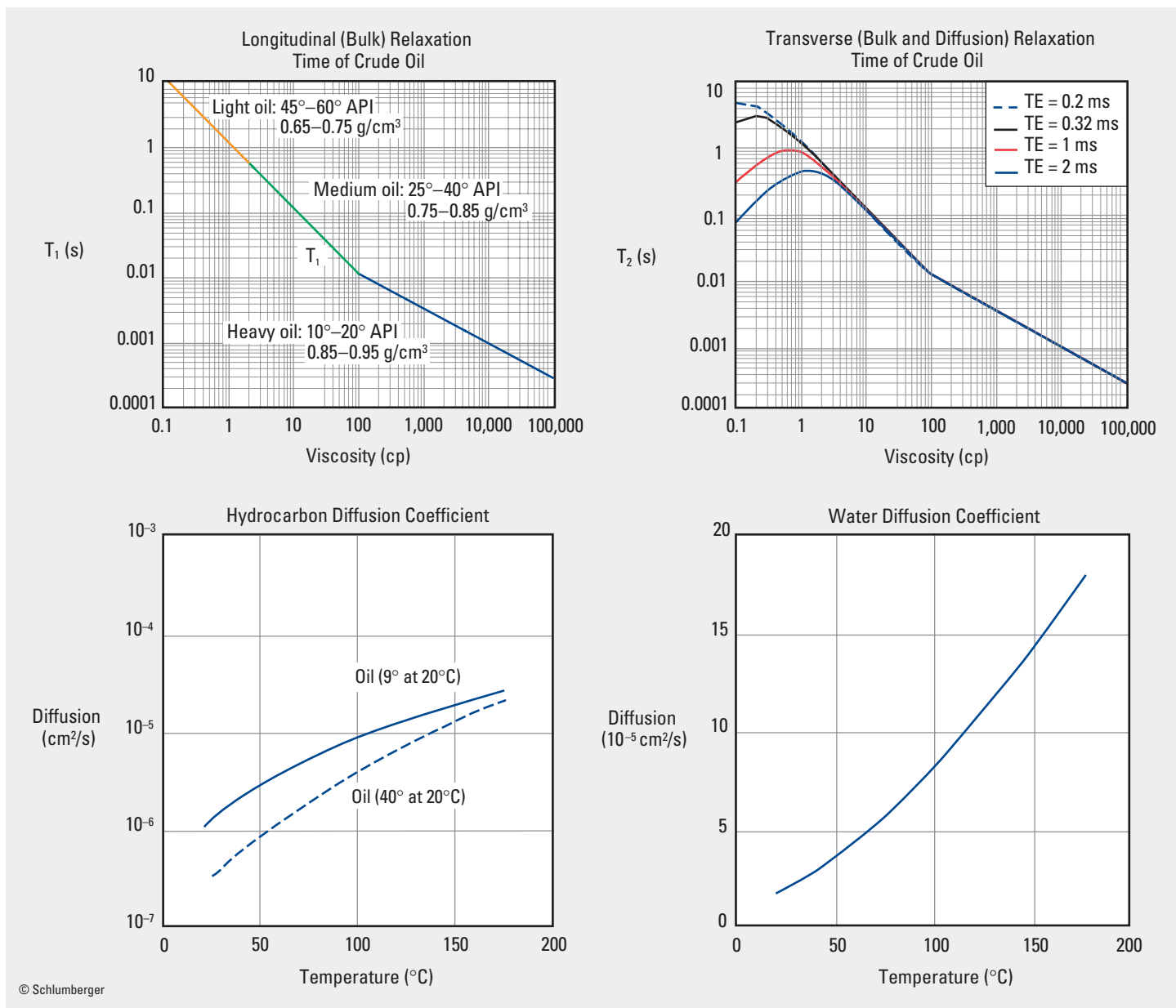
The chart relation is for pure water—the additives in drilling fluids reduce the relaxation time (T_1) of water in the invaded zone. The two major contributors to the reduction are surfactants added to the drilling fluid and the molecular interactions of the mud filtrate contained in the pore spaces and matrix minerals of the formation.

Transverse Relaxation Time

The relaxation time (T_2) determination is based on the formation temperature and echo spacing used to acquire the measurement. The TE value is listed in the parameter section of the log. Using the T_2 measurement from a known water sand or based on local experience further aids in determining whether a zone of interest contains hydrocarbons, water, or both.

Nuclear Magnetic Resonance Relaxation Times of Hydrocarbons

Gen-11a

**Purpose****Longitudinal (Bulk) Relaxation Time of Crude Oil**

This chart is used to predict the T_1 of crude oils with various viscosities and densities or specific gravities to assist in interpretation of the fluid content of the formation of interest.

Transverse (Bulk and Diffusion) Relaxation Time

Known values of T_2 and TE can be used to approximate the viscosity by using this chart.

Diffusion Coefficients for Hydrocarbon and Water

These charts are used to predict the diffusion coefficient of hydrocarbon as a function of formation temperature and viscosity and of water as a function of formation temperature.

Description**Longitudinal (Bulk) Relaxation Time**

This chart is divided into three distinct sections based on the composition of the oil measured. The type of oil contained in the formation can be determined from the measured T_1 and viscosity determined from the transverse relaxation time chart.

Transverse (Bulk and Diffusion) Relaxation Time

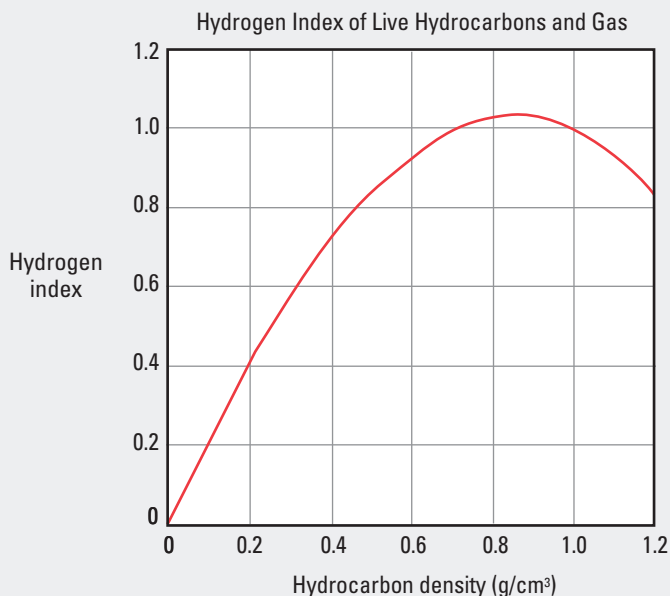
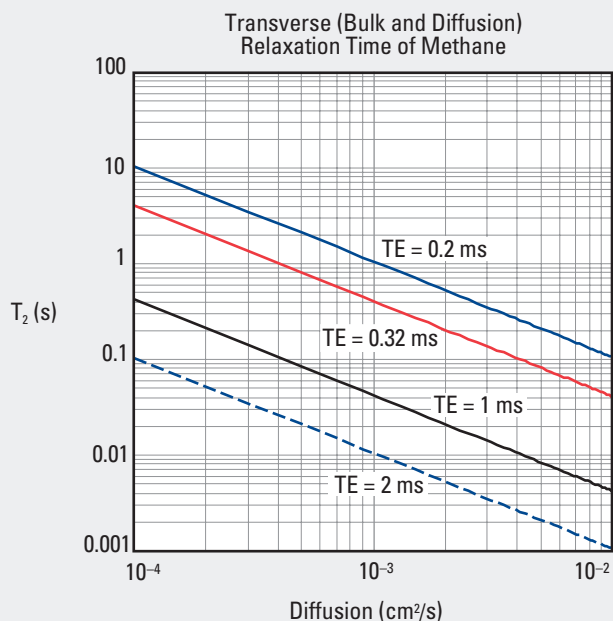
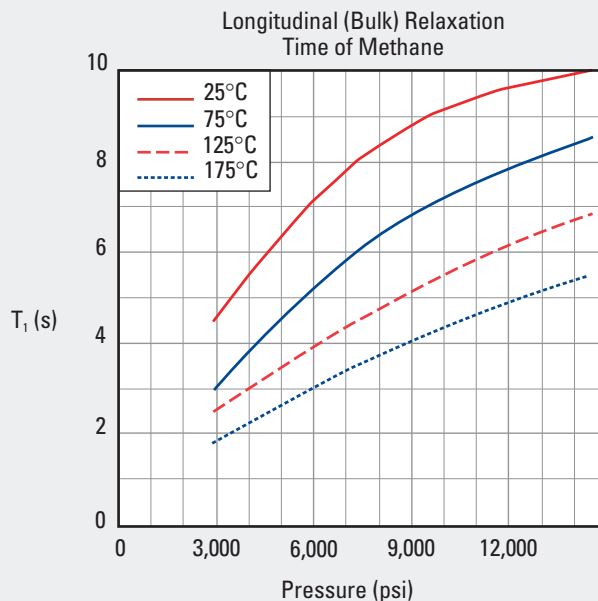
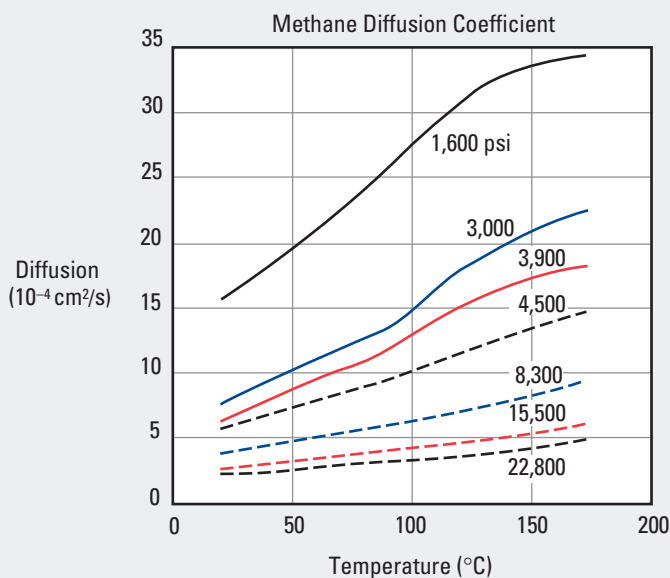
The viscosity can be determined with values of the measured T_2 and TE for input to the longitudinal relaxation time chart to identify the type of oil in the formation.

Gen

Nuclear Magnetic Resonance Relaxation Times of Hydrocarbons

Gen-11b

Gen



© Schlumberger

Purpose

Methane Diffusion Coefficient

This chart is used to determine the diffusion coefficient of methane at a known formation temperature and pressure.

Longitudinal and Transverse Relaxation Times of Methane

These charts are used to determine the longitudinal relaxation time (T_1) of methane by using the formation temperature and pressure (see Reference 48) and the transverse relaxation time (T_2) of methane by using the diffusion and echo spacing (TE), respectively.

Hydrogen Index of Live Hydrocarbons and Gas

This chart is used to determine the hydrogen index from the hydrocarbon density.

Capture Cross Section of NaCl Water Solutions

Purpose

The sigma value (Σ_w) of a saltwater solution can be determined from this chart. The sigma water value is used to calculate the water saturation of a formation.

Description

Charts Gen-12 and Gen-13 define sigma water for pressure conditions of ambient through 20,000 psi [138 MPa] and temperatures from 68° to 500°F [20° to 260°C]. Enter the appropriate chart for the pressure value with the known water salinity on the y-axis and move horizontally to intersect the formation temperature. The sigma of the formation water for the intersection point is on the x-axis.

Example

Given: Water salinity = 125,000 ppm, temperature = 68°F at ambient pressure, and formation temperature = 190°F at 5,000 psi.

Find: Σ_w at ambient conditions and Σ_w of the formation.

Answer: $\Sigma_w = 69$ c.u. and Σ_w of the formation = 67 c.u.

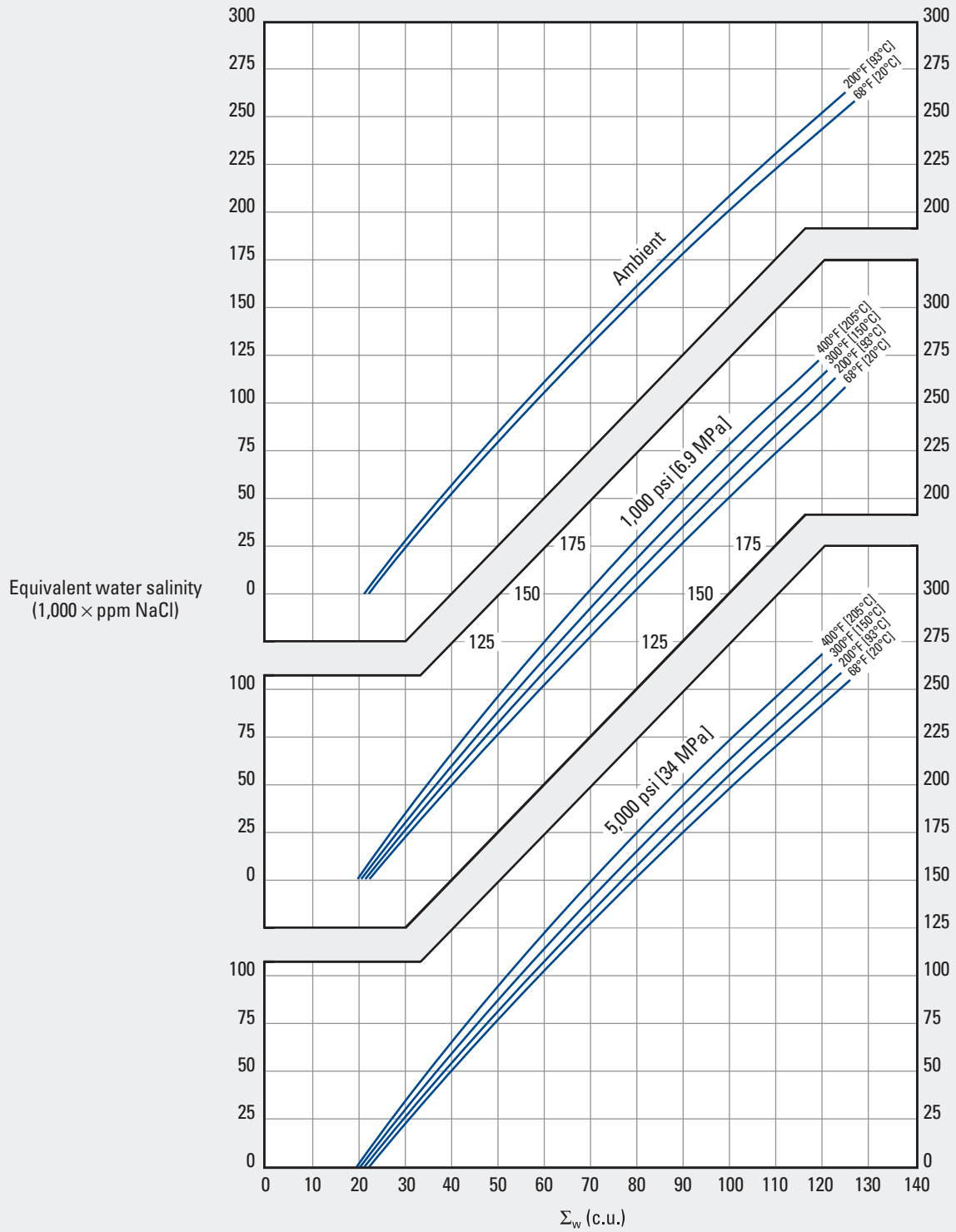
If the sigma water apparent (Σ_{wa}) is known from a clean water sand, then the salinity of the formation can be determined by entering the chart from the sigma water value on the x-axis to intersect the pressure and temperature values.

continued on next page

Capture Cross Section of NaCl Water Solutions

Gen-12
(former Tcor-2a)

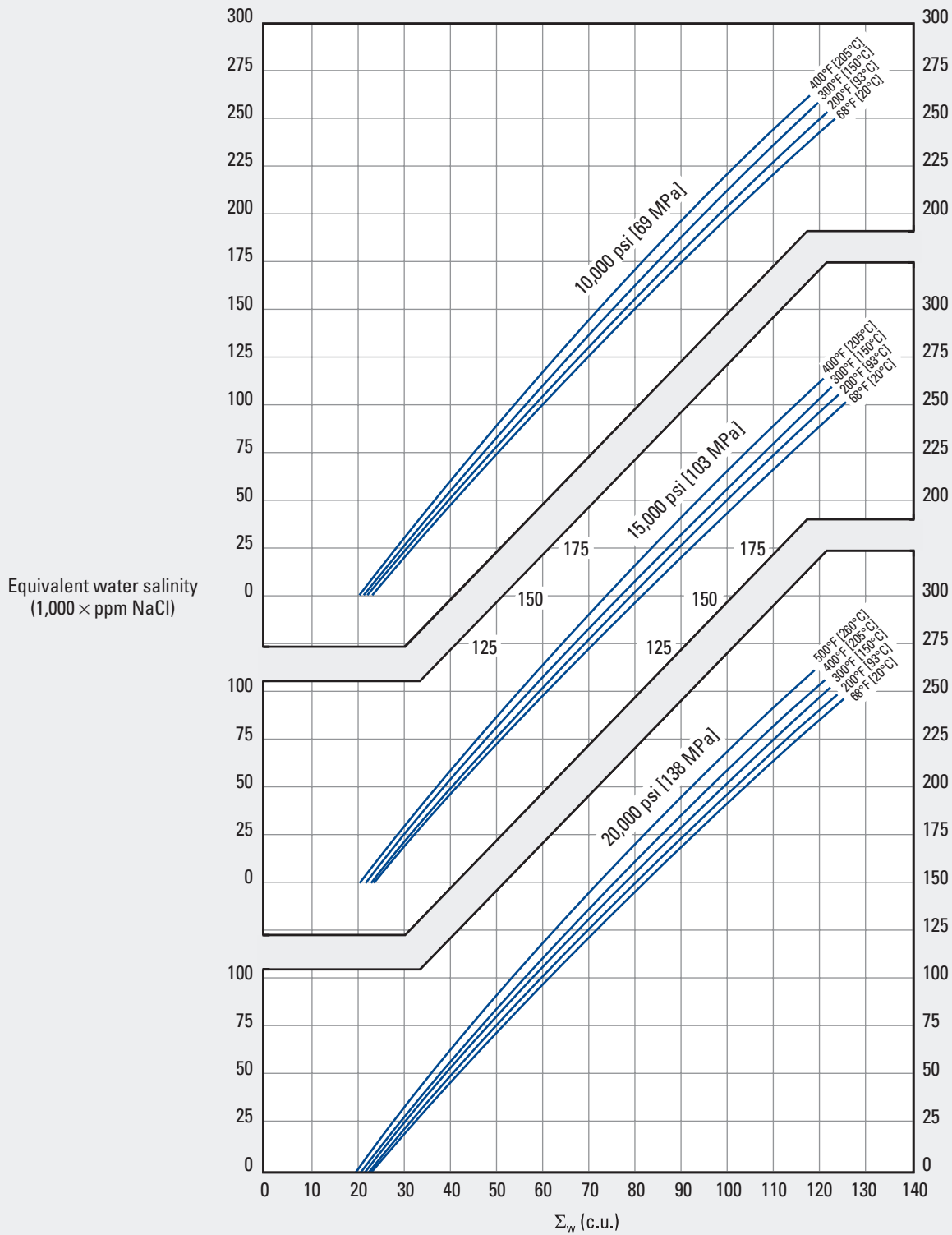
Gen



© Schlumberger

Capture Cross Section of NaCl Water Solutions

Gen-13
(former Tcor-2b)



© Schlumberger

Purpose

Chart Gen-13 continues Chart Gen-12 at higher pressure values for the determination of Σ_w of a saltwater solution.

Capture Cross Section of Hydrocarbons

Purpose

Sigma hydrocarbon (Σ_h) for gas or oil can be determined by using this chart. Sigma hydrocarbon is used to calculate the water saturation of a formation.

Description

One set of charts is for measurement in metric units and the other is for measurements in “customary” oilfield units.

For gas, enter the background chart of a chart set with the reservoir pressure and temperature. At that intersection point move left to the y-axis and read the sigma of methane gas.

For oil, use the foreground chart and enter the solution gas/oil ratio (GOR) of the oil on the x-axis. Move upward to intersect the appropriate API gravity curve for the oil. From this intersection point, move horizontally left and read the sigma of the oil on the y-axis.

Example

Given: Reservoir pressure = 8,000 psi, reservoir temperature = 300°F, gravity of reservoir oil = 30°API, and solution GOR = 200.

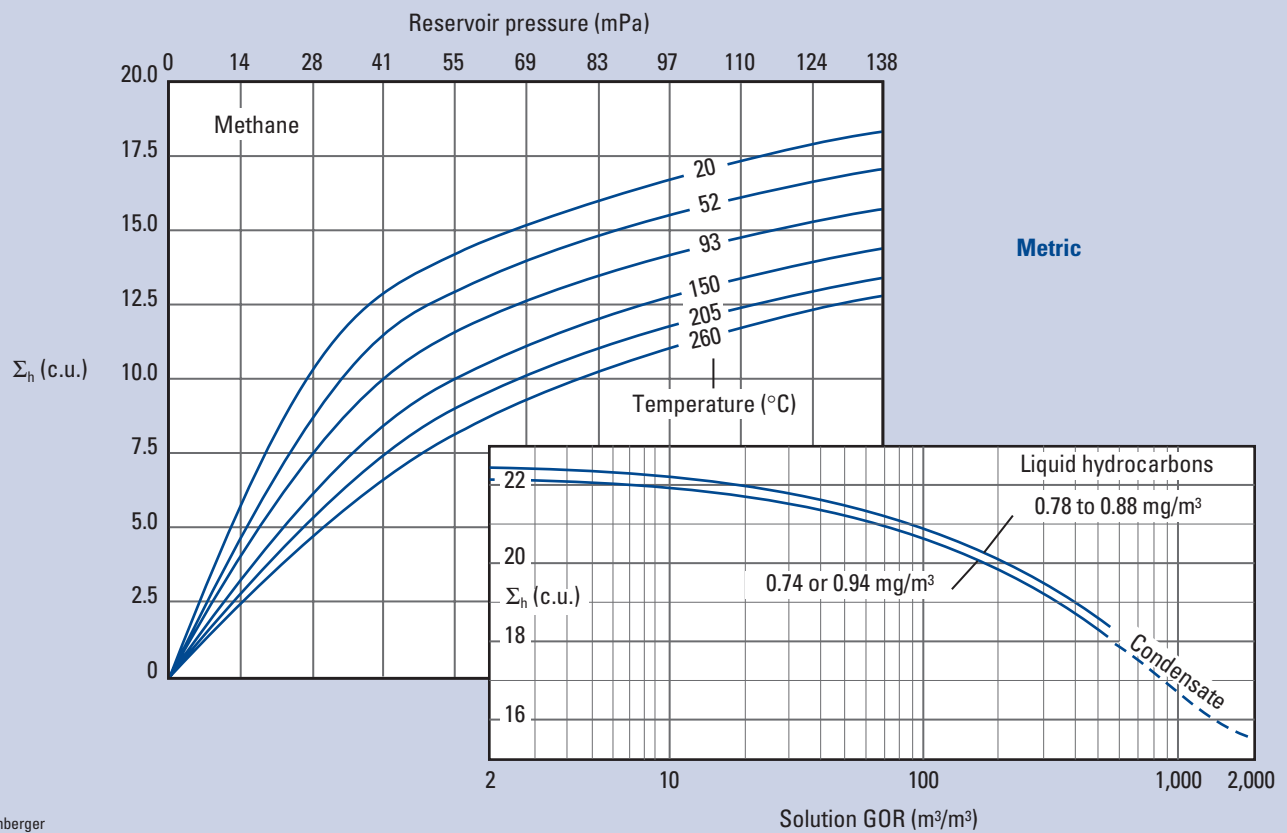
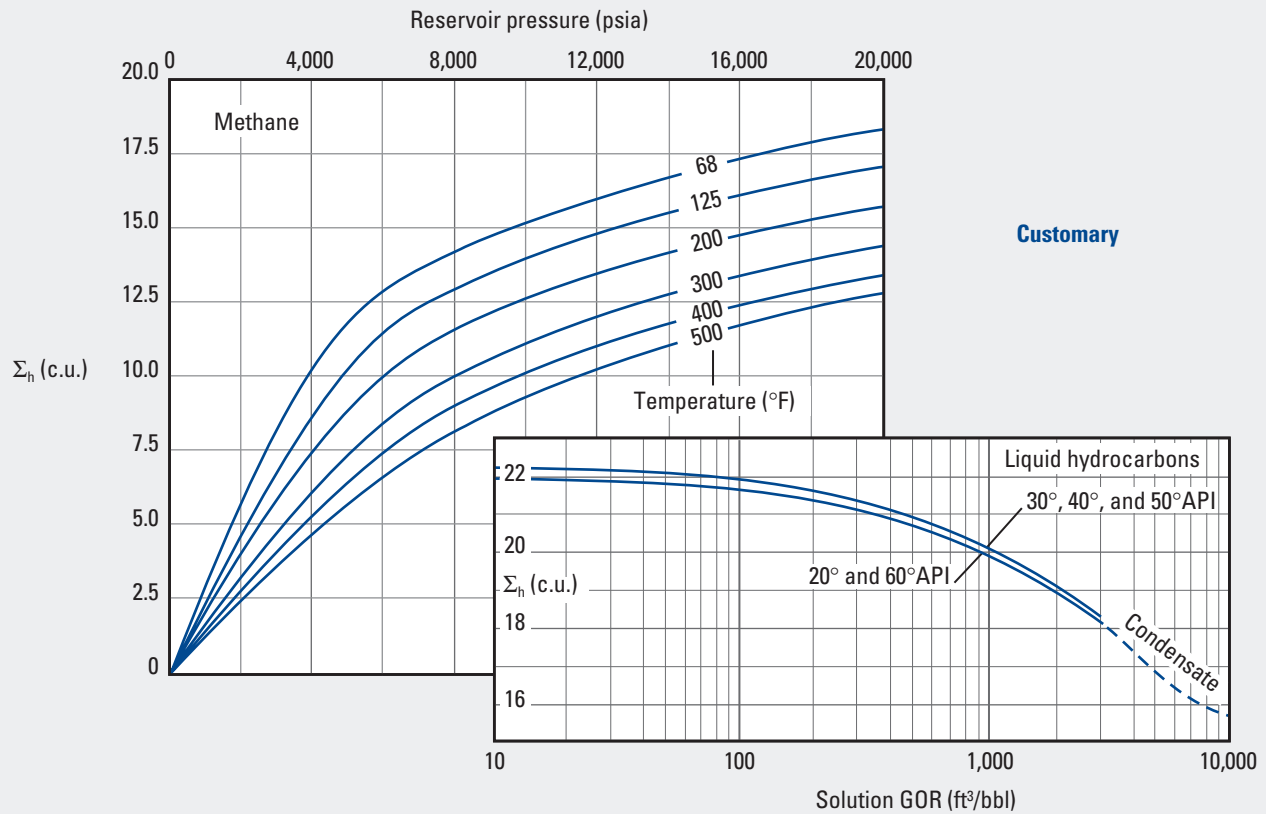
Find: Sigma gas and sigma oil.

Answer: Sigma gas = 10 c.u. and sigma oil = 21.6 c.u.

Capture Cross Section of Hydrocarbons

Gen-14
(former Tcor-1)

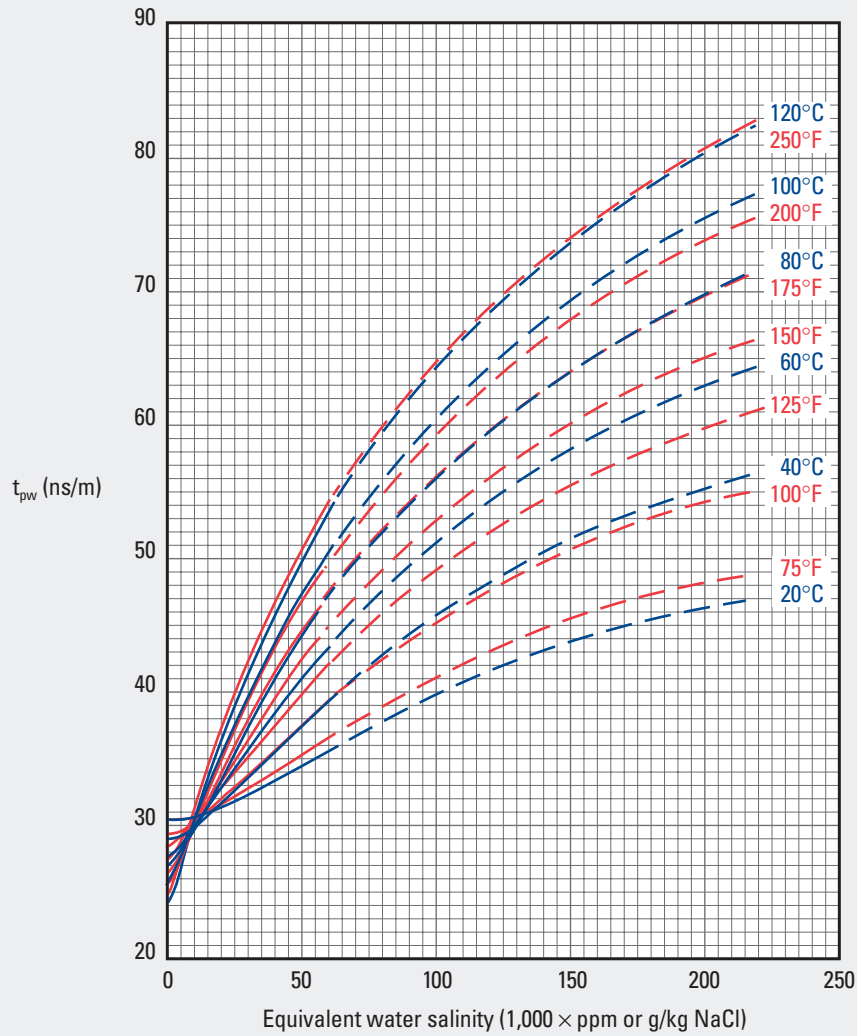
Gen



EPT* Propagation Time of NaCl Water Solutions

Gen-15
(former EPTcor-1)

Gen



*Mark of Schlumberger
© Schlumberger

Purpose

This chart is designed to determine the propagation time (t_{pw}) of saltwater solutions. The value of t_{pw} of a water zone is used to determine the temperature variation of the salinity of the formation water.

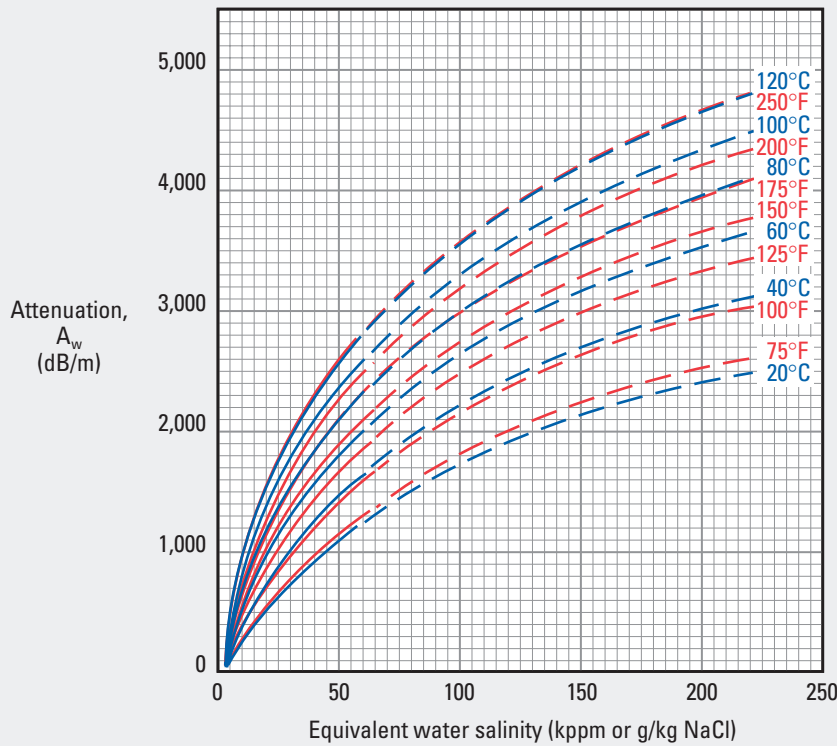
Description

Enter the chart with the known salinity of the zone of interest and move upward to the formation temperature curve. From that intersection point move horizontally left and read the propagation time of the water in the formation on the y-axis. Conversely, enter the chart with a known value of t_{pw} from the EPT Electromagnetic Propagation Tool log to intersect the formation temperature curve and read the water salinity at the bottom of the chart.

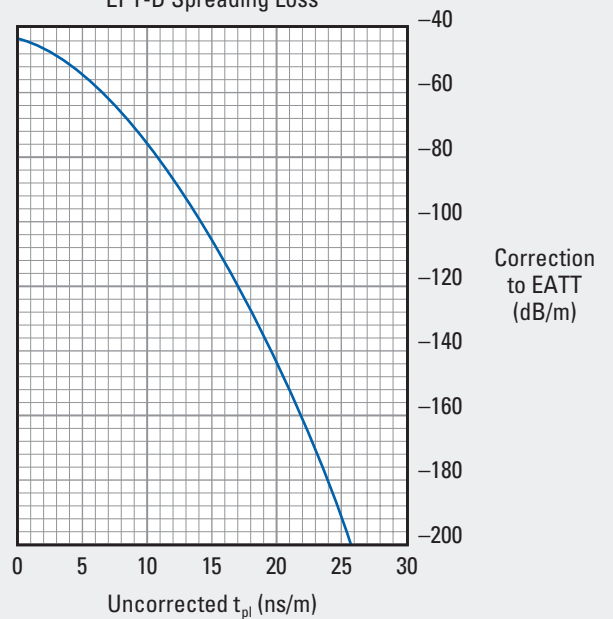
EPT* Attenuation of NaCl Water Solutions

Gen-16
(former EPTcor-2)

Gen



EPT-D Spreading Loss



*Mark of Schlumberger
© Schlumberger

Purpose

This chart is designed to estimate the attenuation of saltwater solutions. The attenuation (A_w) value of a water zone is used in conjunction with the spreading loss determined from the EPT propagation time measurement (t_{pi}) to determine the saturation of the flushed zone by using Chart SatOH-8.

Description

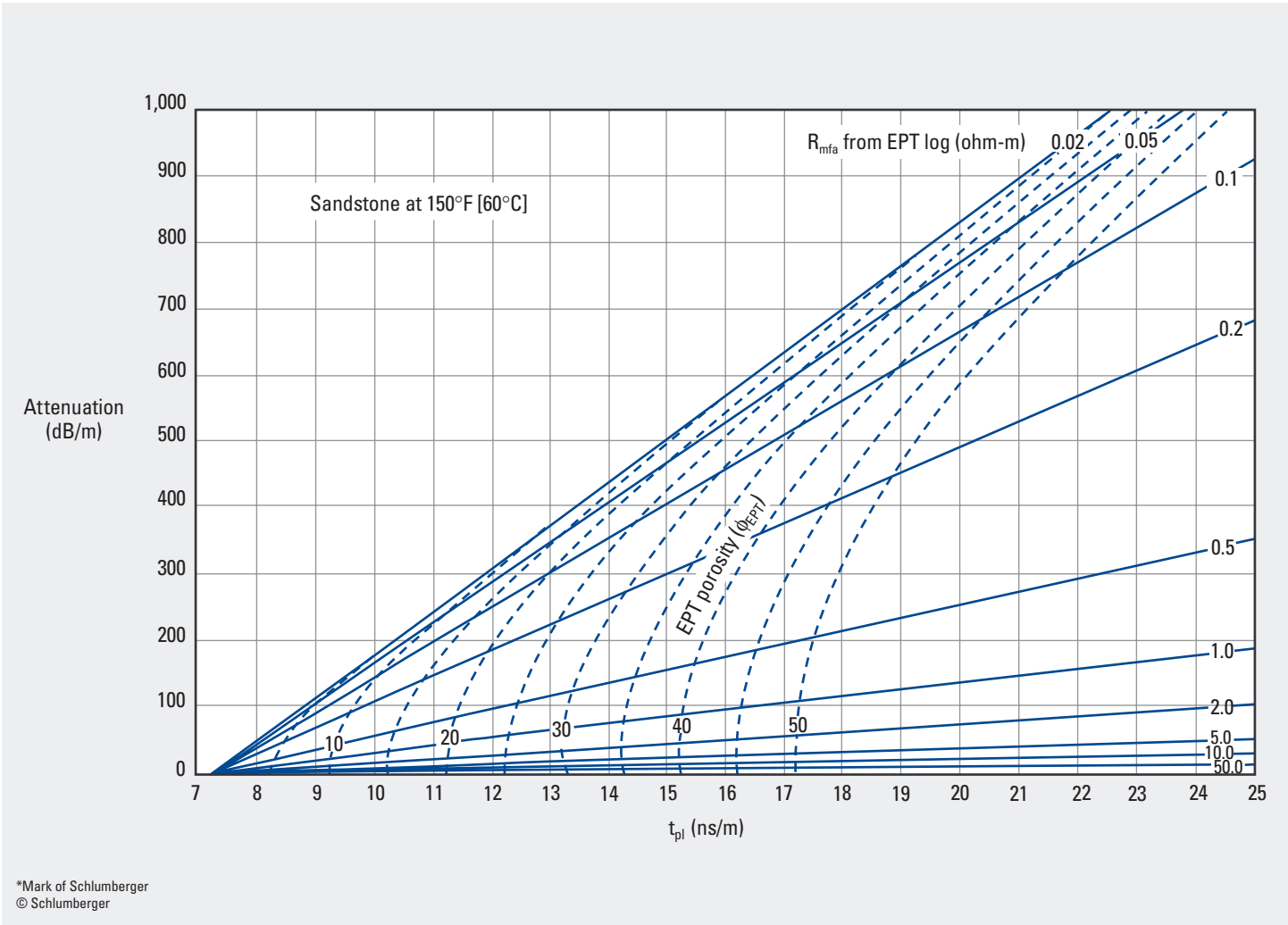
Enter the chart with the known salinity of the zone of interest and move upward to the formation temperature curve. From that intersection point move horizontally left and read the attenuation of the water in the formation on the y-axis. Conversely, enter the chart with a known EATT attenuation value of A_w from the EPT Electromagnetic Propagation Tool log to intersect the formation temperature curve and read the water salinity at the bottom of the chart.

EPT* Propagation Time–Attenuation Crossplot

Sandstone Formation at 150°F [60°C]

Gen-16a

Gen



*Mark of Schlumberger
© Schlumberger

Purpose

This chart is used to determine the apparent resistivity of the mud filtrate (R_{mfa}) from measurements from the EPT Electromagnetic Propagation Tool. The porosity of the formation (ϕ_{EPT}) can also be estimated. Porosity and mud filtrate resistivity values are used in determining the water saturation.

Description

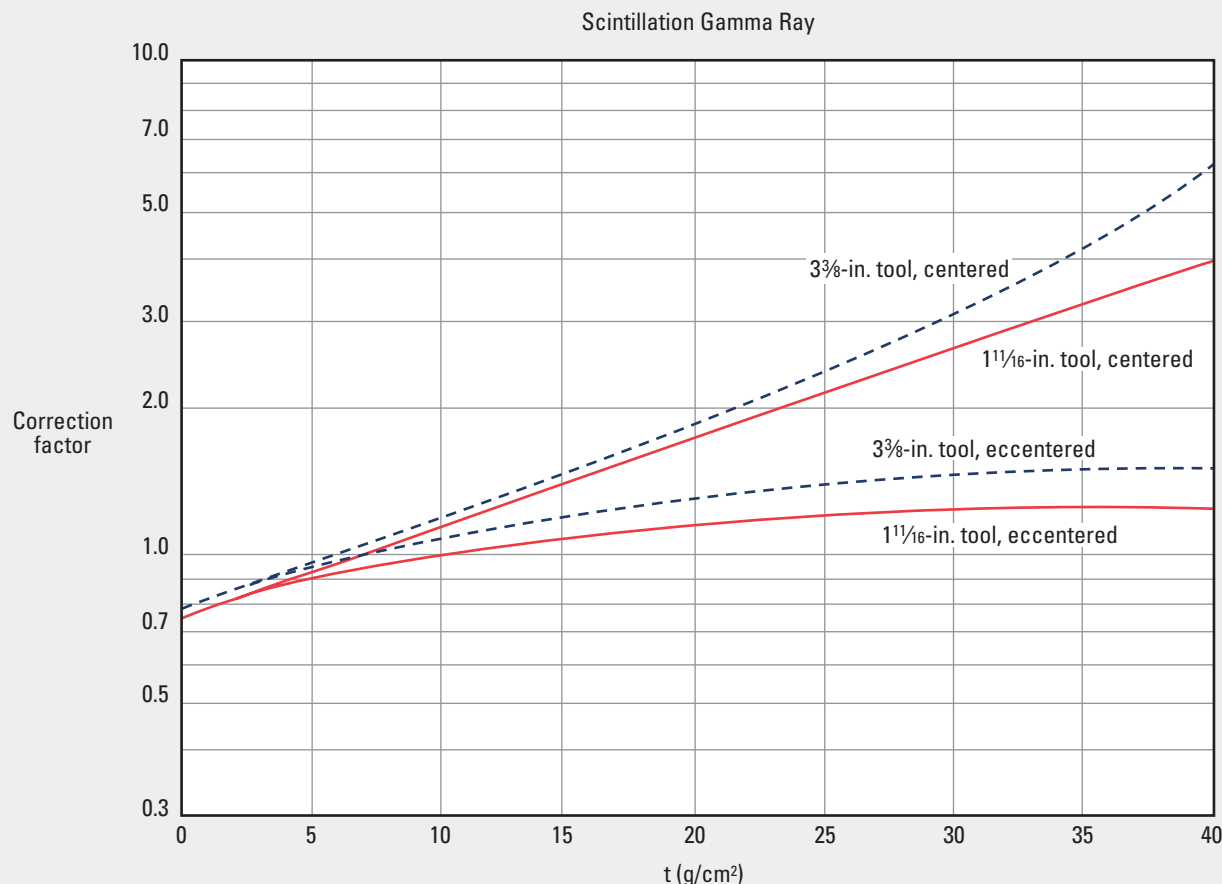
Enter the chart with the known attenuation and propagation time (t_{pi}). The intersection of those values identifies R_{mfa} and ϕ_{EPT} from the two sets of curves. This chart is characterized for a sandstone formation at a temperature of 150°F [60°C].

Example

Given: Attenuation = 300 dB/m and t_{pi} = 13 ns/m.
 Find: Apparent resistivity of the mud filtrate and EPT porosity.
 Answer: R_{mfa} = 0.1 ohm-m and ϕ_{EPT} = 20 p.u.

Scintillation Gamma Ray— $3\frac{3}{8}$ - and $1\frac{1}{16}$ -in. Tools

Gamma Ray Correction for Hole Size and Mud Weight

GR-1
(former GR-1)

© Schlumberger

Purpose

This chart provides a correction factor for measured values of formation gamma ray (GR) in gAPI units. If the mud contains barite, the additional correction of Chart GR-2 should also be made.

Description

The semilog chart has the t factor on the x-axis and the correction factor on the y-axis.

The input parameter, t , in g/cm^2 , is calculated as follows:

$$t = \frac{W_{\text{mud}}}{8.345} \left(\frac{2.54(d_h)}{2} - \frac{2.54(d_{\text{sonde}})}{2} \right),$$

where

W_{mud} = mud weight (lbm/gal)

d_h = diameter of wellbore (in.)

d_{sonde} = outside diameter (OD) of tool (in.).

The correction for standoff is

$$CF' = CF'_m + (CF'_o - CF'_m) \left(\frac{S - S_m}{S_m} \right)^2.$$

CF'_m is the correction factor for centered tools, while CF'_o is the correction factor for eccentered tools. Both are corrected for barite if it is present in the borehole. S is the actual standoff, and S_m is the standoff with the tool centered.

Example

Given: GR = 36 API units (gAPI), $d_h = 12$ in., mud weight = 12 lbm/gal, tool OD = $3\frac{3}{8}$ in., and the tool is centered.

Find: Corrected GR value.

Answer:

$$t = \frac{12}{8.345} \left(\frac{2.54(12)}{2} - \frac{2.54(3.375)}{2} \right) = 15.8 \text{ g}/\text{cm}^2.$$

Enter the chart at 15.8 on the x-axis and move upward to intersect the $3\frac{3}{8}$ -in. centered curve. The corresponding correction factor is 1.6.

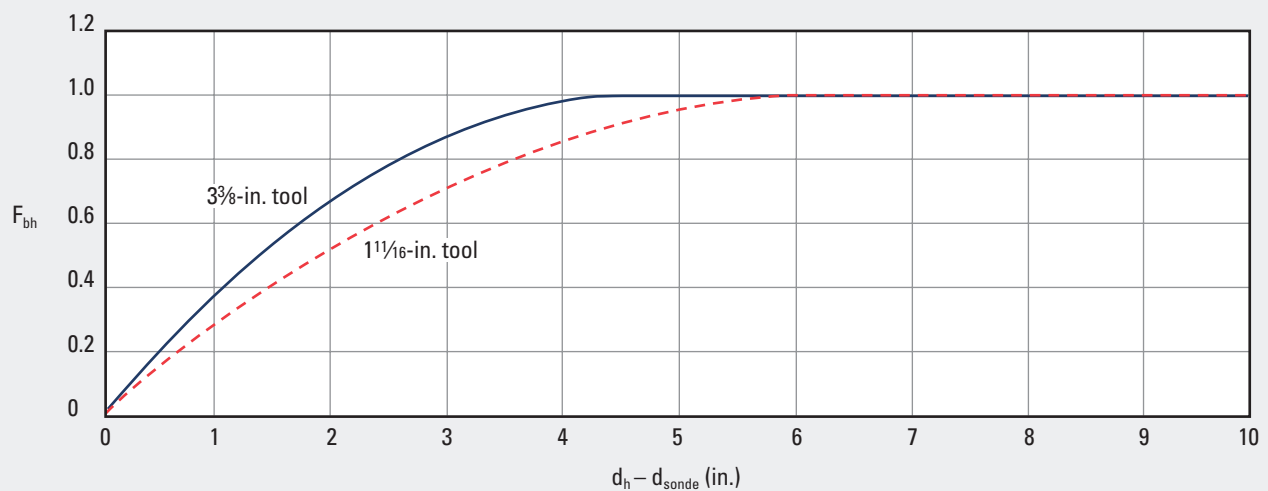
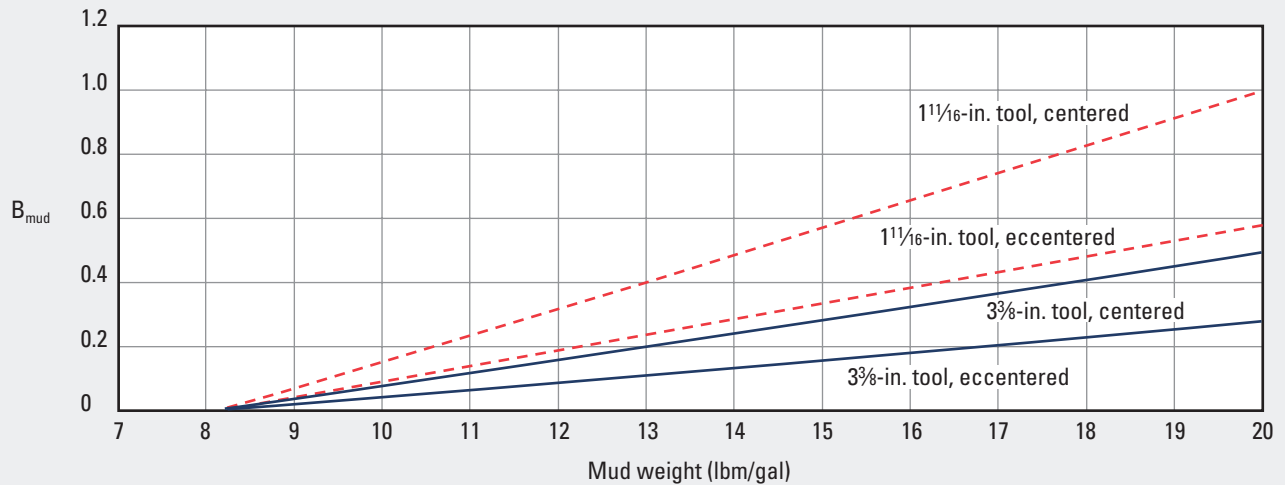
$$1.6 \times 36 \text{ gAPI} = 58 \text{ gAPI}.$$

Scintillation Gamma Ray— $3\frac{3}{8}$ - and $1\frac{1}{16}$ -in. Tools

Additional Gamma Ray Correction for Barite Mud in Various-Size Boreholes

GR-2

(former GR-2)



© Schlumberger

Purpose

Once the GR reading has been corrected with Chart GR-1, these charts are an additional correction to be applied if the mud contains barite.

Description

Two components needed to complete correction of the GR reading are determined with these charts: barite mud factor (B_{mud}) and borehole function factor (F_{bh}).

Example

Given: Borehole diameter = 6.0 in., tool OD = $3\frac{3}{8}$ in., the tool is centered, mud weight = 12 lbm/gal, measured GR = 36 gAPI.

Find: Corrected GR value.

Answer: Enter the upper chart for B_{mud} versus mud weight at 12 lbm/gal on the x-axis. The intersection point with the $3\frac{3}{8}$ -in. centered curve is $B_{mud} = 0.15$ on the y-axis.

Determine $(d_h - d_{sonde})$ as $6 - 3.375 = 2.625$ in. and enter that value on the lower chart for F_{bh} versus $(d_h - d_{sonde})$ on the x-axis. Move upward to intersect the $3\frac{3}{8}$ -in. curve, at which $F_{bh} = 0.81$.

Determine the new value of t using the equation from Chart GR-1:

$$t = \frac{W_{mud}}{8.345} \left(\frac{2.54(d_h)}{2} - \frac{2.54(d_{sonde})}{2} \right)$$

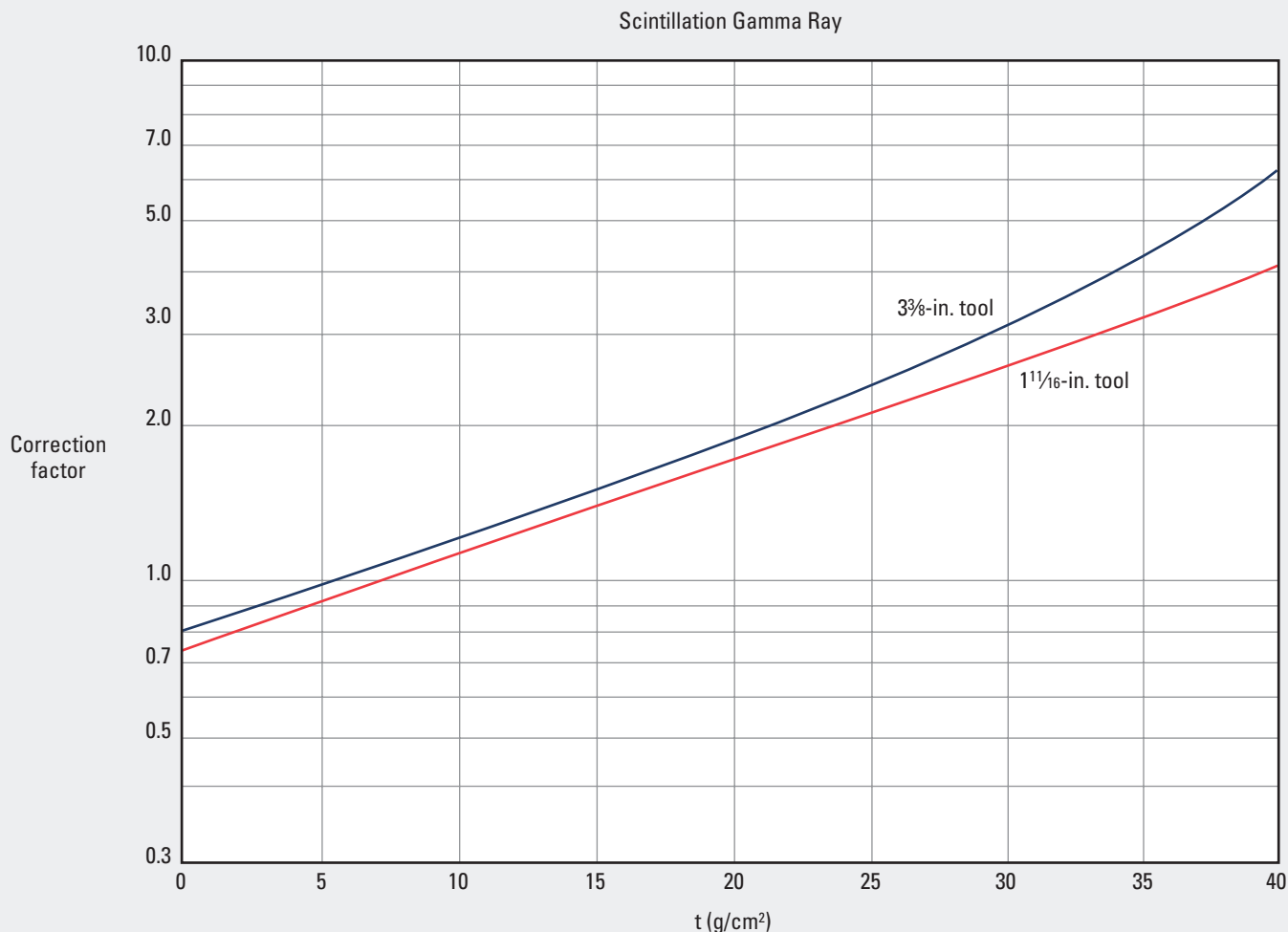
$$= \frac{12}{8.345} \left(\frac{2.54(6)}{2} - \frac{2.54(3.375)}{2} \right) = 4.8 \text{ g/cm}^3$$

The correction factor determined from Chart GR-1 is 0.95.

The complete correction factor is
 (Chart GR-1 correction factor) \times $[1 + (B_{mud} \times F_{bh})]$
 $= 1.12 \times [1 + (0.15 \times 0.81)] = 1.26$
 Corrected GR = $36 \times 1.26 = 45.4$ gAPI.

Scintillation Gamma Ray— $3\frac{3}{8}$ - and $1\frac{1}{16}$ -in. Tools

Borehole Correction for Cased Hole

GR-3
(former GR-3)

© Schlumberger

Purpose

This chart is used to compensate for the effects of the casing, cement sheath, and borehole fluid on the GR count rate in cased holes for conditions of an eccentric $3\frac{3}{8}$ -in. tool in an 8-in. borehole with 10-lbm/gal mud.

Description

In small boreholes the count rate can be too large, and in larger boreholes the count rate can be too small. The chart is based on openhole Chart GR-1, modified by laboratory and Monte Carlo calculations to provide a correction factor for application to the measured GR count rate in cased hole environments:

$$t = \frac{2.54}{2} \left[\frac{W_m}{8.345} (d_{IDcsg} - d_{sonde}) + \rho_{csg} (d_{ODcsg} - d_{IDcsg}) + \rho_{cement} (d_h - d_{ODcsg}) \right]$$

Example

Given: GR = 19 gAPI, hole diameter (d_h) = 12 in., casing OD (d_{ODcsg}) = $9\frac{5}{8}$ in. and 43.5 lbm/ft, casing ID (d_{IDcsg}) = 8.755 in., casing density (ρ_{csg}) = 7.96 g/cm³, tool OD (d_{sonde}) = $3\frac{3}{8}$ in., cement density (ρ_{cement}) = 2.0 g/cm³, and mud weight (W_m) = 8.345 lbm/gal.

Find: Corrected cased hole GR value.

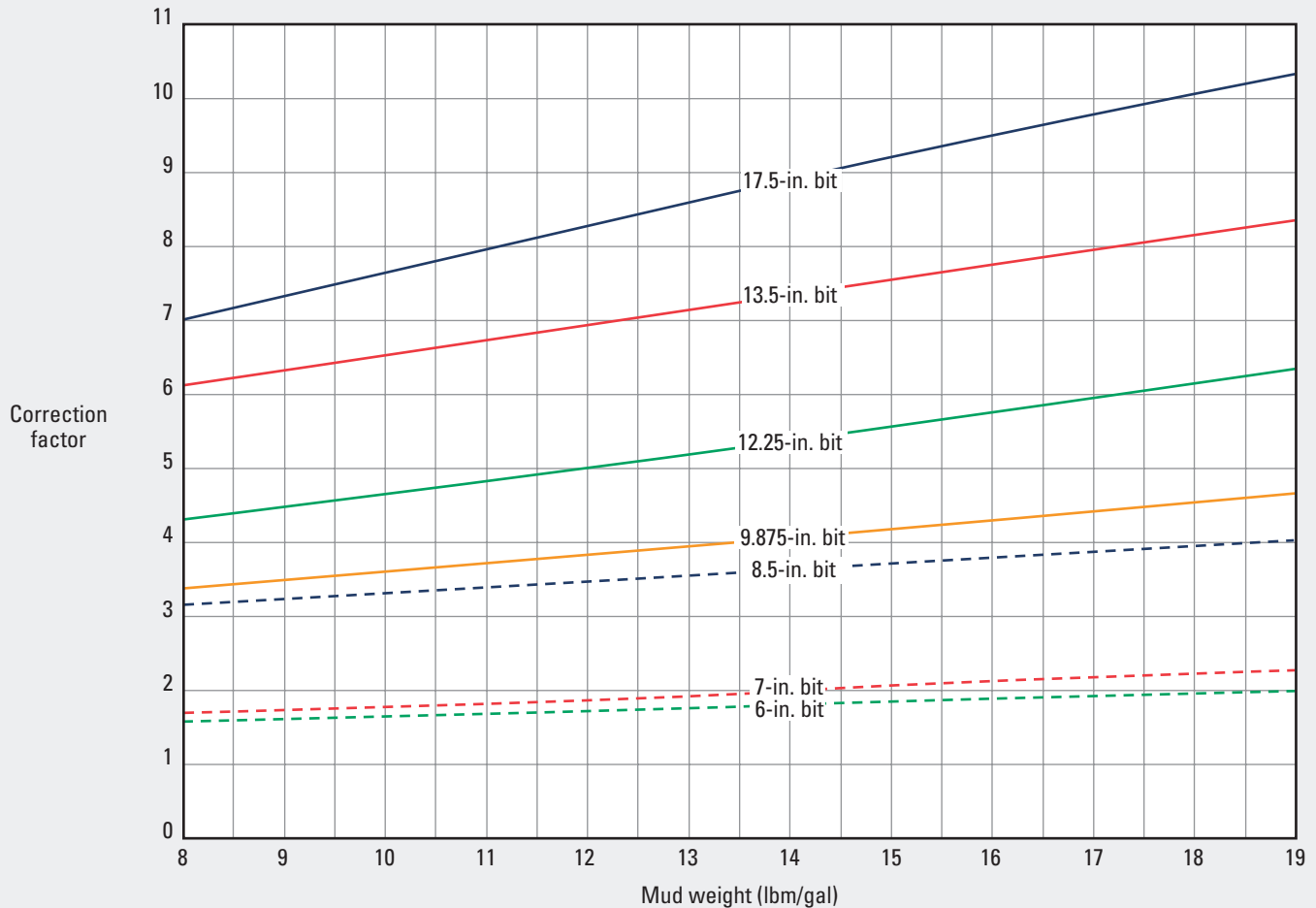
Answer: The chart input factor calculated with the equation is $t = 21.7$ g/cm². Enter the chart at 21.7 on the x-axis. At the intersection point with the $3\frac{3}{8}$ -in. curve, the value of the correction factor on the y-axis is 2.0. The GR value is corrected by multiplying by the correction factor:
19 gAPI \times 2.0 = 38 gAPI.

SlimPulse* and E-Pulse* Gamma Ray Tools

Borehole Correction for Open Hole

GR-6

GR



*Mark of Schlumberger
© Schlumberger

Purpose

This chart is used to provide a correction factor for gamma ray values measured with the SlimPulse third-generation slim measurements-while-drilling (MWD) tool or the E-Pulse electromagnetic telemetry tool. These environmental corrections for mud weight and bit size are already applied to the gamma ray presented on the logs.

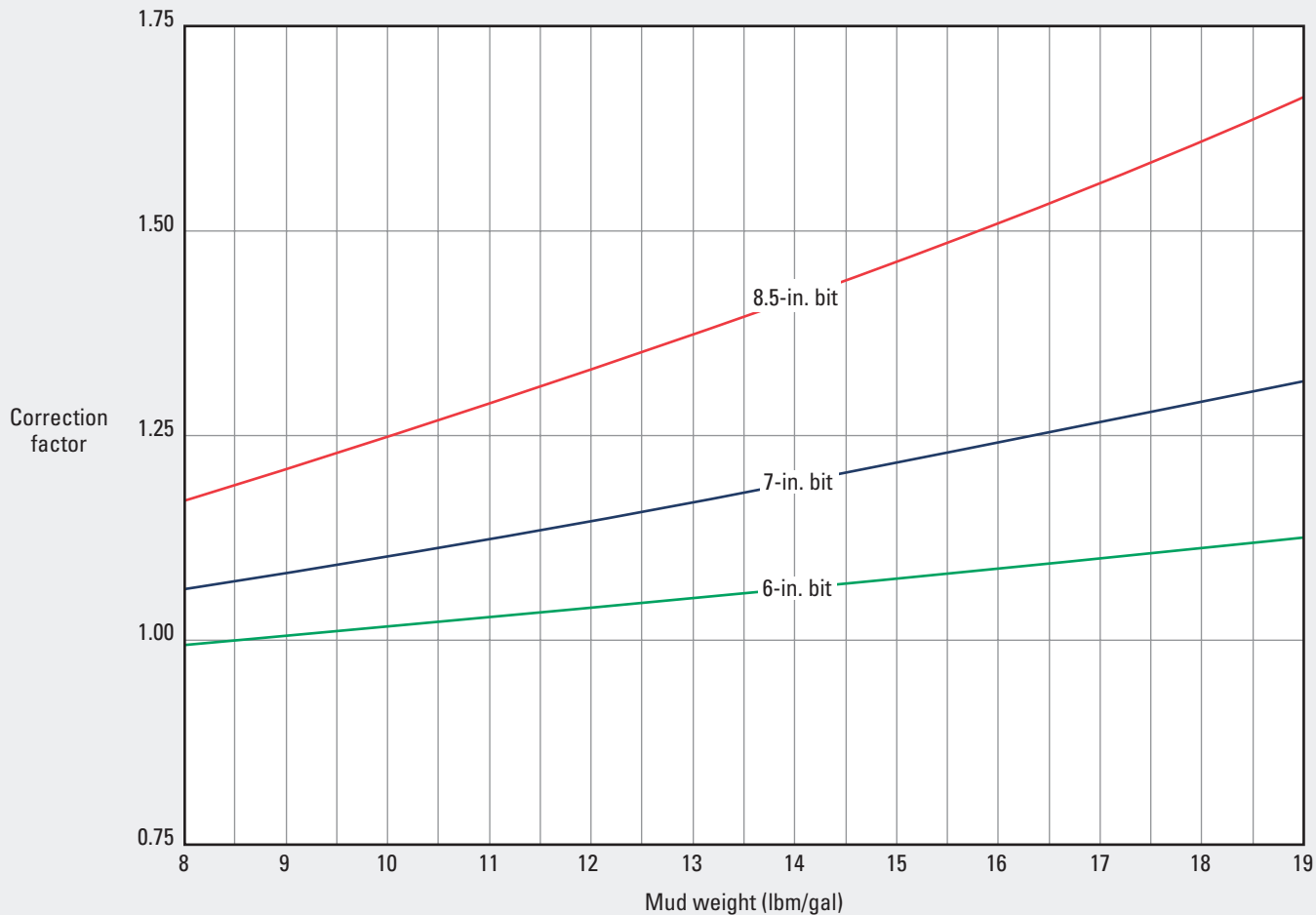
Description

Enter the chart with the mud weight on the x-axis and move upward to intersect the appropriate openhole size. Interpolate between lines as necessary. At the intersection point, move horizontally left to the y-axis to read the correction factor that the SlimPulse or E-Pulse gamma ray value was multiplied by to obtain the corrected gamma ray value in gAPI units.

ImPulse* Gamma Ray—4.75-in. Tool

Borehole Correction for Open Hole

GR-7



*Mark of Schlumberger
© Schlumberger

Purpose

This chart is used to provide a correction factor for gamma ray values measured with the ImPulse integrated MWD platform. These environmental corrections for mud weight and bit size are already applied to the gamma ray presented on the logs.

Description

Enter the chart with the mud weight on the x-axis and move upward to intersect the appropriate bit size. Interpolate between lines as necessary. At the intersection point, move horizontally left to the y-axis to read the correction factor that the ImPulse gamma ray value was multiplied by to obtain the corrected gamma ray value in gAPI units.

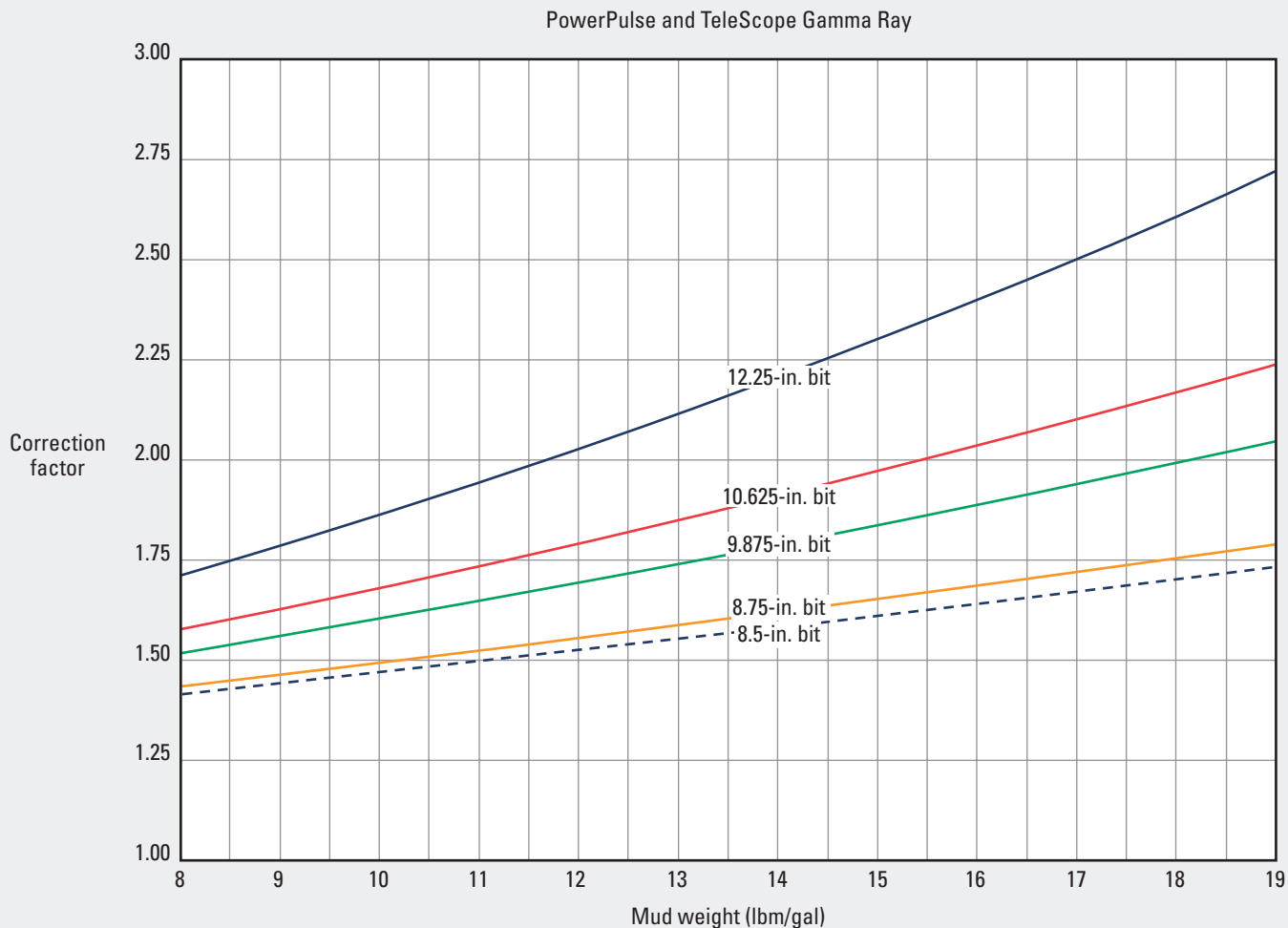
GR

PowerPulse* and TeleScope* Gamma Ray—6.75-in. Tools

Borehole Correction for Open Hole

GR-9

GR



*Mark of Schlumberger
© Schlumberger

Purpose

This chart is used to provide a correction factor for gamma ray values measured with the PowerPulse 6.75-in. MWD telemetry system and TeleScope 6.75-in. high-speed telemetry-while-drilling service. These environmental corrections for mud weight and bit size are already applied to the gamma ray presented on the logs.

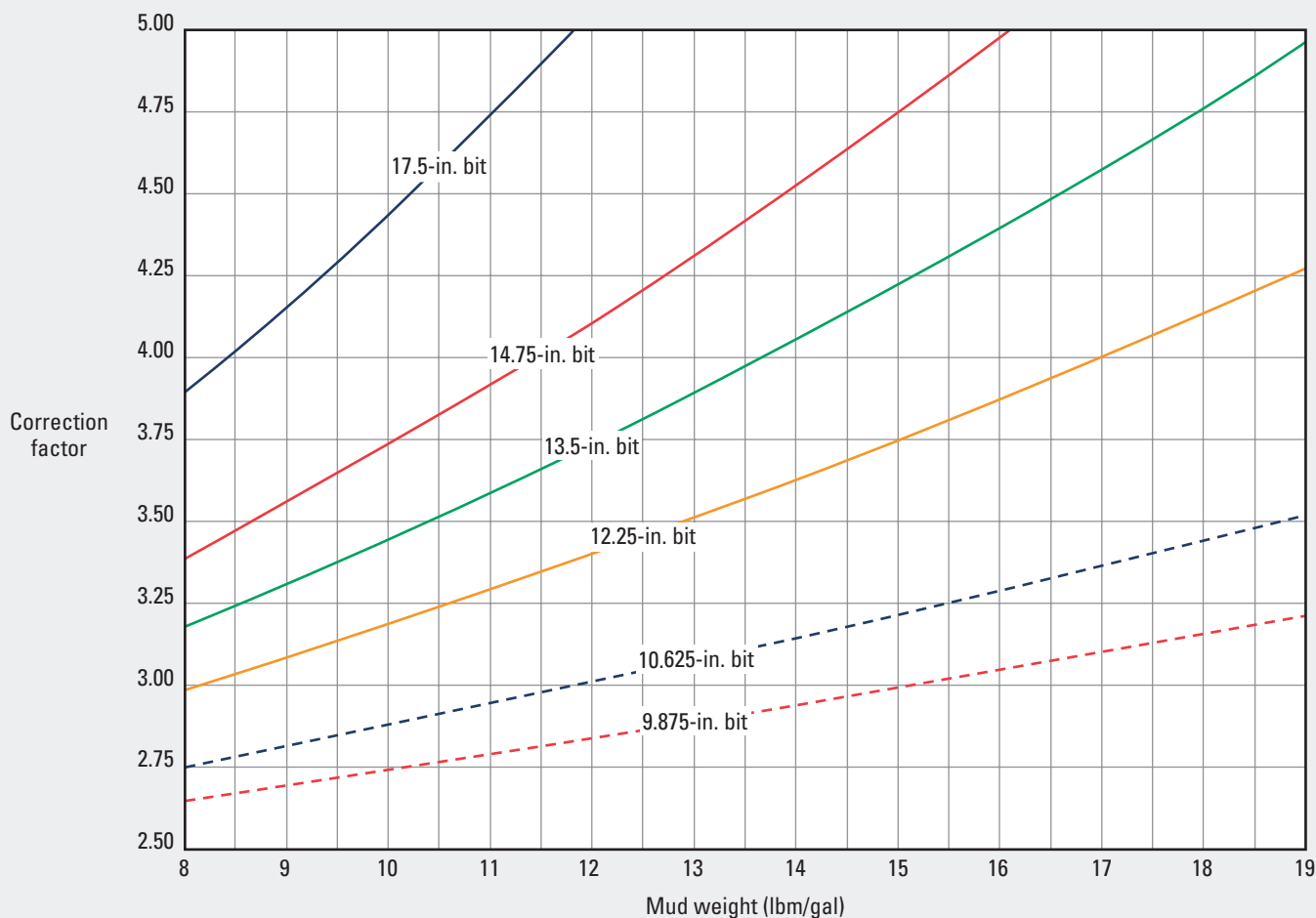
Description

Enter the chart with the mud weight on the x-axis and move upward to intersect the appropriate bit size. Interpolate between lines as necessary. At the intersection point, move horizontally left to the y-axis to read the correction factor that the PowerPulse or TeleScope gamma ray value was multiplied by to obtain the corrected gamma ray value in gAPI units.

PowerPulse* Gamma Ray—8.25-in. Normal-Flow Tool

Borehole Correction for Open Hole

GR-10



*Mark of Schlumberger
© Schlumberger

Purpose

This chart is used to provide a correction factor for gamma ray values measured with the PowerPulse 8.25-in. normal-flow MWD telemetry system. These environmental corrections for mud weight and bit size are already applied to the gamma ray presented on the logs.

Description

Enter the chart with the mud weight on the x-axis and move upward to intersect the appropriate bit size. Interpolate between lines as necessary. At the intersection point, move horizontally left to the y-axis to read the appropriate correction factor that the PowerPulse gamma ray value was multiplied by to obtain the corrected GR value in GAPI units.

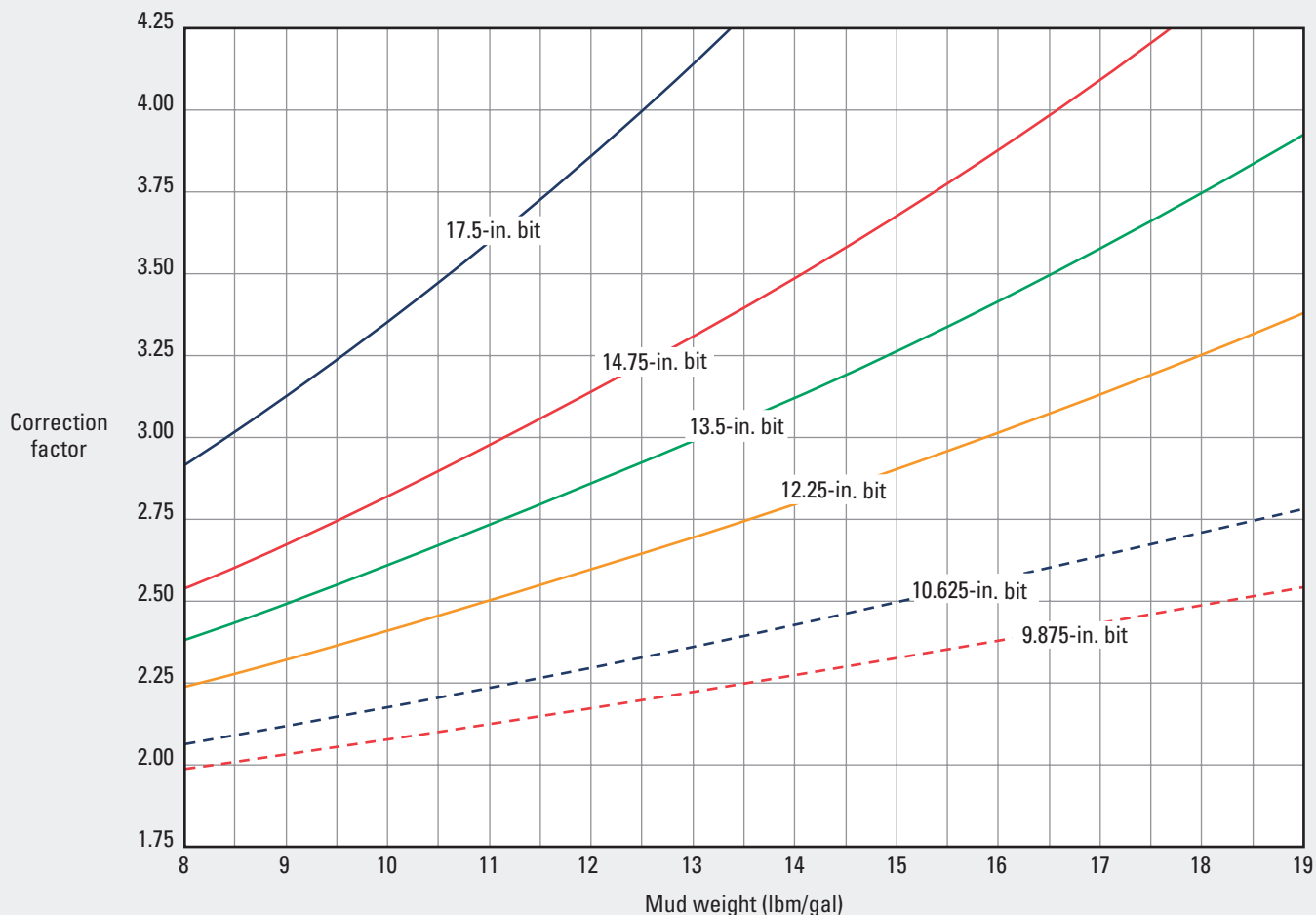
GR

PowerPulse* Gamma Ray—8.25-in. High-Flow Tool

Borehole Correction for Open Hole

GR-11

GR



*Mark of Schlumberger
© Schlumberger

Purpose

This chart is used to provide a correction factor for gamma ray values measured with the PowerPulse 8.25-in. high-flow MWD telemetry system. These environmental corrections for mud weight and bit size are already applied to the gamma ray presented on the logs.

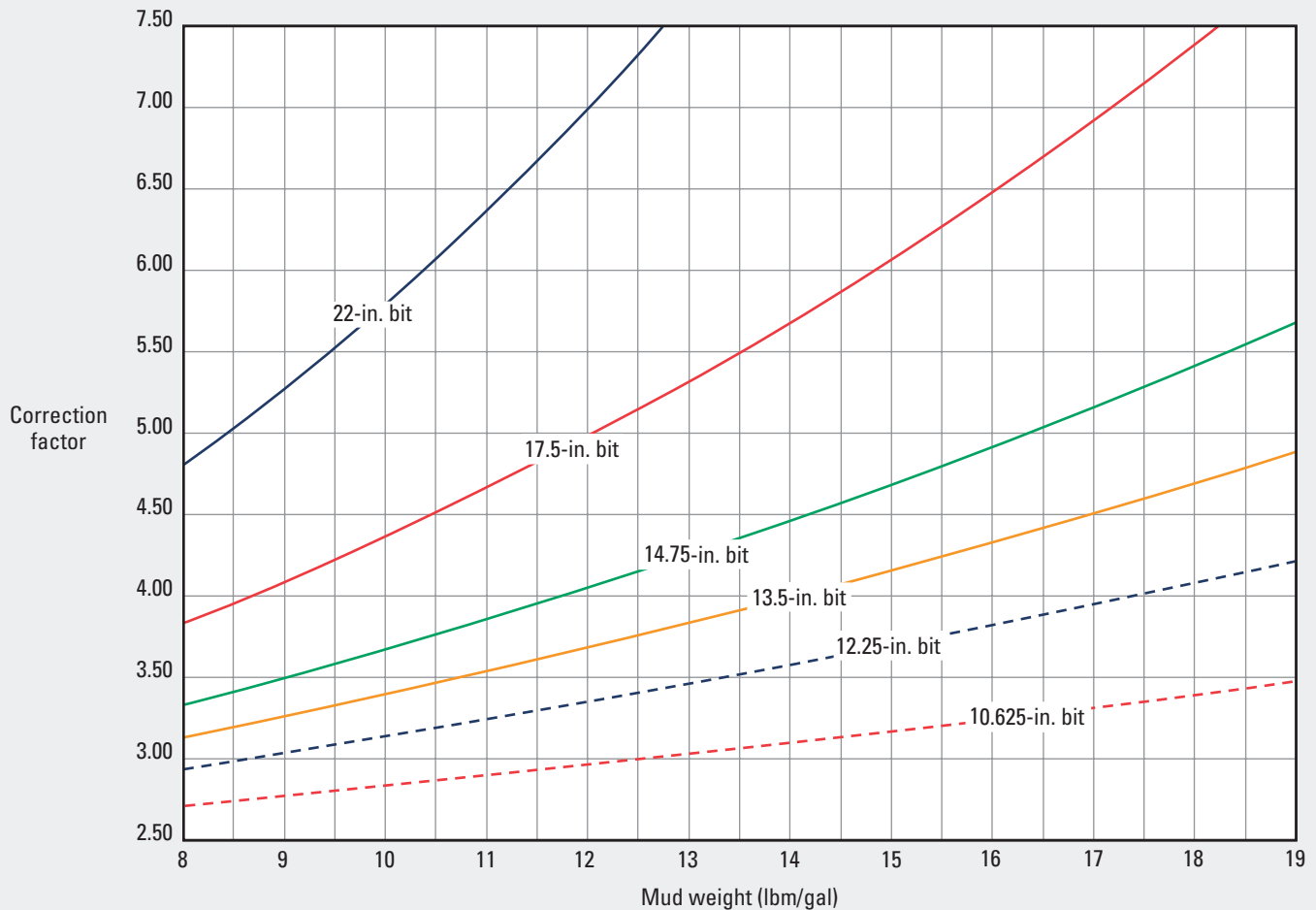
Description

Enter the chart with the mud weight on the x-axis and move upward to intersect the appropriate bit size. Interpolate between lines as necessary. At the intersection point, move horizontally left to the y-axis to read the correction factor that the PowerPulse gamma ray value was multiplied by to obtain the corrected gamma ray value in gAPI units.

PowerPulse* Gamma Ray—9-in. Tool

Borehole Correction for Open Hole

GR-12



*Mark of Schlumberger
© Schlumberger

Purpose

This chart is used to provide a correction factor for gamma ray values measured with the PowerPulse 9-in. MWD telemetry system. These environmental corrections for mud weight and bit size are already applied to the gamma ray presented on the logs.

Description

Enter the chart with the mud weight on the x-axis and move upward to intersect the appropriate bit size. Interpolate between lines as necessary. At the intersection point, move horizontally left to the y-axis to read the correction factor that the PowerPulse gamma ray value was multiplied by to obtain the corrected gamma ray value in gAPI units.

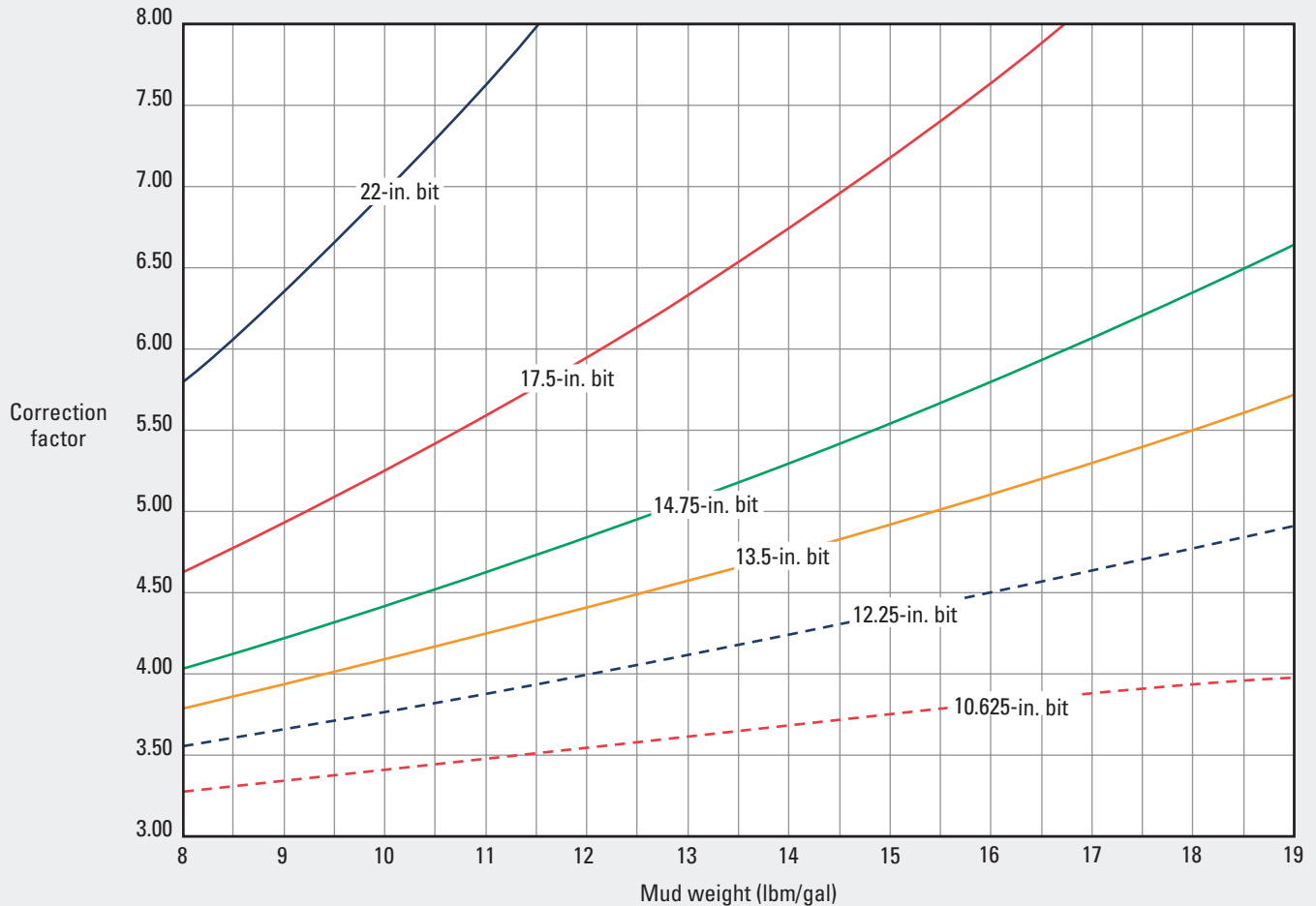
GR

PowerPulse* Gamma Ray—9.5-in. Normal-Flow Tool

Borehole Correction for Open Hole

GR-13

GR



*Mark of Schlumberger
© Schlumberger

Purpose

This chart is used to provide a correction factor for gamma ray values measured with the PowerPulse 9.5-in. normal-flow MWD telemetry system. These environmental corrections for mud weight and bit size are already applied to the gamma ray presented on the logs.

Description

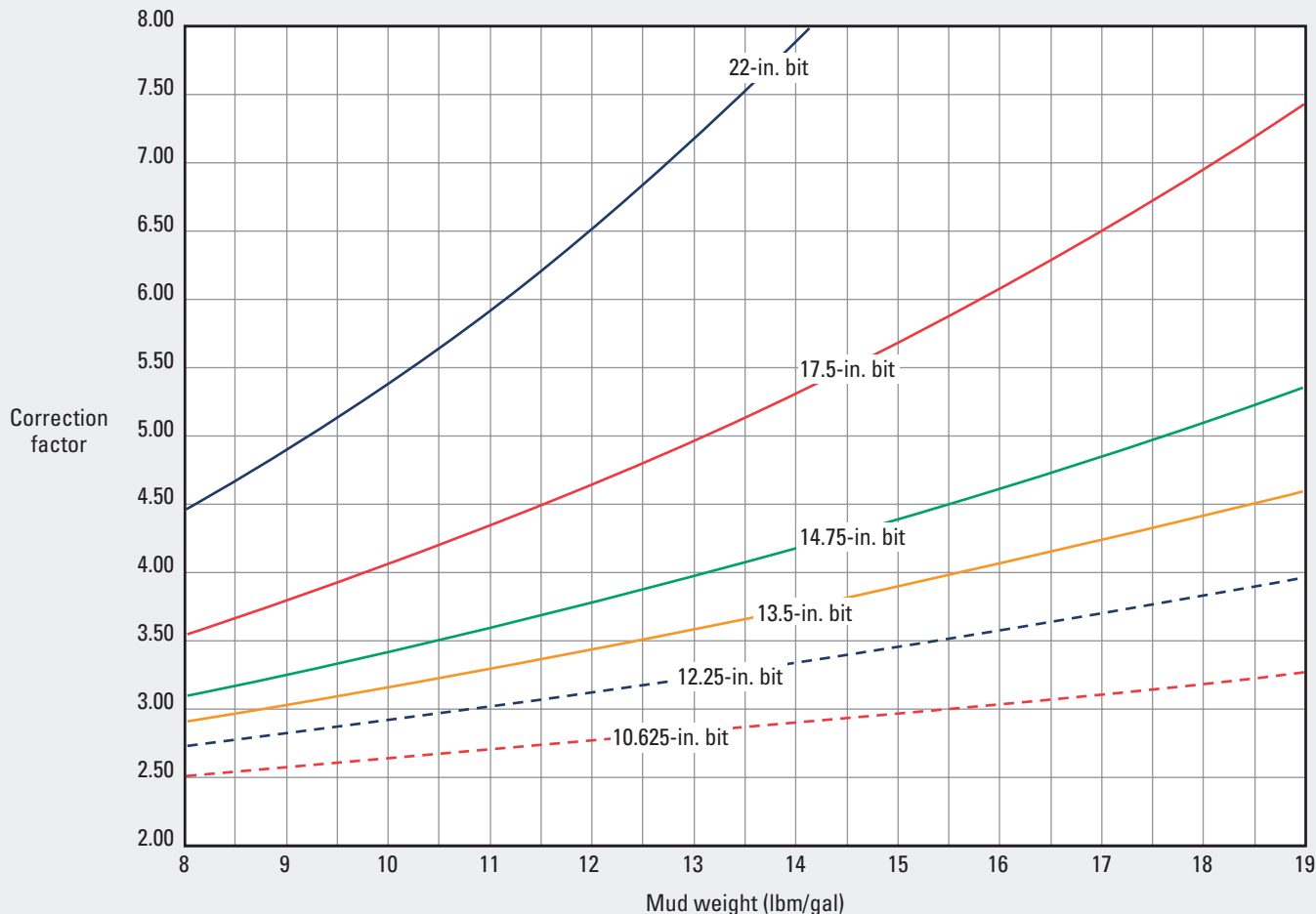
Enter the chart with the mud weight on the x-axis and move upward to intersect the appropriate bit size. Interpolate between lines as necessary. At the intersection point, move horizontally left to the y-axis to read the correction factor that the PowerPulse gamma ray value was multiplied by to obtain the corrected gamma ray value in gAPI units.

PowerPulse* Gamma Ray—9.5-in. High-Flow Tool

Borehole Correction for Open Hole

GR-14

GR



*Mark of Schlumberger
© Schlumberger

Purpose

This chart is used to provide a correction factor for gamma ray values measured by the PowerPulse 9.5-in. high-flow MWD telemetry system. These environmental corrections for mud weight and bit size are already applied to the gamma ray presented on the logs.

Description

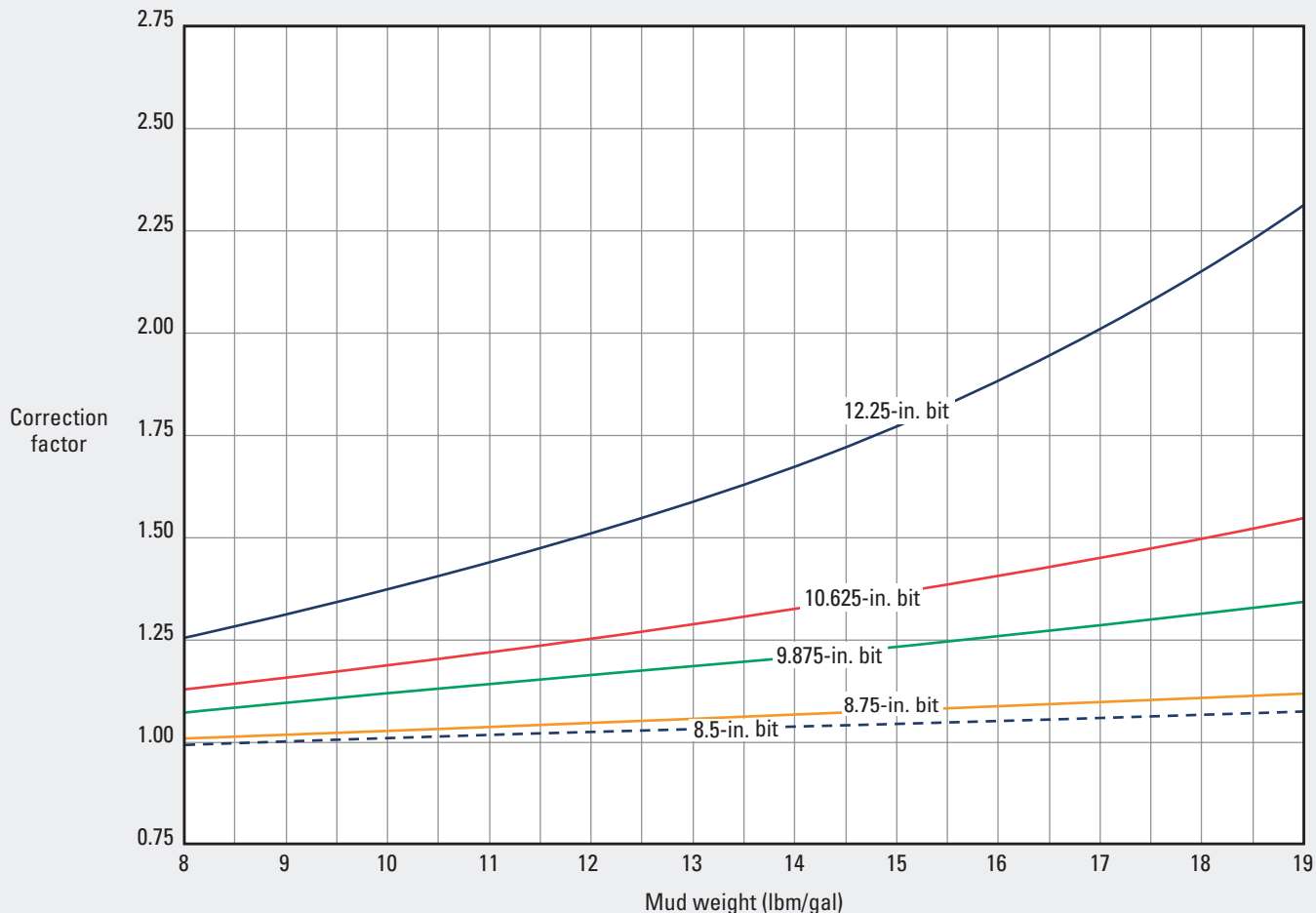
Enter the chart with the mud weight on the x-axis and move upward to intersect the appropriate bit size. Interpolate between lines as necessary. At the intersection point, move horizontally left to the y-axis to read the correction factor that the PowerPulse gamma ray value was multiplied by to obtain the corrected gamma ray value in gAPI units.

geoVISION675* GVR* Gamma Ray—6.75-in. Tool

Borehole Correction for Open Hole

GR-15

GR



*Mark of Schlumberger
© Schlumberger

Purpose

This chart is used to provide a correction factor for gamma ray values measured with the GVR resistivity sub of the geoVISION 6¾-in. MWD/LWD imaging system. These environmental corrections for mud weight and bit size are already applied to the gamma ray presented on the logs.

Description

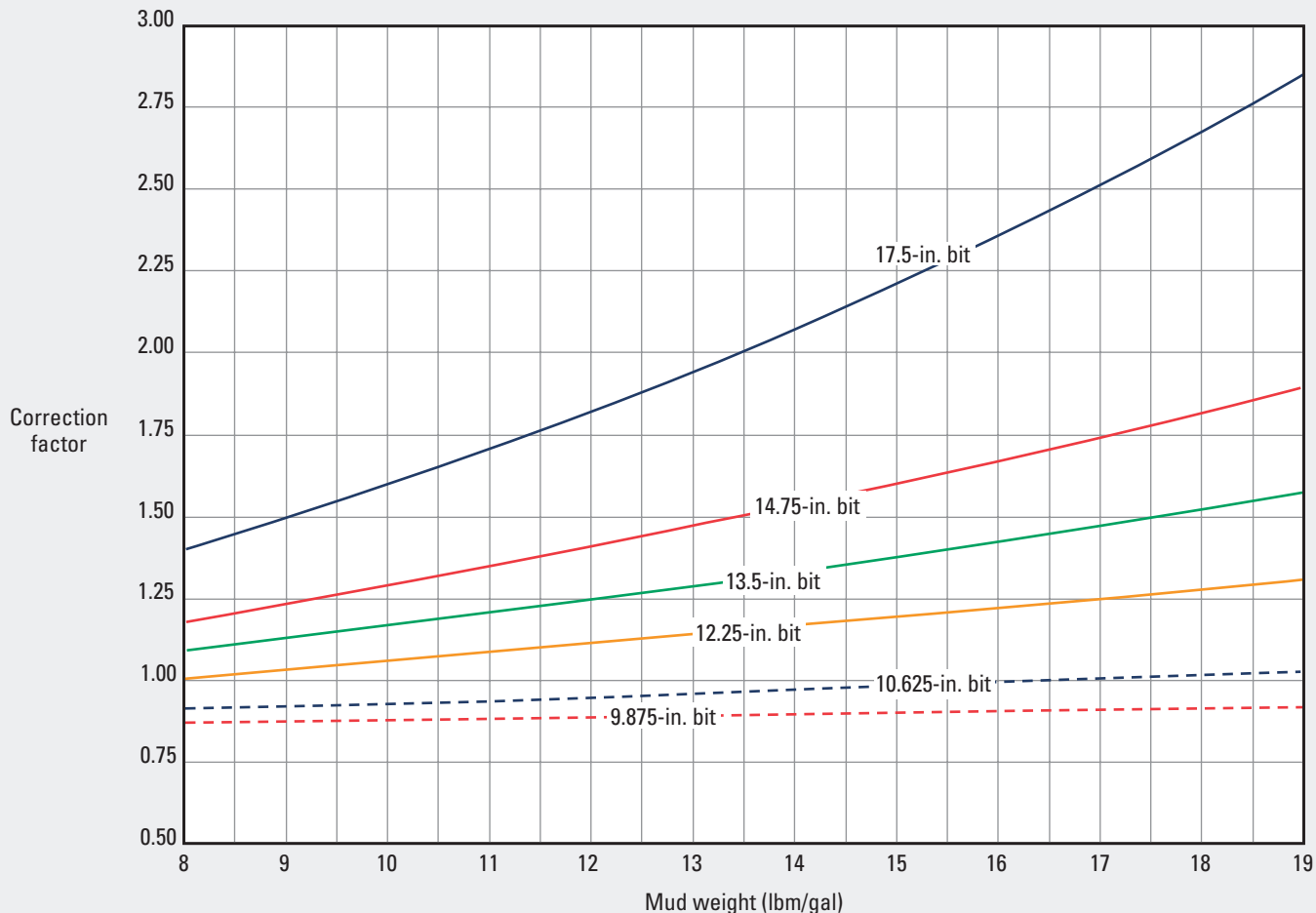
Enter the chart with the mud weight on the x-axis and move upward to intersect the appropriate bit size. Interpolate between lines as necessary. At the intersection point, move horizontally left to the y-axis to read the correction factor that the GVR gamma ray value was multiplied by to obtain the corrected gamma ray value in gAPI units.

RAB* Gamma Ray—8.25-in. Tool

Borehole Correction for Open Hole

GR-16

GR



*Mark of Schlumberger
© Schlumberger

Purpose

This chart is used to provide a correction factor for gamma ray values measured with the RAB Resistivity-at-the-Bit 8.25-in. tool. These environmental corrections for mud weight and bit size are already applied to the gamma ray presented on the logs.

Description

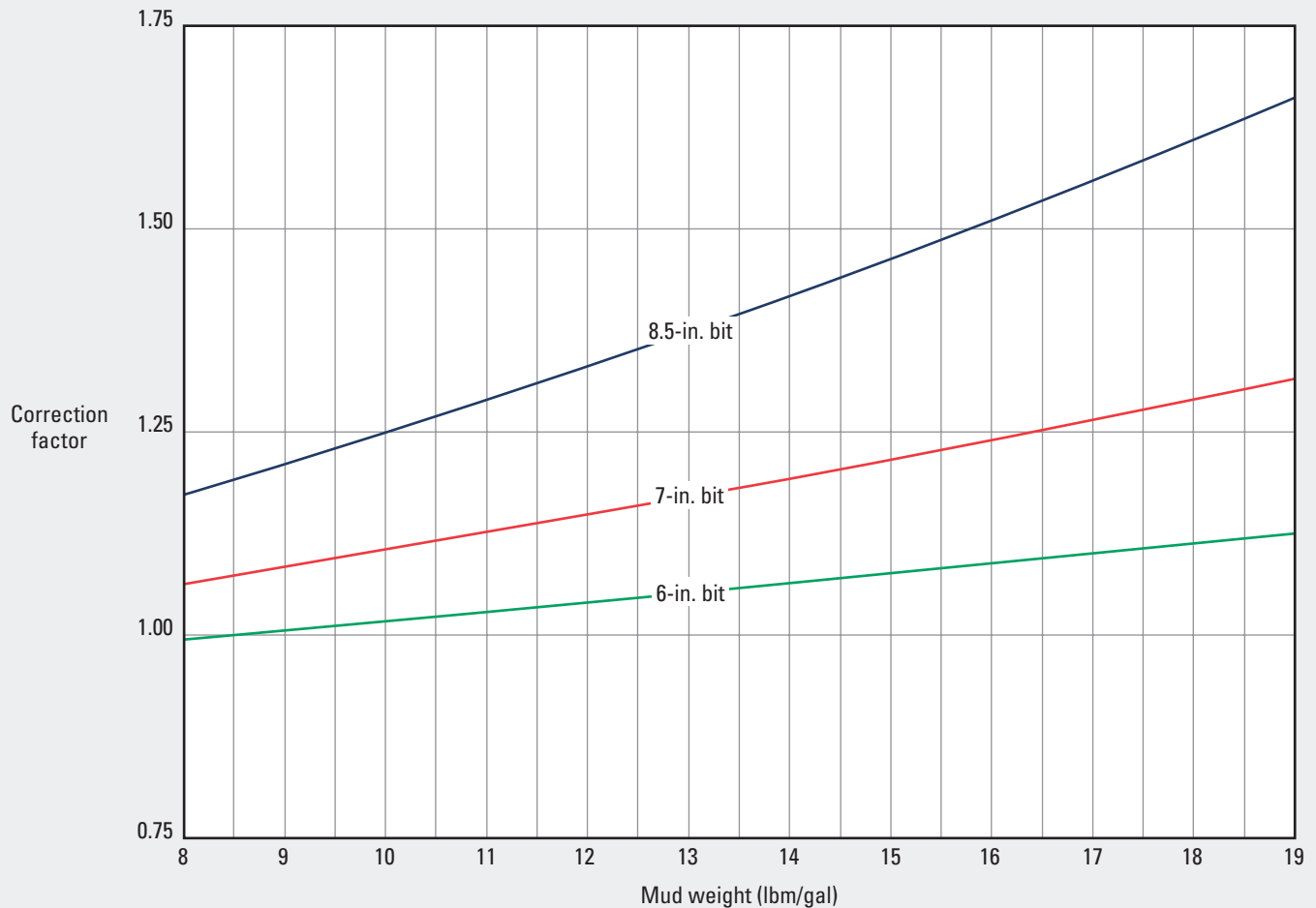
Enter the chart with the mud weight on the x-axis and move upward to intersect the appropriate bit size. Interpolate between lines as necessary. At the intersection point, move horizontally left to the y-axis to read the correction factor that the RAB gamma ray value was multiplied by to obtain the corrected gamma ray value in gAPI units.

arcVISION475* Gamma Ray—4.75-in. Tool

Borehole Correction for Open Hole

GR-19

GR



*Mark of Schlumberger
© Schlumberger

Purpose

This chart is used to provide a correction factor for gamma ray values measured with the arcVISION475 4¾-in. drill collar resistivity tool. These environmental corrections for mud weight and bit size are already applied to the gamma ray presented on the logs.

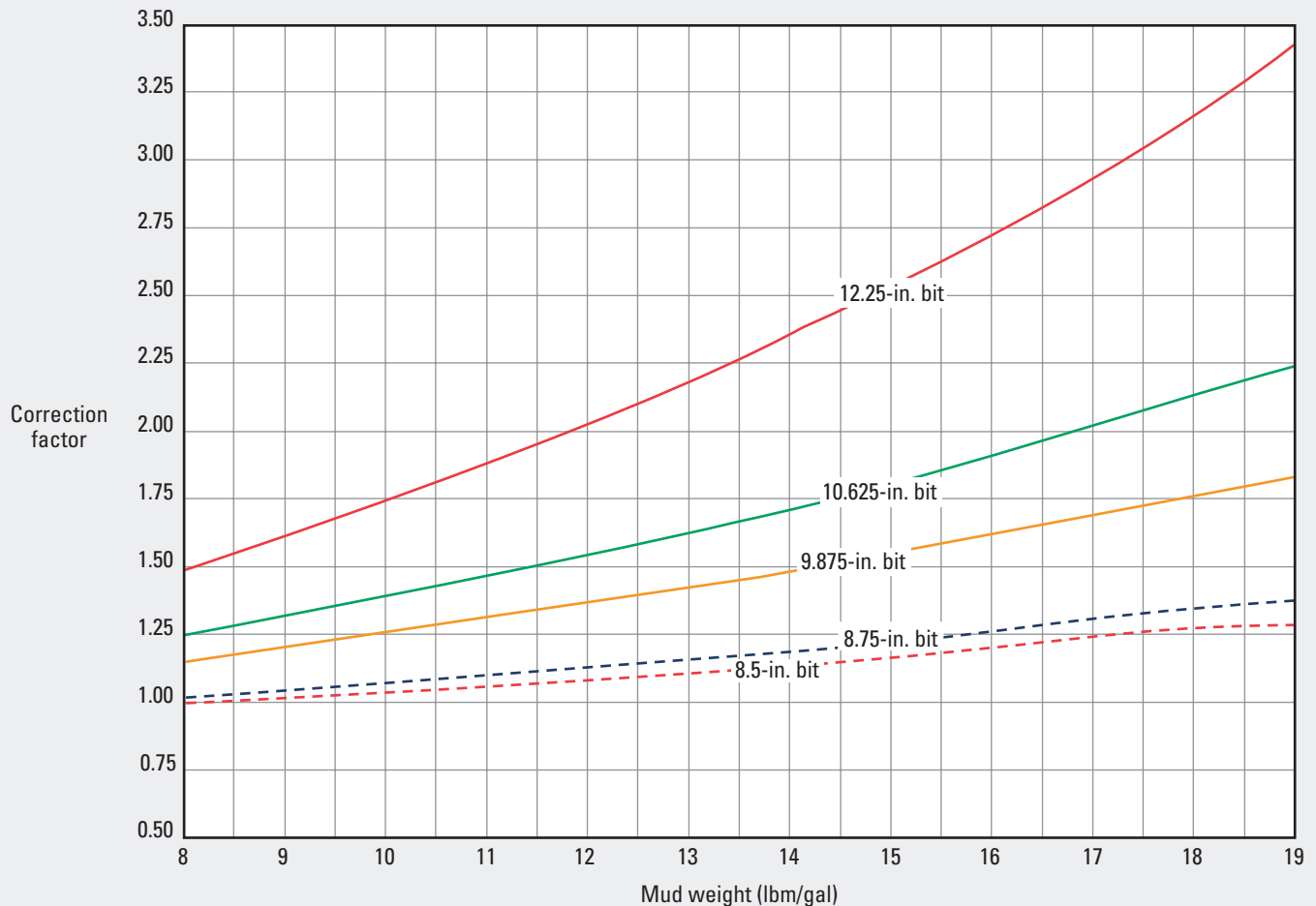
Description

Enter the chart with the mud weight on the x-axis and move upward to intersect the appropriate bit size. Interpolate between lines as necessary. At the intersection point, move horizontally left to the y-axis to read the correction factor that the arcVISION475 gamma ray value was multiplied by to obtain the corrected gamma ray value in GAPI units.

arcVISION675* Gamma Ray—6.75-in. Tool

Borehole Correction for Open Hole

GR-20



*Mark of Schlumberger
© Schlumberger

Purpose

This chart is used to provide a correction factor for gamma ray values measured with the arcVISION675 6¾-in. drill collar resistivity tool. These environmental corrections for mud weight and bit size are already applied to the gamma ray presented on the logs.

Description

Enter the chart with the mud weight on the x-axis and move upward to intersect the appropriate bit size. Interpolate between lines as necessary. At the intersection point, move horizontally left to the y-axis to read the appropriate correction factor that the arcVISION675 gamma ray value was multiplied by to obtain the corrected gamma ray value in GAPI units.

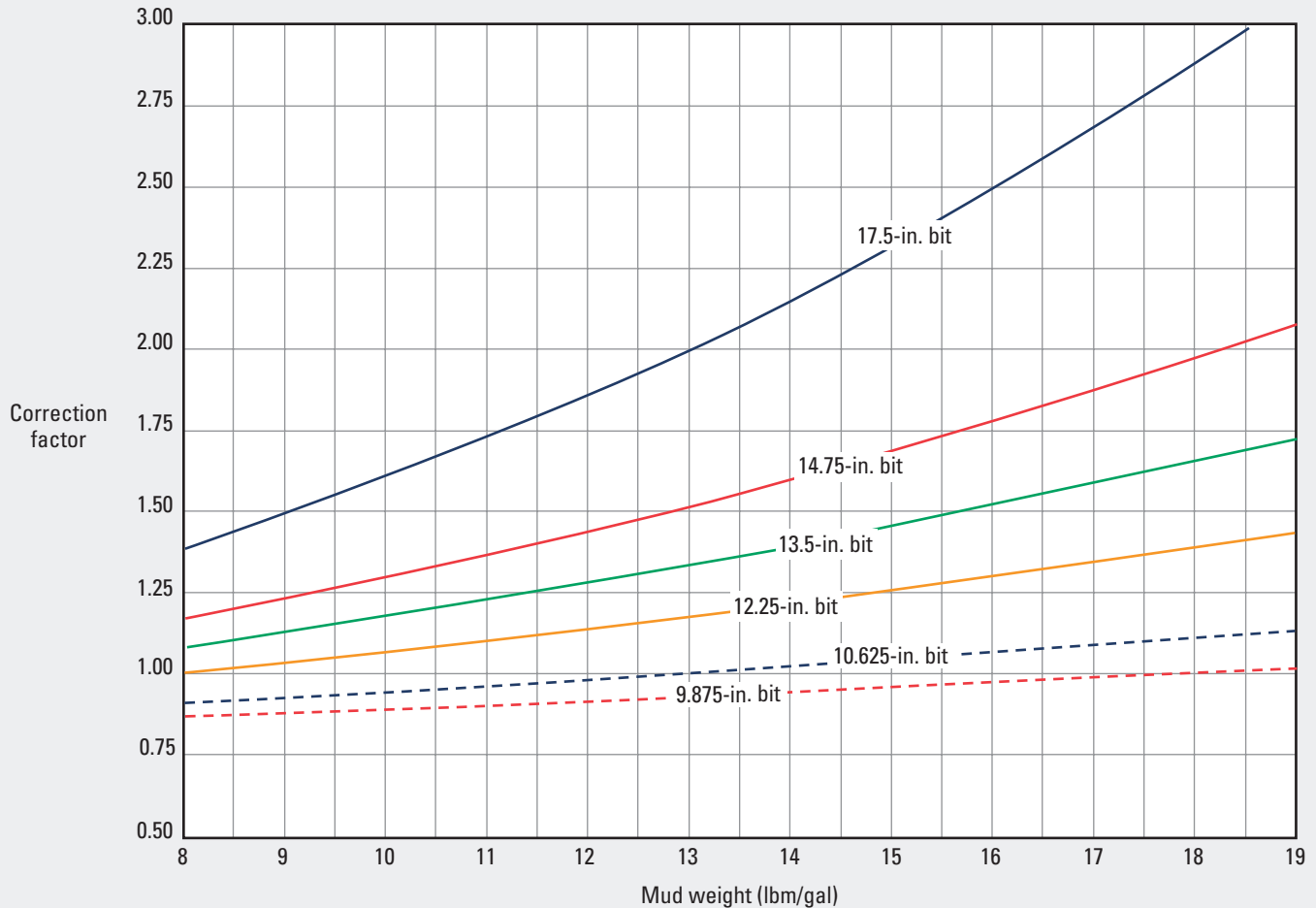
GR

arcVISION825* Gamma Ray—8.25-in. Tool

Borehole Correction for Open Hole

GR-21

GR



*Mark of Schlumberger
© Schlumberger

Purpose

This chart is used to provide a correction factor for gamma ray values measured with the arcVISION825 8¼-in. drill collar resistivity tool. These environmental corrections for mud weight and bit size are already applied to the gamma ray presented on the logs.

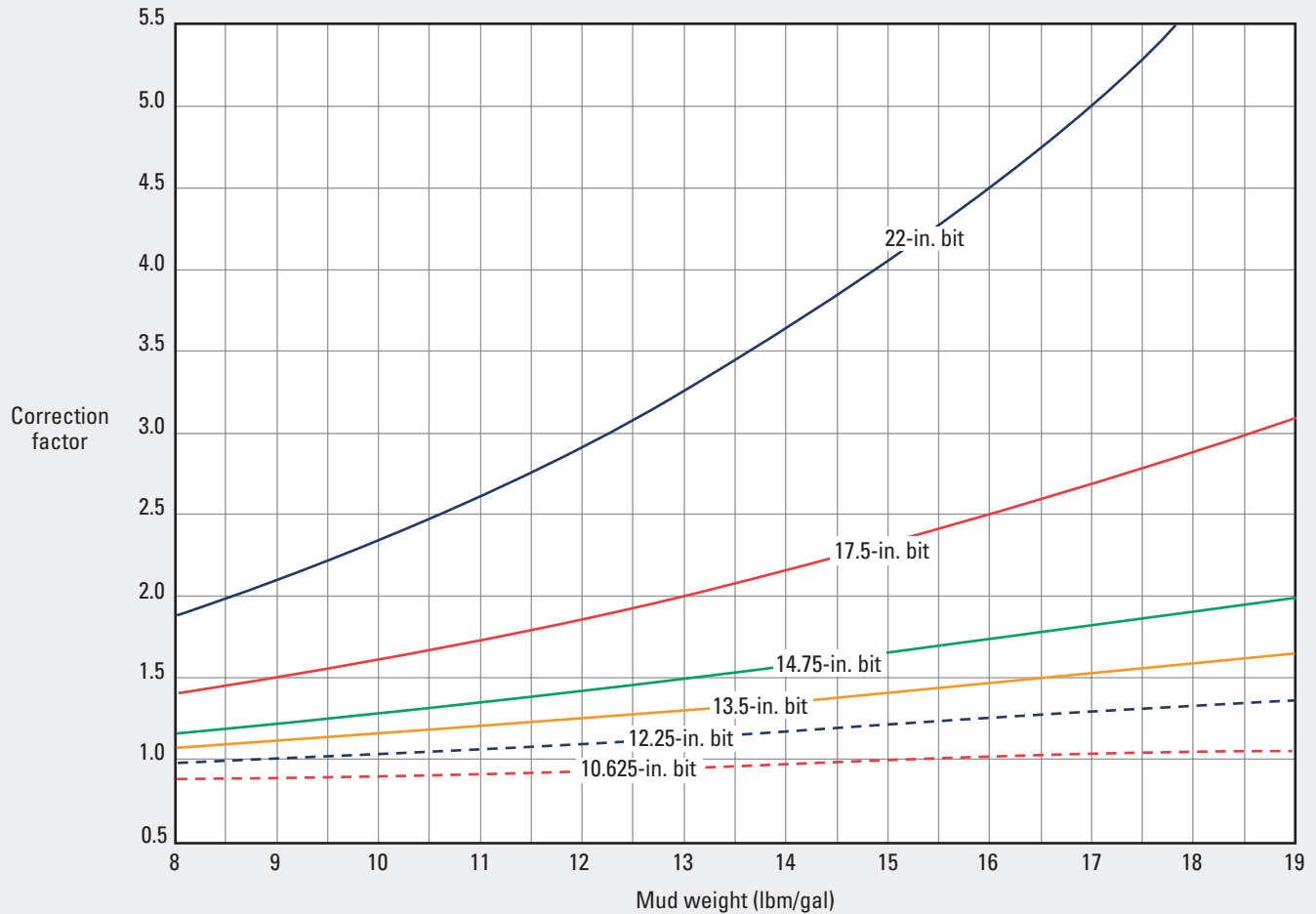
Description

Enter the chart with the mud weight on the x-axis and move upward to intersect the appropriate bit size. Interpolate between lines as necessary. At the intersection point, move horizontally left to the y-axis and read the appropriate correction factor that the arcVISION825 gamma ray value was multiplied by to obtain the corrected gamma ray value in gAPI units.

arcVISION900* Gamma Ray—9-in. Tool

Borehole Correction for Open Hole

GR-22



*Mark of Schlumberger
© Schlumberger

Purpose

This chart is used to provide a correction factor for gamma ray values measured with the arcVISION900 9-in. drill collar resistivity tool. These environmental corrections for mud weight and bit size are already applied to the gamma ray presented on the logs.

Description

Enter the chart with the mud weight on the x-axis and move upward to intersect the appropriate bit size. Interpolate between lines as necessary. At the intersection point, move horizontally left to the y-axis and read the appropriate correction factor that the arcVISION900 gamma ray value was multiplied by to obtain the corrected gamma ray value in GAPI units.

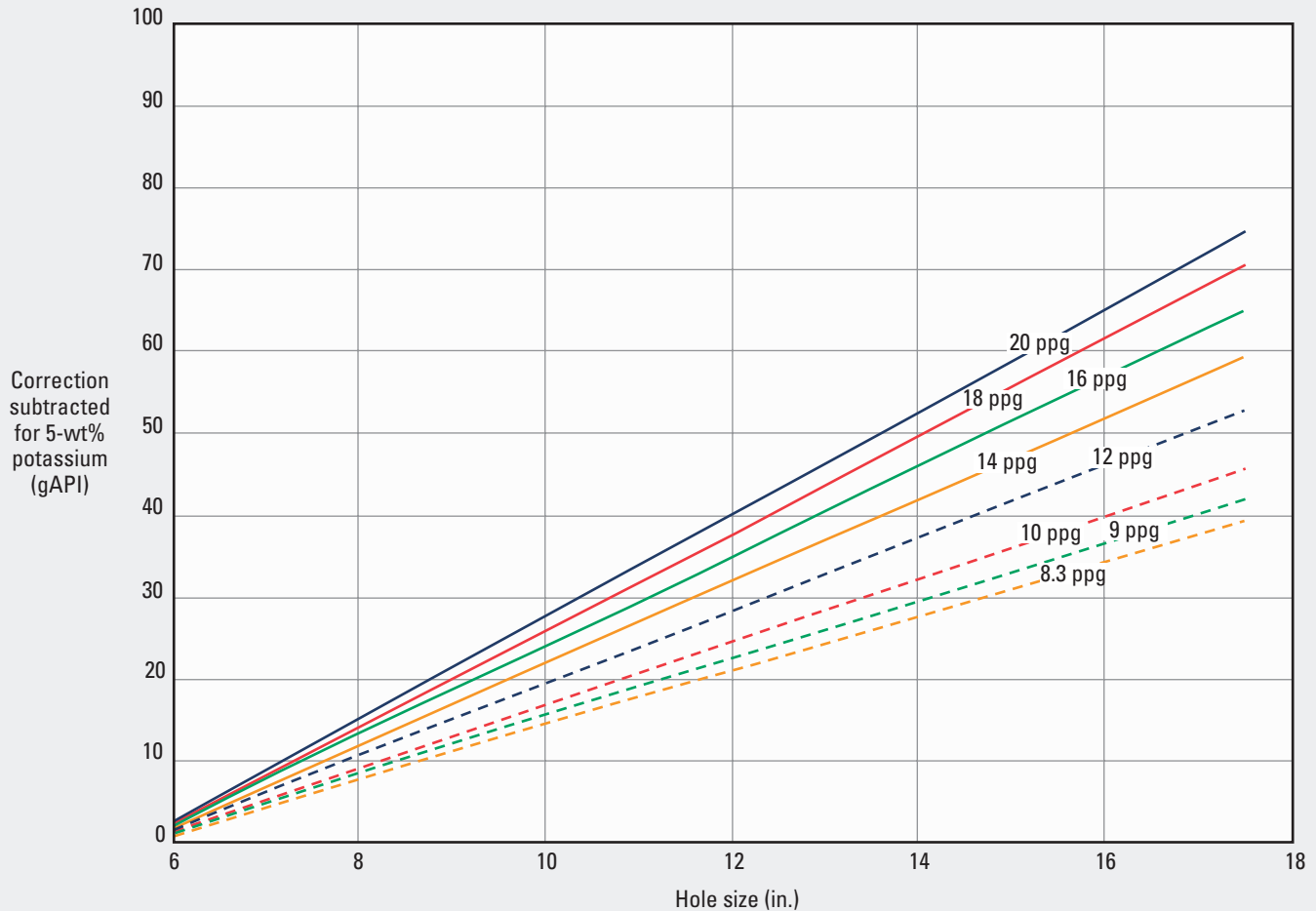
GR

arcVISION475* Gamma Ray—4.75-in. Tool

Potassium Correction for Open Hole

GR-23

GR



*Mark of Schlumberger
© Schlumberger

Purpose

This chart is used to provide a correction that is subtracted from the borehole-corrected gamma ray from the arcVISION475 4¾-in. tool. Environmental corrections for mud weight and bit size are already applied to the gamma ray presented on the logs.

Description

This chart is for illustrative purposes only. The indicated correction is already applied to the gamma ray log.

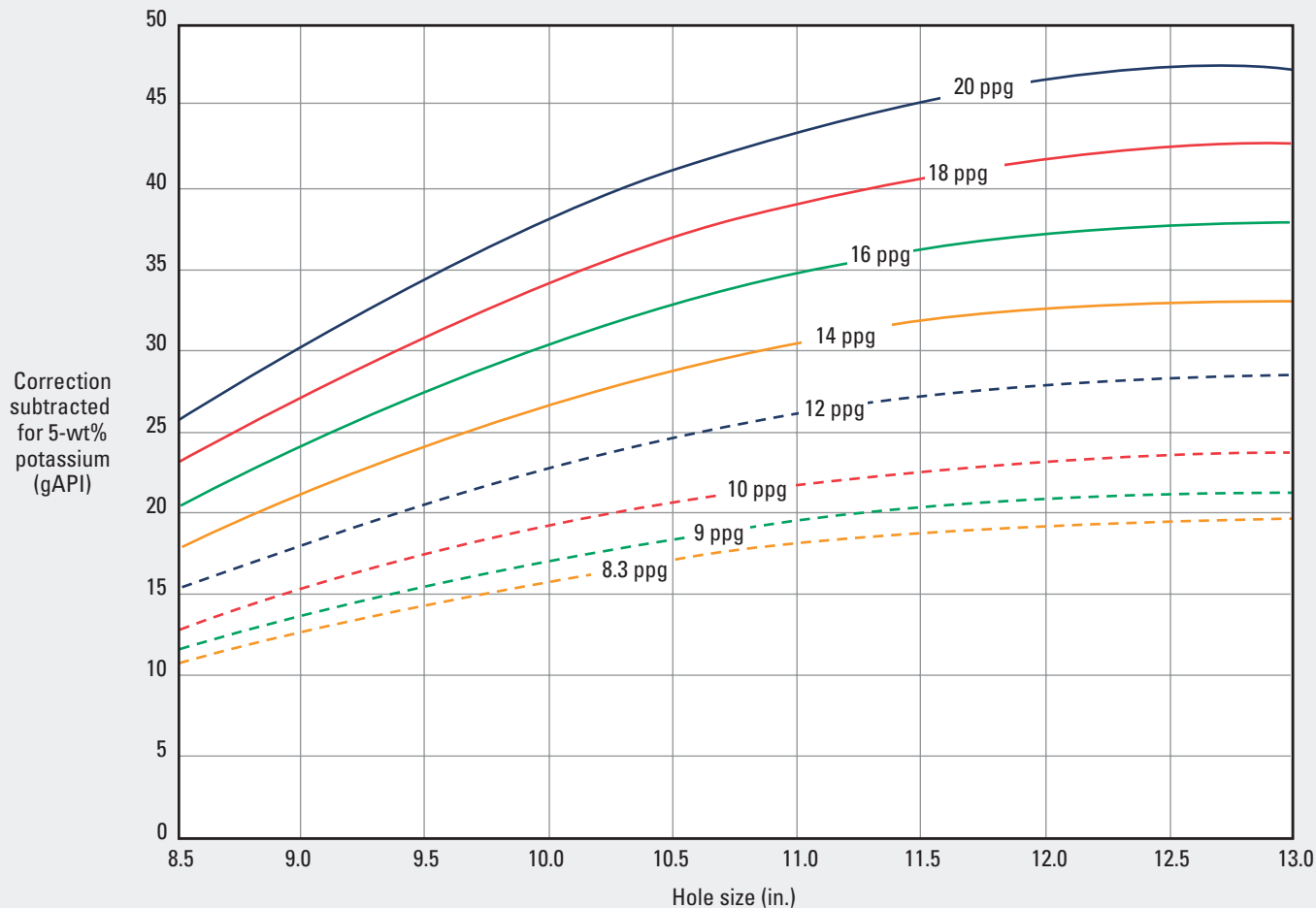
To determine the correction that was applied to the log output, enter the chart with the borehole size on the x-axis and move upward to intersect the downhole mud weight. From the intersection point move horizontally left to read the correction in gAPI units that was subtracted from the borehole-corrected data.

Charts GR-24 through GR-26 are similar to Chart GR-23 for different arcVISION tool sizes.

arcVISION675* Gamma Ray—6.75-in. Tool

Potassium Correction for Open Hole

GR-24



*Mark of Schlumberger
© Schlumberger

Purpose

This chart is used to provide a correction that is subtracted from the borehole-corrected gamma ray from the arcVISION675 6¾-in. tool. Environmental corrections for mud weight and bit size are already applied to the gamma ray presented on the logs.

Description

This chart is for illustrative purposes only. The indicated correction is already applied on the gamma ray log.

To determine the correction that was applied to the log output, enter the chart with the borehole size on the x-axis and move upward to intersect the downhole mud weight. From the intersection point move horizontally left to read the correction in gAPI units that was subtracted from the borehole-corrected data.

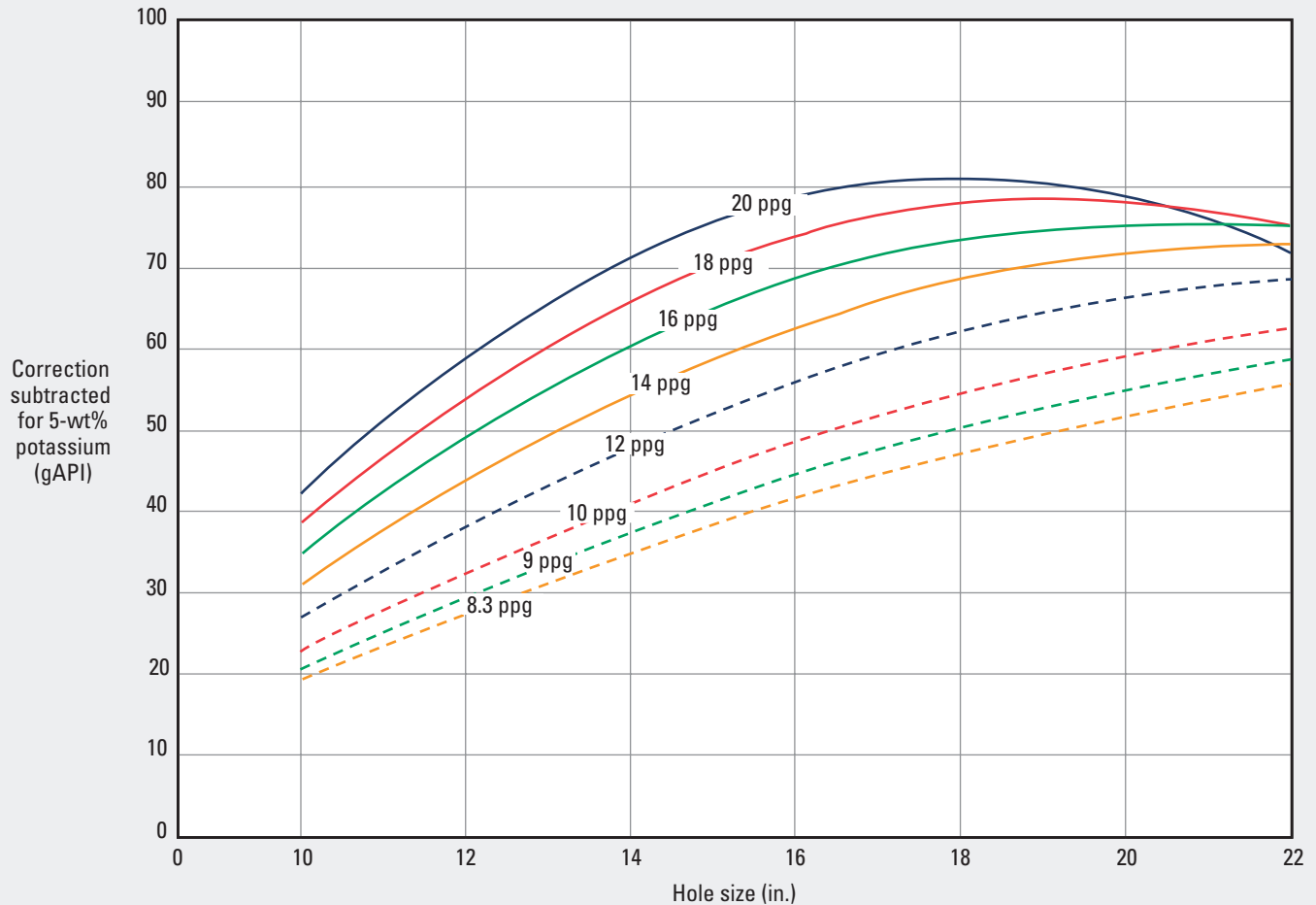
GR

arcVISION825* Gamma Ray—8.25-in. Tool

Potassium Correction for Open Hole

GR-25

GR



*Mark of Schlumberger
© Schlumberger

Purpose

This chart is used to provide a correction that is subtracted from the borehole-corrected gamma ray from the arcVISION825 8¼-in. tool. Environmental corrections for mud weight and bit size are already applied to the gamma ray presented on the logs.

Description

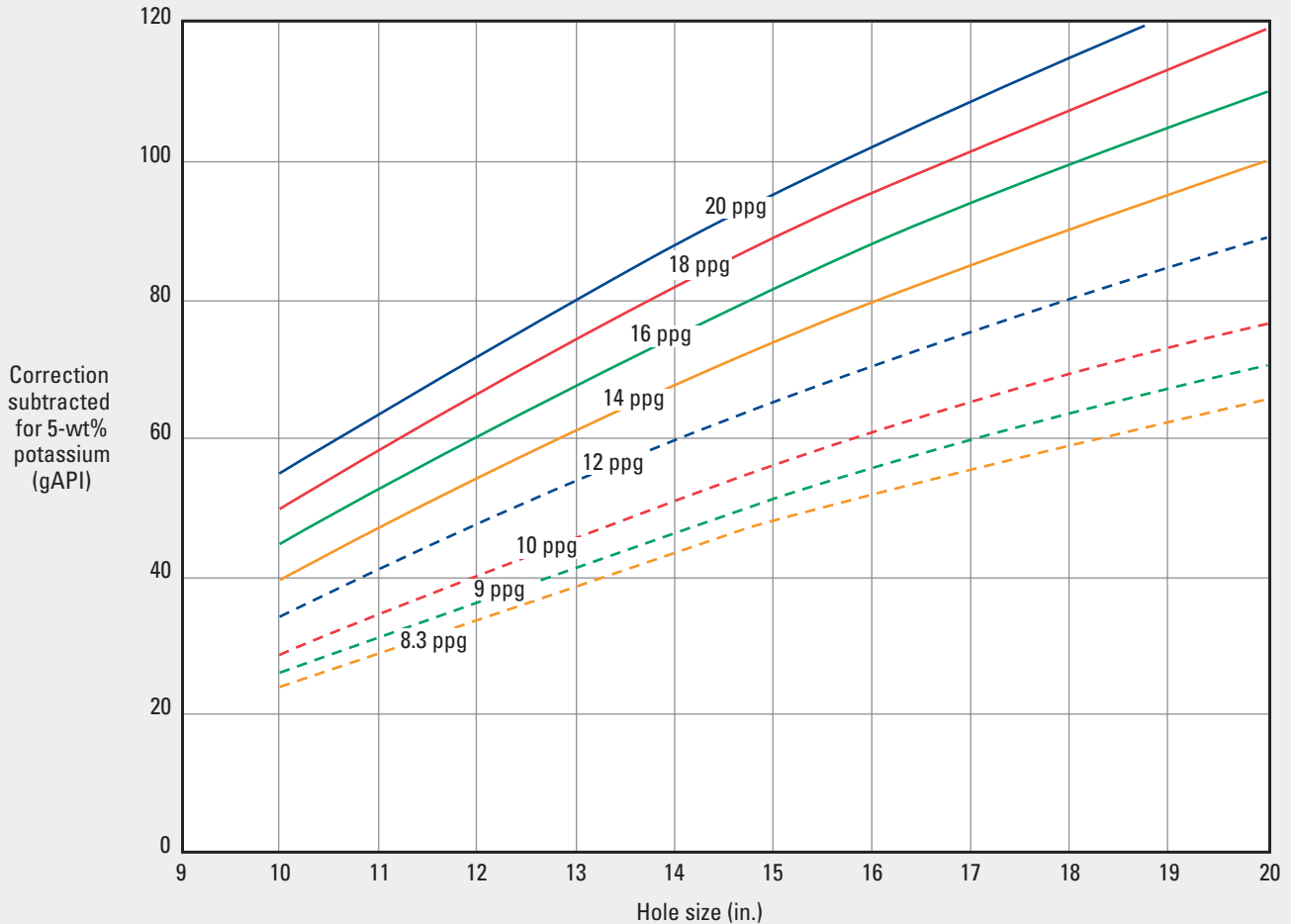
This chart is for illustrative purposes only. The indicated correction is already applied on the gamma ray log.

To determine the correction that was applied to the log output, enter the chart with the borehole size on the x-axis and move upward to intersect the downhole mud weight. From the intersection point move horizontally left to read the correction in gAPI units that was subtracted from the borehole-corrected data.

arcVISION900* Gamma Ray—9-in. tool

Potassium Correction for Open Hole

GR-26



*Mark of Schlumberger
© Schlumberger

Purpose

This chart is used to provide a correction that is subtracted from the borehole-corrected gamma ray from the arcVISION900 9-in. tool. Environmental corrections for mud weight and bit size are already applied to the gamma ray presented on the logs.

Description

This chart is for illustrative purposes only. The indicated correction is already applied on the gamma ray log.

To determine the correction that was applied to the log output, enter the chart with the borehole size on the x-axis and move upward to intersect the downhole mud weight. From the intersection point move horizontally left to read the correction curve in gAPI units that was subtracted from the borehole-corrected data.

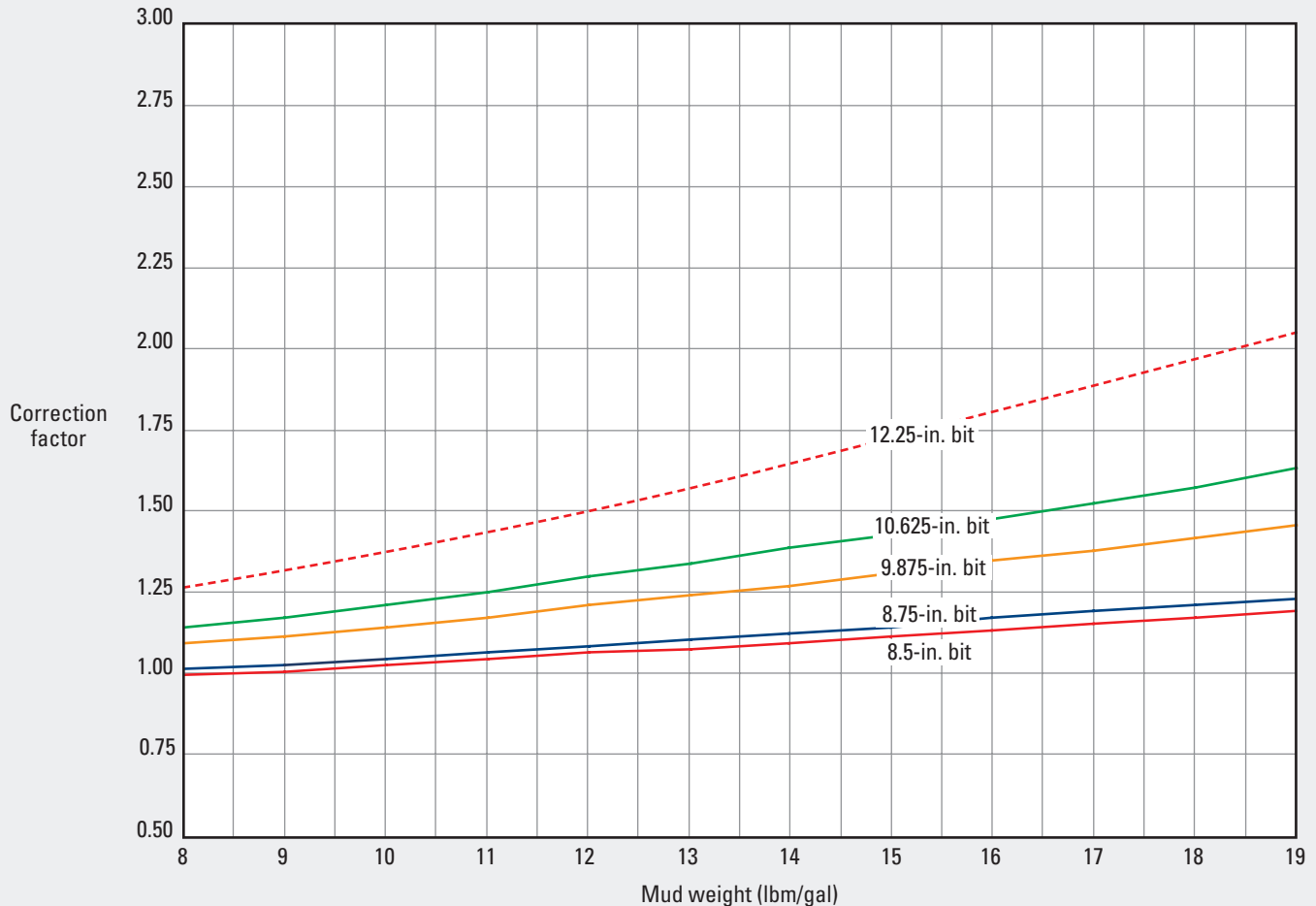
GR

EcoScope* Integrated LWD Gamma Ray—6.75-in. Tool

Borehole Correction for Open Hole

GR-27

GR



*Mark of Schlumberger
© Schlumberger

Purpose

This chart is used to provide a correction factor for gamma ray values measured with the EcoScope 6.75-in. Integrated LWD tool. These environmental corrections for mud weight and bit size are normally already applied to the gamma ray presented on the field logs.

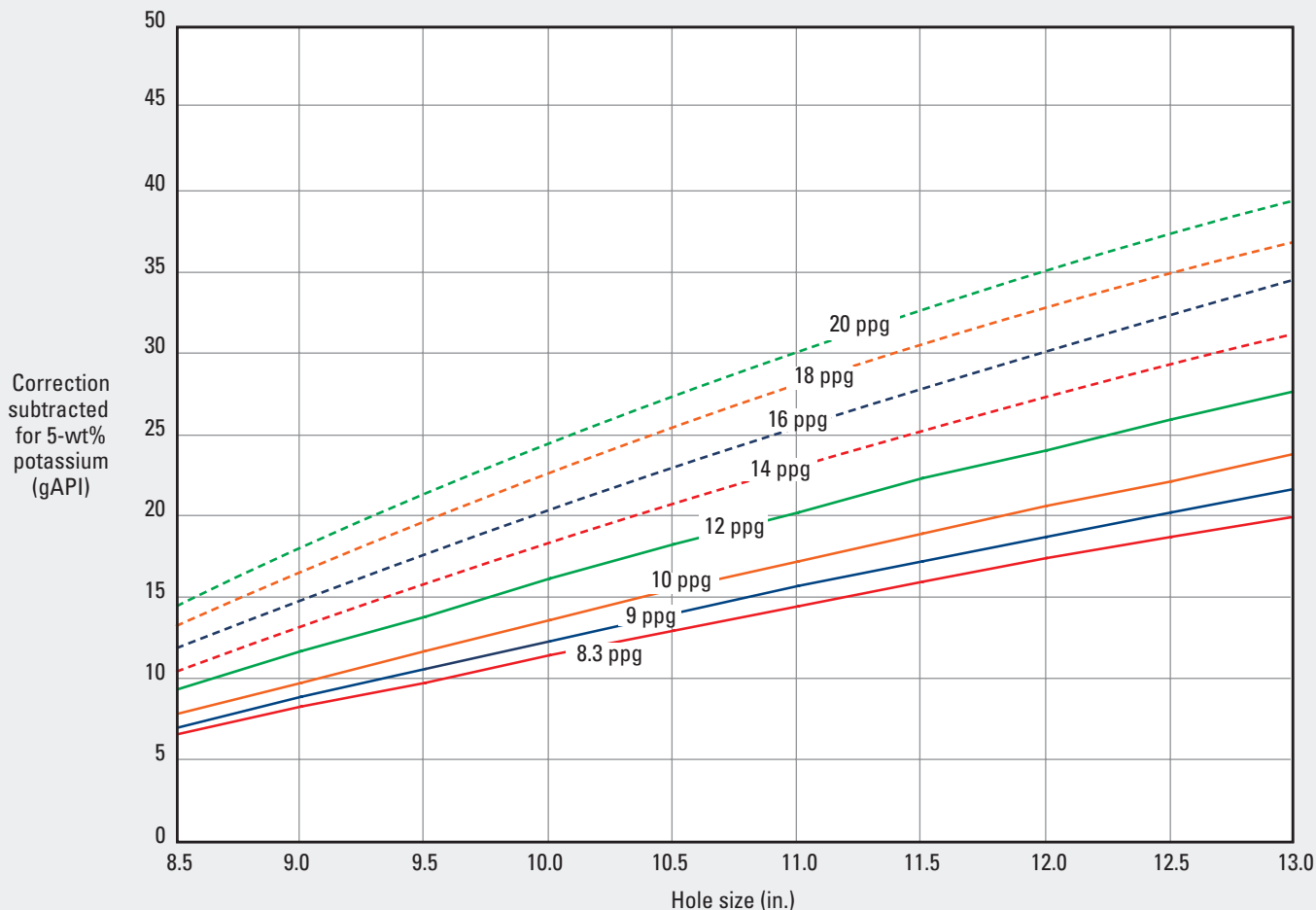
Description

Enter the chart with the mud weight on the x-axis and move upward to intersect the appropriate bit size. Interpolate between lines as necessary. At the intersection point, move horizontally left to the y-axis to read the appropriate correction factor that the EcoScope 6.75-in. gamma ray value was multiplied by to obtain the corrected gamma ray value in gAPI units.

EcoScope* Integrated LWD Gamma Ray—6.75-in. Tool

Potassium Correction for Open Hole

GR-28



*Mark of Schlumberger
© Schlumberger

Purpose

This chart is used to illustrate the potassium correction that is subtracted from the borehole-corrected gamma ray from the EcoScope 6.75-in. Integrated LWD tool. Environmental corrections for mud weight, bit size, and potassium are normally already applied to the gamma ray presented on the field logs.

Description

This chart is for illustrative purposes only. The indicated correction is already applied on the gamma ray log. The chart shows the correction for a typical 5-wt% potassium concentration.

To determine the correction that was applied to the log output, enter the chart with the borehole size on the x-axis and move upward to intersect the downhole mud weight. From the intersection point move horizontally left to read the correction curve in gAPI units that was subtracted from the borehole-corrected data.

GR

R_{weq} Determination from E_{SSP}

Purpose

This chart and nomograph are used to calculate the equivalent formation water resistivity (R_{weq}) from the static spontaneous potential (E_{SSP}) measured in clean formations. The value of R_{weq} is used in Chart SP-2 to determine the resistivity of the formation water (R_w). R_w is used in Archie's water saturation equation.

Description

Enter the chart with E_{SSP} in millivolts on the x-axis and move upward to intersect the appropriate temperature line. From the intersection point move horizontally to intersect the right y-axis for R_{mfeq}/R_{weq} . From this point, draw a straight line through the equivalent mud filtrate resistivity (R_{mf}) point on the R_{mfeq} nomograph to intersect the value of R_{weq} on the far-right nomograph.

The spontaneous potential (SP) reading corrected for the effect of bed thickness (E_{SPcor}) from Chart SP-4 can be substituted for E_{SSP} .

Example

First determine the value of R_{mfeq} :

- If R_{mf} at 75°F is greater than 0.1 ohm-m, correct R_{mf} to the formation temperature by using Chart Gen-6, and use $R_{mfeq} = 0.85R_{mf}$.
- If R_{mf} at 75°F is less than 0.1 ohm-m, use Chart SP-2 to derive a value of R_{mfeq} at formation temperature.

Given: $E_{SSP} = -100$ mV at 250°F and resistivity of the mud filtrate (R_{mf}) = 0.7 ohm-m at 100°F, converted to 0.33 at 250°F.

Find: R_{weq} at 250°F.

Answer: $R_{mfeq} = 0.85R_{mf} = 0.85 \times 0.33 = 0.28$ ohm-m.

Draw a straight line from the point on the R_{mfeq}/R_{weq} line that corresponds to the intersection of $E_{SSP} = -100$ mV and the interpolated 250°F temperature curve through the value of 0.28 ohm-m on the R_{mfeq} line to the R_{weq} line to determine that the value of R_{weq} is 0.025 ohm-m.

The value of R_{mfeq}/R_{weq} can also be determined from the equation

$$E_{SSP} = K_c \log (R_{mfeq}/R_{weq}),$$

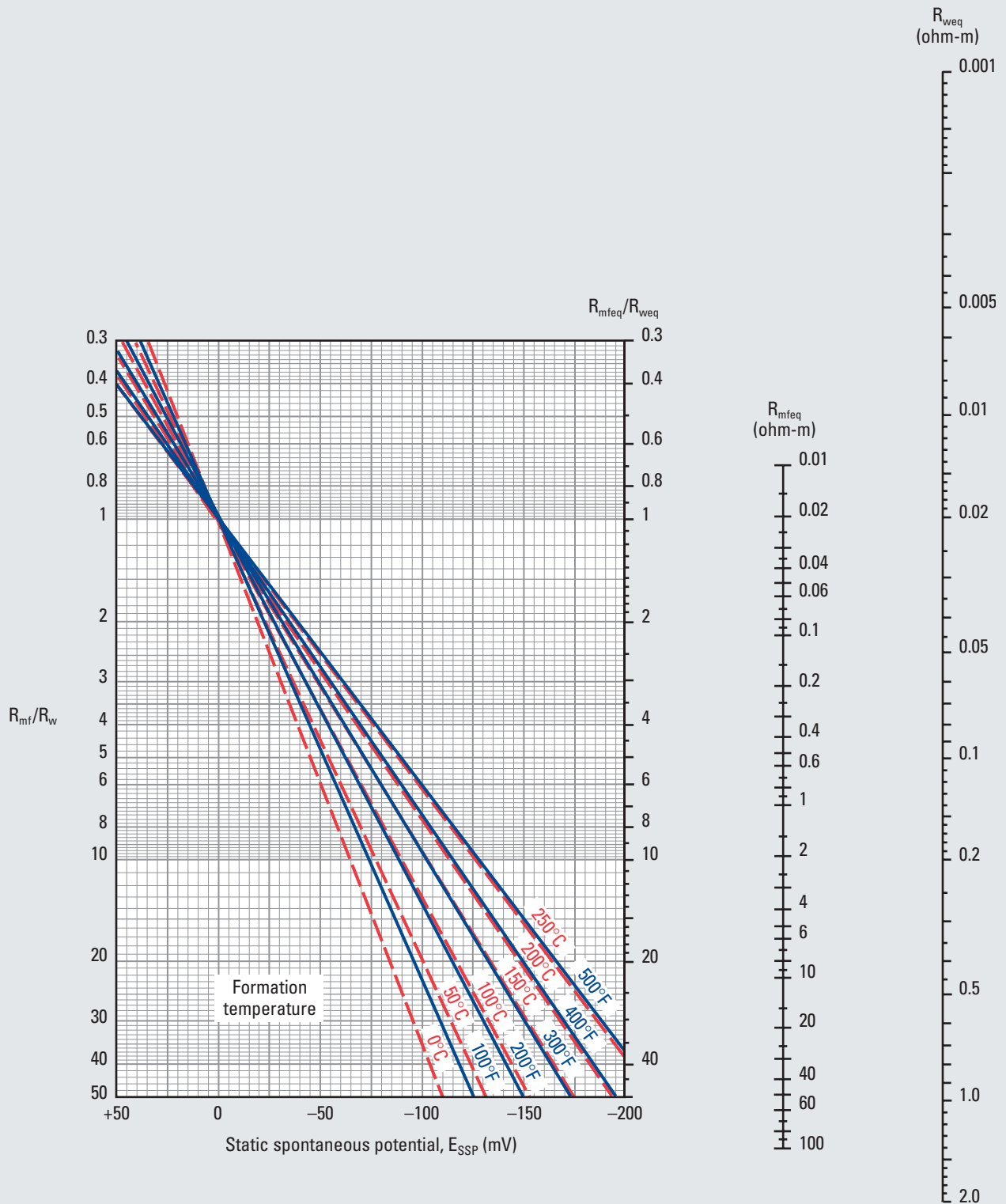
where K_c is the electrochemical spontaneous potential coefficient:

$$K_c = 61 + (0.133 \times \text{Temp}^\circ\text{F})$$

$$K_c = 65 + (0.24 \times \text{Temp}^\circ\text{C}).$$

R_{weq} Determination from E_{SSP}

SP-1
(former SP-1)

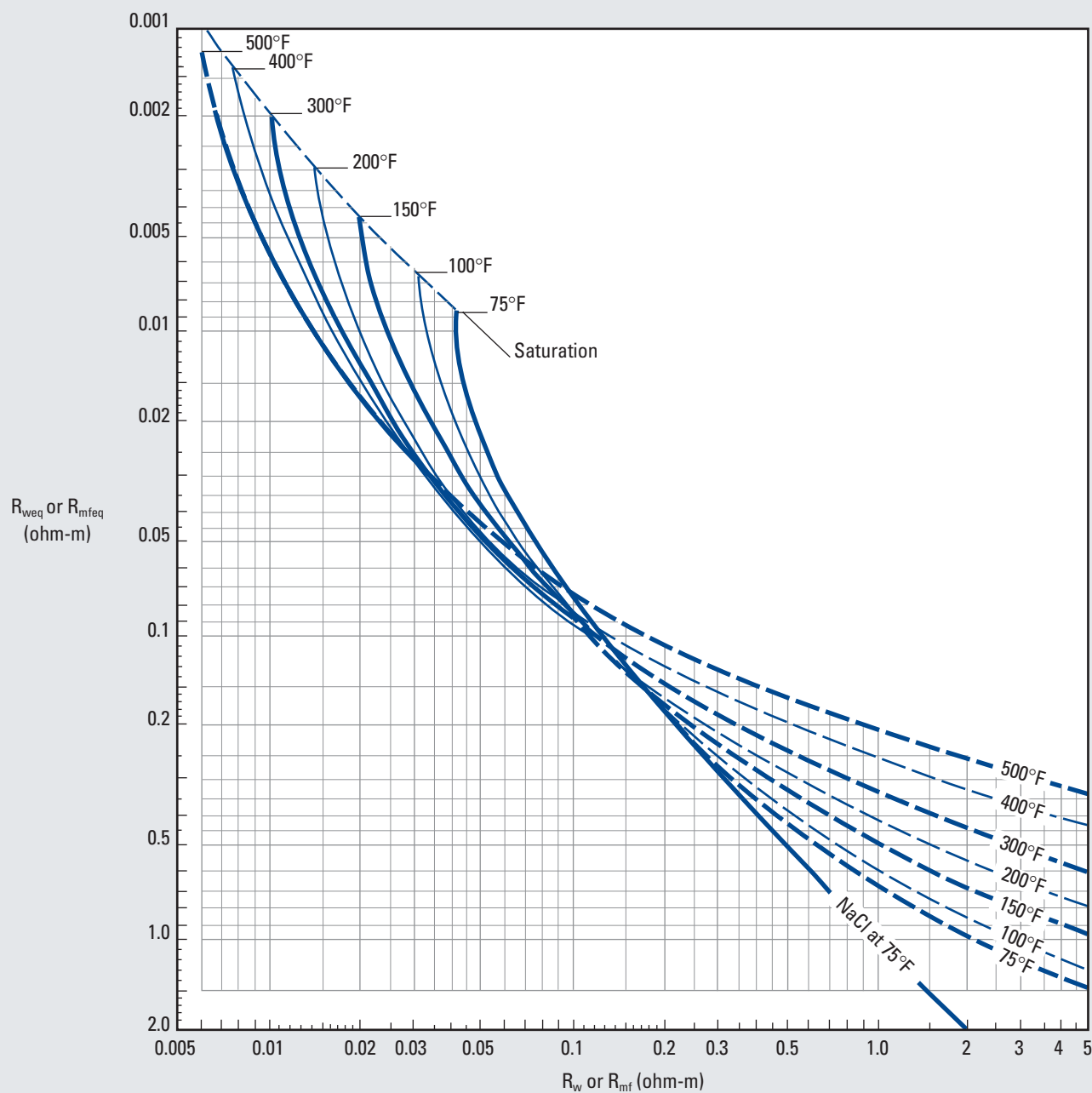


SP

R_{weq} versus R_w and Formation Temperature

SP-2

(customary, former SP-2)



© Schlumberger

Purpose

This chart is used to convert equivalent water resistivity (R_{weq}) from Chart SP-1 to actual water resistivity (R_w). It can also be used to convert the mud filtrate resistivity (R_{mf}) to the equivalent mud filtrate resistivity (R_{mfeq}) in saline mud. The metric version of this chart is Chart SP-3 on page 49.

Description

The solid lines are used for predominantly NaCl waters. The dashed lines are approximations for “average” fresh formation waters (for which the effects of salts other than NaCl become significant).

The dashed lines can also be used for gypsum-base mud filtrates.

Example

Given: From Chart SP-1, $R_{weq} = 0.025$ ohm-m at 250°F in predominantly NaCl water.

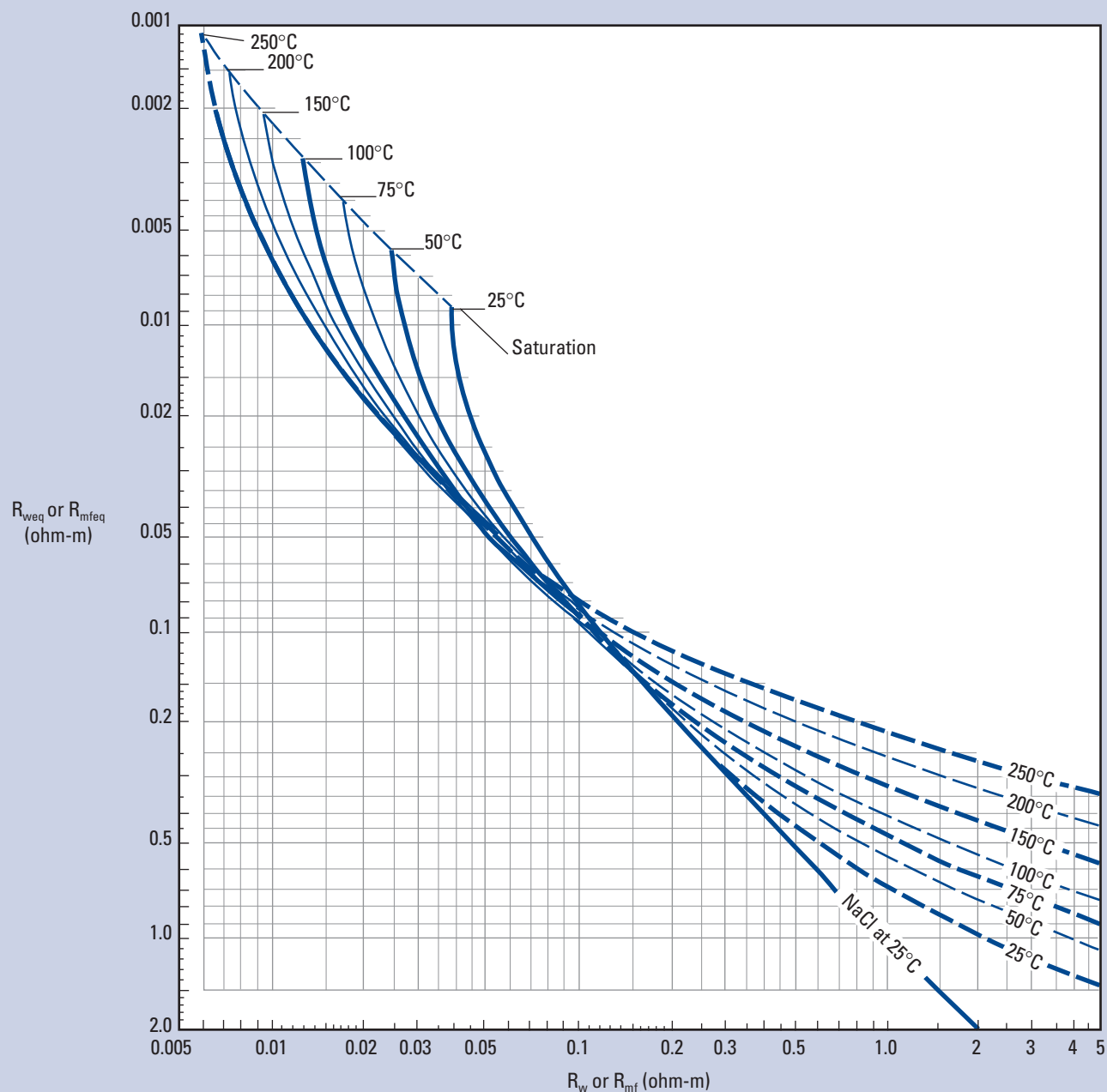
Find: R_w at 250°F.

Answer: Enter the chart at the R_{weq} value on the y-axis and move horizontally right to intersect the solid 250°F line. From the intersection point, move down to find the R_w value on the x-axis. $R_w = 0.03$ ohm-m at 250°F.

R_{weq} versus R_w and Formation Temperature

SP-3
(metric, former SP-2m)

SP



© Schlumberger

Purpose

This chart is the metric version of Chart SP-2 for converting equivalent water resistivity (R_{weq}) from Chart SP-1 to actual water resistivity (R_w). It can also be used to convert the mud filtrate resistivity (R_{mf}) to the equivalent mud filtrate resistivity (R_{mfeq}) in saline mud.

Description

The solid lines are used for predominantly NaCl waters. The dashed lines are approximations for “average” fresh formation waters

(for which the effects of salts other than NaCl become significant). The dashed lines can also be used for gypsum-base mud filtrates.

Example

Given: From Chart SP-1, $R_{weq} = 0.025$ ohm-m at 121°C in predominantly NaCl water.

Find: R_w at 121°C.

Answer: $R_w = 0.03$ ohm-m at 121°C.

Bed Thickness Correction—Open Hole

Purpose

Chart SP-4 is used to correct the SP reading from the well log for the effect of bed thickness. Generally, water sands greater than 20 ft in thickness require no or only a small correction.

Description

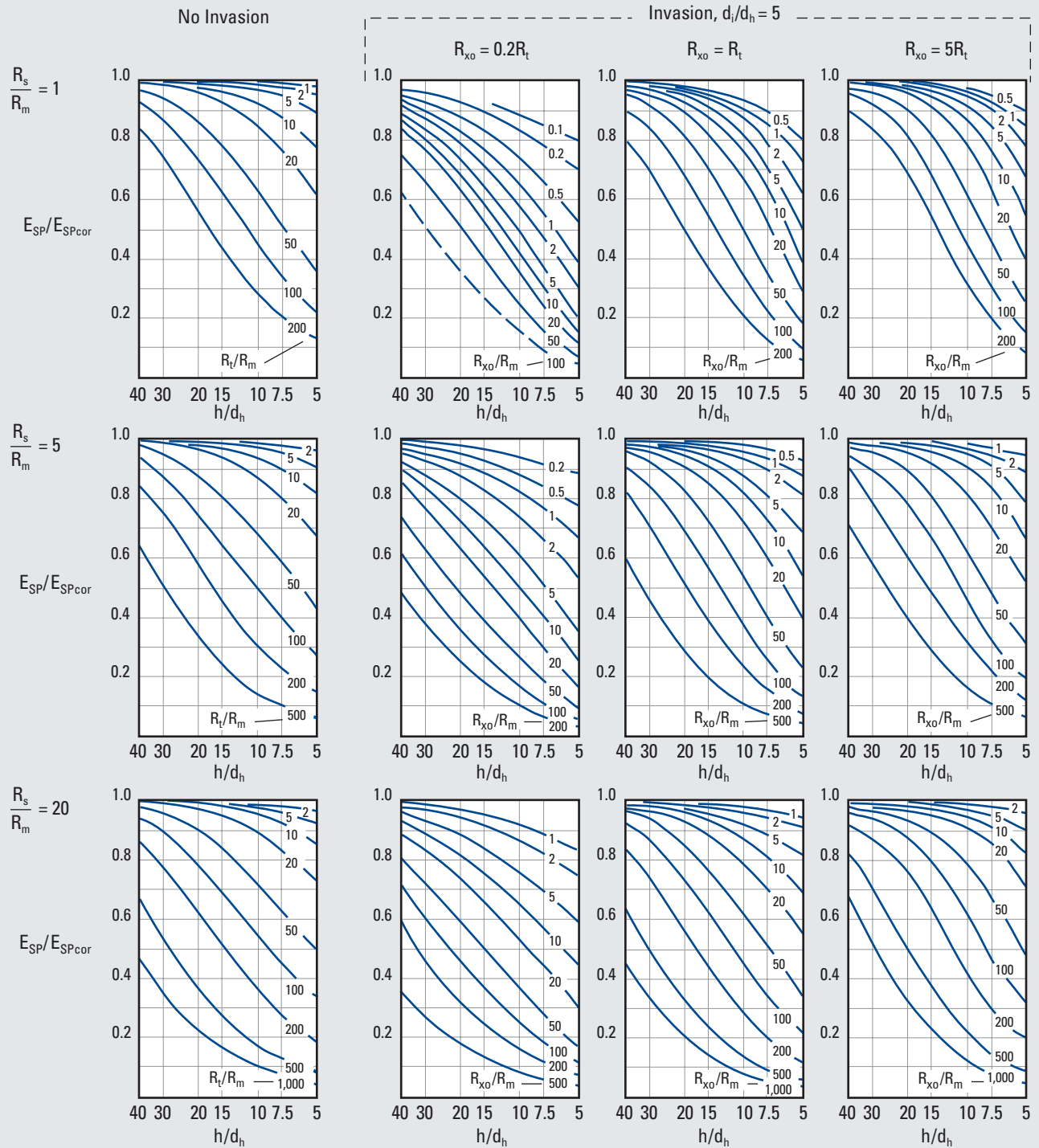
Chart SP-4 incorporates correction factors for a number of conditions that can affect the value of the SP in water sands.

The appropriate chart is selected on the basis of resistivity, invasion, hole diameter, and bed thickness. First, select the row of charts with the most appropriate value of the ratio of the resistivity of shale (R_s) to the resistivity of mud (R_m). On that row, select a chart for no invasion or for invasion for which the ratio of the diameter of invasion to the diameter of the wellbore (d_i/d_h) is 5. Enter the x-axis with the value of the ratio of bed thickness to wellbore diameter (h/d_h). Move upward to intersect the appropriate curve of the ratio of the true formation resistivity to the resistivity of the mud (R_t/R_m) for no invasion or the ratio of the resistivity of the flushed zone to the resistivity of the mud (R_{xo}/R_m) for invaded zones, interpolating between the curves as necessary. Read the ratio of the SP read from the log to the corrected SP (E_{SP}/E_{SPcor}) on the y-axis for the point of intersection. Calculate $E_{SPcor} = E_{SP}/(E_{SP}/E_{SPcor})$. The value of E_{SPcor} can be used in Chart SP-1 for E_{SSP} .

Bed Thickness Correction—Open Hole

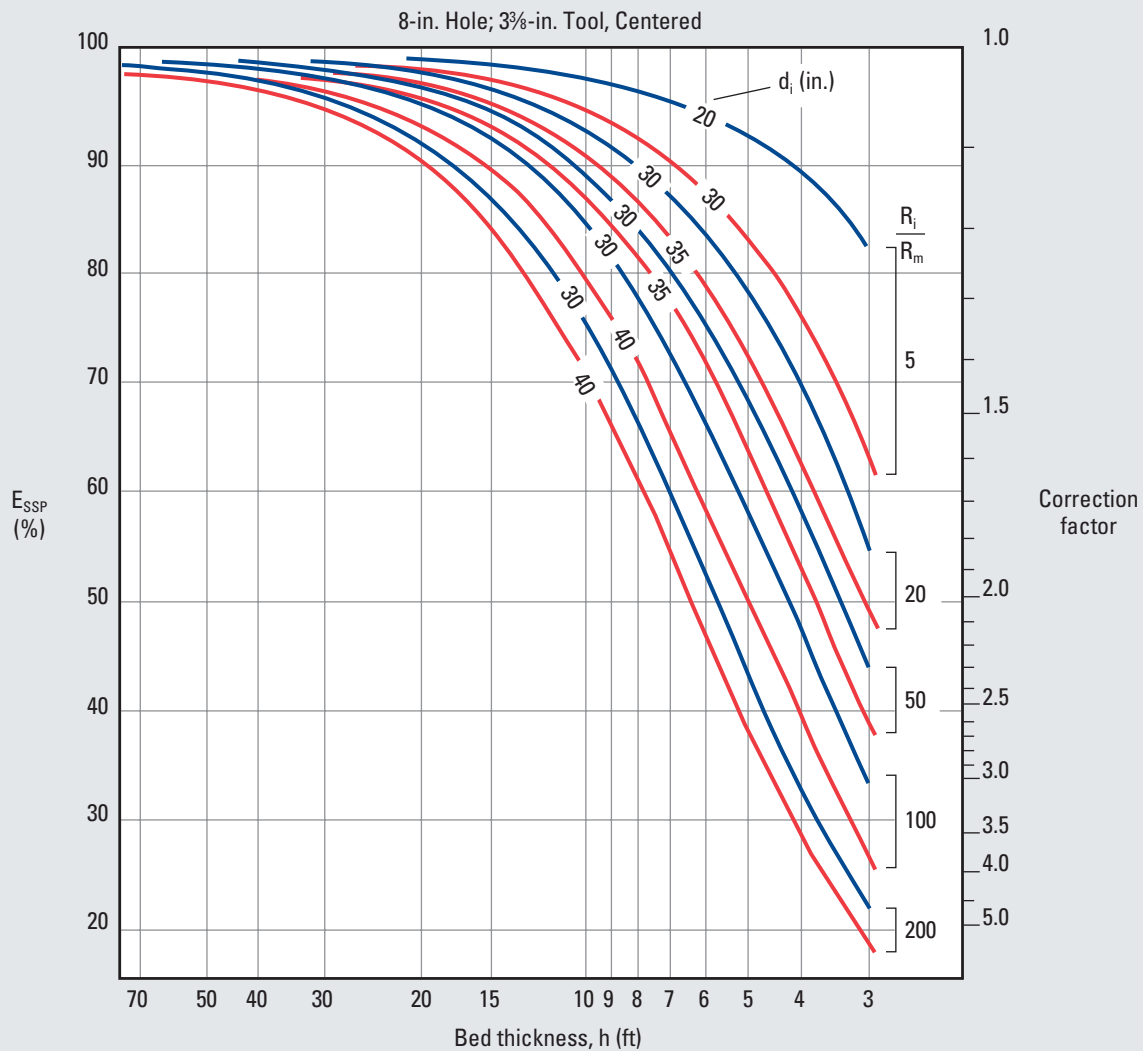
SP-4
(former SP-3)

SP



Bed Thickness Correction—Open Hole (Empirical)

SP-5
(customary, former SP-4)



© Schlumberger

Purpose

This chart is used to provide an empirical correction to the SP for the effects of invasion and bed thickness. The correction was obtained by averaging a series of thin-bed corrections in Reference 4. The resulting value of static spontaneous potential (E_{SSP}) can be used in Chart SP-1.

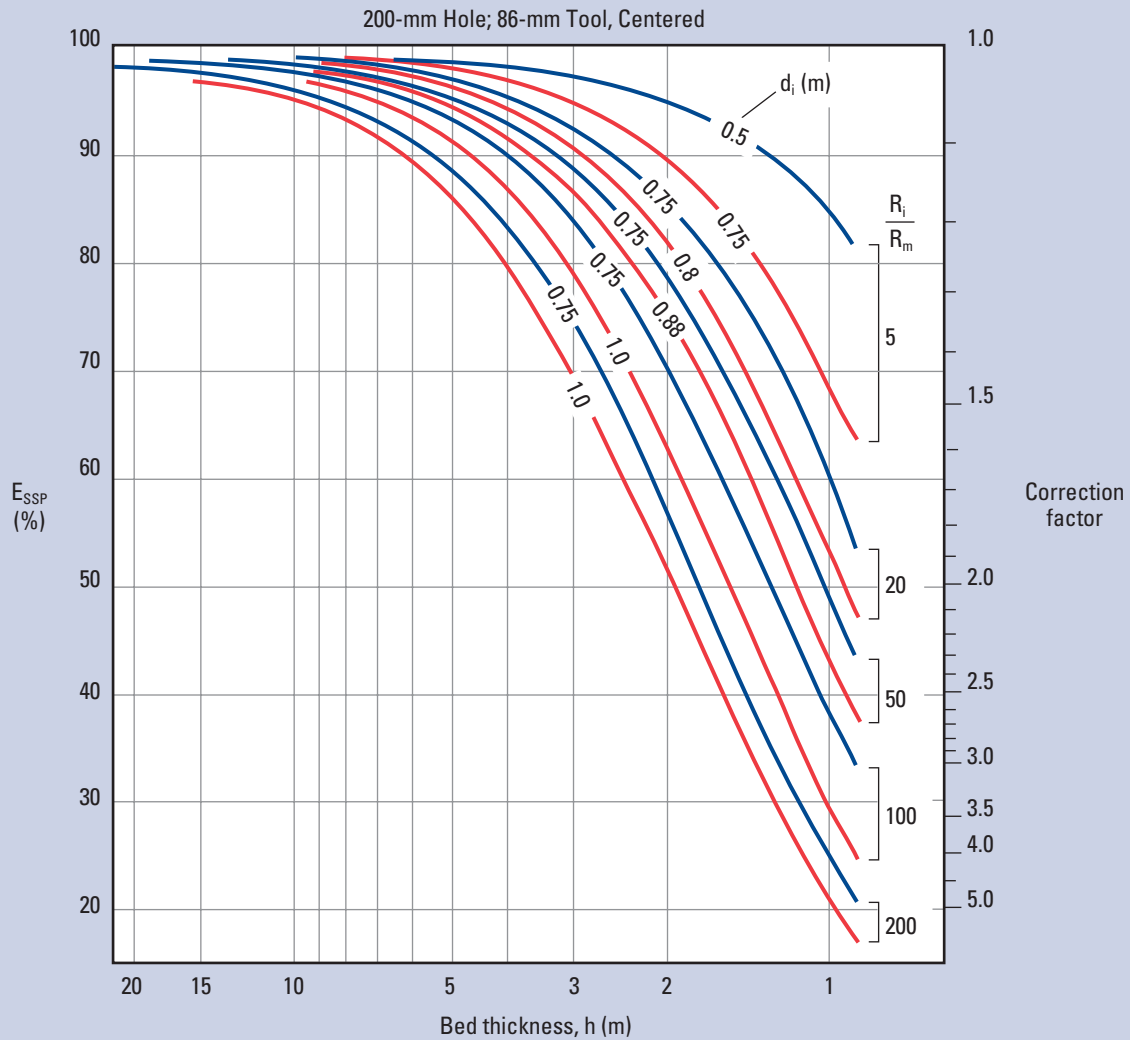
Description

This chart considers bed thickness (h) as a variable, and the ratio of the resistivity of the invaded zone to the resistivity of the mud (R_i/R_m) and the diameter of invasion (d_i) as parameters of fixed value. The borehole diameter is fixed at 8 in. and the tool size at 3 3/8 in.

To obtain the correction factor, enter the chart on the x-axis with the value of h. Move upward to the appropriate d_i curve for the range of R_i/R_m. The correction factor on the y-axis corresponding to the intersection point is multiplied by the SP from the log to obtain the corrected SP.

Bed Thickness Correction—Open Hole (Empirical)

SP-6
(metric, former SP-4m)



© Schlumberger

Purpose

This chart is the metric version of Chart SP-5 for providing an empirical correction to the SP for the effects of invasion and bed thickness. The correction was obtained by averaging a series of thin-bed corrections in Reference 4. The resulting value of E_{SSP} can be used in Chart SP-1.

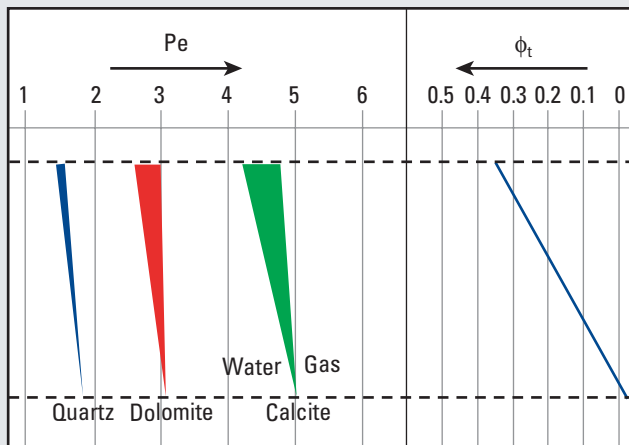
Description

This chart considers bed thickness (h) as a variable, and R_i/R_m and d_i as parameters of fixed value. The borehole diameter is fixed at 203 mm and the tool size at 86 mm.

SP

Porosity Effect on Photoelectric Cross Section

Dens-1



Matrix	ϕ_t	100% H ₂ O	100% CH ₄
Quartz	0.00	1.81	1.81
	0.35	1.54	1.76
Calcite	0.00	5.08	5.08
	0.35	4.23	4.96
Dolomite	0.00	3.14	3.14
	0.35	2.66	3.07
Specific gravity	—	1.00	0.10

© Schlumberger

Purpose

This chart and accompanying table illustrate the effect that porosity, matrix, formation water, and methane (CH₄) have on the recorded photoelectric cross section (P_e).

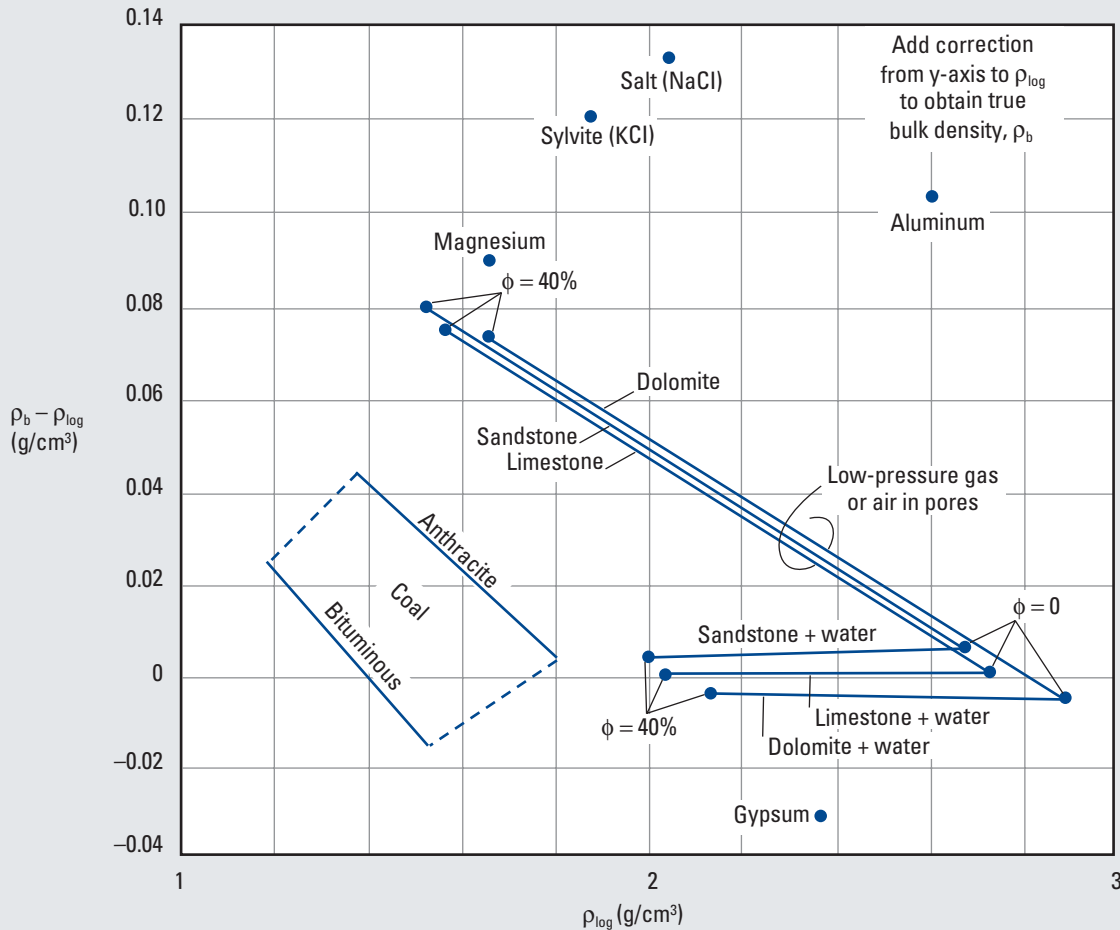
Description

The table lists the data from which the chart was made. As the porosity increases the effect is greater for each mineral. Calcite has the largest effect in the presence of gas or water as the porosity increases.

Enter the chart with the total porosity (ϕ_t) from the log and move downward to intersect the angled line. From this point move to the left and intersect the line representing the appropriate matrix material: quartz, dolomite, or calcite minerals. From this intersection move upward to read the correct P_e .

Apparent Log Density to True Bulk Density

Dens-2



© Schlumberger

Purpose

This chart is used to determine the true bulk density (ρ_b) from the “apparent” recorded log value (ρ_{log}).

Description

Enter the chart with the log density reading on the x-axis and move upward to intersect the mineral line that best represents the formation. At this point, move horizontally left to read the value to be added to the log density. The individual mineral points reflect the log-derived density and the correction factor to be added or subtracted from the log value to obtain the true density of that mineral.

The long diagonal lines representing zero porosity at the lower right and 40% porosity at the upper left are for dry gas in the formation. The three points at the lower right of the diagonal lines represent zero dry gas in the formation and are the endpoints for

sandstone, limestone, and dolomite with water in the pores. This shows that there is a slight correction for water-filled formations from the log density value.

Example

Given: Log density = 2.40 g/cm³ in a sandstone formation (dry gas).

Find: Corrected bulk density.

Answer: Enter the x-axis at 2.4 g/cm³ and move upward to intersect the sandstone line. The correction from the y-axis is 0.02 g/cm³. The correction value is added to the log density to obtain the true value of the bulk density:

$$2.40 + 0.02 = 2.42 \text{ g/cm}^3$$

Dens

Dual-Spacing Compensated Neutron Tool Charts

This section contains interpretation charts to cover developments in compensated neutron tool (CNT) porosity transforms, environmental corrections, and porosity and lithology determination.

CSU* software (versions CP-30 and later) and MAXIS* software compute three thermal porosities: NPHI, TNPH, and NPOR.

NPHI is the “classic NPHI,” computed from instantaneous near and far count rates, using “Mod-8” ratio-to-porosity transform with a caliper correction.

TNPH is computed from deadtime-corrected, depth- and resolution-matched count rates, using an improved ratio-to-porosity transform and performing a complete set of environmental corrections in real time. These corrections may be turned on or off by the field engineer at the wellsite. For more information see Reference 32.

NPOR is computed from the near-detector count rate and TNPH to give an enhanced resolution porosity. The accuracy of NPOR is equivalent to the accuracy of TNPH if the environmental effects on the near detector change less rapidly than the formation porosity. For more information on enhanced resolution processing, see Reference 35.

Cased hole CNT logs are recorded on NPHI, computed from instantaneous near and far count rates, with a cased hole ratio-to-porosity transform.

Using the Neutron Correction Charts

For logs labeled NPHI:

1. Enter Chart Neu-5 with NPHI and caliper reading to convert to uncorrected neutron porosity.
2. Enter Charts Neu-1 and Neu-3 to obtain corrections for each environmental effect. Corrections are summed with the uncorrected porosity to give a corrected value.
3. Use crossplot Charts Por-11 and Por-12 for porosity and lithology determination.

For logs labeled TNPH or NPOR, the CSU wellsite surface instrumentation and MAXIS software have applied environmental corrections as indicated on the log heading. If the CSU and MAXIS software has applied all corrections, TNPH or NPOR can be used directly with the crossplot charts. In this case:

1. Use crossplot Charts Por-11 and Por-12 to determine porosity and lithology.

Compensated Neutron Tool

Environmental Correction—Open Hole

Purpose

Chart Neu-1 is used to correct the compensated neutron log porosity index if the caliper correction was not applied. If the caliper correction is applied, it must be “backed out” to use this chart.

Description

This chart is used only if the caliper correction was not applied to the logged data. The parameter section of the log heading lists whether correction was applied.

Example 1: Backed-Out Correction of TNPH Porosity

Given: Thermal neutron porosity (TNPH) from the log = 32 p.u. (apparent limestone units) and borehole size = 12 in.

Find: Uncorrected TNPH with the correction backed out.

Answer: Enter the top chart for actual borehole size at the intersection point of the standard conditions 8-in. horizontal line and 32 p.u. on the scale above the chart.

From this point, follow the closest trend line to intersect the 12-in. line for the borehole size.

The intersection is the uncorrected TNPH value of 34 p.u.

To use the uncorrected value on Chart Neu-1, draw a vertical line from this intersection through the remainder of the charts, as shown by the red line.

Example 2: Environmentally Corrected THPH

Given: Neutron porosity of 32 p.u. (apparent limestone units), without environmental correction, 12-in. borehole, ¼-in. thick mudcake, 100,000-ppm borehole salinity, 11-lbm/gal natural mud weight (water-base mud [WBM]), 150°F borehole temperature, 5,000-psi pressure (WBM), and 100,000-ppm formation salinity.

Find: Environmentally corrected TNPH porosity.

Answer: If there is standoff (which is not uncommon), use Chart Neu-3. Then use Chart Neu-1 by drawing a vertical line through the charts for the previously determined backed-out (uncorrected) 34-p.u. neutron porosity value.

On each environmental correction chart, enter the y-axis at the given value and move horizontally left to intersect the porosity value vertical line.

For example, on the mudcake thickness chart the line extends from ¼ in. on the y-axis.

At the intersection point, move parallel to the closest blue trend line to intersect the standard conditions, as indicated by the bullet.

The point of intersection with the standard conditions for the chart is the value of porosity corrected for the particular environment. The change in porosity value (either positive or negative) is summed for the charts and referred to as delta porosity ($\Delta\phi$).

The $\Delta\phi$ net correction applied to the uncorrected log neutron porosity is listed in the table for the two examples.

CNT Neutron Porosity Correction Examples

		Correction		
		Example 1	Example 2	$\Delta\phi$
Log porosity	32 p.u.			
Borehole size	12 in.	-2		
Mudcake thickness	¼ in.		0	
Borehole salinity	100,000 ppm		+1	
Mud weight	11 lbm/gal		+2	
Borehole temperature	150°F		+4	
Wellbore pressure	5,000 psi		-1	
Formation salinity	100,000 ppm		-3	
Standoff (from Chart Neu-3)	1 in.		-4	
Net environmental correction			-1	
Backed-out corrected porosity		34 p.u.		
Environmentally corrected porosity			33 p.u.	
Net correction				-3
Backed-out, environmentally corrected porosity				31 p.u.

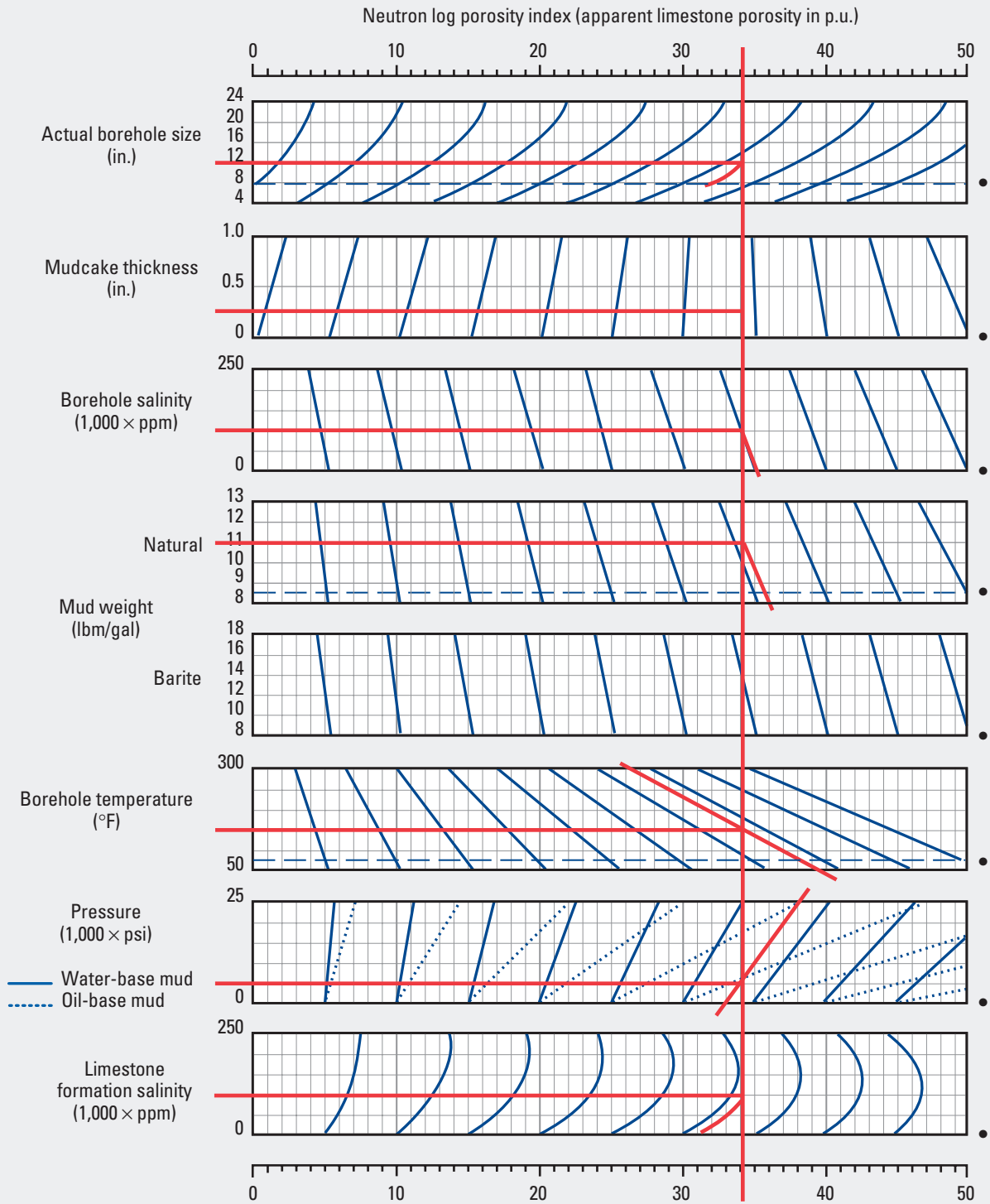
continued on next page

Compensated Neutron Tool

Environmental Correction—Open Hole

Neu-1

(customary, former Por-14c)



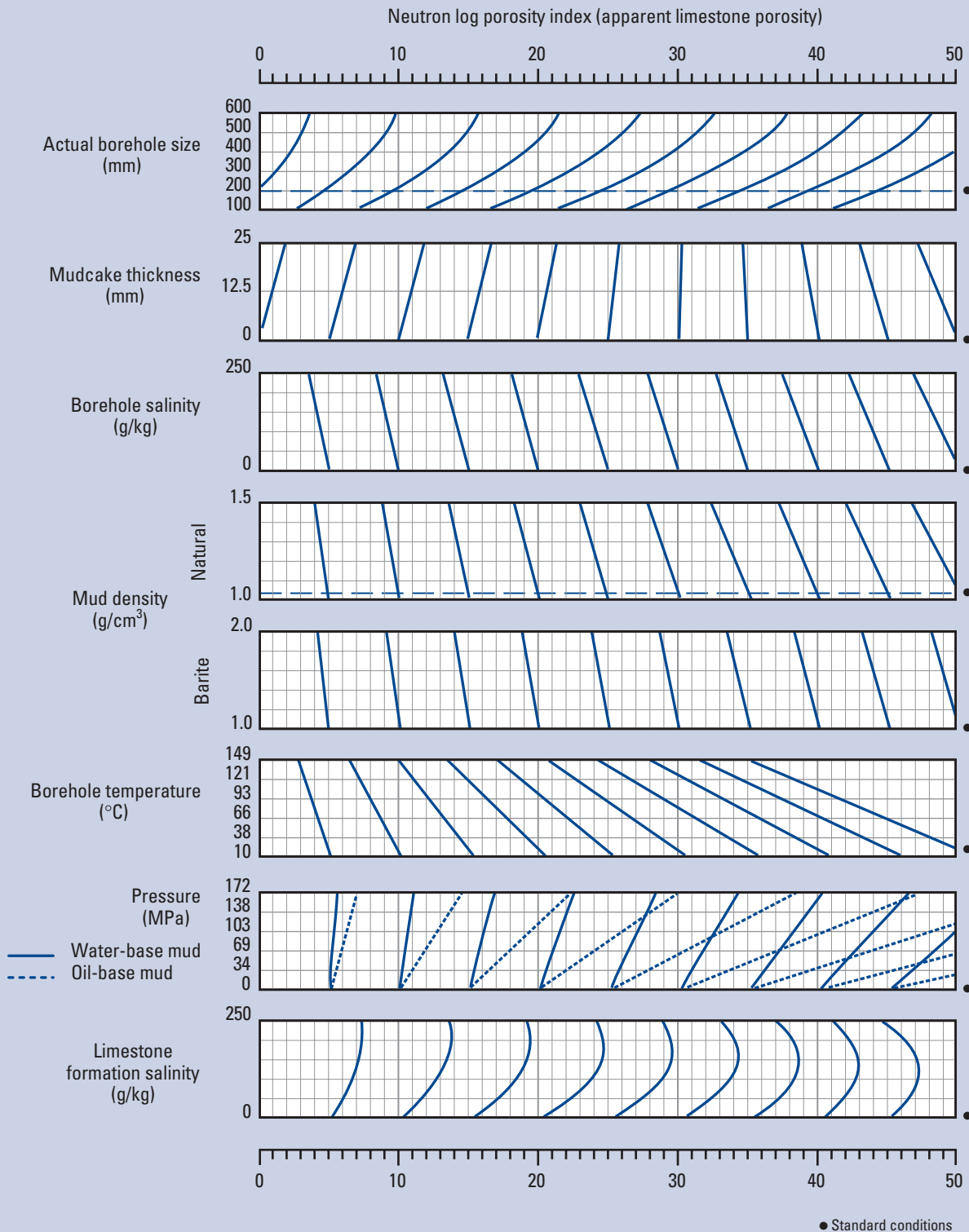
● Standard conditions

Compensated Neutron Tool

Environmental Correction—Open Hole

Neu-2

(metric, former Por-14cm)



© Schlumberger

Purpose

This chart is the metric version of Chart Neu-1 for correcting the compensated neutron tool porosity index.

Compensated Neutron Tool

Standoff Correction—Open Hole

Purpose

Chart Neu-3 is used to determine the porosity change caused by standoff to the uncorrected thermal neutron porosity TNPH from Chart Neu-1.

Description

Enter the appropriate borehole size chart at the estimated neutron tool standoff on the y-axis. Move horizontally to intersect the uncorrected porosity. At the intersection point, move along the closest trend line to the standard conditions line defined by the bullet to the right of the chart. This point is the porosity value corrected for tool standoff. The difference between the standoff-corrected porosity and the uncorrected porosity is the correction itself.

Example

Given: TNPH = 34 p.u., borehole size = 12 in., and standoff = 0.5 in.

Find: Porosity corrected for standoff.

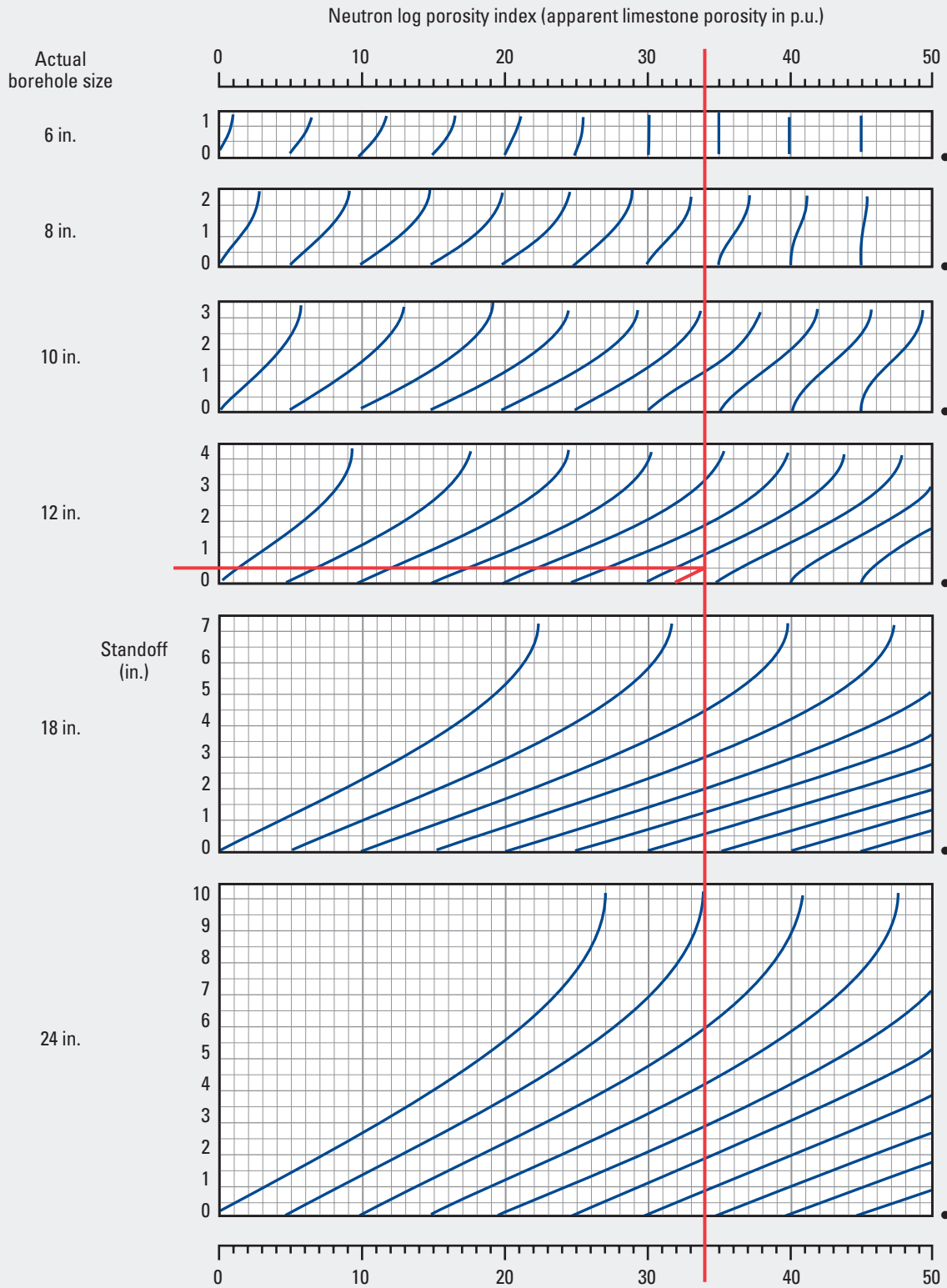
Answer: Draw a vertical line from the uncorrected neutron log porosity of 34 p.u. Enter the 12-in. borehole chart at 0.5-in. standoff and move horizontally right to intersect the vertical porosity line. From the point of intersection move parallel to the closest trend line to intersect the standard conditions line (standoff = 0 in.). The standoff-corrected porosity is 32 p.u. The correction is -2 p.u.

Compensated Neutron Tool

Standoff Correction—Open Hole

Neu-3

(customary, former Por-14d)

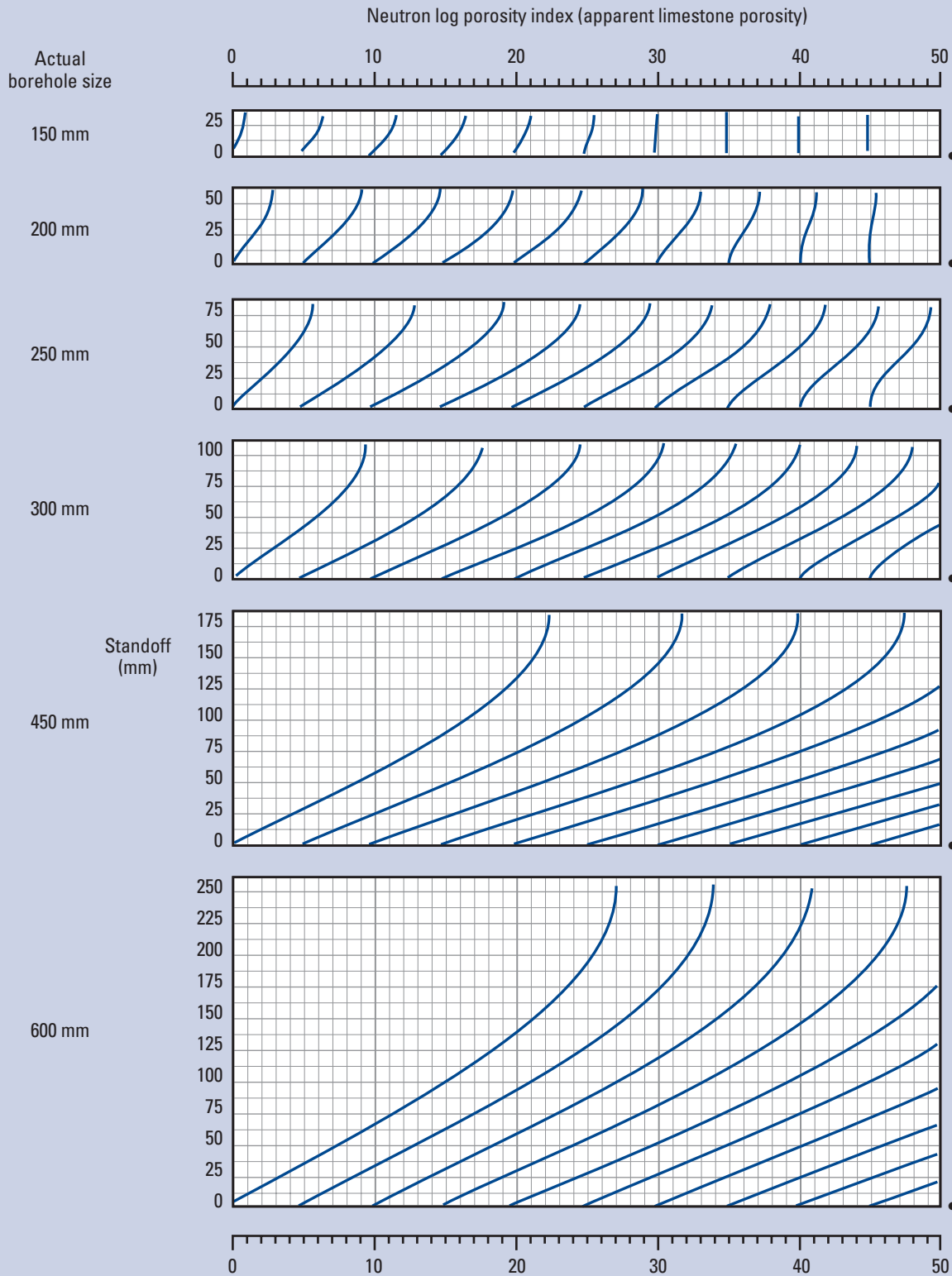


Compensated Neutron Tool

Standoff Correction—Open Hole

Neu-4

(metric, former Por-14dm)



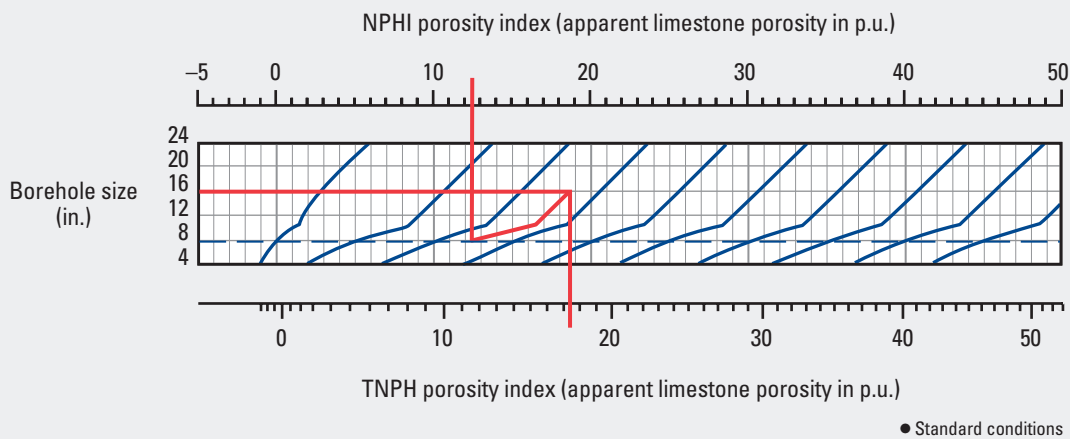
Purpose

This chart is the metric version of Chart Neu-3 for determining the porosity change caused by standoff.

Compensated Neutron Tool

Conversion of NPHI to TNPH—Open Hole

Neu-5
(former Por-14e)



© Schlumberger

Purpose

This chart is used to determine the porosity change caused by the borehole size to the neutron porosity NPHI and convert the porosity to thermal neutron porosity (TNPH). This chart corrects NPHI only for the borehole sizes that differ from the standard condition of 8 in. Refer to Chart Neu-1 to complete the environmental corrections for the TPNH value obtained.

Description

Enter the scale at the top of the chart with the NPHI porosity.

Example

Given: NPHI porosity = 12.5% and borehole size = 16 in.

Find: Porosity correction for nonstandard borehole size.

Answer: Enter the chart with the uncorrected porosity value of 12.5 at the scale at the top. Move down vertically to intersect the standard conditions line indicated by the bullet to the right. Enter the chart on the y-axis with the actual borehole size at the zone of interest and move horizontally right across the chart.

At the point of intersection of the vertical line and the standard conditions line, move parallel to the closest trend line to intersect the actual borehole size line.

At that intersection point move vertically down to the bottom scale to determine the TNPH porosity corrected only for borehole size. This value is also used to determine the change in porosity as a result of tool standoff.

$$\text{TNPH} = 12.5 + 5 = 17.5 \text{ p.u.}$$

Compensated Neutron Tool

Formation Σ Correction for Environmentally Corrected TNPH—Open Hole

Purpose

This chart is used to further correct the environmentally corrected TNPH porosity from Chart Neu-1 for the effect of the total formation capture cross section, or sigma (Σ), of the formation of interest. This correction is applied after all environmental corrections determined with Chart Neu-1 have been applied.

Description

Enter the chart with Σ for the appropriate formation along the y-axis and the corrected TNPH porosity along the x-axis. Where the lines drawn from these points intersect, move parallel to the closest trend line to intersect the appropriate fresh- or saltwater line to read the corrected porosity.

The chart at the bottom of the page is used to correct the Σ -corrected porosity for salt displacement if the formation Σ is due to salinity. However, this correction is not made if the borehole salinity correction from Chart Neu-1 has been applied.

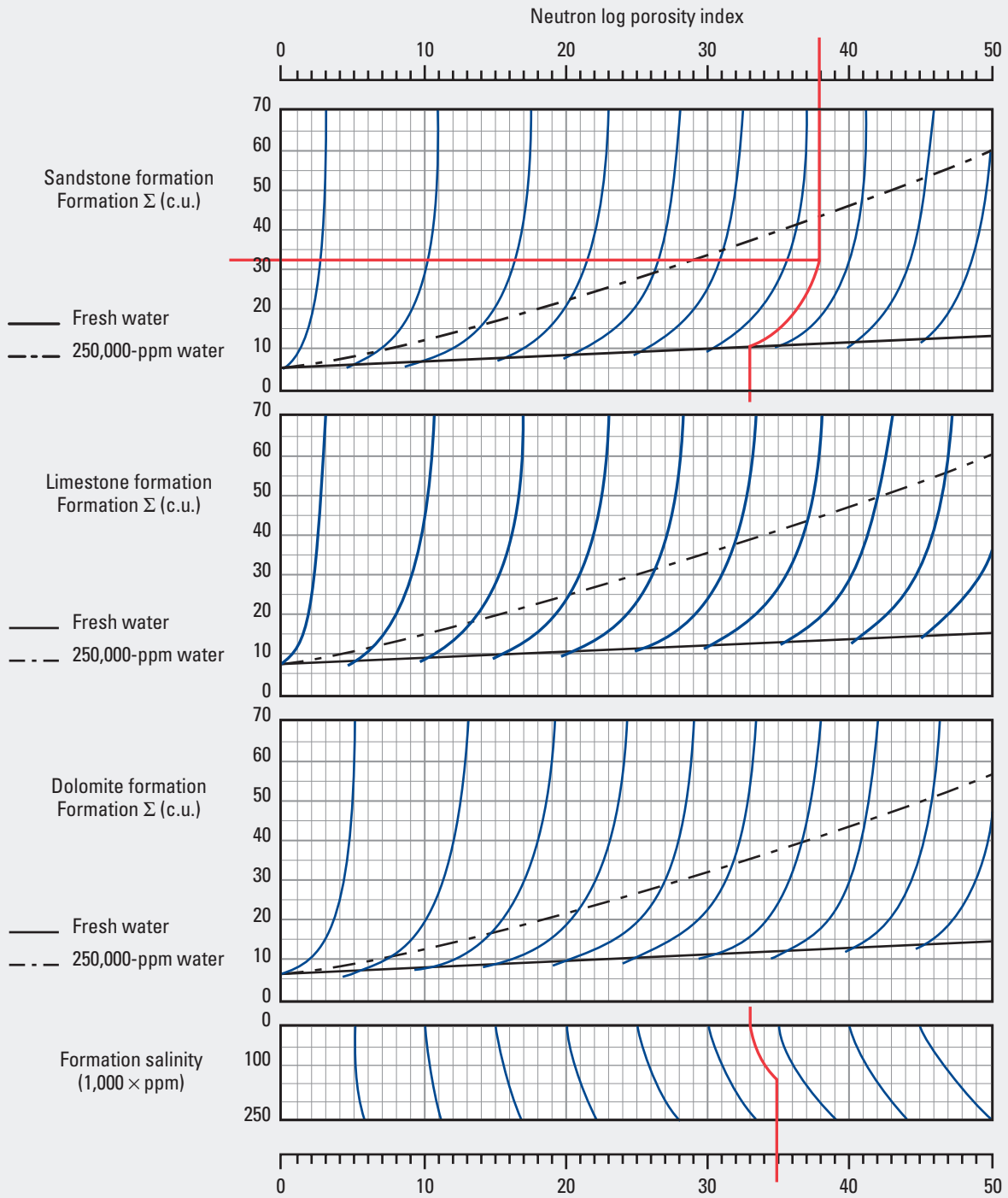
Example

- Given:** Corrected TNPH from Chart Neu-1 = 38 p.u., Σ of the sandstone formation = 33 c.u., and formation salinity = 150,000 ppm (indicating a freshwater formation).
- Find:** TNPH porosity corrected with Chart Neu-1 and for Σ of the formation.
- Answer:** Enter the appropriate chart with the Σ value on the y-axis and the corrected TNPH value on the x-axis. At the intersection of the sigma and porosity lines, parallel the closest trend line to intersect the freshwater line. (If the water in the formation is salty, the 250,000-ppm line should be used.)
- Move straight down from the intersection point to the formation salinity chart at the bottom.
- From the point where the straight line intersects the top of the salinity correction chart, parallel the closest trend line to intersect the formation salinity line.
- Draw a vertical line to the bottom scale to read the corrected formation sigma TNPH porosity, which is 35 p.u.

Compensated Neutron Tool

Formation Σ Correction for Environmentally Corrected TNPH—Open Hole

Neu-6
(former Por-16)



Neu

Compensated Neutron Tool

Mineral Σ Correction for Environmentally Corrected TNPH—Open Hole

Purpose

This chart is used to further correct the environmentally corrected TNPH porosity from Chart Neu-1 for the effect of the mineral sigma (Σ). This correction is applied after all environmental corrections determined with Chart Neu-1 have been applied.

Description

Enter the chart for the formation type with the mineral Σ value along the y-axis and the Chart Neu-1 corrected TNPH porosity along the x-axis. Where lines drawn from these points intersect, move parallel to the closest trend line to intersect the freshwater line to read the corrected porosity on the scale at the bottom. The choice of chart depends on the type of mineral in the formation.

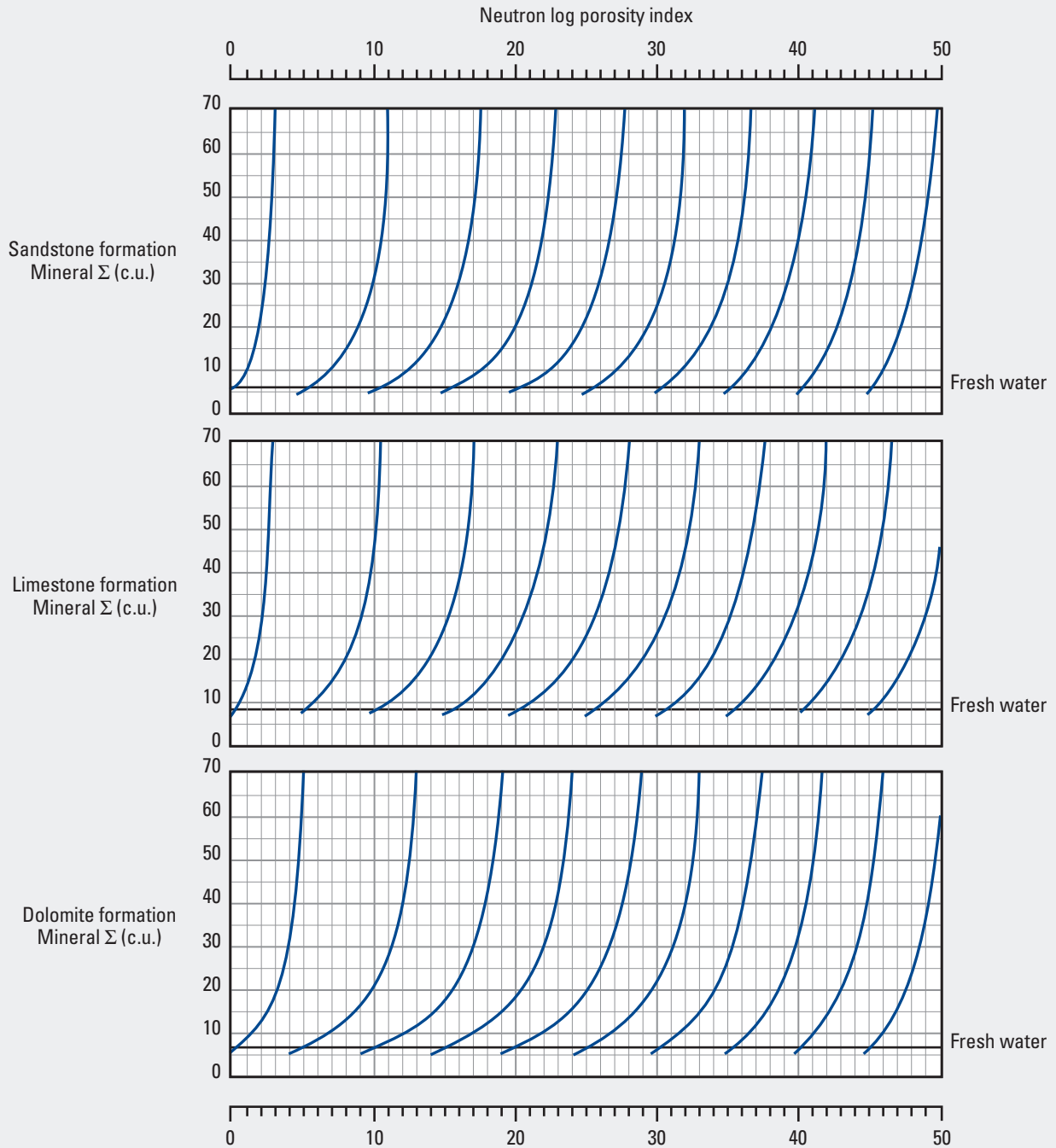
Example

- Given:** Corrected TNPH from Chart Neu-1 = 38 p.u., sandstone formation $\Sigma = 35$ c.u., and formation salinity = 150,000 ppm (indicating a freshwater formation).
- Find:** TNPH porosity corrected with Chart Neu-1 and for the mineral Σ .
- Answer:** At the intersection of the Σ and porosity value lines move parallel to the closest trend line to intersect the freshwater line. Move straight down to intersect the bottom porosity scale to read the TNPH porosity corrected for mineral Σ , which is 33 p.u.

Compensated Neutron Tool

Mineral Σ Correction for Environmentally Corrected TNPH—Open Hole

Neu-7
(former Por-17)



Neu

Compensated Neutron Tool

Fluid Σ Correction for Environmentally Corrected TNPH—Open Hole

Purpose

This chart is used to correct the environmentally corrected TNPH porosity from Chart Neu-1 for the effect of the fluid sigma (Σ) in the formation. This correction is applied after all environmental corrections determined with Chart Neu-1 have been applied.

Description

Enter the appropriate formation chart with the formation fluid Σ value on the y-axis and the Chart Neu-1 corrected TNPH porosity on the x-axis. Where the lines drawn from these points intersect, move parallel to the closest trend line to intersect the appropriate fresh- or saltwater line. If the borehole salinity correction from Chart Neu-1 has not been applied, from this point extend a line down to intersect the formation salinity chart at the bottom. Move parallel to the closest trend line to intersect the formation salinity line. Move straight down to read the corrected porosity on the scale below the chart.

Example

Given: Corrected TNPH from Chart Neu-1 = 30 p.u. (without borehole salinity correction), fluid Σ = 80 c.u., fluid salinity = 150,000 ppm, and sandstone formation.

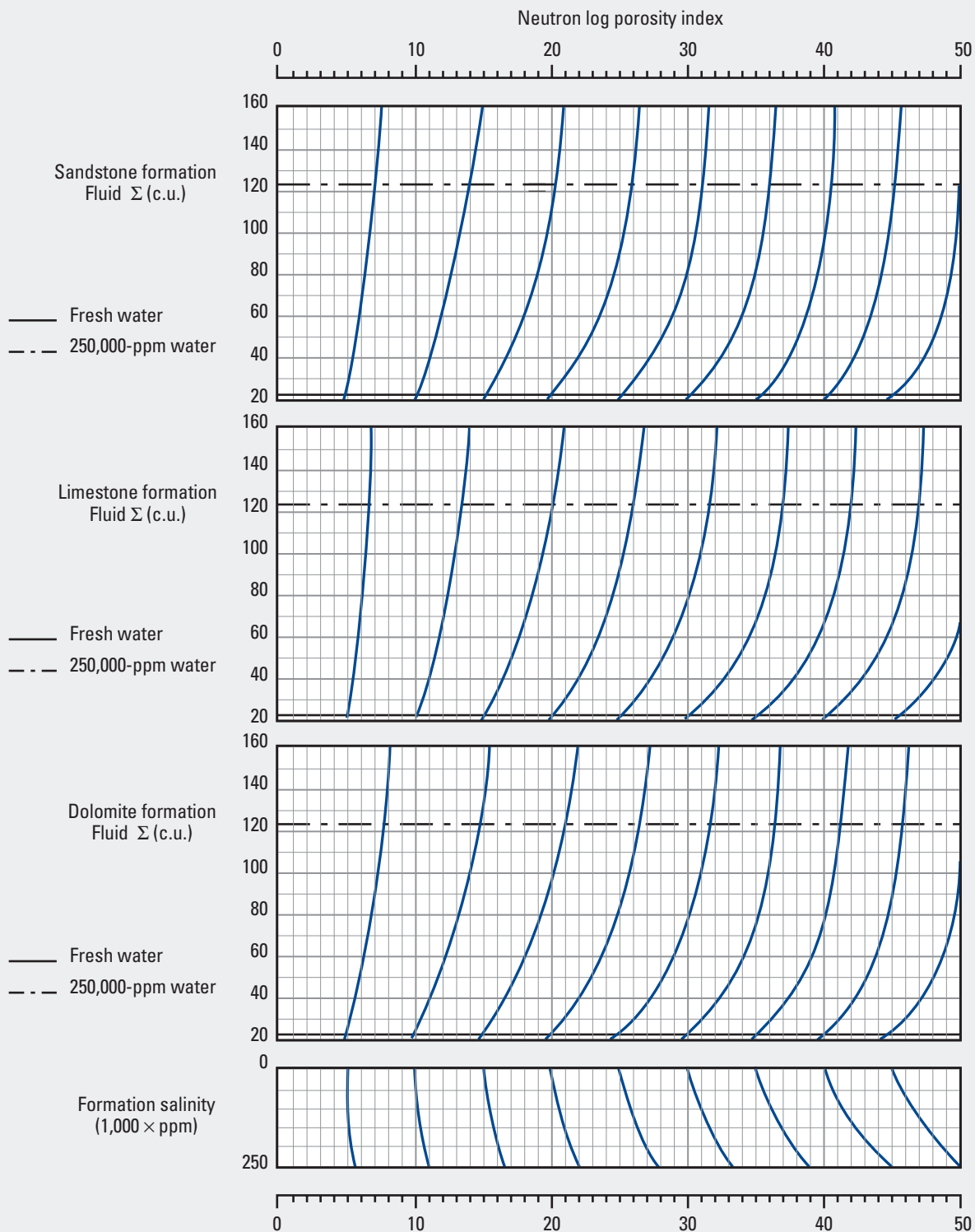
Find: TNPH corrected with Chart Neu-1 and for fluid Σ .

Answer: At the intersection of the fluid Σ and Chart Neu-1 corrected TNPH porosity (30-p.u.) line, move parallel to the closest trend line to intersect the freshwater line. From that point go straight down to the formation salinity correction chart at the bottom. Move parallel to the closest trend line to intersect the formation salinity line (150,000 ppm), and then draw a vertical line to the bottom scale to read the corrected TNPH value (26 p.u.).

Compensated Neutron Tool

Fluid Σ Correction for Environmentally Corrected TNPH—Open Hole

Neu-8
(former Por-18)



Compensated Neutron Tool

Environmental Correction—Cased Hole

Purpose

This chart is used to obtain the correct porosity from the neutron porosity index logged with the compensated neutron tool in casing, where the effects of the borehole size, casing thickness, and cement sheath thickness influence the true value of formation porosity.

Description

Enter the scale at the top of the chart with a whole-number (not fractional) porosity value. Draw a straight line vertically through the three charts representing borehole size, casing thickness, and cement thickness. Draw a horizontal line on each chart from the appropriate value on the y-axis. At the intersection point of the vertical line and the horizontal line on each chart proceed to the blue dashed horizontal line by following the slope of the blue solid lines on each chart. At that point read the change in porosity index. The cumulative change in porosity is added to the logged porosity to obtain the corrected value. As can be seen, the major influences to the casing-derived porosity are the borehole size and the cement thickness. The same procedure applies to the metric chart.

The blue dashed lines represent the standard conditions from which the charts were developed: 8¾-in. open hole, 5½-in. 17-lbm casing, and 1.62-in. annular cement thickness.

The neutron porosity equivalence nomographs at the bottom are used to convert from the log standard of limestone porosity to porosity for other matrix materials.

The porosity value corrected with Chart Neu-9 is entered into Chart Neu-1 to provide environmental corrections necessary for determining the correct cased hole porosity value.

Example

Given: Log porosity index = 27%, borehole diameter = 11 in., casing thickness = 0.304 in., and cement thickness = 1.62 in.

Cement thickness is defined as the annular space between the outside wall of the casing and the borehole wall. The value is determined by subtracting the casing outside diameter from the borehole diameter and dividing by 2.

Find: Porosity corrected for borehole size, casing thickness, and cement thickness.

Answer: Draw a vertical line (shown in red) through the three charts at 27 p.u.

Borehole-diameter correction chart: From the intersection of the vertical line and the 11-in. borehole-diameter line (shown in red dashes) move upward along the curved blue line as shown on the chart.

The porosity is reduced to 26% by -1 p.u.

Casing thickness chart: The porosity index is changed by 0.3 p.u.

Cement thickness chart: The porosity index is changed by 0.5 p.u.

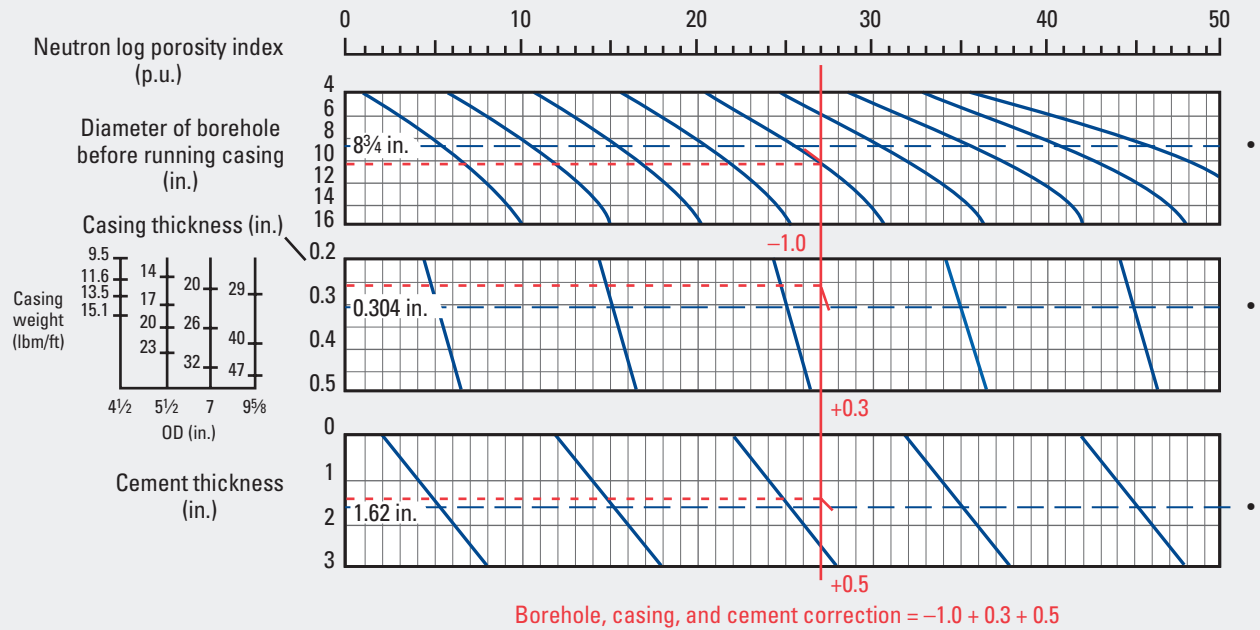
The resulting corrected porosity for borehole, casing, and cement is $27 - 1 + 0.3 + 0.5 = 26.8$ p.u.

Compensated Neutron Tool

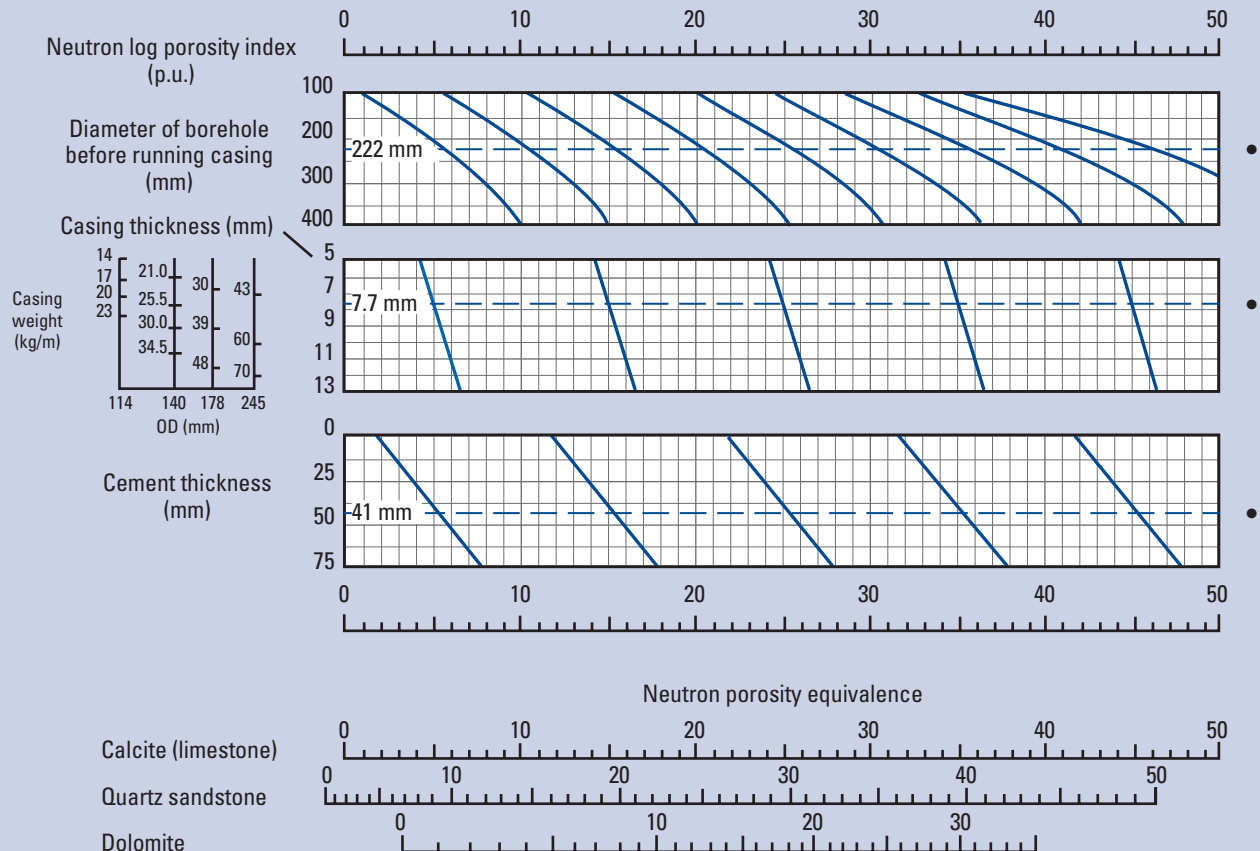
Environmental Correction—Cased Hole

Neu-9
(former Por-14a)

Customary



Metric



● Standard conditions

APS* Accelerator Porosity Sonde

Environmental Correction—Open Hole

Purpose

The Neu-10 charts pair is used to correct the APS Accelerator Porosity Sonde apparent limestone porosity for mud weight and actual borehole size. The charts are for the near-to-array and near-to-far porosity measurements. The design of the APS sonde resulted in a significant reduction in environmental correction. The answer determined with this chart is used in conjunction with the correction from Chart Neu-11.

Description

Enter the appropriate chart pair (mud weight and actual borehole size) for the APS near-to-array apparent limestone porosity (APLU) or APS near-to-far apparent limestone porosity (FPLU) with the uncorrected porosity from the APS log by drawing a straight vertical line (shown in red) through both of the charts. At the intersection with the mud weight value, move parallel to the closest trend line to intersect the standard conditions line. This point represents a change in porosity resulting from the correction for mud weight. Follow the same procedure for the borehole size chart to determine that correction change. Because the borehole size correction has a dependency on mud weight, even with natural muds, there are two sets of curves on the borehole size chart—solid for light muds (8.345 lbm/gal) and dashed for heavy muds (16 lbm/gal). Intermediate mud weights are interpolated. The two differences are summed for the total correction to the APS log value.

This answer is used in Chart Neu-11 to complete the environmental corrections for corrected APLU or FPLU porosity.

Example

Given: APS neutron APLU uncorrected porosity = 34 p.u.,
mud weight = 10 lbm/gal, and borehole size = 12 in.

Find: Corrected APLU porosity.

Answer: Draw a vertical line on the APLU mud weight chart from 34 p.u. on the scale above. At the intersection with the 10-lbm/gal mud weight line, move parallel to the trend line to intersect the standard conditions line. This point represents a change in porosity of -0.75 p.u.

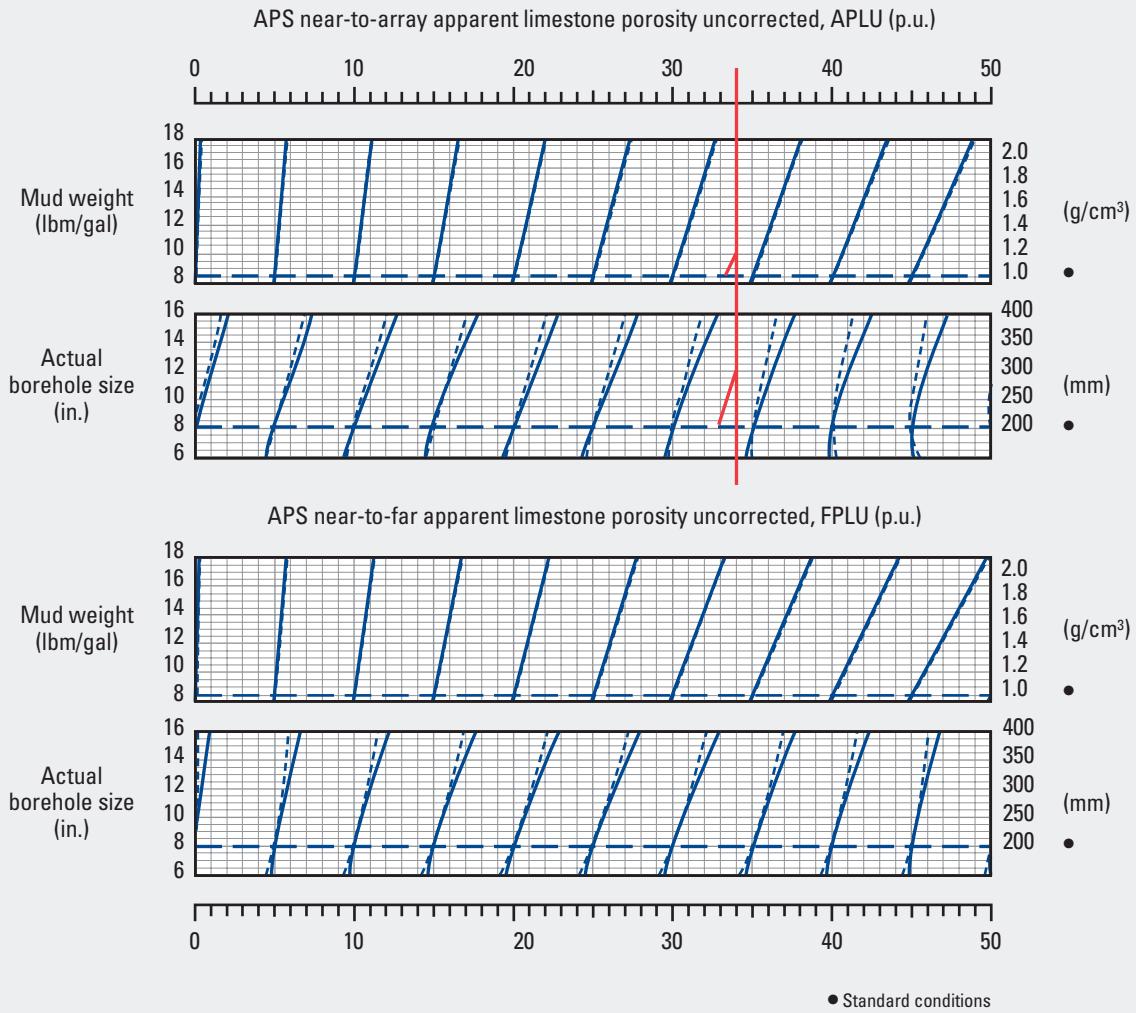
On the actual borehole size chart, move parallel to the closest trend line from the intersection of the 34-p.u. line and the actual borehole size (12 in.) to intersect the 8-in. standard conditions line. This point represents a change in porosity of -1.0 p.u.

The total correction is $-0.75 + -1.0 = -1.75$ p.u., which results in a corrected APLU porosity of $34 - 1.75 = 32.25$ p.u.

APS* Accelerator Porosity Sonde

Environmental Correction—Open Hole

Neu-10
(former Por-23a)



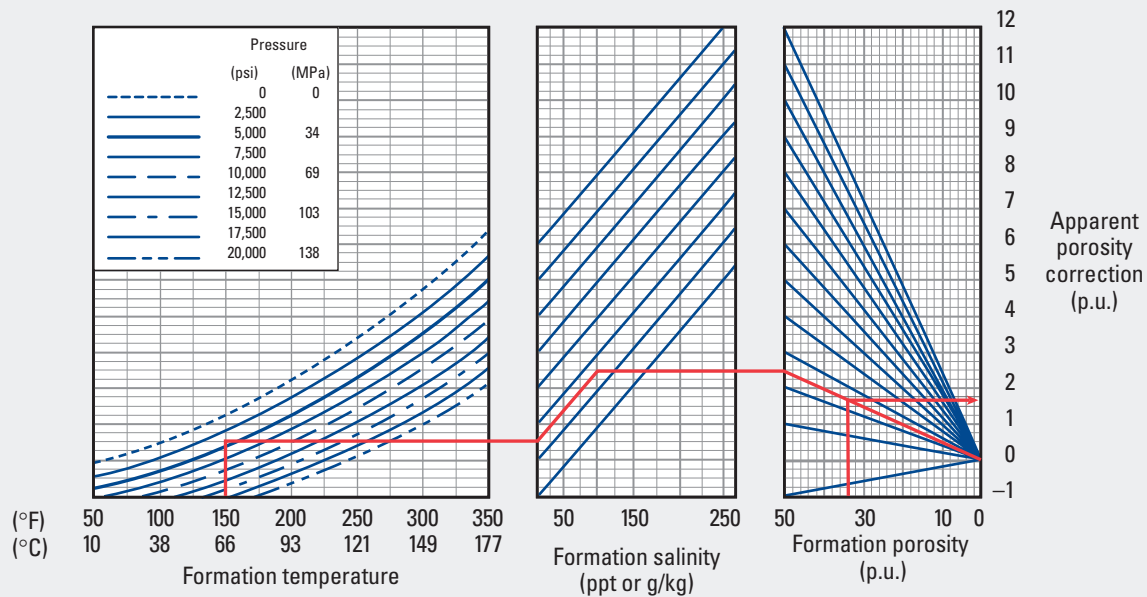
*Mark of Schlumberger
© Schlumberger

Neu

APS* Accelerator Porosity Sonde Without Environmental Corrections

Environmental Correction—Open Hole

Neu-11
(former Por-23b)



*Mark of Schlumberger
© Schlumberger

Purpose

This chart is used to complete the environmental correction for APLU and FPLU porosities from the APS log.

Description

Enter the left-hand chart on the x-axis with the temperature of the formation of interest. Move vertically to intersect the appropriate formation pressure line. From that point, move horizontally right to intersect the left edge of the formation salinity chart. Move parallel to the trend lines to intersect the formation salinity value. From that point move horizontally to intersect the left edge of the formation porosity chart. Move parallel to the trend lines to intersect the uncorrected APLU or FPLU porosity. At that intersection, move horizontally right to read the apparent porosity correction.

Example

Given: APLU or FPLU porosity = 34 p.u., formation temperature = 150°F, formation pressure = 5,000 psi, and formation salinity = 150,000 ppm.

Find: Environmentally corrected APLU or FPLU porosity.

Answer: Enter the formation temperature chart at 150°F to intersect the 5,000-psi curve. From that point move horizontally right to intersect the left edge of the formation salinity chart. Move parallel to the trend lines to intersect the formation salinity of 150,000. At this point, again move horizontally to the left edge of the next chart. Move parallel to the trend lines to intersect the 34-p.u. porosity line. At that point on the y-axis, the change in porosity is +1.6 p.u.

The total correction for a corrected APLU or FPLU from Charts Neu-10 and Neu-11 is
 $34 + (-0.75 + -1) + 1.6 = 33.85$ p.u.

CDN* Compensated Density Neutron, adnVISION* Azimuthal Density Neutron, and EcoScope* Integrated LWD Tools

Mud Hydrogen Index Determination

Purpose

This chart is used to determine one of several environmental corrections for neutron porosity values recorded with the CDN Compensated Density Neutron, adnVISION Azimuthal Density Neutron, and EcoScope Integrated LWD tools. The value of hydrogen index (H_m) is used in the following porosity correction charts.

Description

To determine the H_m of the drilling mud, the mud weight, temperature, and hydrostatic mud pressure at the zone of interest must be known.

Example

Given: Barite mud weight = 14 lbm/gal, mud temperature = 150°F, and hydrostatic mud pressure = 5,000 psi.

Find: Hydrogen index of the drilling mud.

Answer: Enter the bottom chart for mud weight at 14 lbm/gal on the y-axis. Move horizontally to intersect the barite line. Move vertically to the bottom of the mud temperature chart and move upward parallel to the closest trend line to intersect the formation temperature. From the intersection point move vertically to the bottom of the mud pressure chart.

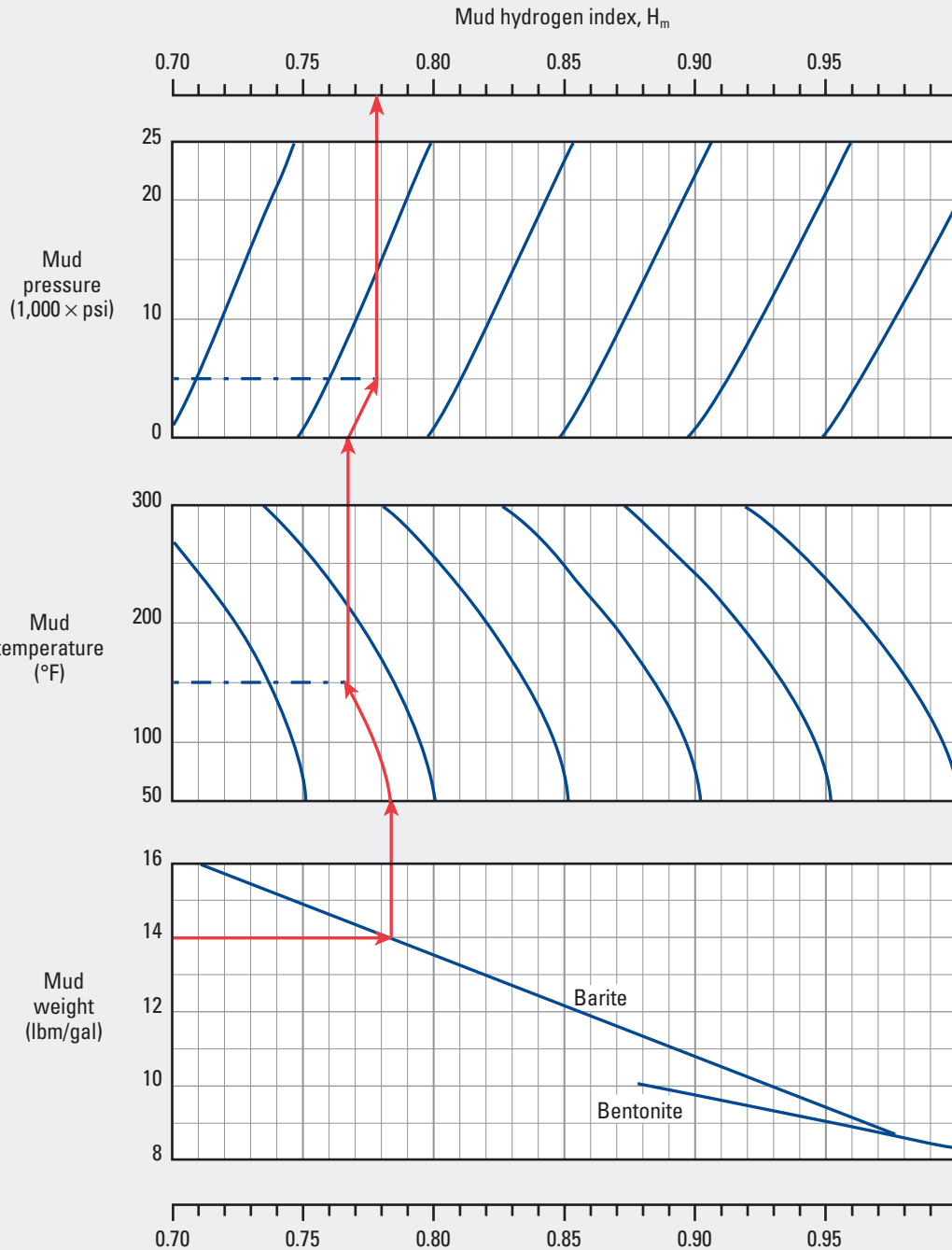
Move parallel to the closest trend line to intersect the formation pressure. Draw a line vertically to intersect the mud hydrogen index scale and read the result.

Mud hydrogen index = 0.78.

CDN* Compensated Density Neutron, adnVISION* Azimuthal Density Neutron, and EcoScope* Integrated LWD Tools

Neu-30
(former Por-19)

Mud Hydrogen Index Determination



*Mark of Schlumberger
© Schlumberger

adnVISION475* Azimuthal Density Neutron—4.75-in. Tool and 6-in. Borehole

Environmental Correction—Open Hole

Purpose

This is one of a series of charts used to correct adnVISION475 4.75-in. Azimuthal Density Neutron tool porosity for several environmental effects by using the mud hydrogen index (H_m) determined from Chart Neu-30 in conjunction with the parameters on the chart.

Description

This chart incorporates the parameters of borehole size, mud temperature, mud hydrogen index (from Chart Neu-30), mud salinity, and formation salinity for the correction of adnVISION475 porosity.

The following charts are used with the same interpretation procedure as Chart Neu-31. The charts differ for tool size and borehole size.

Example

Given: adnVISION475 uncorrected porosity = 34 p.u., borehole size = 10 in., mud temperature = 150°F, hydrogen index = 0.78, borehole salinity = 100,000 ppm, and formation salinity = 100,000 ppm.

Find: Corrected adnVISION475 porosity.

Answer: From the adnVISION475 porosity of 34 p.u. on the top scale, enter the borehole size chart to intersect the borehole size of 10 in. From the point of intersection move parallel to the closest trend line to intersect the standard conditions line.

From this intersection point move straight down to enter the mud temperature chart and intersect the mud temperature of 150°F. From the point of intersection move parallel to the closest trend line to intersect the standard conditions line.

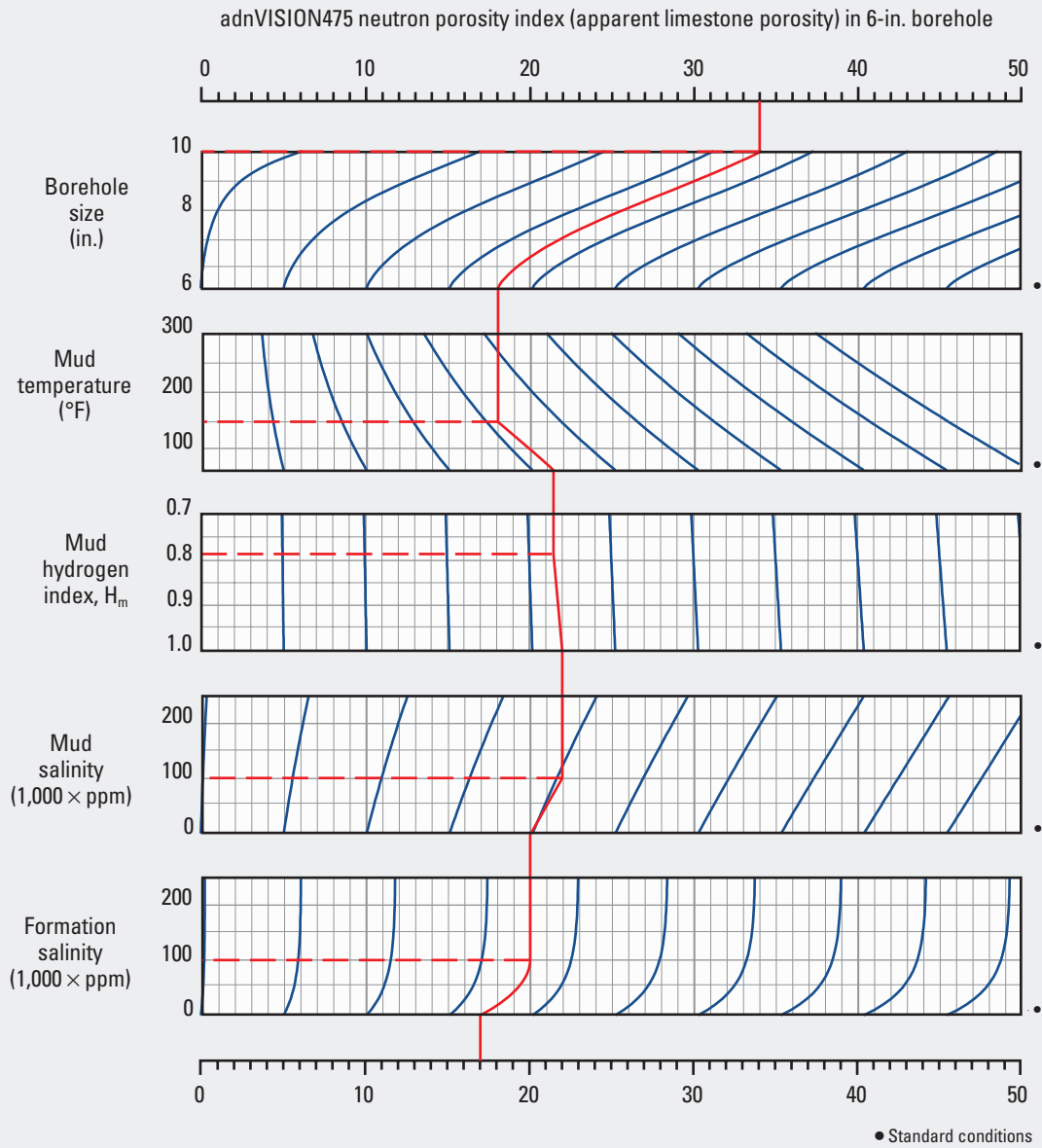
Continue this pattern through the charts to read the corrected porosity from the scale at the bottom of the charts.

The corrected adnVISION475 porosity is 17 p.u.

adnVISION475* Azimuthal Density Neutron—4.75-in. Tool and 6-in. Borehole

Environmental Correction—Open Hole

Neu-31

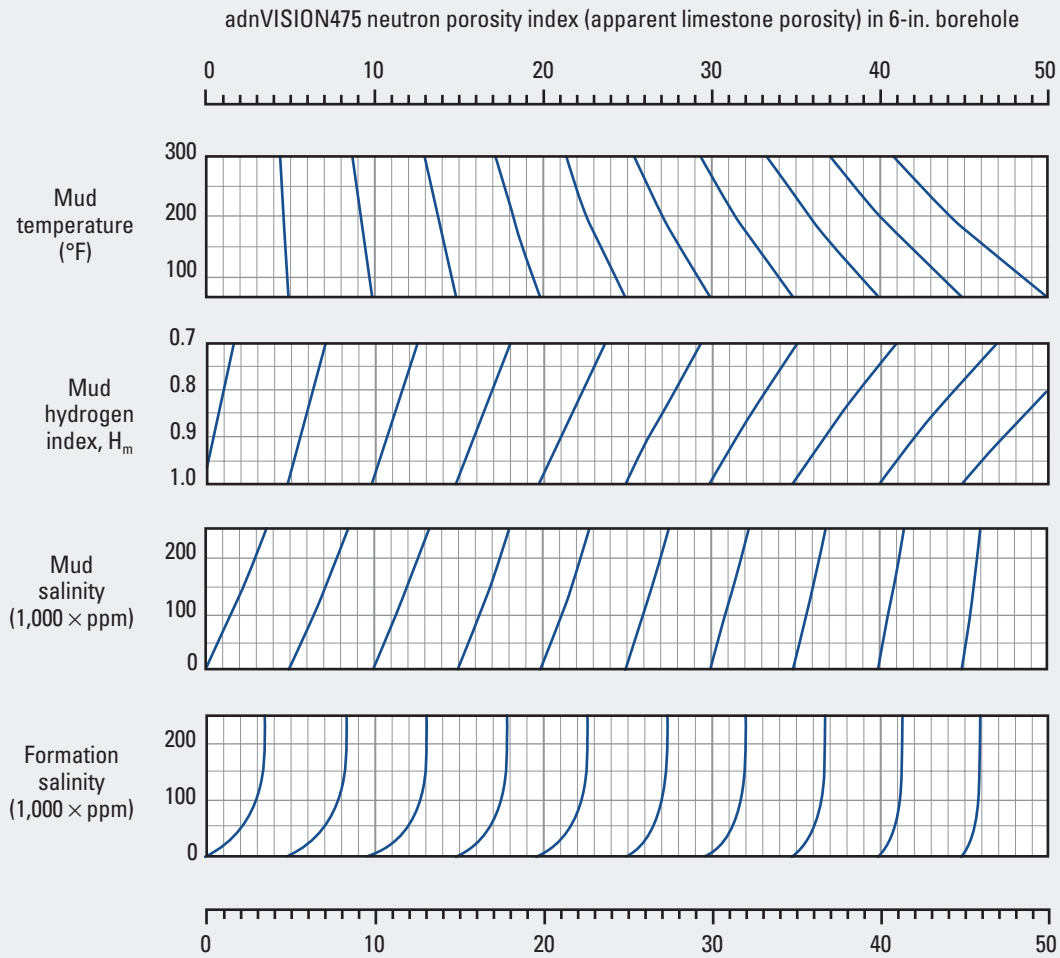


*Mark of Schlumberger
© Schlumberger

adnVISION475* BIP Neutron—4.75-in. Tool and 6-in. Borehole

Environmental Correction—Open Hole

Neu-32



*Mark of Schlumberger
© Schlumberger

Purpose

This chart is used similarly to Chart Neu-31 to correct adnVISION475 borehole-invariant porosity (BIP) measurements.

Description

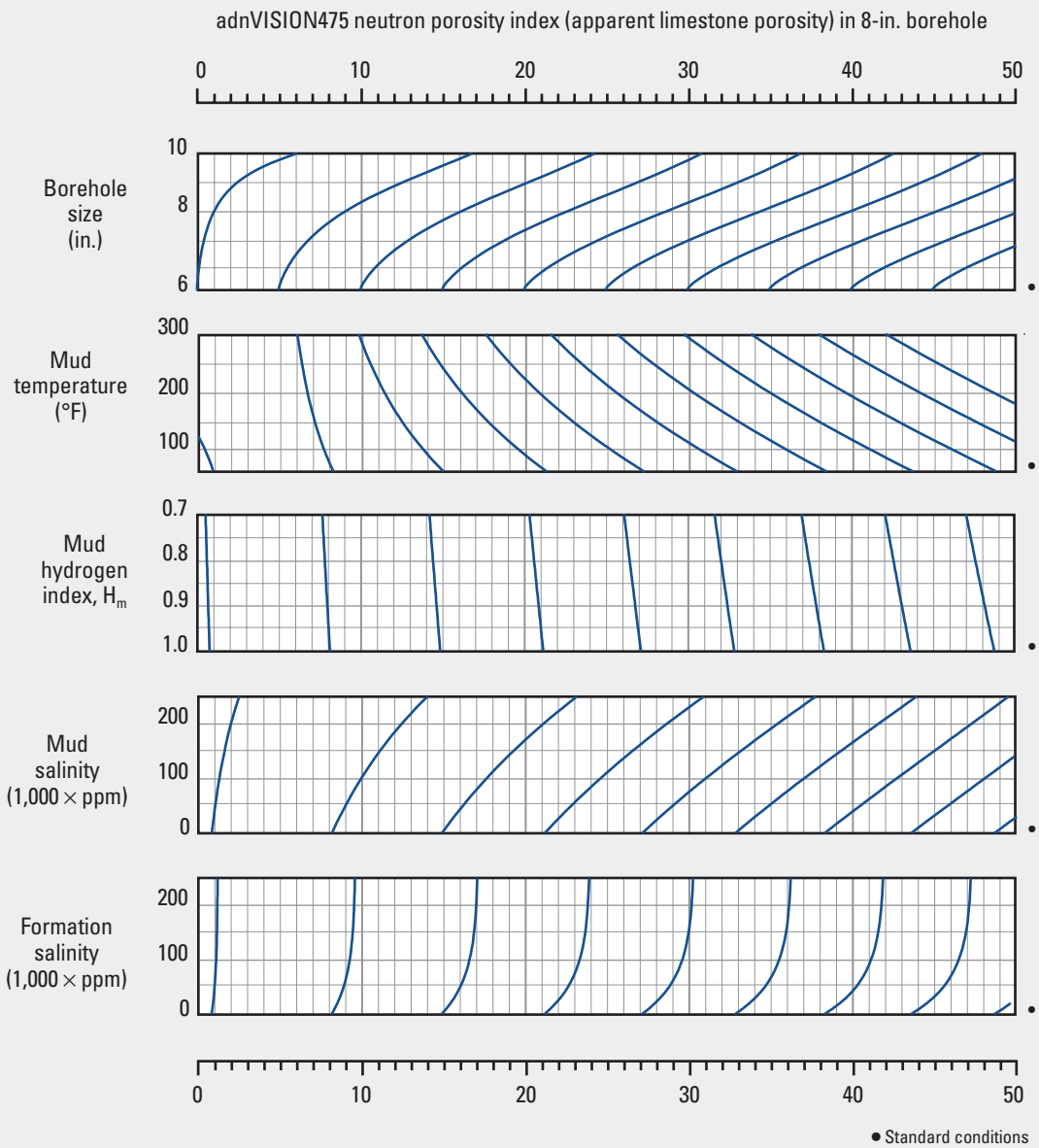
Enter the top scale with the BIP neutron porosity (BNPH) to incorporate corrections for mud temperature, mud hydrogen index, and mud and formation salinity.

Neu

adnVISION475* Azimuthal Density Neutron—4.75-in. Tool and 8-in. Borehole

Neu-33

Environmental Correction—Open Hole



*Mark of Schlumberger
© Schlumberger

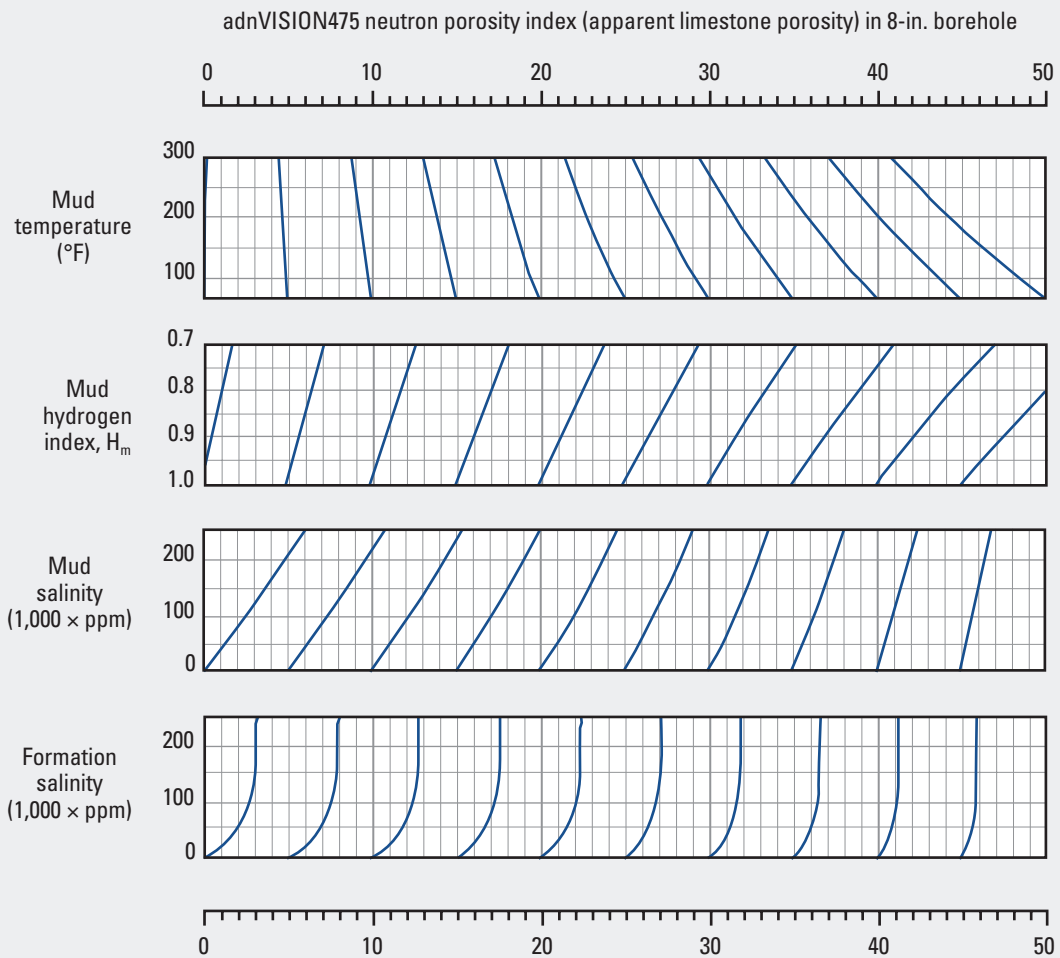
Purpose

This chart is used similarly to Chart Neu-31 to correct adnVISION475 porosity.

adnVISION475* BIP Neutron—4.75-in. Tool and 8-in. Borehole

Environmental Correction—Open Hole

Neu-34



*Mark of Schlumberger
© Schlumberger

Purpose

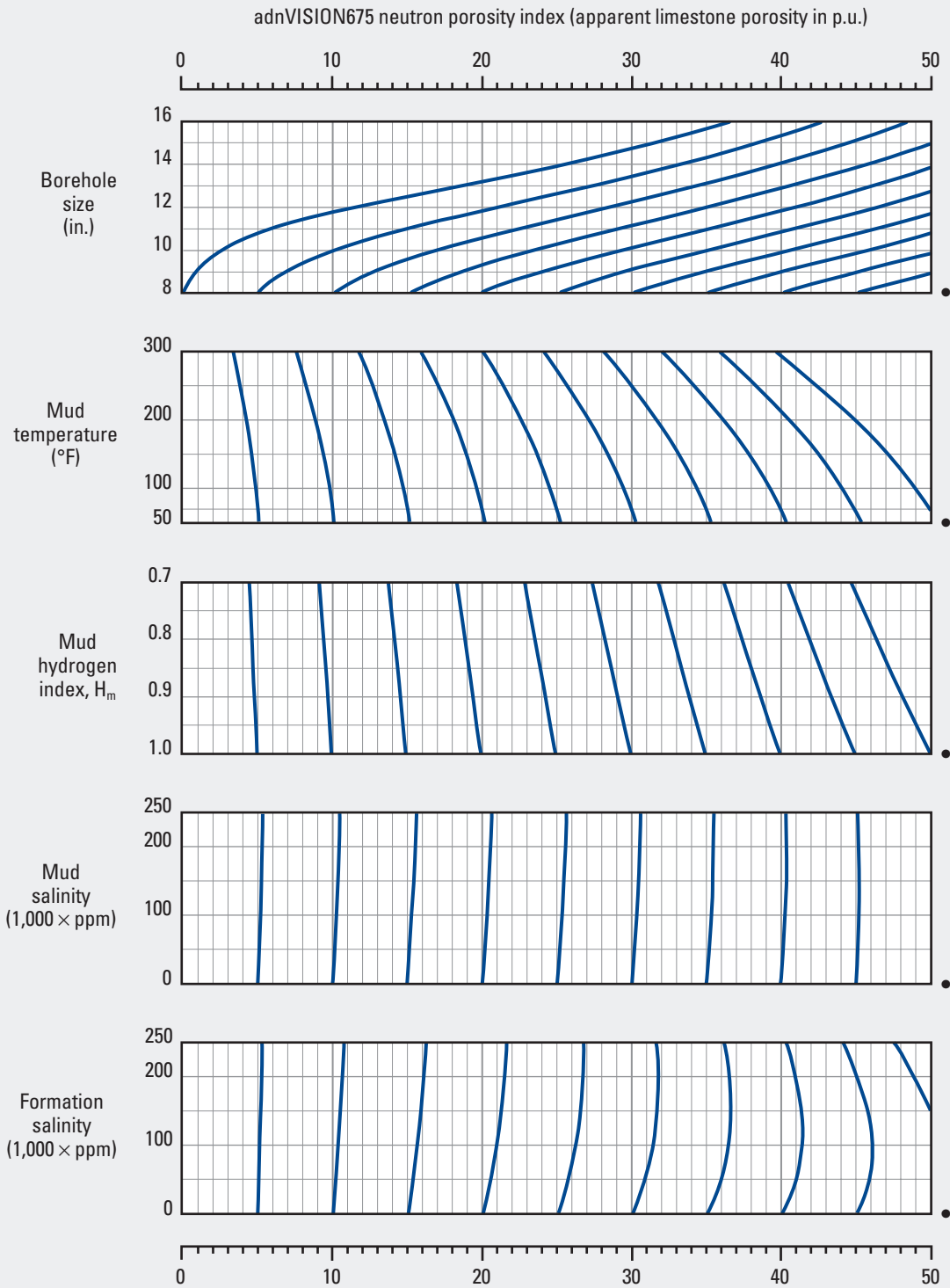
This chart is used similarly to Chart Neu-32 to correct adnVISION475 borehole-invariant porosity (BIP) measurements.

Neu

adnVISION675* Azimuthal Density Neutron—6.75-in. Tool and 8-in. Borehole

Environmental Correction—Open Hole

Neu-35
(former Por-26a)



*Mark of Schlumberger
© Schlumberger

● Standard conditions

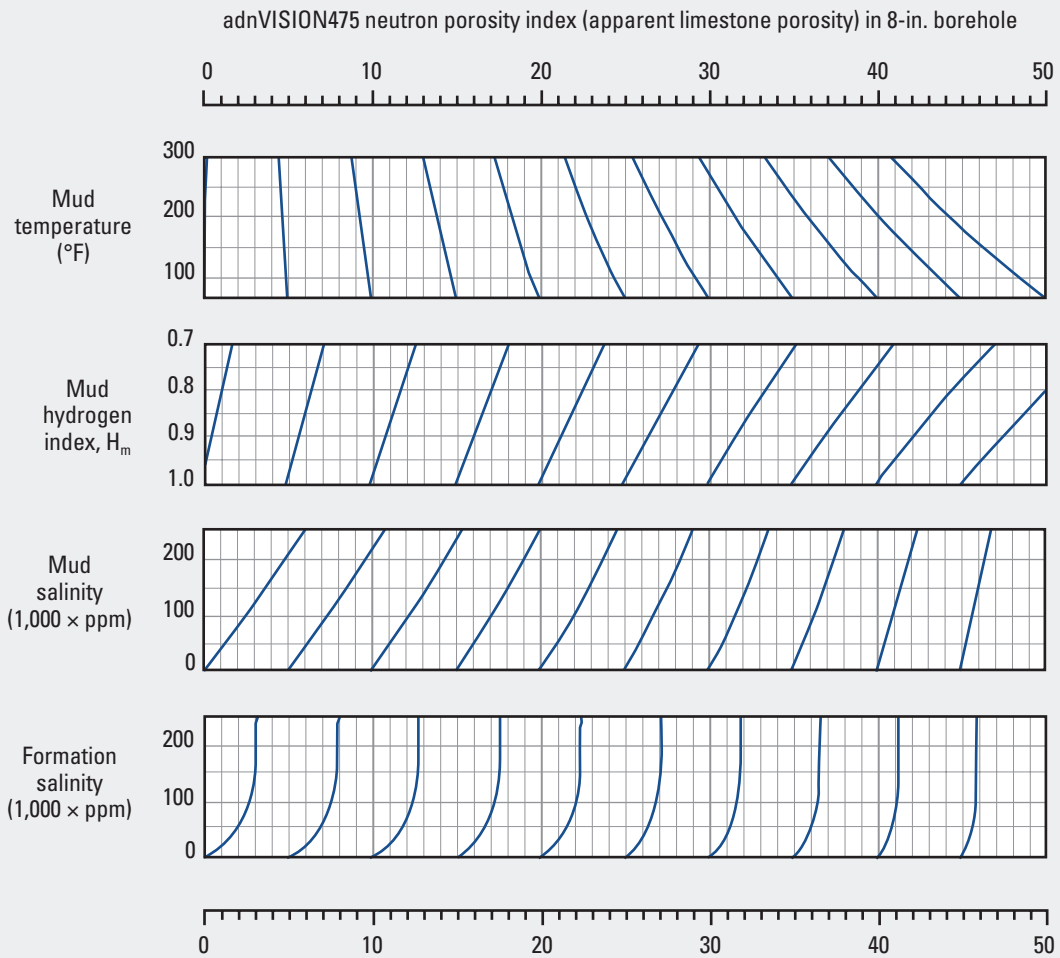
Purpose

This chart is used similarly to Chart Neu-31 to correct adnVISION675 porosity.

adnVISION675* BIP Neutron—6.75-in. Tool and 8-in. Borehole

Environmental Correction—Open Hole

Neu-34



*Mark of Schlumberger
© Schlumberger

Purpose

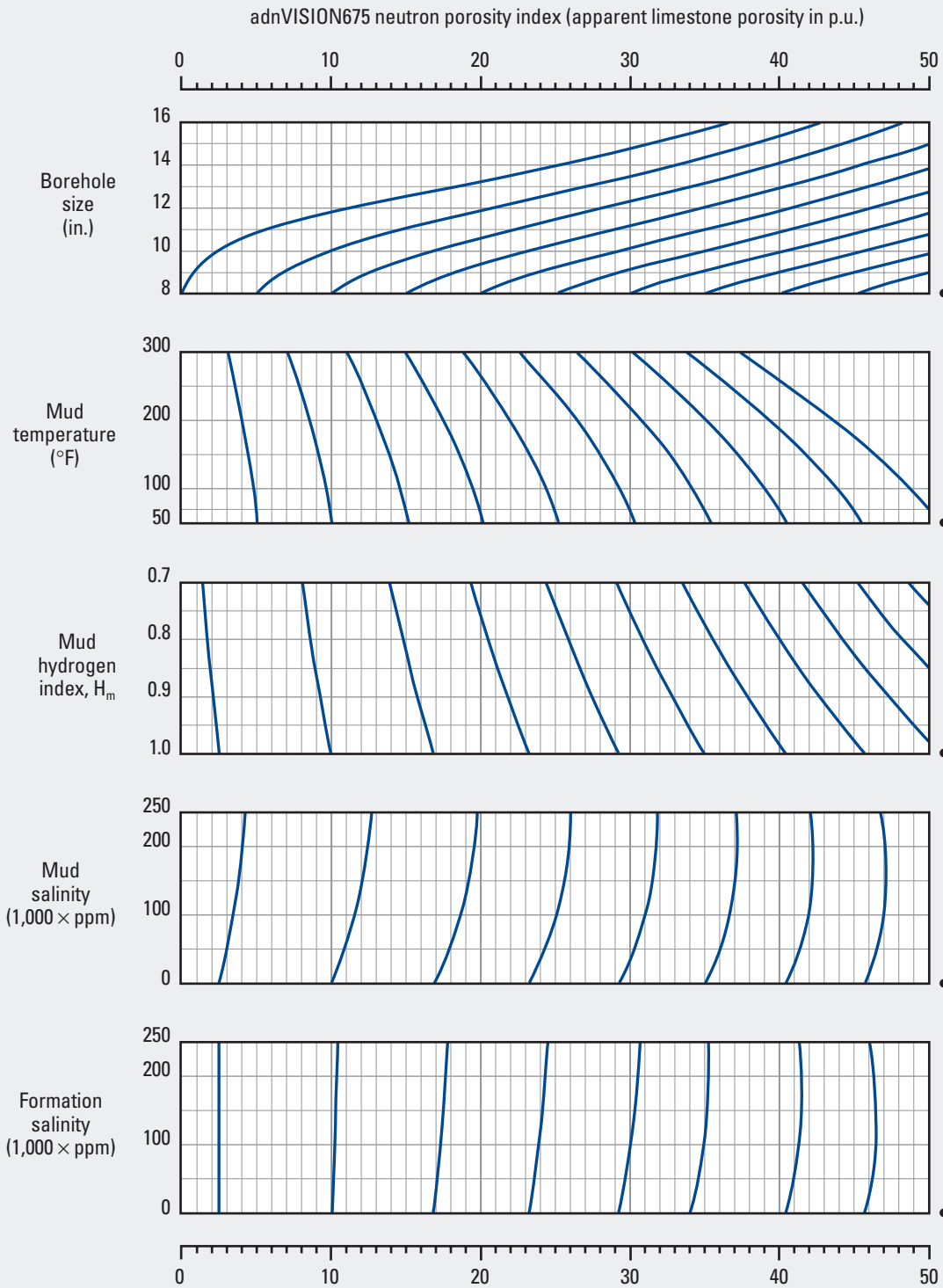
This chart is used similarly to Chart Neu-32 to correct adnVISION675 borehole-invariant porosity (BIP) measurements.

Neu

adnVISION675* Azimuthal Density Neutron—6.75-in. Tool and 10-in. Borehole

Environmental Correction—Open Hole

Neu-37
(former Por-26b)



*Mark of Schlumberger
© Schlumberger

● Standard conditions

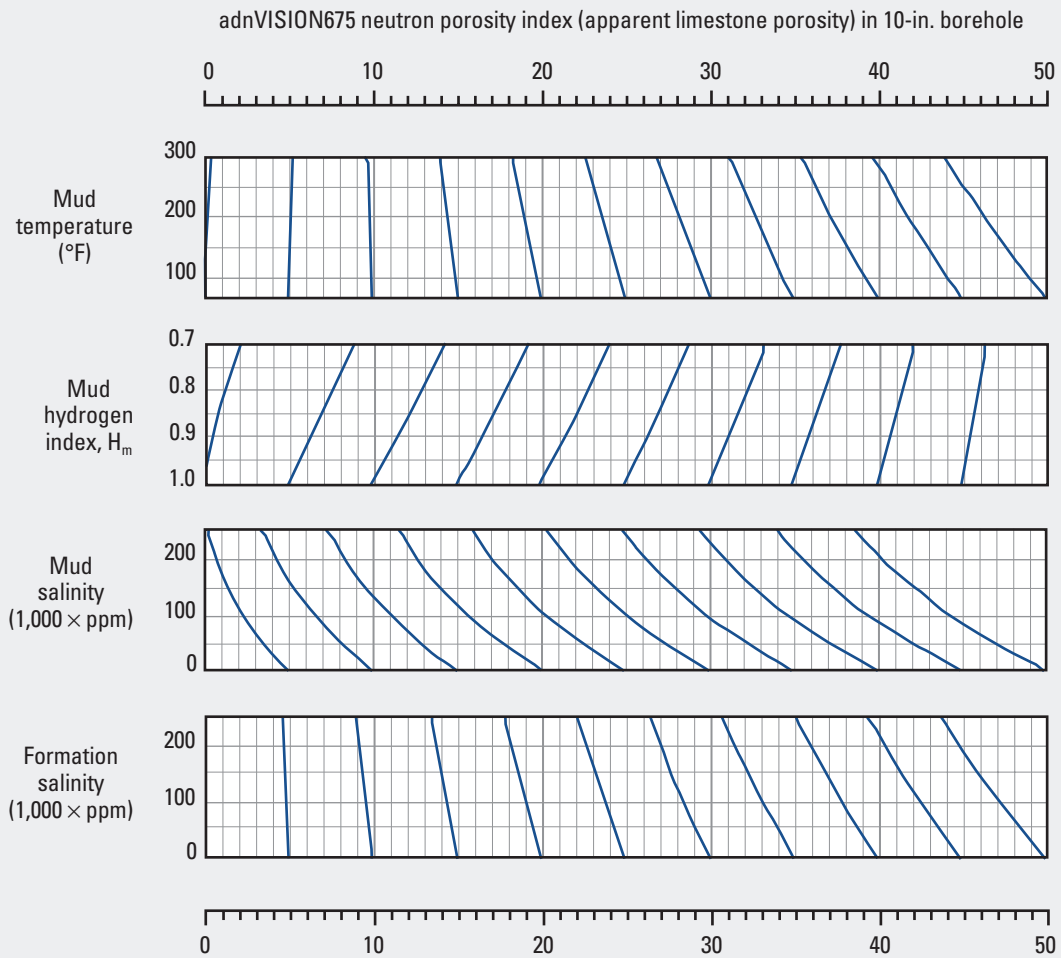
Purpose

This chart is used similarly to Chart Neu-31 to correct adnVISION675 porosity.

adnVISION675* BIP Neutron—6.75-in. Tool and 10-in. Borehole

Environmental Correction—Open Hole

Neu-38



*Mark of Schlumberger
© Schlumberger

Purpose

This chart is used similarly to Chart Neu-32 to correct adnVISION675 borehole-invariant porosity (BIP) measurements.

Neu

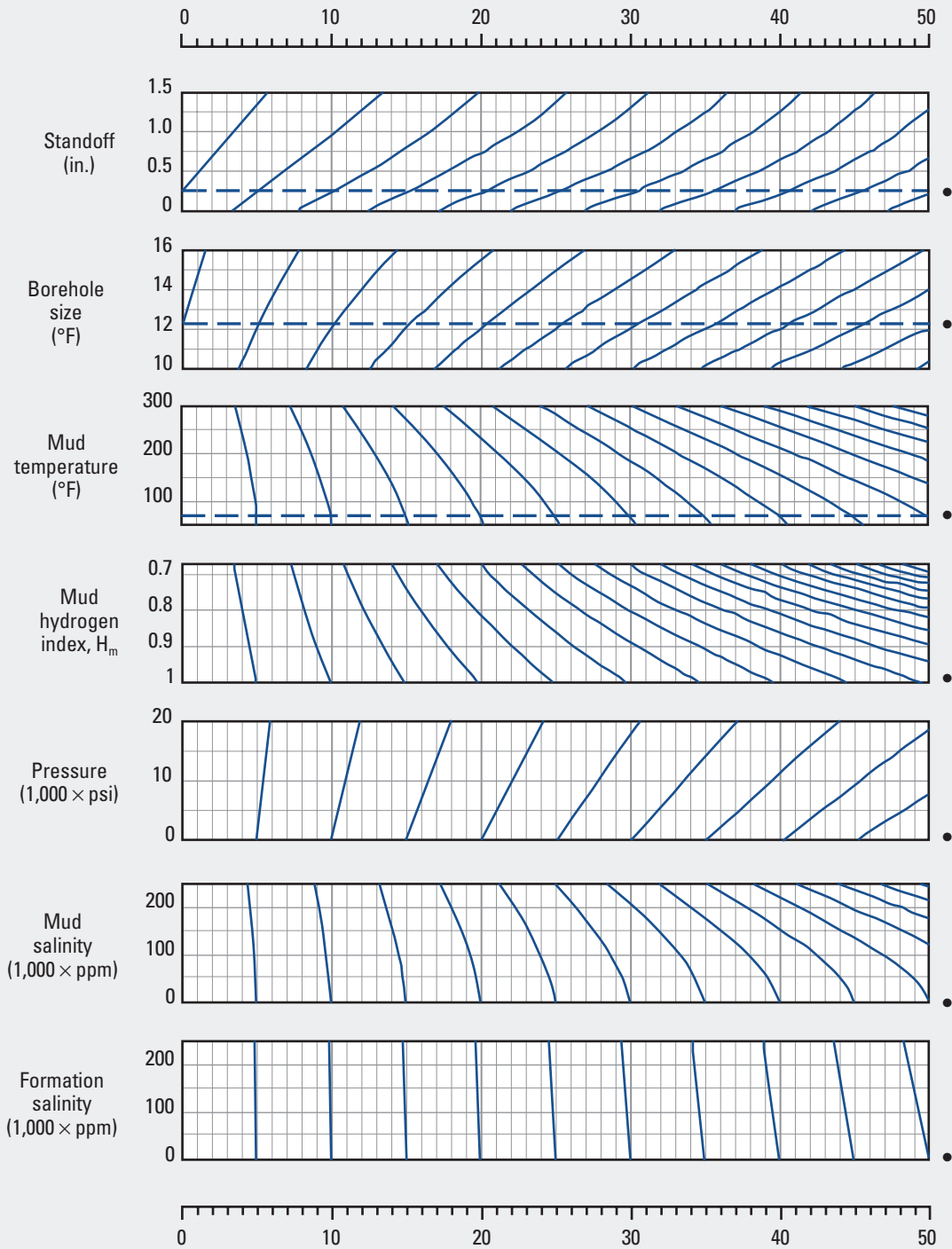
adnVISION825* Azimuthal Density Neutron—8.25-in. Tool and 12.25-in. Borehole

Neu-39

Environmental Correction—Open Hole

Standoff = 0.25 in.

adnVISION825 neutron porosity index (apparent limestone porosity) in 12.25-in. borehole



*Mark of Schlumberger
© Schlumberger

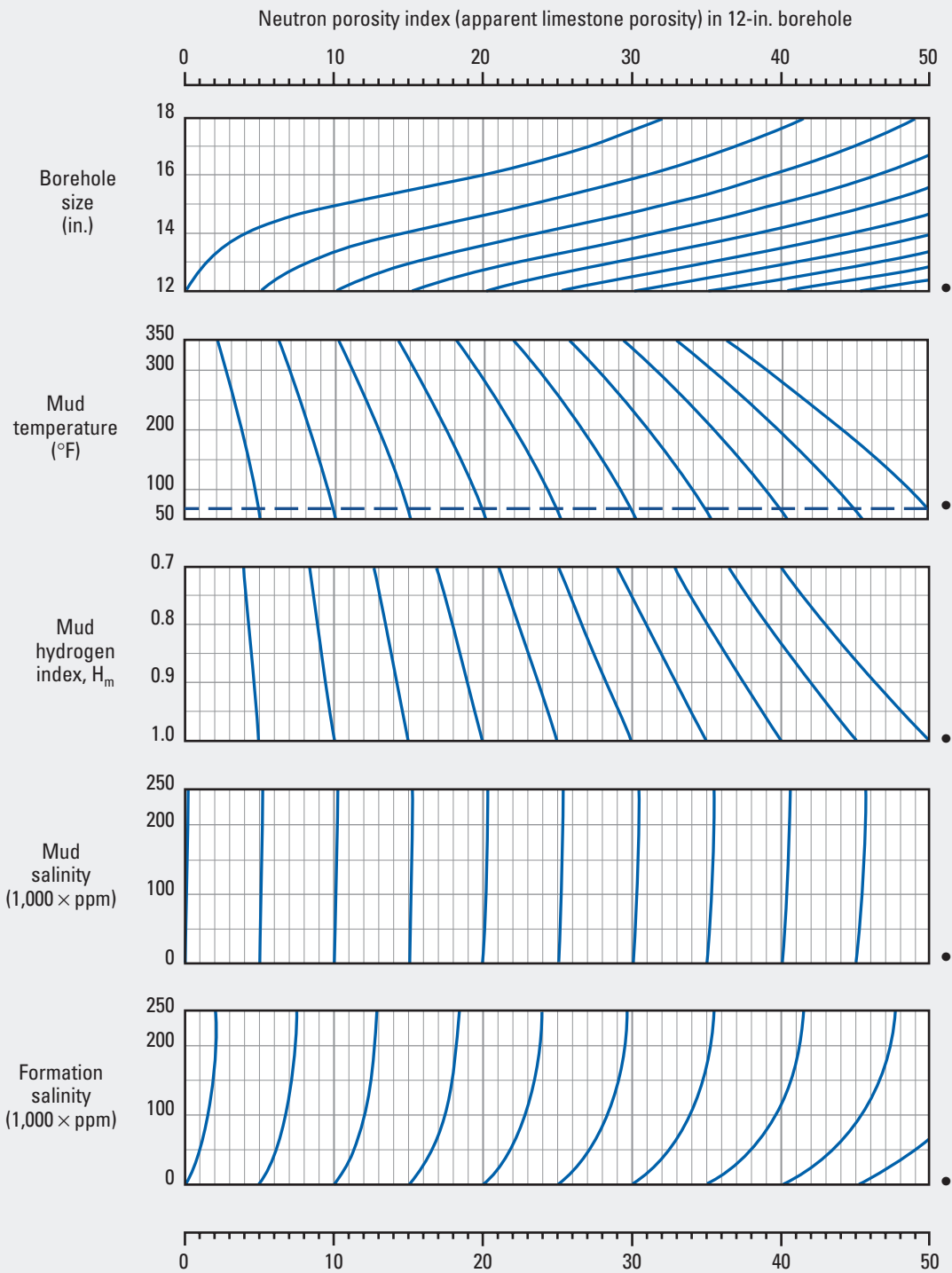
● Standard conditions

Purpose

This chart is used similarly to Chart Neu-31 to correct adnVISION825 porosity.

CDN* Compensated Density Neutron and adnVISION825s*
Azimuthal Density Neutron—8-in. Tool and 12-in. Borehole
Environmental Correction—Open Hole

Neu-40
(former Por-24c)



*Mark of Schlumberger
© Schlumberger

• Standard conditions

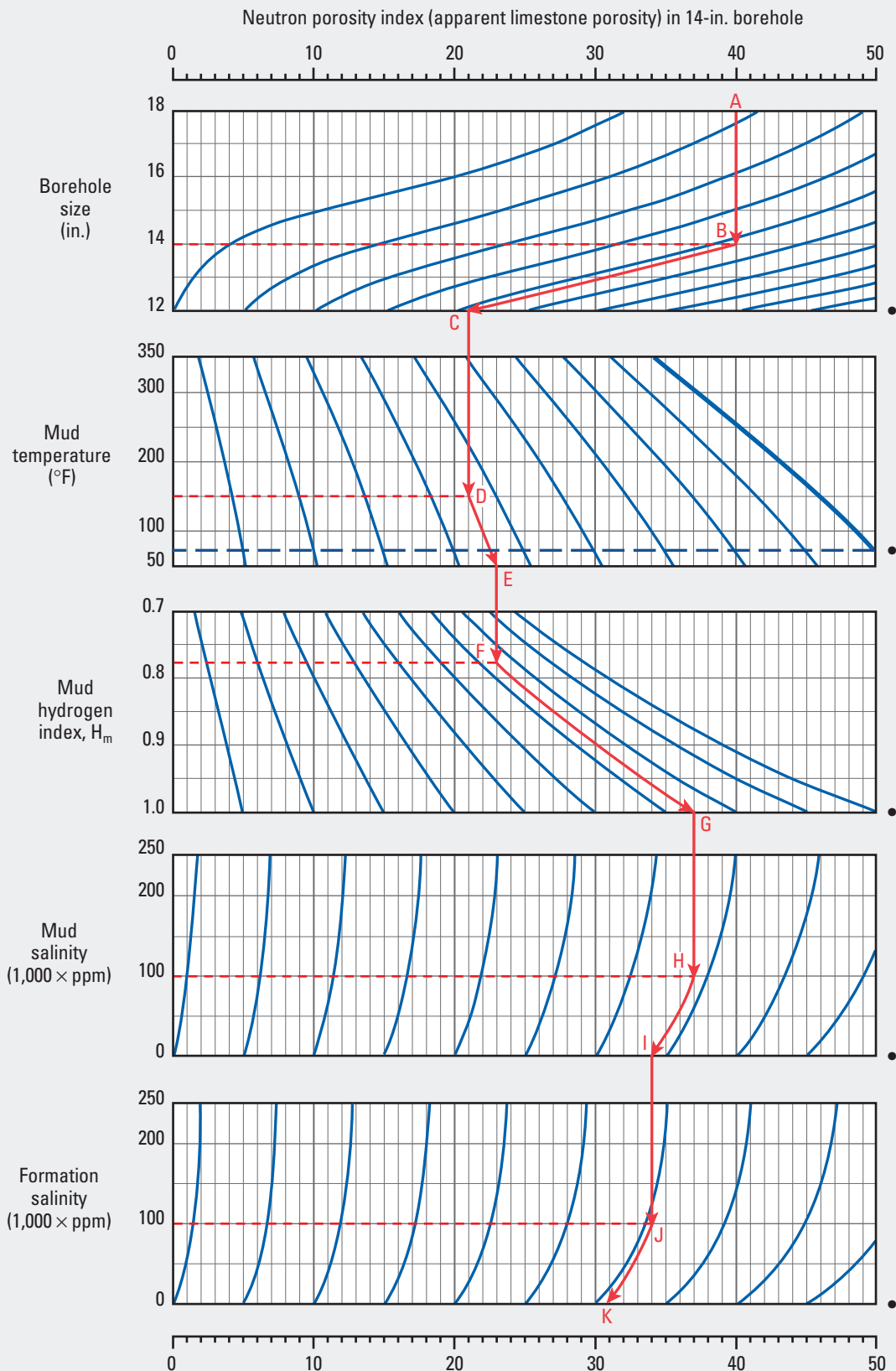
Purpose

This chart is used similarly to Chart Neu-31 to correct CDN Compensated Density Neutron tool and adnVISION825s Azimuthal Density Neutron porosity.

CDN* Compensated Density Neutron and adnVISION825s*
Azimuthal Density Neutron—8-in. Tool and 14-in. Borehole

Neu-41
(former Por-24d)

Environmental Correction—Open Hole

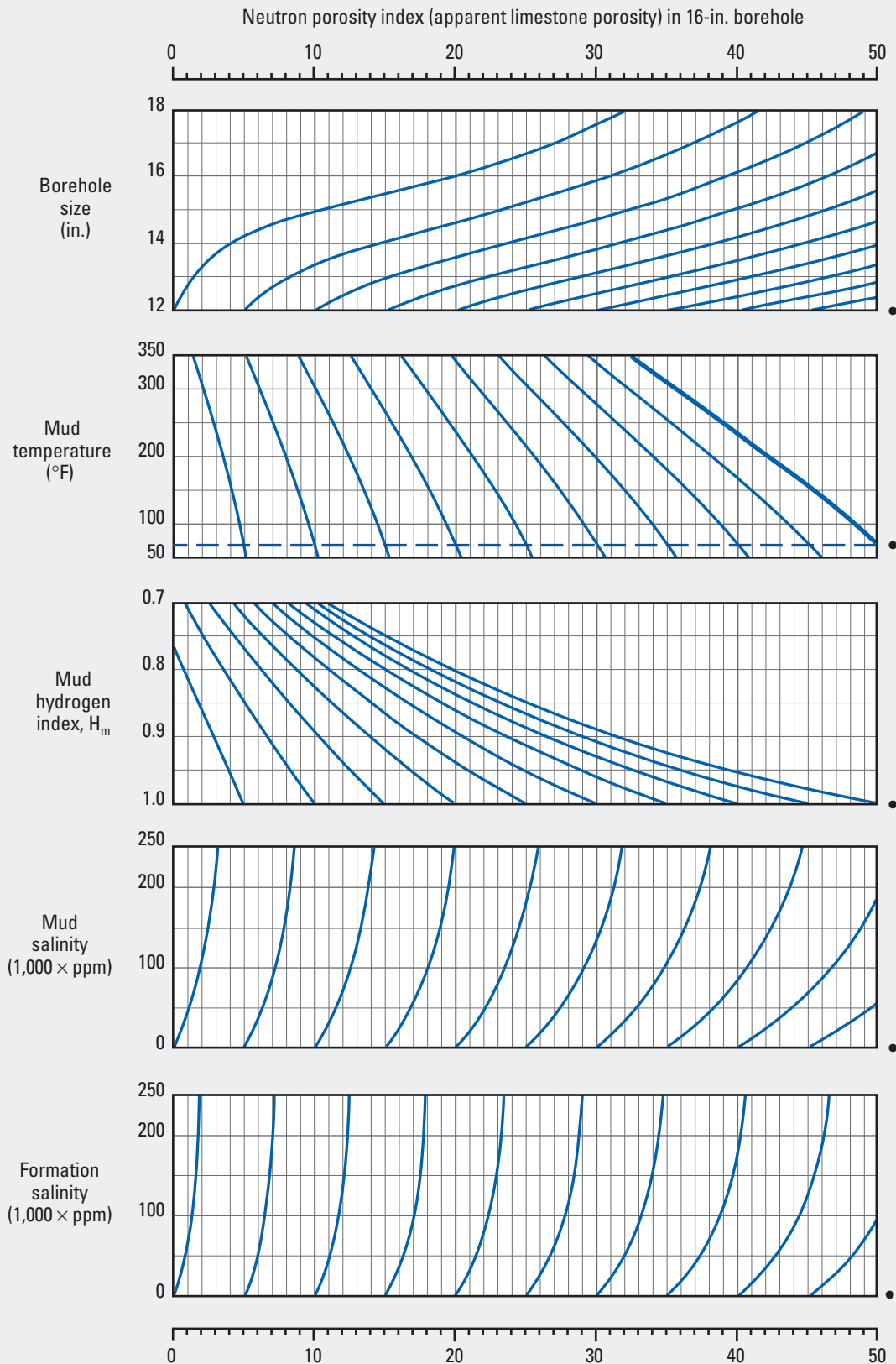


*Mark of Schlumberger
© Schlumberger

• Standard conditions

CDN* Compensated Density Neutron and adnVISION825s*
Azimuthal Density Neutron—8-in. Tool and 16-in. Borehole
Environmental Correction—Open Hole

Neu-42
(former Por-24e)



*Mark of Schlumberger
© Schlumberger

• Standard conditions

EcoScope* Integrated LWD Neutron Porosity—6.75-in. Tool

Environmental Correction—Open Hole

Purpose

Charts Neu-43 through Neu-46 show the environmental corrections that are applied to EcoScope 6.75-in. Integrated LWD Tool neutron porosity measurements. These charts can be used to estimate the correction that is normally already applied to the field logs.

Description

The charts incorporate the parameters of borehole size, mud temperature, mud hydrogen index (from Chart Neu-30), mud salinity, and formation salinity for the correction of EcoScope 6.75-in. neutron porosity.

Select the appropriate chart based on both the hole size and the measurement type: thermal neutron porosity (TNPH) or best thermal neutron porosity (BPHI).

Enter the charts with the uncorrected neutron porosity data.

Charts Neu-43 and Neu-44 are for use with BPHI_UNC, and Charts Neu-45 and Neu-46 are for use with TNPH_UNC. Because the borehole size correction is applied to the field logs, including the _UNC channels, do not include the borehole size correction, which is in the charts for illustrative purposes only.

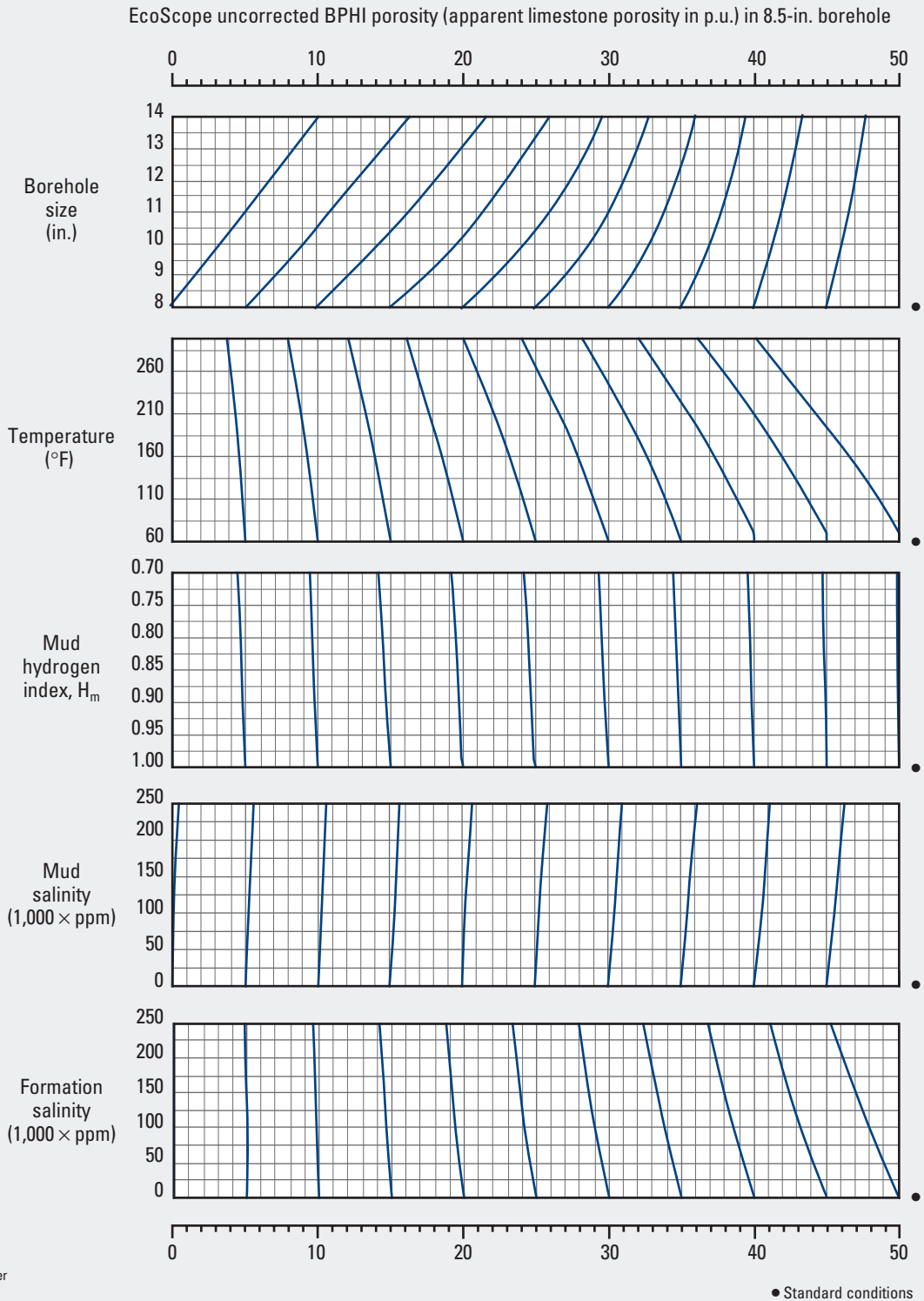
A correction for eccentricity effects is normally also applied to the field BPHI measurement. Because this correction is not included in these charts, there may be a small difference between the correction estimated from the charts and that actually applied to the field data, depending on the tool position in the borehole.

The charts are used with a similar procedure to that described for Chart Neu-31.

EcoScope* Integrated LWD BPHI Porosity—6.75-in. Tool and 8.5-in. Borehole

Environmental Correction—Open Hole

Neu-43



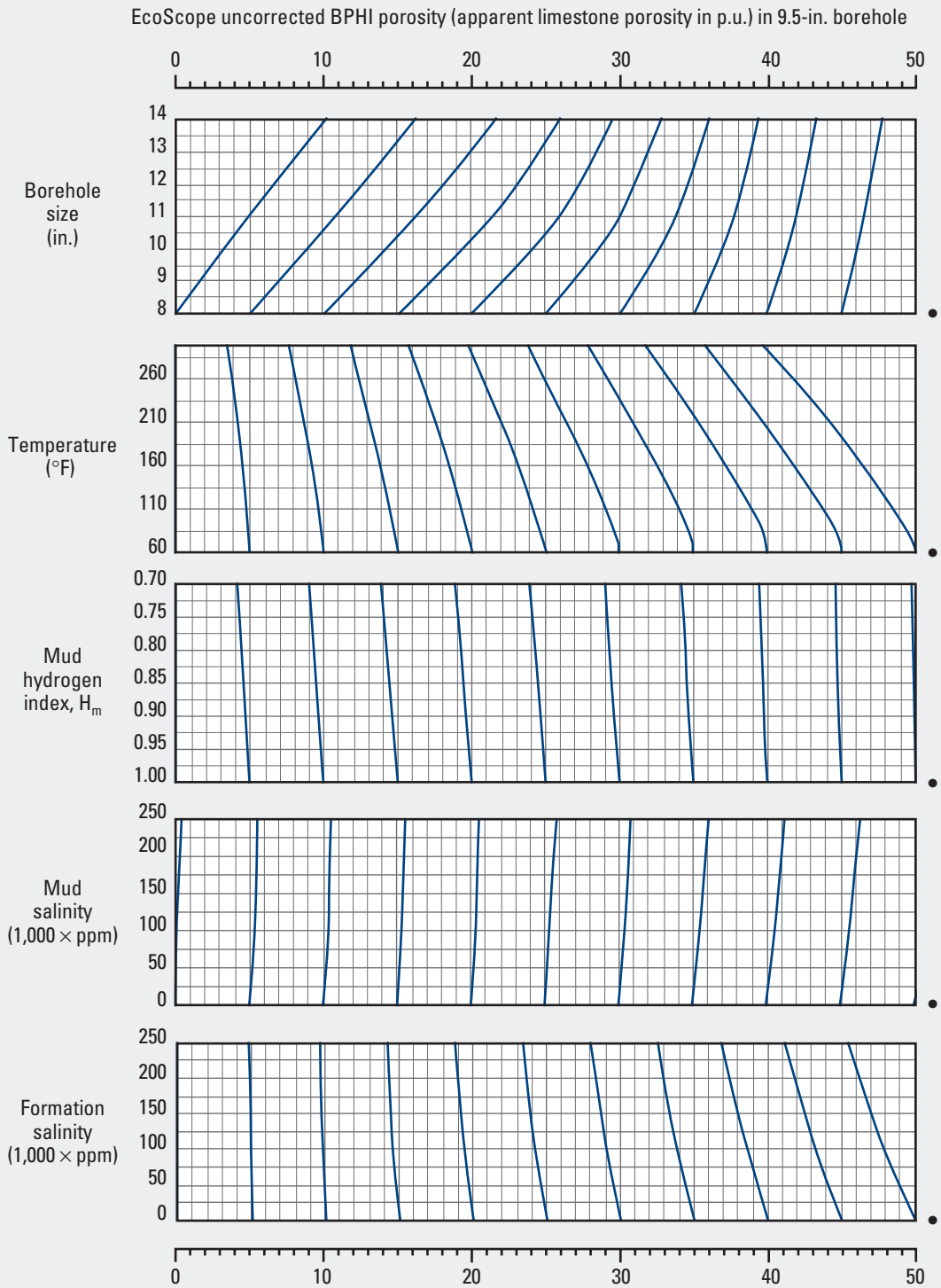
Purpose

This chart is used similarly to Chart Neu-31 to estimate the correction applied to EcoScope 6.75-in. Integrated LWD Tool best thermal neutron porosity (BPHI) measurements.

Use this chart only with EcoScope BPHI neutron porosity; use Chart Neu-45 with EcoScope thermal neutron porosity (TNPH) measurements.

EcoScope* Integrated LWD BPHI Porosity—6.75-in. Tool and 9.5-in. Borehole
 Environmental Correction—Open Hole

Neu-44



*Mark of Schlumberger
 © Schlumberger

● Standard conditions

Purpose

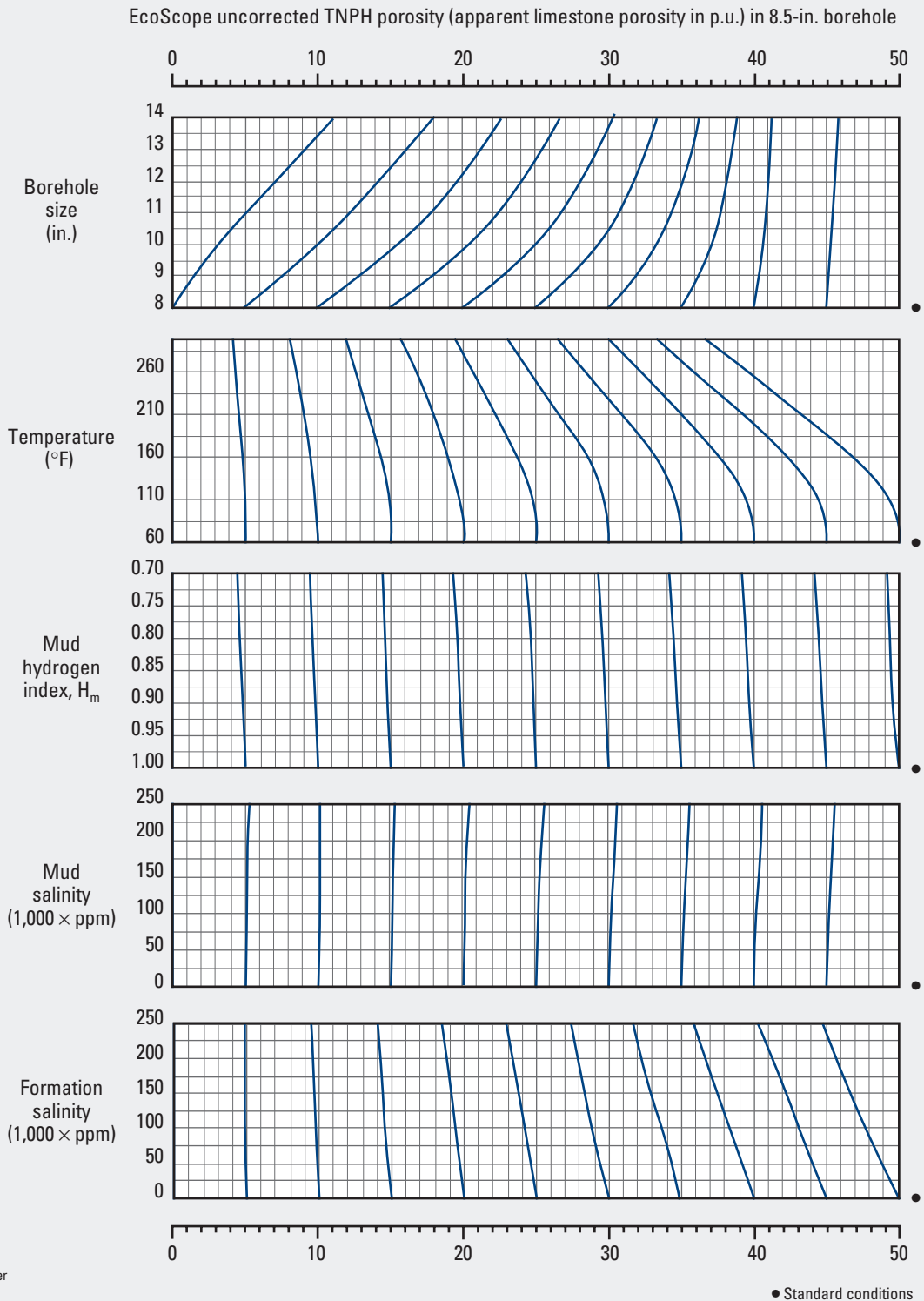
This chart is used similarly to Chart Neu-31 to estimate the correction applied to EcoScope 6.75-in. Integrated LWD Tool best thermal neutron porosity (BPHI) measurements.

Use this chart only with EcoScope BPHI neutron porosity; use Chart Neu-46 with EcoScope thermal neutron porosity (TNPH) measurements.

EcoScope* Integrated LWD TNPH Porosity—6.75-in. Tool and 8.5-in. Borehole

Environmental Correction—Open Hole

Neu-45



Purpose

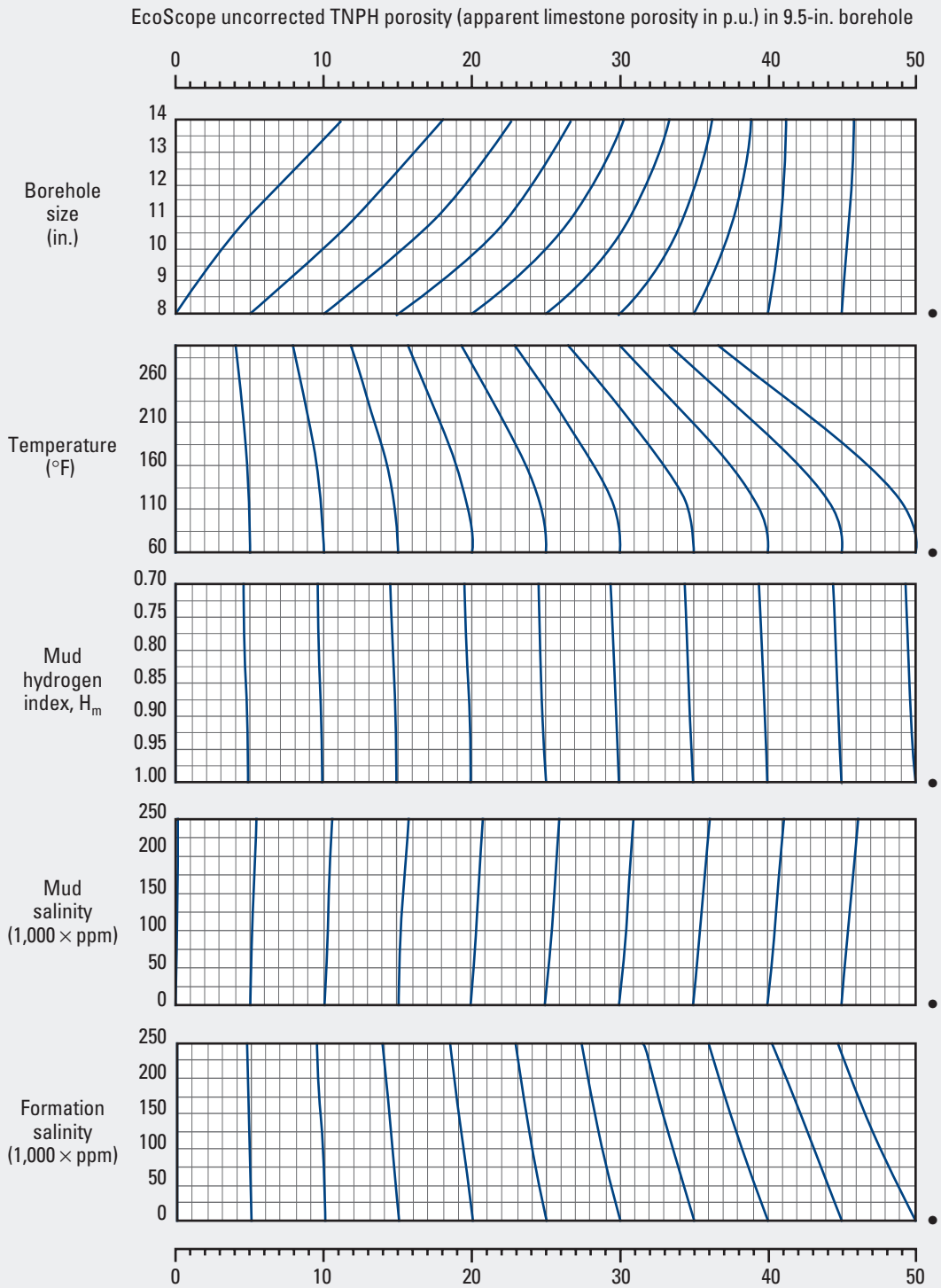
This chart is used similarly to Chart Neu-31 to estimate the correction applied to EcoScope 6.75-in. Integrated LWD Tool thermal neutron porosity (TNPH) measurements.

Use this chart only with EcoScope TNPH measurements. Use Chart Neu-43 with EcoScope best thermal neutron porosity (BPHI) measurements.

EcoScope* Integrated LWD TNPH Porosity—6.75-in. Tool and 9.5-in. Borehole

Environmental Correction—Open Hole

Neu-46



*Mark of Schlumberger
© Schlumberger

● Standard conditions

Purpose

This chart is used similarly to Chart Neu-31 to estimate the correction applied to EcoScope 6.75-in. Integrated LWD Tool thermal neutron porosity (TNPH) measurements.

Use this chart only with EcoScope TNPH neutron porosity; use Chart Neu-44 with EcoScope best thermal neutron porosity (BPHI) measurements.

EcoScope* Integrated LWD—6.75-in. Tool

Formation Sigma Environmental Correction—Open Hole

Purpose

This chart is used to environmentally correct the raw sigma (RFSA) measurement for porosity, borehole size, and mud salinity. The fully corrected sigma (SIFA) measurement is normally presented on the logs.

Description

Chart Neu-47 includes (from top to bottom) the moments sigma transform, diffusion correction based on porosity, and borehole correction.

Example

Given: Raw sigma (24 c.u.), porosity (30 p.u.), borehole size (10 in.), and mud salinity (200,000 ppm).

Find: Corrected sigma (SIFA).

Answer: Enter the chart from the scale at the top with the raw sigma value of 24 c.u.

Moments Sigma Transform

Move parallel to the closest trend line to intersect the x-axis of the moments sigma transform chart. The difference between the x-axis value and the raw sigma value is the moments sigma transform correction ($19.8 - 24 = -4.2$ c.u.).

EcoScope Sigma Correction Example

		Correction
Raw sigma	24 c.u.	
Porosity	30 p.u.	
Borehole size	10 in.	
Mud salinity	200,000 ppm	
Moments sigma transform		-4.2 c.u.
Porosity correction		+1.3 c.u.
Borehole correction		-1.2 c.u.
Net correction		-4.1 c.u.
Environmentally corrected sigma		19.9 c.u.

Diffusion Correction

Move down vertically from the scale at the top to intersect the 30-p.u. line on the porosity chart. At the intersection point, move parallel to the closest trend line to intersect the x-axis of the porosity chart.

The difference between the x-axis value and the raw sigma value is the diffusion correction ($25.3 - 24 = +1.3$ c.u.).

Borehole Correction

Move down vertically from the scale at the top to intersect the 10-in. borehole size line. At the intersection point, move parallel to the closest trend line corresponding to the mud salinity to intersect the x-axis of the borehole correction chart.

The difference between the x-axis value and the raw sigma value is the borehole correction ($22.8 - 24 = -1.2$ c.u.).

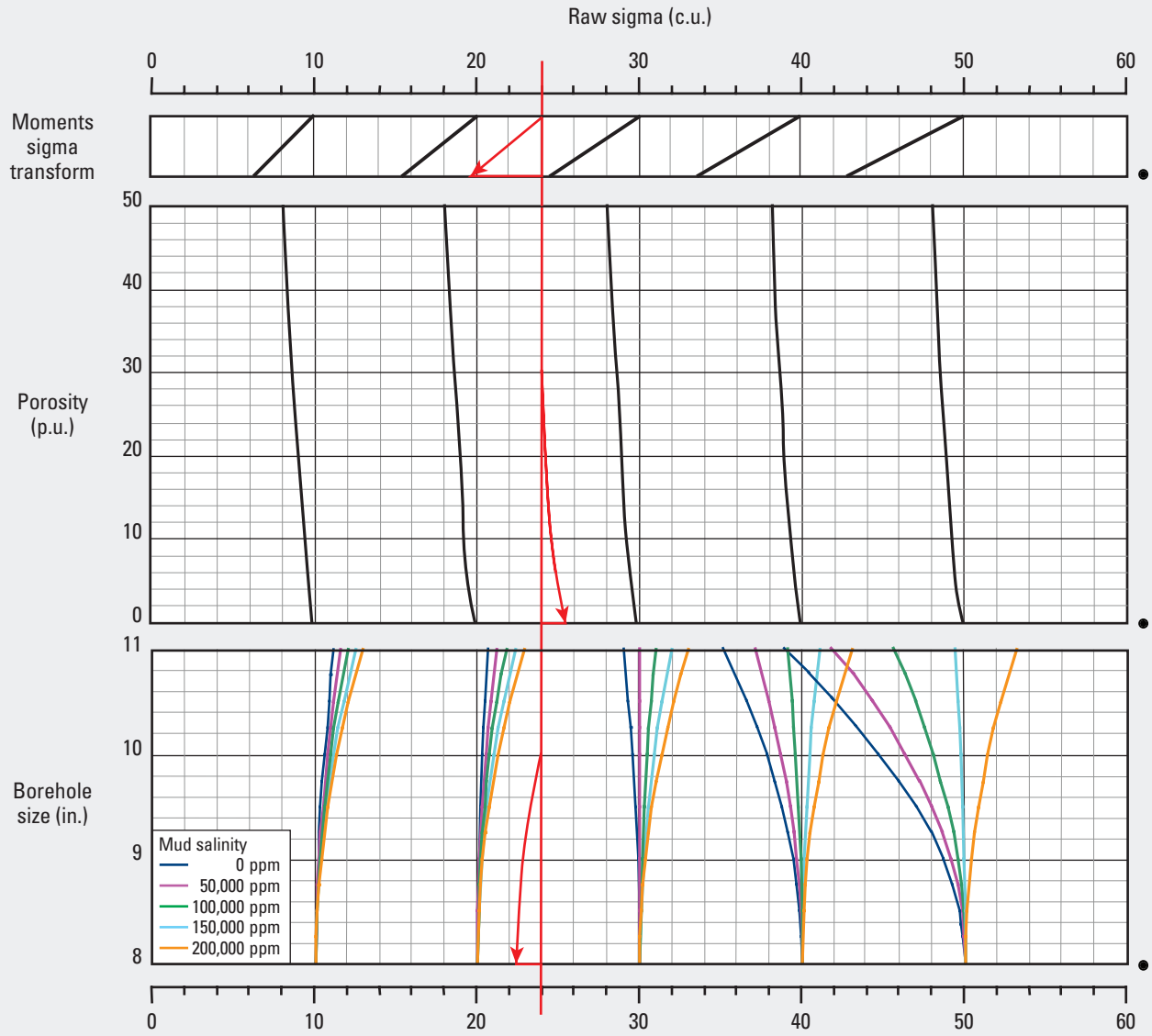
Net Correction

The net correction to apply to the raw sigma value is the sum the three corrections ($-4.2 + 1.3 + -1.2 = -4.1$ c.u.). The environmentally corrected sigma is the sum of the net correction and the raw sigma value ($24 + -4.1 = 19.9$ c.u.).

EcoScope* Integrated LWD—6.75-in. Tool

Formation Sigma Environmental Correction—Open Hole

Neu-47



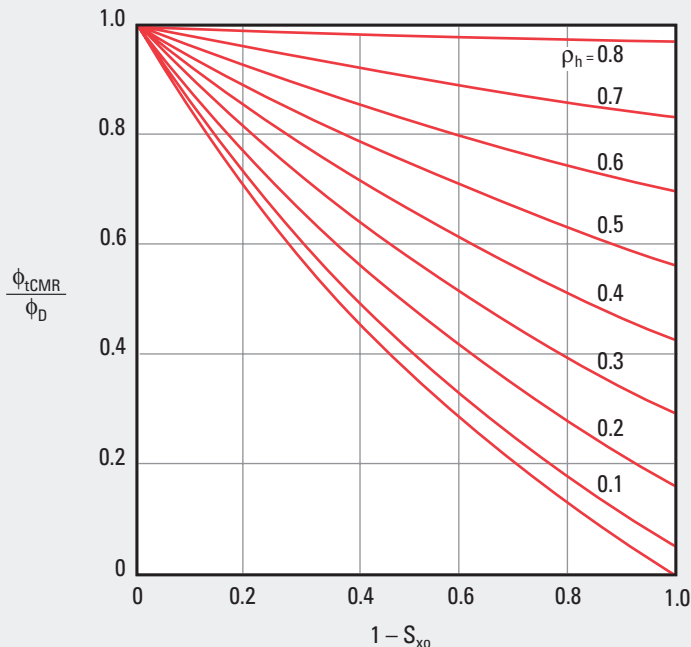
*Mark of Schlumberger
© Schlumberger

● Standard conditions

CMR* Tool

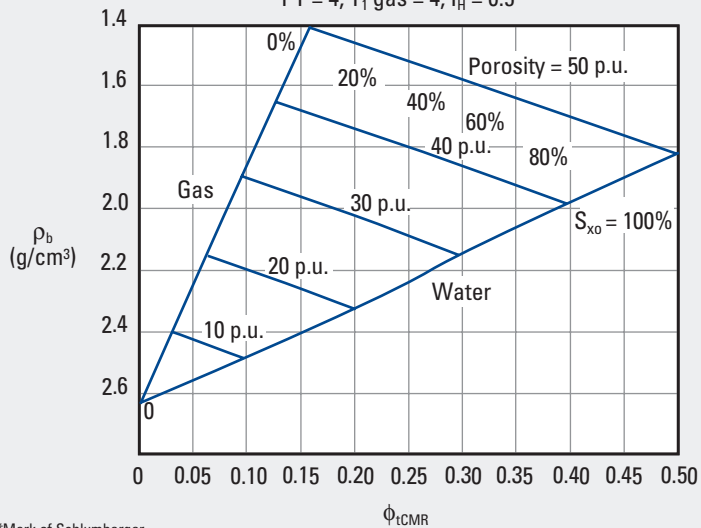
Hydrocarbon Effect on NMR/Density Porosity Ratio

CMR-1



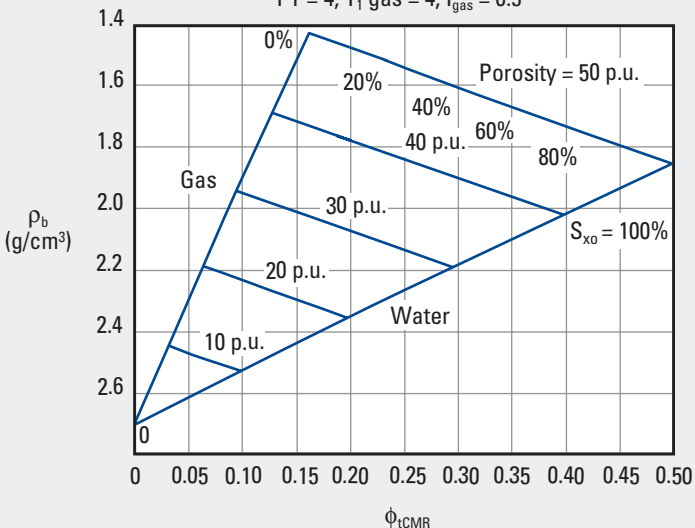
Fresh Mud and Dry Gas at 700 psi

$\rho_{ma} = 2.65, \rho_f = 1, I_f = 1, \rho_{gas} = 0.25,$
 $PT = 4, T_1 \text{ gas} = 4, I_H = 0.5$



Fresh Mud and Dry Gas at 700 psi

$\rho_{ma} = 2.71, \rho_f = 1, I_f = 1, \rho_{gas} = 0.25,$
 $PT = 4, T_1 \text{ gas} = 4, I_{gas} = 0.5$



*Mark of Schlumberger
 © Schlumberger

Purpose

This chart is used to determine the saturation of the flushed zone (S_{xo}) and hydrocarbon density (ρ_h) by using density (ρ) and CMR Combinable Magnetic Resonance data.

Description

The top chart has three components: ratio of total CMR porosity to density porosity (ϕ_{tCMR}/ϕ_D) on the y-axis, $(1 - S_{xo})$ values on the x-axis, and ρ_h defined by the radiating lines from the value of unity on the y-axis. Enter the chart with the values for $(1 - S_{xo})$ and the ϕ_{tCMR}/ϕ_D ratio. The intersection point indicates the hydrocarbon

density value. The bottom charts are used to determine the S_{xo} value in sandstone (left) and limestone (right).

Example

Given: CMR porosity = 25 p.u., $\phi_D = 30$ p.u., and $S_{xo} = 80\%$.

Find: Hydrocarbon density of the fluid in the formation.

Answer: ϕ_{tCMR}/ϕ_D ratio = $25/30 = 0.83$.

$1 - S_{xo} = 1 - 0.8 = 0.20$ or 20%.

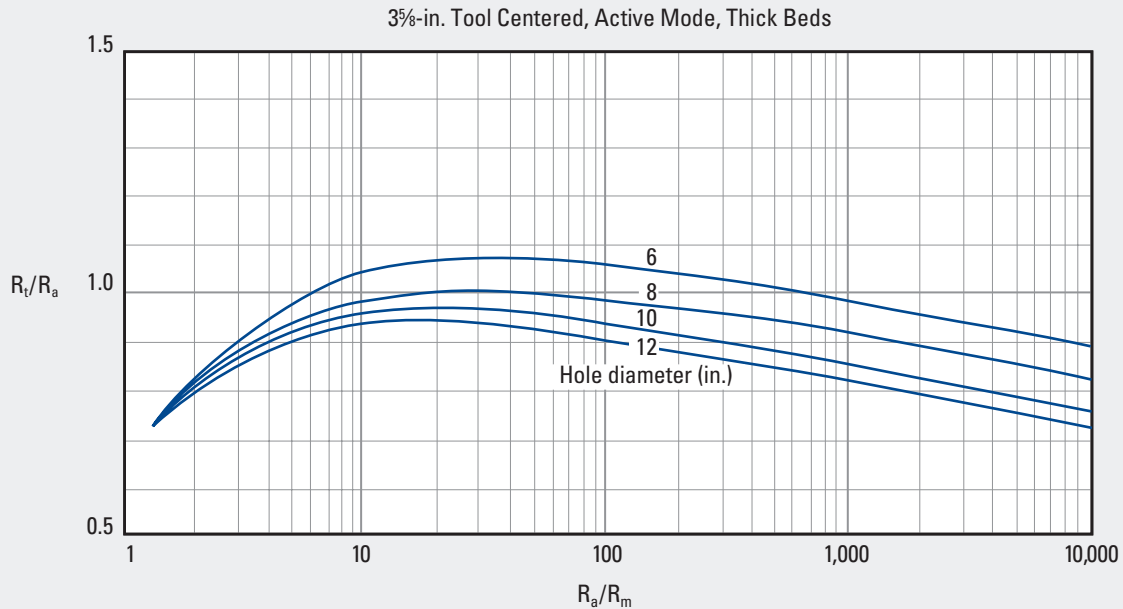
For these values, $\rho_h = 0.40$.

NMR

This page intentionally left blank.

ARI* Azimuthal Resistivity Imager

Environmental Correction—Open Hole

RLI-1
(former Rcor-14)*Mark of Schlumberger
© Schlumberger

RLI

Purpose

This chart is used to environmentally correct the ARI Azimuthal Resistivity Imager high-resolution resistivity (LL_{hr}) curve for the effect of borehole size.

Description

For a known value of resistivity of the borehole mud (R_m) at the zone of interest, a correction for the recorded log azimuthal resistivity (R_a) is determined by using this chart. The resistivity measured by the ARI tool is equal to or higher than the corrected resistivity (R_t) for borehole sizes of 8 to 12 in. However, the measured ARI resistivity is lower than R_t in 6-in. boreholes and for values of R_a/R_m between 6 and 600.

Example

Given: ARI LL_{hr} resistivity (R_a) = 20 ohm-m, mud resistivity (R_m) = 0.02 ohm-m, and borehole size at the zone of interest = 10 in.

Find: True resistivity (R_t).

Answer: Enter the chart at the x-axis with the ratio $R_a/R_m = 20/0.02 = 1,000$.

Move vertically upward to intersect the 10-in. line. Move horizontally left to read the R_t/R_a value on the y-axis of 0.86.

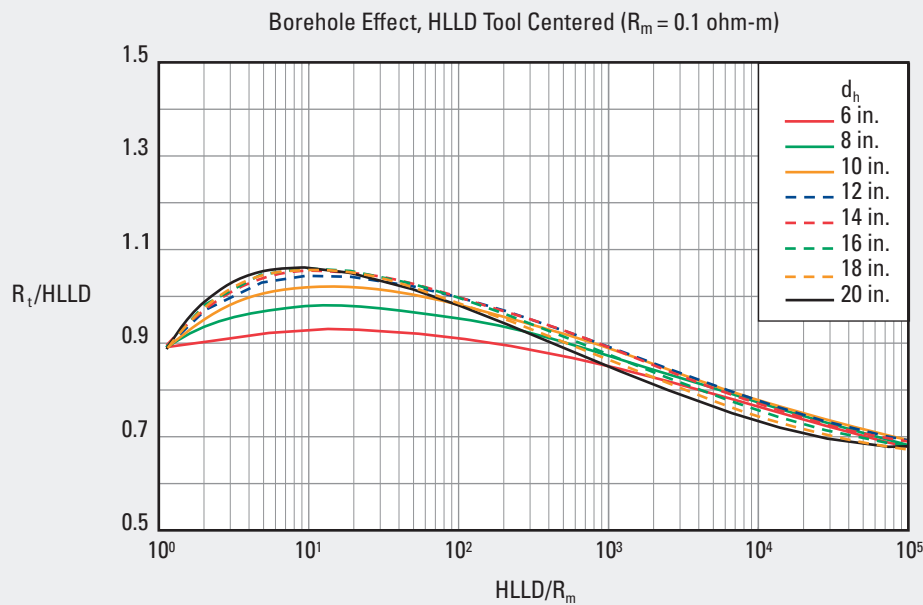
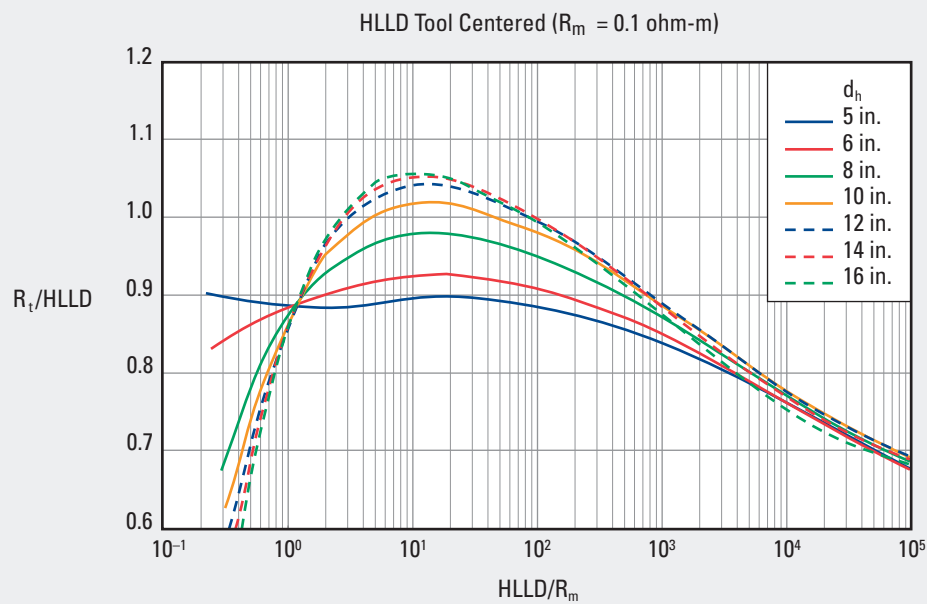
Multiply the ratio by R_a to obtain the corrected LL_{hr} resistivity:

$$R_t = 0.86 \times 20 = 17.2 \text{ ohm-m.}$$

High-Resolution Azimuthal Laterolog Sonde (HALS)

HLLD Borehole Correction—Open Hole

RLI-2



© Schlumberger

Purpose

This chart is used to correct the HALS laterolog deep resistivity (HLLD) for borehole and drilling mud effects.

Description

Enter the chart on the x-axis with the value of HLLD divided by the mud resistivity (R_m) at formation temperature. Move upward to intersect the curve representing the borehole diameter (d_h), and then move horizontally left to read the value of the ratio $R_t/HLLD$ on the y-axis. Multiply this value by the HLLD value to obtain R_t . Charts

RLI-3 through RLI-14 are similar to Chart RLI-2 for different resistivity measurements and values of tool standoff.

Example

Given: HLLD = 100 ohm-m, $R_m = 0.02$ ohm-m at formation temperature, and borehole size = 10 in.

Find: R_t .

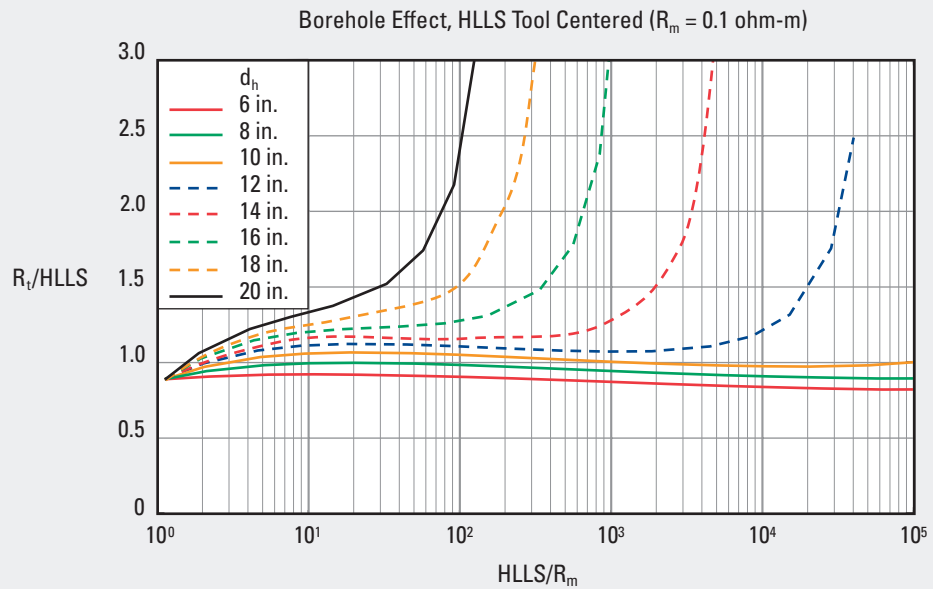
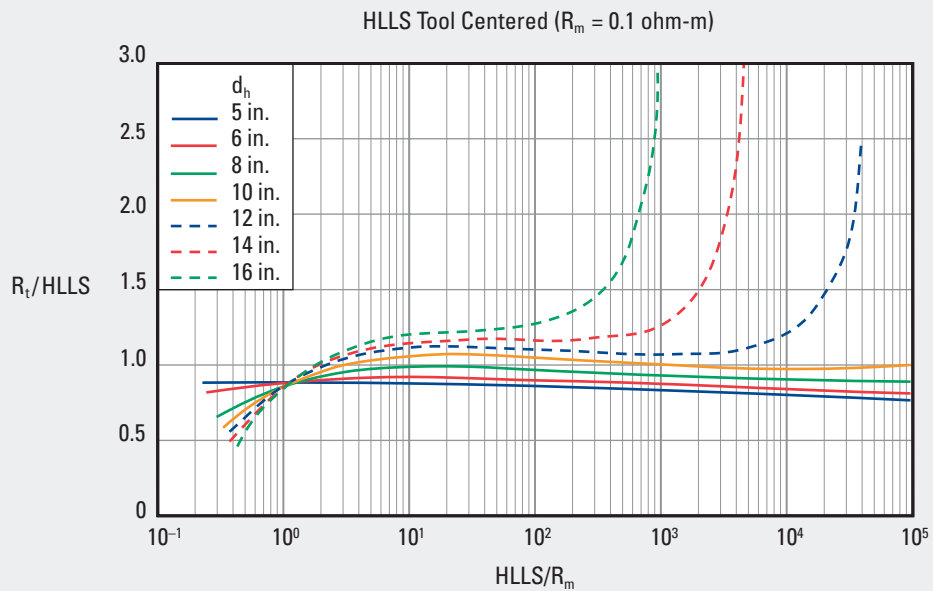
Answer: Ratio of $HLLD/R_m = 100/0.02 = 5,000$.

$R_t = 0.80 \times 100 = 80$ ohm-m.

High-Resolution Azimuthal Laterolog Sonde (HALS)

HLLS Borehole Correction—Open Hole

RLI-3



© Schlumberger

Purpose

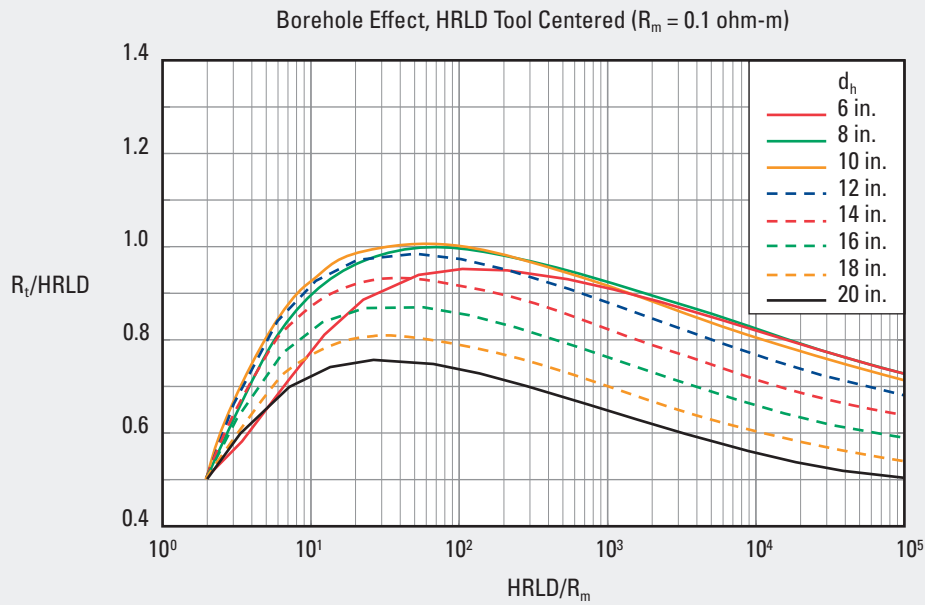
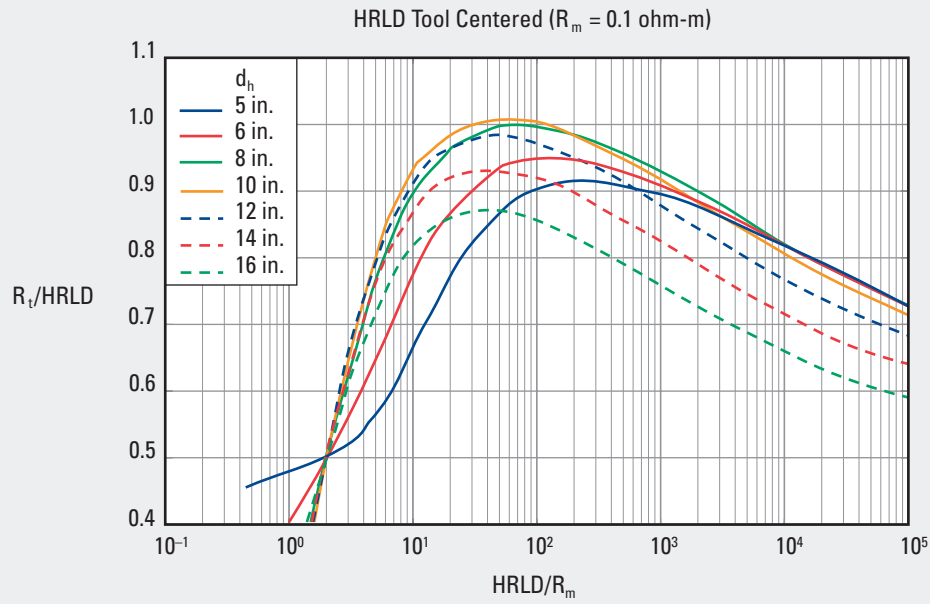
This chart is used similarly to Chart RLI-2 to correct HALS laterolog shallow resistivity (HLLS) for borehole and drilling mud effects.

RLI

High-Resolution Azimuthal Laterolog Sonde (HALS)

HRLD Borehole Correction—Open Hole

RLI-4



© Schlumberger

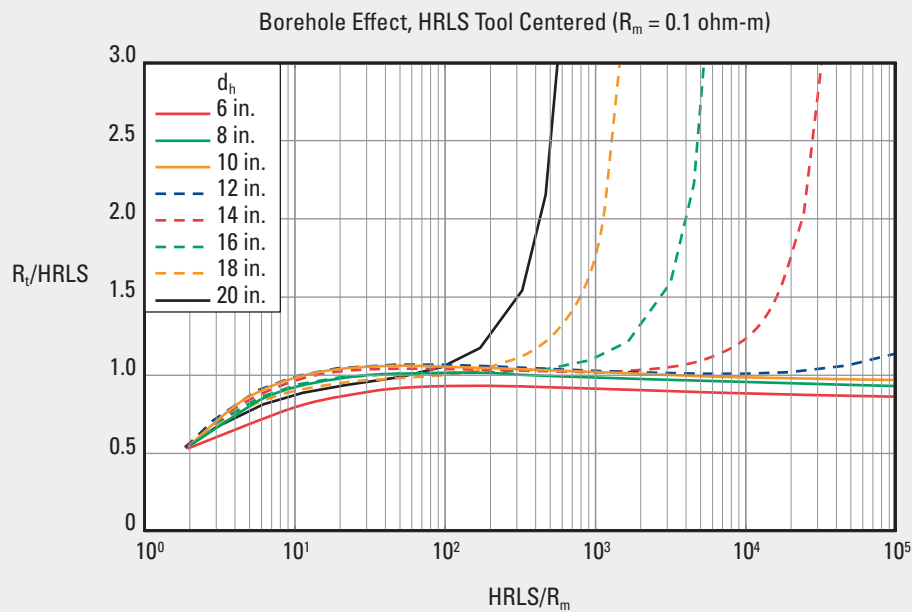
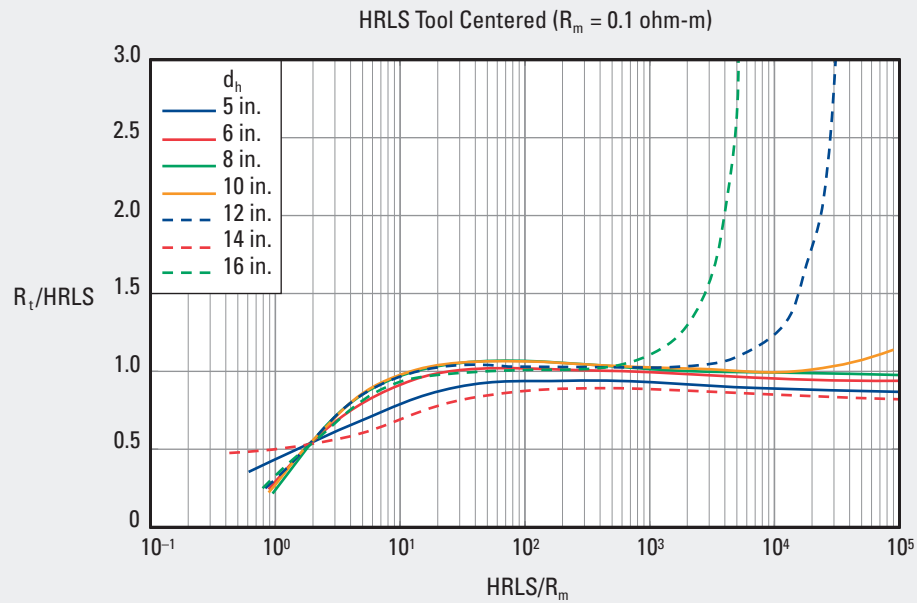
Purpose

This chart is used to similarly to Chart RLI-2 to correct the HALS high-resolution deep resistivity (HRLD) for borehole and drilling mud effects.

High-Resolution Azimuthal Laterolog Sonde (HALS)

HRLS Borehole Correction—Open Hole

RLI-5



© Schlumberger

Purpose

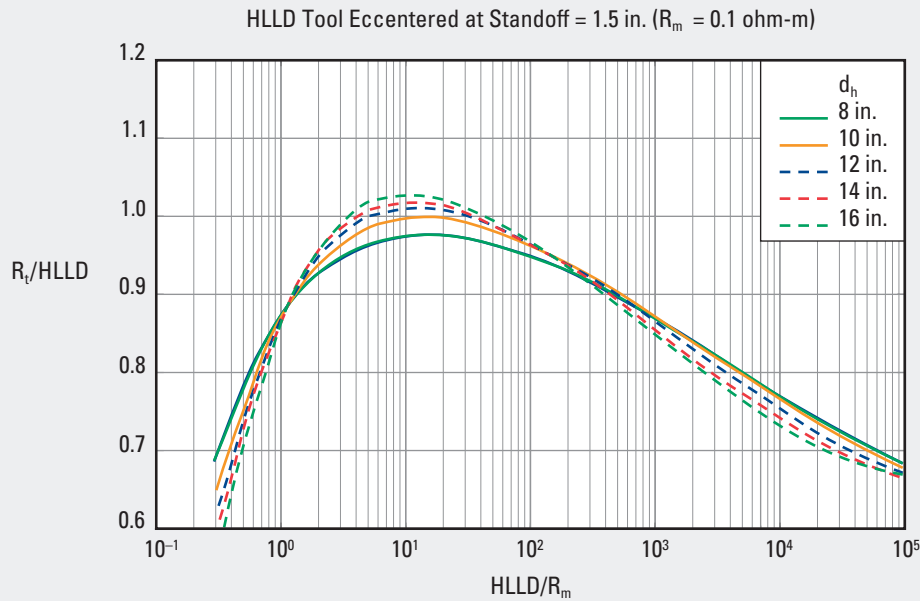
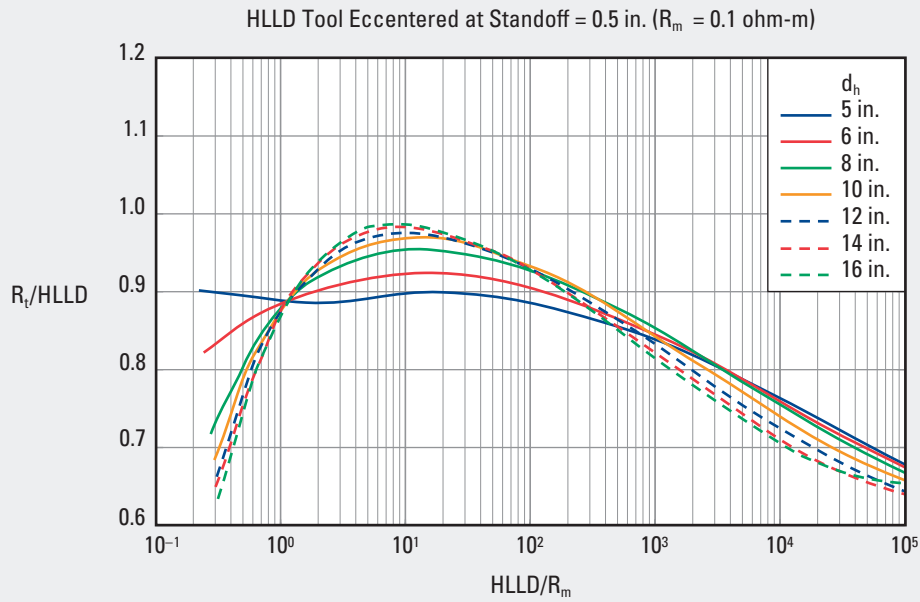
This chart is used to similarly to Chart RLI-2 to correct the HALS high-resolution shallow resistivity (HRLS) for borehole and drilling mud effects.

RLI

High-Resolution Azimuthal Laterolog Sonde (HALS)

HLLD Borehole Correction—Eccentered in Open Hole

RLI-6



© Schlumberger

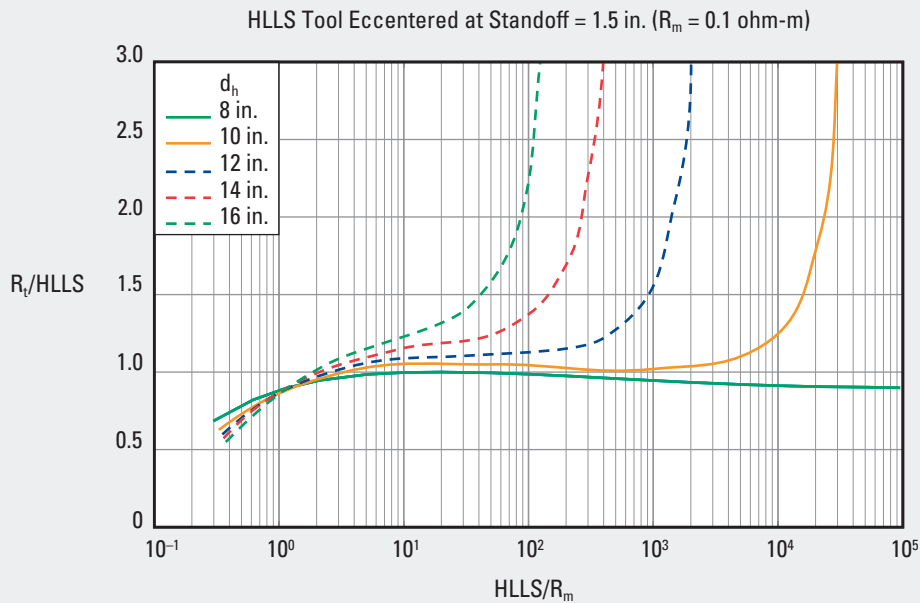
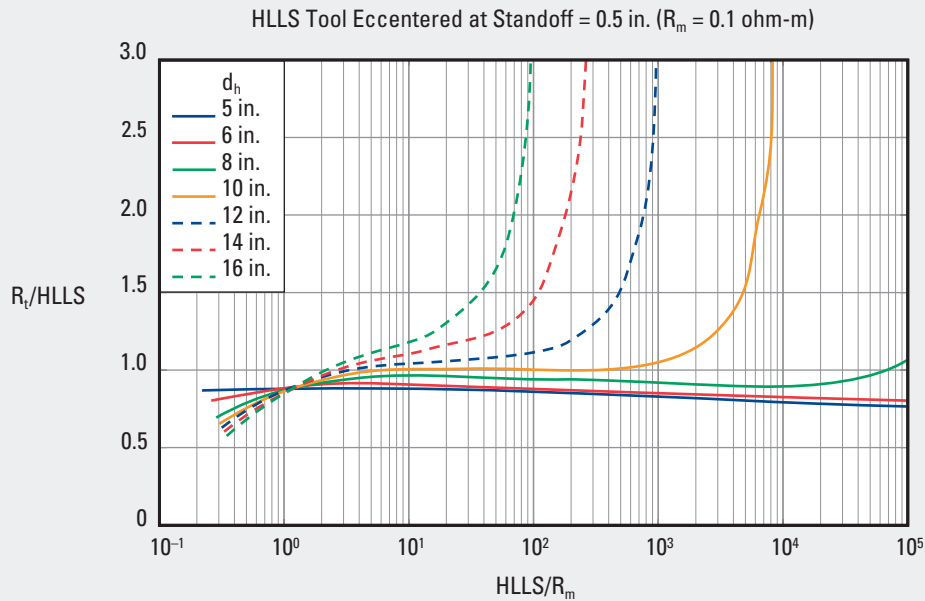
Purpose

This chart is used to similarly to Chart RLI-2 to correct the HALS laterolog deep resistivity (HLLD) for borehole and drilling mud effects at 0.5- and 1.5-in. standoffs.

High-Resolution Azimuthal Laterolog Sonde (HALS)

HLLS Borehole Correction—Eccentered in Open Hole

RLI-7



© Schlumberger

Purpose

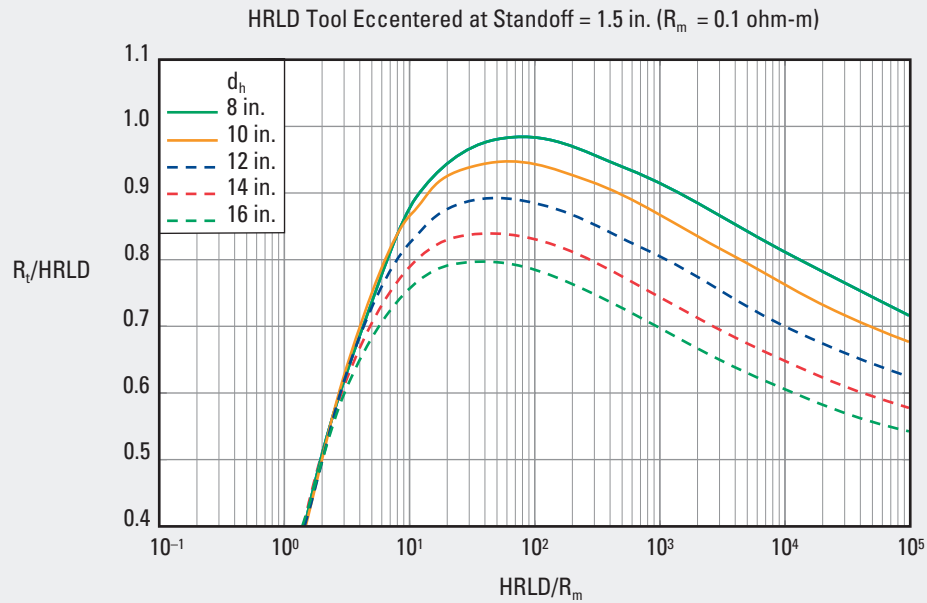
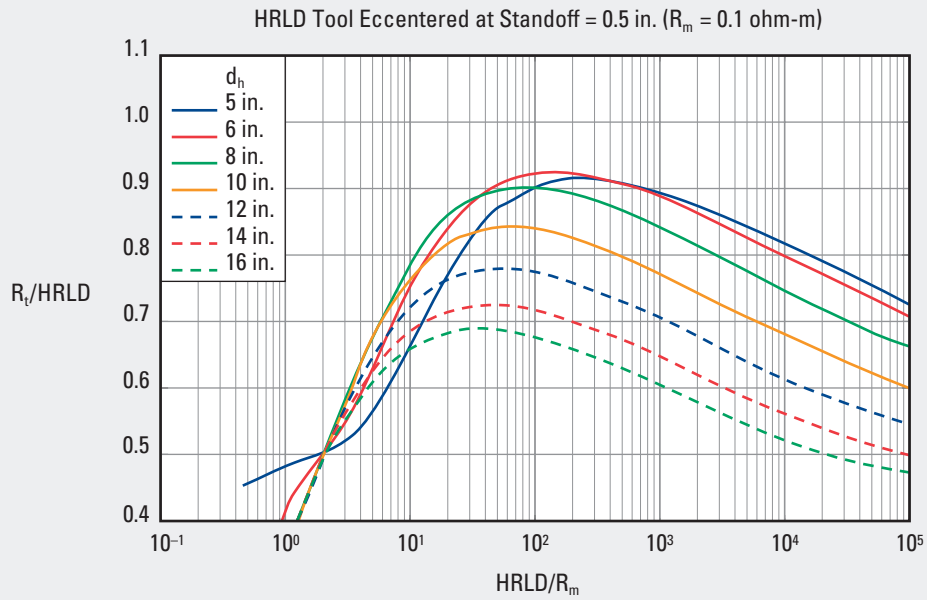
This chart is used to similarly to Chart RLI-2 to correct the HALS laterolog shallow resistivity (HLLS) for borehole and drilling mud effects at 0.5- and 1.5-in. standoffs.

RLI

High-Resolution Azimuthal Laterolog Sonde (HALS)

HRLD Borehole Correction—Eccentered in Open Hole

RLI-8



© Schlumberger

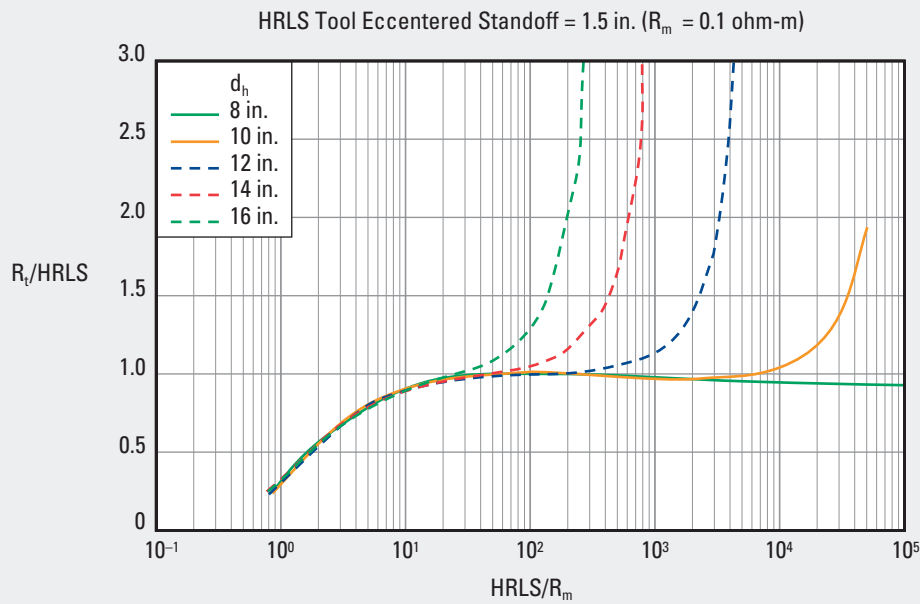
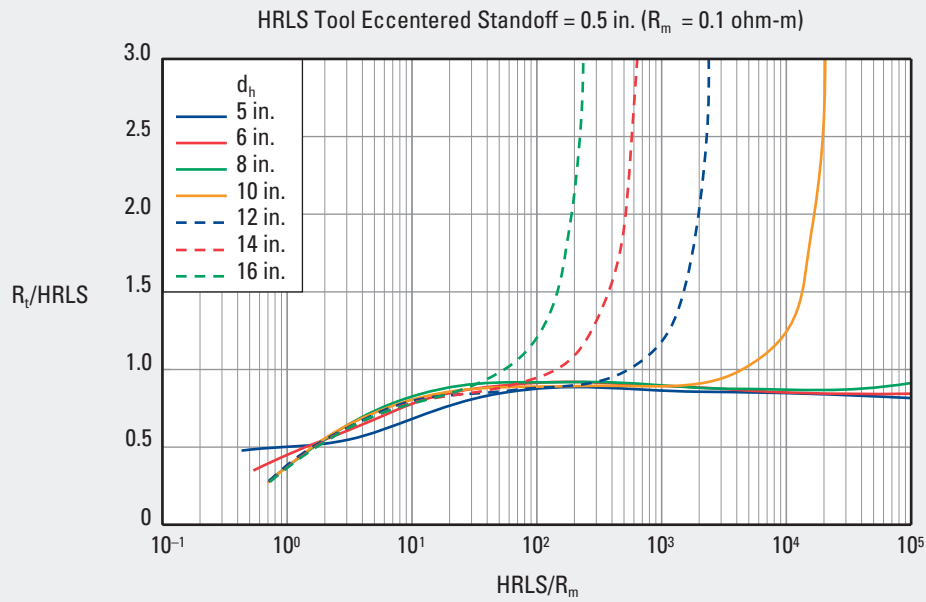
Purpose

This chart is used to similarly to Chart RLI-2 to correct the HALS high-resolution deep resistivity (HRLD) for borehole and drilling mud effects at 0.5- and 1.5-in. standoffs.

High-Resolution Azimuthal Laterolog Sonde (HALS)

HRLS Borehole Correction—Eccentered in Open Hole

RLI-9



© Schlumberger

Purpose

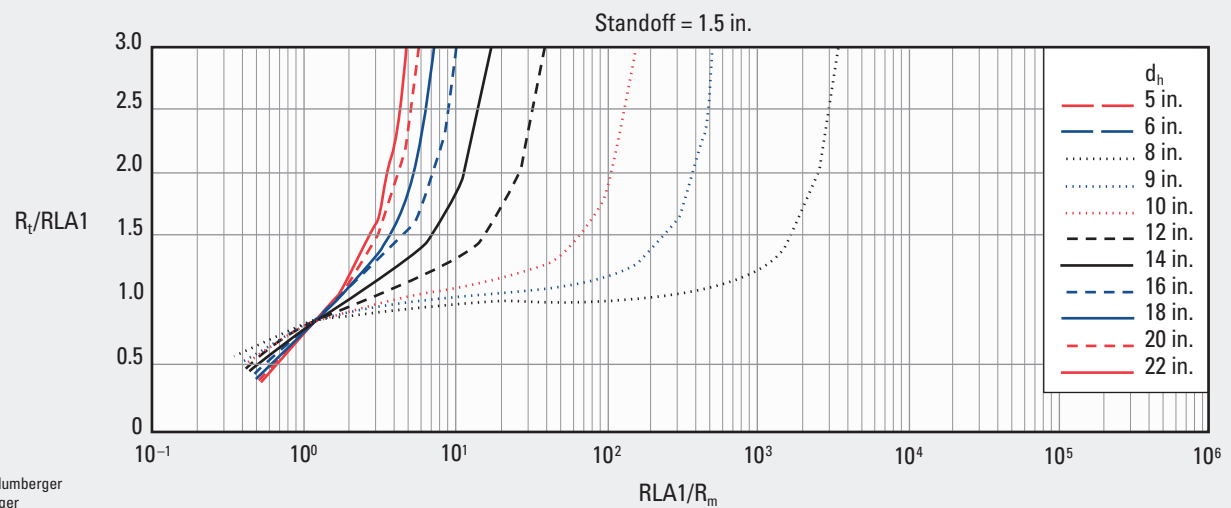
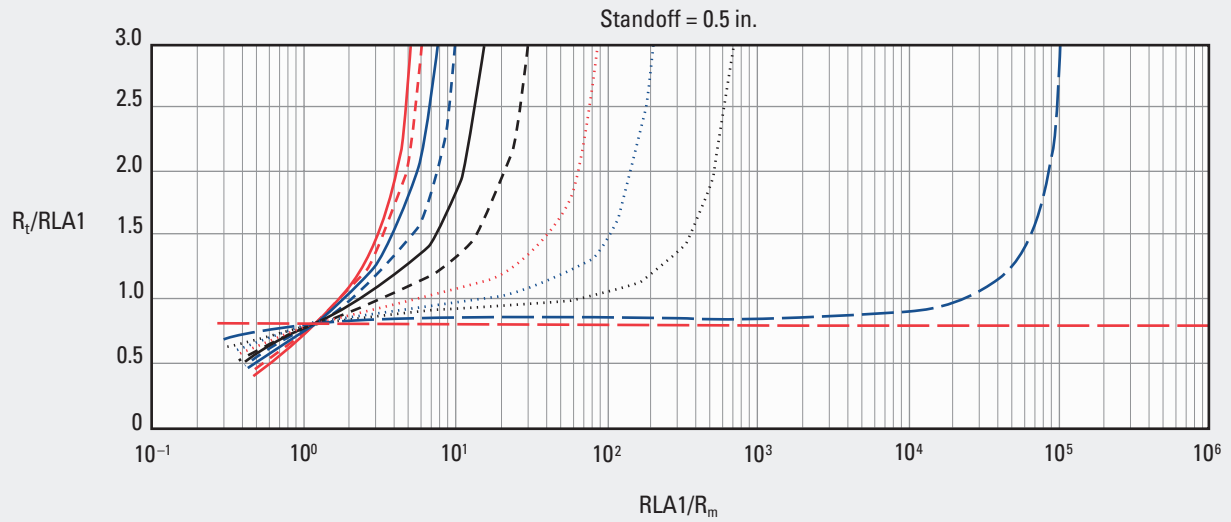
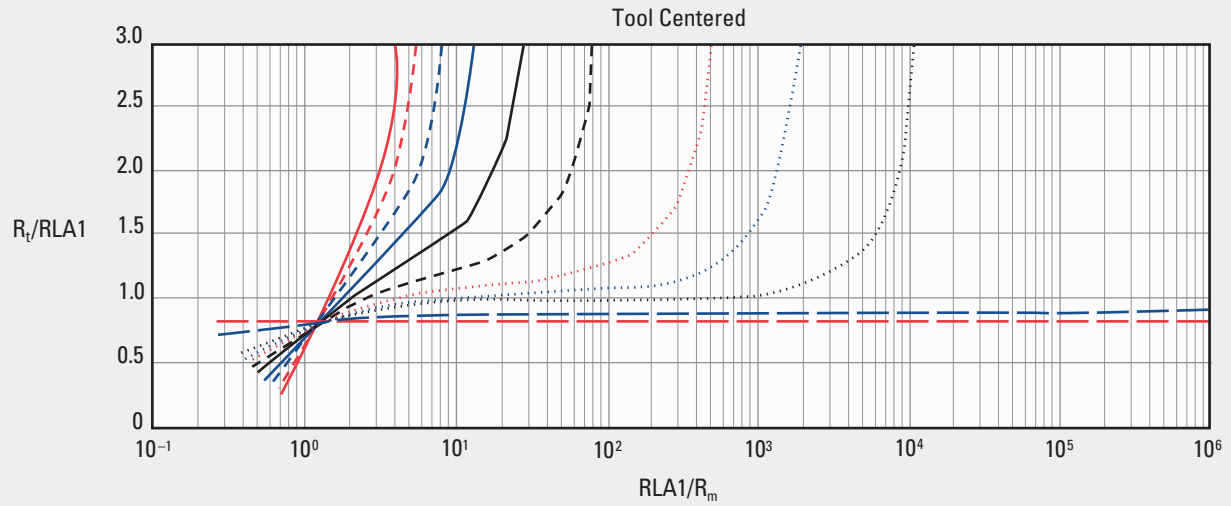
This chart is used to similarly to Chart RLI-2 to correct the HALS high-resolution shallow resistivity (HRLS) for borehole and drilling mud effects at 0.5- and 1.5-in. standoffs.

RLI

HRLA* High-Resolution Laterolog Array

Borehole Correction—Open Hole

RLI-10



*Mark of Schlumberger
© Schlumberger

Purpose

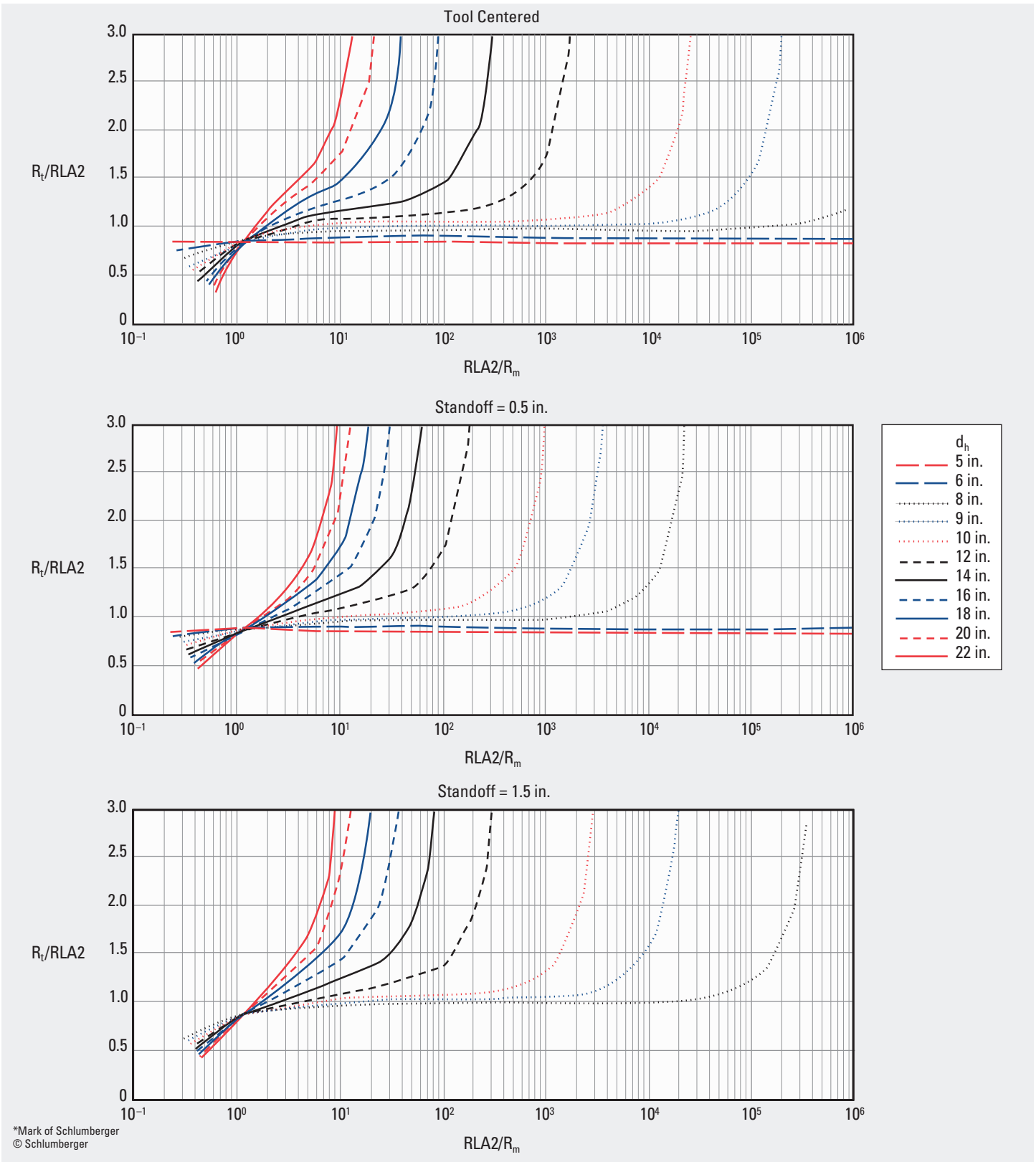
This chart is used to similarly to Chart RLI-2 to correct HRLA High-Resolution Laterolog Array resistivity for borehole and drilling mud

effects. RLA1 is the apparent resistivity from computed focusing mode 1.

HRLA* High-Resolution Laterolog Array

Borehole Correction—Open Hole

RLI-11



*Mark of Schlumberger
© Schlumberger

Purpose

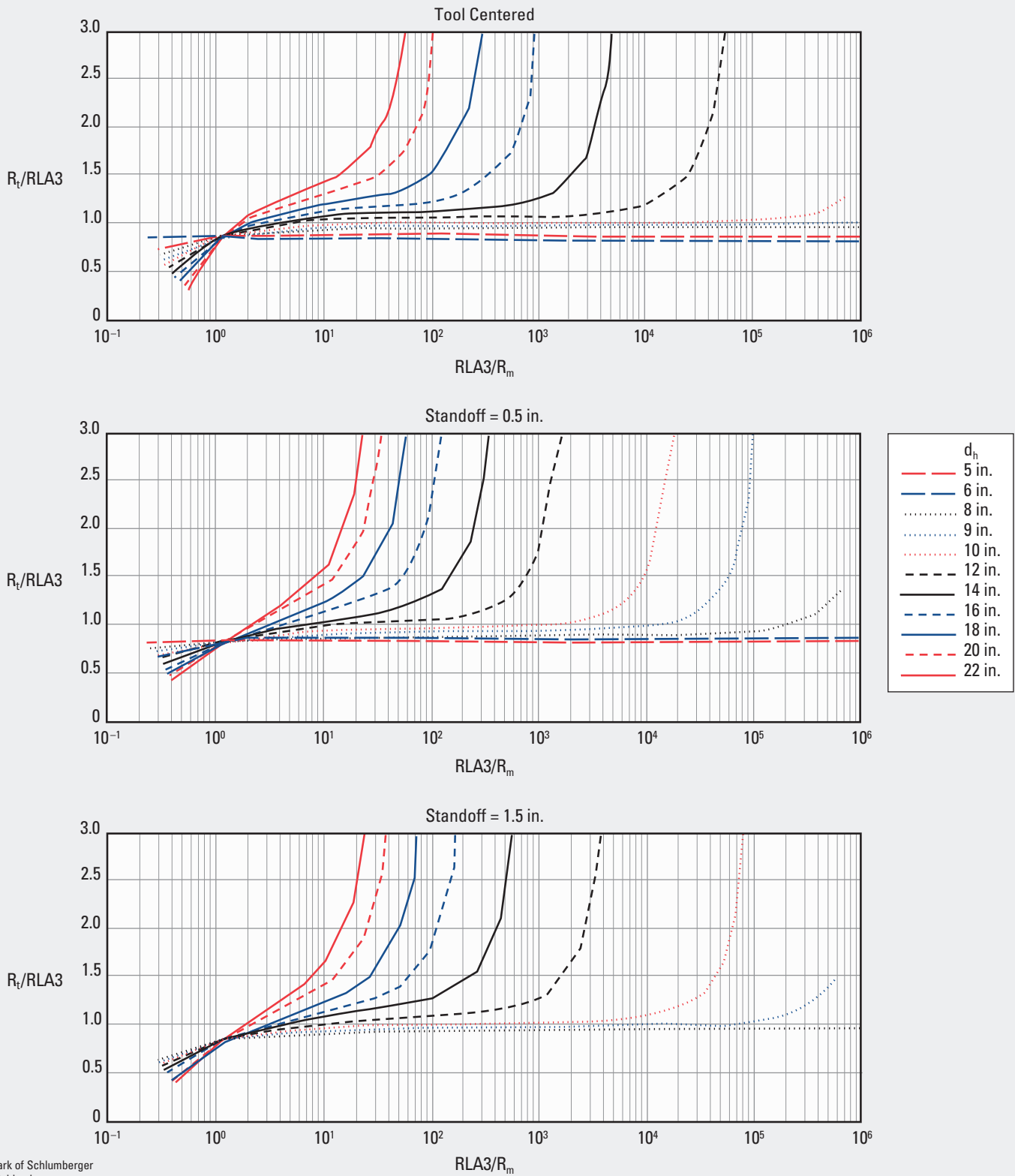
This chart is used to similarly to Chart RLI-2 to correct HRLA High-Resolution Laterolog Array resistivity for borehole and drilling mud

effects. RLA2 is the apparent resistivity from computed focusing mode 2.

HRLA* High-Resolution Laterolog Array

Borehole Correction—Open Hole

RLI-12



*Mark of Schlumberger
© Schlumberger

Purpose

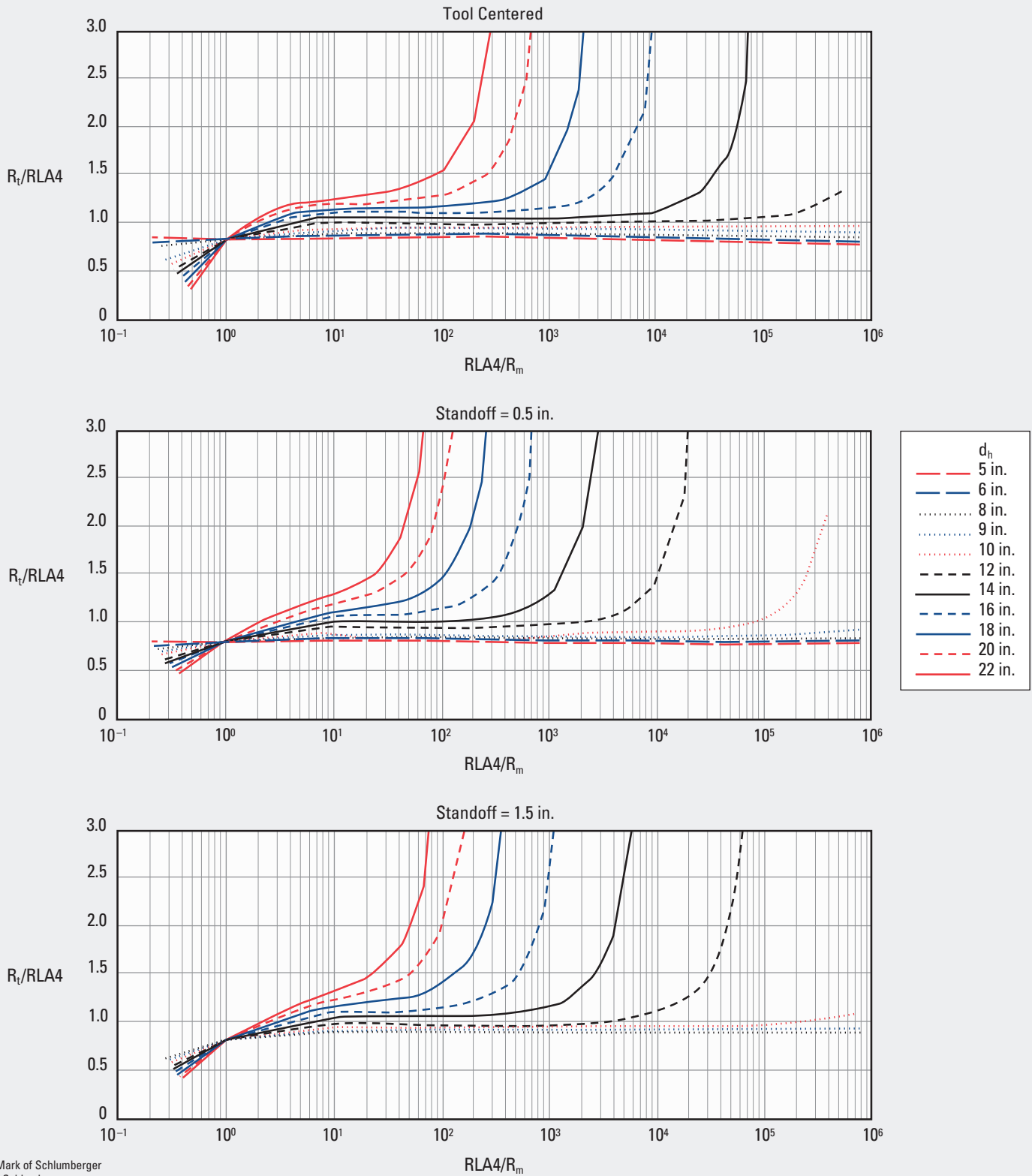
This chart is used to similarly to Chart RLI-2 to correct HRLA High-Resolution Laterolog Array resistivity for borehole and drilling mud

effects. RLA3 is the apparent resistivity from computed focusing mode 3.

HRLA* High-Resolution Laterolog Array

Borehole Correction—Open Hole

RLI-13



*Mark of Schlumberger
© Schlumberger

Purpose

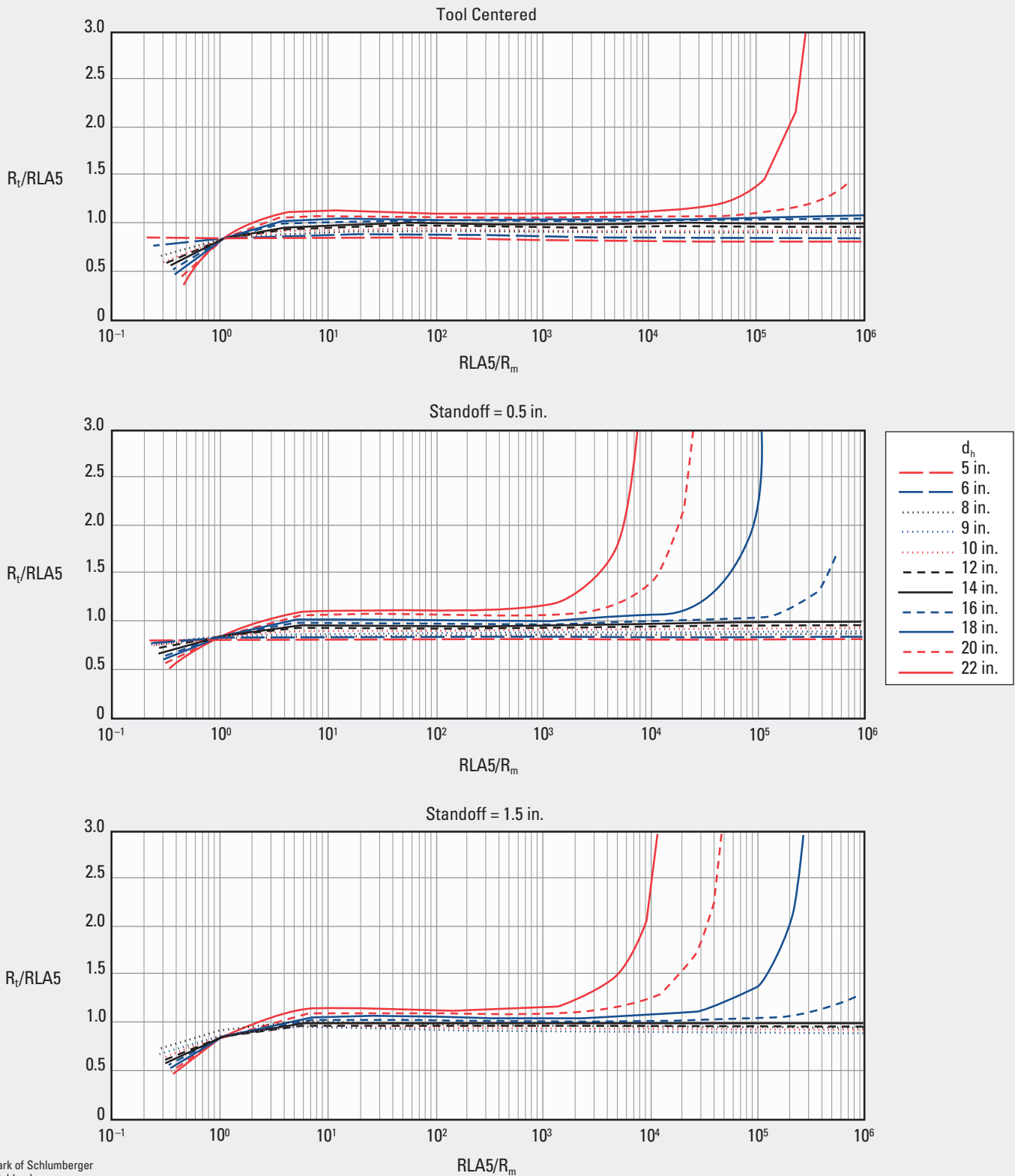
This chart is used to similarly to Chart RLI-2 to correct HRLA High-Resolution Laterolog Array resistivity for borehole and drilling mud

effects. RLA4 is the apparent resistivity from computed focusing mode 4.

HRLA* High-Resolution Laterolog Array

Borehole Correction—Open Hole

RLI-14



*Mark of Schlumberger
© Schlumberger

Purpose

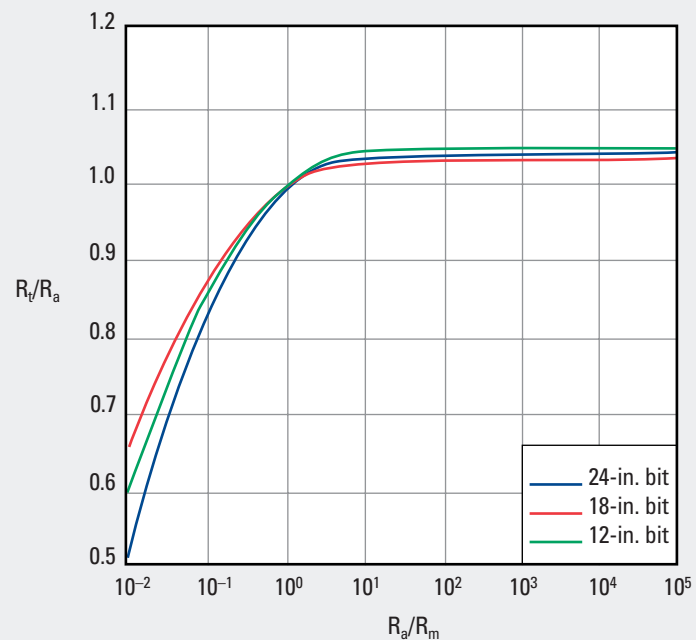
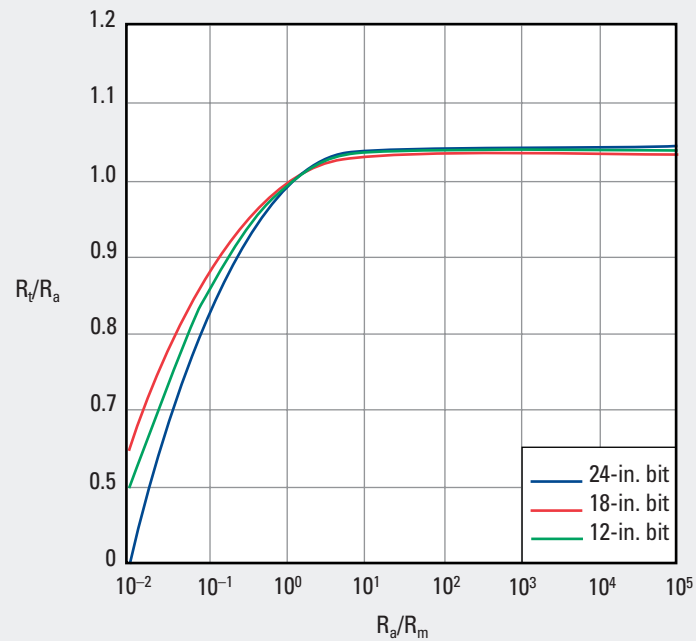
This chart is used to similarly to Chart RLI-2 to correct HRLA High-Resolution Laterolog Array resistivity for borehole and drilling mud

effects. $RLA5$ is the apparent resistivity from computed focusing mode 5.

GeoSteering* Bit Resistivity—6.75-in. Tool

Borehole Correction—Open Hole

RLI-20



*Mark of Schlumberger
© Schlumberger

Purpose

This chart is used to derive the borehole correction for the GeoSteering bit-measured resistivity. The bit resistivity corrected to the true resistivity (R_t) is then used in the calculation of water saturation.

Description

Enter the chart on the x-axis with the ratio of the bit resistivity and mud resistivity (R_a/R_m) at formation temperature. Move upward to

intersect the appropriate bit size. Move horizontally left to intersect the correction factor on the y-axis. Multiply the correction factor by the R_a value to obtain R_t . Charts RLI-21, RLI-23, and RLI-24 are similar to Chart RLI-20 for different tools and bit sizes.

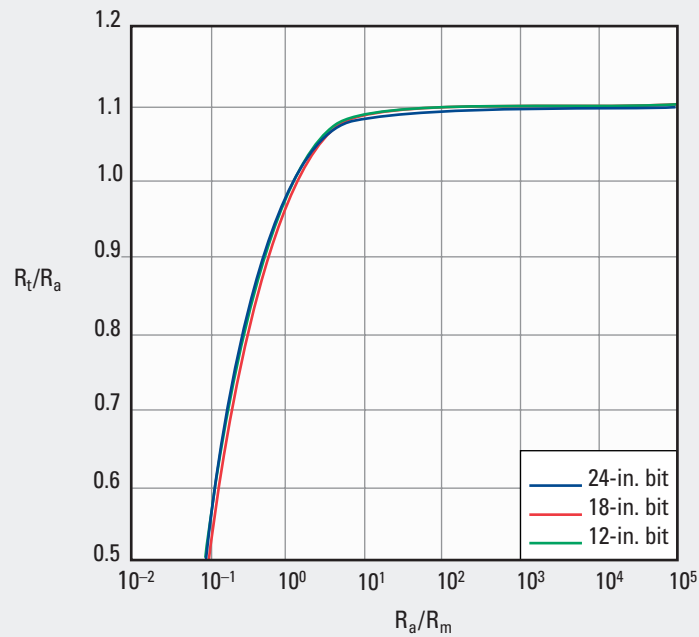
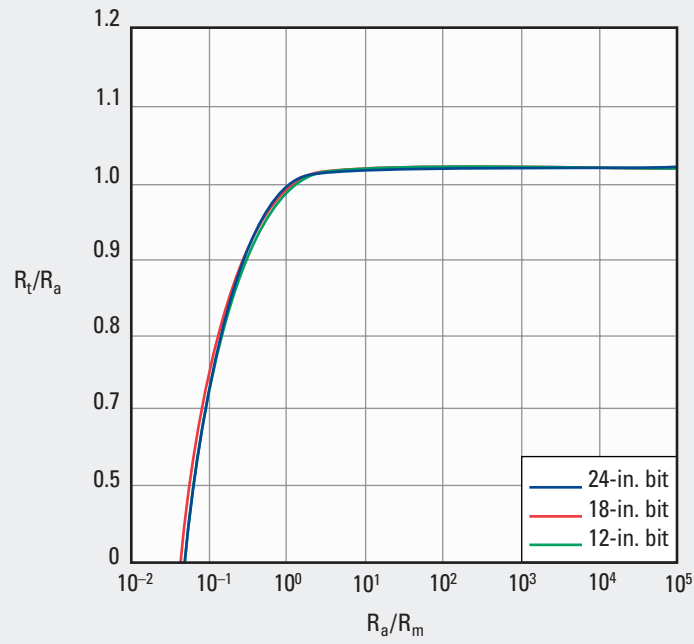
Chart RLI-22 differs in that it is for reaming-down mode as opposed to drilling mode.

RLI

GeoSteering* arcVISION675* Resistivity—6.75-in. Tool

Borehole Correction—Open Hole

RLI-21



*Mark of Schlumberger
© Schlumberger

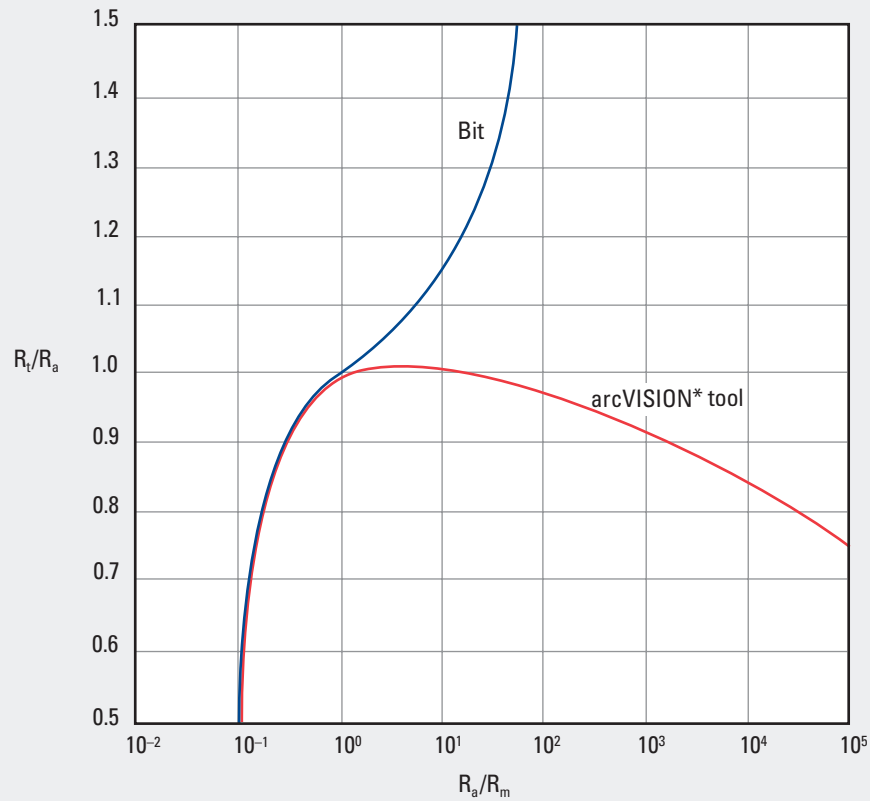
Purpose

This chart is used similarly to Chart RLI-20 to derive the borehole correction for the GeoSteering bit-measured arcVISION675 resistivity.

GeoSteering* Bit Resistivity in Reaming Mode—6.75-in. Tool

Borehole Correction—Open Hole

RLI-22



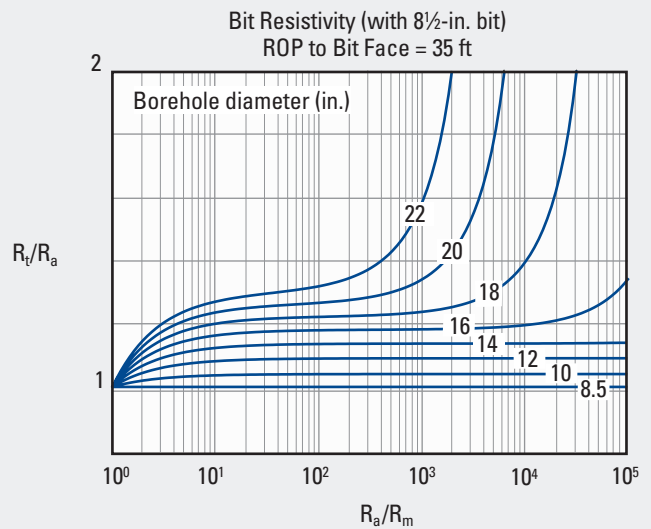
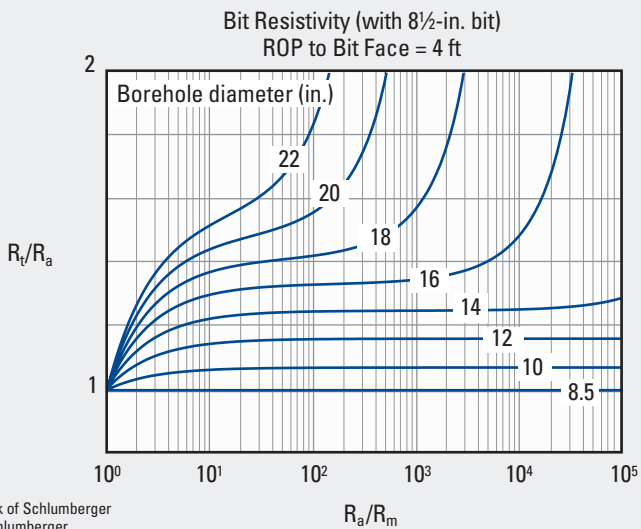
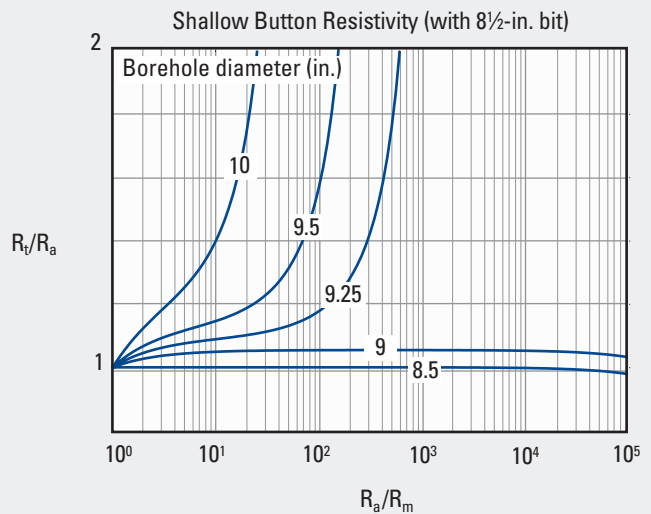
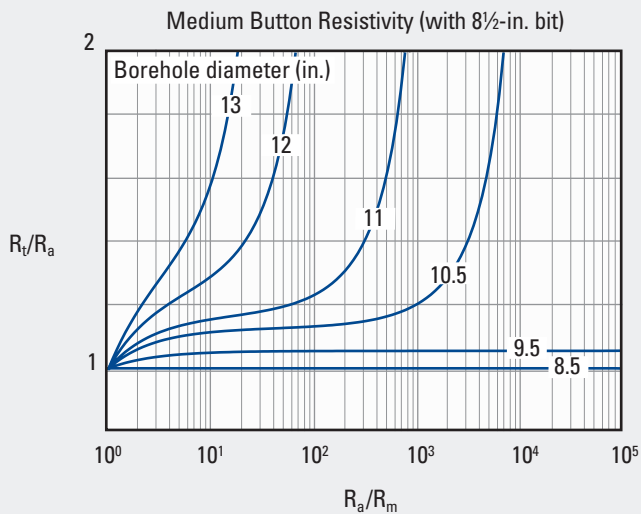
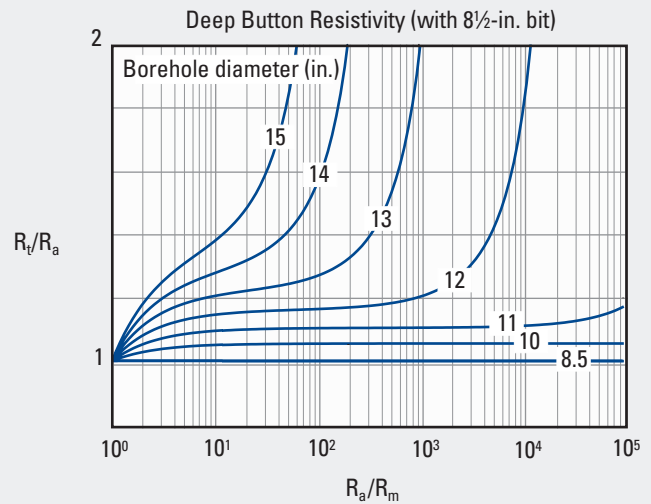
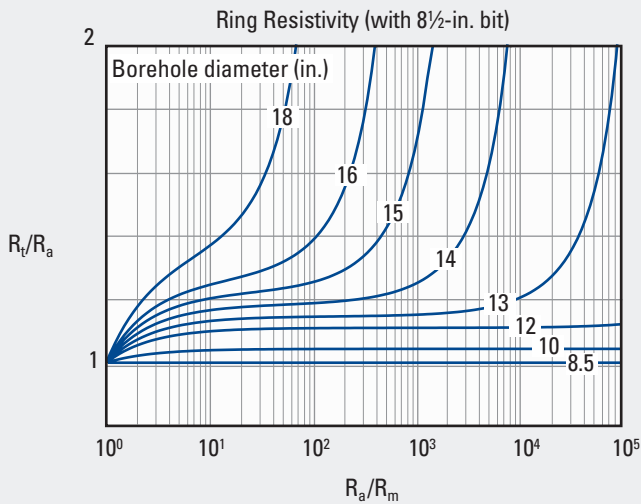
*Mark of Schlumberger
© Schlumberger

Purpose

This chart is used similarly to Chart RLI-20 to derive the borehole correction for the GeoSteering bit-measured resistivity while reaming down.

geoVISION® Resistivity Sub—6.75-in. Tool
Borehole Correction—Open Hole

RLI-23



*Mark of Schlumberger
© Schlumberger

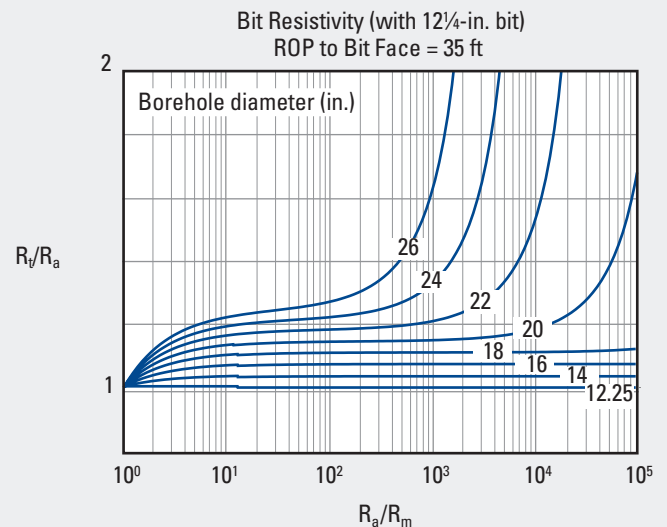
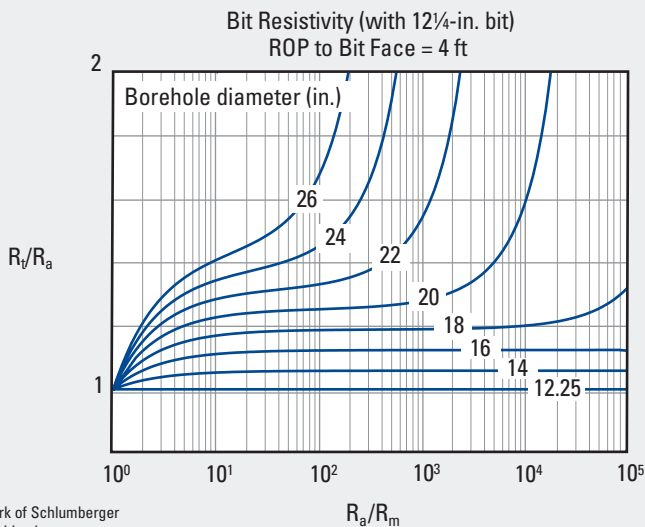
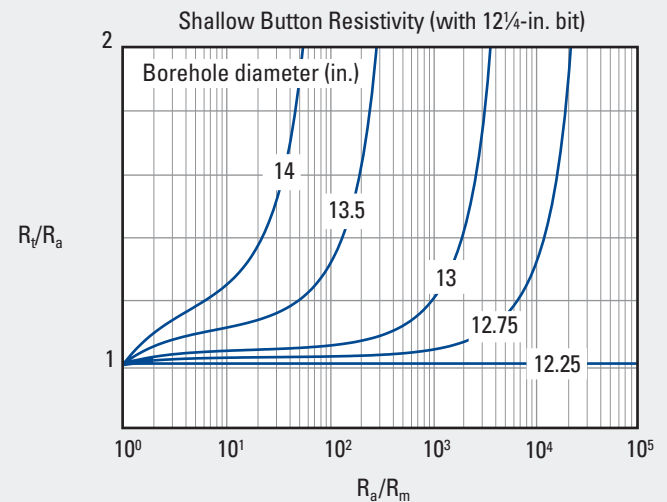
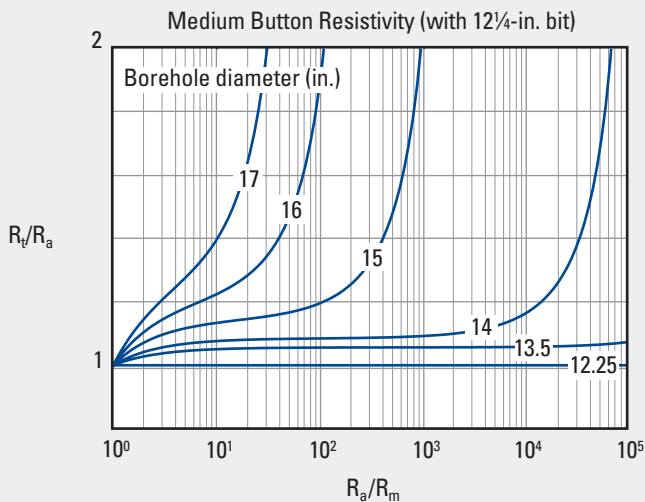
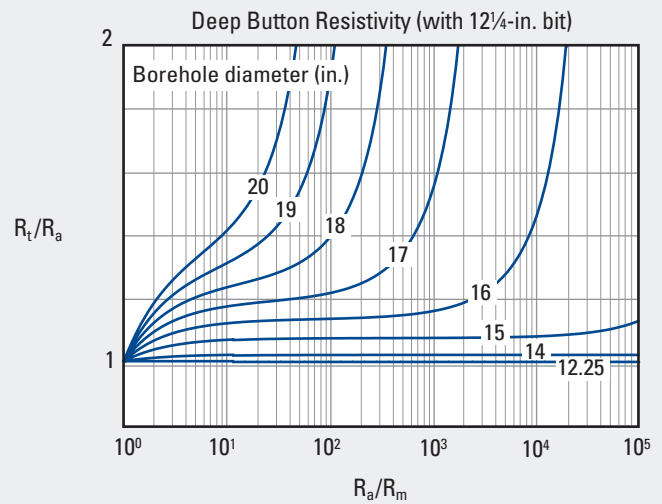
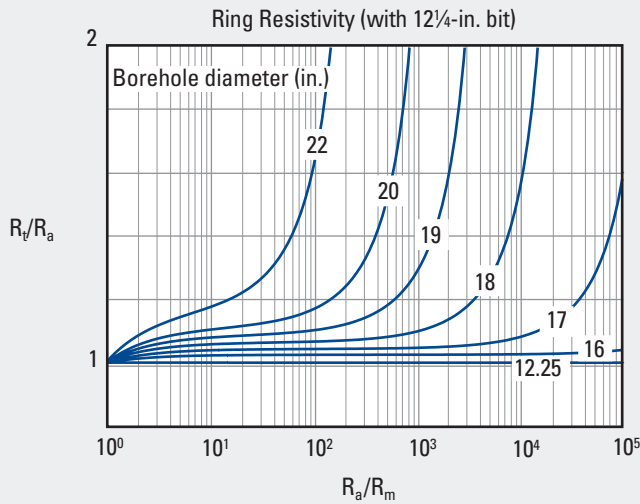
Purpose

This chart is used similarly to Chart RLI-20 to derive the borehole correction for the bit-measured resistivity from the GVR* resistivity

sub of the geoVISION 6.75-in. tool. The bottom row of charts specifies the bit readout point (ROP) to the bit face.

geoVISION® Resistivity Sub—8.25-in. Tool
Borehole Correction—Open Hole

RLI-24



*Mark of Schlumberger
© Schlumberger

RLI

Purpose

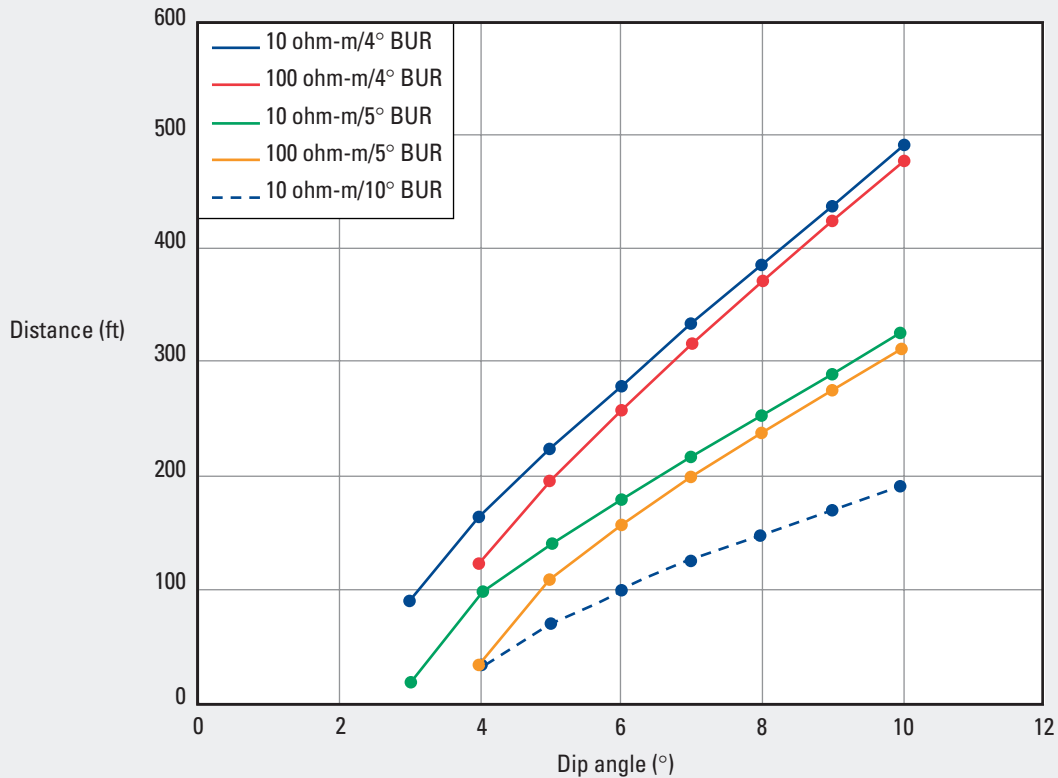
This chart is used similarly to Chart RLI-20 to derive the borehole correction for the bit-measured resistivity from the GVR* resistivity

sub of the geoVISION 8.25-in. tool. The bottom row of charts specifies the bit readout point (ROP) to the bit face.

GeoSteering* Bit Resistivity—6.75-in. Tool

Distance Out of Formation—Open Hole

RLI-25



*Mark of Schlumberger
© Schlumberger

Purpose

This chart is used to calculate the distance the GeoSteering bit must travel to return to the target formation.

Description

When drilling is at very high angles from vertical, the bit may wander out of formation. If this occurs, how far the bit must travel to get back into the formation must be determined.

Enter the chart with the known dip angle of the formation on the x-axis. Move upward to intersect the appropriate “buildup rate” (BUR) curve. Move horizontally left from the intersection point to the y-axis and read the distance back into the formation.

Example

Given: Formation dip angle = 6° , formation resistivity during drilling = 10 ohm-m, and buildup rate = 4° .

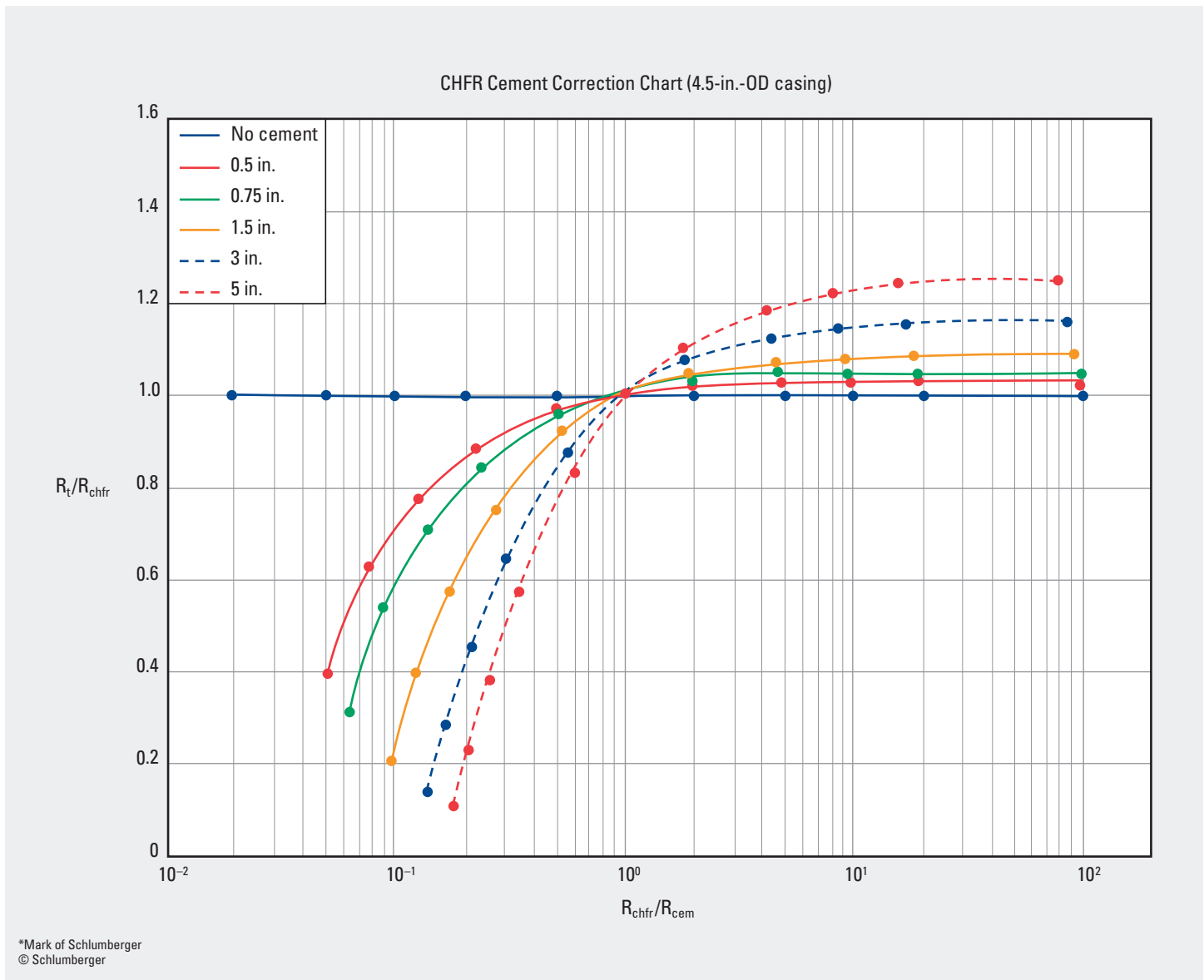
Find: Distance to return to the target formation.

Answer: Enter the chart at 6° on the x-axis. Move upward to the 10 ohm-m/ 4° BUR curve. Move horizontally left to the y-axis to read approximately 290 ft.

CHFR* Cased Hole Formation Resistivity Tool

Cement Correction—Cased Hole

RLI-50

**Purpose**

This chart is used to correct the raw cased hole resistivity measurement of the CHFR Cased Hole Formation Resistivity tool (R_{chfr}) for the thickness of the cement sheath. The resulting value of true resistivity (R_t) is used to calculate the water saturation.

Description

Enter the chart on the x-axis with the ratio of R_{chfr} and the resistivity of the cement sheath (R_{cem}). The value of R_{cem} is obtained with laboratory measurements. Move upward to the appropriate cement sheath thickness curve, which represents the annular space between the outside of the casing and the borehole wall. Move horizontally left to the y-axis and read the R_t/R_{chfr} value. Multiply this value by R_{chfr} to obtain R_t .

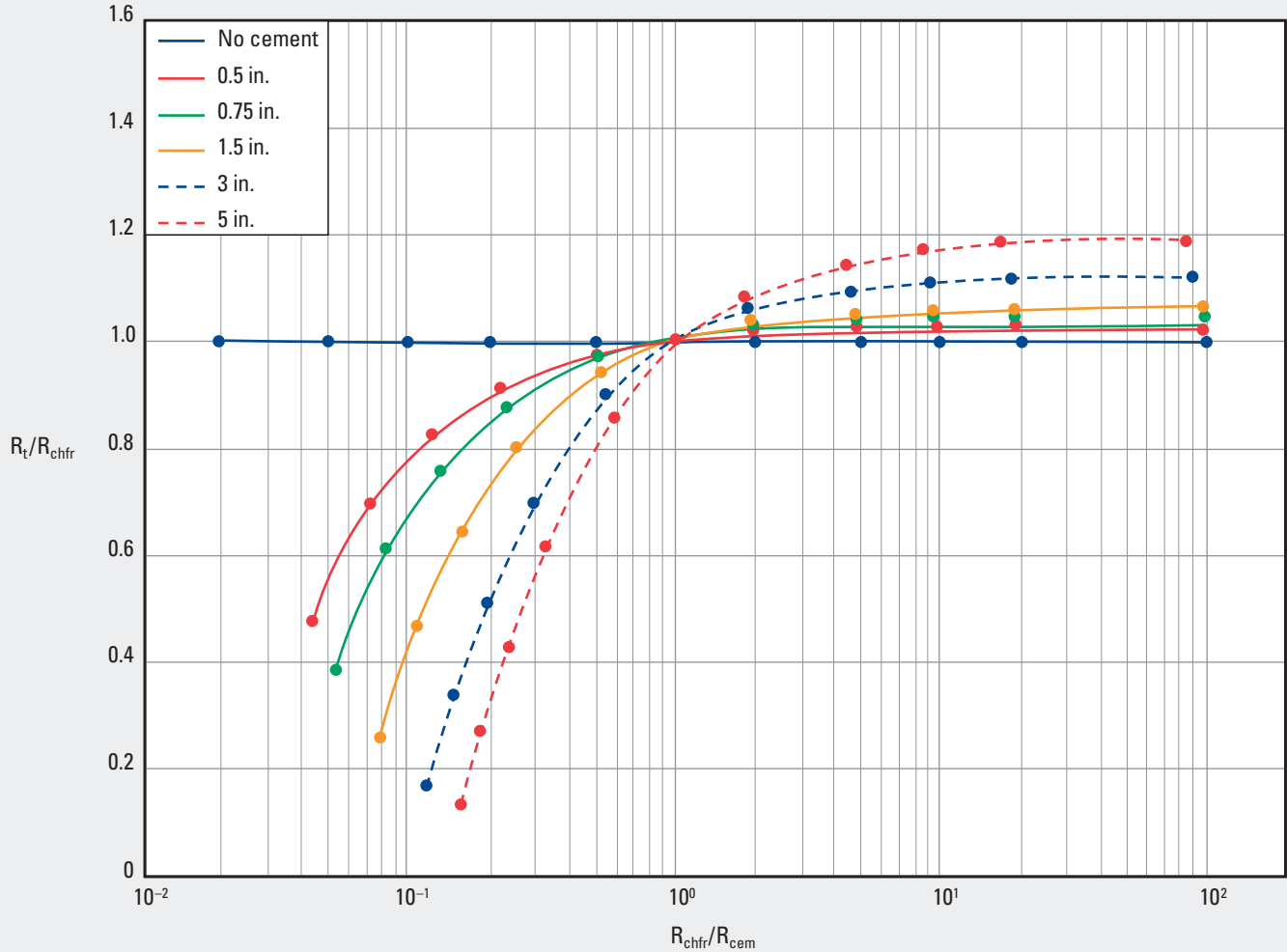
Charts RLI-51 and RLI-52 are for making the correction in larger casing sizes.

CHFR* Cased Hole Formation Resistivity Tool

Cement Correction—Cased Hole

RLI-51

CHFR Cement Correction Chart (7-in.-OD casing)



*Mark of Schlumberger
© Schlumberger

Purpose

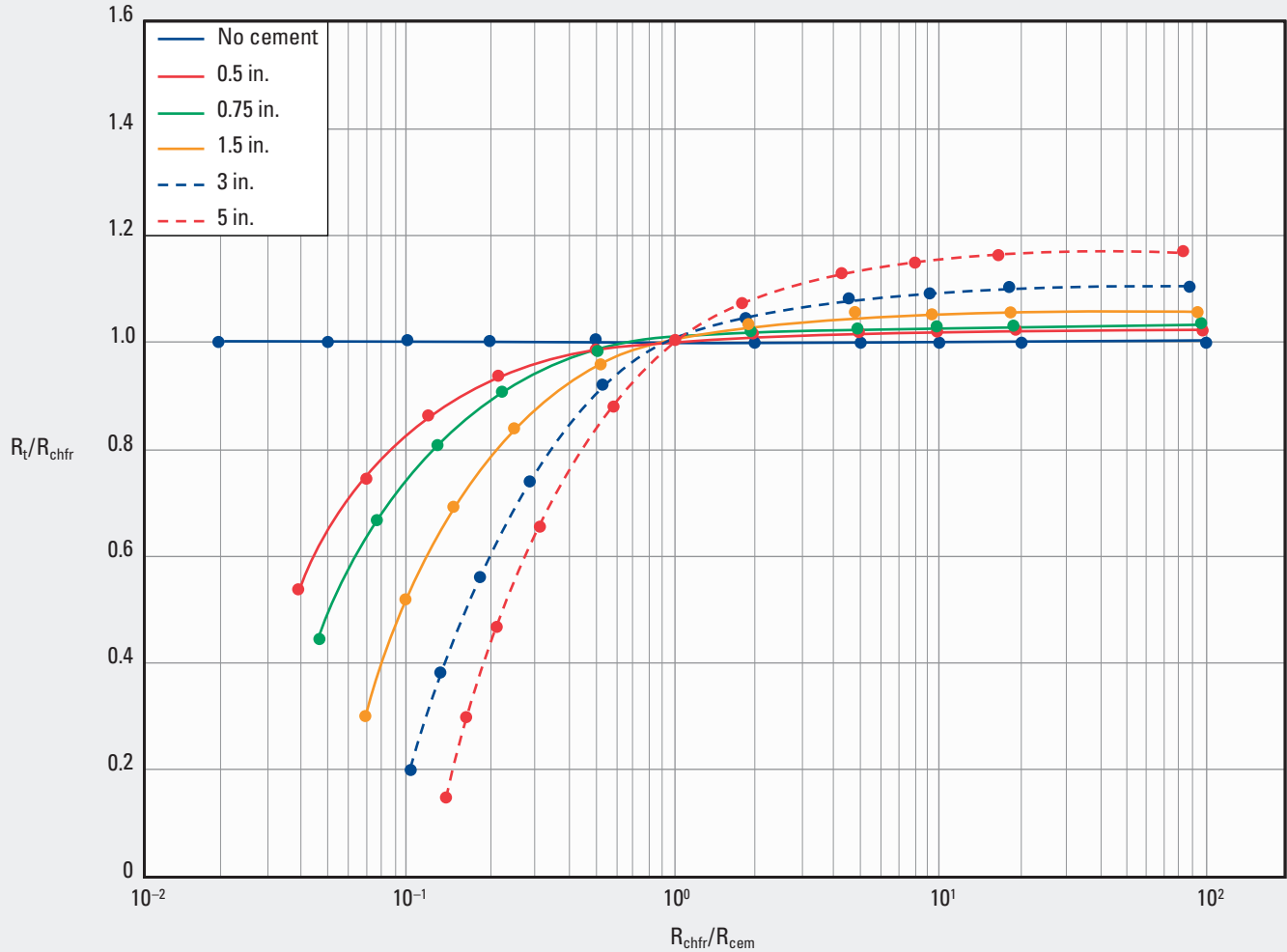
This chart is used similarly to Chart RLI-50 to obtain the cased hole resistivity of the CHFR Cased Hole Formation Resistivity tool corrected for the thickness of the cement sheath in 7-in.-OD casing.

CHFR* Cased Hole Formation Resistivity Tool

Cement Correction—Cased Hole

RLI-52

CHFR Cement Correction Chart (9.625-in.-OD casing)



*Mark of Schlumberger
© Schlumberger

Purpose

This chart is used similarly to Chart RLI-50 to obtain the cased hole resistivity of the CHFR Cased Hole Formation Resistivity tool corrected for the thickness of the cement sheath in 9.625-in.-OD casing.

RLI

AIT* Array Induction Imager Tool

Operating Range—Open Hole

Purpose

This chart is used to determine the limit of application for the AIT Array Induction Imager Tool measurement in a salt-saturated borehole.

Description

When the AIT tool logs a large salt-saturated borehole, the 10- and 20-in. induction curves may well be unusable because of the large conductive borehole. In a borehole with a diameter (d_h) of 8 in., the 10- and 20-in. curve data are usable if $R_t < 300R_m$. The ratio of the true resistivity to the mud resistivity (R_t/R_m) is proportional to $(d_h/8)^2$.

A general rule is that a 12-in. borehole must have a ratio of $R_t/R_m \leq 133$ to have usable shallow log data. Additional requirements are that the borehole must be round and the AIT tool standoff is 2.5 in. The value of R_t/R_m is further reduced if the borehole is irregular or the standoff requirement is not met.

Chart RInd-1 summarizes these requirements. The expected values of R_t , R_m , borehole size, and standoff size are entered to accurately determine the usable resolution in a smooth hole. The lower chart summarizes which AIT resistivity tools typically provide the most accurate deep resistivity data.

Example: Salt-Saturated Borehole

Given: Borehole size = 10 in., $R_t = 5$ ohm-m, $R_m = 0.0135$ ohm-m, and standoff (so) = 2.5 in.

Find: Which, if any, of the AIT curves are valid.

Answer: From the x-axis equation:

$$\left(\frac{R_t}{R_m}\right)\left(\frac{d_h}{8}\right)^2\left(\frac{1.5}{so}\right) =$$

$$\left(\frac{5}{0.0135}\right)\left(\frac{10}{8}\right)^2\left(\frac{1.5}{2.5}\right) =$$

$$(370)(1.5625)(0.6) = 346.$$

Enter the chart on the x-axis at 346 and move upward to intersect $R_t = 5$ ohm-m on the y-axis. The intersection point is in an error zone for which the shallow induction curves are not valid even in a round borehole. The deeper induction curves are valid only with a 2-ft or larger vertical resolution.

The limits for the 1-, 2-, and 4-ft curves are integral to the chart. As illustrated, a 1-ft 90-in. curve is not usable in a large salt-saturated borehole. Also, under these conditions, the 1-, 2-, and 4-ft curves cannot have the same resistivity response.

Example: Freshwater Mud Borehole

Given: Borehole size = 10 in., $R_t = 5$ ohm-m, $R_m = 0.135$ ohm-m, and standoff (so) = 1.5 in.

Find: Which, if any, of the AIT curves are valid.

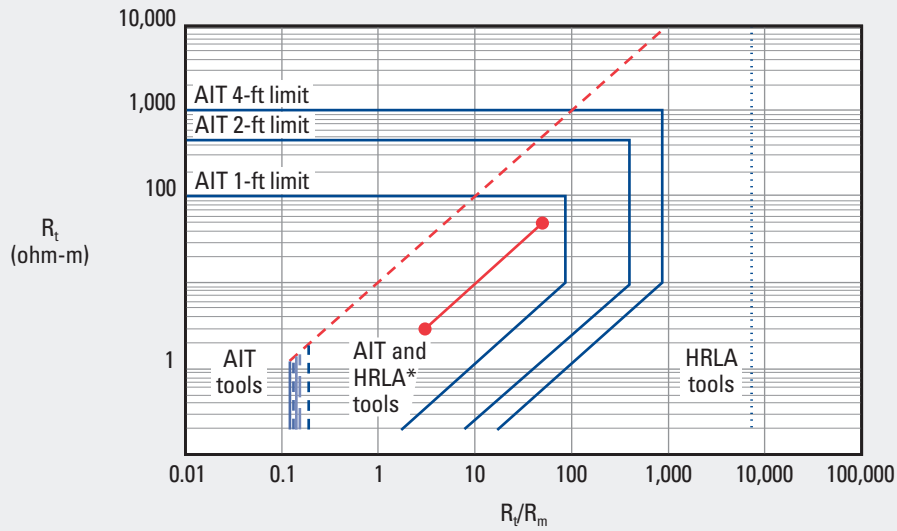
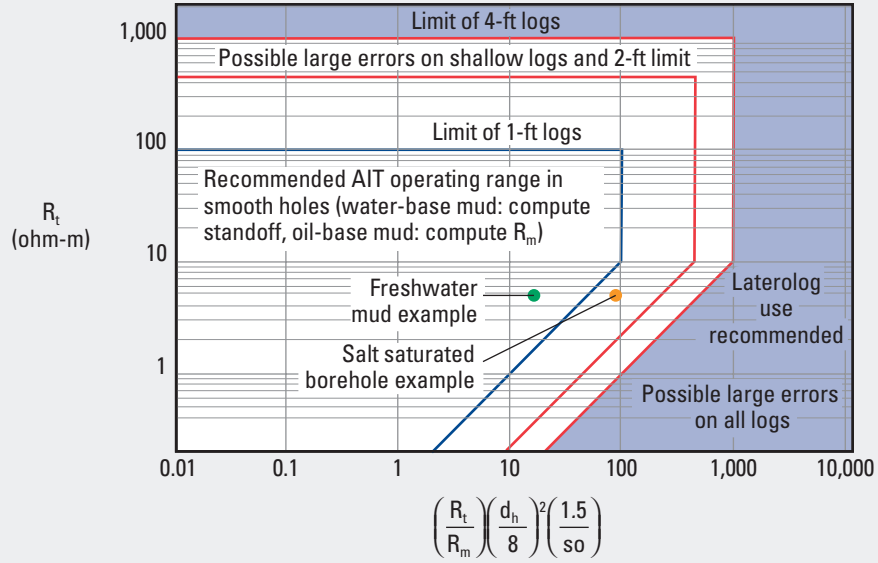
Answer: $R_t/R_m = 37.0$, $(d_h/8)^2 = (10/8)^2 = 1.5625$, and $(1.5/so) = 1.5/1.5 = 1$. The resulting value from the x-axis equation is $37.0 \times 1.5625 \times 1 = 57.9$.

Enter the chart at 57.9 on the x-axis and intersect $R_t = 5$ ohm-m on the y-axis. The intersection point is within the limit of the 1-ft vertical resolution boundary. All the AIT induction curves are usable.

AIT* Array Induction Imager Tool

Operating Range—Open Hole

RInd-1



*Mark of Schlumberger
© Schlumberger

RInd

AIT* Array Induction Imager Tool

Borehole Correction—Open Hole

Introduction

The AIT tools (AIT-B, AIT-C, AIT-H, AIT-M, Slim Array Induction Imager Tool [SAIT], Hostile Environment Induction Imager Tool [HIT], and SlimXtreme* Array Induction Imager Tool [QAIT]) do not have chartbook corrections for environmental effects. The normal effects that required correction charts in the past (borehole correction, shoulder effect, and invasion interpretation) are now all made using real-time algorithms for the AIT tools. In reality, the charts for the older dual induction tools were inadequate for the complexity of environmental effects on induction tools. The very large volume of investigation required to obtain an adequate radial depth of investigation to overcome invasion makes the resulting set of charts too extensive for a book of this size. The volume that affects the logs can be tens of feet above and below the tool. To make useful logs, the effects of the volume above and below the layer of interest must be carefully removed. This can be done only by either signal processing or inversion-based processing. This section briefly describes the wellsite processing and advanced processing available at computing centers.

Wellsite Processing

Borehole Correction

The first step of AIT log processing is to correct the raw data from all eight arrays for borehole effects. Borehole corrections for the AIT tools are based on inversion through an iterative forward model to find the borehole parameters that best reproduce the logs from the four shortest arrays—the 6-, 9-, 12-, and 15-in. arrays (Grove and Minerbo, 1991). The borehole forward model is based on a solution to Maxwell's equations in a cylindrical borehole of radius r with the mud resistivity (R_m) surrounded by a homogeneous formation of resistivity R_f . The tool can be located anywhere in the borehole, but is parallel to the borehole axis at a certain tool standoff (so). The borehole is characterized by its radius (r). In this model, the signal in a given AIT array is a function of only these four parameters.

The four short arrays overlap considerably in their investigation depth, so only two of the borehole parameters can be uniquely determined in an inversion. The others must be supplied by outside measurements or estimates. Because the greatest sensitivity to the formation resistivity is in the contrast between R_m and R_f , no external measurement is satisfactory for fitting to R_f . Therefore, R_f is always solved for. This leaves one other parameter that can be determined. The three modes of the borehole correction operation depend on which parameter is being determined:

- compute mud resistivity: requires hole diameter and standoff
- compute hole diameter: requires a mud resistivity measurement and standoff
- compute standoff: requires hole diameter and mud resistivity measurement.

Because the AIT borehole model is a circular hole, either axis from a multiaxis caliper can be used. If the tool standoff is adequate, the process finds the circular borehole parameters that best match the input logs. Control of adequate standoff is important because the changes in the tool reading are very large for small changes in tool position when the tool is very close to the borehole wall. Near the center of the hole the changes are very small. A table of recommended standoff sizes is as follows.

AIT Tool Recommended Standoff

Hole Size (in.)	Recommended Standoff (in.)	
	AIT-B, AIT-C, AIT-H, AIT-M, HIT	SAIT, QAIT
<5.0	–	0.5
5.0 to 5.5	–	1.0
5.5 to 6.5	0.5	1.5
6.5 to 7.75	1.0	2.0
7.75 to 9.5	1.5	2.5
9.5 to 11.5	2.0 + bowspring [†]	2.5
>11.5	2.5 + bowspring [†]	2.5

Note: Do not run AIT tools slick.

[†] Only for AIT-H tool

Each type of AIT tool requires a slightly different approach to the borehole correction method. For example, the AIT-B tool requires the use of an auxiliary R_m measurement (Environmental Measurement Sonde [EMS]) to compute R_m or to compute hole size by using a recalibration of the mud resistivity method internal to the borehole correction algorithm. The Platform Express*, SlimAccess*, and Xtreme* AIT tools have integral R_m sensors that meet the accuracy requirements for the compute standoff mode.

Log Formation

AIT tools are designed to produce a high-resolution log response with reduced cave effect in comparison with the induction log deep (ILD) in most formations. The log processing (Barber and Rosthal, 1991) is a weighted sum of the raw array data:

$$\sigma_{\log}(z) = \sum_{n=1}^N \sum_{z=z_{\min}}^{z=z_{\max}} w_n(z') \sigma_a^{(n)}(z-z')$$

where $\Sigma_{\log}(z)$ is the output log conductivity in mS/m, $\Sigma_a^{(n)}$ is the skin-effect-corrected conductivity from the n th array, and the weights (w) represent a deconvolution filter applied to each of the raw array measurements. The log depth is z , and z' refers to the distance above or below the log depth to where the weights are applied. The skin effect correction consists of fitting the X-signal to the skin-effect-error signal (Moran, 1964; Barber, 1984) at high conductivities and the R-signal to the error signal at low conductivi-

AIT* Array Induction Imager Tool

Borehole Correction—Open Hole

ties, with the crossover occurring between 100 and 200 mS/m. The use of the R-signal at low conductivities overcomes the errors in the X-signal associated with the normal magnetic susceptibilities of sedimentary rock layers (Barber et al., 1995).

The weights w in the equation can profit from further refinement. The method used to compute the weights introduces a small amount of noise in the matrix inversion, so the fit is about $\pm 1\%$ to $\pm 2\%$ to the defined target response. A second refinement filter is used to correct for this error. The AIT wellsite processing sequence, from raw, calibrated data to corrected logs, is shown in Fig. 1.

(Freedman and Minerbo, 1991, 1993; Zhang et al., 1994). Maximum-Entropy Resistivity Log Inversion (MERLIN) processing (Barber et al., 1999) follows Freedman and Minerbo (1991) closely, and that paper is the basic reference for the mathematical formulation. The problem is set up as the simplest parametric model that can fit the data: a thinly layered formation with each layer the same thickness (Fig. 2). The inversion problem is to solve for the conductivity of each layer so that the computed logs from the layered formation are the closest match to the measured logs.

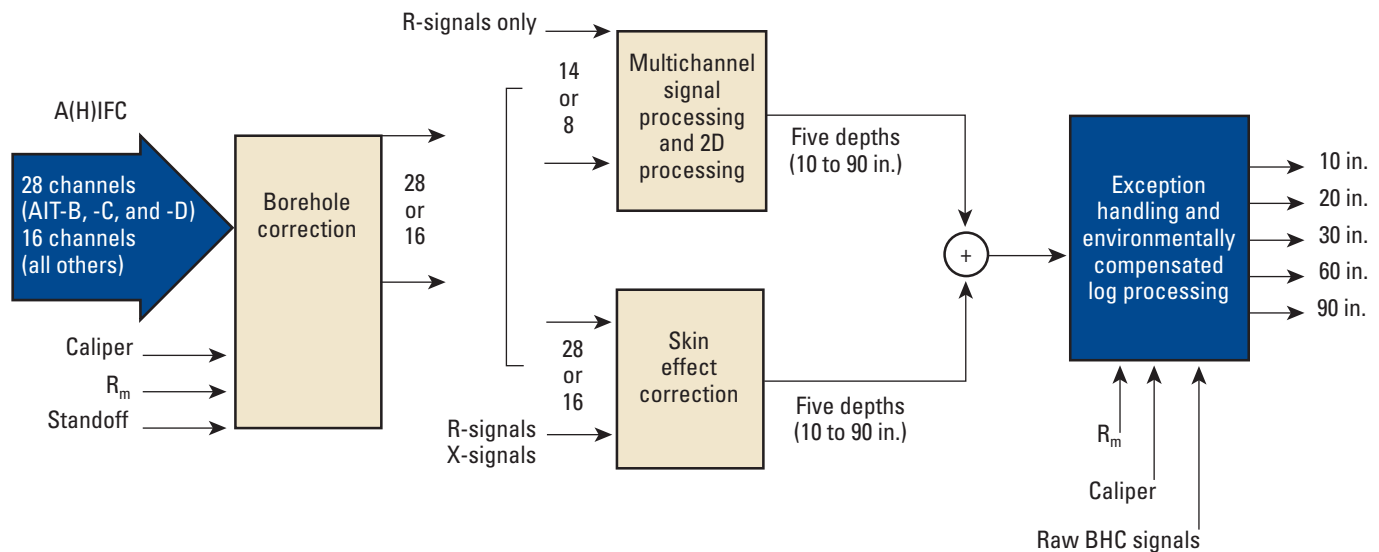


Figure 1. Block diagram of the real-time log processing chain from raw, calibrated array data to finished logs.

There are only two versions of this processing—one for AIT-B, AIT-C, and AIT-D tools and one for all other AIT tools (AIT-H, AIT-M, SAIT, HIT, and QAIT) (Anderson and Barber, 1995). Only two versions are required because the tools were carefully designed with the same coil spacings to produce the same two-dimensional (2D) response to the formation.

Advanced Processing

Logs in Deviated Wells or Dipping Formations

The interpretation of induction logs is complicated by the large volume of investigation of these tools. The AIT series of induction tools is carefully focused to limit the contributions from outside a relatively thin layer of response (Barber and Rosthal, 1991). In beds at high relative dip, the focused response cuts across several beds, and the focusing developed for vertical wells no longer isolates the response to a single layer. The effect of the high relative dip angle is to blur the response and to introduce horns at the bed boundaries.

Maximum Entropy Inversion: MERLIN Processing

The maximum entropy inversion method was first applied by Dyos (1987) to induction log data. For beds at zero dip angle, it has been shown to give well-controlled results when applied to deep induction (ID) and medium induction (IM) from the dual induction tool

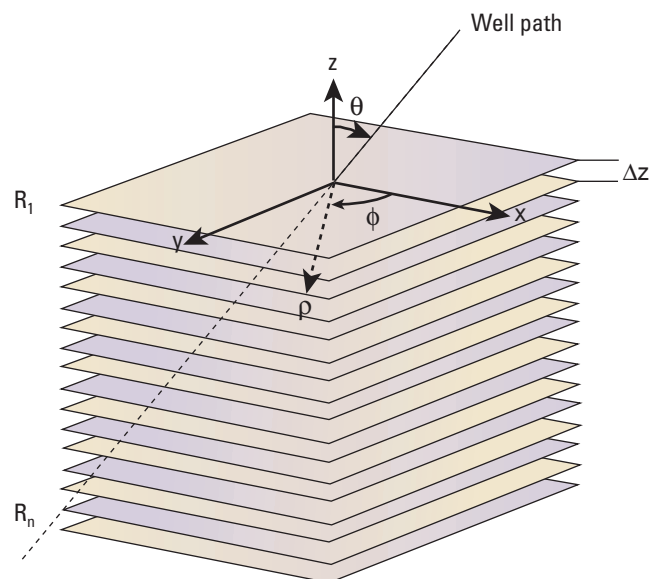


Figure 2. The parametric model used in MERLIN inversion. All layers are the same thickness, and the inversion solves for the conductivity of each layer with maximum-entropy constraints.

AIT* Array Induction Imager Tool

Borehole Correction—Open Hole

The flow of MERLIN processing is shown in Fig. 3. The borehole-corrected raw resistive and reactive (R- and X-) signals are used as a starting point. The conductivity of a set of layers is estimated from the log values, and the iterative modeling is continued until the logs converge. The set of formation layer conductivity values is then converted to resistivity and output as logs.

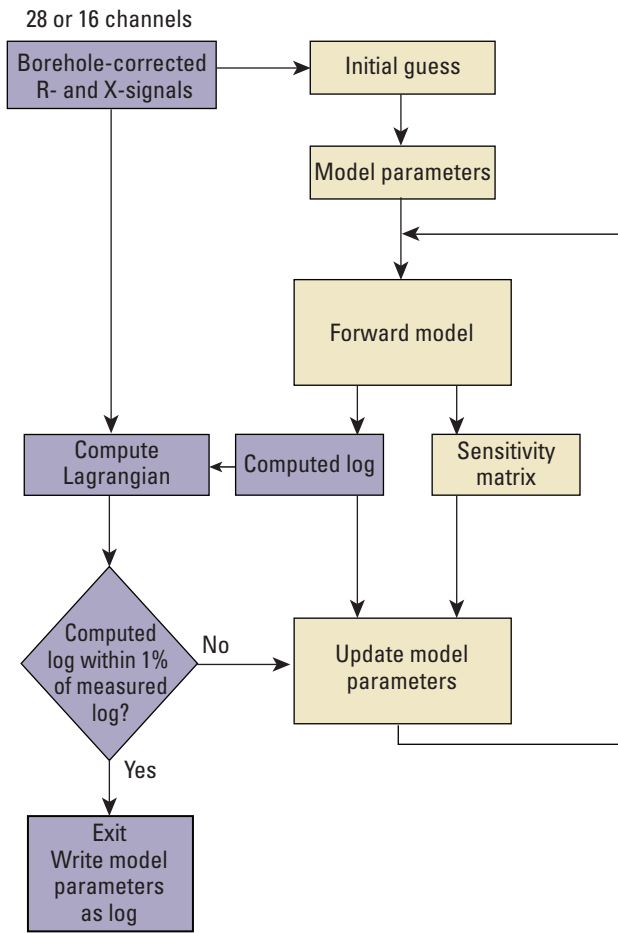


Figure 3. Data flow in the MERLIN inversion algorithm. The output is the final set of model parameters after the iterations converge.

Invasion Processing

The wellsite interpretation for invasion is a one-dimensional (1D) inversion of the processed logs into a four-parameter invasion model (R_{x0} , R_t , r_1 , and r_2 , shown in Fig. 4). The forward model is based on the Born model of the radial response of the tools and is accurate for most radial contrasts in which induction logs should be used. The inversion can be run in real time. The model is also available in the Invasion Correction module of the GeoFrame* Invasion 2 application, which also includes the step-invasion model and annulus model (Fig. 4).

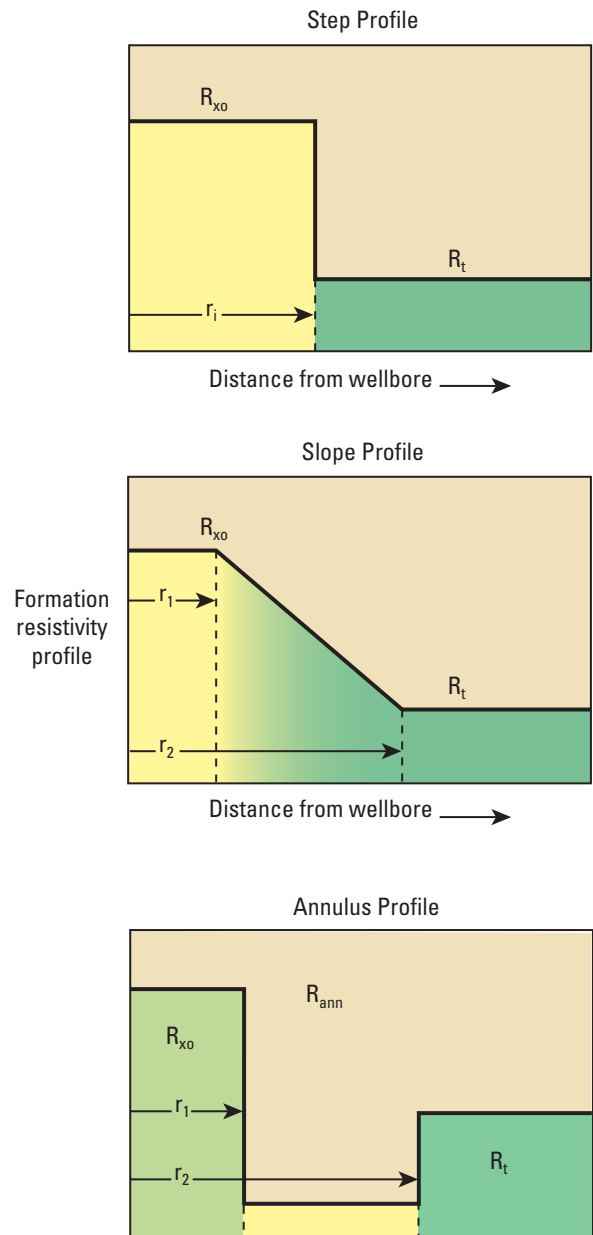


Figure 4. Parametric models used in AIT invasion processing. The slope profile model is used for real-time processing; the others are available at the computing centers. R_{x0} = resistivity of the flushed zone, R_t = true resistivity, r_1 = radius of invasion, R_{ann} = resistivity of the annulus.

AIT* Array Induction Imager Tool

Borehole Correction—Open Hole

Another approach is also used in the Invasion 2 application module. If the invaded zone is more conductive than the noninvaded zone, some 2D effects on the induction response can complicate the 1D inversion. Invasion 2 conducts a full 2D inversion using a 2D forward model (Fig. 5) to produce a more accurate answer for situations of conductive invasion and in thin beds.

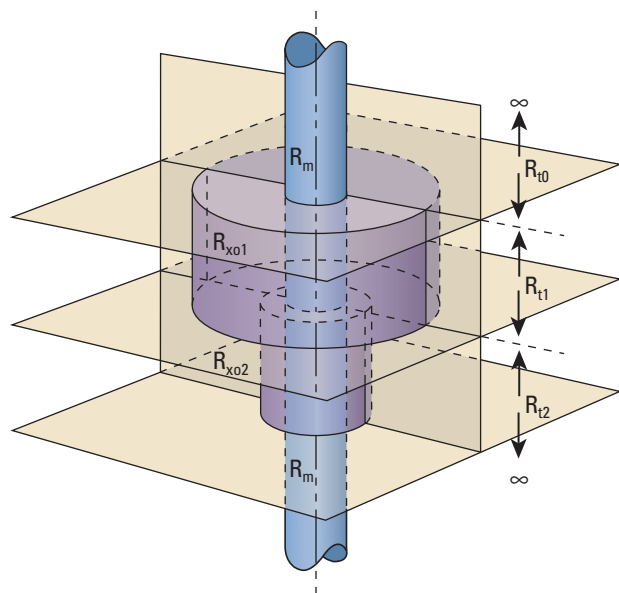


Figure 5. The parametric 2D formation model used in Invasion 2.

References

Anderson, B., and Barber, T.: *Induction Logging*, Sugar Land, TX, USA, Schlumberger SMP-7056 (1995).

Barber, T.D.: "Phasor Processing of Induction Logs Including Shoulder and Skin Effect Correction," US Patent No. 4,513,376 (September 11, 1984).

Barber, T., *et al.*: "Interpretation of Multiarray Induction Logs in Invaded Formations at High Relative Dip Angles," *The Log Analyst*, (May–June 1999) 40, No. 3, 202–217.

Barber, T., Anderson, B., and Mowat, G.: "Using Induction Tools to Identify Magnetic Formations and to Determine Relative Magnetic Susceptibility and Dielectric Constant," *The Log Analyst* (July–August 1995) 36, No. 4, 16–26.

Barber, T., and Rosthal, R.: "Using a Multiarray Induction Tool to Achieve Logs with Minimum Environmental Effects," paper SPE 22725 presented at the SPE Annual Technical Conference and Exhibition, Dallas, Texas, USA (October 6–9, 1991).

Dyos, C.J.: "Inversion of the Induction Log by the Method of Maximum Entropy," *Transactions of the SPWLA 28th Annual Logging Symposium*, London, UK (June 29–July 2, 1987), paper T.

Freedman, R., and Minerbo, G.: "Maximum Entropy Inversion of the Induction Log," *SPE Formation Evaluation* (1991), 259–267; also paper SPE 19608 presented at the SPE Annual Technical Conference and Exhibition, San Antonio, TX, USA (October 8–11, 1989).

Freedman, R., and Minerbo, G.: "Method and Apparatus for Producing a More Accurate Resistivity Log from Data Recorded by an Induction Sonde in a Borehole," US Patent 5,210,691 (January 1993).

Grove, G.P., and Minerbo, G.N.: "An Adaptive Borehole Correction Scheme for Array Induction Tools," *Transactions of the SPWLA 32nd Annual Logging Symposium*, Midland, Texas, USA (June 16–19, 1991), paper P.

Moran, J.H.: "Induction Method and Apparatus for Investigating Earth Formations Utilizing Two Quadrature Phase Components of a Detected Signal," US Patent No. 3,147,429 (September 1, 1964).

Zhang, Y-C., Shen, L., and Liu, C.: "Inversion of Induction Logs Based on Maximum Flatness, Maximum Oil, and Minimum Oil Algorithms," *Geophysics* (September 1994), 59, No. 9, 1320–1326.

arcVISION475* and ImPulse* 4³/₄-in. Array Resistivity Compensated Tools—2 MHz

Borehole Correction—Open Hole

Purpose

This chart is used to determine the borehole correction applied by the surface acquisition system to arcVISION475 and ImPulse phase-shift (R_{ps}) and attenuation resistivity (R_{ad}) curves on the log. The value of R_t is used in the calculation of water saturation.

Description

Enter the appropriate chart for the borehole environmental conditions and tool used to measure the various formation resistivities with the either the uncorrected phase-shift or attenuation resistivity value (not the resistivity shown on the log) on the x-axis. Move upward to intersect the appropriate resistivity spacing line, and then move horizontally left to read the ratio value on the y-axis. Multiply the ratio value by the resistivity value entered on the x-axis to obtain R_t .

Charts REm-12 through REm-38 are used similarly to Chart REm-11 for different borehole conditions and arcVISION* and ImPulse tool combinations.

Example

Given: $R_{ps} = 400$ ohm-m (uncorrected) from arcVISION475 (2-MHz) phase-shift 10-in. resistivity, borehole size = 6 in., and mud resistivity (R_m) = 0.02 ohm-m at formation temperature.

Find: Formation resistivity (R_t).

Answer: Enter the top left chart at 400 ohm-m on the x-axis and move upward to intersect the 10-in. resistivity curve (green).

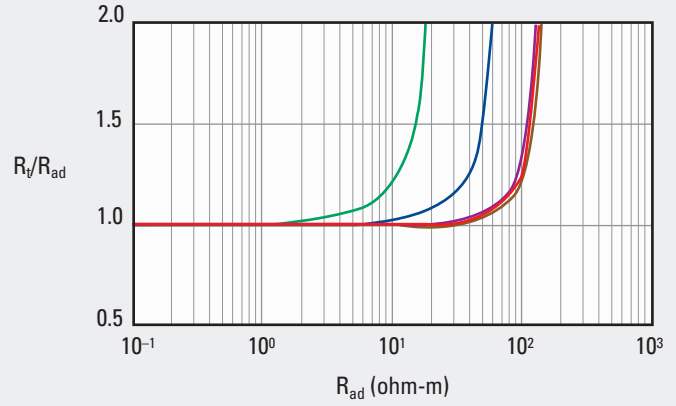
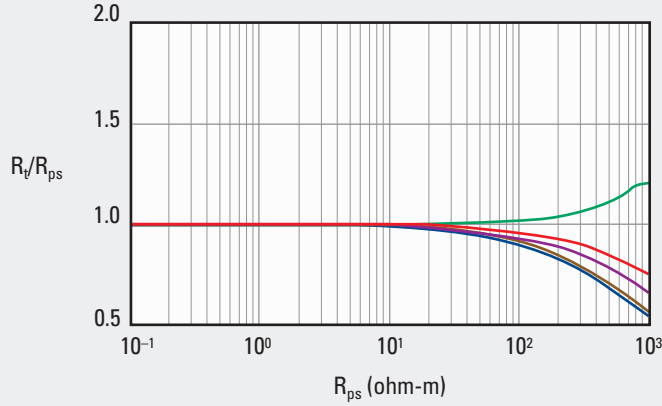
Move left and read approximately 1.075 on the y-axis.

$$R_t = 1.075 \times 400 = 430 \text{ ohm-m.}$$

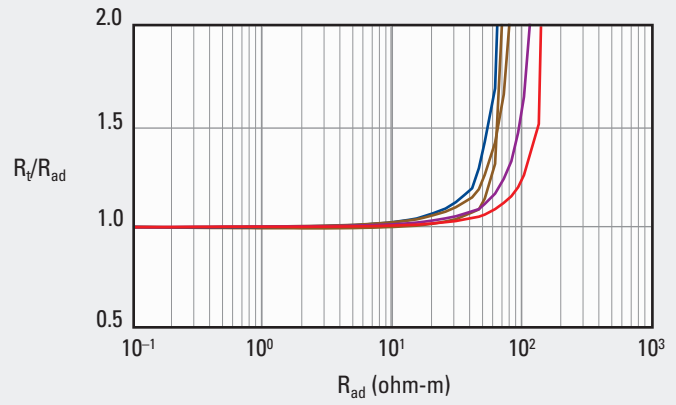
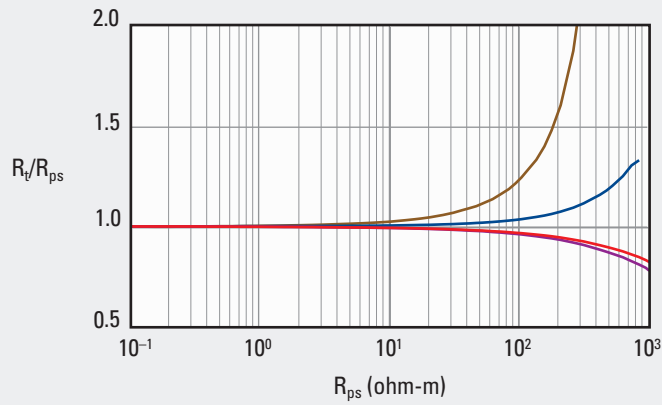
arcVISION475* and ImPulse* 4¾-in. Array
 Resistivity Compensated Tools—2 MHz
 Borehole Correction—Open Hole

REm-11

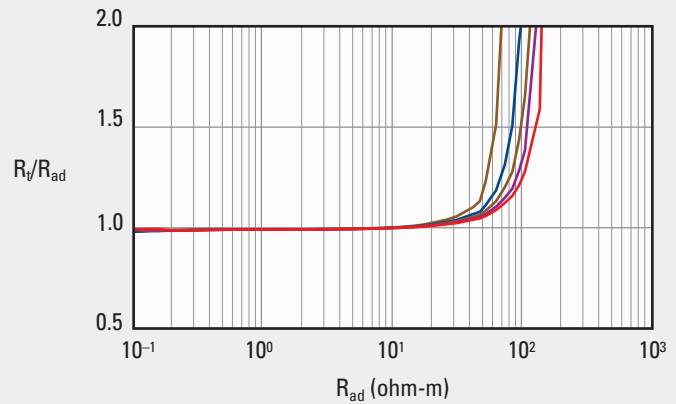
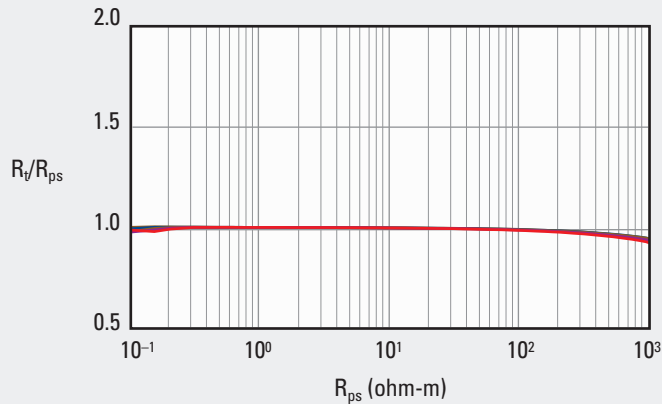
arcVISION475 and ImPulse Borehole Correction for 2 MHz, $d_h = 6$ in., $R_m = 0.02$ ohm-m



arcVISION475 and ImPulse Borehole Correction for 2 MHz, $d_h = 6$ in., $R_m = 0.1$ ohm-m



arcVISION475 and ImPulse Borehole Correction for 2 MHz, $d_h = 6$ in., $R_m = 1.0$ ohm-m

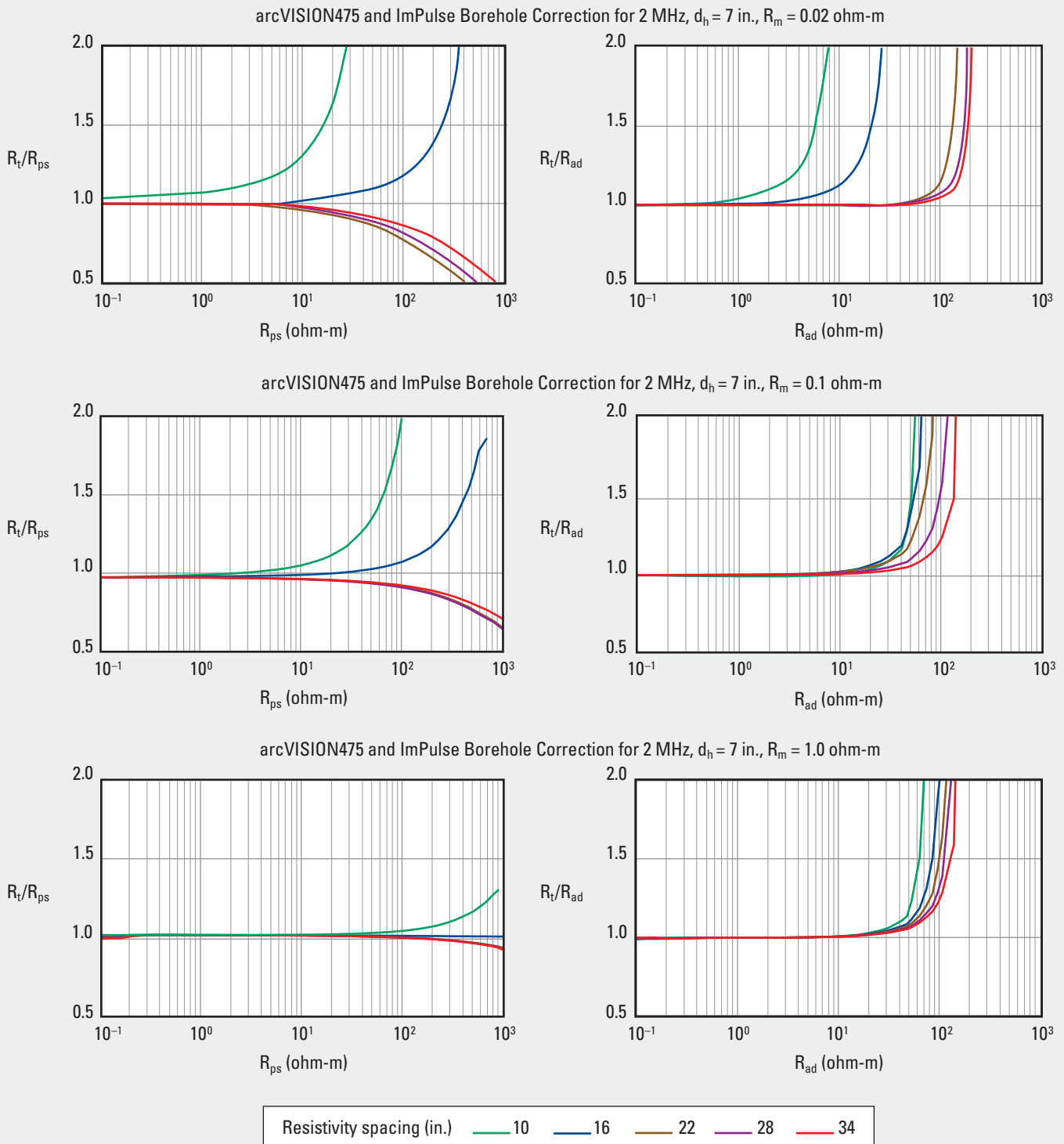


*Mark of Schlumberger
 © Schlumberger

REm

arcVISION475* and ImPulse* 4¾-in. Array
Resistivity Compensated Tools—2 MHz
Borehole Correction—Open Hole

REm-12



*Mark of Schlumberger
© Schlumberger

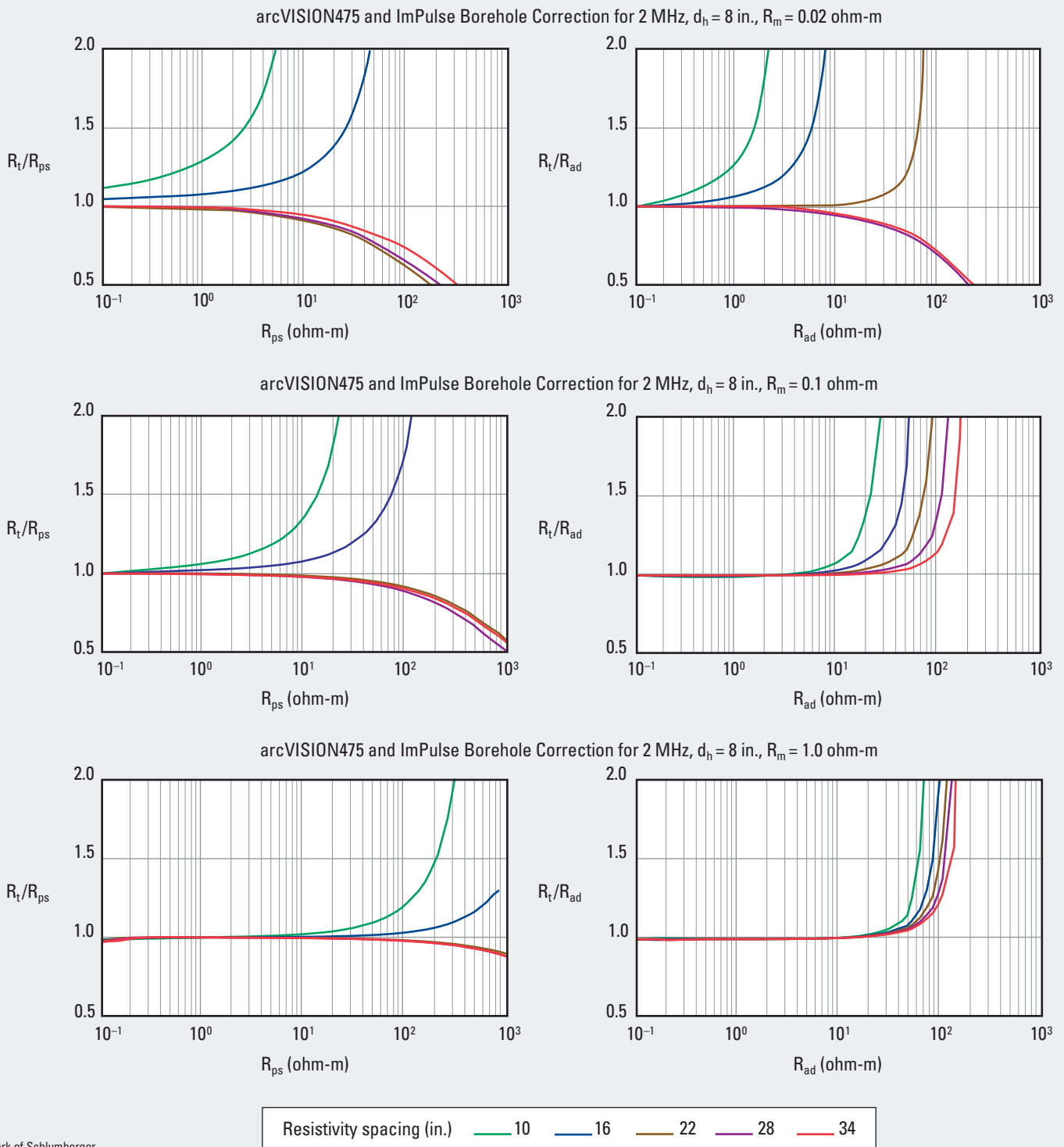
Purpose

This chart is used similarly to Chart REm-11 to determine the borehole correction applied by the surface acquisition system

to arcVISION475 and ImPulse resistivity measurements. Uncorrected resistivity is entered on the x-axis, not the resistivity shown on the log.

arcVISION475* and ImPulse* 4¾-in. Array
Resistivity Compensated Tools—2 MHz
Borehole Correction—Open Hole

REm-13



REm

Purpose

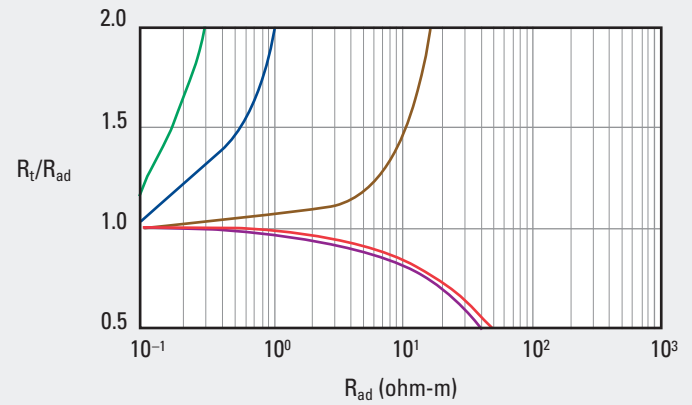
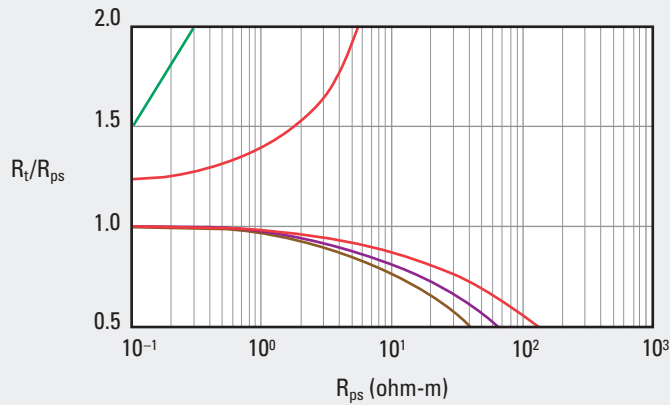
This chart is used similarly to Chart REm-11 to determine the borehole correction applied by the surface acquisition system

to arcVISION475 and ImPulse resistivity measurements. Uncorrected resistivity is entered on the x-axis, not the resistivity shown on the log.

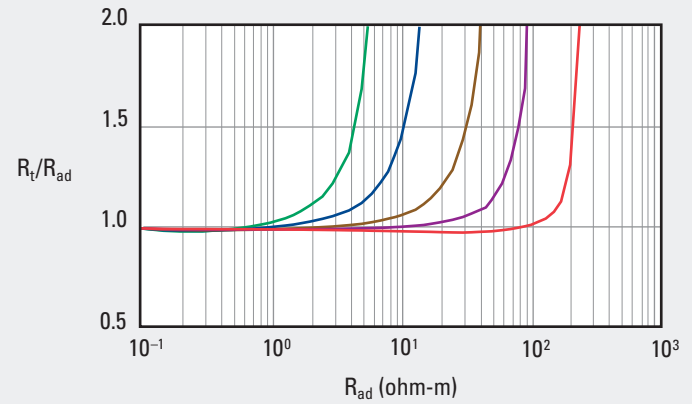
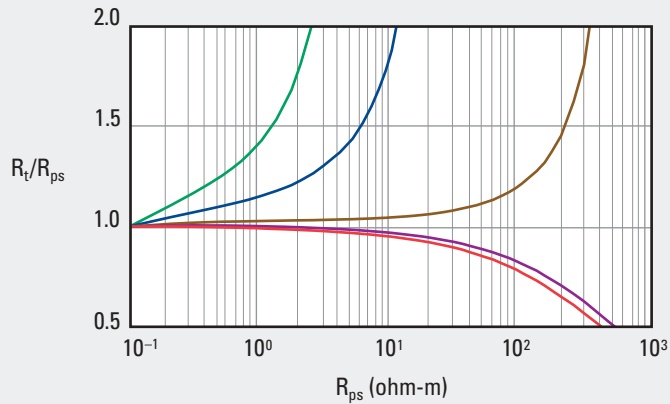
arcVISION475* and ImPulse* 4¾-in. Array
Resistivity Compensated Tools—2 MHz
Borehole Correction—Open Hole

REm-14

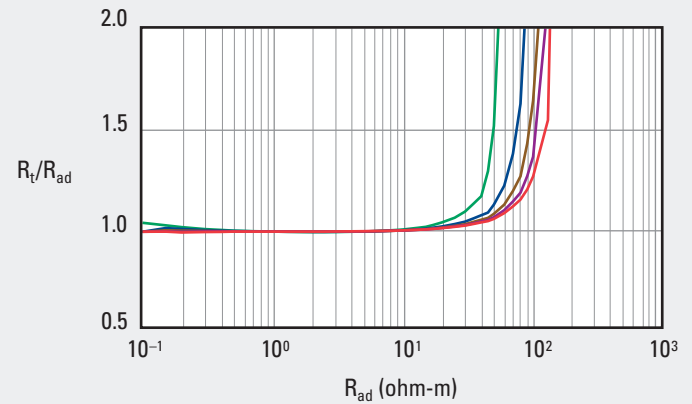
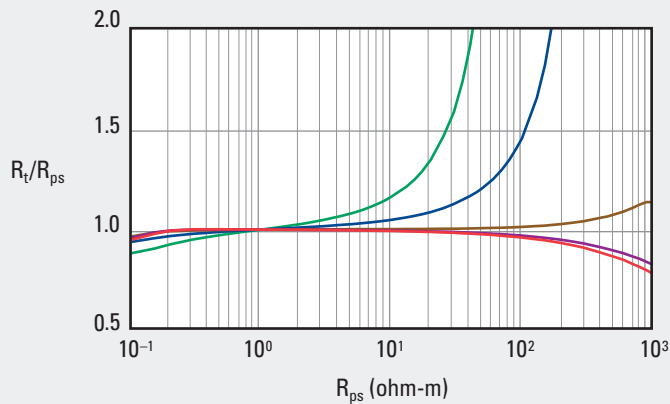
arcVISION475 and ImPulse Borehole Correction for 2 MHz, $d_h = 10$ in., $R_m = 0.02$ ohm-m



arcVISION475 and ImPulse Borehole Correction for 2 MHz, $d_h = 10$ in., $R_m = 0.1$ ohm-m



arcVISION475 and ImPulse Borehole Correction for 2 MHz, $d_h = 10$ in., $R_m = 1.0$ ohm-m



Resistivity spacing (in.) — 10 — 16 — 22 — 28 — 34

*Mark of Schlumberger
© Schlumberger

Purpose

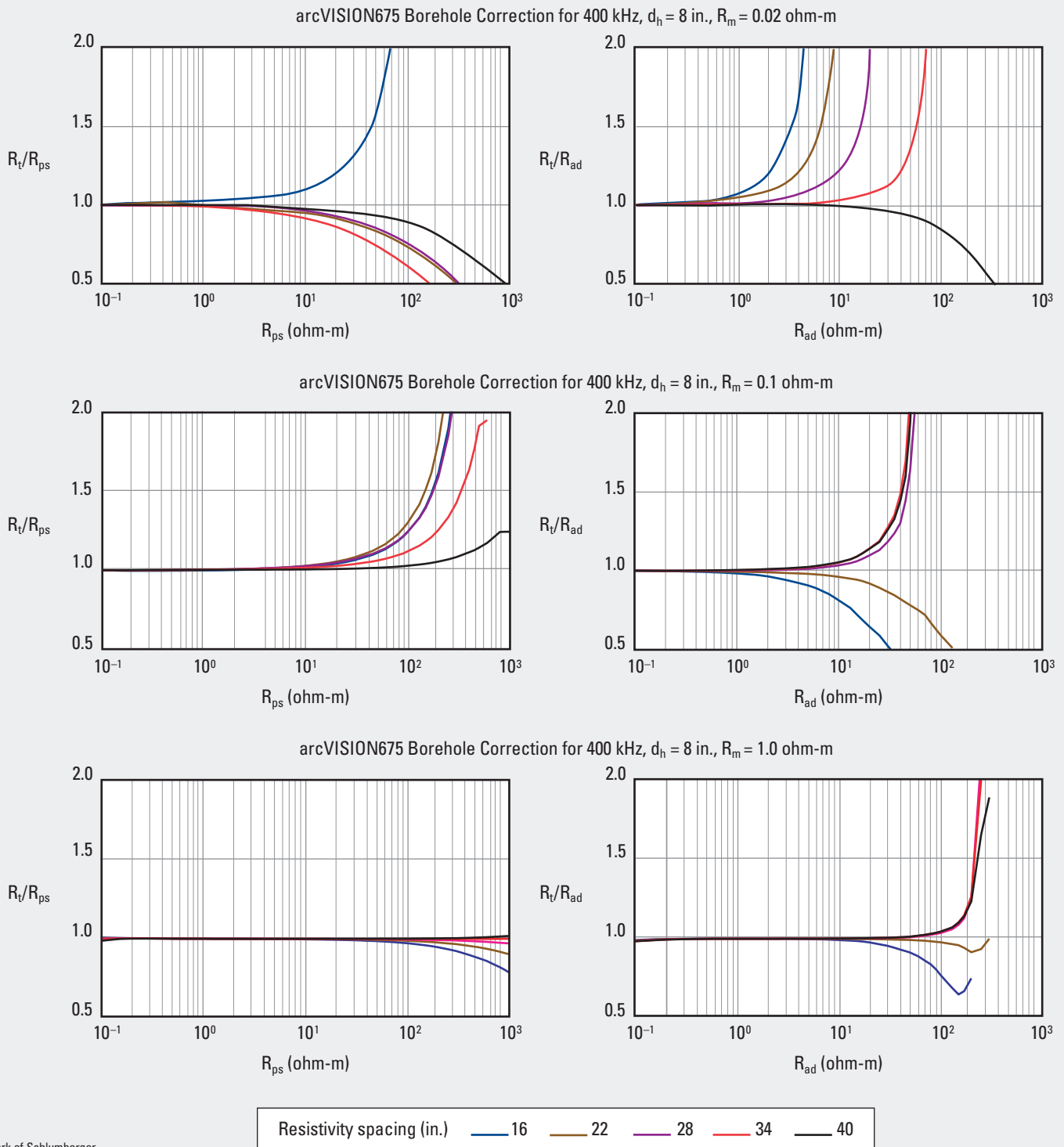
This chart is used similarly to Chart REm-11 to determine the borehole correction applied by the surface acquisition system

to arcVISION475 and ImPulse resistivity measurements. Uncorrected resistivity is entered on the x-axis, not the resistivity shown on the log.

arcVISION675* 6¾-in. Array Resistivity Compensated Tool—400 kHz

Borehole Correction—Open Hole

REm-15



*Mark of Schlumberger
© Schlumberger

Purpose

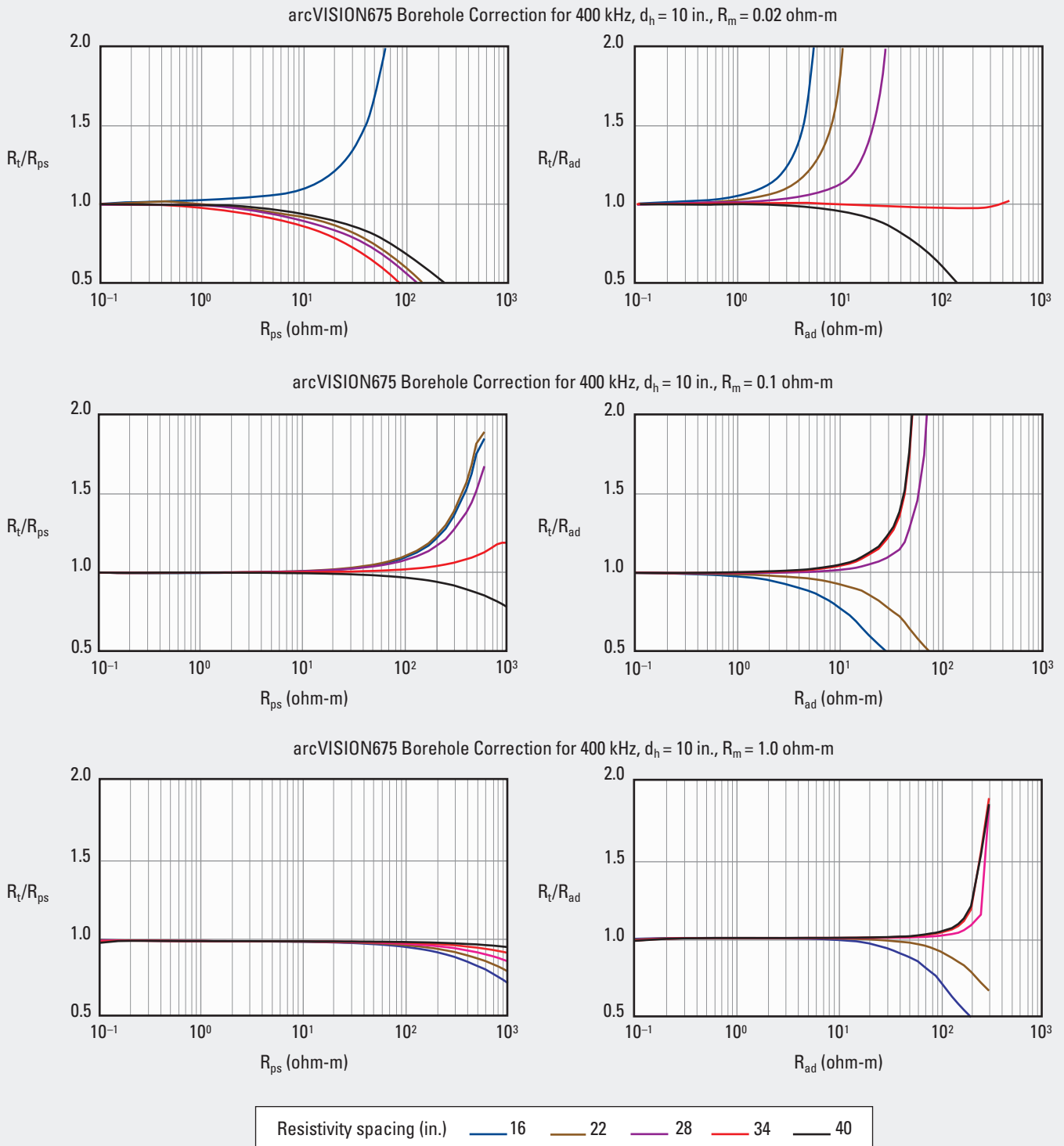
This chart is used similarly to Chart REm-11 to determine the borehole correction applied by the surface acquisition system

to arcVISION675 resistivity measurements. Uncorrected resistivity is entered on the x-axis, not the resistivity shown on the log.

arcVISION675* 6¾-in. Array Resistivity Compensated Tool—400 kHz

Borehole Correction—Open Hole

REm-16



*Mark of Schlumberger
© Schlumberger

Purpose

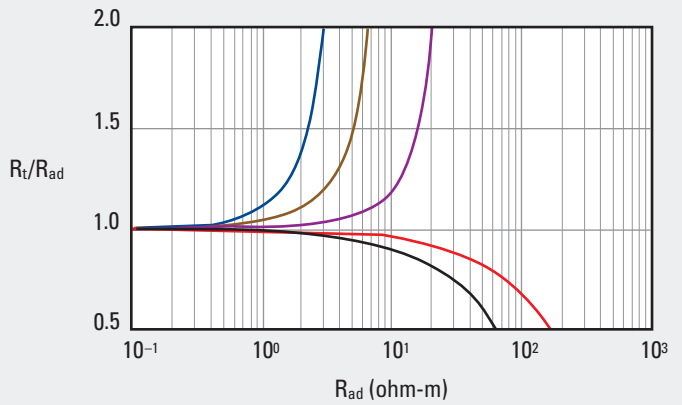
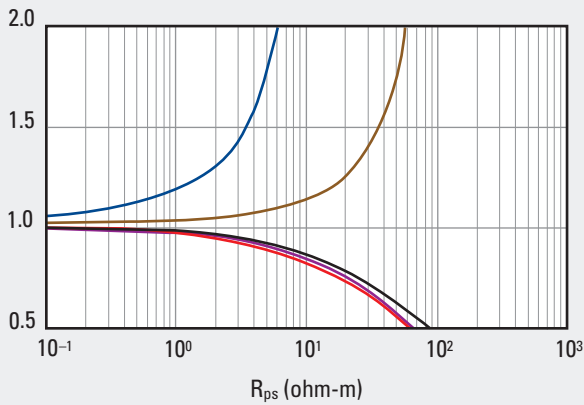
This chart is used similarly to Chart REm-11 to determine the borehole correction applied by the surface acquisition system

to arcVISION675 resistivity measurements. Uncorrected resistivity is entered on the x-axis, not the resistivity shown on the log.

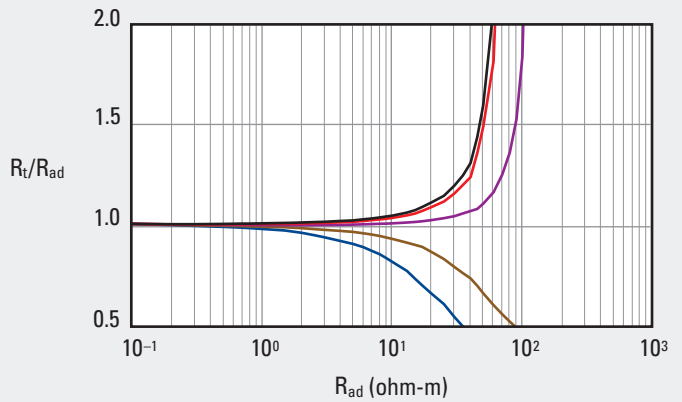
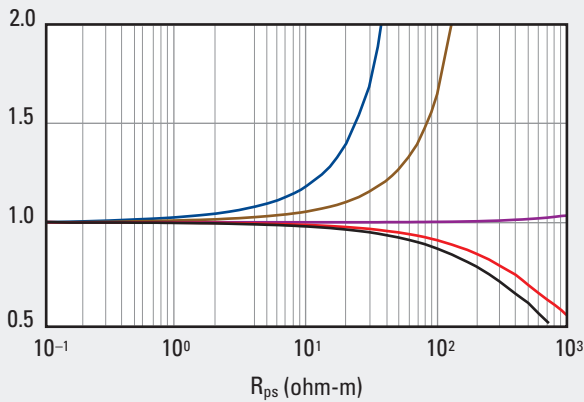
arcVISION675* 6¾-in. Array Resistivity Compensated Tool—400 kHz

Borehole Correction—Open Hole

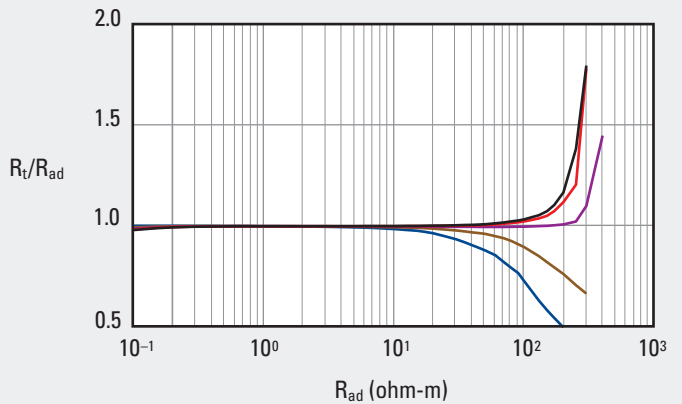
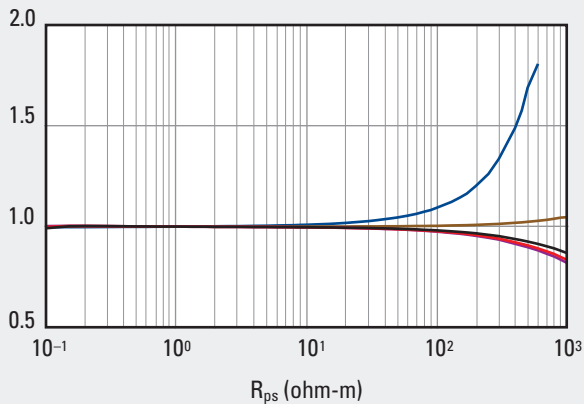
REm-17



arcVISION675 Borehole Correction for 400 kHz, $d_h = 12$ in., $R_m = 0.1$ ohm-m



arcVISION675 Borehole Correction for 400 kHz, $d_h = 12$ in., $R_m = 1.0$ ohm-m



Resistivity spacing (in.) — 16 — 22 — 28 — 34 — 40

*Mark of Schlumberger
© Schlumberger

Purpose

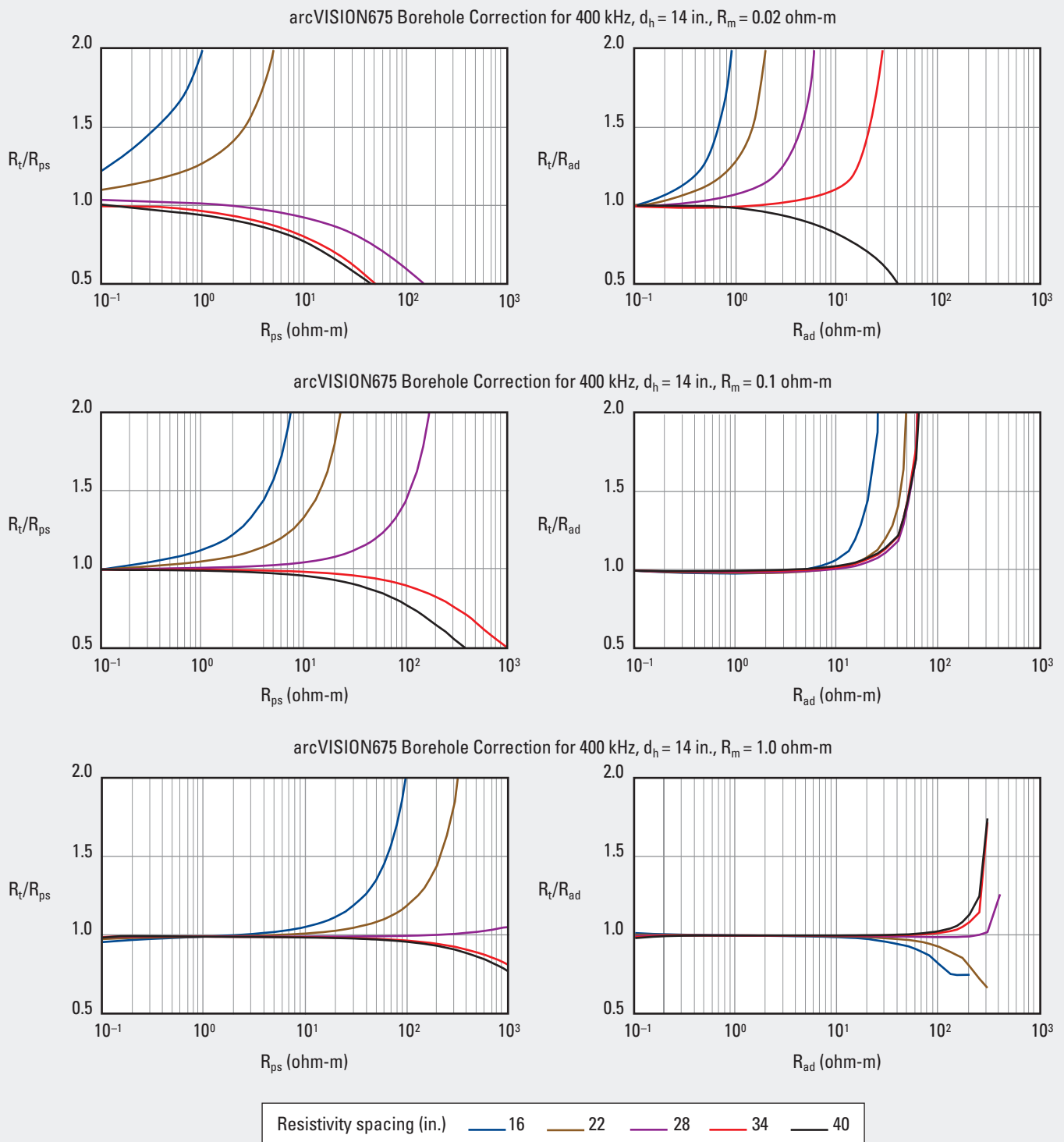
This chart is used similarly to Chart REm-11 to determine the borehole correction applied by the surface acquisition system

to arcVISION675 resistivity measurements. Uncorrected resistivity is entered on the x-axis, not the resistivity shown on the log.

arcVISION675* 6¾-in. Array Resistivity Compensated Tool—400 kHz

Borehole Correction—Open Hole

REm-18



*Mark of Schlumberger
© Schlumberger

Purpose

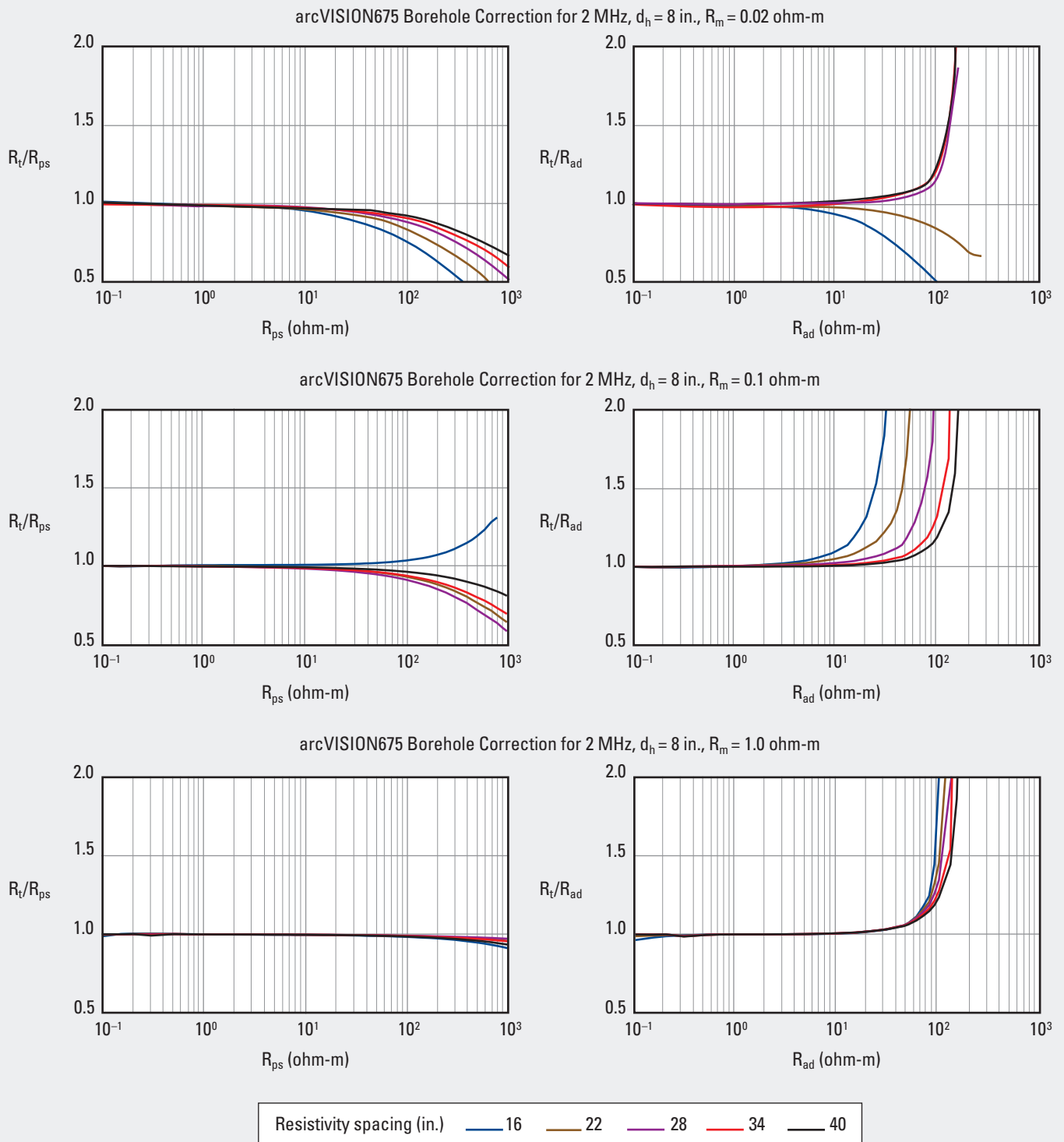
This chart is used similarly to Chart REm-11 to determine the borehole correction applied by the surface acquisition system

to arcVISION675 resistivity measurements. Uncorrected resistivity is entered on the x-axis, not the resistivity shown on the log.

arcVISION675* 6¾-in. Array Resistivity Compensated Tool—2 MHz

Borehole Correction—Open Hole

REm-19



*Mark of Schlumberger
© Schlumberger

Purpose

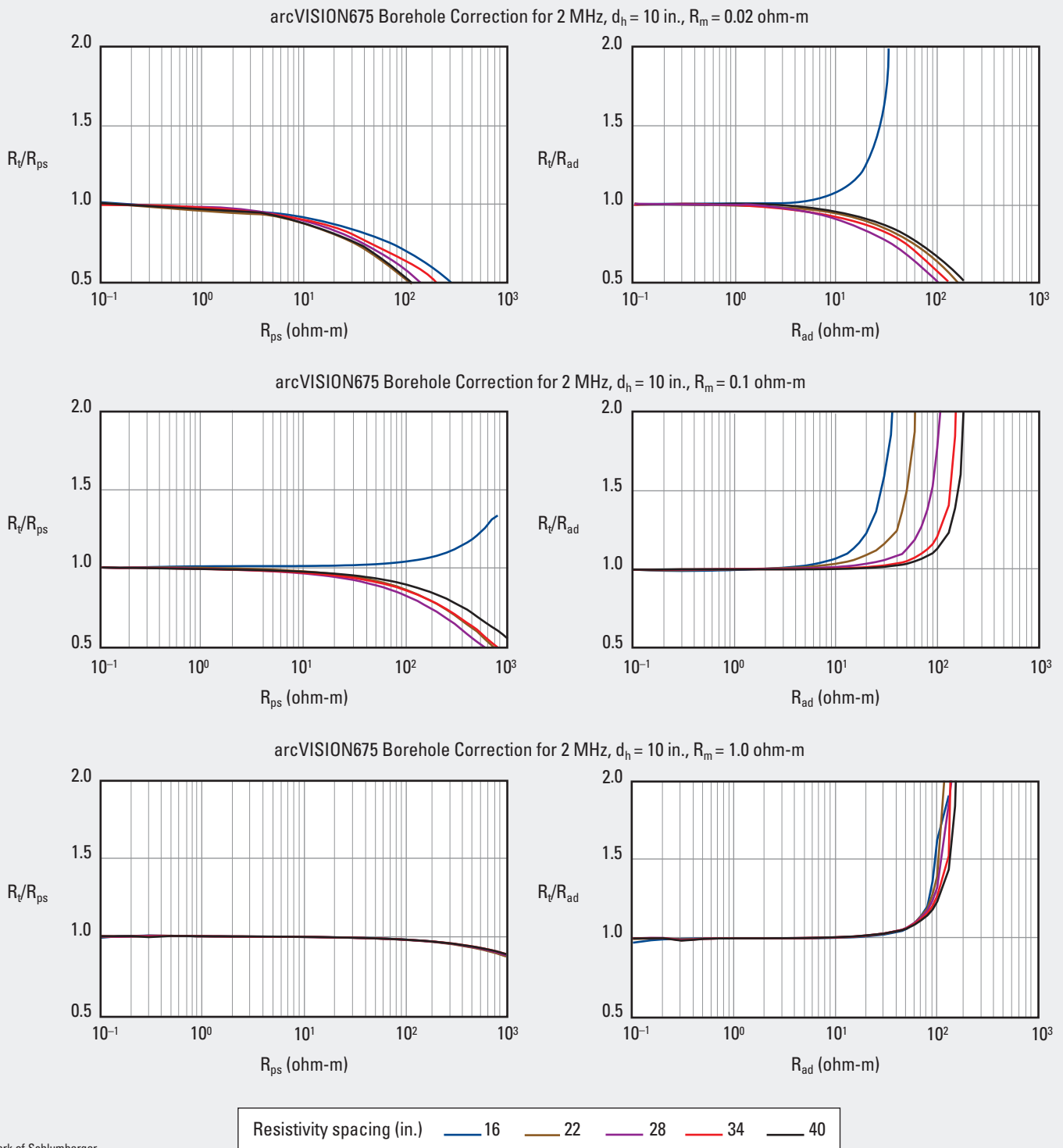
This chart is used similarly to Chart REm-11 to determine the borehole correction applied by the surface acquisition system

to arcVISION675 resistivity measurements. Uncorrected resistivity is entered on the x-axis, not the resistivity shown on the log.

arcVISION675* 6¾-in. Array Resistivity Compensated Tool—2 MHz

Bed Thickness Correction—Open Hole

REm-20



*Mark of Schlumberger
© Schlumberger

Purpose

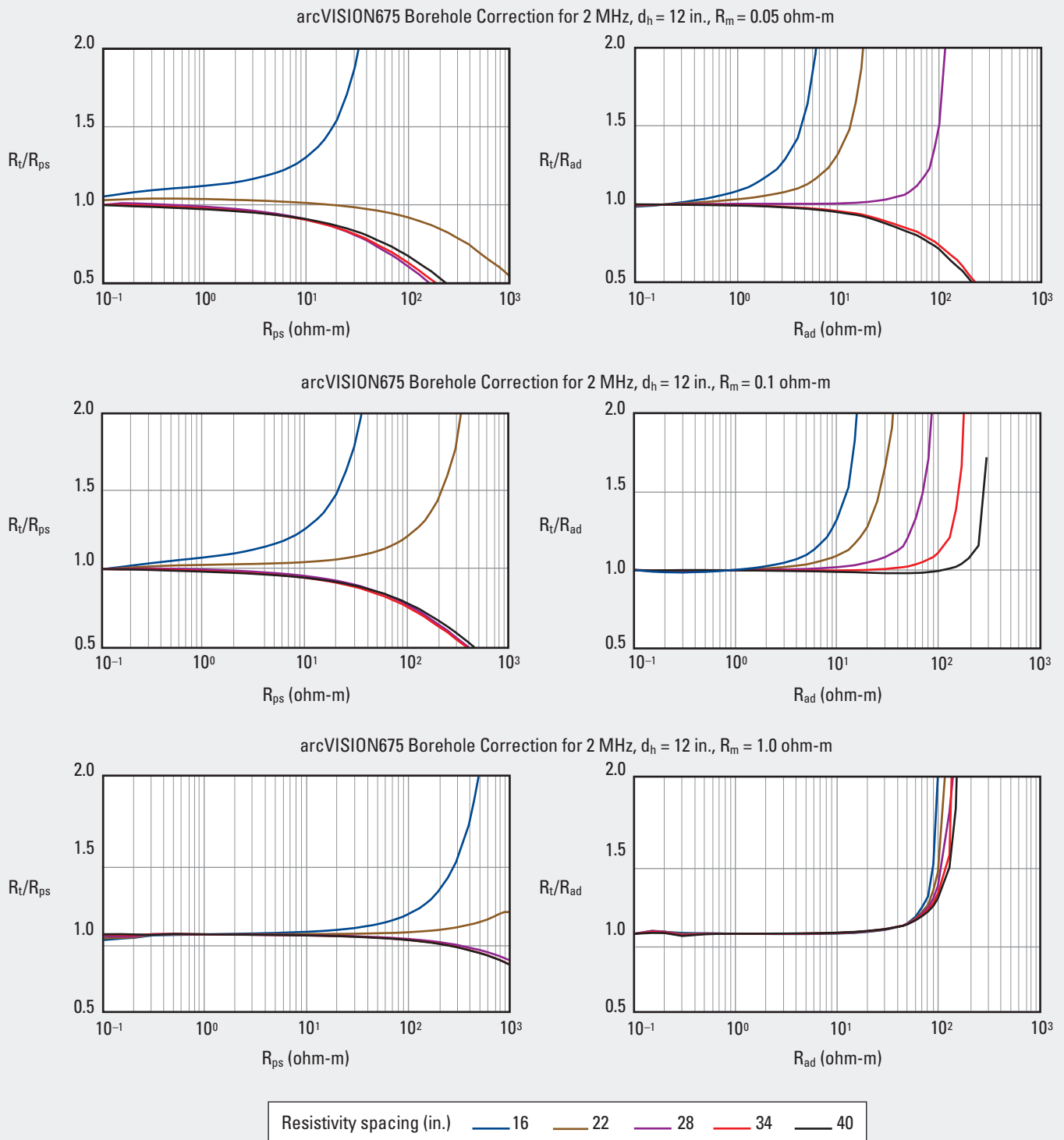
This chart is used similarly to Chart REm-11 to determine the borehole correction applied by the surface acquisition system

to arcVISION675 resistivity measurements. Uncorrected resistivity is entered on the x-axis, not the resistivity shown on the log.

arcVISION675* 6¾-in. Array Resistivity Compensated Tool—2 MHz

Borehole Correction—Open Hole

REm-21



*Mark of Schlumberger
© Schlumberger

Purpose

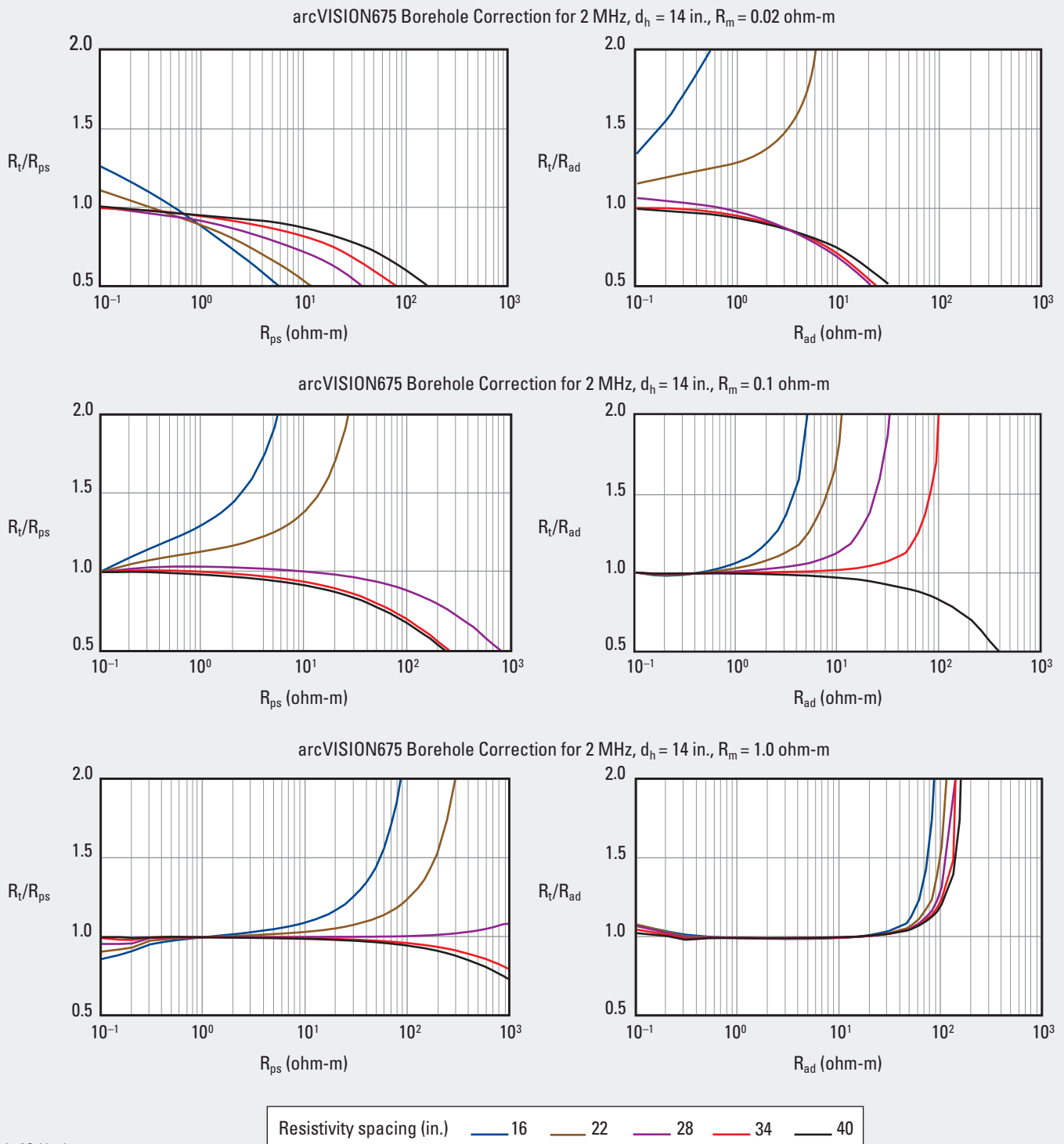
This chart is used similarly to Chart REm-11 to determine the borehole correction applied by the surface acquisition system

to arcVISION675 resistivity measurements. Uncorrected resistivity is entered on the x-axis, not the resistivity shown on the log.

arcVISION675* 6¾-in. Array Resistivity Compensated Tool—2 MHz

Borehole Correction—Open Hole

REm-22



*Mark of Schlumberger
© Schlumberger

Purpose

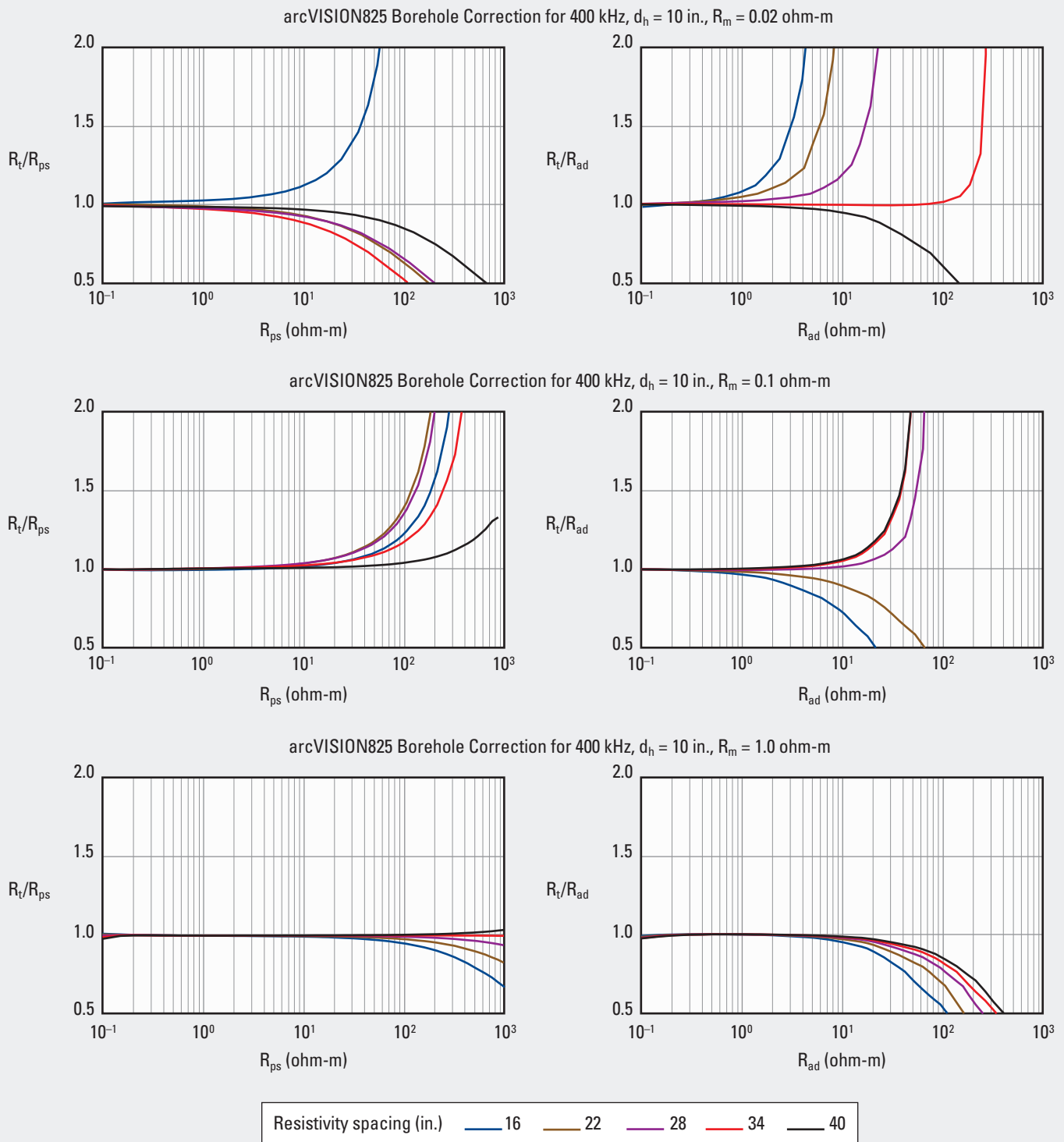
This chart is used similarly to Chart REm-11 to determine the borehole correction applied by the surface acquisition system

to arcVISION675 resistivity measurements. Uncorrected resistivity is entered on the x-axis, not the resistivity shown on the log.

arcVISION825* 8¼-in. Array Resistivity Compensated Tool—400 kHz

Borehole Correction—Open Hole

REm-23



*Mark of Schlumberger
© Schlumberger

Purpose

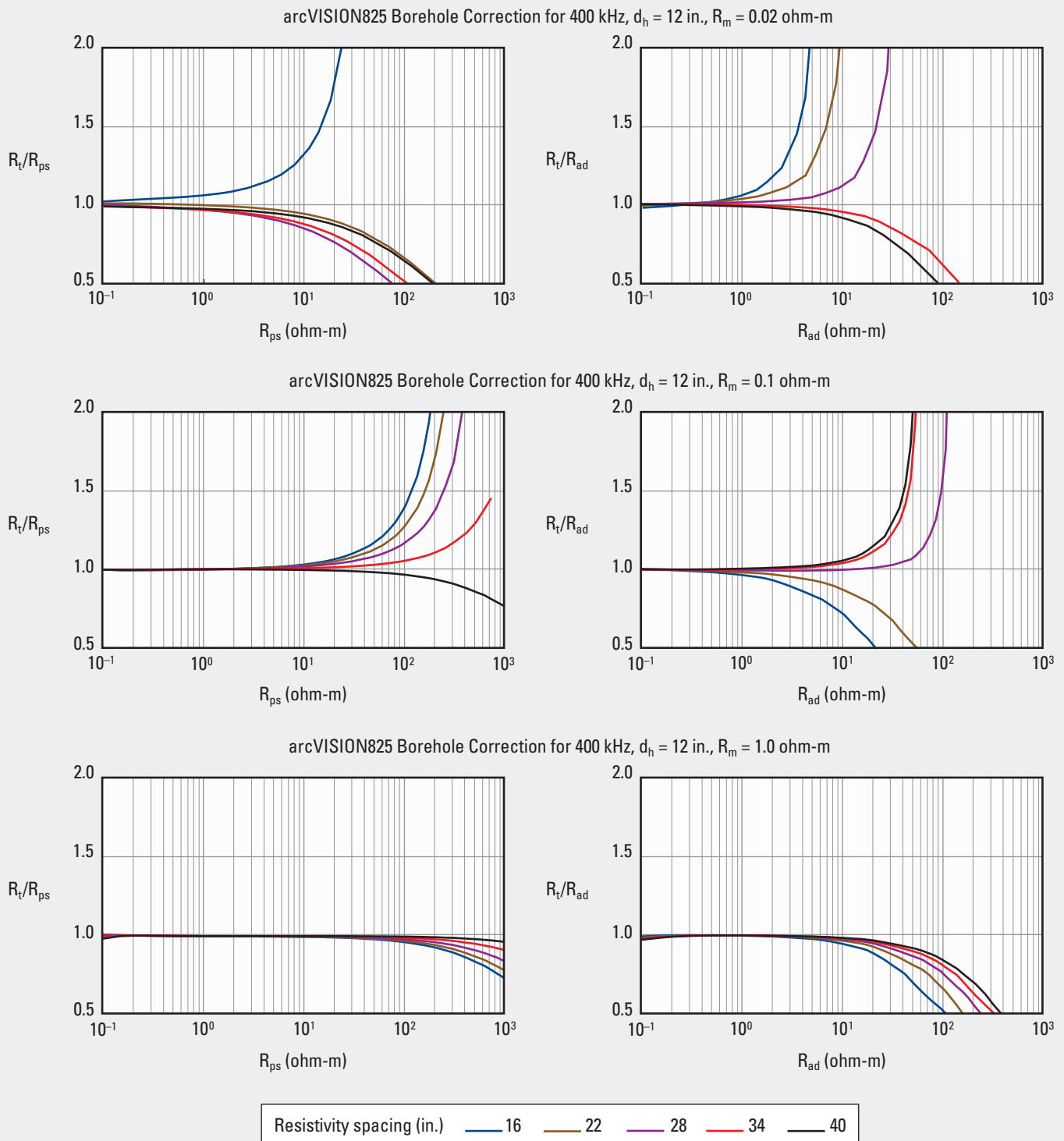
This chart is used similarly to Chart REm-11 to determine the borehole correction applied by the surface acquisition system

to arcVISION825 resistivity measurements. Uncorrected resistivity is entered on the x-axis, not the resistivity shown on the log.

arcVISION825* 8¼-in. Array Resistivity Compensated Tool—400 kHz

Bed Thickness Correction—Open Hole

REm-24



*Mark of Schlumberger
© Schlumberger

Purpose

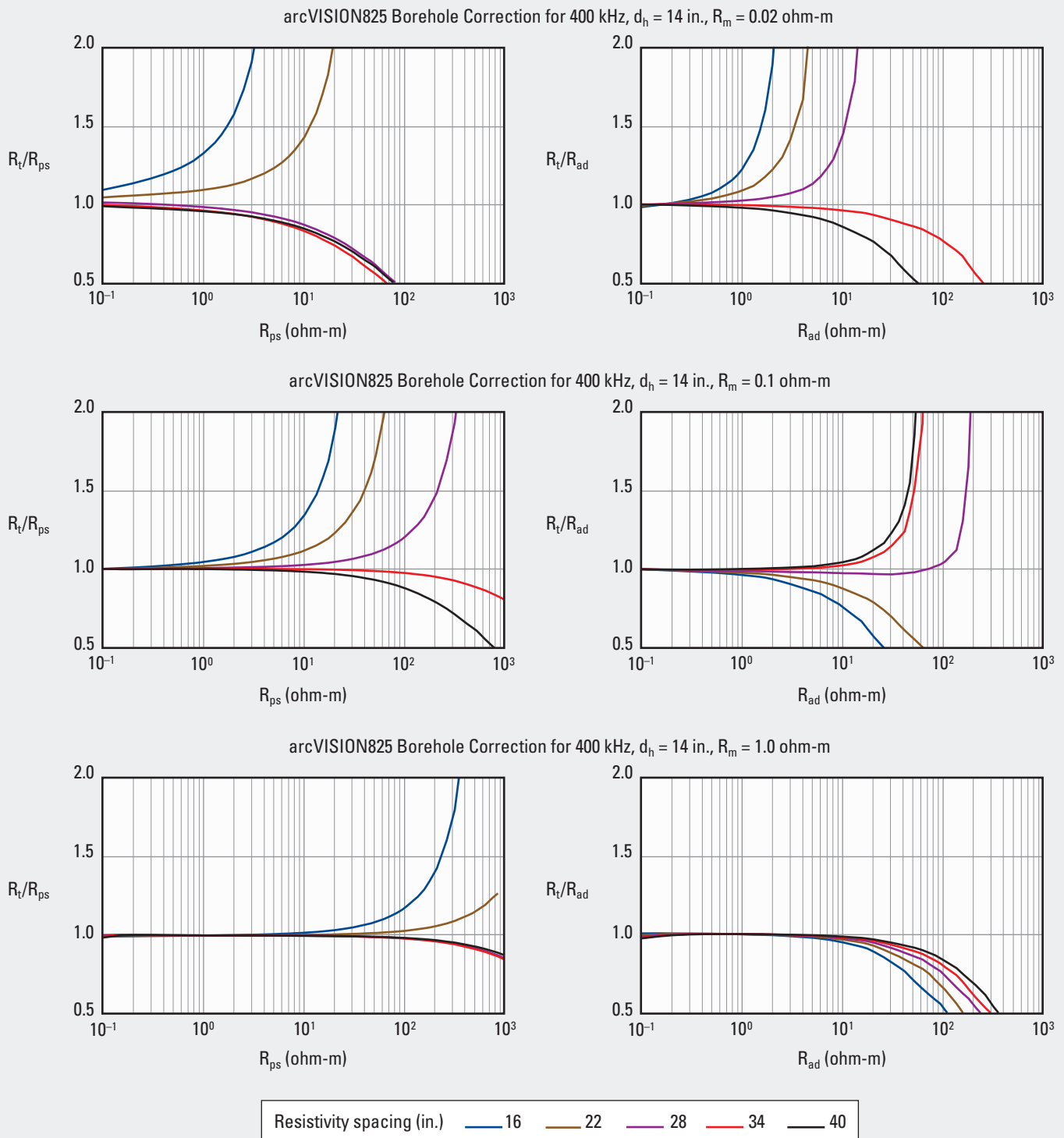
This chart is used similarly to Chart REm-11 to determine the borehole correction applied by the surface acquisition system

to arcVISION825 resistivity measurements. Uncorrected resistivity is entered on the x-axis, not the resistivity shown on the log.

arcVISION825* 8¼-in. Array Resistivity Compensated Tool—400 kHz

Borehole Correction—Open Hole

REm-25



*Mark of Schlumberger
© Schlumberger

Purpose

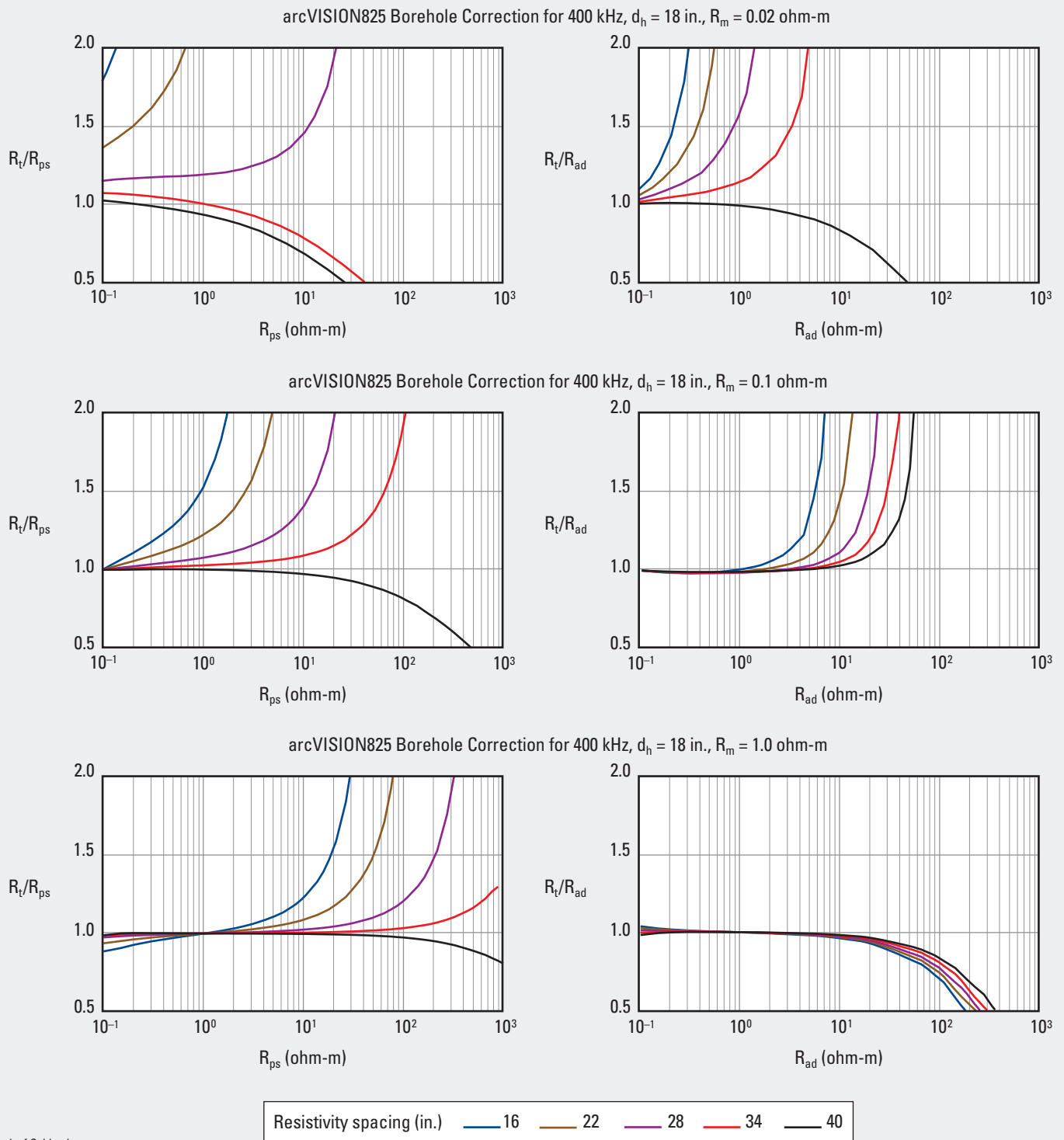
This chart is used similarly to Chart REm-11 to determine the borehole correction applied by the surface acquisition system

to arcVISION825 resistivity measurements. Uncorrected resistivity is entered on the x-axis, not the resistivity shown on the log.

arcVISION825* 8¼-in. Array Resistivity Compensated Tool—400 kHz

Borehole Correction—Open Hole

REm-26



*Mark of Schlumberger
© Schlumberger

Purpose

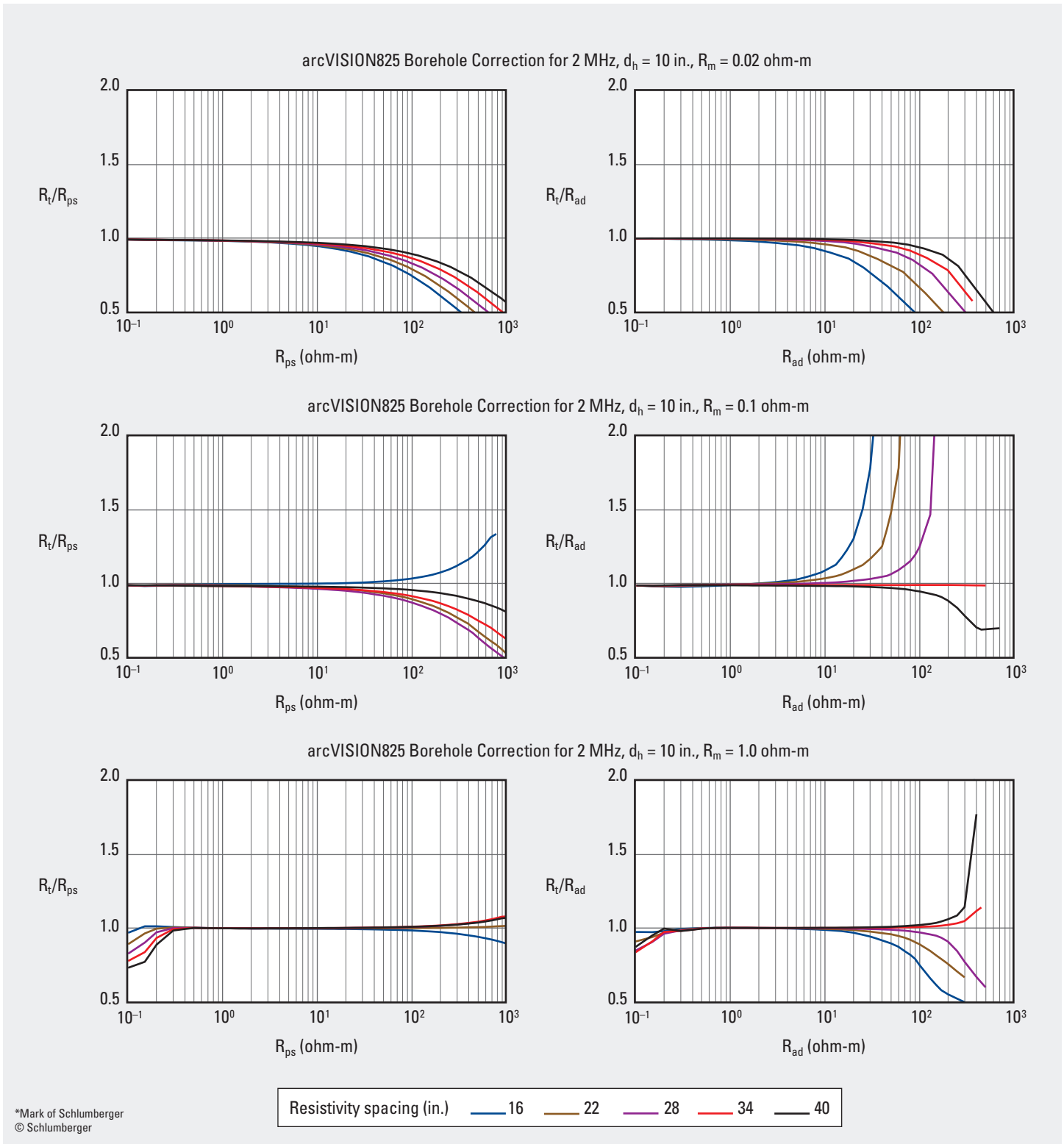
This chart is used similarly to Chart REm-11 to determine the borehole correction applied by the surface acquisition system

to arcVISION825 resistivity measurements. Uncorrected resistivity is entered on the x-axis, not the resistivity shown on the log.

arcVISION825* 8¼-in. Array Resistivity Compensated Tool—2 MHz

Borehole Correction—Open Hole

REm-27



REm

Purpose

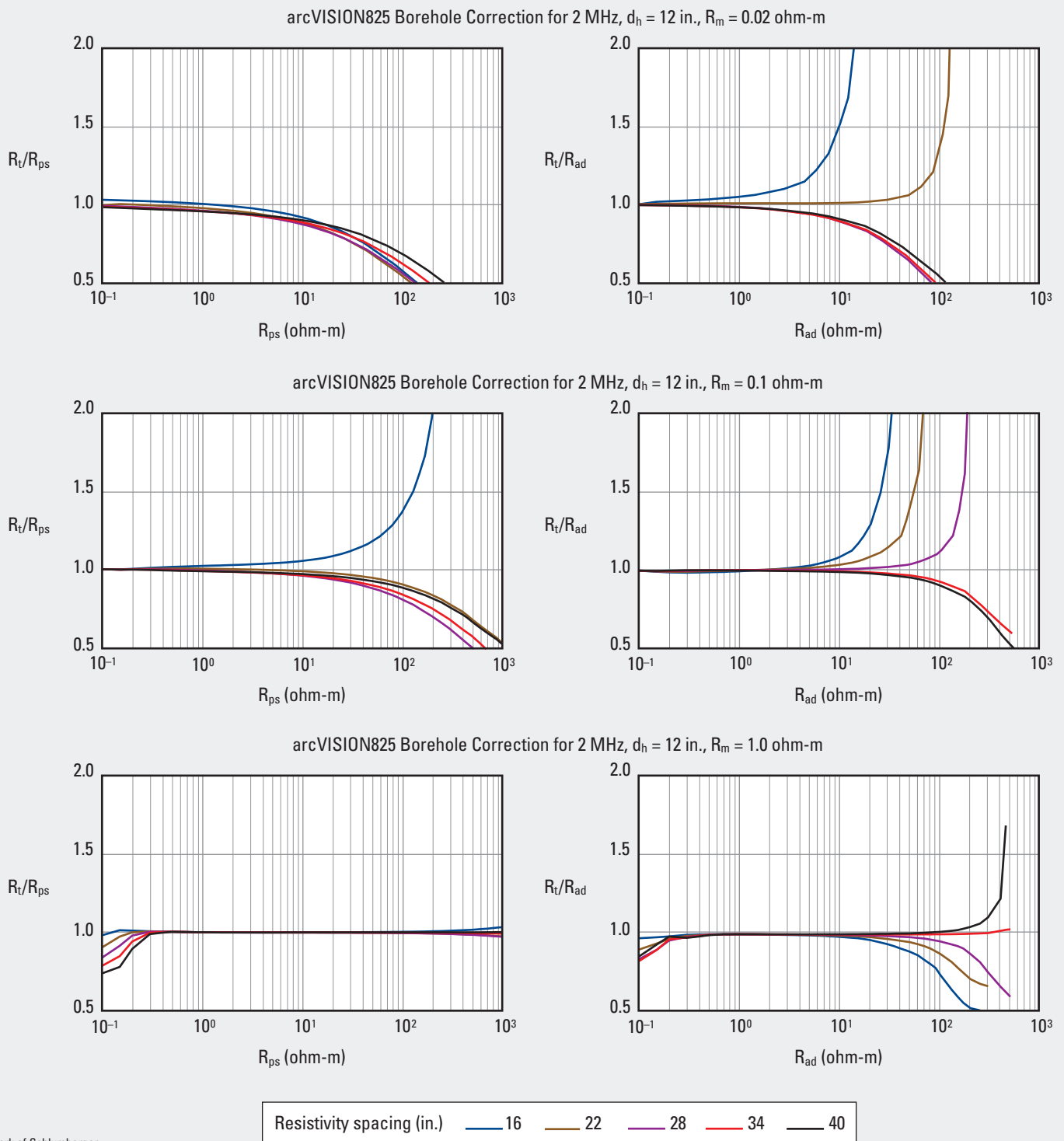
This chart is used similarly to Chart REm-11 to determine the borehole correction applied by the surface acquisition system

to arcVISION825 resistivity measurements. Uncorrected resistivity is entered on the x-axis, not the resistivity shown on the log.

arcVISION825* 8¼-in. Array Resistivity Compensated Tool—2 MHz

Borehole Correction—Open Hole

REm-28



*Mark of Schlumberger
© Schlumberger

Purpose

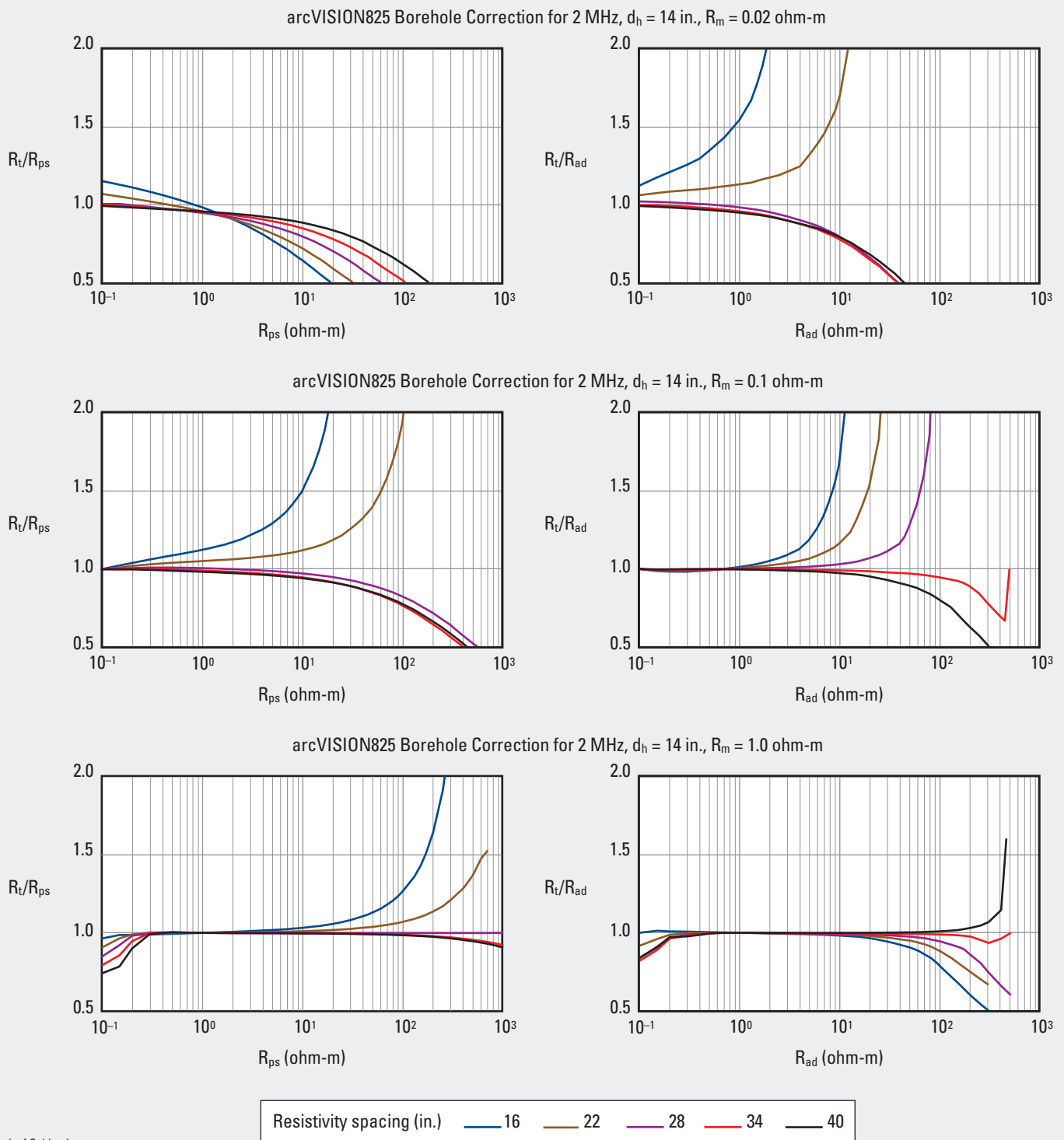
This chart is used similarly to Chart REm-11 to determine the borehole correction applied by the surface acquisition system

to arcVISION825 resistivity measurements. Uncorrected resistivity is entered on the x-axis, not the resistivity shown on the log.

arcVISION825* 8¼-in. Array Resistivity Compensated Tool—2 MHz

Borehole Correction—Open Hole

REm-29



*Mark of Schlumberger
© Schlumberger

Purpose

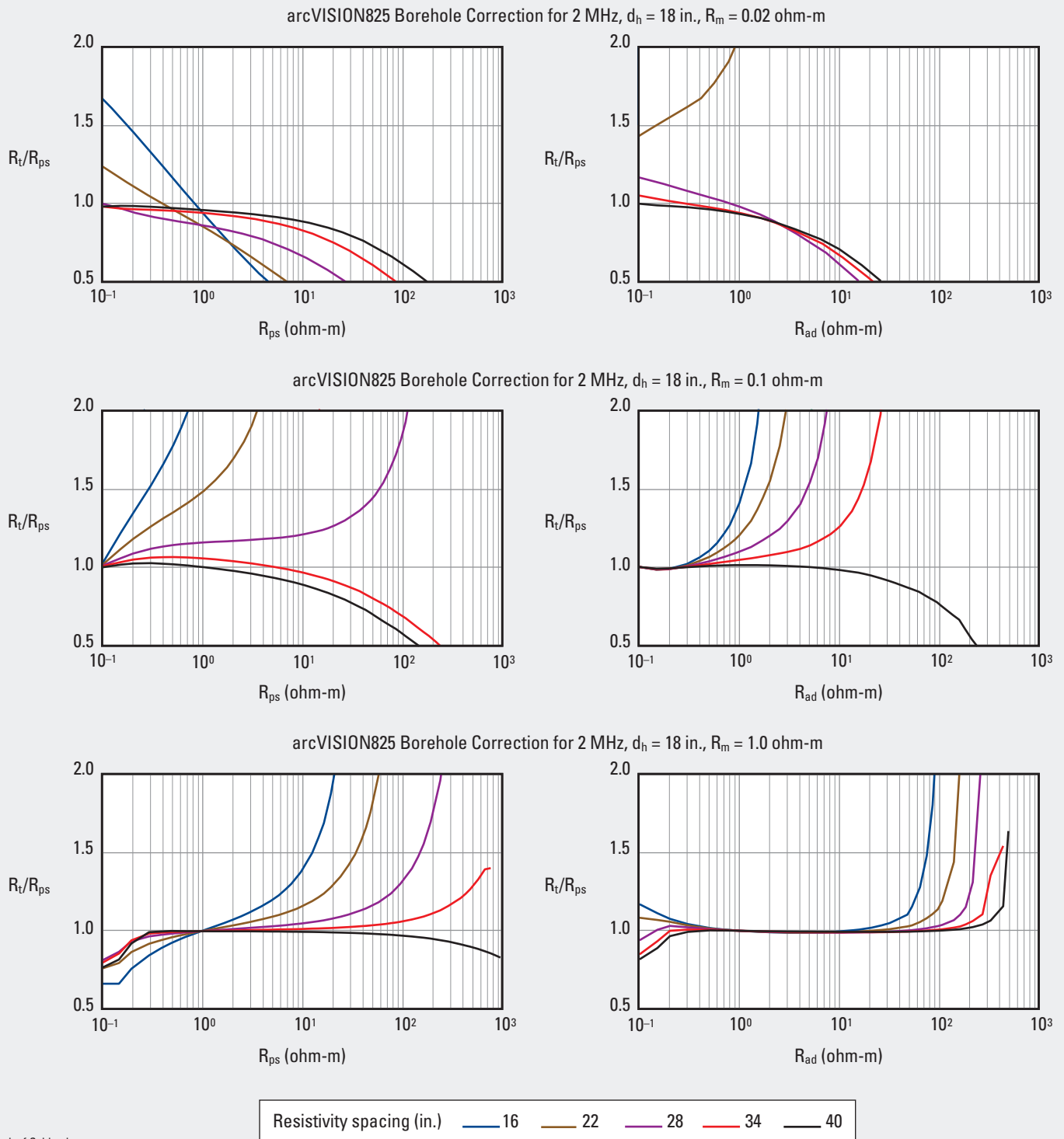
This chart is used similarly to Chart REm-11 to determine the borehole correction applied by the surface acquisition system

to arcVISION825 resistivity measurements. Uncorrected resistivity is entered on the x-axis, not the resistivity shown on the log.

arcVISION825* 8¼-in. Array Resistivity Compensated Tool—2 MHz

Borehole Correction—Open Hole

REm-30



*Mark of Schlumberger
© Schlumberger

Purpose

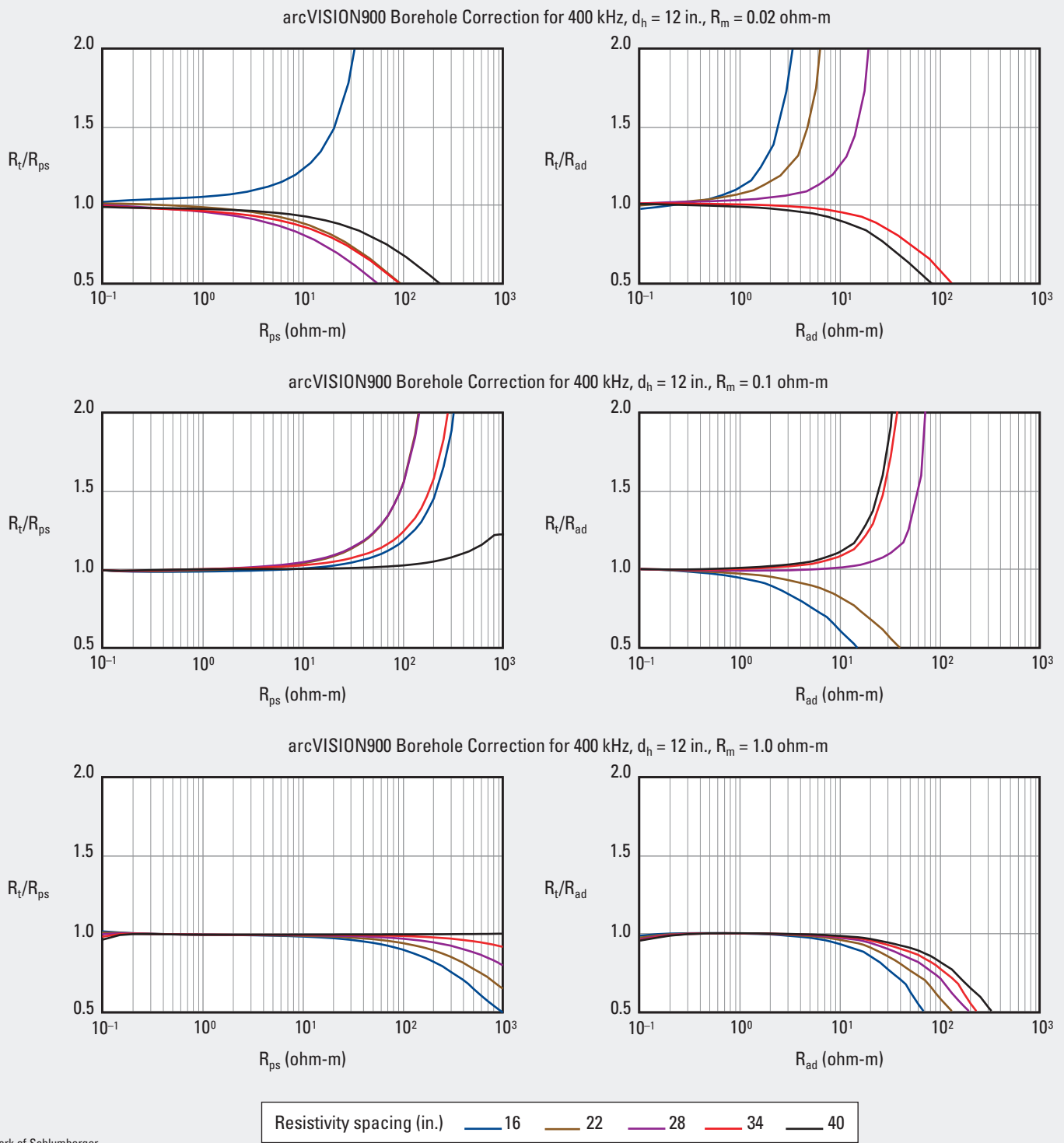
This chart is used similarly to Chart REm-11 to determine the borehole correction applied by the surface acquisition system

to arcVISION825 resistivity measurements. Uncorrected resistivity is entered on the x-axis, not the resistivity shown on the log.

arcVISION900* 9-in. Array Resistivity Compensated Tool—400 kHz

Borehole Correction—Open Hole

REm-31



*Mark of Schlumberger
© Schlumberger

Purpose

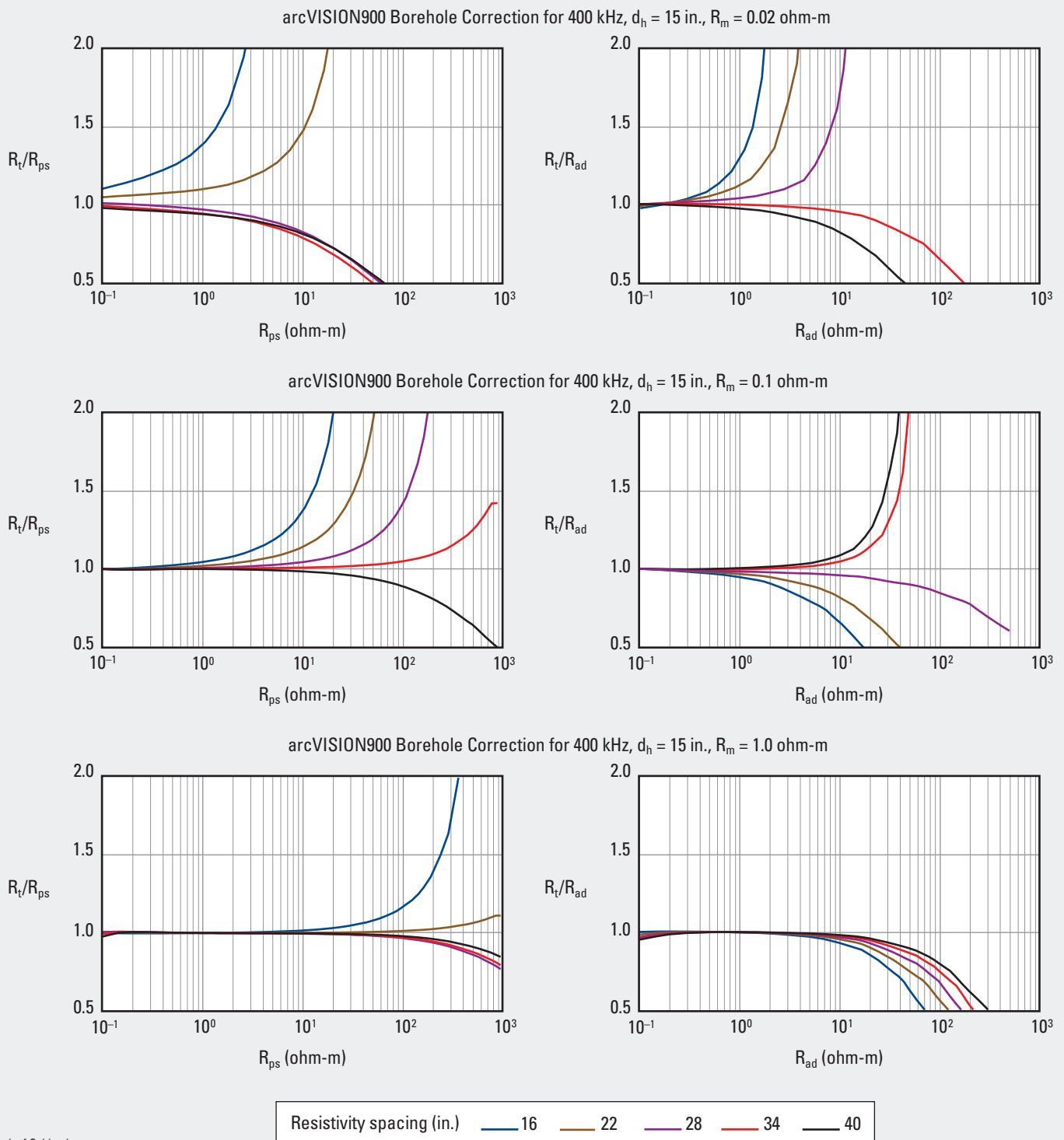
This chart is used similarly to Chart REm-11 to determine the borehole correction applied by the surface acquisition system

to arcVISION900 resistivity measurements. Uncorrected resistivity is entered on the x-axis, not the resistivity shown on the log.

arcVISION900* 9-in. Array Resistivity Compensated Tool—400 kHz

Borehole Correction—Open Hole

REm-32



REm

*Mark of Schlumberger
© Schlumberger

Purpose

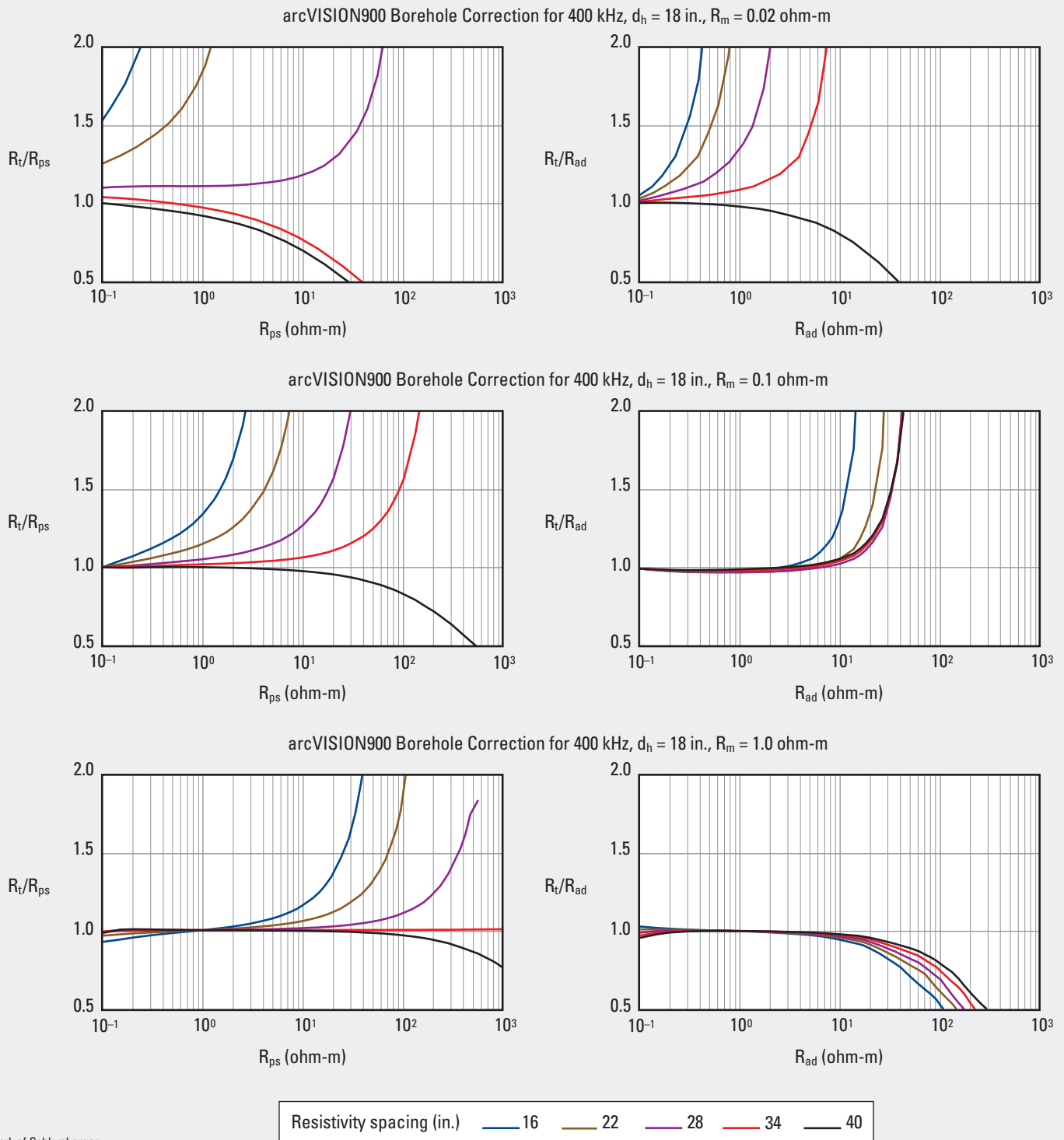
This chart is used similarly to Chart REm-11 to determine the borehole correction applied by the surface acquisition system

to arcVISION900 resistivity measurements. Uncorrected resistivity is entered on the x-axis, not the resistivity shown on the log.

arcVISION900* 9-in. Array Resistivity Compensated Tool—400 kHz

Borehole Correction—Open Hole

REm-33



*Mark of Schlumberger
© Schlumberger

Purpose

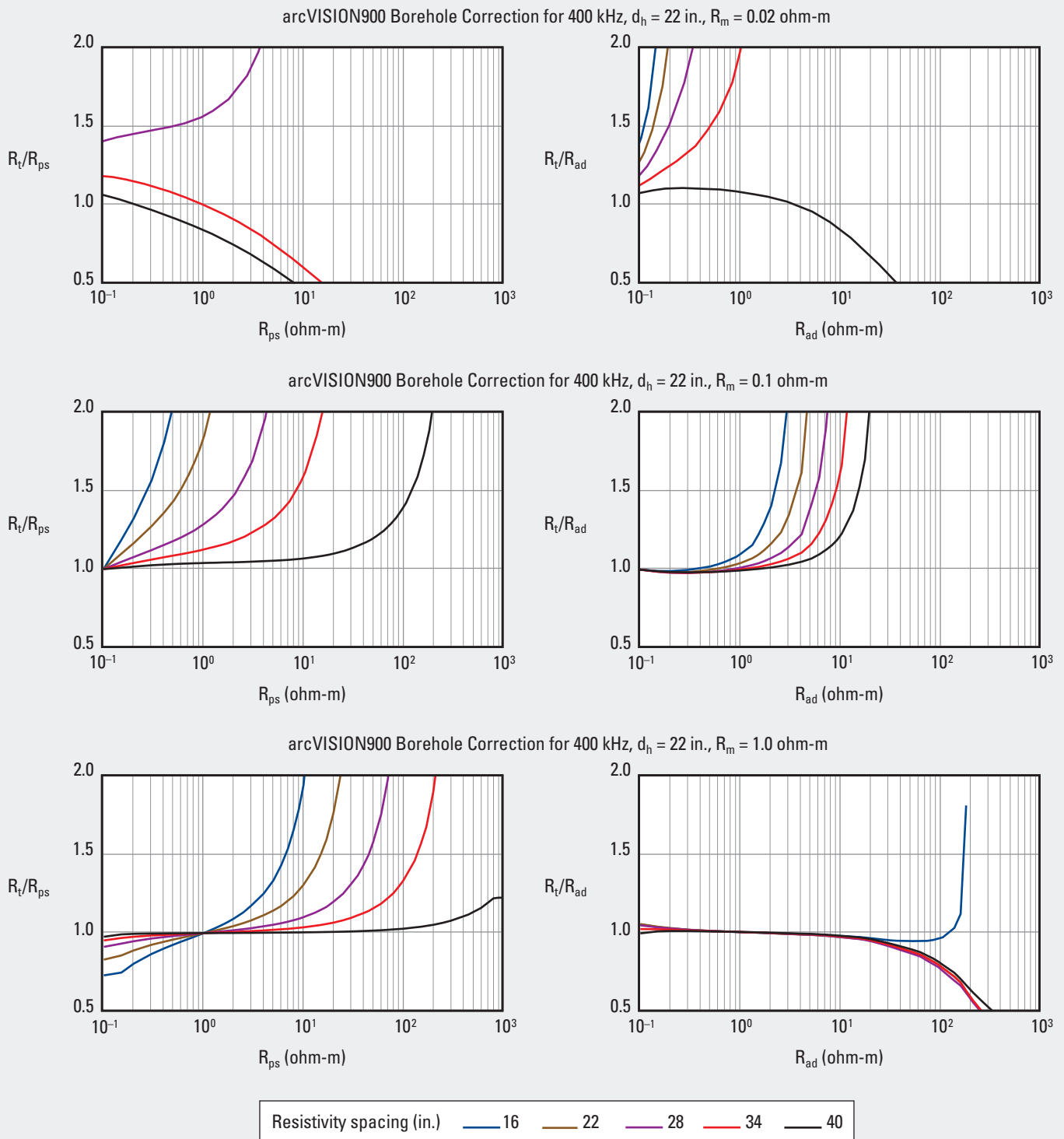
This chart is used similarly to Chart REm-11 to determine the borehole correction applied by the surface acquisition system

to arcVISION900 resistivity measurements. Uncorrected resistivity is entered on the x-axis, not the resistivity shown on the log.

arcVISION900* 9-in. Array Resistivity Compensated Tool—400 kHz

Borehole Correction—Open Hole

REm-34



*Mark of Schlumberger
© Schlumberger

Purpose

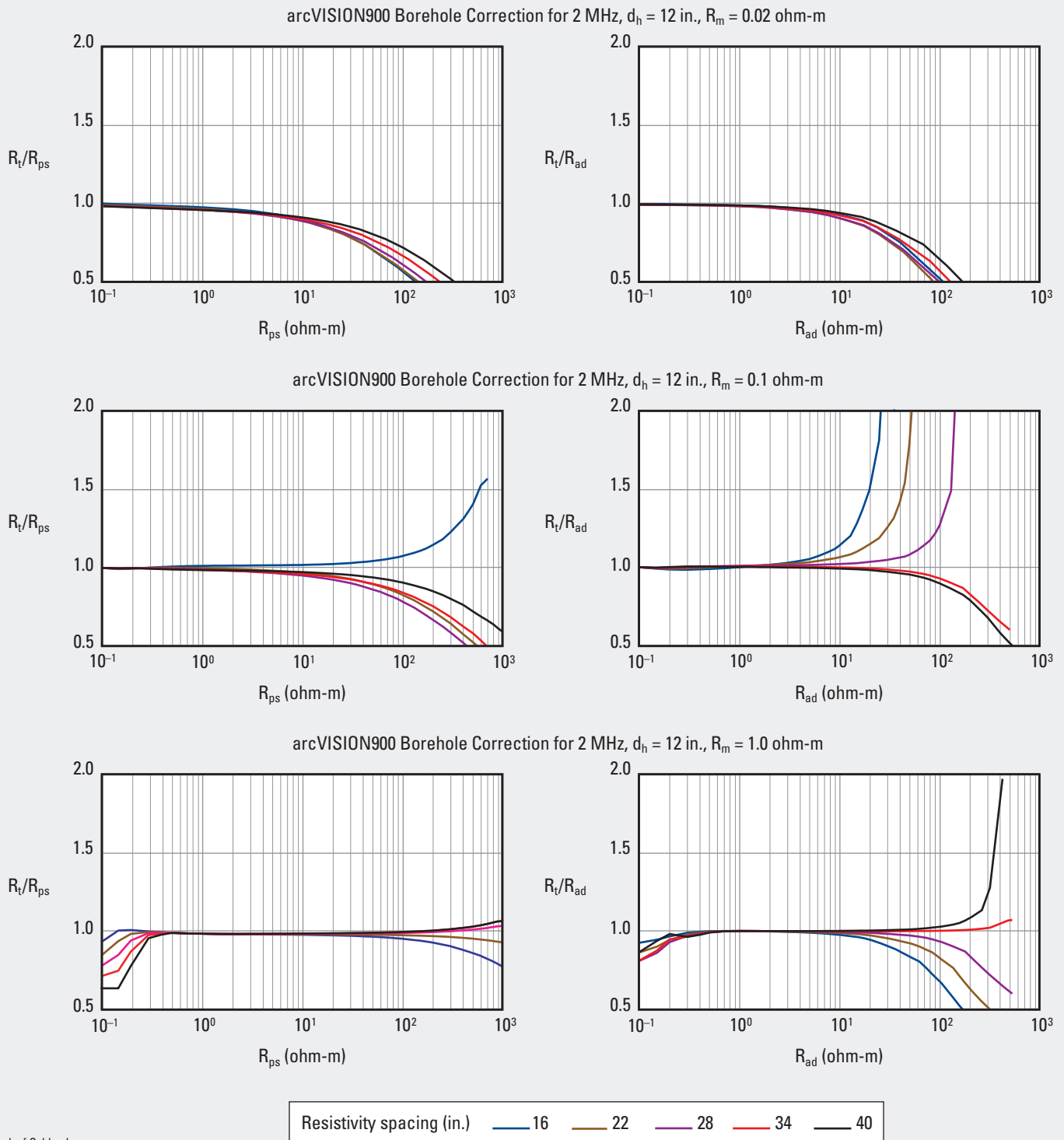
This chart is used similarly to Chart REm-11 to determine the borehole correction applied by the surface acquisition system

to arcVISION900 resistivity measurements. Uncorrected resistivity is entered on the x-axis, not the resistivity shown on the log.

arcVISION900* 9-in.Array Resistivity Compensated Tool—2 MHz

Borehole Correction—Open Hole

REm-35



*Mark of Schlumberger
© Schlumberger

Purpose

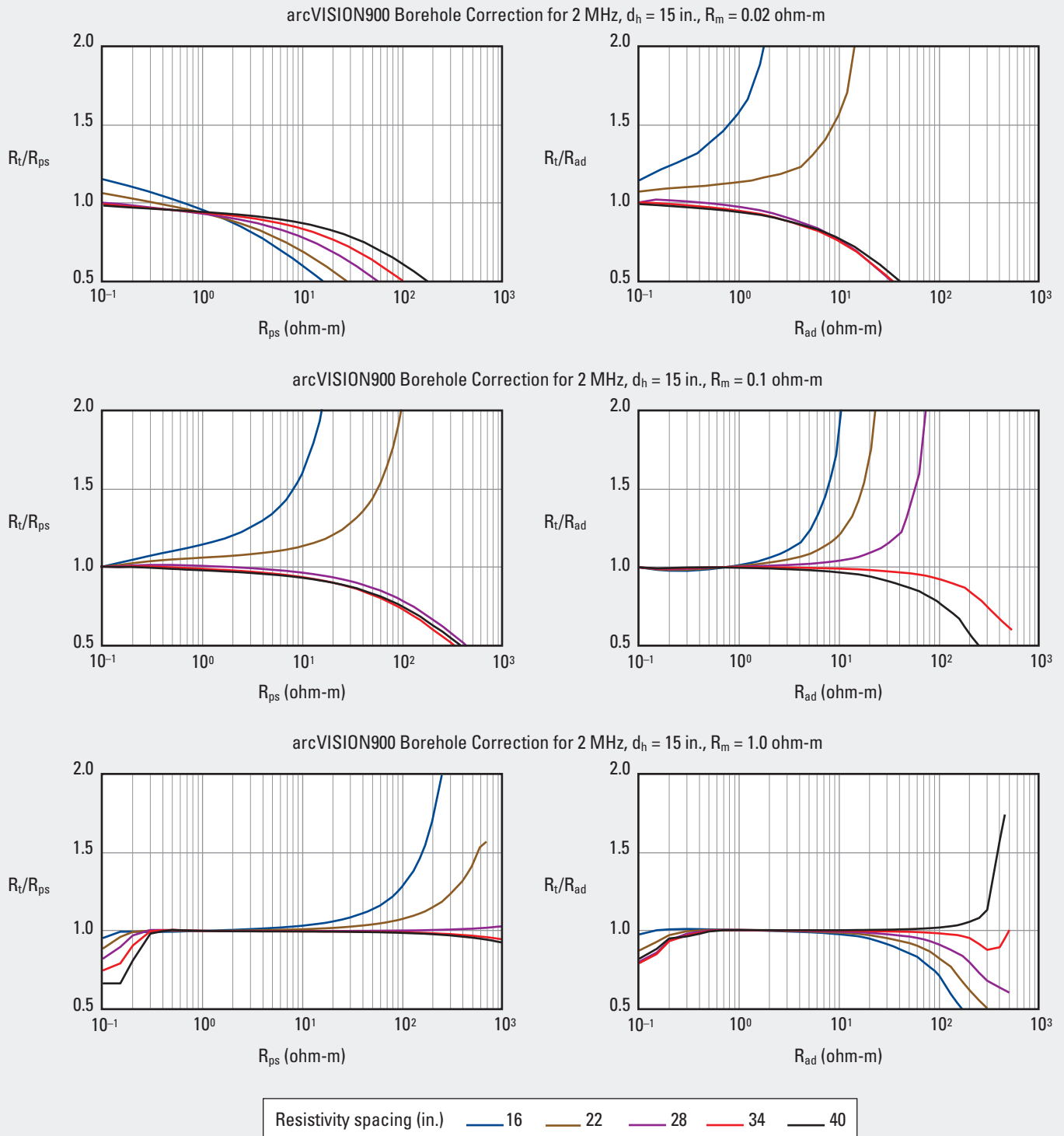
This chart is used similarly to Chart REm-11 to determine the borehole correction applied by the surface acquisition system

to arcVISION900 resistivity measurements. Uncorrected resistivity is entered on the x-axis, not the resistivity shown on the log.

arcVISION900* 9-in. Array Resistivity Compensated Tool—2 MHz

Borehole Correction—Open Hole

REm-36



*Mark of Schlumberger
© Schlumberger

Purpose

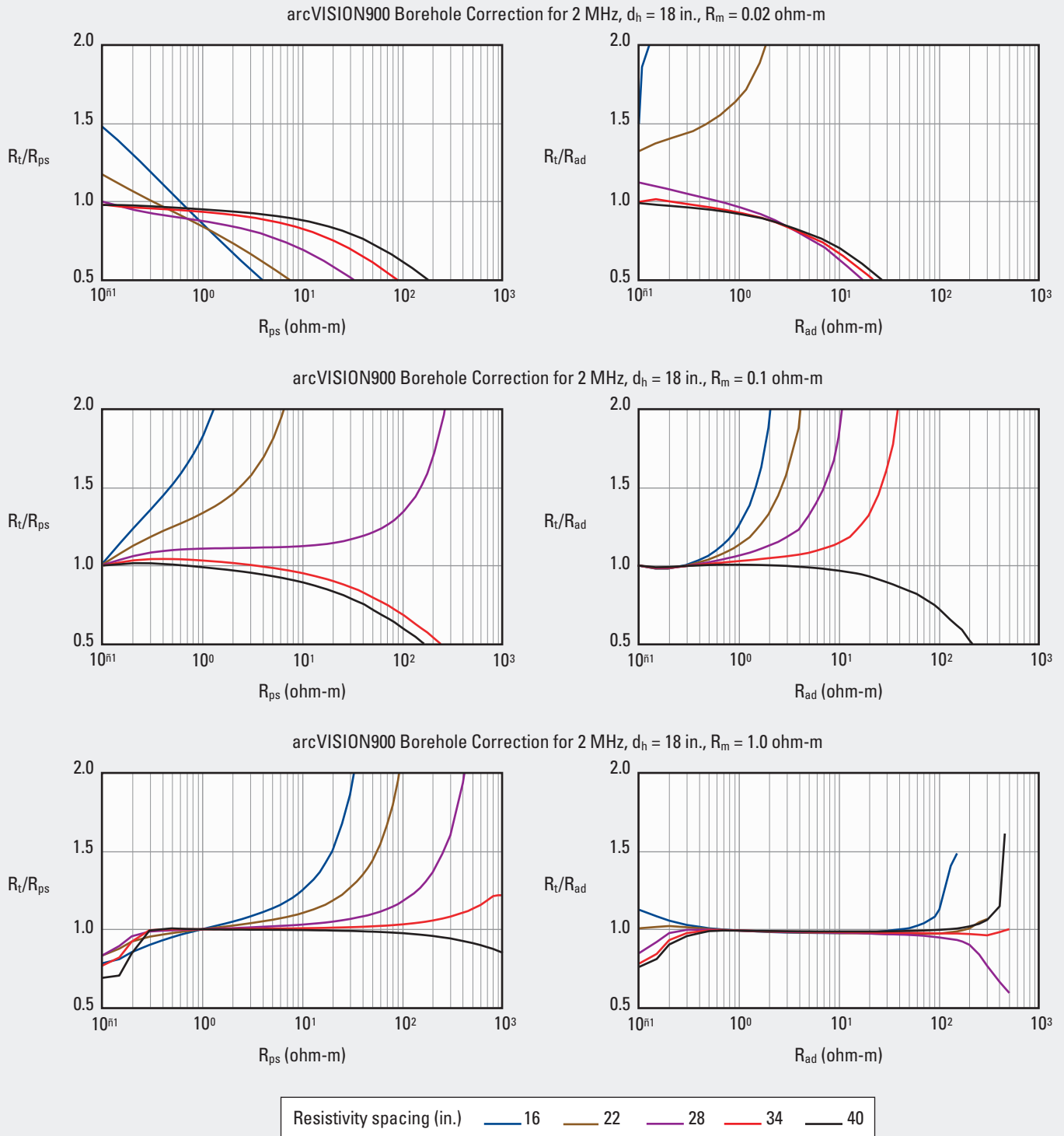
This chart is used similarly to Chart REm-11 to determine the borehole correction applied by the surface acquisition system

to arcVISION900 resistivity measurements. Uncorrected resistivity is entered on the x-axis, not the resistivity shown on the log.

arcVISION900* 9-in. Array Resistivity Compensated Tool—2 MHz

Borehole Correction—Open Hole

REm-37



*Mark of Schlumberger
© Schlumberger

Purpose

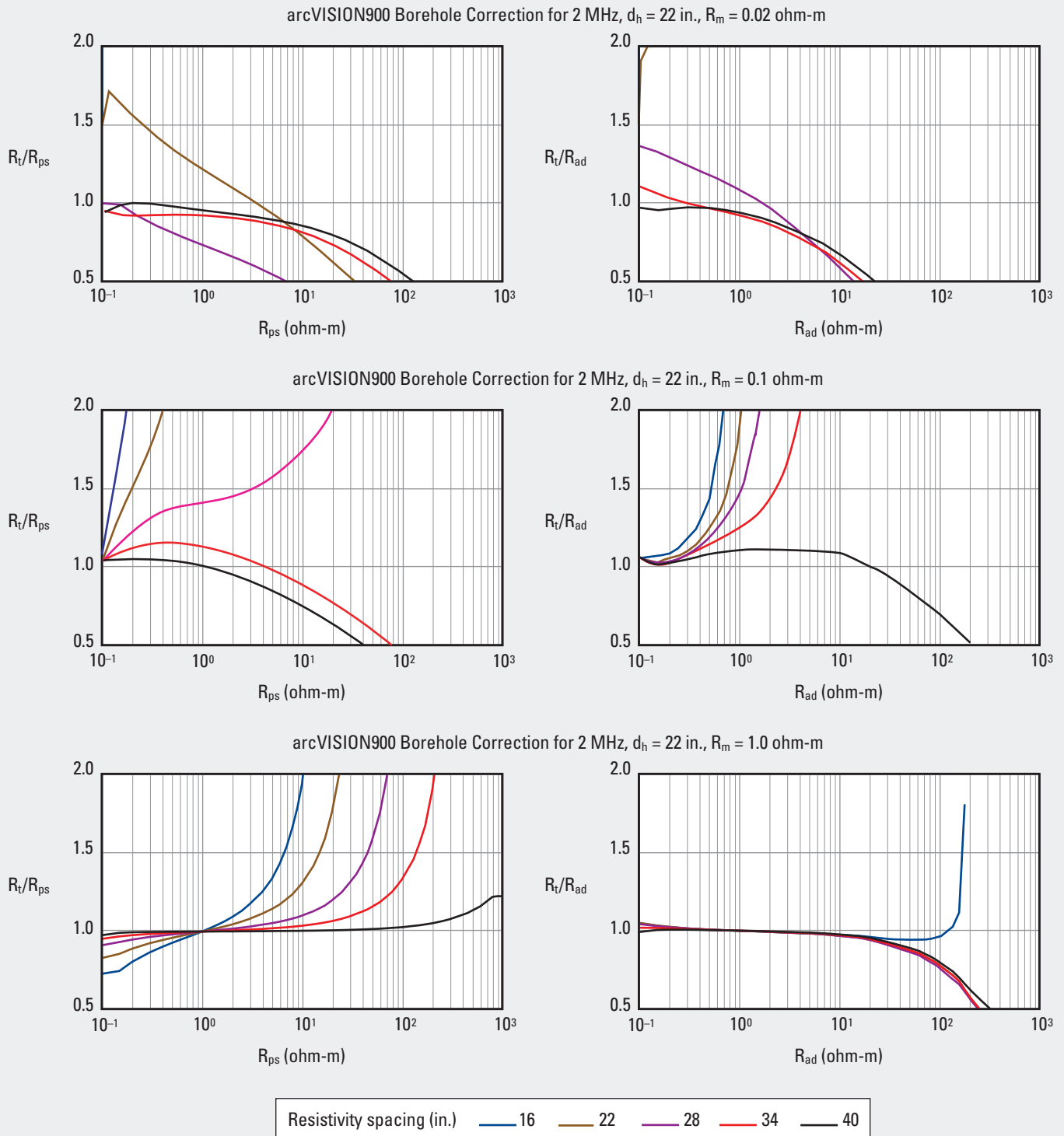
This chart is used similarly to Chart REm-11 to determine the borehole correction applied by the surface acquisition system

to arcVISION900 resistivity measurements. Uncorrected resistivity is entered on the x-axis, not the resistivity shown on the log.

arcVISION900* 9-in. Array Resistivity Compensated Tool—2 MHz

Borehole Correction—Open Hole

REm-38



*Mark of Schlumberger
© Schlumberger

Purpose

This chart is used similarly to Chart REm-11 to determine the borehole correction applied by the surface acquisition system

to arcVISION900 resistivity measurements. Uncorrected resistivity is entered on the x-axis, not the resistivity shown on the log.

arcVISION675*, arcVISION825*, and arcVISION900* Array Resistivity Compensated Tools—400 kHz

Bed Thickness Correction—Open Hole

Purpose

This chart is used to determine the correction factor applied by the surface acquisition system for bed thickness to the phase-shift and attenuation resistivity on the logs of arcVISION675, arcVISION825, and arcVISION900 tools.

Description

The six bed thickness correction charts on this page are paired for phase-shift and attenuation resistivity at different values of true (R_t) and shoulder bed (R_s) resistivity. Only uncorrected resistivity values are entered on the chart, not the resistivity shown on the log.

Chart REm-56 is also used to find the bed thickness correction applied by the surface acquisition system for 2-MHz arcVISION* and ImPulse* logs.

Example

Given: $R_t/R_s = 10/1$, R_{ps} uncorrected = 20 ohm-m (34 in.), and bed thickness = 6 ft.

Find: R_t .

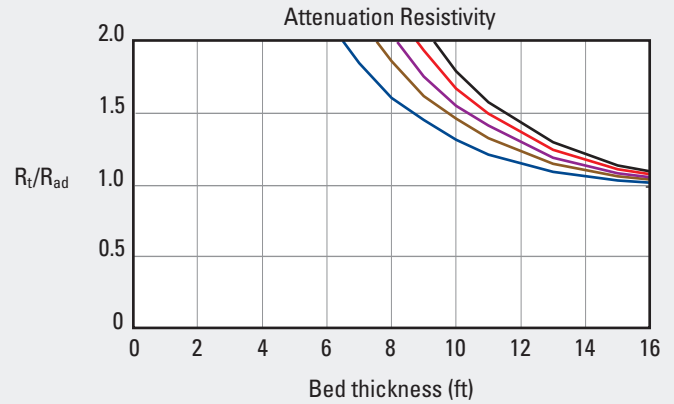
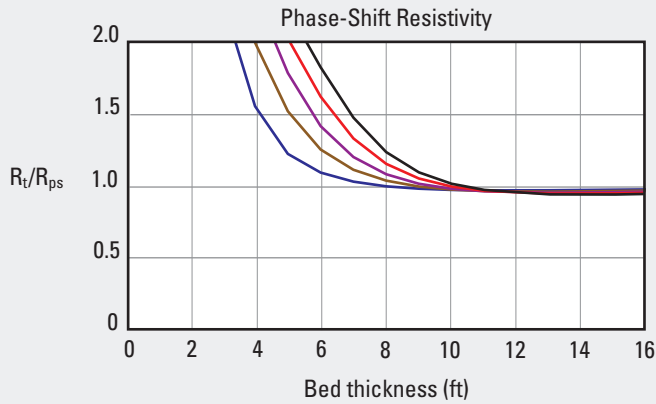
Answer: The appropriate chart to use is the phase-shift resistivity chart in the first row, for $R_t = 10$ ohm-m and $R_s = 1$ ohm-m. Enter the chart on the x-axis at 6 ft and move upward to intersect the 34-in. spacing line. The corresponding value of R_t/R_{ps} is 1.6; $R_t = 20 \times 1.6 = 32$ ohm-m.

arcVISION675*, arcVISION825*, and arcVISION900*
 Array Resistivity Compensated Tools—400 kHz

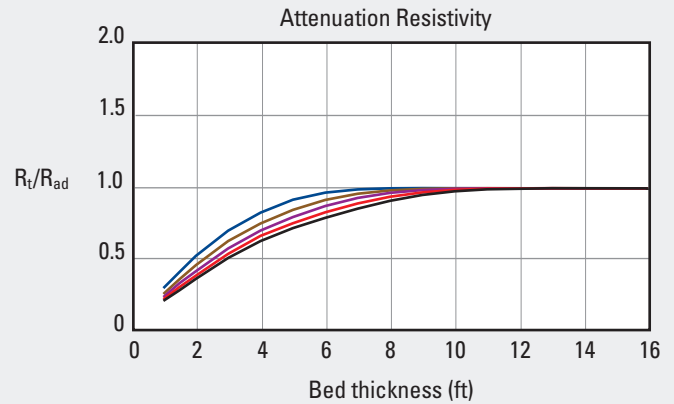
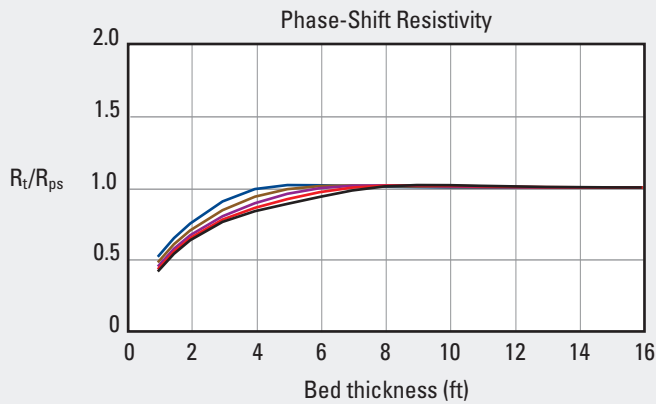
REm-55

Bed Thickness Correction—Open Hole

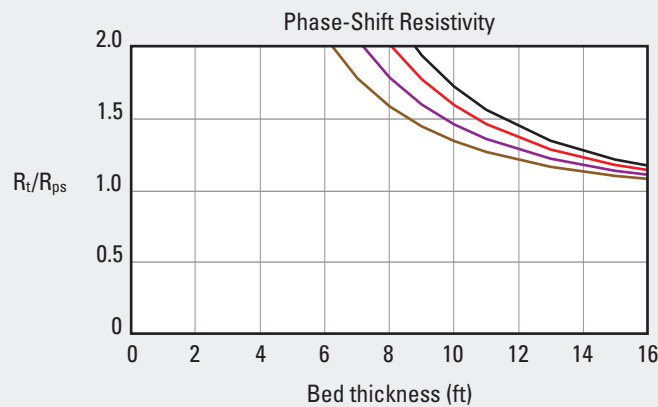
arcVISION675, arcVISION825, and arcVISION900 400-kHz
 Bed Thickness Correction for $R_t = 10$ ohm-m and $R_s = 1$ ohm-m at Center of Bed



arcVISION675, arcVISION825, and arcVISION900 400-kHz
 Bed Thickness Correction for $R_t = 1$ ohm-m and $R_s = 10$ ohm-m at Center of Bed



arcVISION675, arcVISION825, and arcVISION900 400-kHz
 Bed Thickness Correction for $R_t = 100$ ohm-m and $R_s = 10$ ohm-m at Center of Bed



Resistivity spacing (in.) — 16 — 22 — 28 — 34 — 40

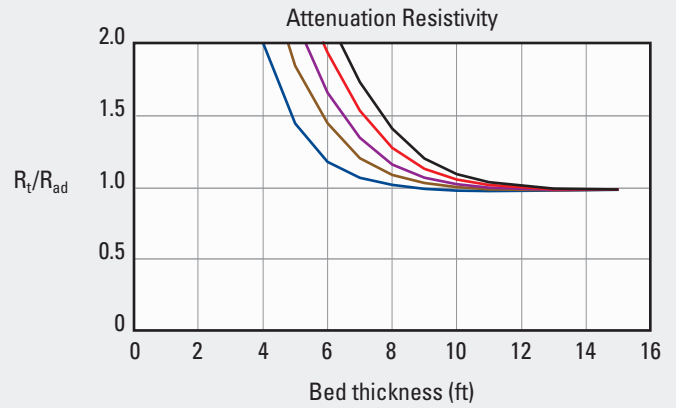
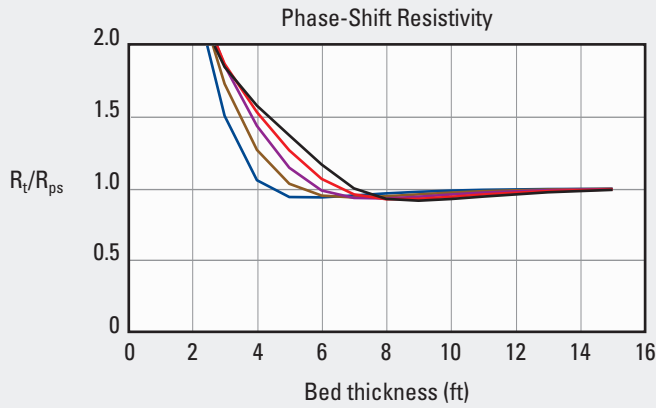
*Mark of Schlumberger
 © Schlumberger

arcVISION* and ImPulse* Array Resistivity Compensated Tools—2 MHz

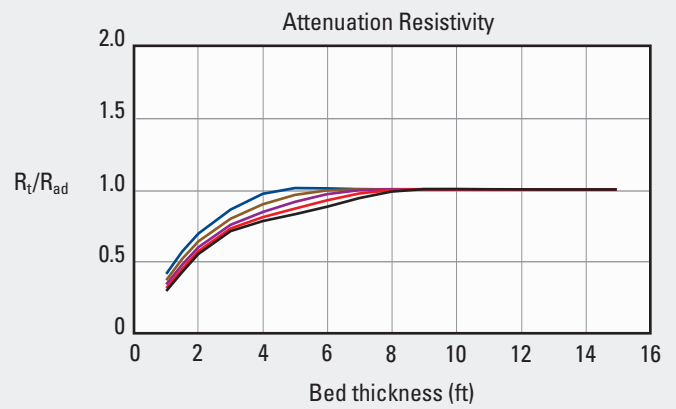
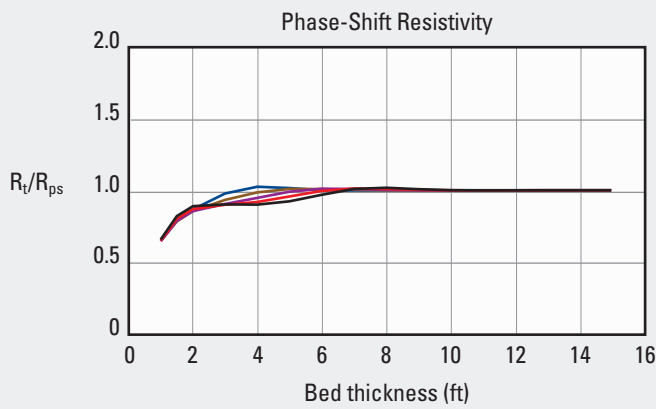
Bed Thickness Correction—Open Hole

REm-56

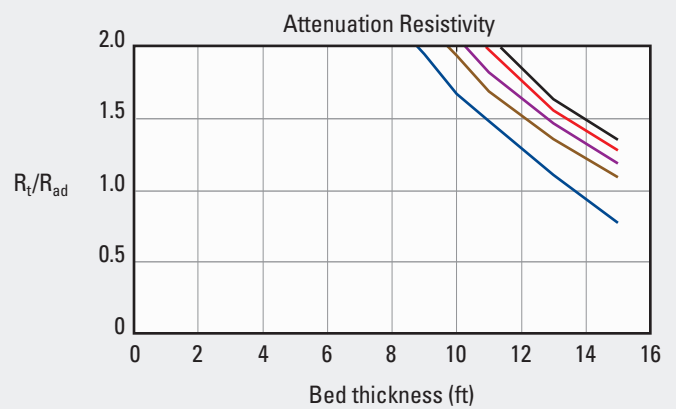
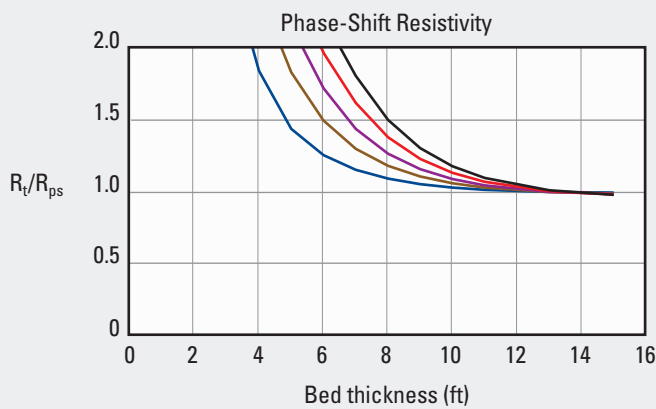
arcVISION and ImPulse 2-MHz Bed Thickness Correction for $R_t = 10$ ohm-m and $R_s = 1$ ohm-m at Center of Bed



arcVISION and ImPulse 2-MHz Bed Thickness Correction for $R_t = 1$ ohm-m and $R_s = 10$ ohm-m at Center of Bed



arcVISION and ImPulse 2-MHz Bed Thickness Correction for $R_t = 100$ ohm-m and $R_s = 10$ ohm-m at Center of Bed



Resistivity spacing (in.) — 16 — 22 — 28 — 34 — 40

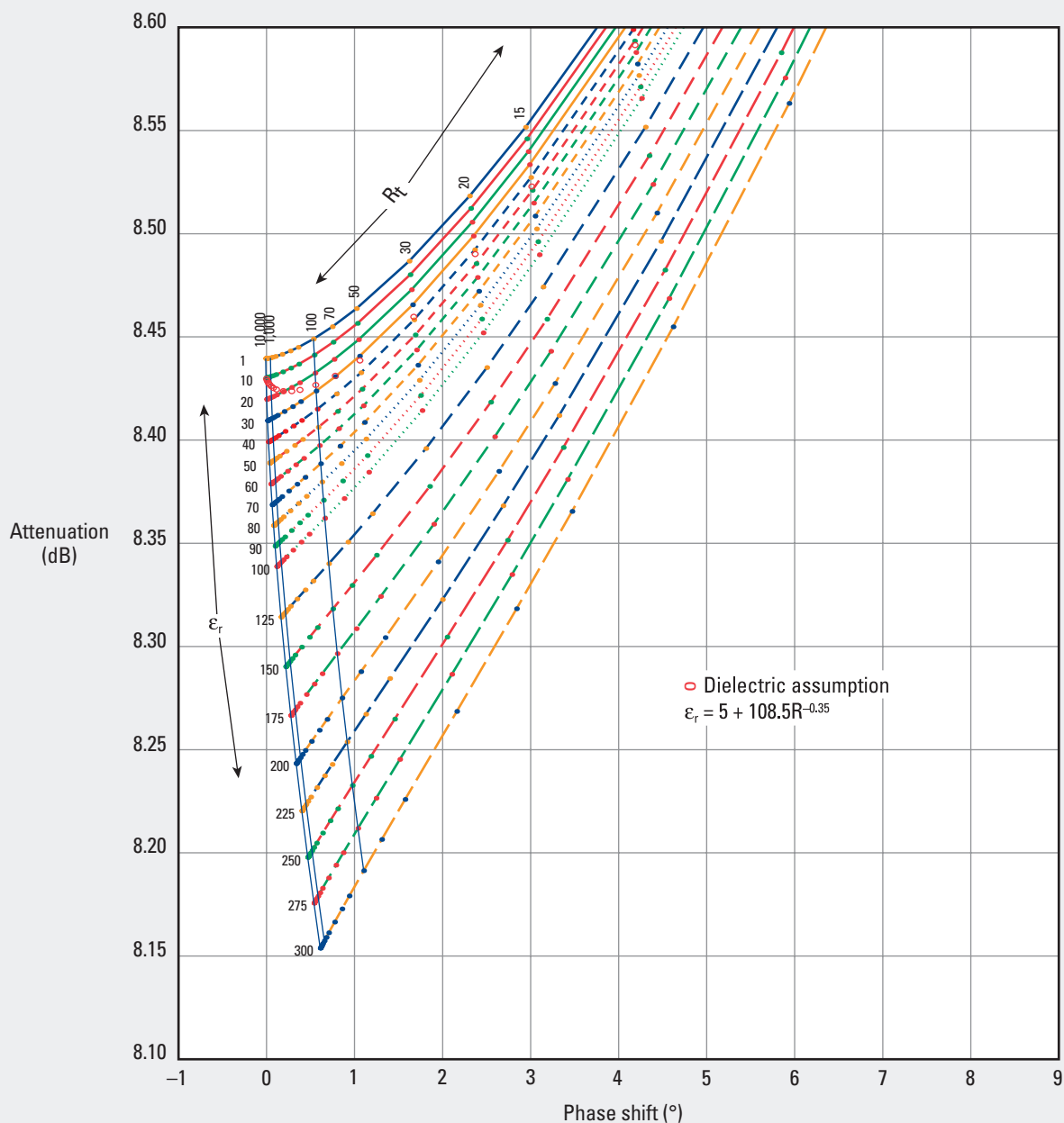
*Mark of Schlumberger
© Schlumberger

REm

arcVISION675* and ImPulse* Array Resistivity Compensated Tools—2 MHz and 16-in. Spacing

REm-58

Dielectric Correction—Open Hole



*Mark of Schlumberger
© Schlumberger

Purpose

This chart is used to estimate the true resistivity (R_t) and dielectric correction (ϵ_r). R_t is used in water saturation calculation.

Description

Enter the chart with the uncorrected (not those shown on the log) phase-shift and attenuation values from the arcVISION675 or ImPulse resistivity tool. The intersection point of the two values is used to determine R_t and the dielectric correction. R_t is interpolated from the subvertical lines described by the dots originating at the

listed R_t values. The ϵ_r is interpolated from the radial lines originating from the ϵ_r values listed on the left-hand side of the chart. Charts REm-59 through REm-62 are used to determine R_t and ϵ_r at larger spacings.

Example

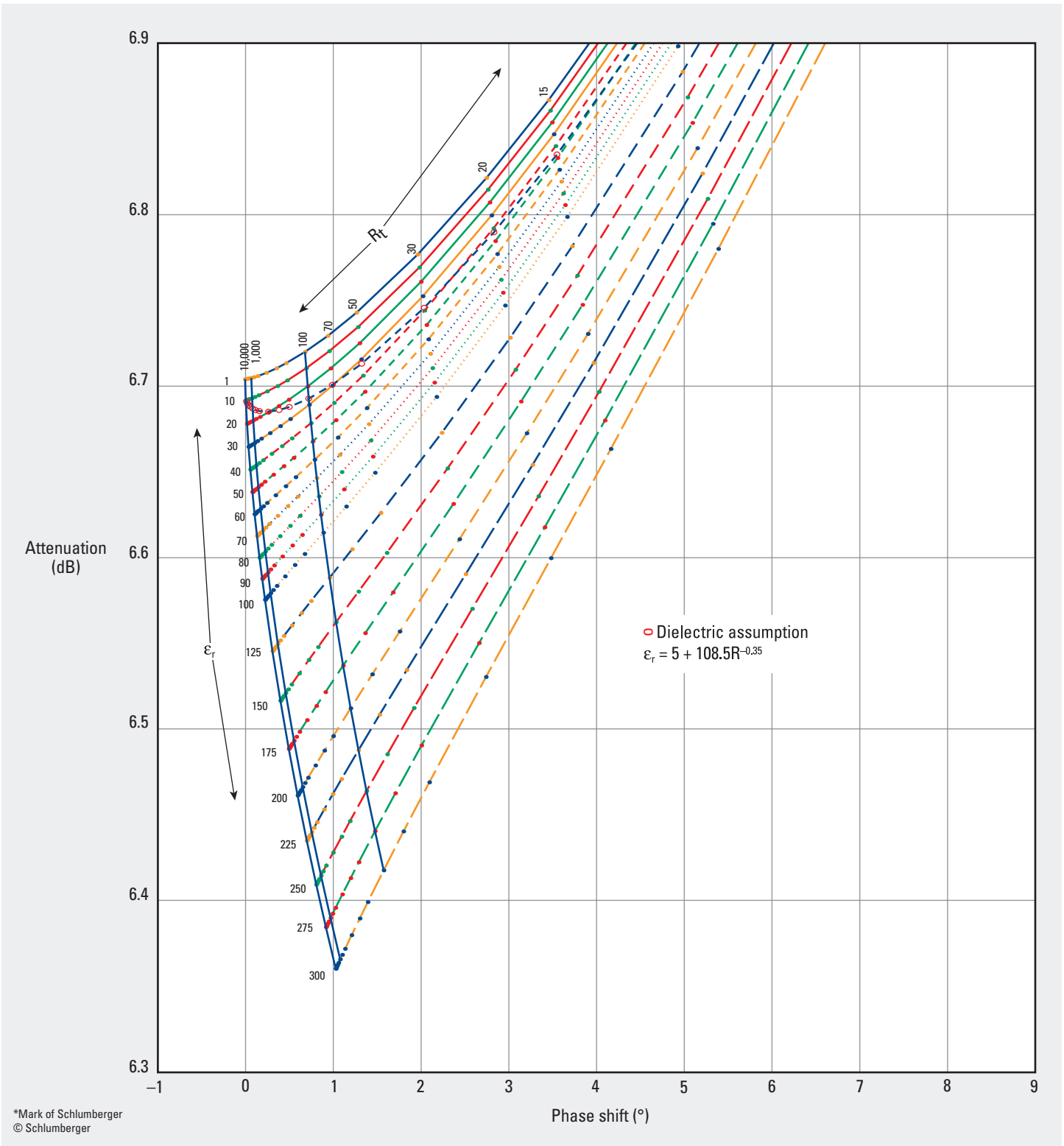
Given: Phase shift = 2° and attenuation = 8.45 dB for 16-in. spacing.

Find: R_t and ϵ_r .

Answer: $R_t = 26$ ohm-m and $\epsilon_r = 70$ dB.

arcVISION675* and ImPulse* Array Resistivity
Compensated Tools—2 MHz and 22-in. Spacing
Dielectric Correction—Open Hole

REm-59



*Mark of Schlumberger
© Schlumberger

Purpose

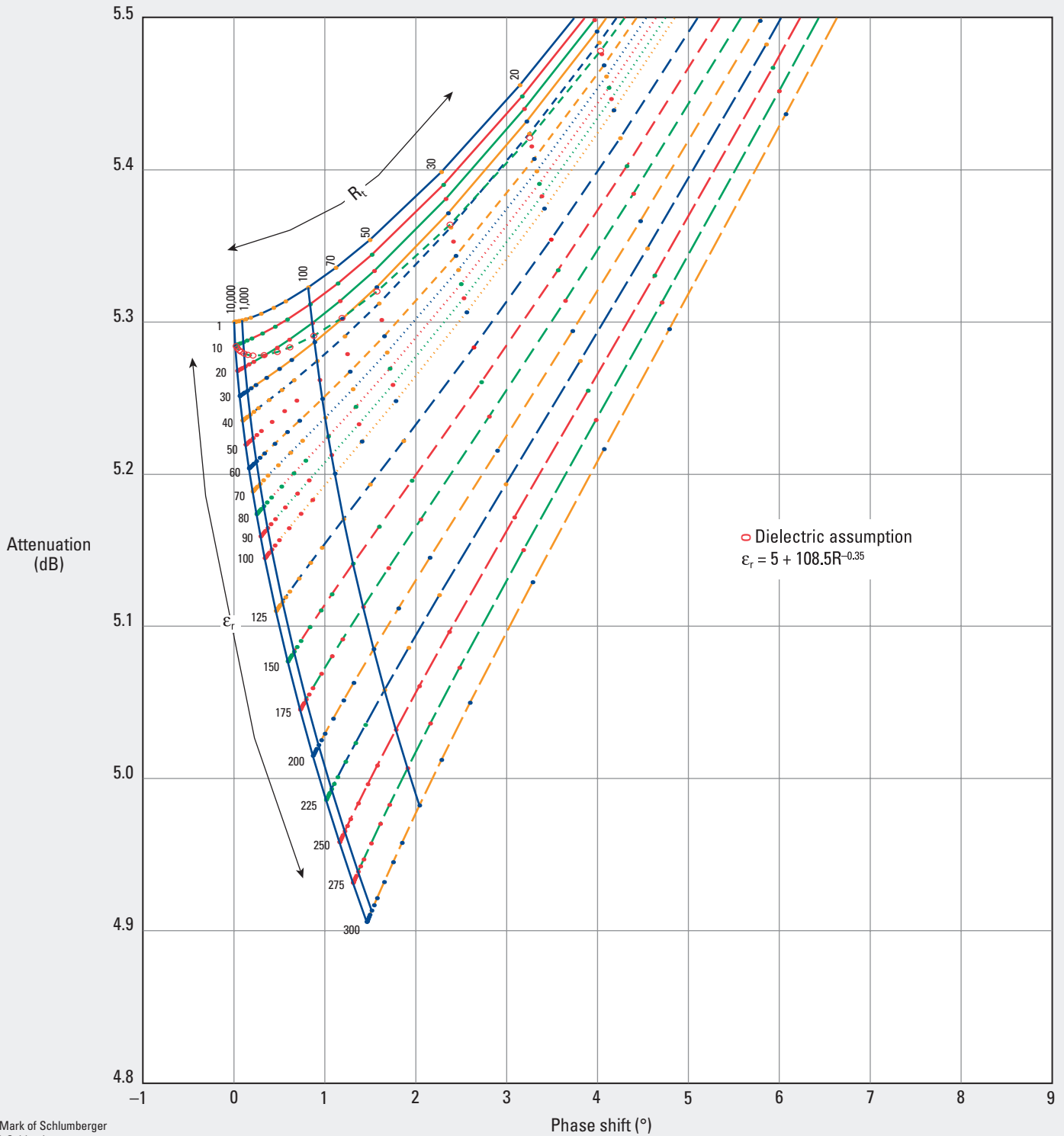
Charts REm-59 through REm-62 are identical to Chart REm-58 for determining R_t and ϵ_r at larger spacings of the arcVISION675 and ImPulse 2-MHz tools.

REm

arcVISION675* and ImPulse* Array Resistivity Compensated Tools—2 MHz and 28-in. Spacing

REm-60

Dielectric Correction—Open Hole



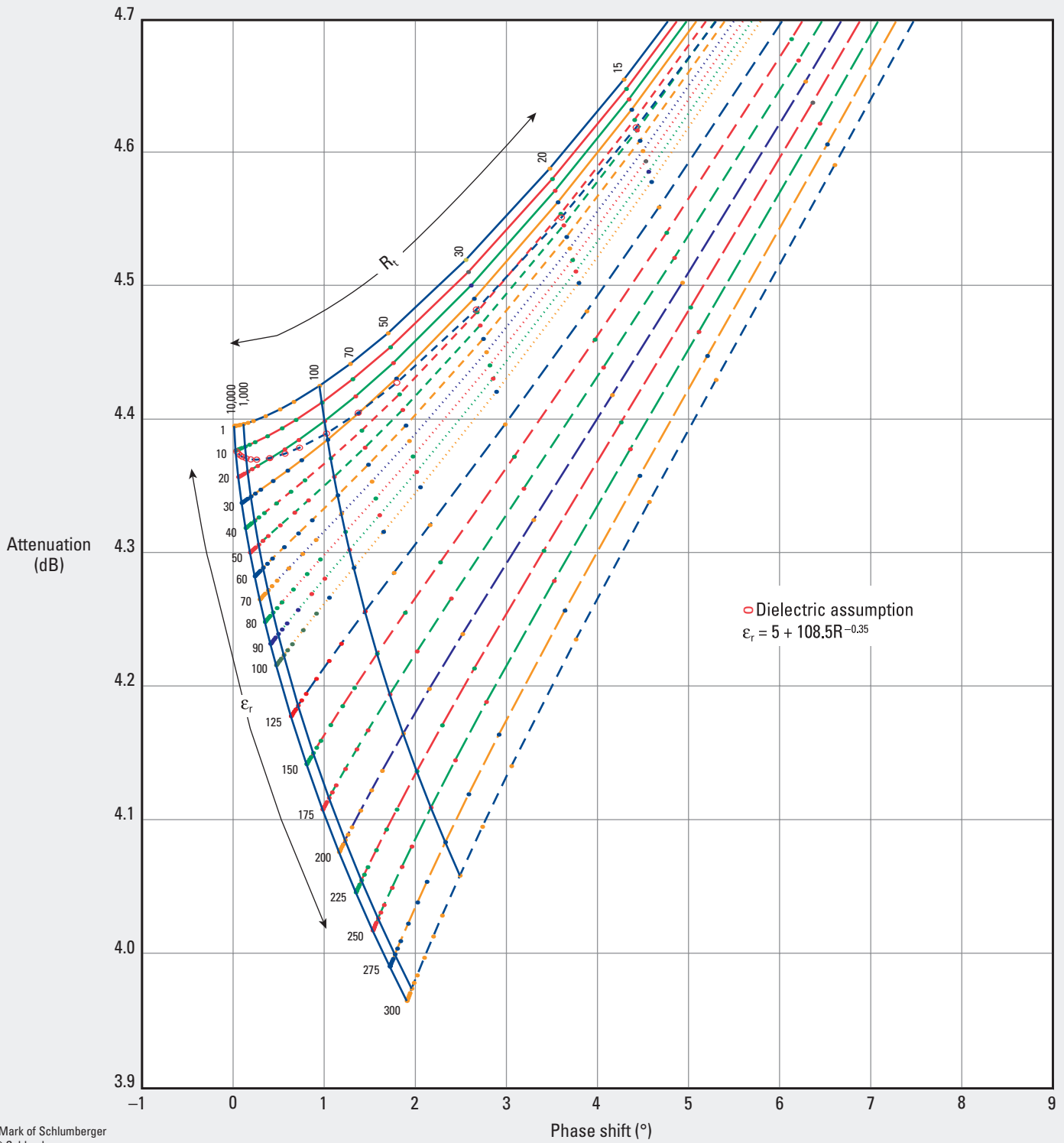
*Mark of Schlumberger
© Schlumberger

Purpose

Charts REm-59 through REm-62 are identical to Chart REm-58 for determining R_t and ϵ_r at larger spacings of the arcVISION675 and ImPulse 2-MHz tools.

arcVISION675* and ImPulse* Array Resistivity
Compensated Tools—2 MHz and 34-in. Spacing
Dielectric Correction—Open Hole

REm-61



REm

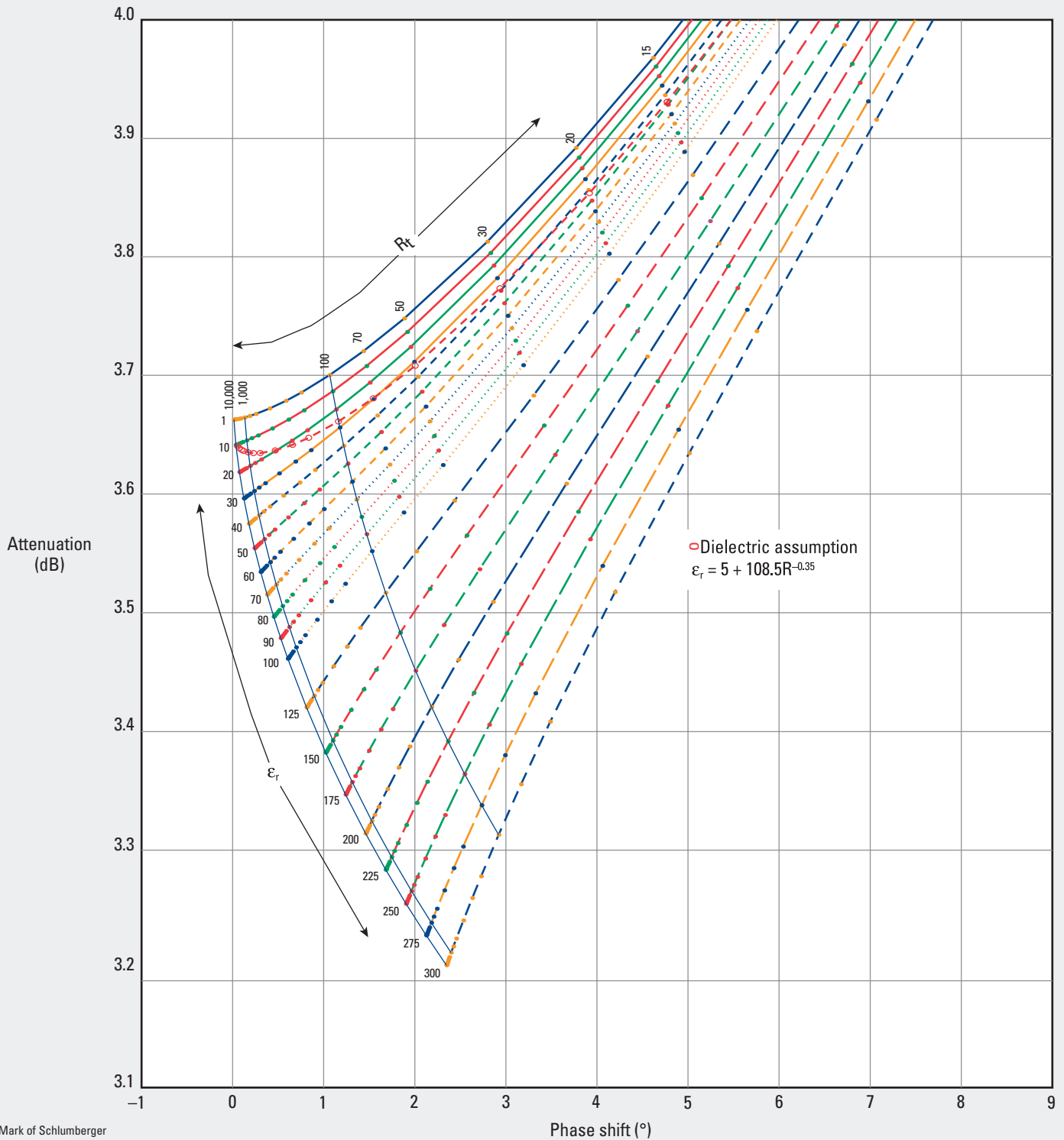
Purpose

Charts REm-59 through REm-62 are identical to Chart REm-58 for determining R_t and ϵ_r at larger spacings of the arcVISION675 and ImPulse 2-MHz tools.

arcVISION675* and ImPulse* Array Resistivity Compensated Tools—2 MHz and 40-in. Spacing

REm-62

Dielectric Correction—Open Hole



*Mark of Schlumberger
© Schlumberger

Purpose

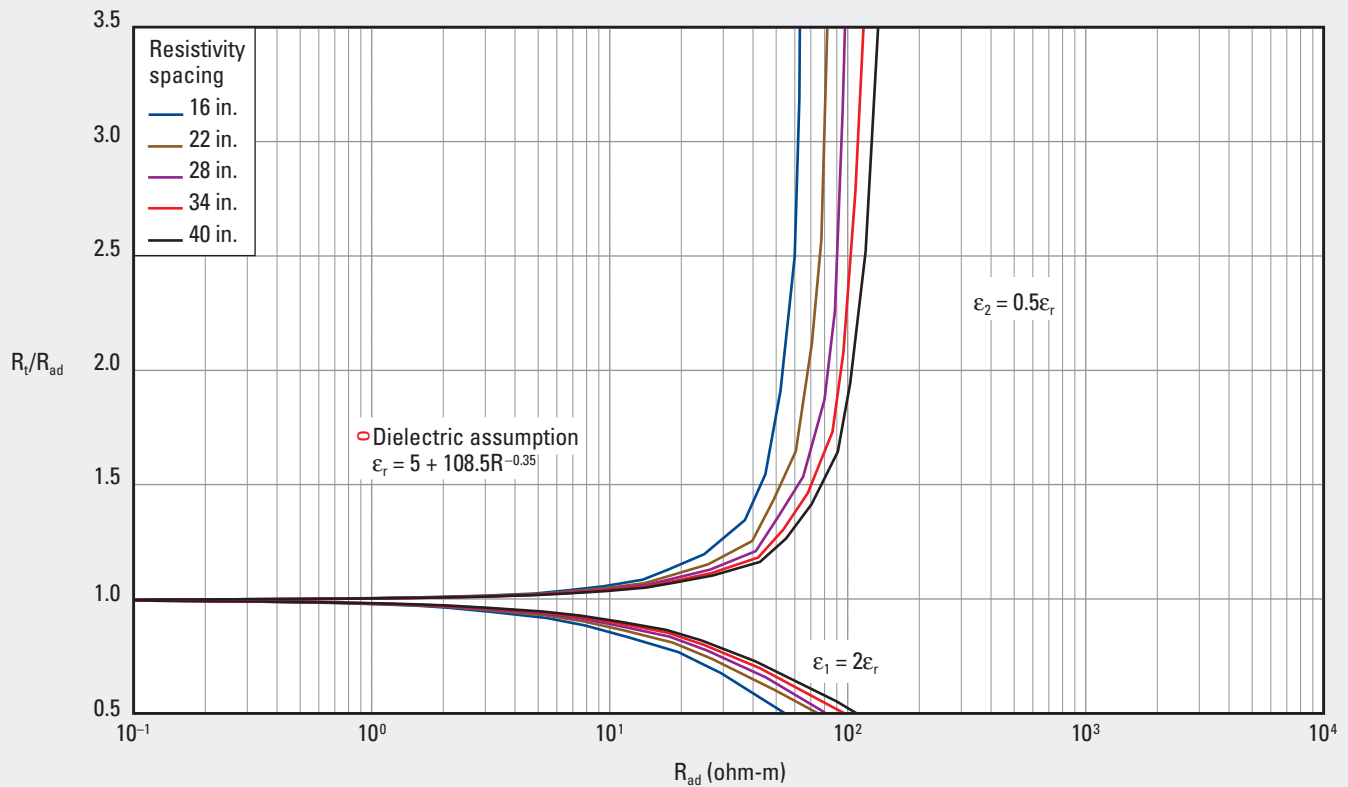
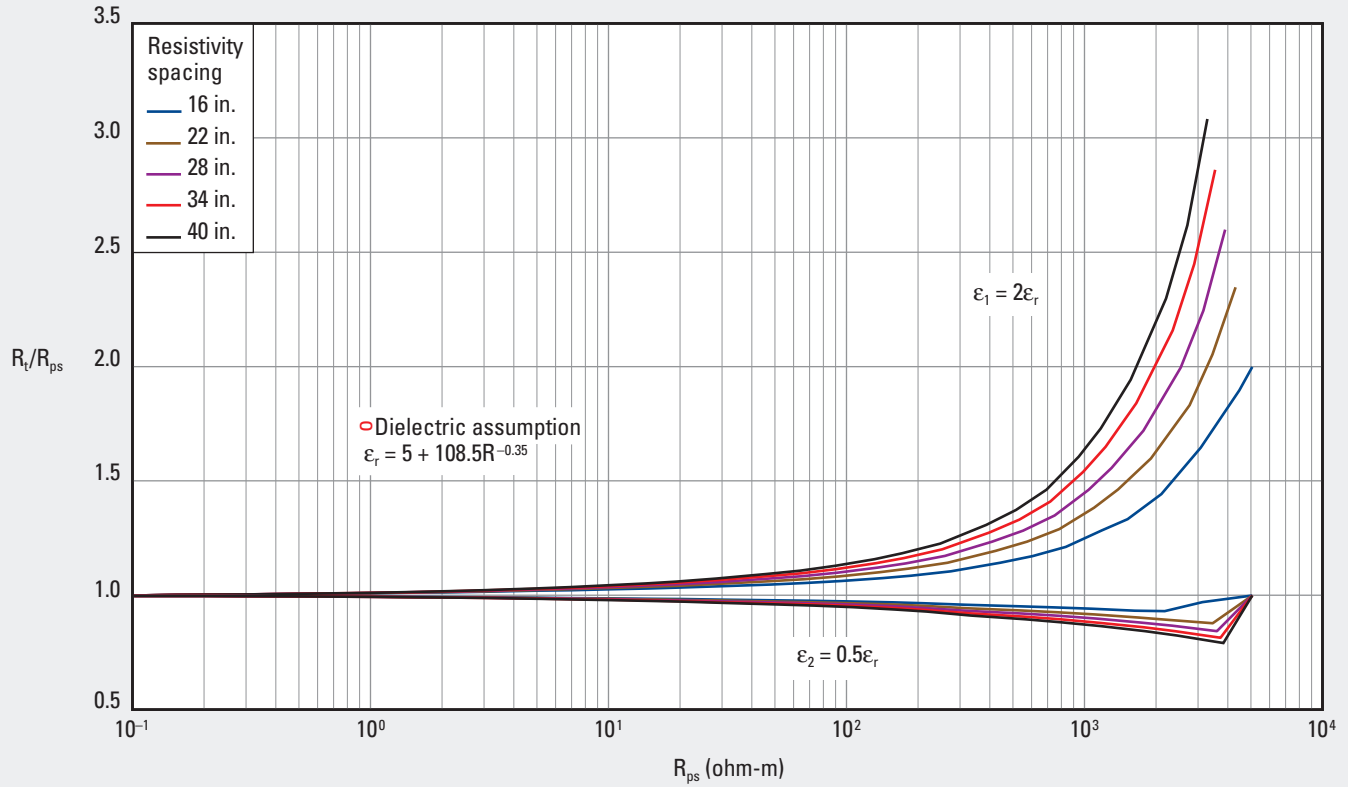
Charts REm-59 through REm-62 are identical to Chart REm-58 for determining R_t and ϵ_r at larger spacings of the arcVISION675 and ImPulse 2-MHz tools.

arcVISION675* and ImPulse* Array Resistivity Compensated Tools—2 MHz with Dielectric Assumption

REm-63

Dielectric Correction—Open Hole

Dielectric Effects of Standard Processed arcVISION675 or ImPulse Log at 2 MHz with Dielectric Assumption



*Mark of Schlumberger
 © Schlumberger

Resistivity Galvanic

Invasion Correction—Open Hole

Rt-1

(former Rint-1)

Purpose

The charts in this chapter are used to determine the correction for invasion effects on the following parameters:

- diameter of invasion (d_i)
- ratio of flushed zone to true resistivity (R_{xo}/R_t)
- R_t from laterolog resistivity tools.

The R_{xo}/R_t and R_t values are used in the calculation of water saturation.

Description

The invasion correction charts, also referred to as “tornado” or “butterfly” charts, assume a step-contact profile of invasion and that all resistivity measurements have already been corrected as necessary for borehole effect and bed thickness by using the appropriate chart from the “Resistivity Laterolog” chapter.

To use any of these charts, enter the y-axis and x-axis with the required resistivity ratios. The point of intersection defines d_i , R_{xo}/R_t , and R_t as a function of one resistivity measurement.

Saturation Determination in Clean Formations

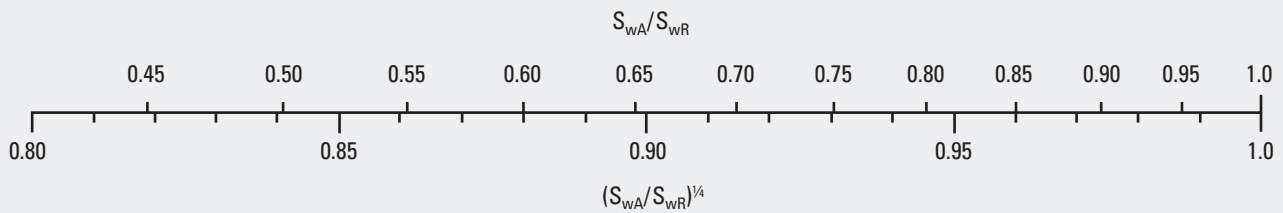
Either of the chart-derived values of R_t and R_{xo}/R_t are used to find values for the water saturation of the formation (S_w). The first of two approaches is the S_w -Archie (S_{wA}), which is found using the Archie saturation formula (or Chart SatOH-3) with the derived R_t value and known values of the formation resistivity factor (F_R) and the resistivity of the water (R_w). The S_w -ratio (S_{wR}) is found by using R_{xo}/R_t and R_{mf}/R_w as in Chart SatOH-4.

If S_{wA} and S_{wR} are equal, the assumption of a step-contact invasion profile is indicated to be correct, and all values determined (S_w , R_t , R_{xo} , and d_i) are considered good.

If $S_{wA} > S_{wR}$, either invasion is very shallow or a transition-type invasion profile is indicated, and S_{wA} is considered a good value for S_w .

If $S_{wA} < S_{wR}$, an annulus-type invasion profile may be indicated, and a more accurate value of water saturation may be estimated by using

$$S_{wcor} = S_{wA} \left(\frac{S_{wA}}{S_{wR}} \right)^{\frac{1}{4}}$$



© Schlumberger

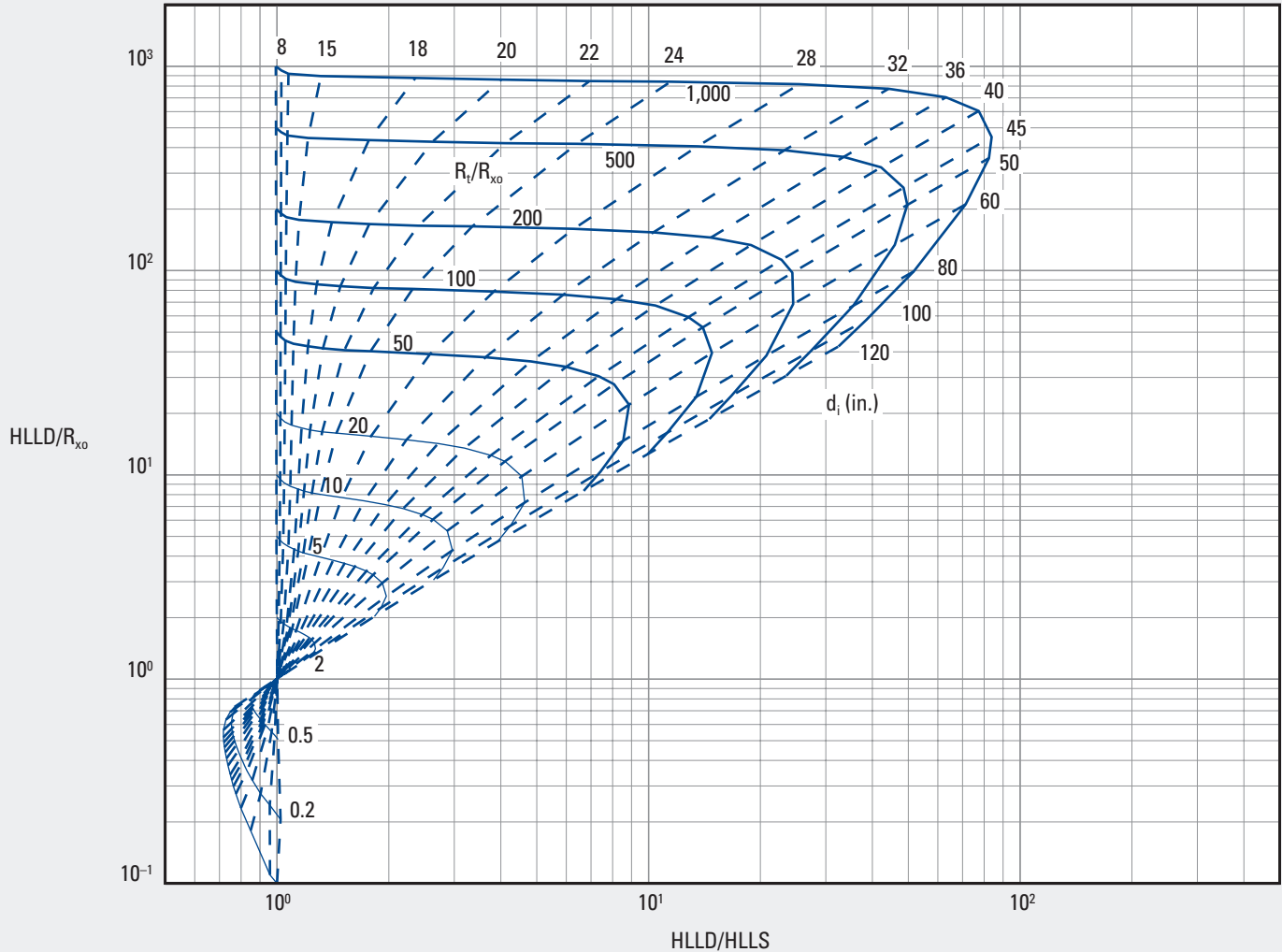
Rt

High-Resolution Azimuthal Laterolog Sonde (HALS)

Formation Resistivity and Diameter of Invasion—Open Hole

Rt-2

Thick Beds, 8-in. Hole, $R_{x0}/R_m = 10$



© Schlumberger

Purpose

The resistivity values of HALS laterolog deep resistivity (HLLD), HALS laterolog shallow resistivity (HLLS), and resistivity of the flushed zone (R_{x0}) measured by the High-Resolution Azimuthal Laterolog Sonde (HALS) are used with this chart to determine values for diameter of invasion (d_i) and true resistivity (R_t).

Description

The conditions for which this chart is used are listed at the top. The chart is entered with the ratios of HLLD/HLLS on the x-axis and HLLD/ R_{x0} on the y-axis. The intersection point defines d_i on the dashed curves and the ratio of R_t/R_{x0} on the solid curves.

Example

Given: HLLD = 50 ohm-m, HLLS = 15 ohm-m, $R_{x0} = 2.0$ ohm-m, and $R_m = 0.2$ ohm-m.

Find: R_t and diameter of invasion.

Answer: Enter the chart with the values of HLLD/HLLS = $50/15 = 3.33$ and HLLD/ $R_{x0} = 50/2 = 25$.

The resulting point of intersection on the chart indicates that $R_t/R_{x0} = 35$ and $d_i = 34$ in.

$R_t = 35 \times 2.0 = 70$ ohm-m.

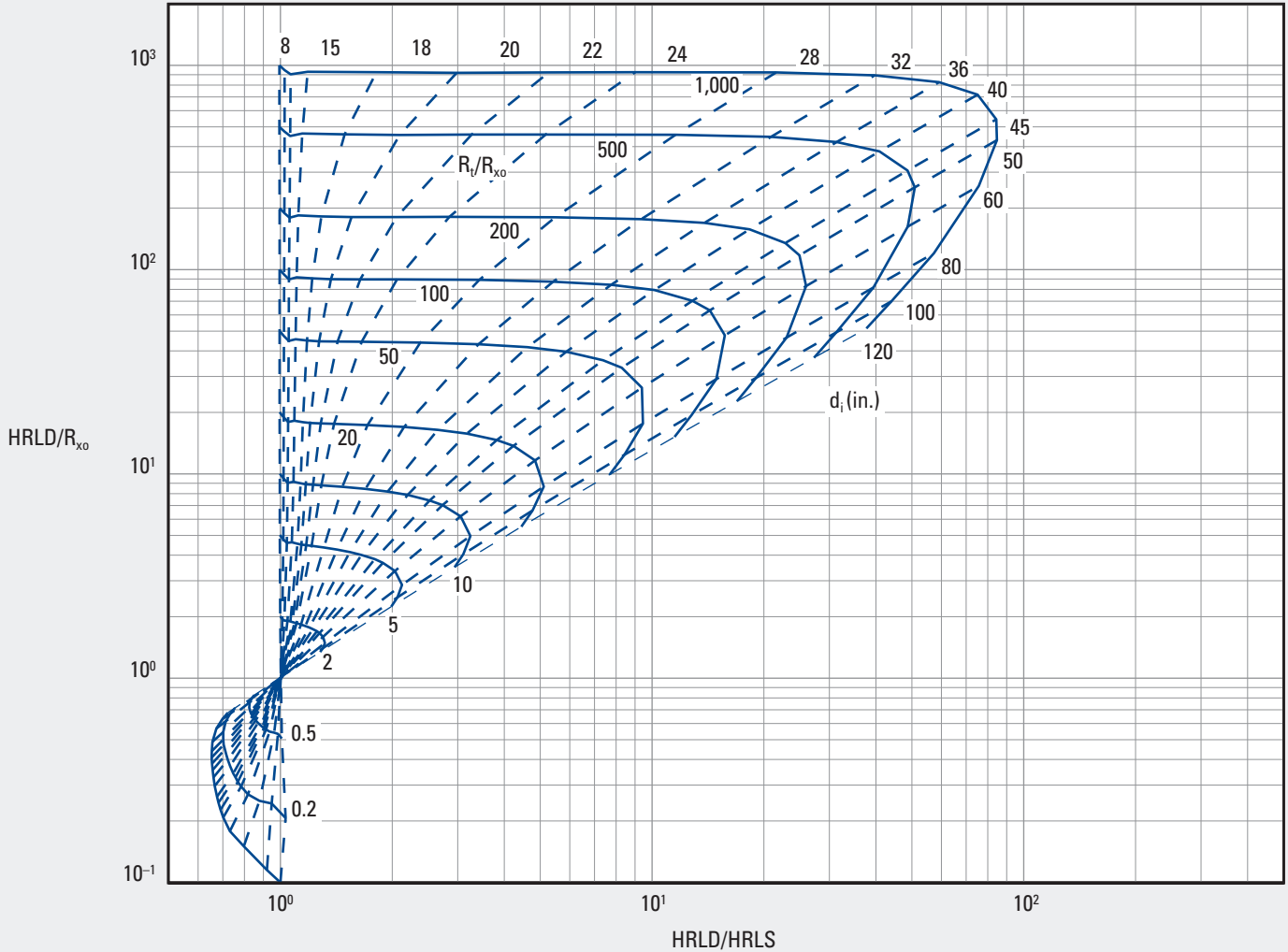
Rt

High-Resolution Azimuthal Laterolog Sonde (HALS)

Formation Resistivity and Diameter of Invasion—Open Hole

Rt-3

Thick Beds, 8-in. Hole, $R_{xo}/R_m = 10$



© Schlumberger

Purpose

The resistivity values of high-resolution deep resistivity (HRLD), high-resolution shallow resistivity (HRLS), and R_{xo} measured by the HALS are used similarly to Chart Rt-2 to determine values for d_i and R_t .

Description

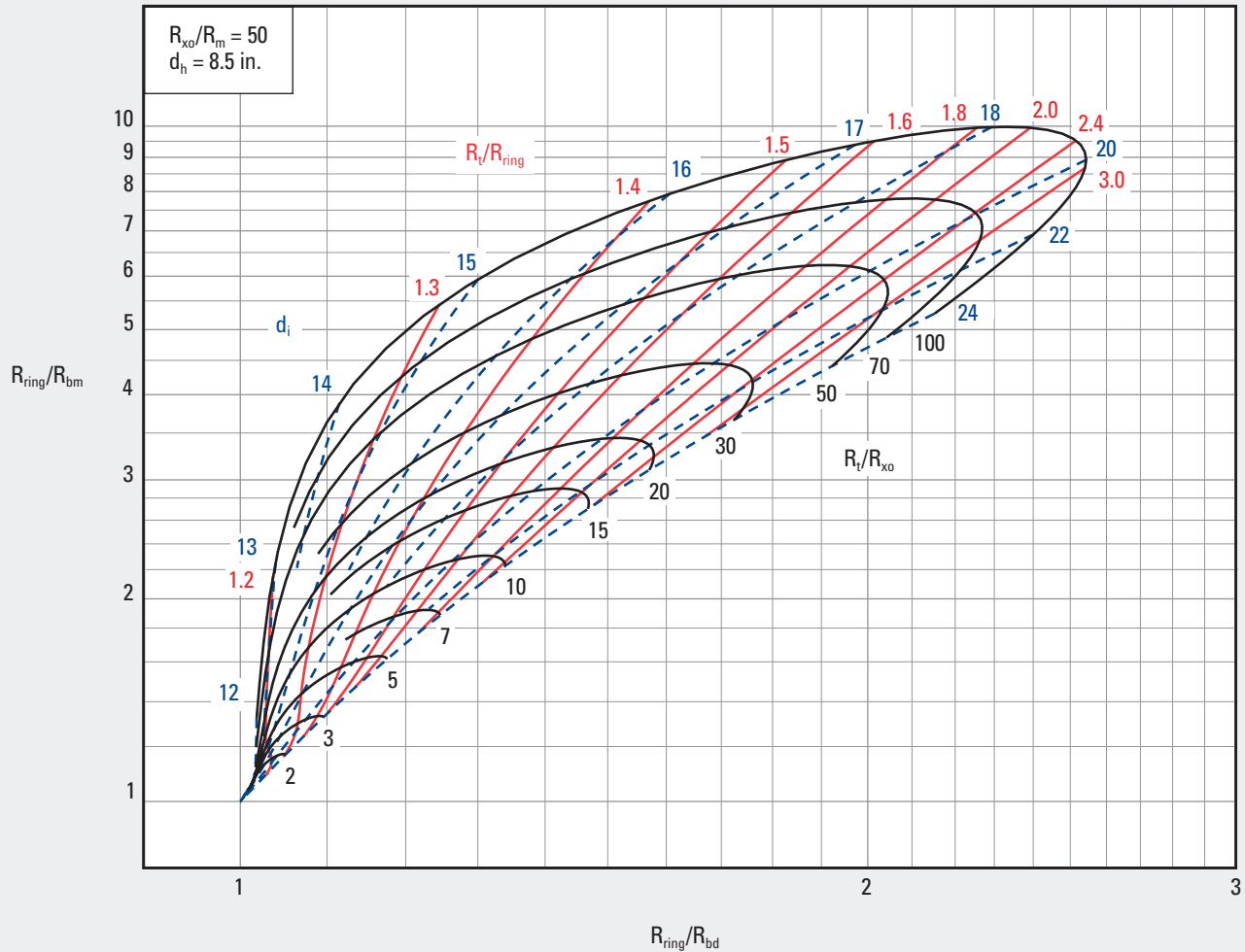
The conditions for which this chart is used are listed at the top. The chart is entered with the ratios of $HRLD/HRLS$ on the x-axis and $HRLD/R_{xo}$ on the y-axis. The intersection point defines d_i on the dashed curves and the ratio of R_t/R_{xo} on the solid curves.

geoVISION675* Resistivity

Formation Resistivity and Diameter of Invasion—Open Hole

Rt-10

Ring, Deep, and Medium Button Resistivity (6.75-in. tool)



*Mark of Schlumberger
© Schlumberger

Purpose

This chart is used to determine the correction applied to the log presentation of R_t and d_i determined from geoVISION675 ring (R_{ring}) and deep (R_{bd}) and medium button (R_{bm}) resistivity values.

Description

Enter the chart with the ratios of R_{ring}/R_{bd} on the x-axis and R_{ring}/R_{bm} on the y-axis. The intersection point defines d_i on the blue dashed curves, R_t/R_{ring} on the red curves, and R_t/R_{xo} on the black curves. Charts Rt-11 through Rt-17 are similar to Chart Rt-10 for different tool sizes, configurations, and resistivity terms.

Example

Given: $R_{ring} = 30$ ohm-m, $R_{xo}/R_m = 50$, $R_{bd} = 15$ ohm-m, and $R_{bm} = 6$ ohm-m.

Find: R_t , d_i , and R_{xo} .

Answer: Enter the chart with values of $R_{ring}/R_{bd} = 30/15 = 2$ on the x-axis and $R_{ring}/R_{bm} = 30/6 = 5$ on the y-axis to find $d_i = 22.5$ in., $R_t/R_{ring} = 3.1$, and $R_t/R_{xo} = 50$. From these ratios, $R_t = 3.1 \times 30 = 93$ ohm-m and $R_{xo} = 93/50 = 1.86$ ohm-m.

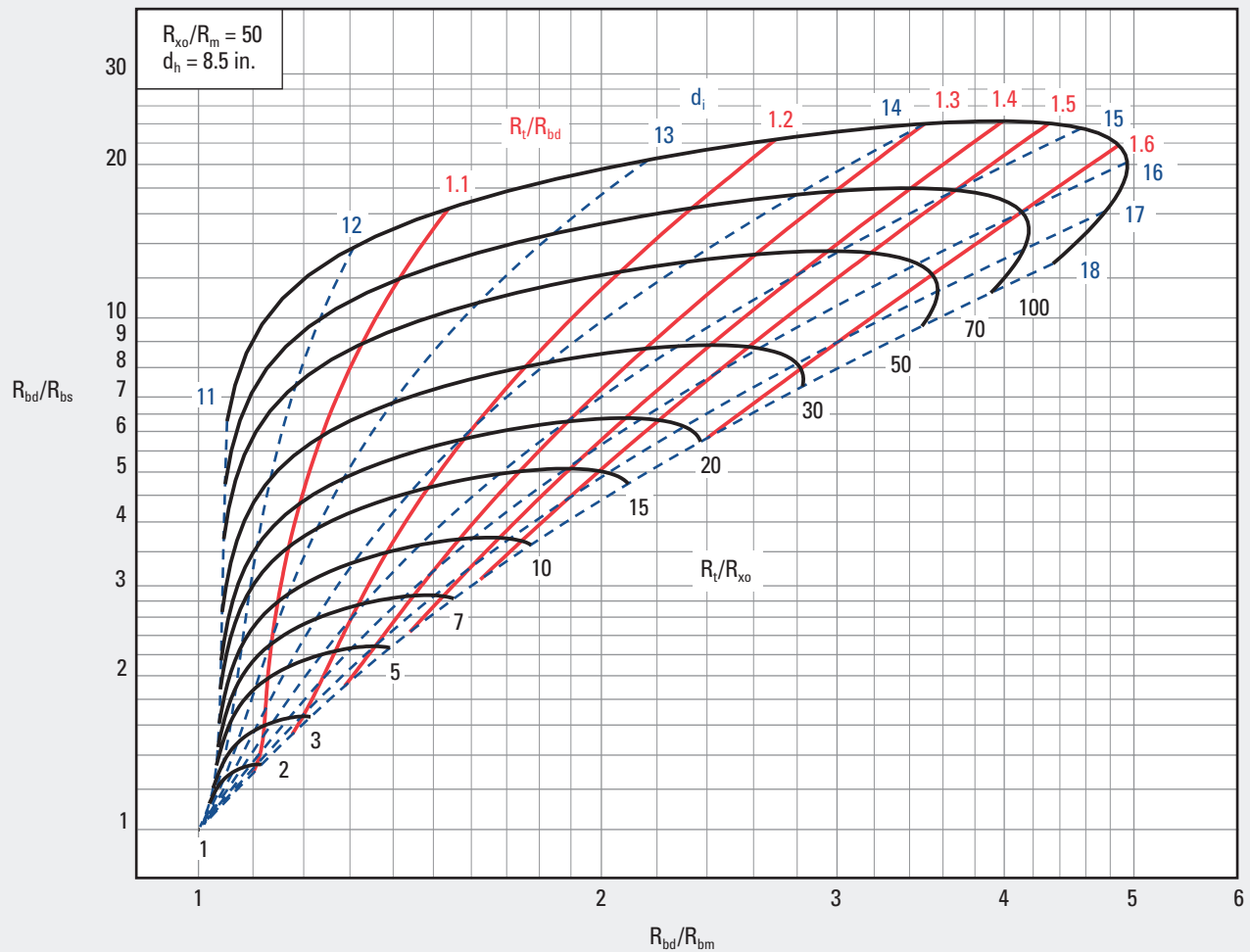
Rt

geoVISION675* Resistivity

Formation Resistivity and Diameter of Invasion—Open Hole

Rt-11

Deep, Medium, and Shallow Button Resistivity (6.75-in. tool)



*Mark of Schlumberger
© Schlumberger

Purpose

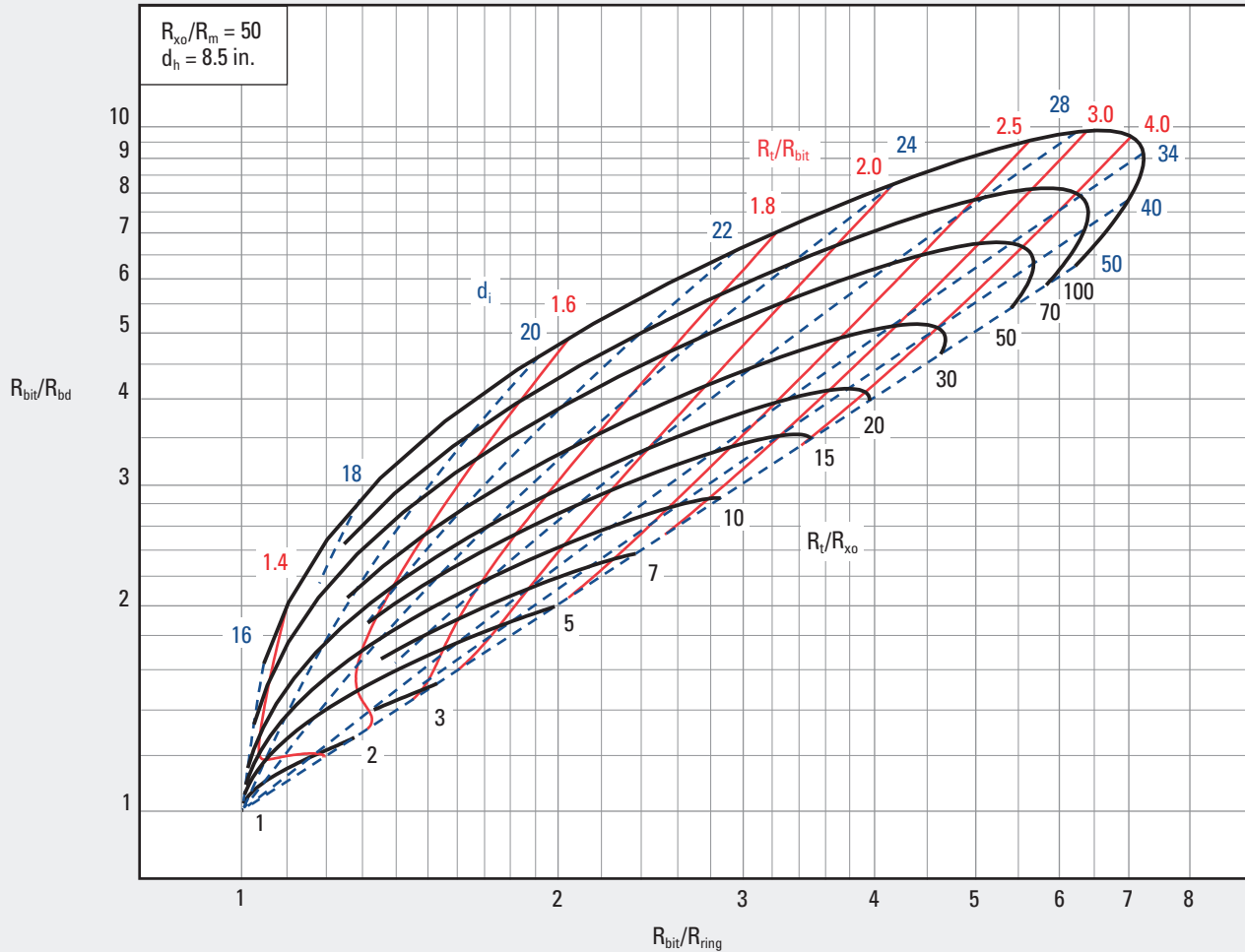
This chart is used similarly to Chart Rt-10 to determine the correction applied to the log presentation of R_t and d_i determined from geoVISION675 deep (R_{bd}), medium (R_{bm}), and shallow button (R_{bs}) resistivity values.

geoVISION675* Resistivity

Formation Resistivity and Diameter of Invasion—Open Hole

Rt-12

Bit, Ring, and Deep Button Resistivity (6.75-in. tool) with ROP to Bit Face = 4 ft



*Mark of Schlumberger
© Schlumberger

Purpose

This chart is used similarly to Chart Rt-10 to determine the correction applied to the log presentation of R_t and d_i determined from geoVISION675 R_{ring} , bit (R_{bit}), and R_{bd} resistivity values.

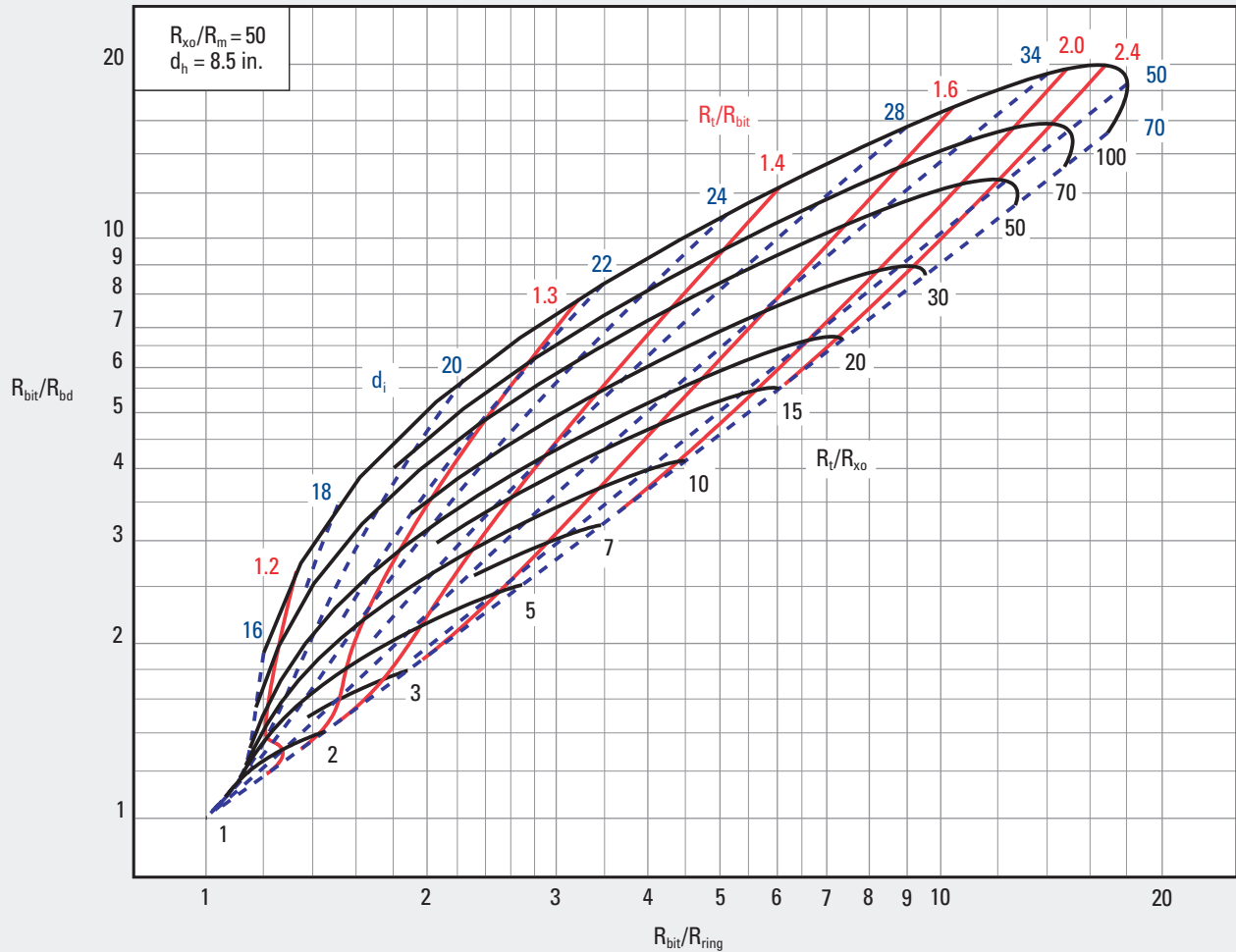
Rt

geoVISION675* Resistivity

Formation Resistivity and Diameter of Invasion—Open Hole

Rt-13

Bit, Ring, and Deep Button Resistivity (6.75-in. tool) with ROP to Bit Face = 35 ft



*Mark of Schlumberger
© Schlumberger

Purpose

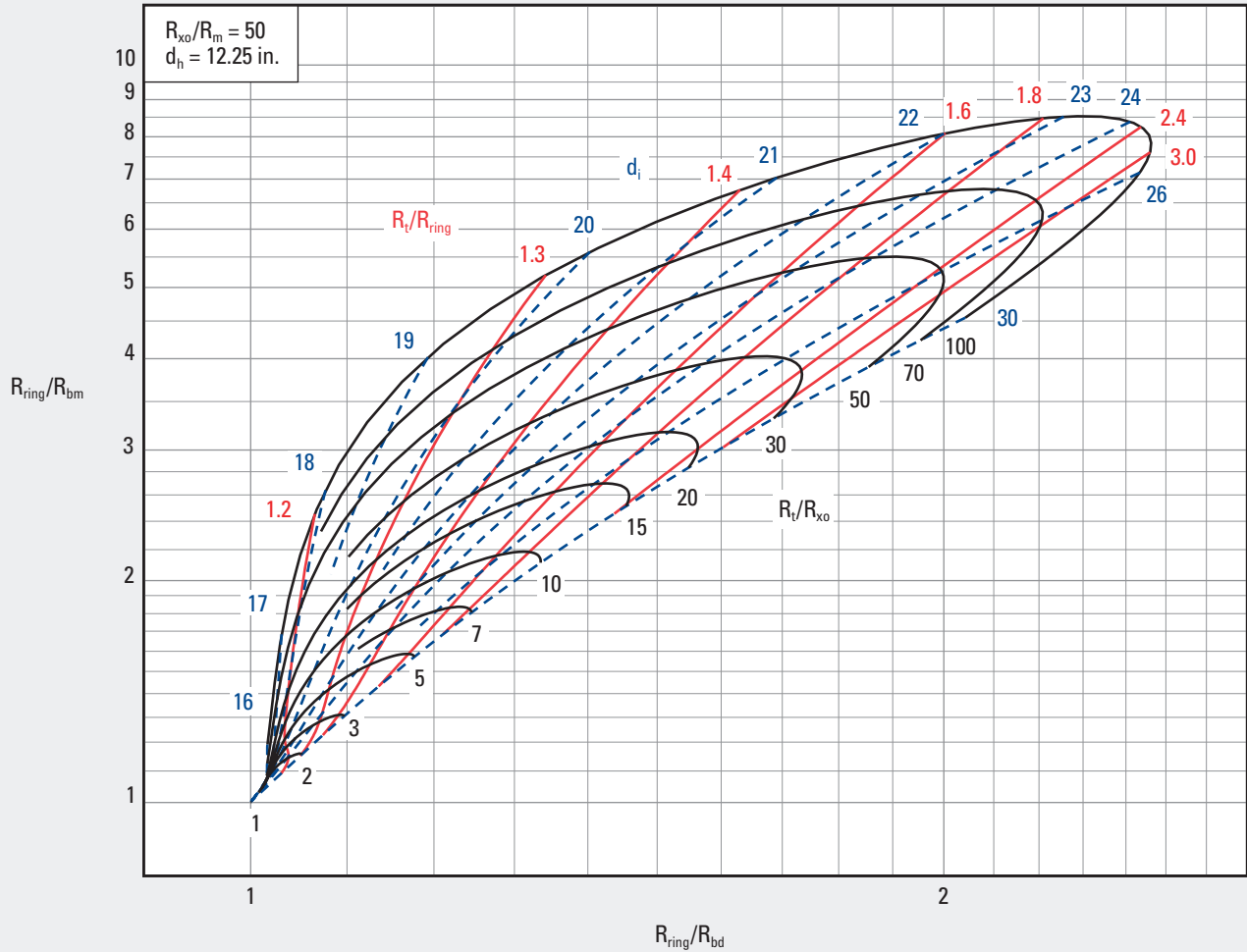
This chart is used similarly to Chart Rt-10 to determine the correction applied to the log presentation of R_t and d_i determined from geoVISION675 R_{ring} , R_{bit} , and R_{bd} resistivity values.

geoVISION825* 8¼-in. Resistivity-at-the-Bit Tool

Formation Resistivity and Diameter of Invasion—Open Hole

Rt-14

Ring, Deep, and Medium Button Resistivity (8¼-in. tool)



*Mark of Schlumberger
© Schlumberger

Purpose

This chart is used similarly to Chart Rt-10 to determine the correction applied to the log presentation of R_t and d_i determined from geoVISION825 R_{ring} , R_{bd} , and R_{bm} resistivity values.

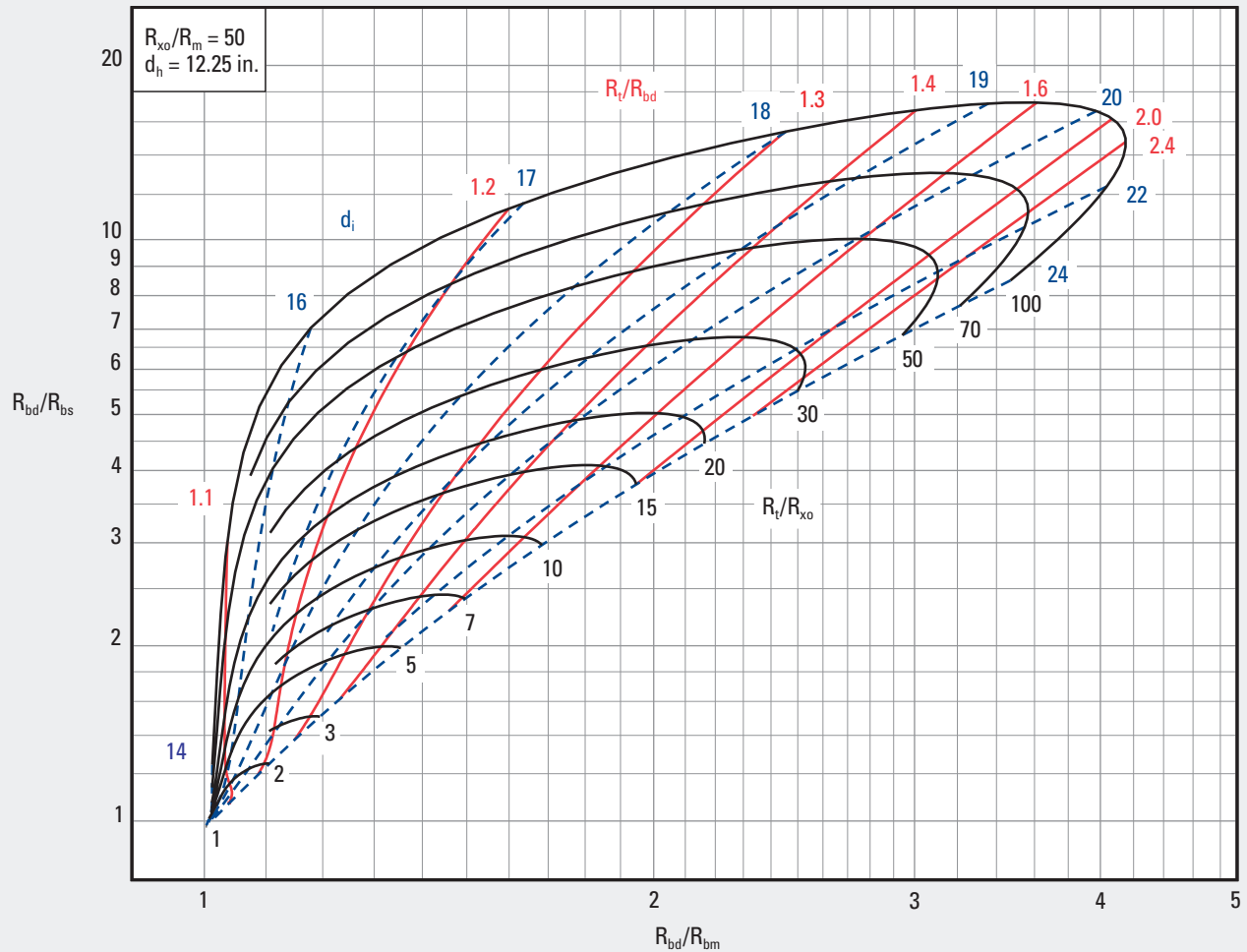
Rt

geoVISION825* 8¼-in. Resistivity-at-the-Bit Tool

Formation Resistivity and Diameter of Invasion—Open Hole

Rt-15

Deep, Medium, and Shallow Button Resistivity (8¼-in. tool)



*Mark of Schlumberger
© Schlumberger

Purpose

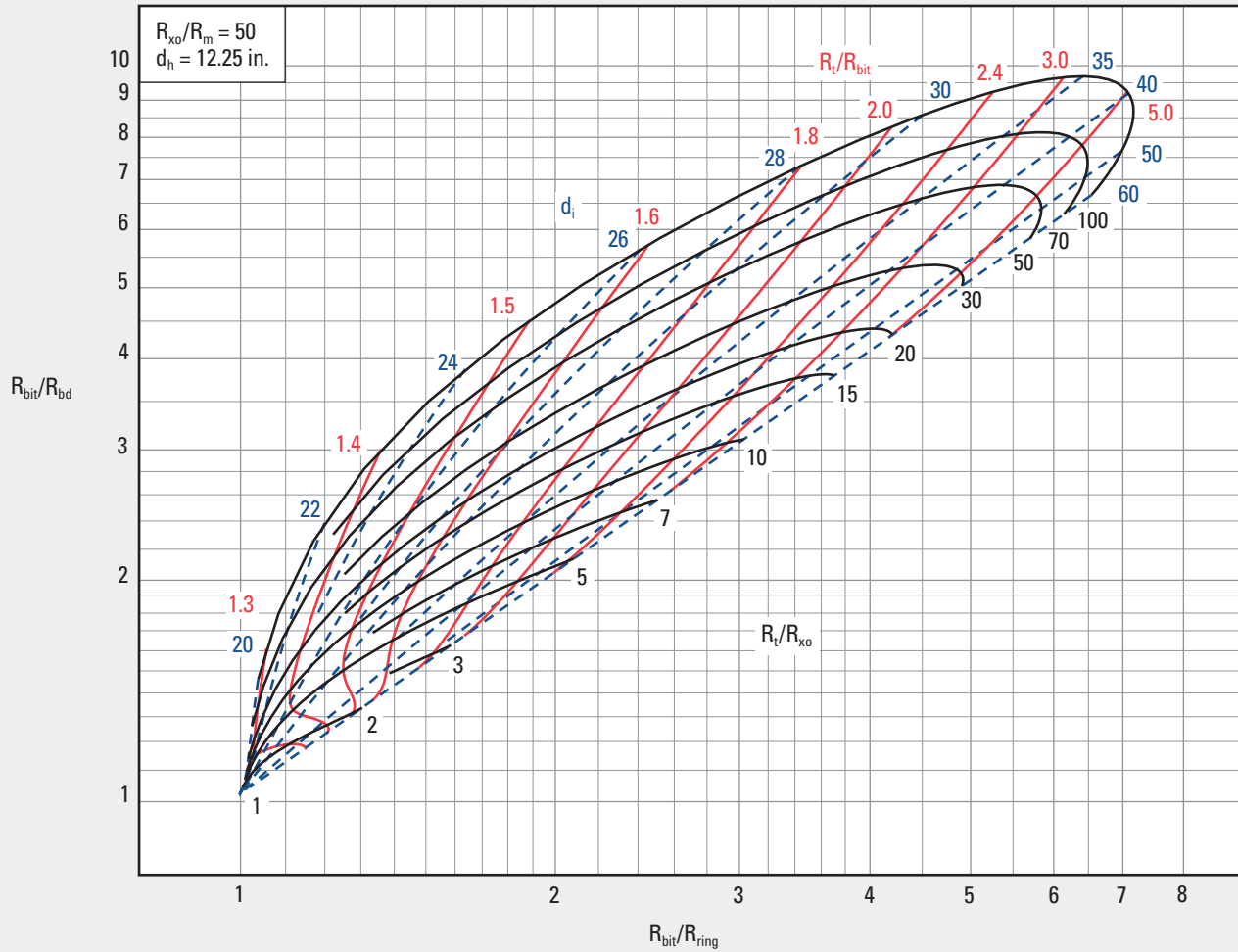
This chart is used similarly to Chart Rt-10 to determine the correction applied to the log presentation of R_t and d_i determined from geoVISION825 R_{bd} , R_{bm} , and R_{bs} resistivity values.

geoVISION825* 8¼-in. Resistivity-at-the-Bit Tool

Formation Resistivity and Diameter of Invasion—Open Hole

Rt-16

Bit, Ring, and Deep Button Resistivity (8¼-in. tool) with ROP to Bit Face = 4 ft



*Mark of Schlumberger
© Schlumberger

Purpose

This chart is used similarly to Chart Rt-10 to determine the correction applied to the log presentation of R_t and d_i determined from geoVISION825 R_{ring} , R_{bit} , and R_{bd} resistivity values.

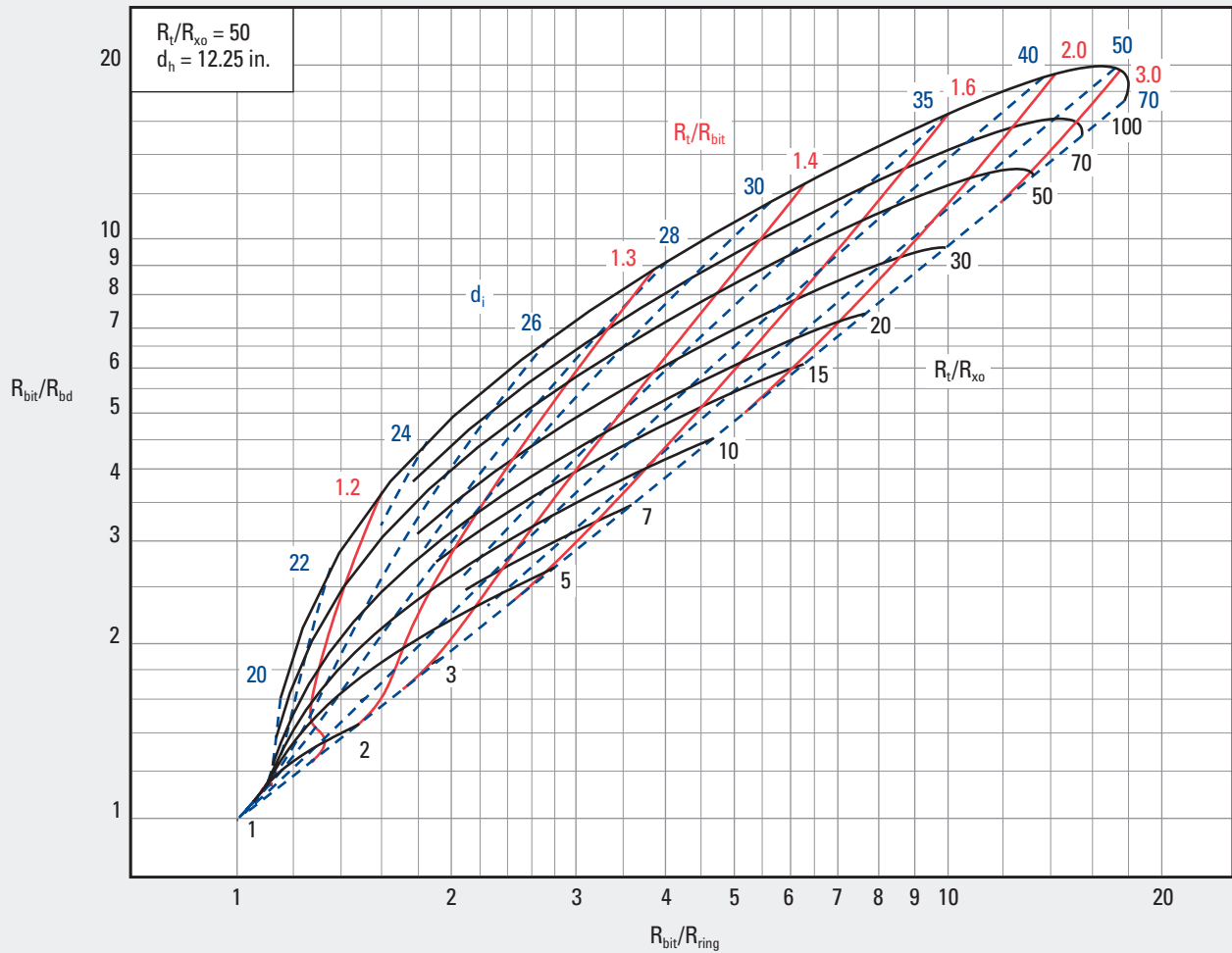
Rt

geoVISION825* 8¼-in. Resistivity-at-the-Bit Tool

Formation Resistivity and Diameter of Invasion—Open Hole

Rt-17

Bit, Ring, and Deep Button Resistivity (8¼-in. tool) with ROP to Bit Face = 35 ft



*Mark of Schlumberger
© Schlumberger

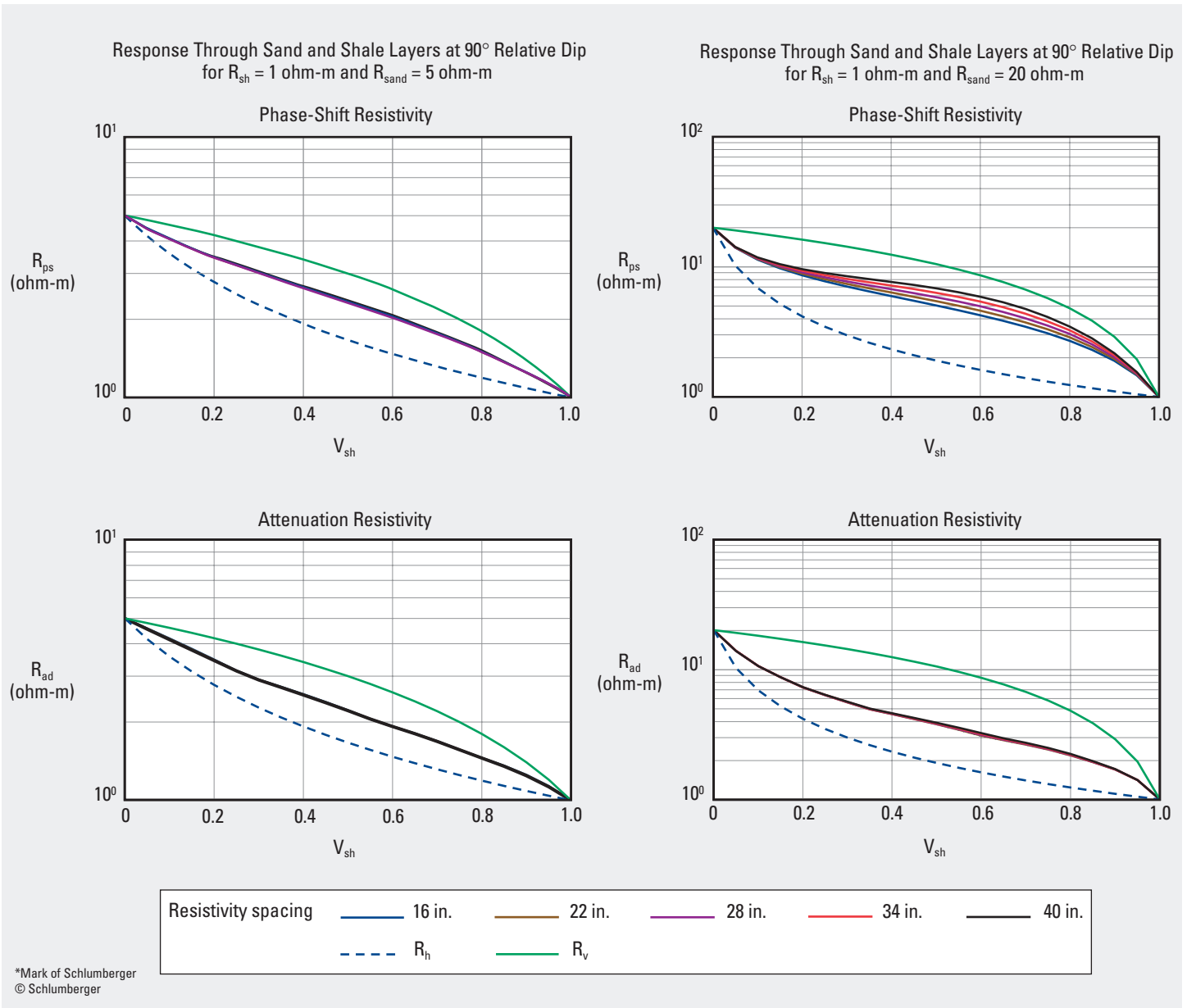
Purpose

This chart is used similarly to Chart Rt-10 to determine the correction applied to the log presentation of R_t and d_i determined from geoVISION825 R_{ring} , R_{bit} , and R_{bd} resistivity values.

arcVISION* Array Resistivity Compensated Tool—400 kHz

Resistivity Anisotropy Versus Shale Volume—Open Hole

Rt-31



Purpose

This chart illustrates the resistivity response, as affected by sand and shale layers, of the arcVISION tool in horizontal wellbores. The chart is used to determine the values of R_h and R_v . These corrections are already applied to the log presentation.

Description

The chart is constructed for shale layers at 90° relative dip to the axis of the arcVISION tool. That is, both the layers of shale and the tool are horizontal to the vertical. Other requirements for use of this chart are that the shale resistivity (R_{sh}) is 1 ohm-m and the sand resistivity is 5 or 20 ohm-m.

Select the appropriate chart for the attenuation (R_{ad}) or phase-shift (R_{ps}) resistivity and values of resistivity of the shale (R_{sh}) and sand (R_{sand}). Enter the chart with the volume of shale (V_{sh}) on the x-axis and the resistivity on the y-axis. At the intersection point of these two values move straight downward to the dashed blue curve to read the value of R_h . Move upward to the solid green curve to read the value of R_v .

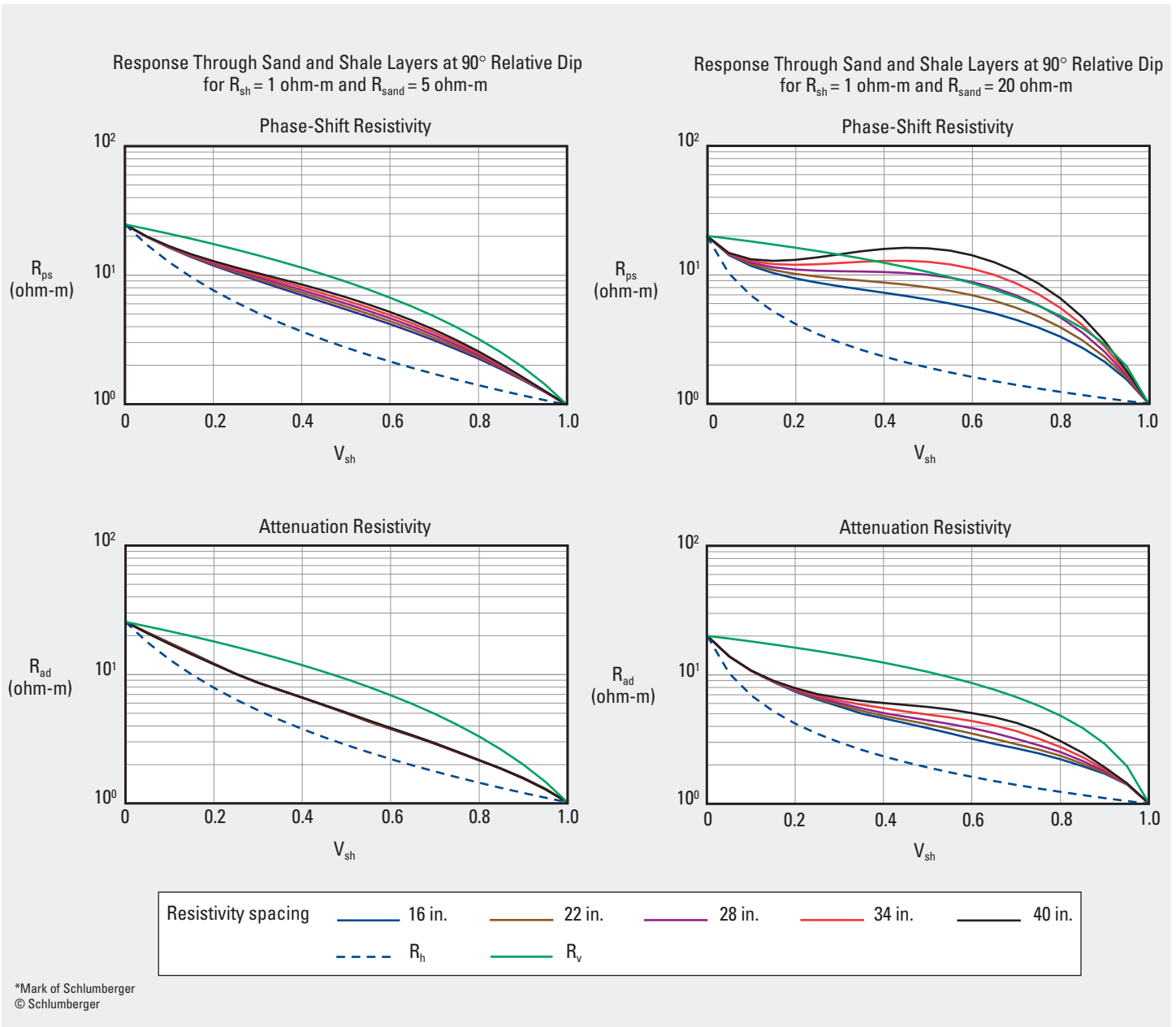
Chart Rt-32 is used to determine R_h and R_v values for the 2-MHz resistivity.

Rt

arcVISION* and ImPulse* Array Resistivity Compensated Tools—2 MHz

Resistivity Anisotropy Versus Shale Volume—Open Hole

Rt-32



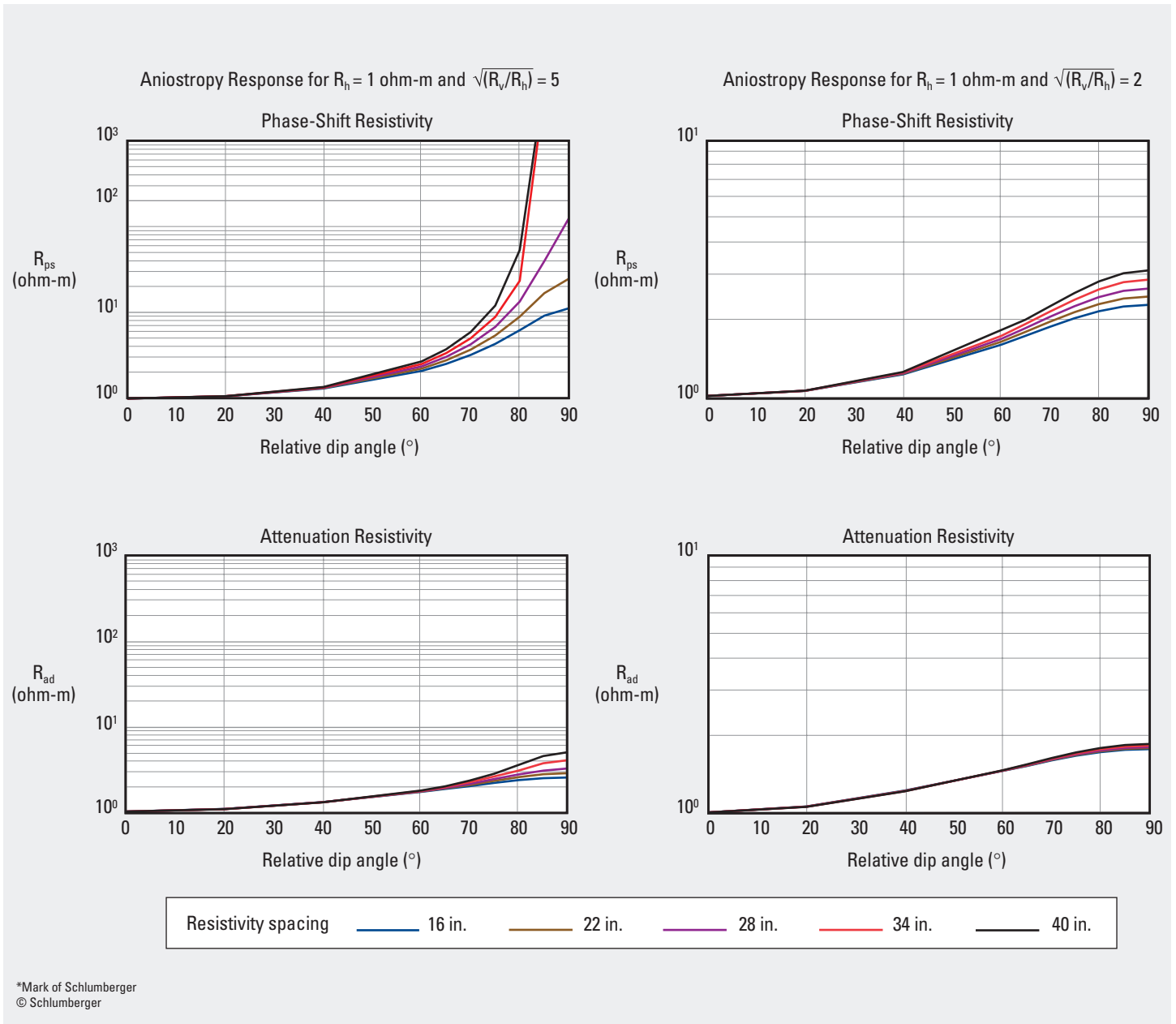
Purpose

This chart is used similarly to Chart Rt-31 for arcVISION and ImPulse 2-MHz resistivity. These corrections are already applied to the log presentation.

arcVISION* Array Resistivity Compensated Tool—400 kHz

Resistivity Anisotropy Versus Dip—Open Hole

Rt-33



Rt

Purpose

This chart is used to determine arcVISION R_{ps} and R_{ad} for relative dip angles from 0 to 90°. These corrections are already applied to the log presentation.

Description

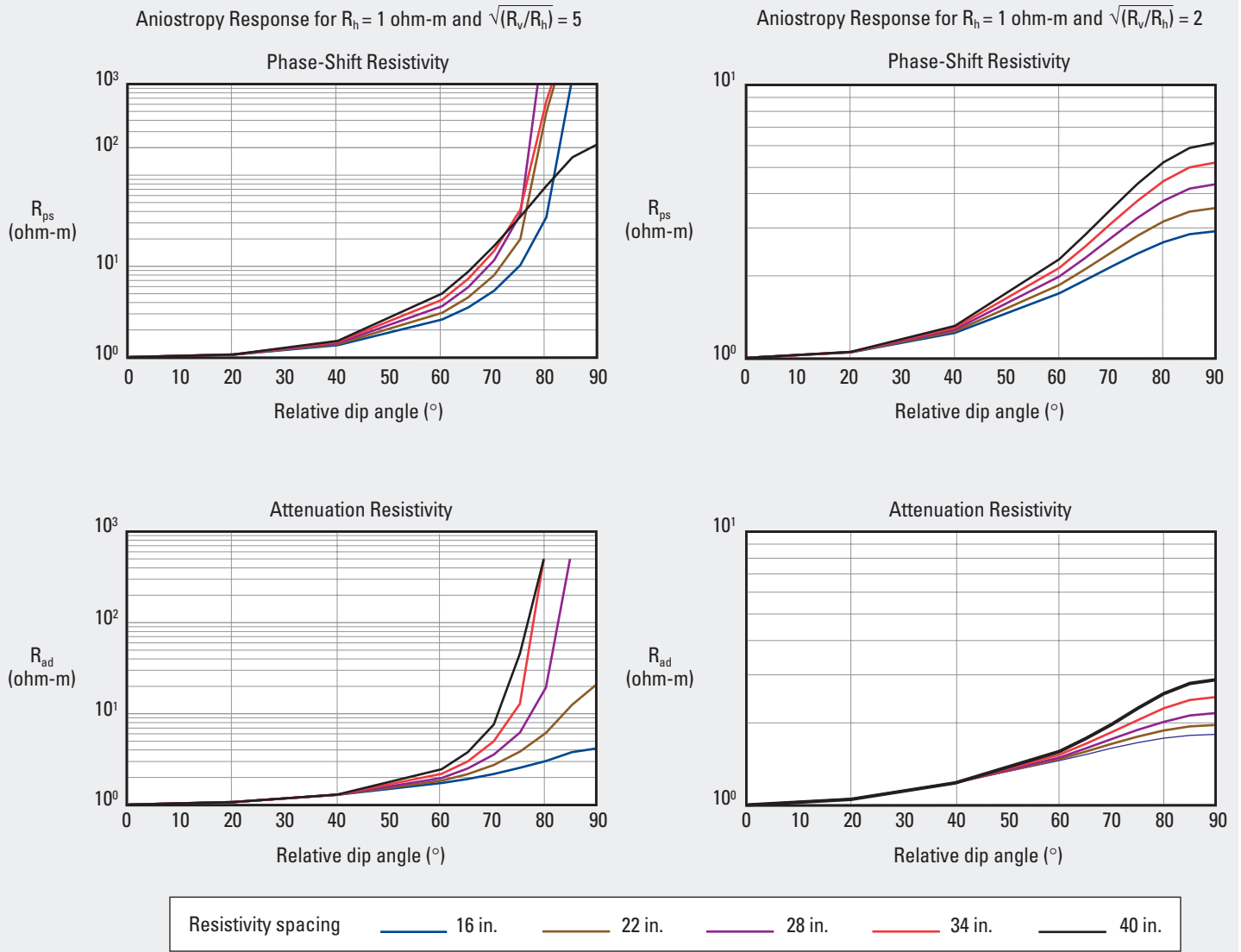
Enter the appropriate chart with the value of relative dip angle and move to intersect the known resistivity spacing. Move horizontally left to read R_{ps} or R_{ad} for the conditions of the horizontal resistivity (R_h) = 1 ohm-m and the square root of the R_v/R_h ratio.

*Mark of Schlumberger
© Schlumberger

arcVISION* and ImPulse* Array Resistivity Compensated Tools—2 MHz

Resistivity Anisotropy Versus Dip—Open Hole

Rt-34



*Mark of Schlumberger
© Schlumberger

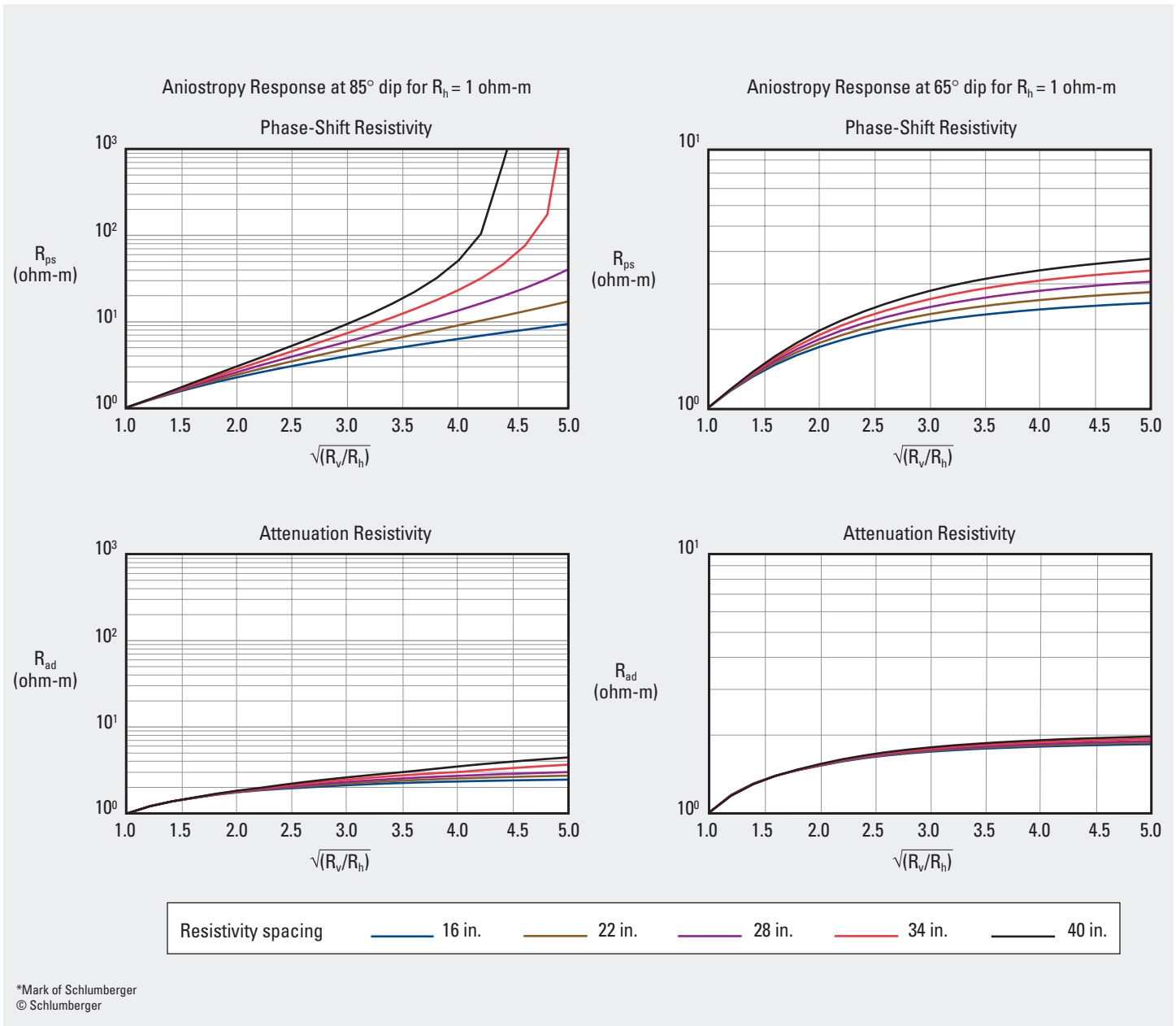
Purpose

This chart is used similarly to Chart Rt-33 for arcVISION and ImPulse 2-MHz resistivity. These corrections are already applied to the log presentation.

arcVISION* Array Resistivity Compensated Tool—400 kHz

Resistivity Anisotropy Versus Square Root of R_v/R_h —Open Hole

Rt-35



Purpose

This chart and Chart Rt-36 reflect the effect of anisotropy on the arcVISION resistivity response. These corrections are already applied to the log presentation. As the square root of the R_v/R_h ratio increases, the effect on the resistivity significantly increases.

Description

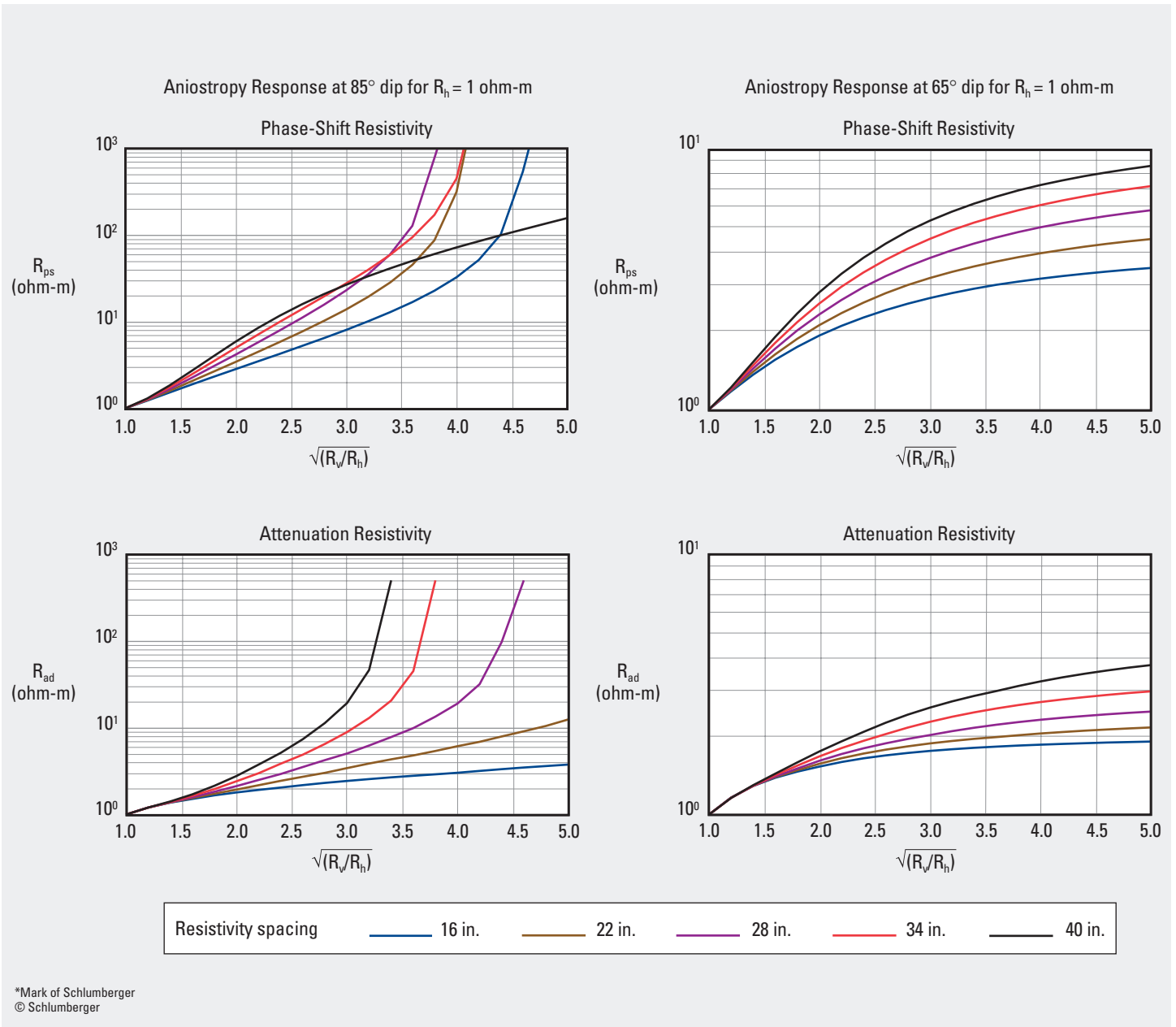
Enter the appropriate chart with the value of the phase-shift or attenuation resistivity on the y-axis. Move horizontally to intersect the resistivity spacing curve. At the intersection point read the value of the square root of the R_v/R_h ratio on the x-axis.

Rt

arcVISION* and ImPulse* Array Resistivity Compensated Tools—2 MHz

Resistivity Anisotropy Versus Square Root of R_v/R_h —Open Hole

Rt-36



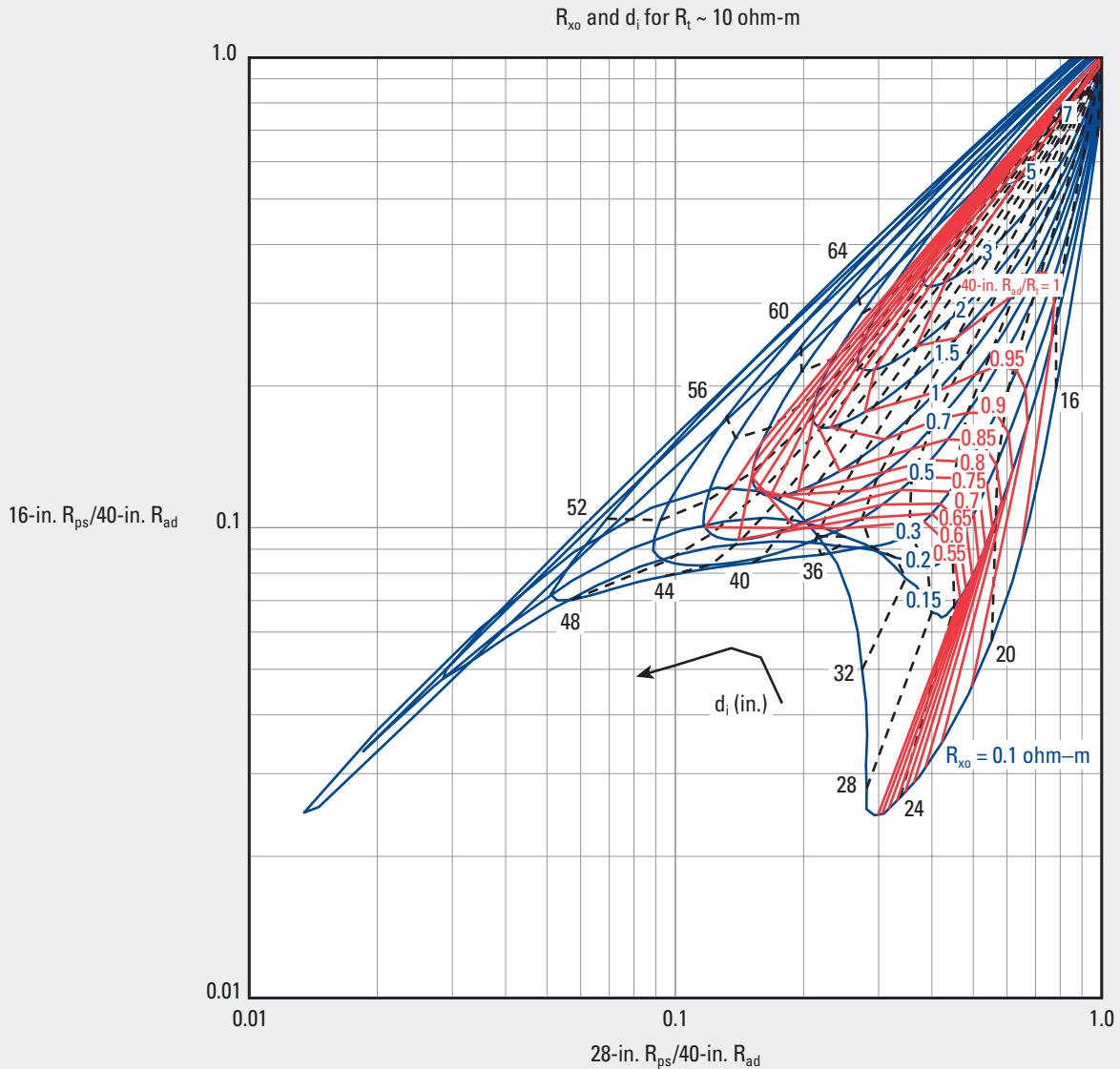
Purpose

This chart is used similarly to Chart Rt-35 for arcVISION and ImPulse for 2-MHz resistivity. These corrections are already applied to the log presentation.

arcVISION675* Array Resistivity Compensated Tool—400 kHz

Conductive Invasion—Open Hole

Rt-37



*Mark of Schlumberger
© Schlumberger

Purpose

This log-log chart is used to determine the correction applied to the log presentation of the 40-in. arcVISION675 resistivity measurements, diameter of invasion (d_i), and resistivity of the flushed zone (R_{xo}). These data are used to evaluate a formation for hydrocarbons.

Description

Enter the chart with the ratio of the 16-in. $R_{ps}/40$ -in. R_{ad} on the y-axis and 28-in. $R_{ps}/40$ -in. R_{ad} on the x-axis. The intersection point defines the following:

- d_i
- R_{xo}
- correction factor for 40-in. attenuation resistivity.

Chart Rt-38 is used for 2-MHz resistivity values. The corresponding charts for resistive invasion are Charts Rt-39 and Rt-40.

Example

Given: 16-in. $R_{ps}/40$ -in. $R_{ad} = 0.2$ and 28-in. $R_{ps}/40$ -in. $R_{ad} = 0.4$.

Find: R_{xo} , d_i , and correction factor for 40-in. R_{ad} .

Answer: At the intersection point of 0.2 on the y-axis and 0.4 on the x-axis, $d_i = 31.9$ in., $R_{xo} = 1.1$ ohm-m, and correction factor = 0.955.

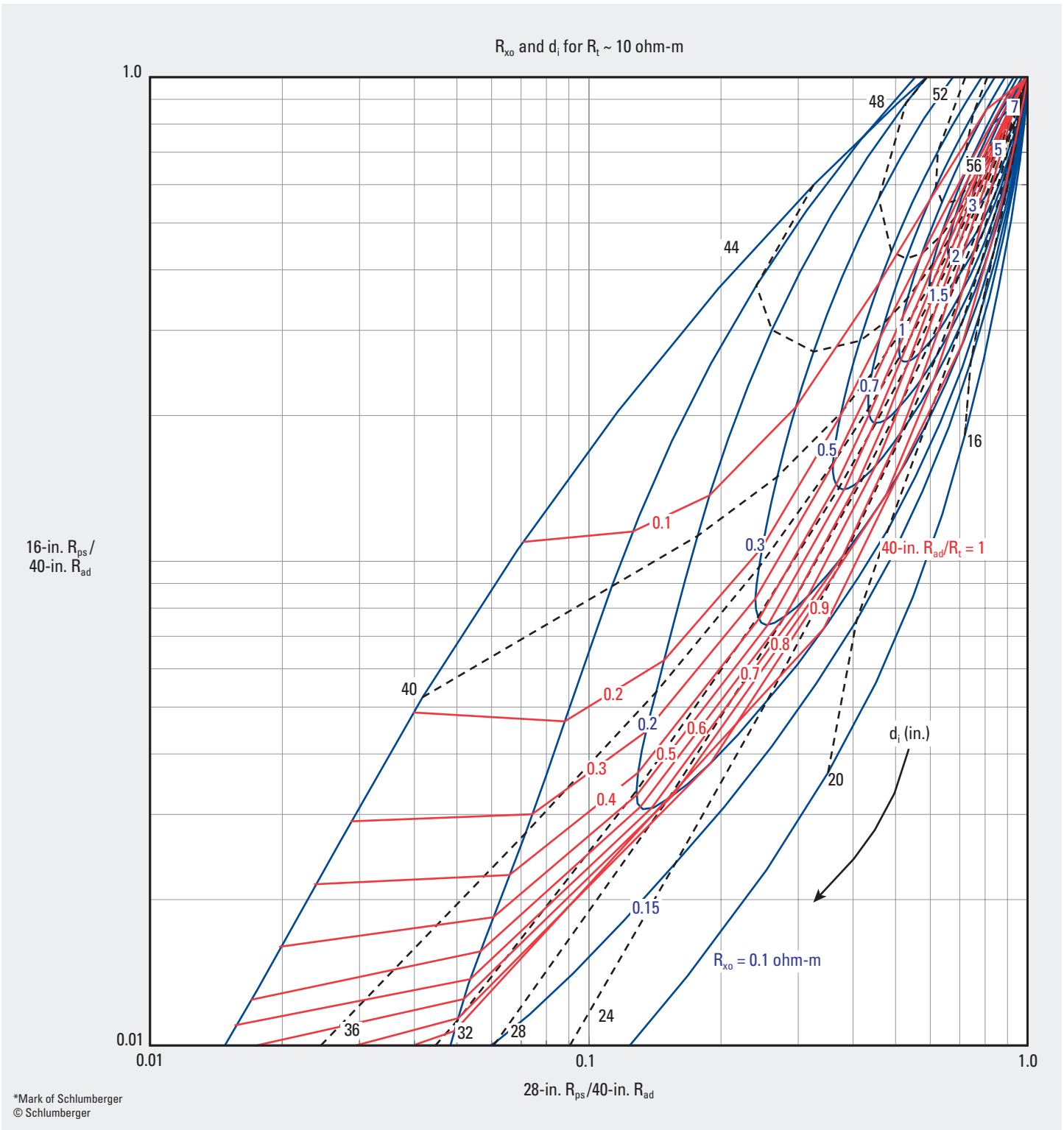
The value of the 40-in. R_{ad} is reduced by the correction factor: 40-in. $R_{ad} \times 0.955$.

Rt

arcVISION675* and ImPulse* Array Resistivity Compensated Tools—2 MHz

Conductive Invasion—Open Hole

Rt-38



*Mark of Schlumberger
© Schlumberger

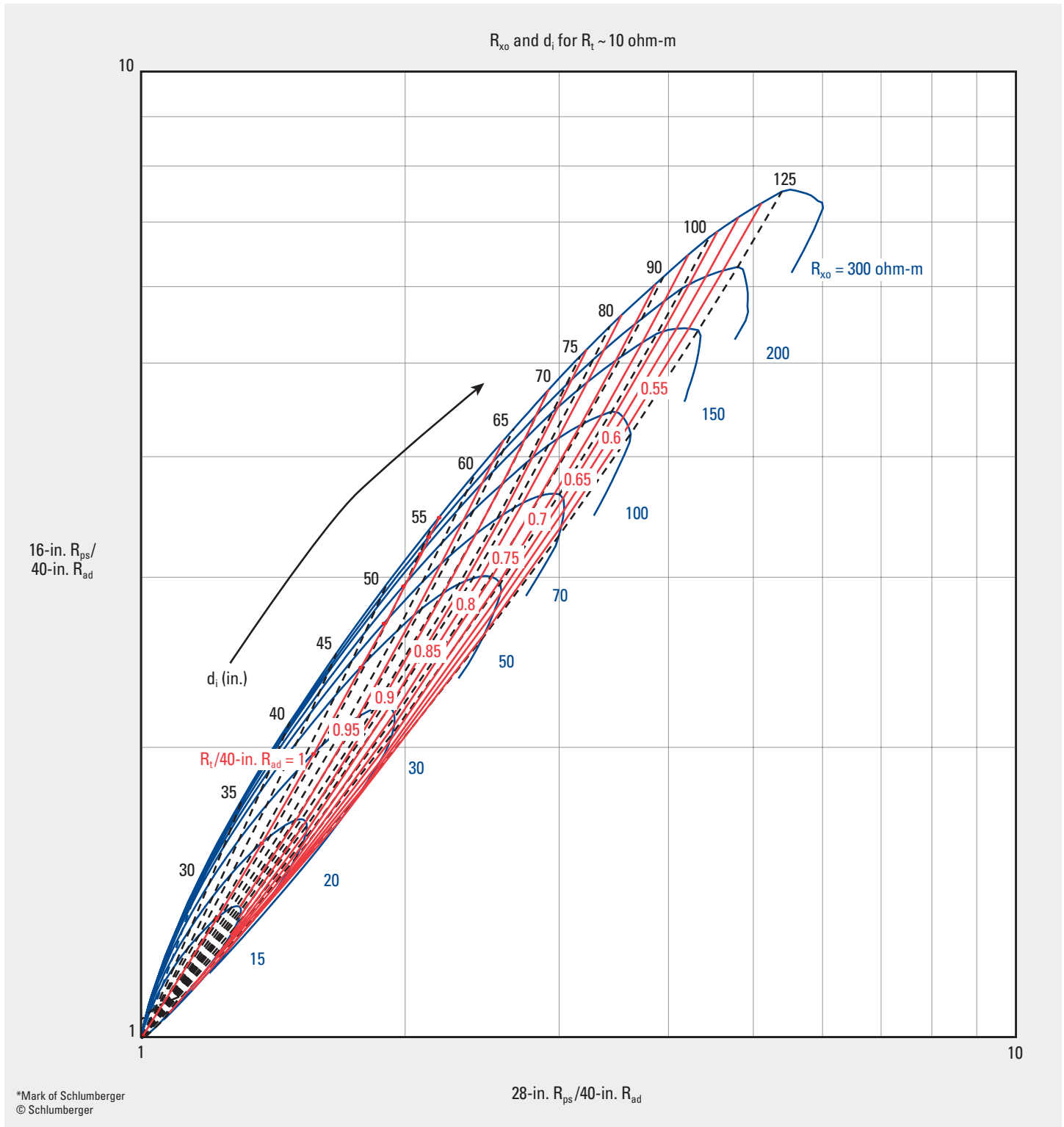
Purpose

This chart is used similarly to Chart Rt-37 for arcVISION675 and ImPulse 2-MHz resistivity. The corrections are already applied to the log presentation.

arcVISION* Array Resistivity Compensated Tool—400 kHz

Resistive Invasion—Open Hole

Rt-39



Rt

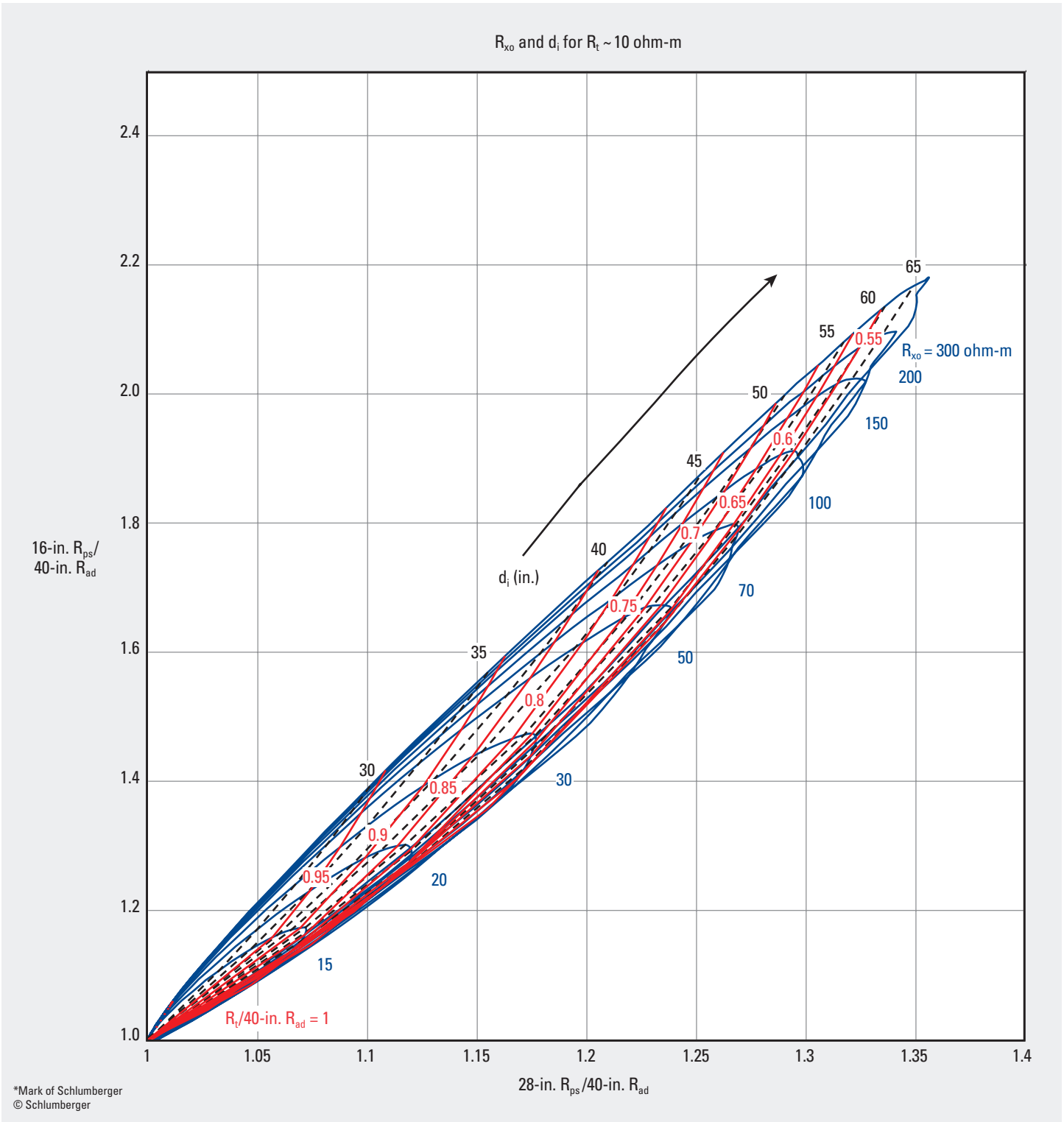
Purpose

This chart is used similarly to Chart Rt-37 to determine the correction applied to the arcVISION log presentation of d_i , R_{xo} , and 40-in. R_{ad} for resistive invasion.

arcVISION* and ImPulse* Array Resistivity Compensated Tools—2 MHz

Resistive Invasion—Open Hole

Rt-40



Purpose

This chart is used similarly to Chart Rt-39 to determine the correction applied to the arcVISION and ImPulse log presentation for 2-MHz resistivity.

arcVISION* Array Resistivity Compensated Tool—400 kHz in Horizontal Well

Bed Proximity Effect—Open Hole

Purpose

Charts Rt-41 and Rt-42 are used to calculate the correction applied to the log presentation of R_t from the arcVISION tool at the approach to a bed boundary. The value of R_t is used to calculate water saturation.

Description

There are two sets of charts for differing conditions:

- shoulder bed resistivity (R_{shoulder}) = 10 ohm-m and $R_t = 1$ ohm-m
- $R_{\text{shoulder}} = 10$ ohm-m and $R_t = 100$ ohm-m.

Example

Given: $R_{\text{shoulder}} = 10$ ohm-m, $R_t = 1$ ohm-m, and 16-in. $R_{\text{ps}} = 1.5$ ohm-m.

Find: Bed proximity effect.

Answer: The top set of charts is appropriate for these resistivity values. The ratio $R_{\text{ps}}/R_t = 1.5/1 = 1.5$.

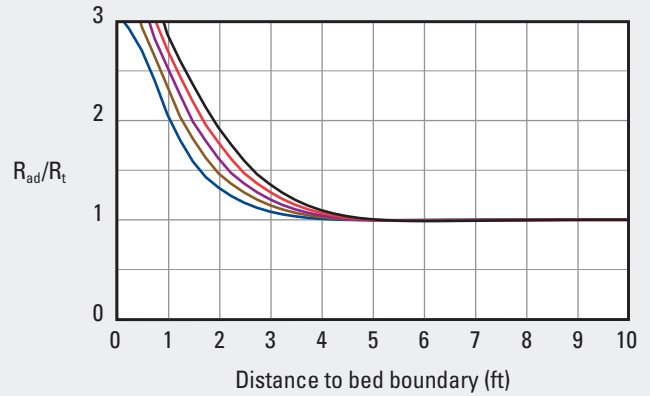
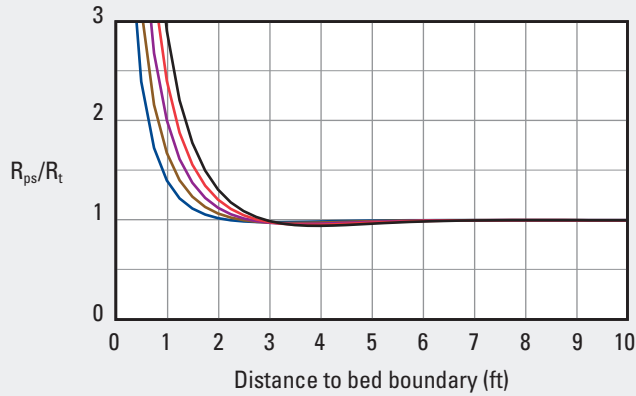
Enter the y-axis of the left-hand chart at 1.5 and move horizontally to intersect the 16-in. curve. The corresponding value on the x-axis is 1 ft, which is the distance of the surrounding bed from the tool. At 2 ft from the bed boundary, the value of 16-in. $R_{\text{ps}} = 1$ ohm-m.

arcVISION* Array Resistivity Compensated Tool—400 kHz in Horizontal Well

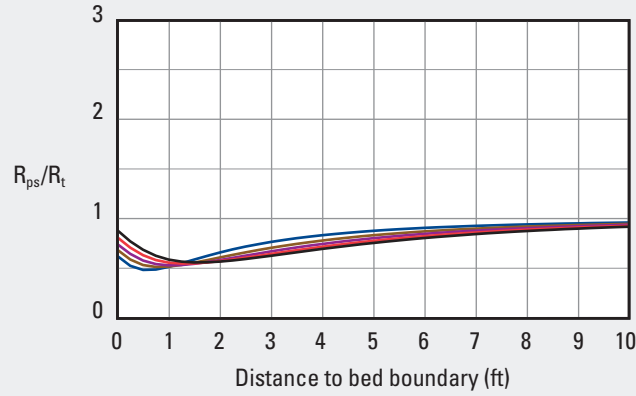
Bed Proximity Effect—Open Hole

Rt-41

Bed Proximity Effect for Horizontal Well: $R_{\text{shoulder}} = 10 \text{ ohm-m}$ and $R_t = 1 \text{ ohm-m}$



Bed Proximity Effect for Horizontal Well: $R_{\text{shoulder}} = 10 \text{ ohm-m}$ and $R_t = 100 \text{ ohm-m}$



Resistivity spacing — 16 in. — 22 in. — 28 in. — 34 in. — 40 in.

*Mark of Schlumberger
© Schlumberger

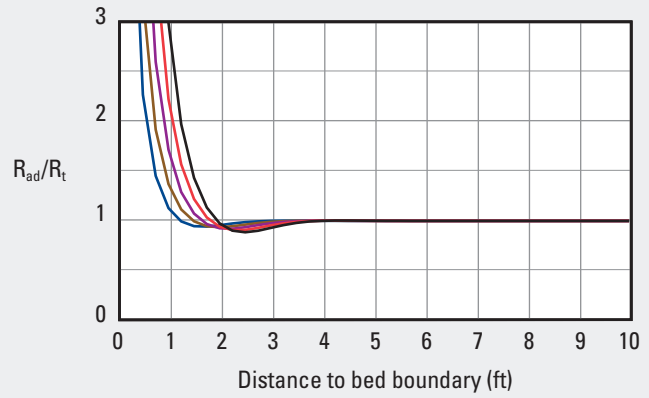
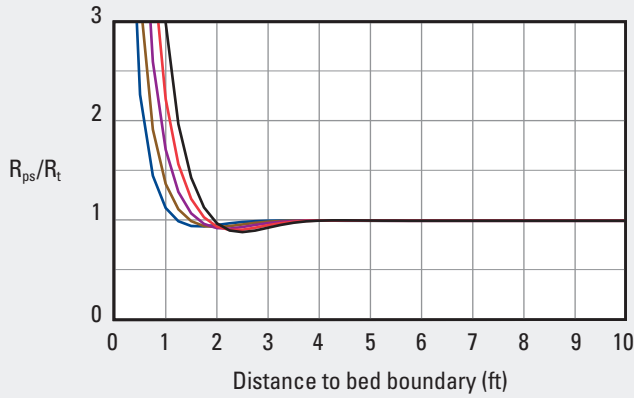
Rt

arcVISION* and ImPulse* Array Resistivity Compensated Tools—2 MHz in Horizontal Well

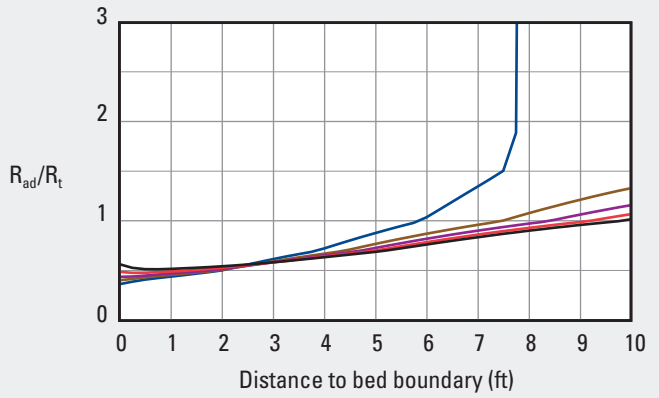
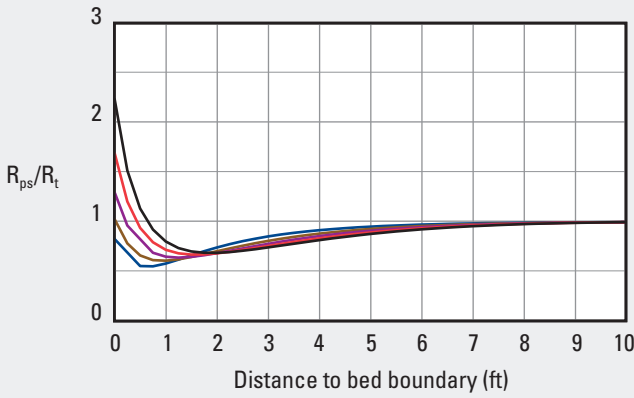
Rt-42

Bed Proximity Effect—Open Hole

Bed Proximity Effect for Horizontal Well: $R_{\text{shoulder}} = 10 \text{ ohm-m}$, $R_t = 1 \text{ ohm-m}$



Bed Proximity Effect for Horizontal Well: $R_{\text{shoulder}} = 10 \text{ ohm-m}$, $R_t = 100 \text{ ohm-m}$



Resistivity spacing — 16 in. — 22 in. — 28 in. — 34 in. — 40 in.

*Mark of Schlumberger
© Schlumberger

Purpose

This chart is used similarly to Chart Rt-41 for arcVISION and ImPulse 2-MHz resistivity. The correction is already applied to the log presentation.

Rt

Density and NGS* Natural Gamma Ray Spectrometry Tool

Mineral Identification—Open Hole

Purpose

This chart is a method for identifying the type of clay in the wellbore. The values of the photoelectric factor (Pe) from the Litho-Density* log and the concentration of potassium (K) from the NGS Natural Gamma Ray Spectrometry tool are entered on the chart.

Description

Enter the upper chart with the values of Pe and K to determine the point of intersection. On the lower chart, plotting Pe and the ratio of thorium and potassium (Th/K) provides a similar mineral evaluation. The intersection points are not unique but are in general areas defined by a range of values.

Example

Given: Environmentally corrected thorium concentration (ThNGScorr) = 10.6 ppm, environmentally corrected potassium concentration (KNGScorr) = 3.9%, and Pe = 3.2.

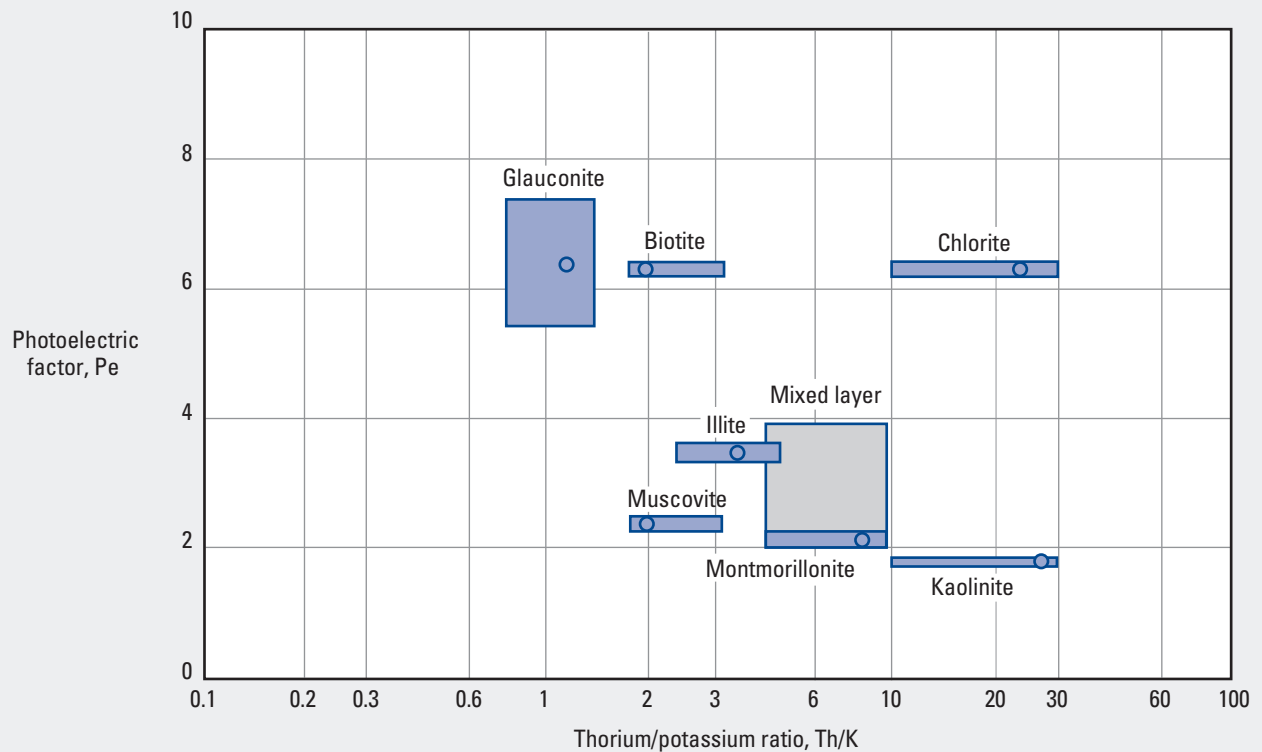
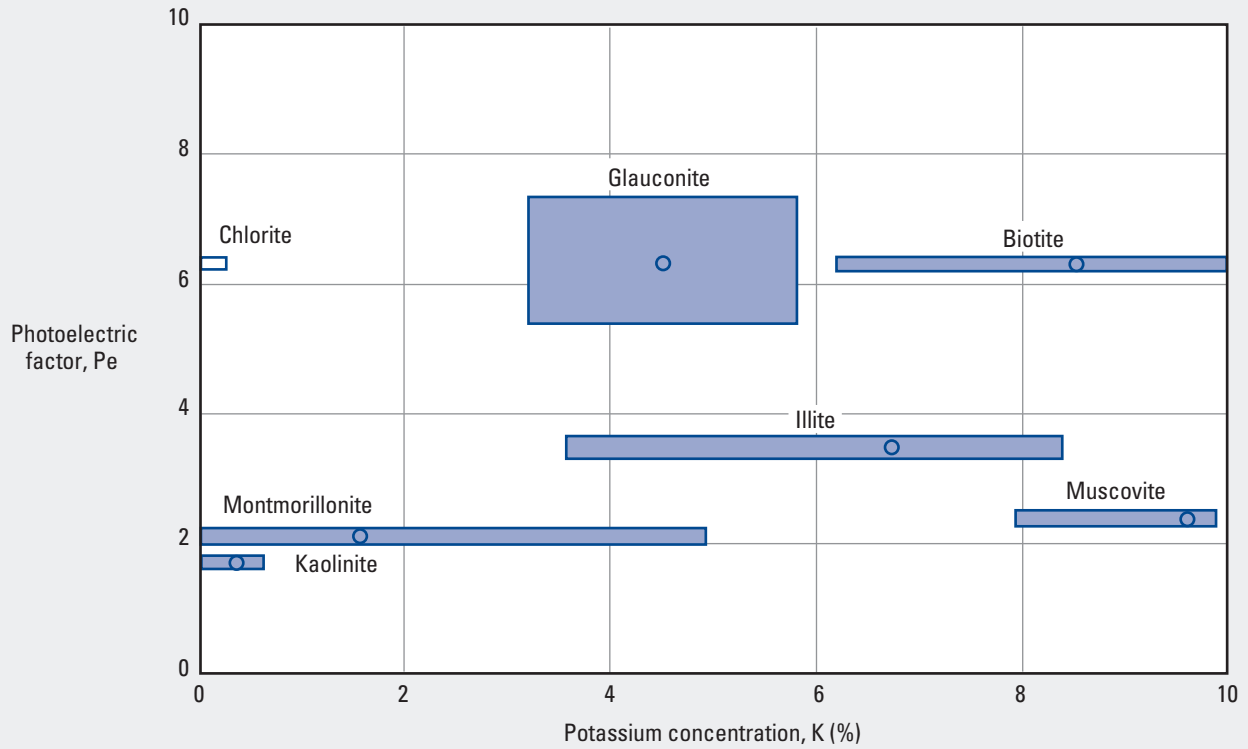
Find: Mineral concentration of the logged clay.

Answer: The intersection points from plotting values of Pe and K on the upper chart and Pe and Th/K ratio = $10.6/3.9 = 2.7$ on the lower chart suggest that the clay mineral is illite.

Density and NGS* Natural Gamma Ray Spectrometry Tool

Mineral Identification—Open Hole

Lith-1
(former CP-18)

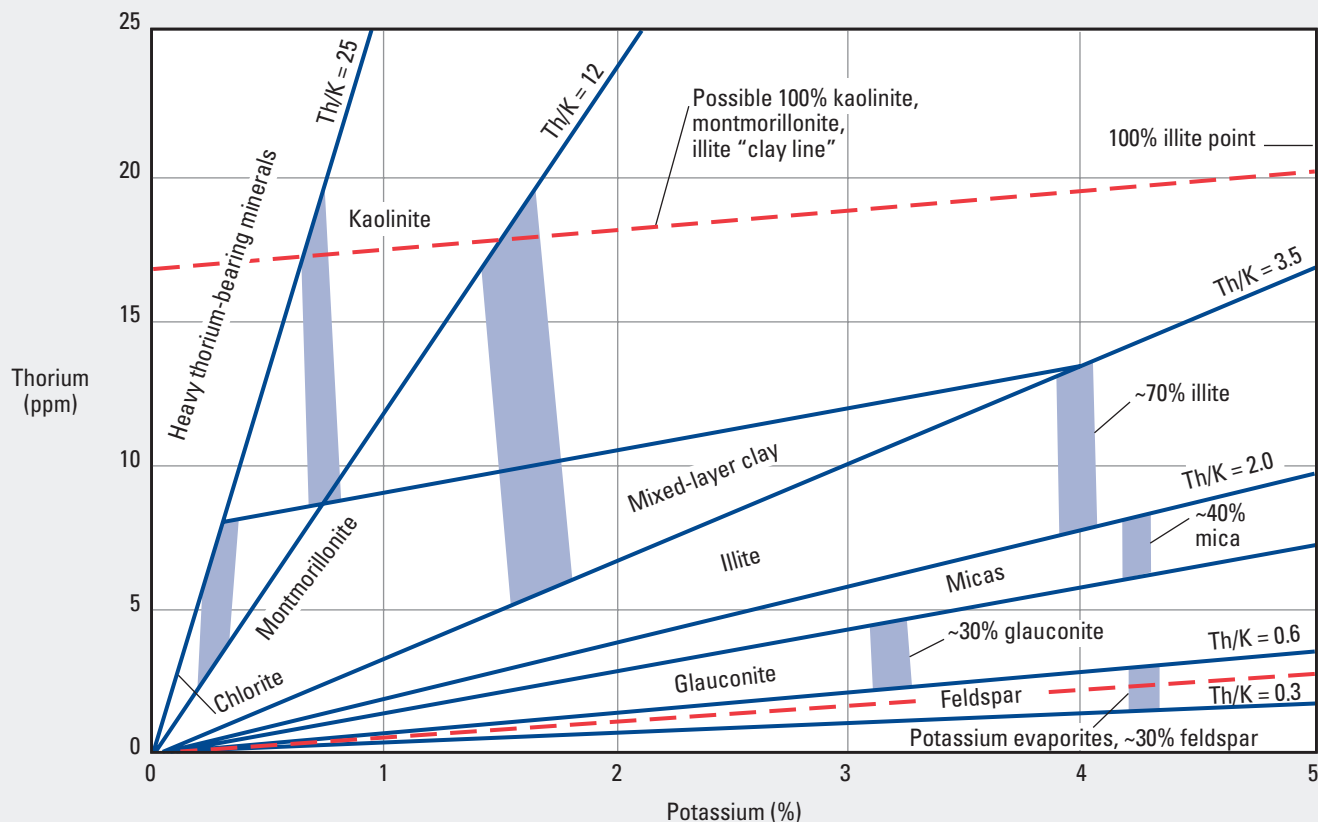


*Mark of Schlumberger
© Schlumberger

Lith

NGS* Natural Gamma Ray Spectrometry Tool

Mineral Identification—Open Hole

Lith-2
(former CP-19)

*Mark of Schlumberger
© Schlumberger

Lith

Purpose

This chart is used to determine the type of minerals in a shale formation from concentrations measured by the NGS Natural Gamma Ray Spectrometry tool.

Description

Entering the chart with the values of thorium and potassium locates the intersection point used to determine the type of radioactive minerals that compose the majority of the clay in the formation.

A sandstone reservoir with varying amounts of shaliness and illite as the principal clay mineral usually plots in the illite segment of the chart with Th/K between 2.0 and 3.5. Less shaly parts of the reservoir plot closer to the origin, and shaly parts plot closer to the 70% illite area.

Platform Express* Three-Detector Lithology Density Tool

Porosity and Lithology—Open Hole

Purpose

This chart is used to determine the lithology and porosity of a formation. The porosity is used for the water saturation determination and the lithology helps to determine the makeup of the logged formation.

Description

Note that this chart is designed for fresh water (fluid density [ρ_f] = 1.0 g/cm³) in the borehole. Chart Lith-4 is used for saltwater (ρ_f = 1.1 g/cm³) formations.

Values of photoelectric factor (Pe) and bulk density (ρ_b) from the Platform Express Three-Detector Lithology Density (TLD) tool are entered into the chart. At the point of intersection, porosity and lithology values can be determined.

Example

Given: Freshwater drilling mud, Pe = 3.0, and bulk density = 2.73 g/cm³.

Freshwater drilling mud, Pe = 1.6, and bulk density = 2.24 g/cm³.

Find: Porosity and lithology.

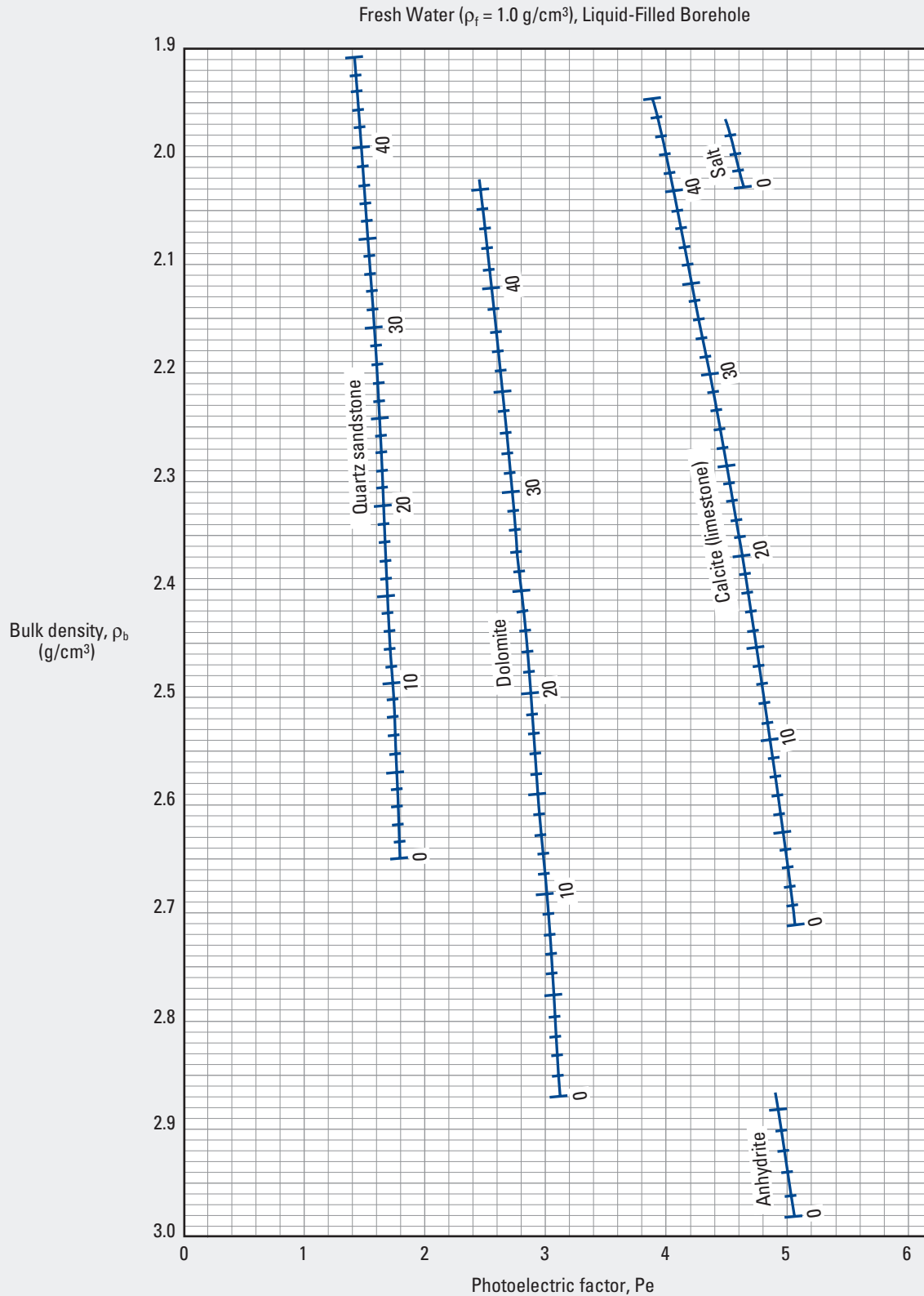
Answer: For the first set of conditions, the formation is a dolomite with 8% porosity.

The second set is for a quartz sandstone formation with 30% porosity.

Platform Express* Three-Detector Lithology Density Tool

Porosity and Lithology—Open Hole

Lith-3
(former CP-16)



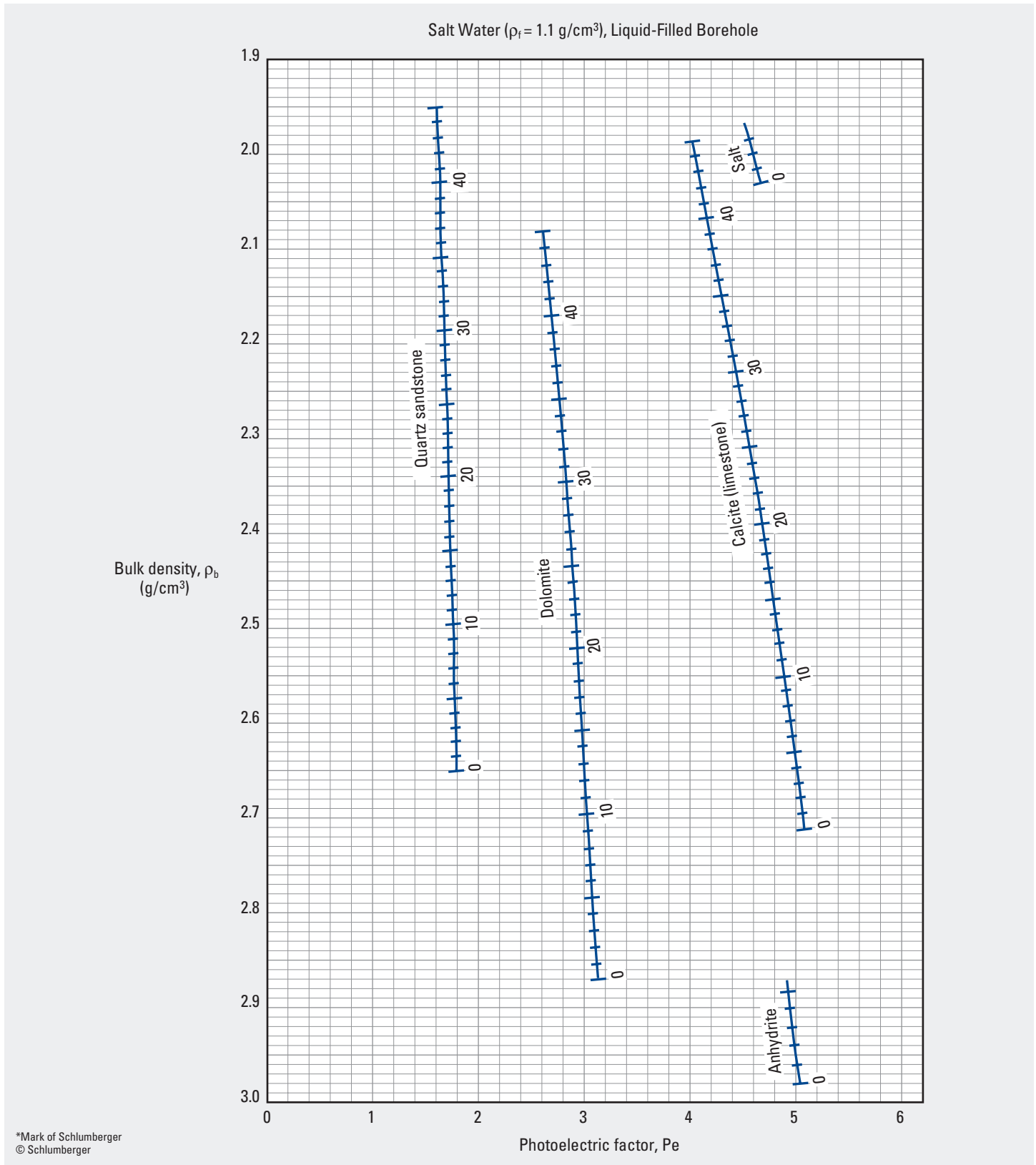
*Mark of Schlumberger
© Schlumberger

Lith

Platform Express* Three-Detector Lithology Density Tool

Porosity and Lithology—Open Hole

Lith-4
(former CP-17)



This chart is used similarly to Chart Lith-3 for lithology and porosity determination with values of photoelectric factor (Pe) and

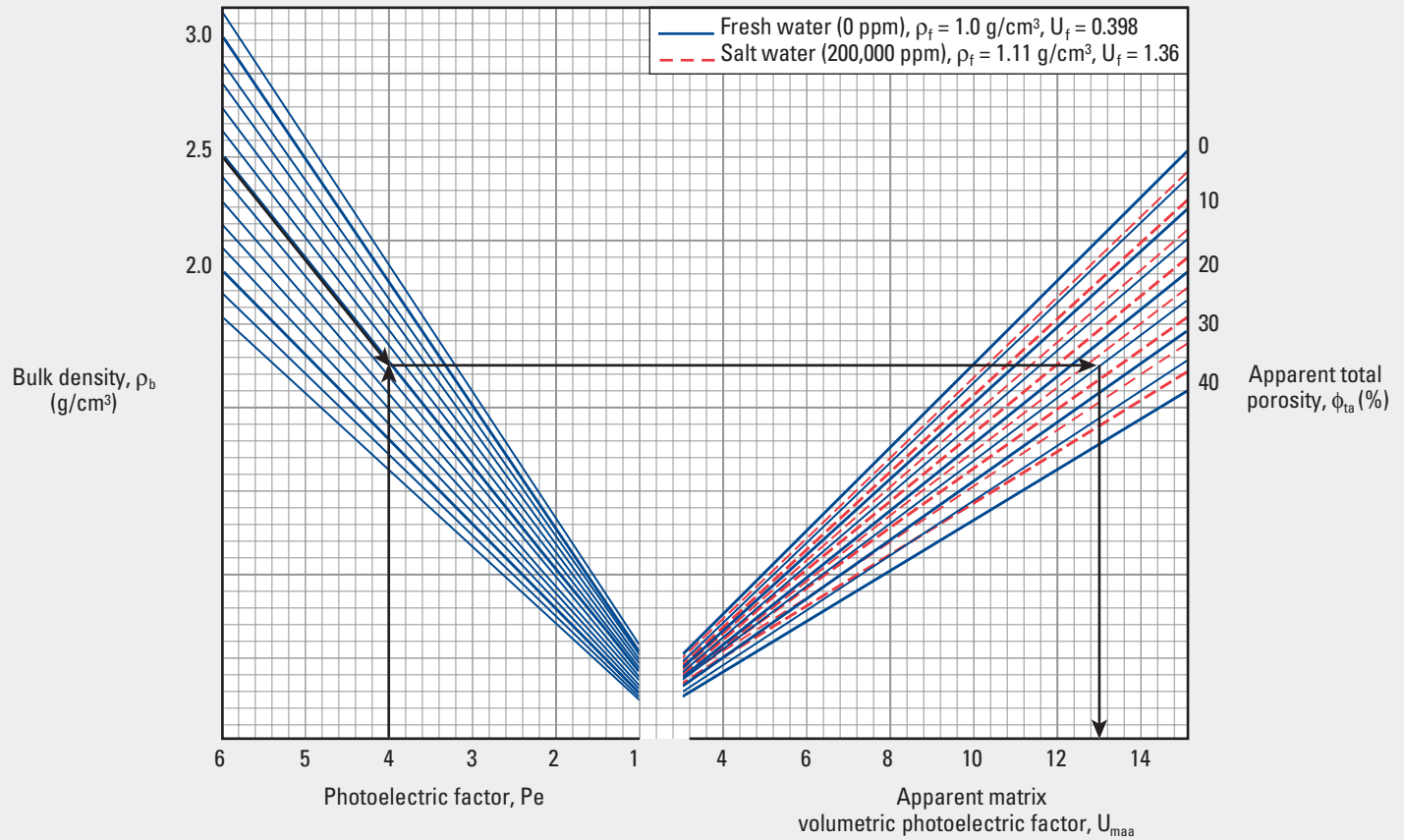
bulk density (ρ_b) from the Platform Express TLD tool in saltwater borehole fluid.

Lith

Density Tool

Apparent Matrix Volumetric Photoelectric Factor—Open Hole

Lith-5
(former CP-20)



© Schlumberger

Lith

Purpose

This chart is used to determine the apparent matrix volumetric photoelectric factor (U_{maa}) for the Chart Lith-6 percent lithology determination.

Description

This chart is entered with the values of bulk density (ρ_b) and Pe from a density log. The value of the apparent total porosity (ϕ_{ta}) must also be known. The appropriate solid lines on the right-hand side of the chart that indicate a freshwater borehole fluid or dotted lines that represent saltwater borehole fluid are used depending on the salinity of the borehole fluid. U_f is the fluid photoelectric factor.

Example

Given: $Pe = 4.0$, $\rho_b = 2.5$ g/cm³, $\phi_{ta} = 25\%$, and freshwater borehole fluid.

Find: Apparent matrix volumetric photoelectric factor (U_{maa}).

Answer: Enter the chart with the Pe value (4.0) on the left-hand x-axis, and move upward to intersect the curve for $\rho_b = 2.5$ g/cm³.

From that intersection point, move horizontally right to intersect the ϕ_{ta} value of 25%, using the blue freshwater curve.

Move vertically downward to determine the U_{maa} value on the right-hand x-axis scale: $U_{maa} = 13$.

Density Tool

Lithology Identification—Open Hole

Purpose

This chart is used to identify the rock mineralogy through comparison of the apparent matrix grain density (ρ_{maa}) and apparent matrix volumetric photoelectric factor (U_{maa}).

Description

The values of ρ_{maa} and U_{maa} are entered on the y- and x-axis, respectively. The rock mineralogy is identified by the proximity of the point of intersection of the two values to the labeled points on the plot. The effect of gas, salt, etc., is to shift data points in the directions shown by the arrows.

Example

Given: $\rho_{\text{maa}} = 2.74 \text{ g/cm}^3$ (from Chart Lith-9 or Lith-10) and $U_{\text{maa}} = 13$ (from Chart Lith-5).

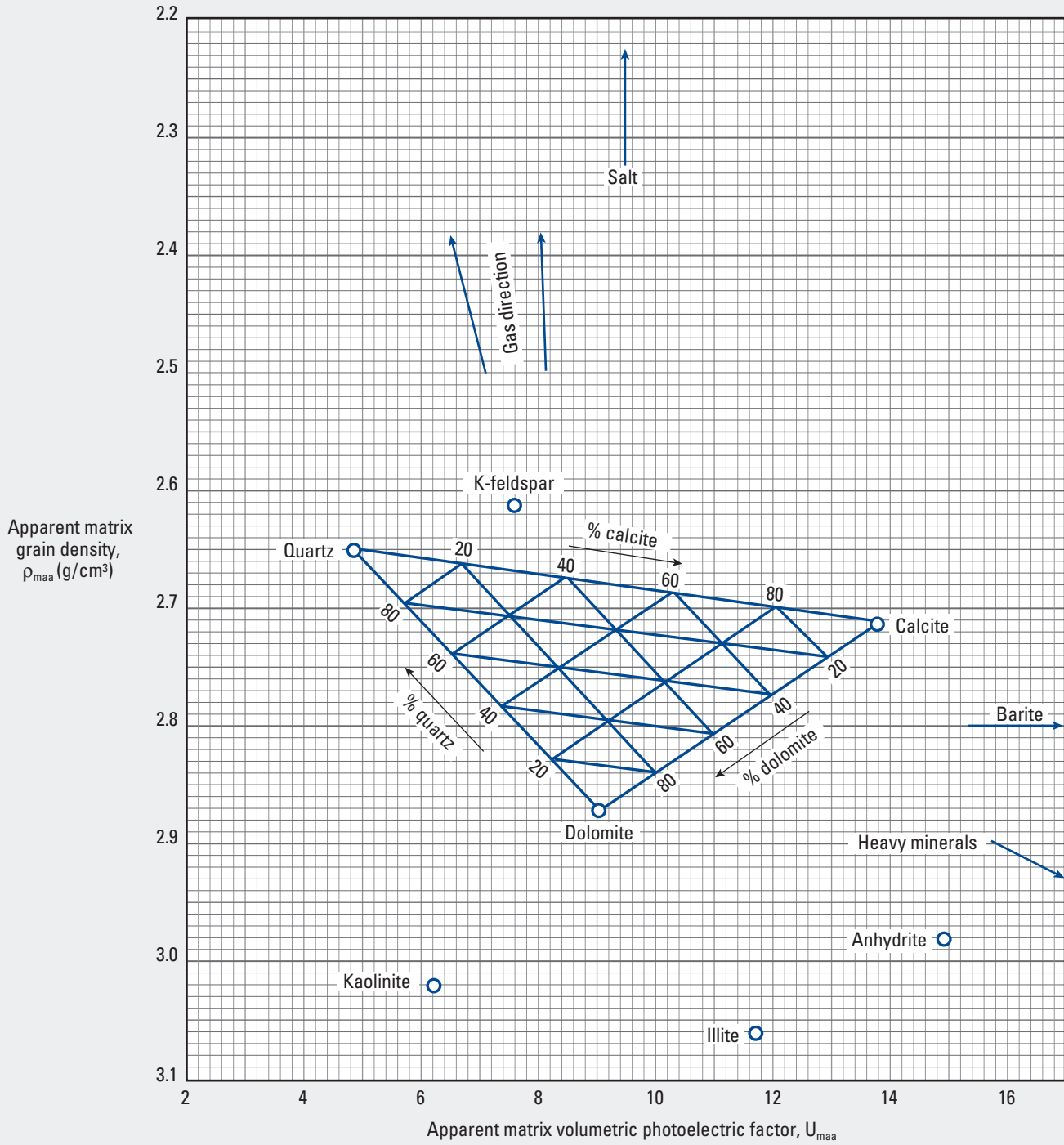
Find: Matrix composition of the formation.

Answer: Enter the chart with $\rho_{\text{maa}} = 2.74 \text{ g/cm}^3$ on the y-axis and $U_{\text{maa}} = 13$ on the x-axis. The intersection point indicates a matrix mixture of 20% dolomite and 80% calcite.

Density Tool

Lithology Identification—Open Hole

Lith-6
(former CP-21)



Environmentally Corrected Neutron Curves

M–N Plot for Mineral Identification—Open Hole

Purpose

This chart is used to help identify mineral mixtures from sonic, density, and neutron logs.

Description

Because M and N slope values are practically independent of porosity except in gas zones, the porosity values they indicate can be correlated with the mineralogy. (See Appendix E for the formulas to calculate M and N from sonic, density, and neutron logs.)

Enter the chart with M on the y-axis and N on the x-axis. The intersection point indicates the makeup of the formation. Points for binary mixtures plot along a line connecting the two mineral points. Ternary mixtures plot within the triangle defined by the three constituent minerals. The effect of gas, shaliness, secondary porosity, etc., is to shift data points in the directions shown by the arrows.

The lines on the chart are divided into numbered groups by porosity range as follows:

1. $\phi = 0$ (tight formation)
2. $\phi = 0$ to 12 p.u.
3. $\phi = 12$ to 27 p.u.
4. $\phi = 27$ to 40 p.u.

Example

Given: $M = 0.79$ and $N = 0.51$.

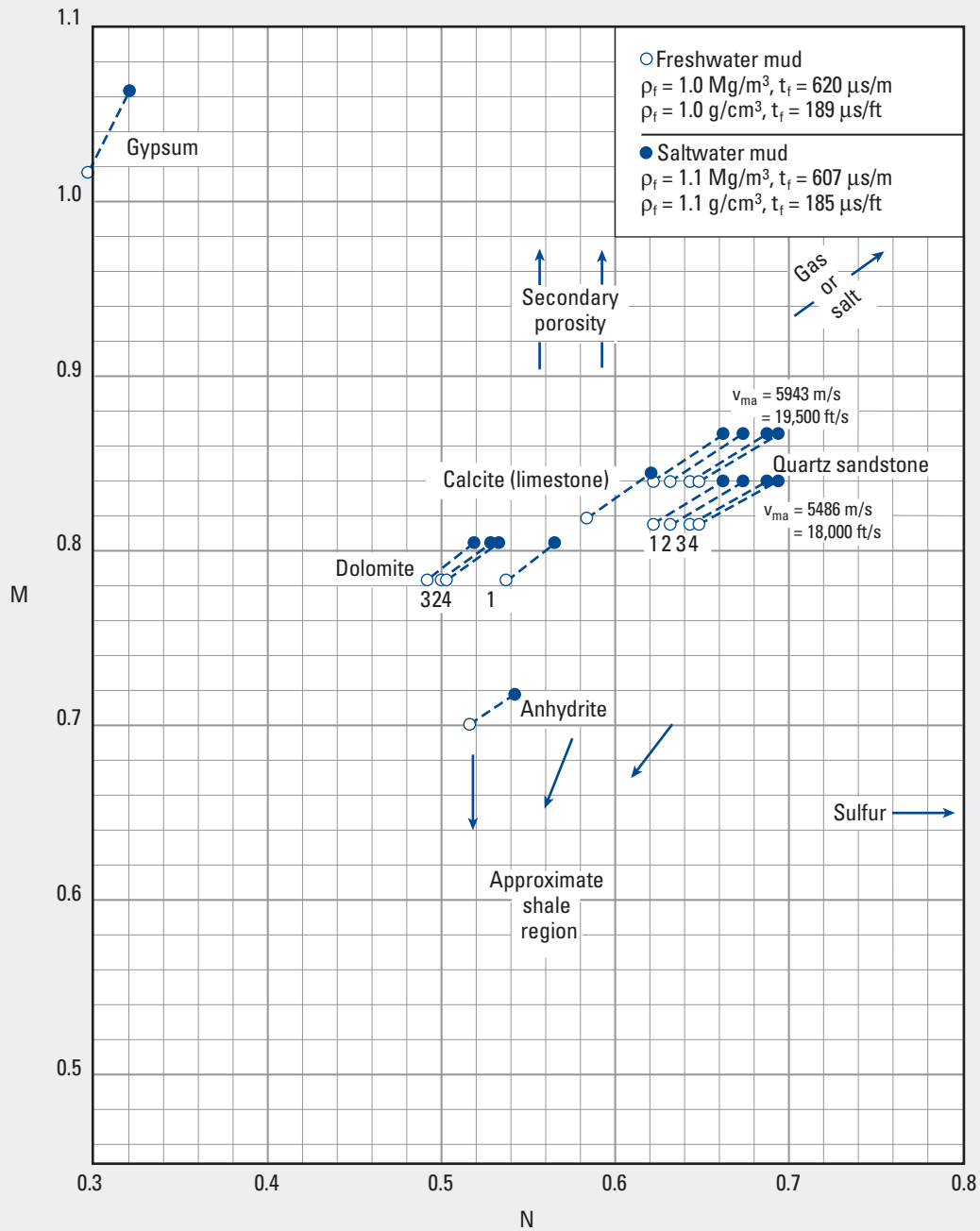
Find: Mineral composition of the formation.

Answer: The intersection of the M and N values indicates dolomite in group 2, which has a porosity between 0 to 12 p.u.

Environmentally Corrected Neutron Curves

M–N Plot for Mineral Identification—Open Hole

Lith-7
(former CP-8)



Lith

Environmentally Corrected APS* Curves

M–N Plot for Mineral Identification—Open Hole

Purpose

This chart is used to help identify mineral mixtures from APS Accelerator Porosity Sonde neutron logs.

Description

Because M and N values are practically independent of porosity except in gas zones, the porosity values they indicate can be correlated with the mineralogy. (See Appendix E for the formulas to calculate M and N from sonic, density, and neutron logs.)

Enter the chart with M on the y-axis and N on the x-axis. The intersection point indicates the makeup of the formation. Points for binary mixtures plot along a line connecting the two mineral points. Ternary mixtures plot within the triangle defined by the three constituent minerals. The effect of gas, shaliness, secondary porosity, etc., is to shift data points in the directions shown by the arrows.

The lines on the chart are divided into numbered groups by porosity range as follows:

1. $\phi = 0$ (tight formation)
2. $\phi = 0$ to 12 p.u.
3. $\phi = 12$ to 27 p.u.
4. $\phi = 27$ to 40 p.u.

Because the dolomite spread is negligible, a single dolomite point is plotted for each mud.

Example

Given: $M = 0.80$ and $N = 0.55$.

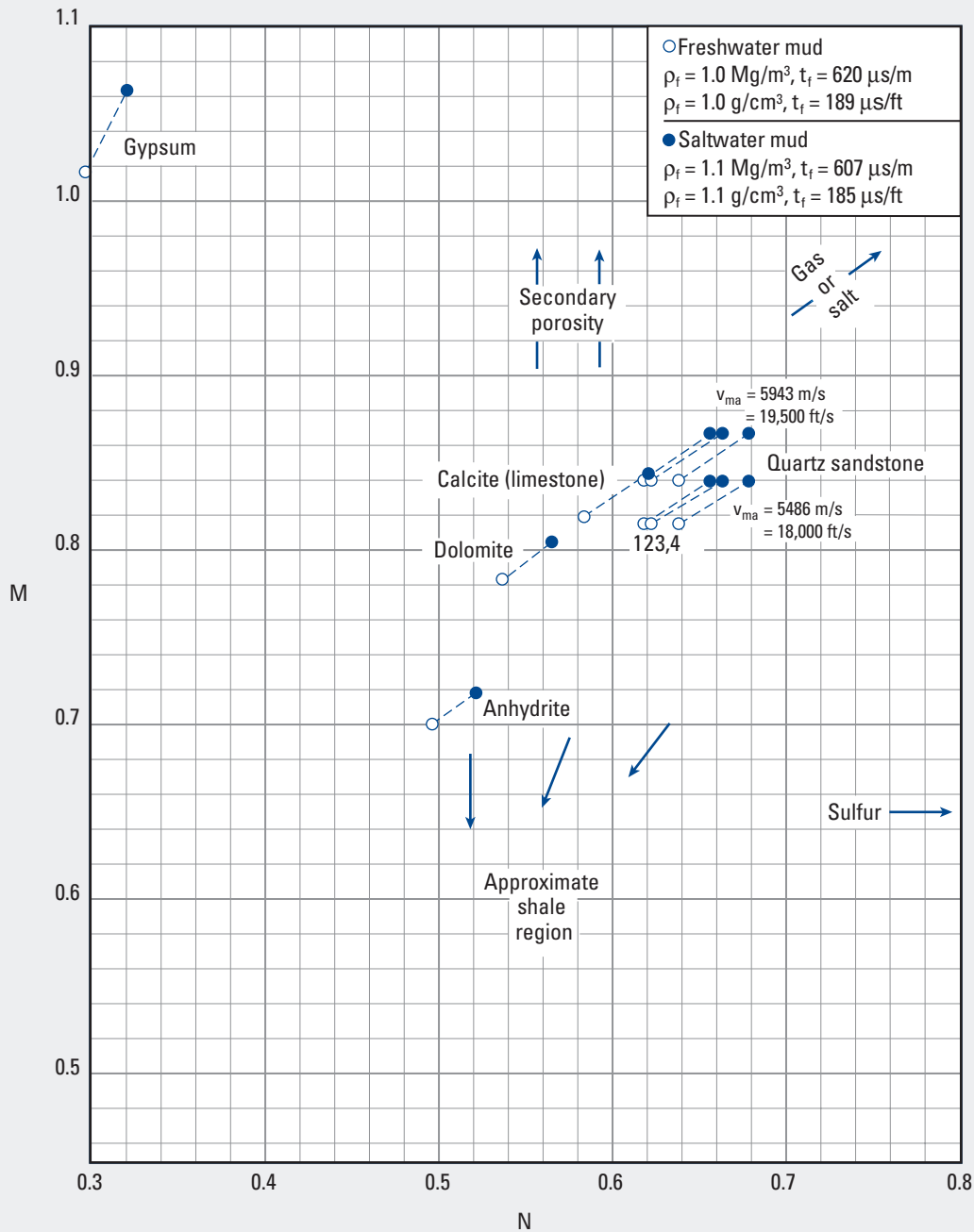
Find: Mineral composition of the formation.

Answer: Dolomite.

Environmentally Corrected APS* Curves

M–N Plot for Mineral Identification—Open Hole

Lith-8
(former CP-8a)



*Mark of Schlumberger
© Schlumberger

Lith

Bulk Density or Interval Transit Time and Apparent Total Porosity

Apparent Matrix Parameters—Open Hole

Purpose

Charts Lith-9 (customary units) and Lith-10 (metric units) provide values of the apparent matrix internal transit time (t_{maa}) and apparent matrix grain density (ρ_{maa}) for the matrix identification (MID) Charts Lith-11 and Lith-12. With these parameters the identification of rock mineralogy or lithology through a comparison of neutron, density, and sonic measurements is possible.

Description

Determining the values of t_{maa} and ρ_{maa} to use in the MID Charts Lith-11 and Lith-12 requires three steps.

First, apparent crossplot porosity is determined using the appropriate neutron-density and neutron-sonic crossplot charts in the “Porosity” section of this book. For data that plot above the sandstone curve on the charts, the apparent crossplot porosity is defined by a vertical projection to the sandstone curve.

Second, enter Chart Lith-9 or Lith-10 with the interval transit time (t) to intersect the previously determined apparent crossplot porosity. This point defines t_{maa} .

Third, enter Chart Lith-9 or Lith-10 with the bulk density (ρ_b) to again intersect the apparent crossplot porosity and define ρ_{maa} .

The values determined from Charts Lith-9 and Lith-10 for t_{maa} and ρ_{maa} are cross plotted on the appropriate MID plot (Charts Lith-11 and Lith-12) to identify the rock mineralogy by its proximity to the labeled points on the plot.

Example

Given: Apparent crossplot porosity from density-neutron = 20%,
 $\rho_b = 2.4 \text{ g/cm}^3$, apparent crossplot porosity from
 neutron-sonic = 30%, and $t = 82 \text{ } \mu\text{s/ft}$.

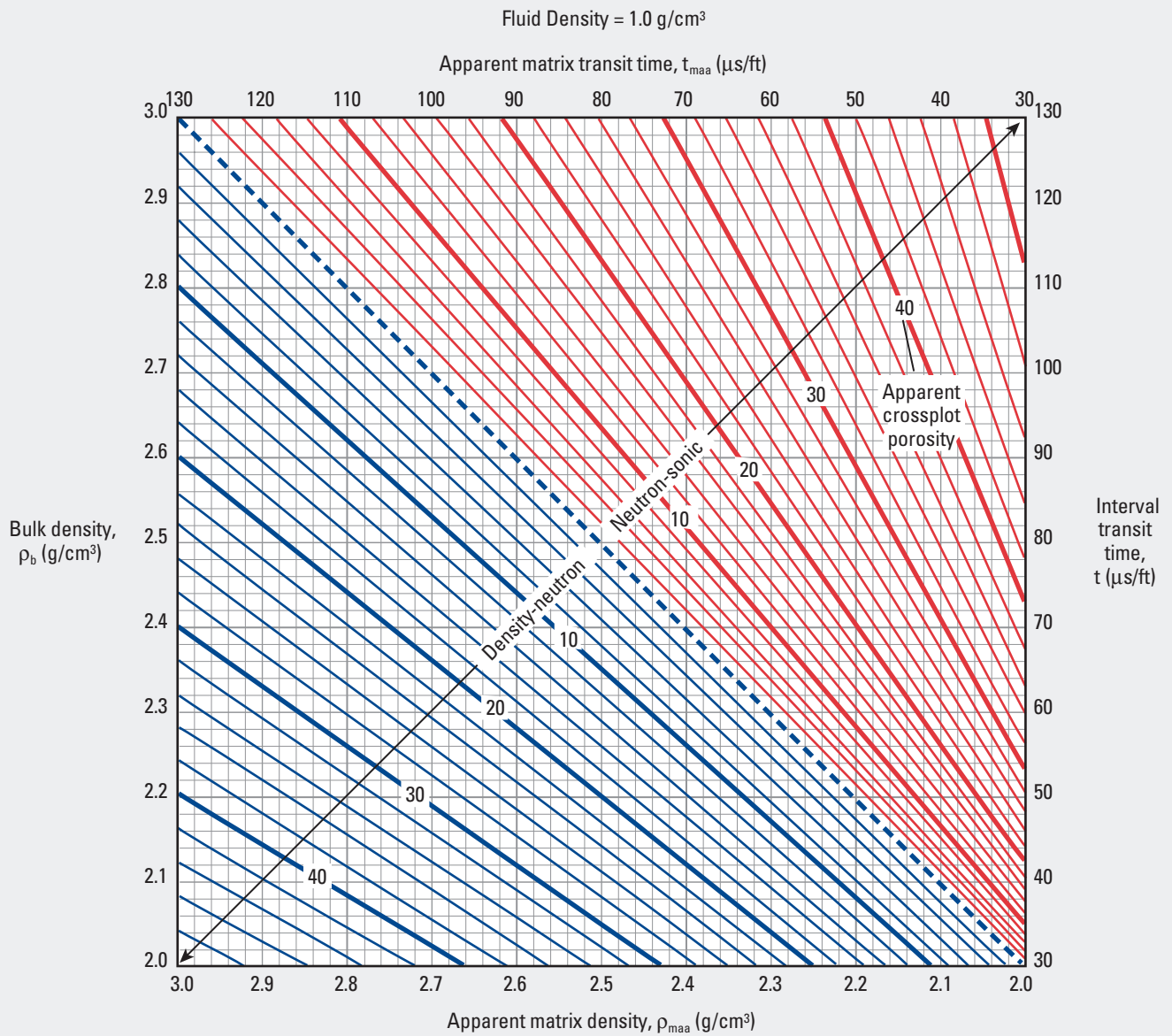
Find: ρ_{maa} and t_{maa} .

Answer: $\rho_{\text{maa}} = 2.75 \text{ g/cm}^3$ and $t_{\text{maa}} = 46 \text{ } \mu\text{s/ft}$.

Bulk Density or Interval Transit Time and Apparent Total Porosity

Apparent Matrix Parameters—Open Hole

Lith-9
(customary, former CP-14)



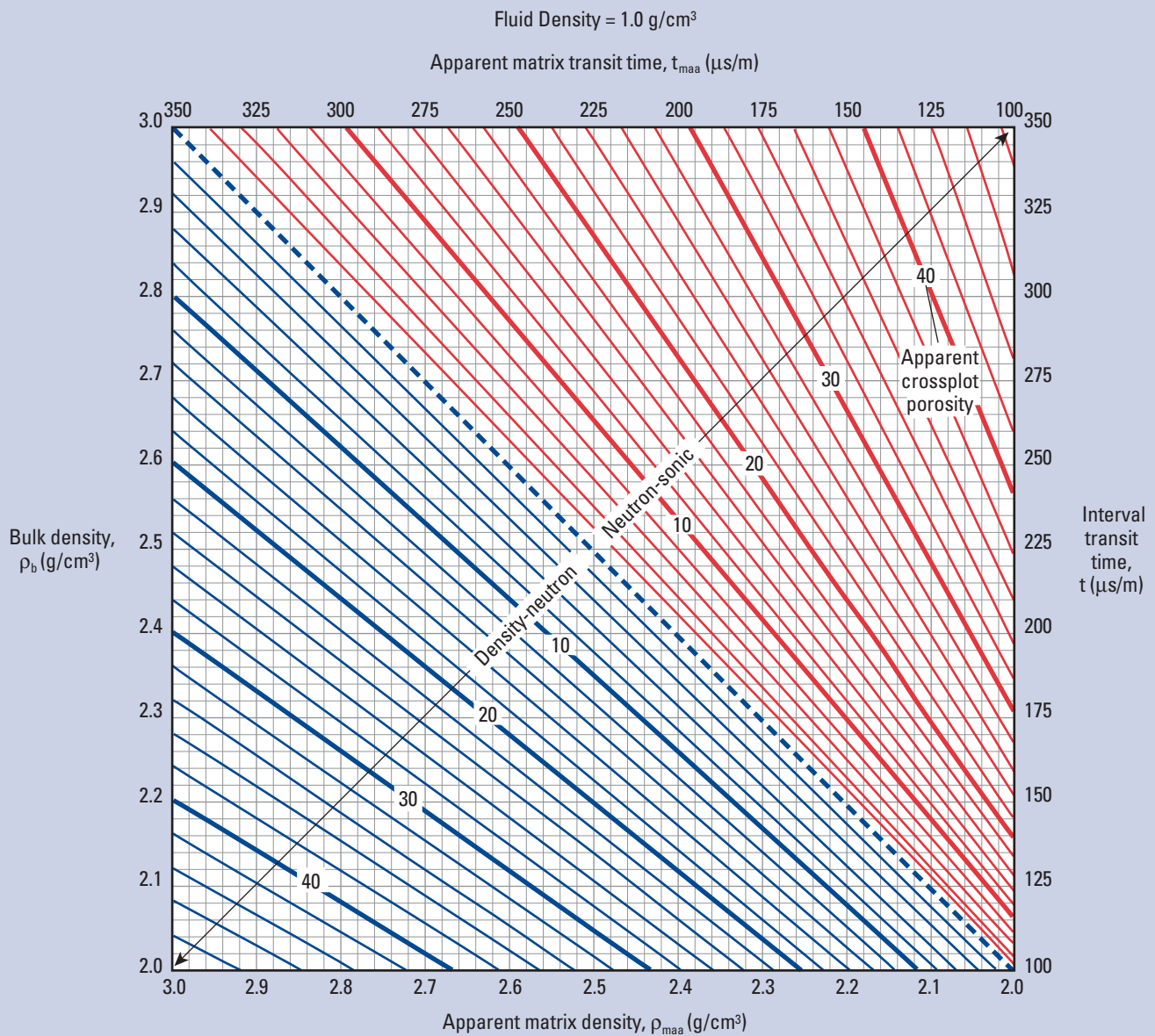
© Schlumberger

Bulk Density or Interval Transit Time and Apparent Total Porosity

Apparent Matrix Parameters—Open Hole

Lith-10

(metric, former CP-14m)

**Purpose**

Charts Lith-9 (customary units) and Lith-10 (metric units) provide values of the apparent matrix internal transit time (t_{maa}) and apparent matrix grain density (ρ_{maa}) for the matrix identification (MID) Charts Lith-11 and Lith-12. With these parameters the identification of rock mineralogy or lithology through a comparison of neutron, density, and sonic measurements is possible.

Density Tool

Matrix Identification (MID)—Open Hole

Purpose

Charts Lith-11 and Lith-12 are used to establish the type of mineral predominant in the formation.

Description

Enter the appropriate (customary or metric units) chart with the values established from Charts Lith-9 or Lith-10 to identify the predominant mineral in the formation. Salt points are defined for two tools, the sidewall neutron porosity (SNP) and the CNL* Compensated Neutron Log. The presence of secondary porosity in the form of vugs or fractures displaces the data points parallel to the apparent matrix internal transit time (t_{maa}) axis. The presence of gas displaces points to the right on the chart. Plotting some shale points to establish the shale trend lines helps in the identification of shaliness. For fluid density (ρ_f) other than 1.0 g/cm^3 use the table to determine the multiplier to correct the apparent total density porosity before entering Chart Lith-11 or Lith-12.

ρ_f	Multiplier
1.00	1.00
1.05	0.98
1.10	0.95
1.15	0.93

Example

Given: $\rho_{maa} = 2.75 \text{ g/cm}^3$, $t_{maa} = 56 \text{ } \mu\text{s/ft}$ (from Chart Lith-9), and $\rho_f = 1.0 \text{ g/cm}^3$.

Find: The predominant mineral.

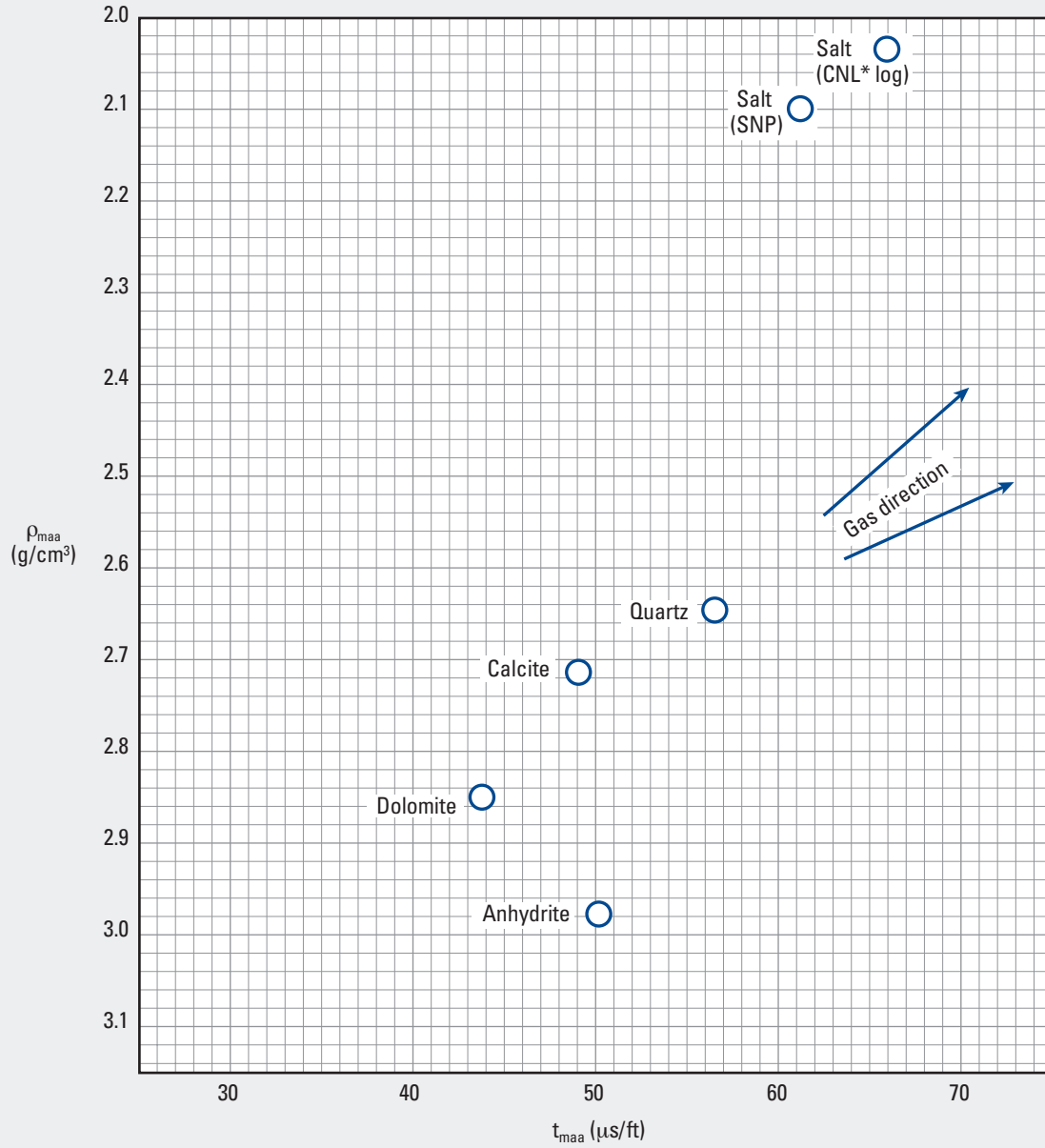
Answer: The formation consists of both dolomite and calcite, which indicates a dolomitized limestone. The formation used in this example is from northwest Florida in the Jay field. The vugs (secondary porosity) created by the dolomitization process displace the data point parallel to the dolomite and calcite points.

Density Tool

Matrix Identification (MID)—Open Hole

Lith-11

(customary, former CP-15)



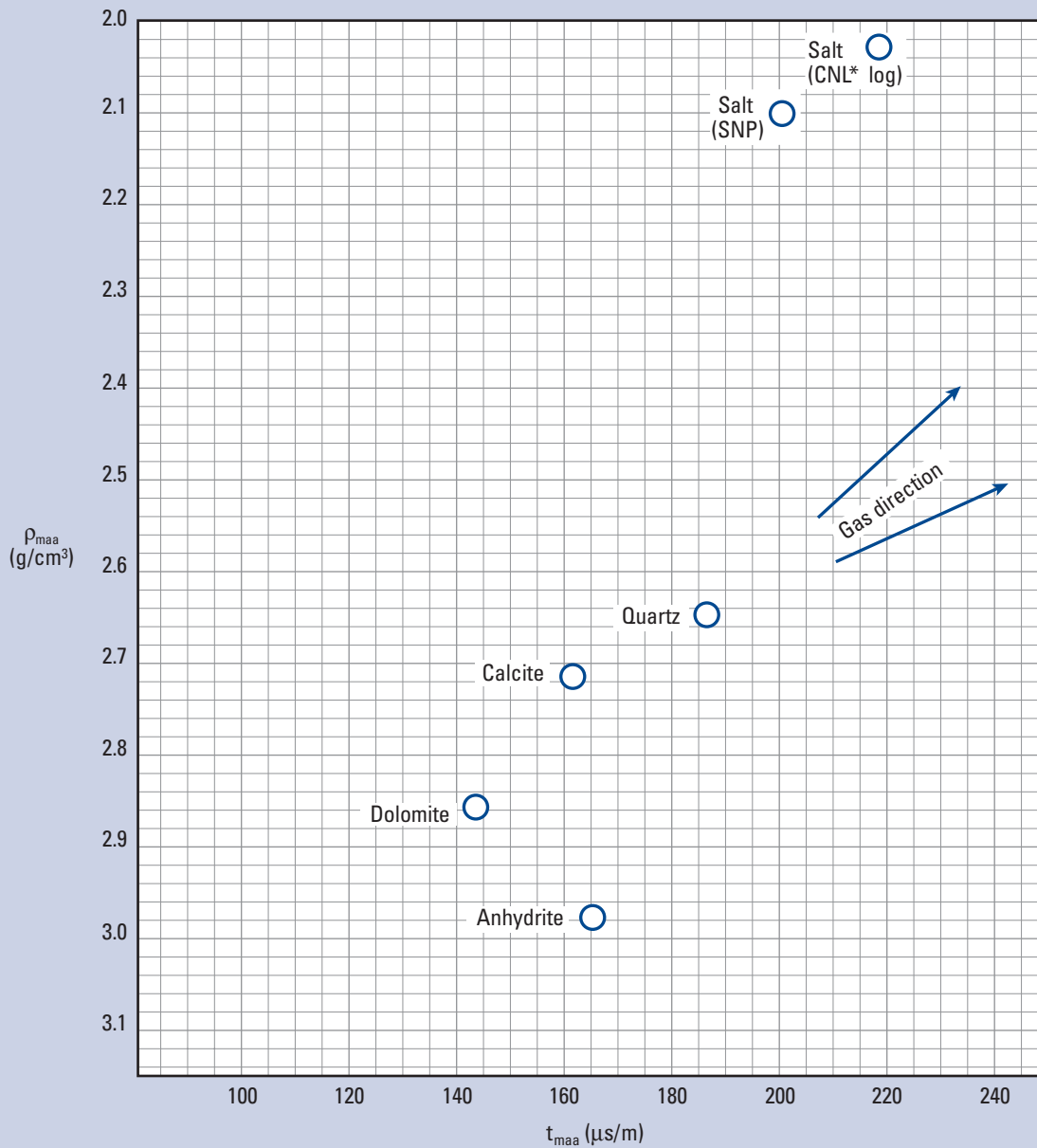
*Mark of Schlumberger
© Schlumberger

Density Tool

Matrix Identification (MID)—Open Hole

Lith-12

(metric, former CP-15m)



*Mark of Schlumberger
© Schlumberger

Purpose

Chart Lith-12 is used similarly to Chart Lith-11 to establish the mineral type of the formation.

Sonic Tool

Porosity Evaluation—Open Hole

Purpose

This chart is used to convert sonic log slowness time (Δt) values into those for porosity (ϕ).

Description

There are two sets of curves on the chart. The blue set for matrix velocity (v_{ma}) employs a weighted-average transform. The red set is based on the empirical observation of lithology (see Reference 20). For both, the saturating fluid is assumed to be water with a velocity (v_f) of 5,300 ft/s (1,615 m/s).

Enter the chart with the slowness time from the sonic log on the x-axis. Move vertically to intersect the appropriate matrix velocity or lithology curve and read the porosity value on the y-axis. For rock mixtures such as limy sandstones or cherty dolomites, intermediate matrix lines may be interpolated.

To use the weighted-average transform for an unconsolidated sand, a lack-of-compaction correction (B_{cp}) must be made. Enter the chart with the slowness time and intersect the appropriate compaction correction line to read the porosity on the y-axis. If the compaction correction is not known, it can be determined by working backward from a nearby clean water sand for which the porosity is known.

Example: Consolidated Formation

Given: $\Delta t = 76 \mu\text{s}/\text{ft}$ in a consolidated formation with $v_{ma} = 18,000 \text{ ft/s}$.

Find: Porosity and the formation lithology (sandstone, dolomite, or limestone).

Answer: 15% porosity and consolidated sandstone.

Example: Unconsolidated Formation

Given: Unconsolidated formation with $\Delta t = 100 \mu\text{s}/\text{ft}$ in a nearby water sand with a porosity of 28%.

Find: Porosity of the formation for $\Delta t = 110 \mu\text{s}/\text{ft}$.

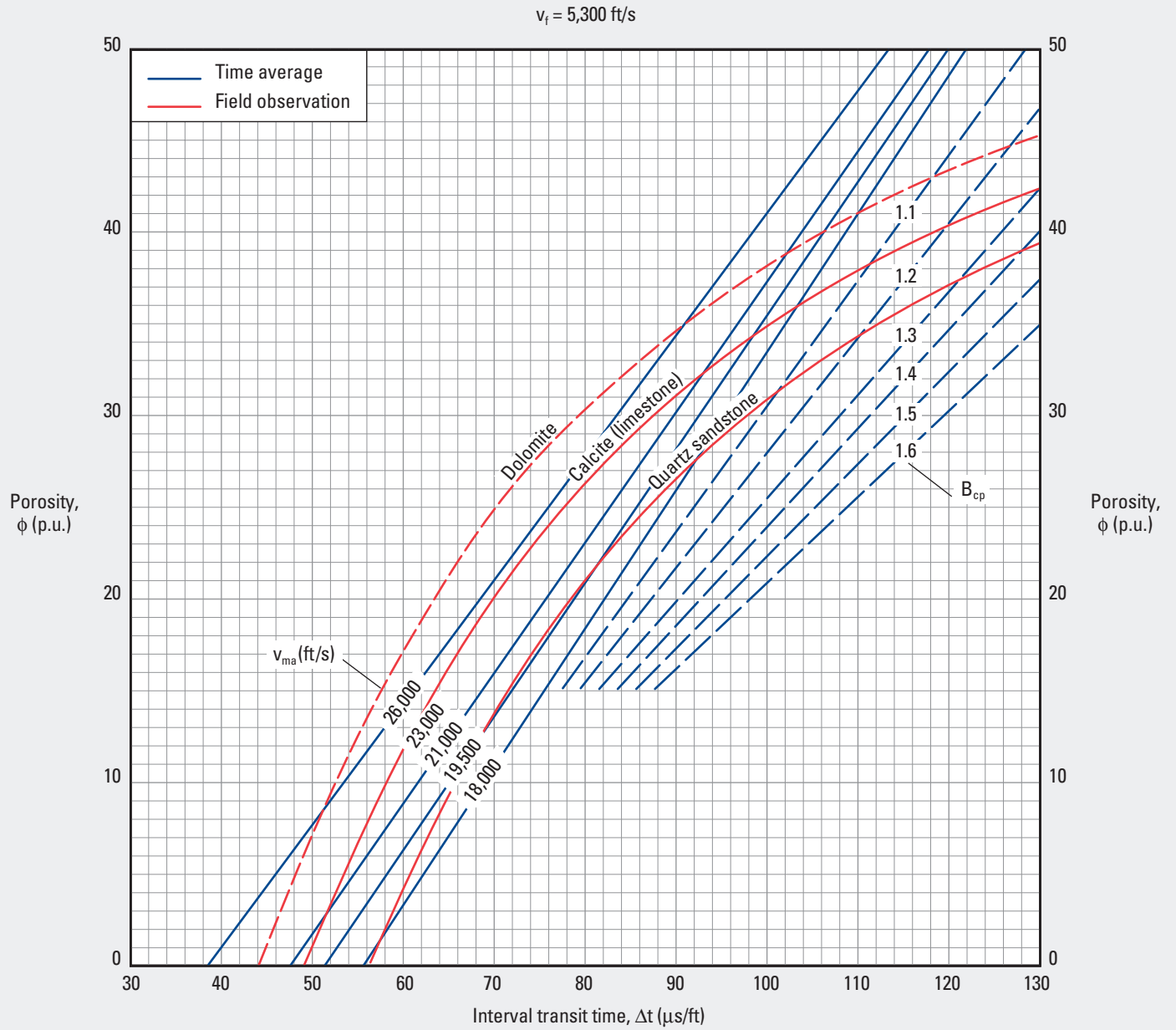
Answer: Enter the chart with 100 $\mu\text{s}/\text{ft}$ on the x-axis and move vertically upward to intersect 28-p.u. porosity. This intersection point indicates the correction factor curve of 1.2. Use the 1.2 correction value to find the porosity for the other slowness time. The porosity of an unconsolidated formation with $\Delta t = 110 \mu\text{s}/\text{ft}$ is 34 p.u.

Lithology	v_{ma} (ft/s)	Δt_{ma} ($\mu\text{s}/\text{ft}$)	v_{ma} (m/s)	Δt_{ma} ($\mu\text{s}/\text{m}$)
Sandstone	18,000–19,500	55.5–51.3	5,486–5,944	182–168
Limestone	21,000–23,000	47.6–43.5	6,400–7,010	156–143
Dolomite	23,000–26,000	43.5–38.5	7,010–7,925	143–126

Sonic Tool

Porosity Evaluation—Open Hole

Por-1
(customary, former Por-3)



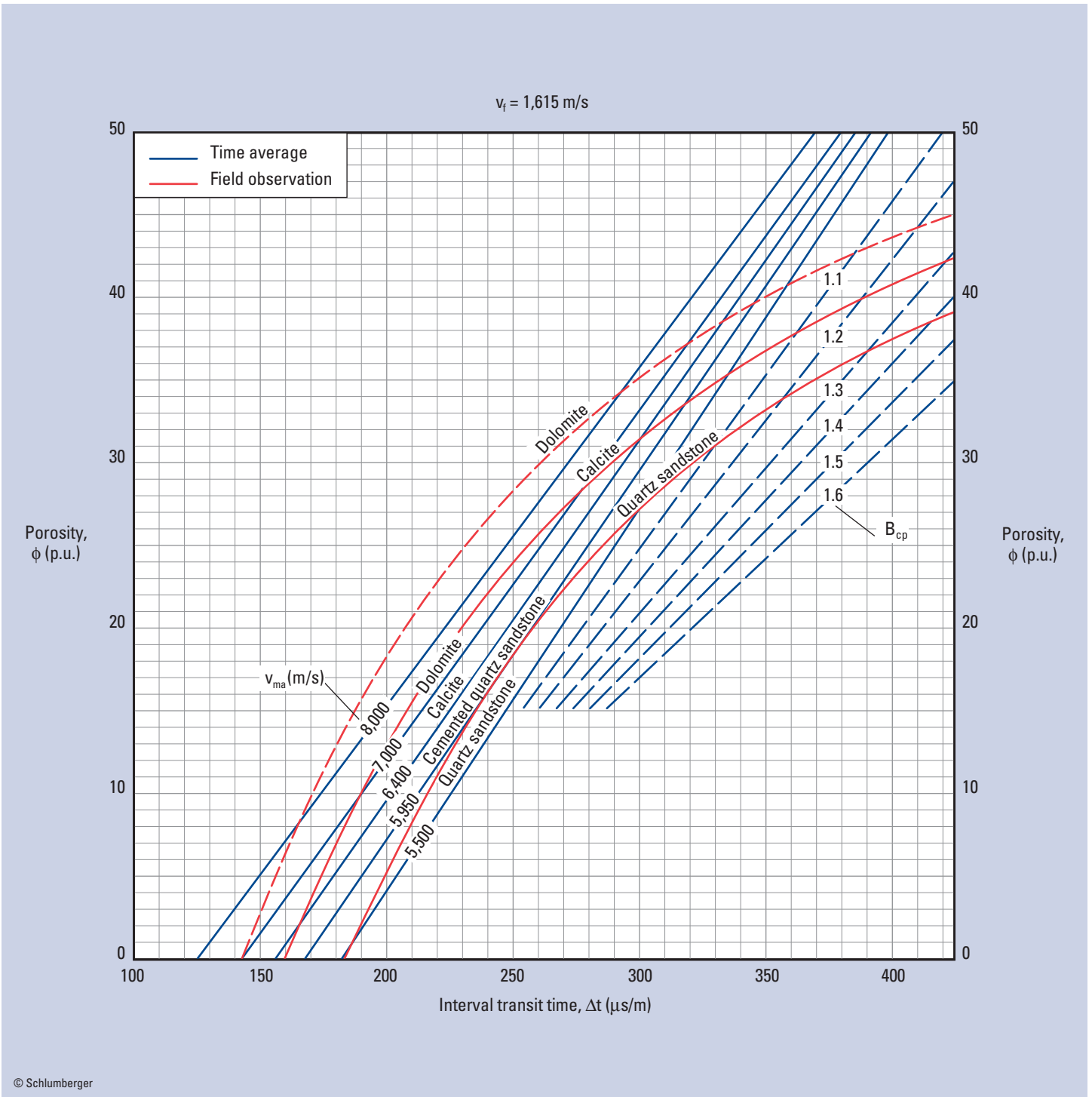
© Schlumberger

Sonic Tool

Porosity Evaluation—Open Hole

Por-2

(metric, former Por-3m)



© Schlumberger

Purpose

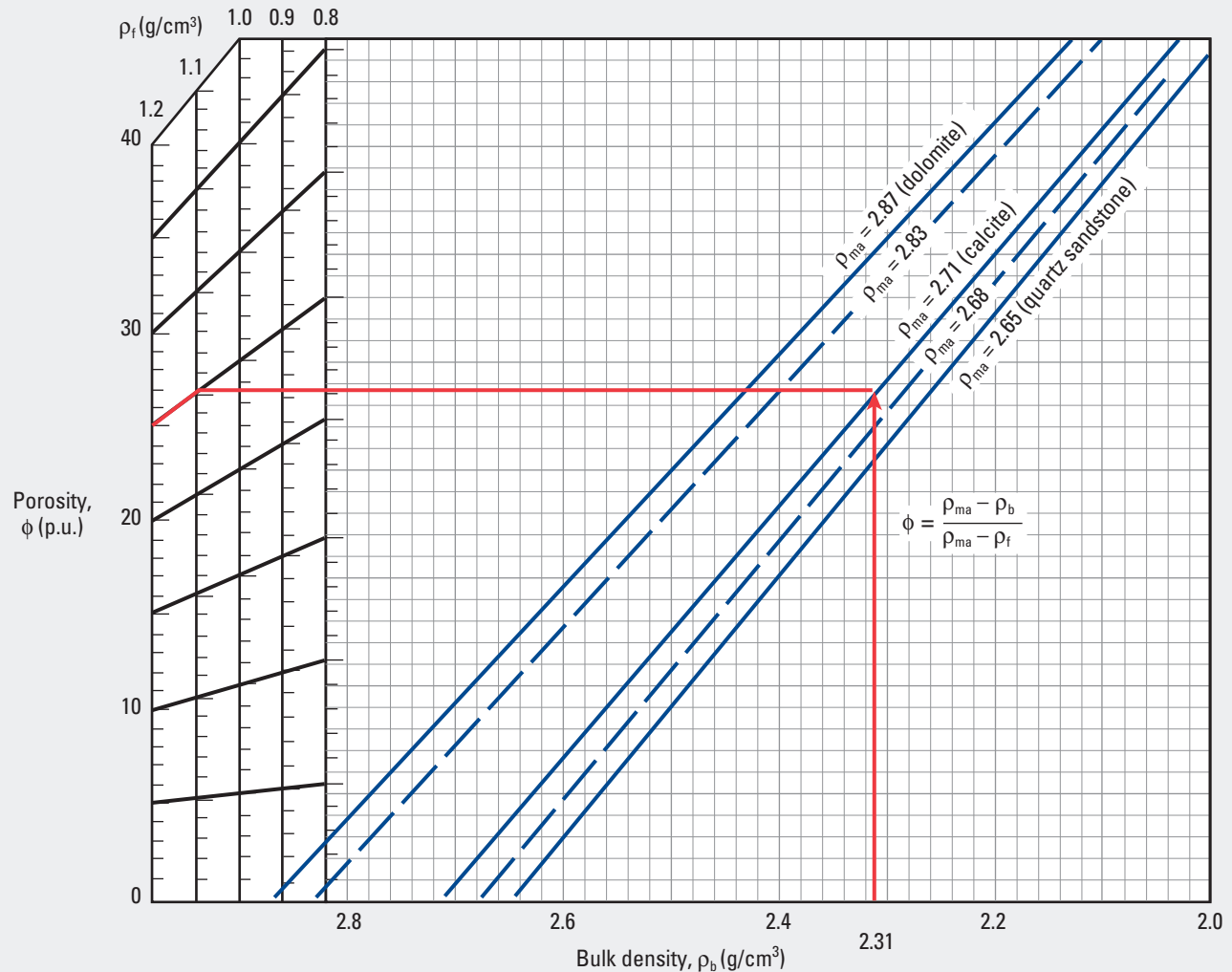
This chart is used similarly to Chart Por-1 with metric units.

Por

Density Tool

Porosity Determination—Open Hole

Por-3
(former Por-5)



*Mark of Schlumberger
© Schlumberger

$$\phi = \frac{\rho_{ma} - \rho_b}{\rho_{ma} - \rho_f}$$

Por

Purpose

This chart is used to convert grain density (g/cm^3) to density porosity.

Description

Values of log-derived bulk density (ρ_b) corrected for borehole size, matrix density of the formation (ρ_{ma}), and fluid density (ρ_f) are used to determine the density porosity (ϕ_D) of the logged formation. The ρ_f is the density of the fluid saturating the rock immediately surrounding the borehole—usually mud filtrate.

Enter the borehole-corrected value of ρ_b on the x-axis and move vertically to intersect the appropriate matrix density curve. From the intersection point move horizontally to the fluid density line. Follow the porosity trend line to the porosity scale to read the formation

porosity as determined by the density tool. This porosity in combination with CNL* Compensated Neutron Log, sonic, or both values of porosity can help determine the rock type of the formation.

Example

Given: $\rho_b = 2.31 \text{ g}/\text{cm}^3$ (log reading corrected for borehole effect), $\rho_{ma} = 2.71 \text{ g}/\text{cm}^3$ (calcite mineral), and $\rho_f = 1.1 \text{ g}/\text{cm}^3$ (salt mud).

Find: Density porosity.

Answer: $\phi_D = 25 \text{ p.u.}$

APS* Near-to-Array (APLC) and Near-to-Far (FPLC) Logs

Epithermal Neutron Porosity Equivalence—Open Hole

Purpose

This chart is used for the apparent limestone porosity recorded by the APS Accelerator Porosity Sonde or sidewall neutron porosity (SNP) tool to provide the equivalent porosity in sandstone or dolomite formations. It can also be used to obtain the apparent limestone porosity (used for the various crossplot porosity charts) for a log recorded in sandstone or dolomite porosity units.

Description

Enter the x-axis with the corrected near-to-array apparent limestone porosity (APLC) or near-to-far apparent limestone porosity (FPLC) and move vertically to the appropriate lithology curve. Then read the equivalent porosity on the y-axis. For APS porosity recorded in sandstone or dolomite porosity units enter that value on the y-axis and move horizontally to the recorded lithology curve. Then read the apparent limestone neutron porosity for that point on the x-axis.

The APLC is the epithermal short-spacing apparent limestone neutron porosity from the near-to-array detectors. The log is automatically corrected for standoff during acquisition. Because it is epithermal this measurement does not need environmental corrections for temperature or chlorine effect. However, corrections for mud weight and actual borehole size should be applied (see Chart Neu-10). The short spacing means that the effect of density and therefore the lithology on this curve is minimal.

The FPLC is the epithermal long-spacing apparent limestone neutron porosity acquired from the near-to-far detectors. Because it is epithermal this measurement does not need environmental corrections for temperature or chlorine effect. However, corrections for mud weight and actual borehole size should be applied (see Chart Neu-10). The long spacing means that the density and therefore lithology effect on this curve is pronounced, as seen on Charts Por-13 and Por-14.

The HPLC curve is the high-resolution version of the APLC curve. The same corrections apply.

Resolution	Short Spacing	Long Spacing
Normal	APLC Epithermal neutron porosity (ENPI) [†]	FPLC
Enhanced	HPLC HNPI [†]	HFLC

[†] Not formation-salinity corrected.

Example: Equivalent Porosity

Given: APLC = 25 p.u. and FPLC = 25 p.u.

Find: Porosity for sandstone and for dolomite.

Answer: Sandstone porosity from APLC = 28.5 p.u. and sandstone porosity from FPLC = 30 p.u.

Dolomite porosity = 24 and 20 p.u., respectively.

Example: Apparent Porosity

Given: Clean sandstone porosity = 20 p.u.

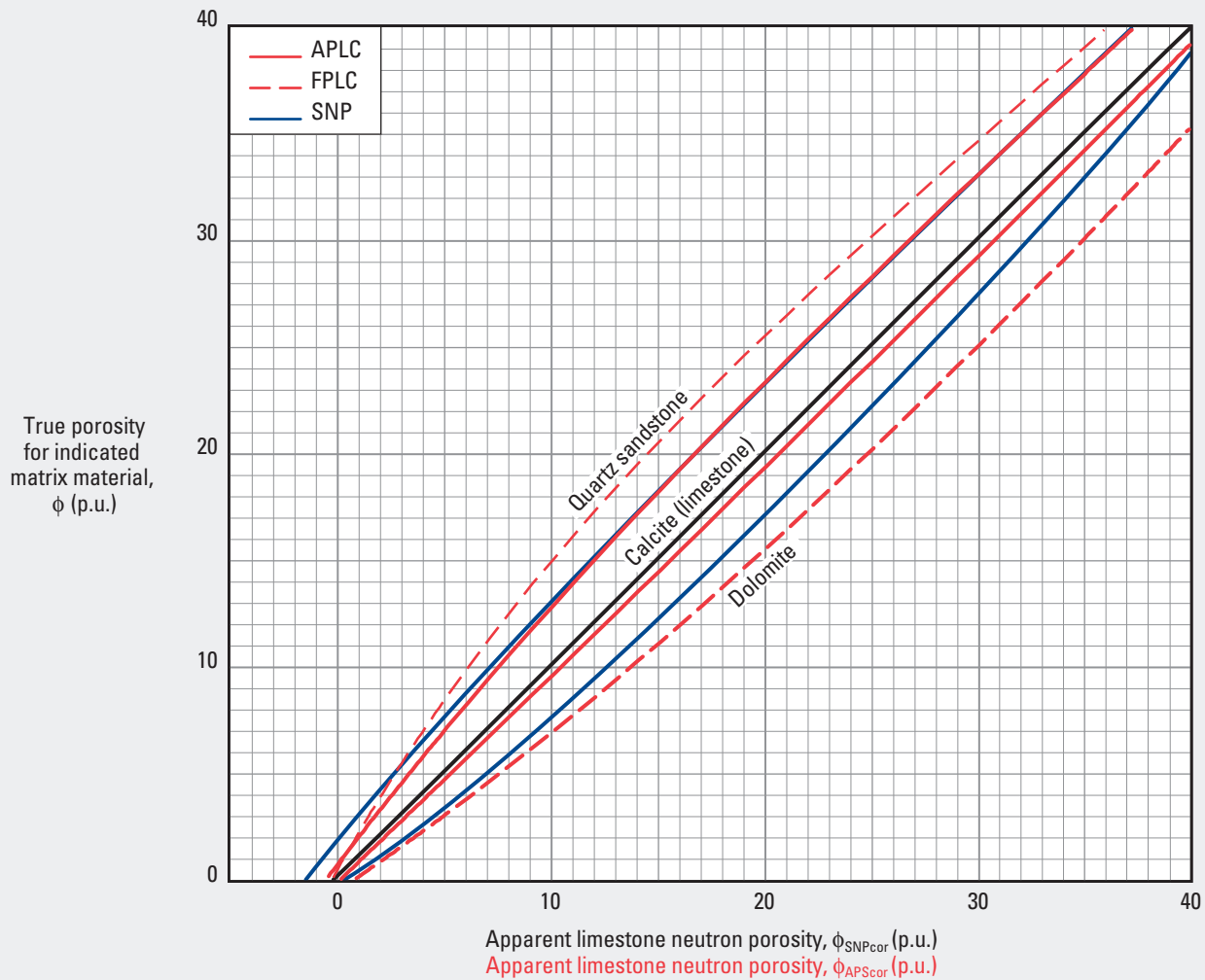
Find: Apparent limestone neutron porosity.

Answer: Enter the y-axis at 20 p.u. and move horizontally to the quartz sandstone matrix curves. Move vertically from the points of intersection to the x-axis and read the apparent limestone neutron porosity values.
APLC = 16.8 p.u. and FPLC = 14.5 p.u.

APS* Near-to-Array (APLC) and Near-to-Far (FPLC) Logs

Epithermal Neutron Porosity Equivalence—Open Hole

Por-4
(former Por-13a)

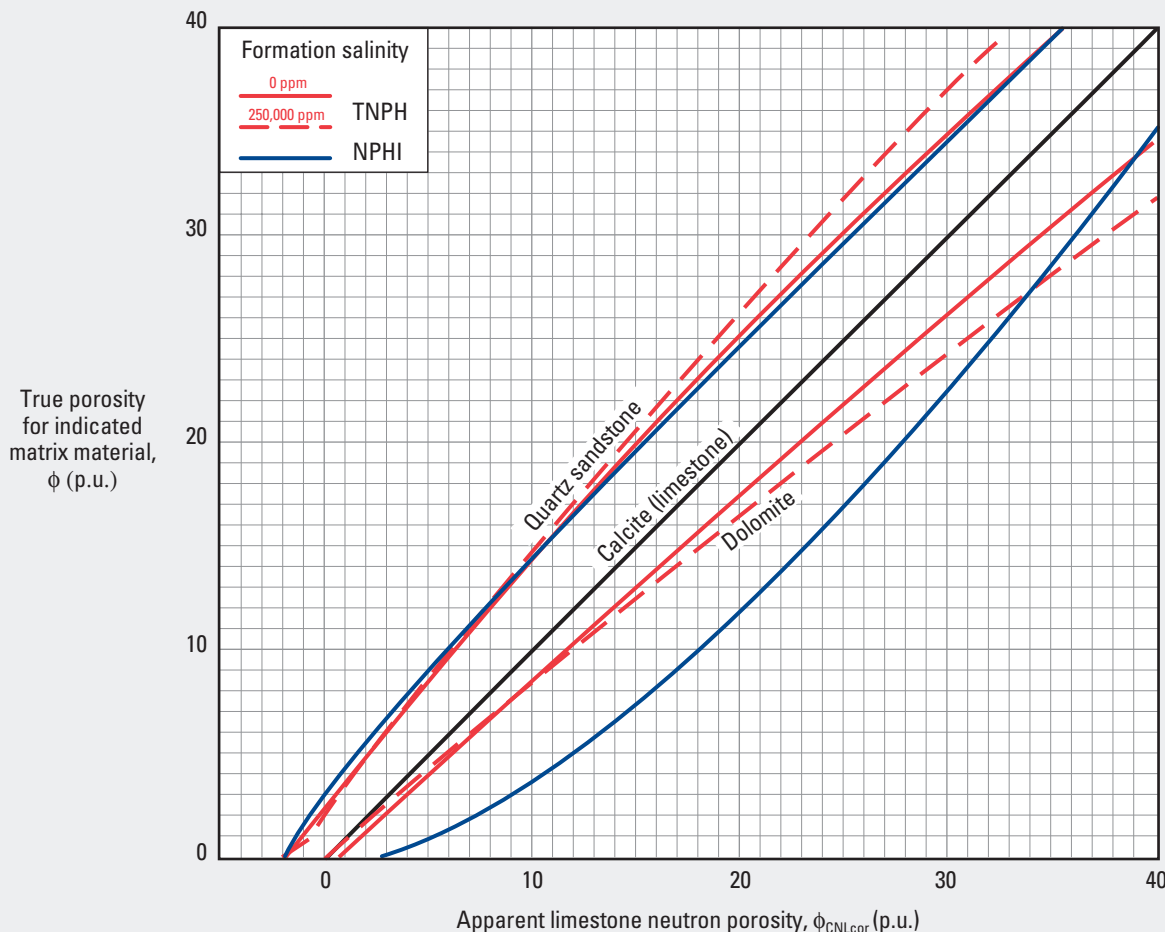


*Mark of Schlumberger
© Schlumberger

Thermal Neutron Tool

Porosity Equivalence—Open Hole

Por-5
(former Por-13b)



*Mark of Schlumberger
© Schlumberger

Purpose

This chart is used to convert CNL* Compensated Neutron Log porosity curves (TNPH or NPHI) from one lithology to another. It can also be used to obtain the apparent limestone porosity (used for the various crossplot porosity charts) from a log recorded in sandstone or dolomite porosity units.

Description

To determine the porosity of either quartz sandstone or dolomite enter the chart with the either the TNPH or NPHI corrected apparent limestone neutron porosity (φ_{CNLcor}) on the x-axis. Move vertically to intersect the appropriate curve and read the porosity for quartz sandstone or dolomite on the y-axis. The chart has a built-in salinity correction for TNPH values.

NPHI	Thermal neutron porosity (ratio method)
NPOR	Neutron porosity (environmentally corrected and enhanced vertical resolution processed)
TNPH	Thermal neutron porosity (environmentally corrected)

Example

Given: Quartz sandstone formation, TNPH = 18 p.u. (apparent limestone neutron porosity), and formation salinity = 250,000 ppm.

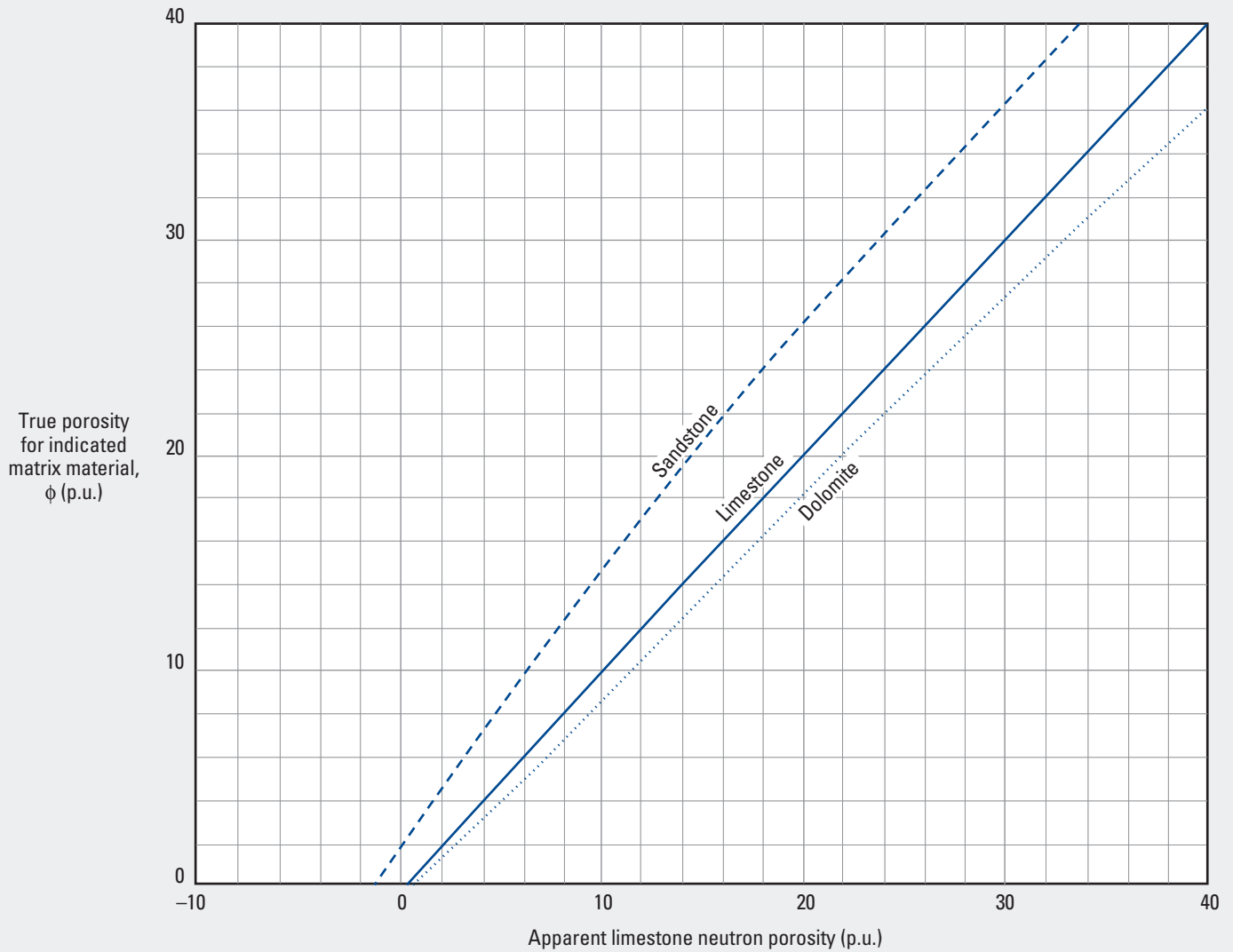
Find: Porosity in sandstone.

Answer: From the TNPH porosity reading of 18 p.u. on the x-axis, project a vertical line to intersect the quartz sandstone dashed red curve. From the y-axis, the porosity of the sandstone is 24 p.u.

Thermal Neutron Tool—CNT-D and CNT-S 2½-in. Tools

Porosity Equivalence—Open Hole

Por-6



© Schlumberger

Por

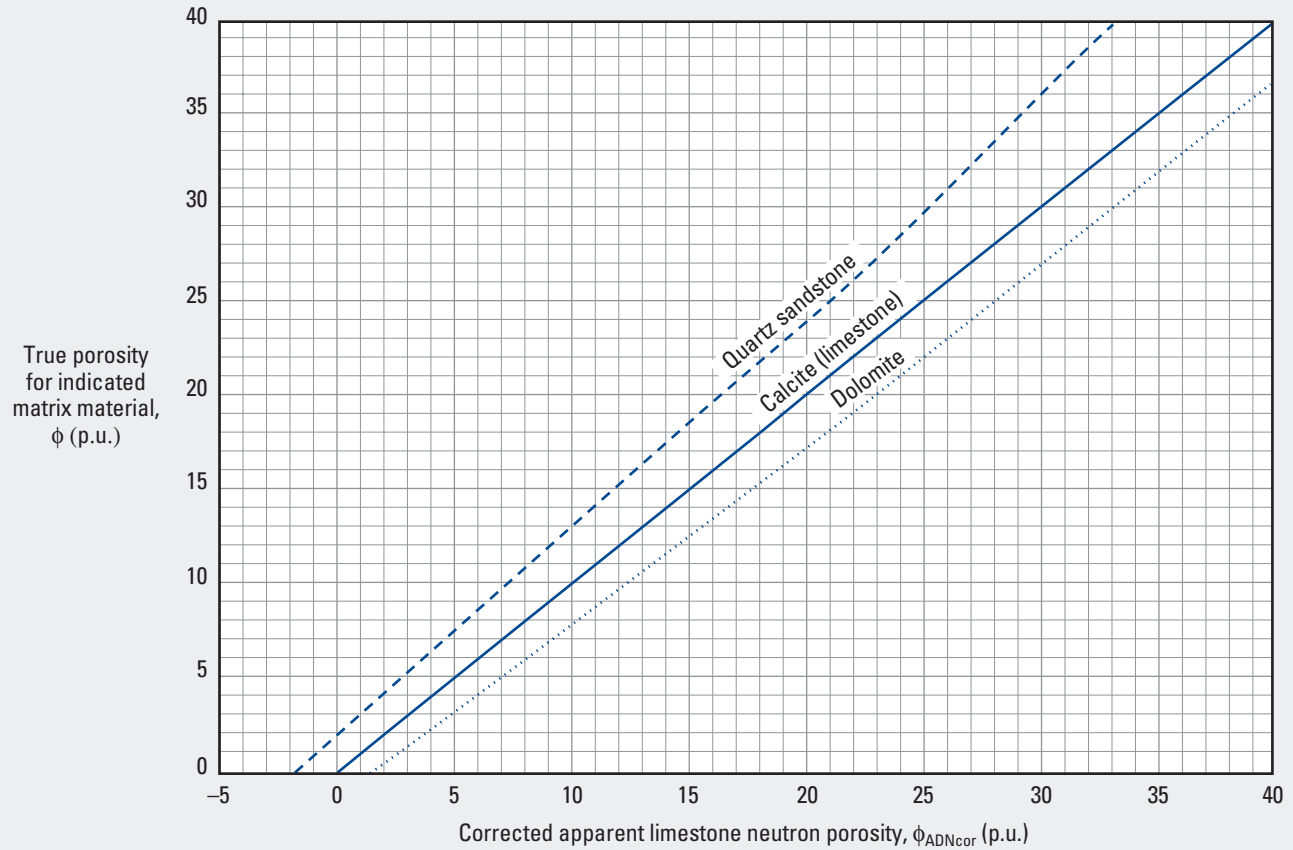
Purpose

This chart is used similarly to Chart Por-5 to convert 2½-in. compensated neutron tool (CNT) porosity values (TNPH) from one lithology to another. Fresh formation water is assumed.

adnVISION475* 4.75-in. Azimuthal Density Neutron Tool

Porosity Equivalence—Open Hole

Por-7



*Mark of Schlumberger
© Schlumberger

Purpose

This chart is used to determine the porosity of sandstone, limestone, or dolomite from the corrected apparent limestone porosity measured with the adnVISION475 4.75-in. tool.

Description

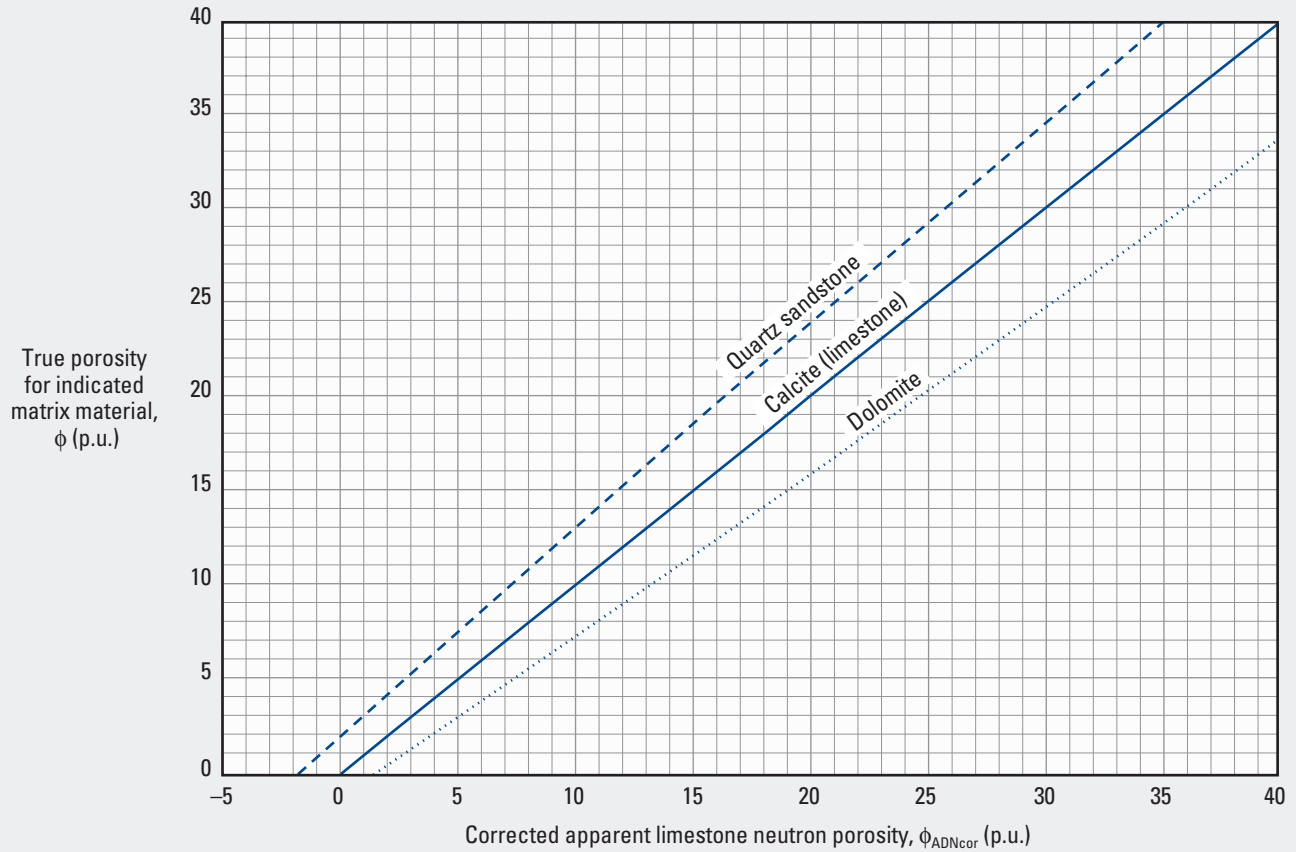
Enter the chart on the x-axis with the corrected apparent limestone porosity from Chart Neu-31 to intersect the curve for the appropriate formation material. Read the porosity on the y-axis.

Por

adnVISION675* 6.75-in. Azimuthal Density Neutron Tool

Porosity Equivalence—Open Hole

Por-8



*Mark of Schlumberger
© Schlumberger

Purpose

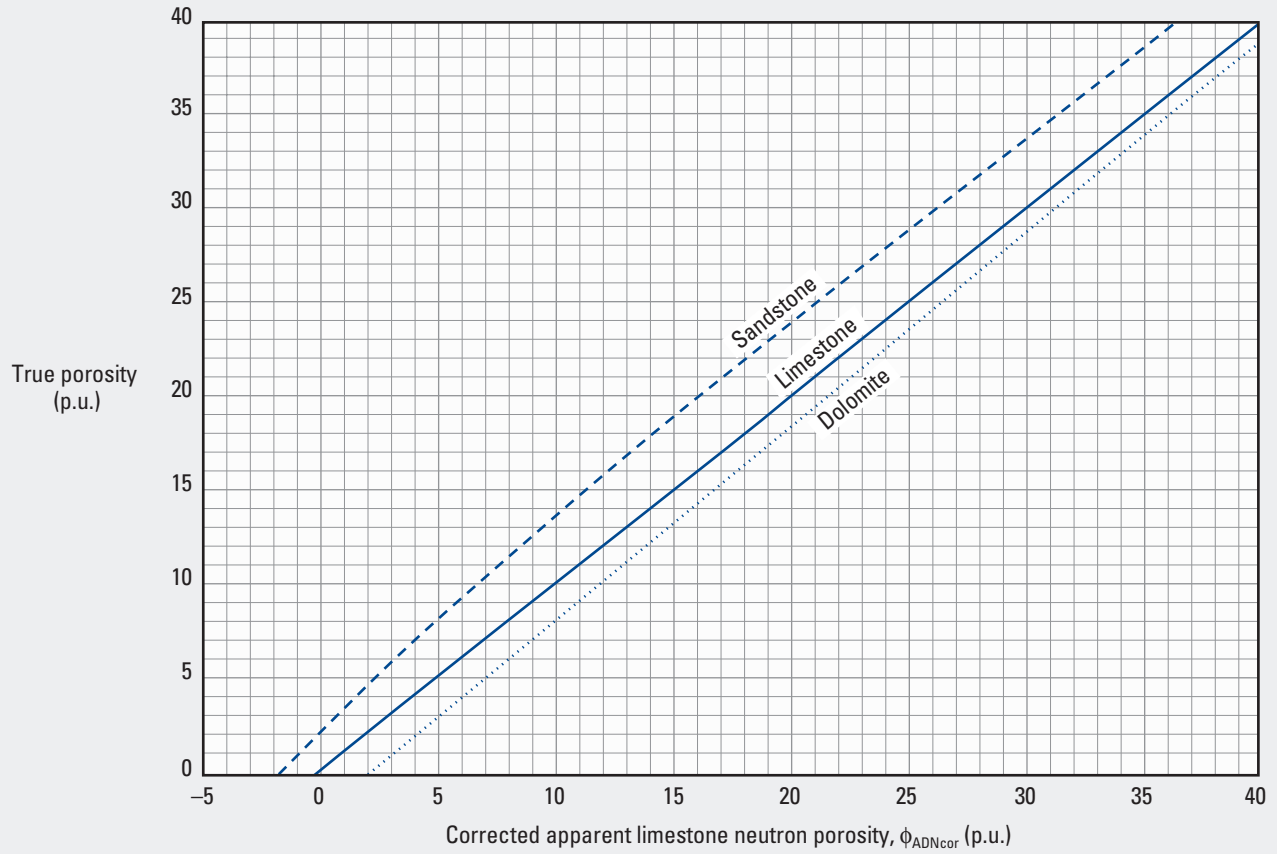
Chart Por-8 is used similarly to Chart Por-7 for determining porosity from the corrected apparent limestone porosity from the adnVISION675 6.75-in. tool.

Por

adnVISION825* 8.25-in. Azimuthal Density Neutron Tool

Porosity Equivalence—Open Hole

Por-9



*Mark of Schlumberger
© Schlumberger

Purpose

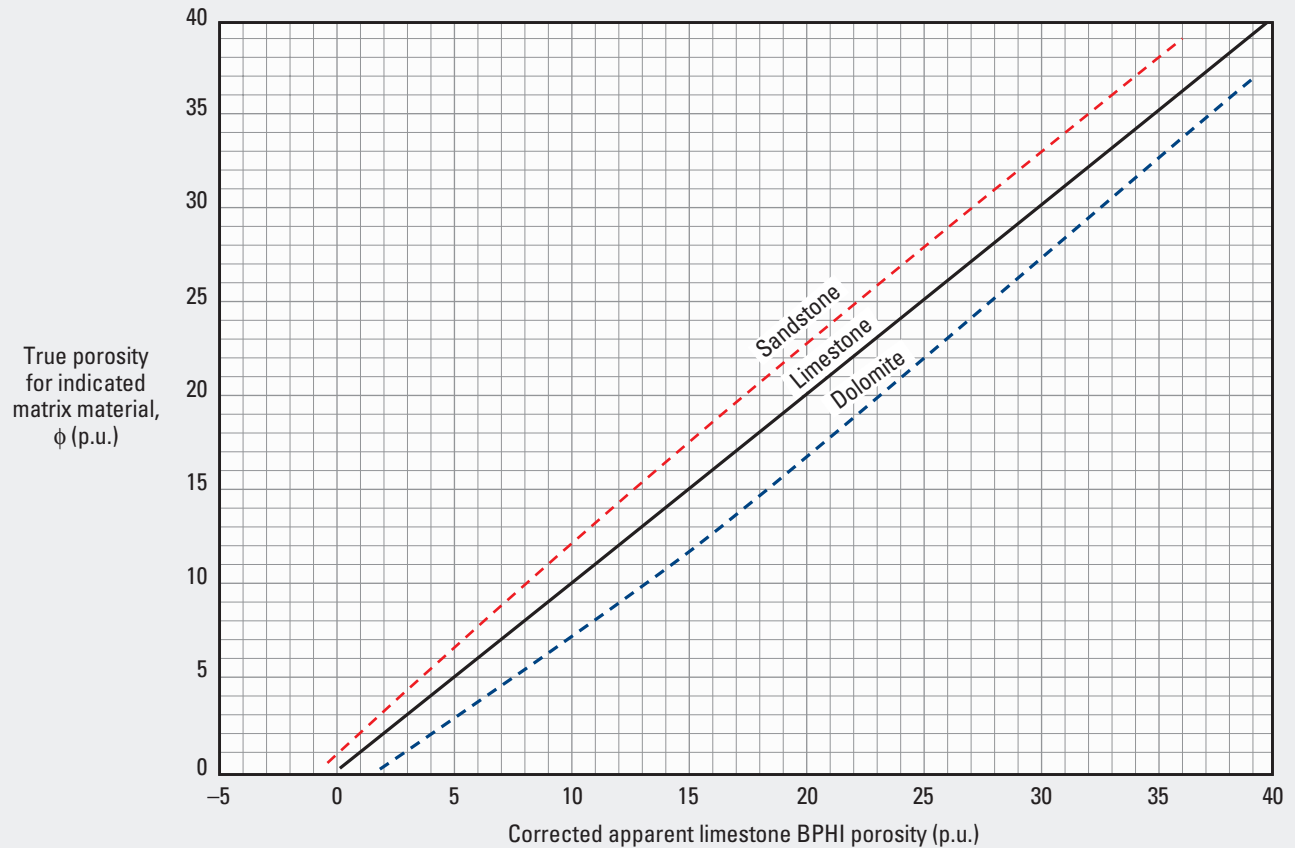
Chart Por-9 is used similarly to Chart Por-7 for determining porosity from the corrected apparent limestone porosity from the adnVISION825 8.25-in. tool.

Por

EcoScope* 6.75-in. Integrated LWD Tool, BPHI Porosity

Porosity Equivalence—Open Hole

Por-10



*Mark of Schlumberger
© Schlumberger

Por

Purpose

This chart is used to determine the porosity of sandstone, limestone, or dolomite from the corrected apparent limestone BPHI porosity measured with the EcoScope 6.75-in. LWD tool.

Use this chart only with EcoScope best thermal neutron porosity (BPHI) measurements; use Chart Por-10a with EcoScope thermal neutron porosity (TNPH) measurements.

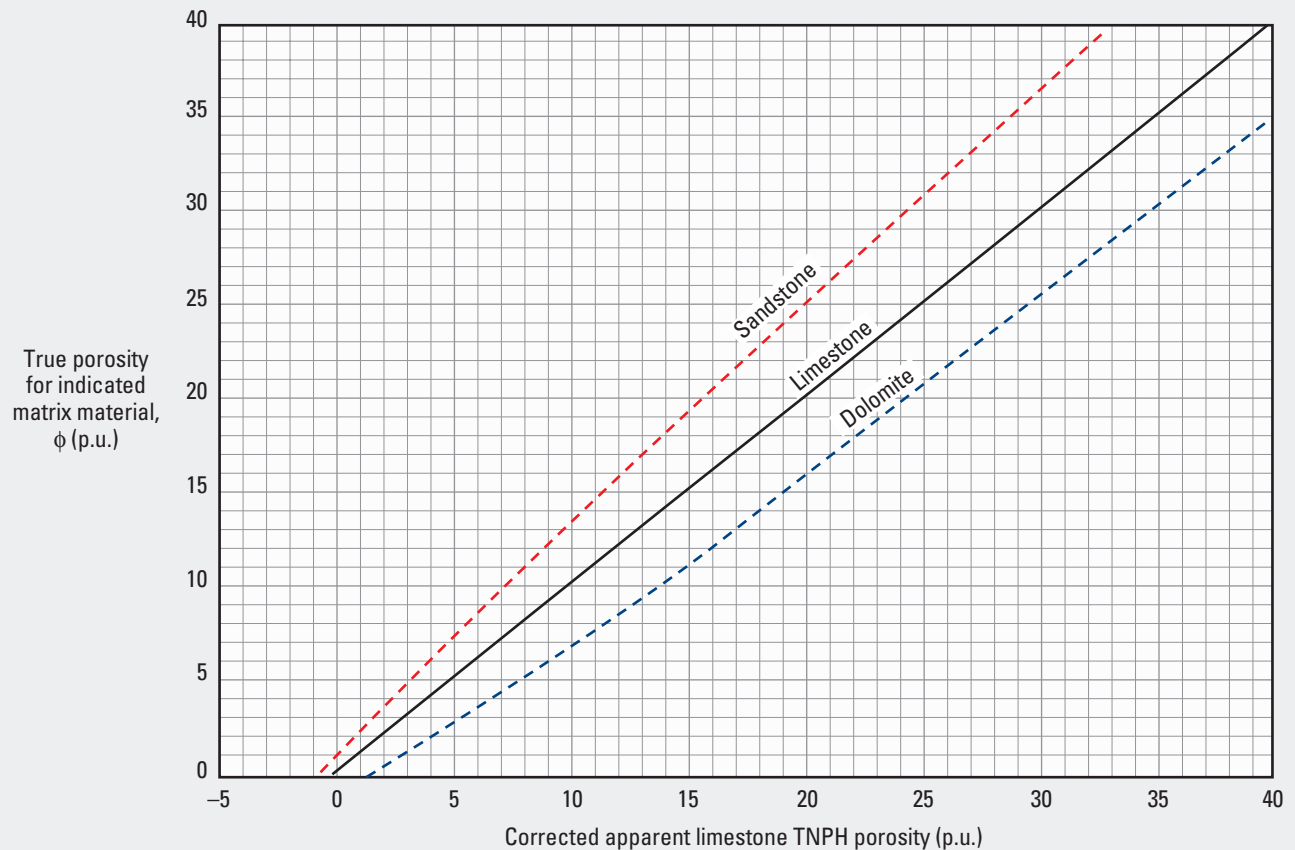
Description

Enter the chart on the x-axis with the corrected apparent limestone BPHI porosity from Chart Neu-43 or Neu-44 to intersect the curve for the appropriate formation material. Read the porosity on the y-axis.

EcoScope* 6.75-in. Integrated LWD Tool, TNPH Porosity

Porosity Equivalence—Open Hole

Por-10a



*Mark of Schlumberger
© Schlumberger

Purpose

This chart is used to determine the porosity of sandstone, limestone, or dolomite from the corrected apparent limestone TNPH porosity measured with the EcoScope 6.75-in. LWD tool.

Use this chart only with EcoScope thermal neutron porosity (TNPH) measurements; use Chart Por-10 with EcoScope best thermal neutron porosity, average (BPHI) measurements.

Description

Enter the chart on the x-axis with the corrected apparent limestone TNPH porosity from Chart Neu-45 or Neu-46 to intersect the curve for the appropriate formation material. Read the porosity on the y-axis.

Por

CNL* Compensated Neutron Log and Litho-Density* Tool (fresh water in invaded zone)

Porosity and Lithology—Open Hole

Purpose

This chart is used with the bulk density and apparent limestone porosity from the CNL Compensated Neutron Log and Litho-Density tools, respectively, to approximate the lithology and determine the crossplot porosity.

Description

Enter the chart with the environmentally corrected apparent neutron limestone porosity on the x-axis and bulk density on the y-axis. The intersection of the two values describes the crossplot porosity and lithology.

If the point is on a lithology curve, that indicates that the formation is primarily that lithology. If the point is between the lithology curves, then the formation is a mixture of those lithologies. The position of the point in relation to the two lithology curves as composition endpoints indicates the mineral percentages of the formation.

The porosity for a point between lithology curves is determined by scaling the crossplot porosity by connecting similar numbers on the two lithology curves (e.g., 20 on the quartz sandstone curve to 20 on the limestone curve). The scale line closest to the point represents the crossplot porosity.

Chart Por-12 is used for the same purpose as this chart for salt-water-invaded zones.

Example

Given: Corrected apparent neutron limestone porosity = 16.5 p.u. and bulk density = 2.38 g/cm³.

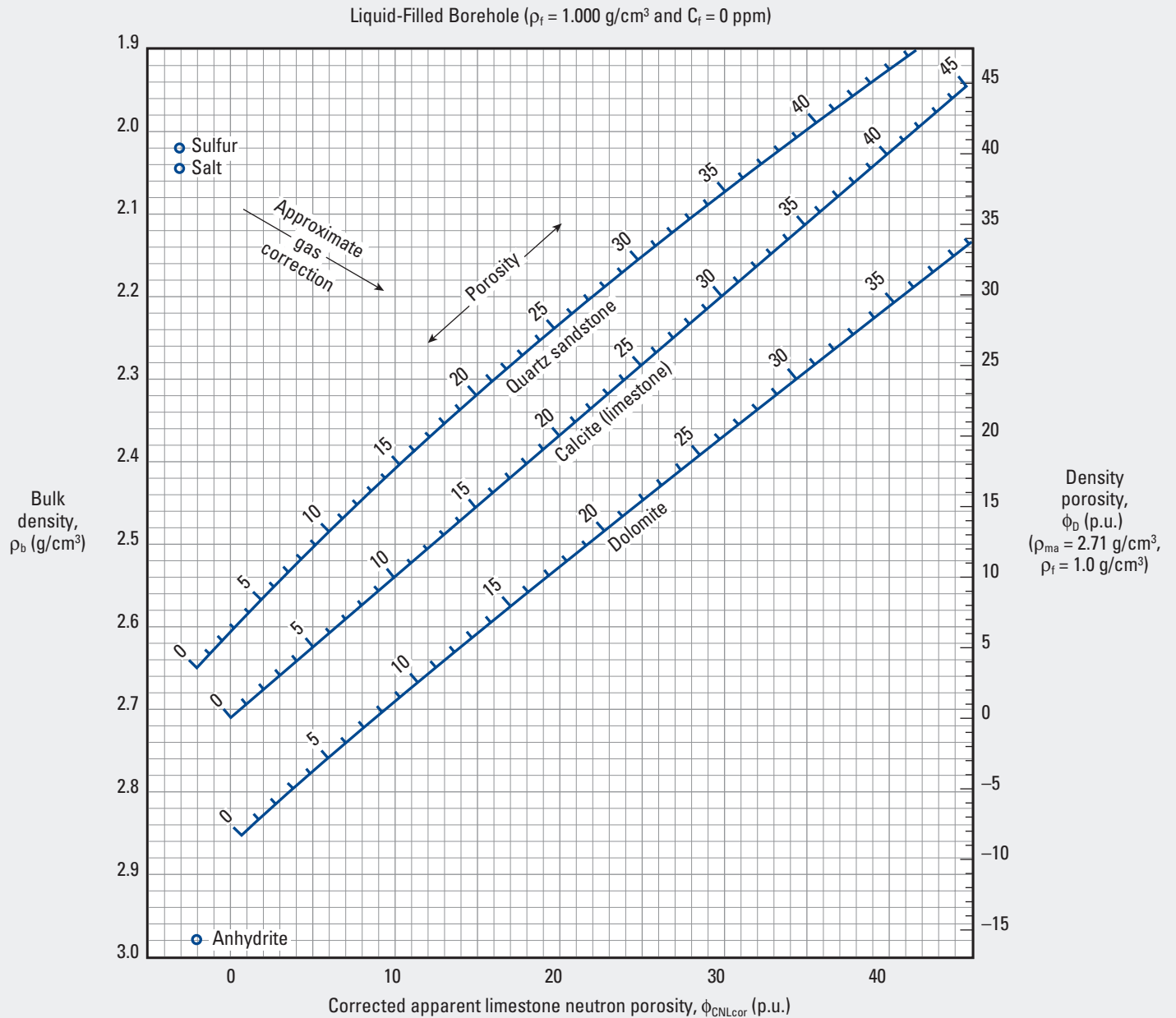
Find: Crossplot porosity and lithology.

Answer: Crossplot porosity = 18 p.u. The lithology is approximately 40% quartz and 60% limestone.

CNL* Compensated Neutron Log and Litho-Density* Tool (fresh water in invaded zone)

Por-11
(former CP-1e)

Porosity and Lithology—Open Hole



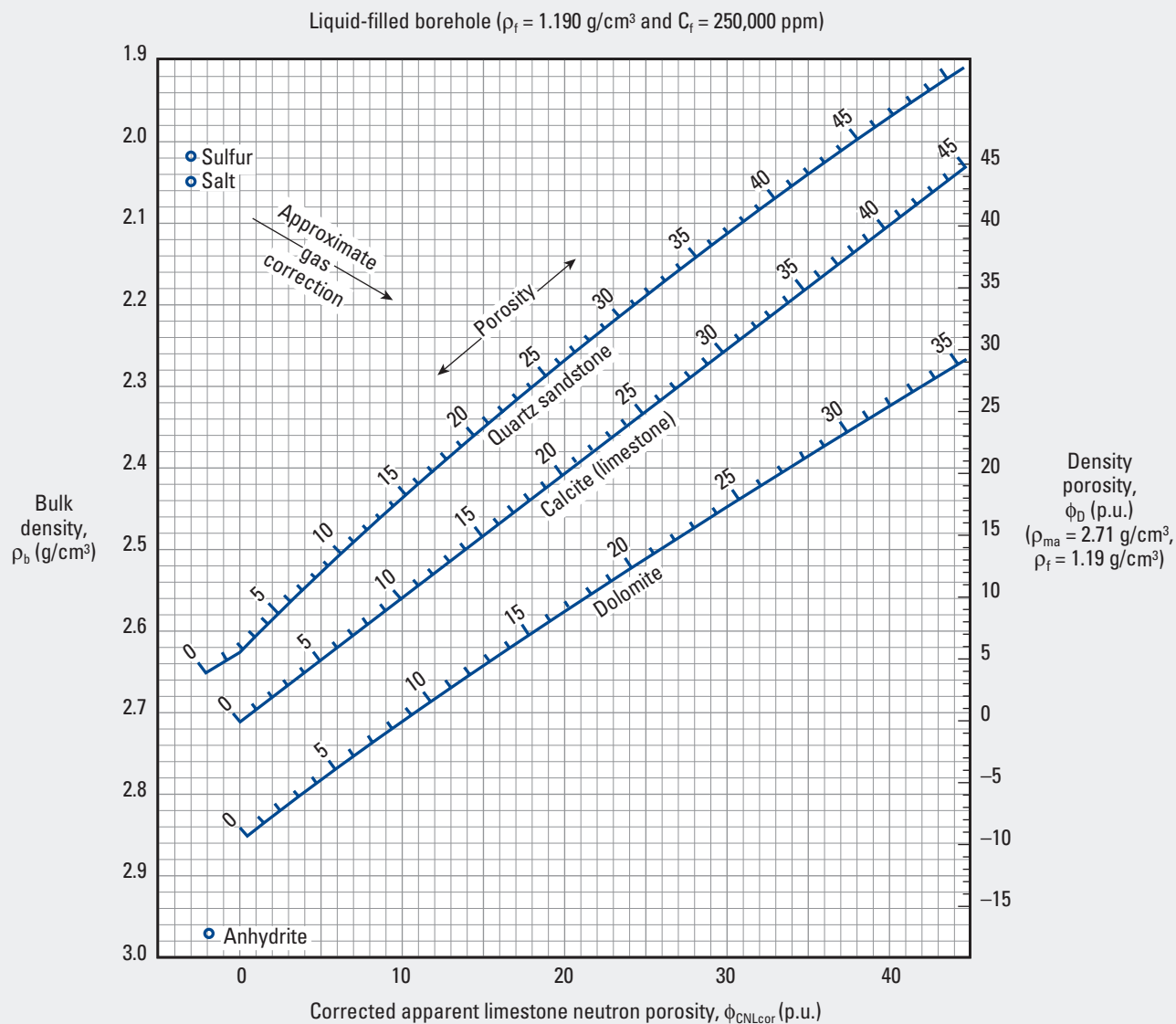
*Mark of Schlumberger
© Schlumberger

Por

CNL* Compensated Neutron Log and Litho-Density* Tool (salt water in invaded zone)

Por-12
(former CP-11)

Porosity and Lithology—Open Hole



*Mark of Schlumberger
© Schlumberger

Por

Purpose

This chart is used similarly to Chart Por-11 with CNL Compensated Neutron Log and Litho-Density values to approximate the lithology and determine the crossplot porosity in the saltwater-invaded zone.

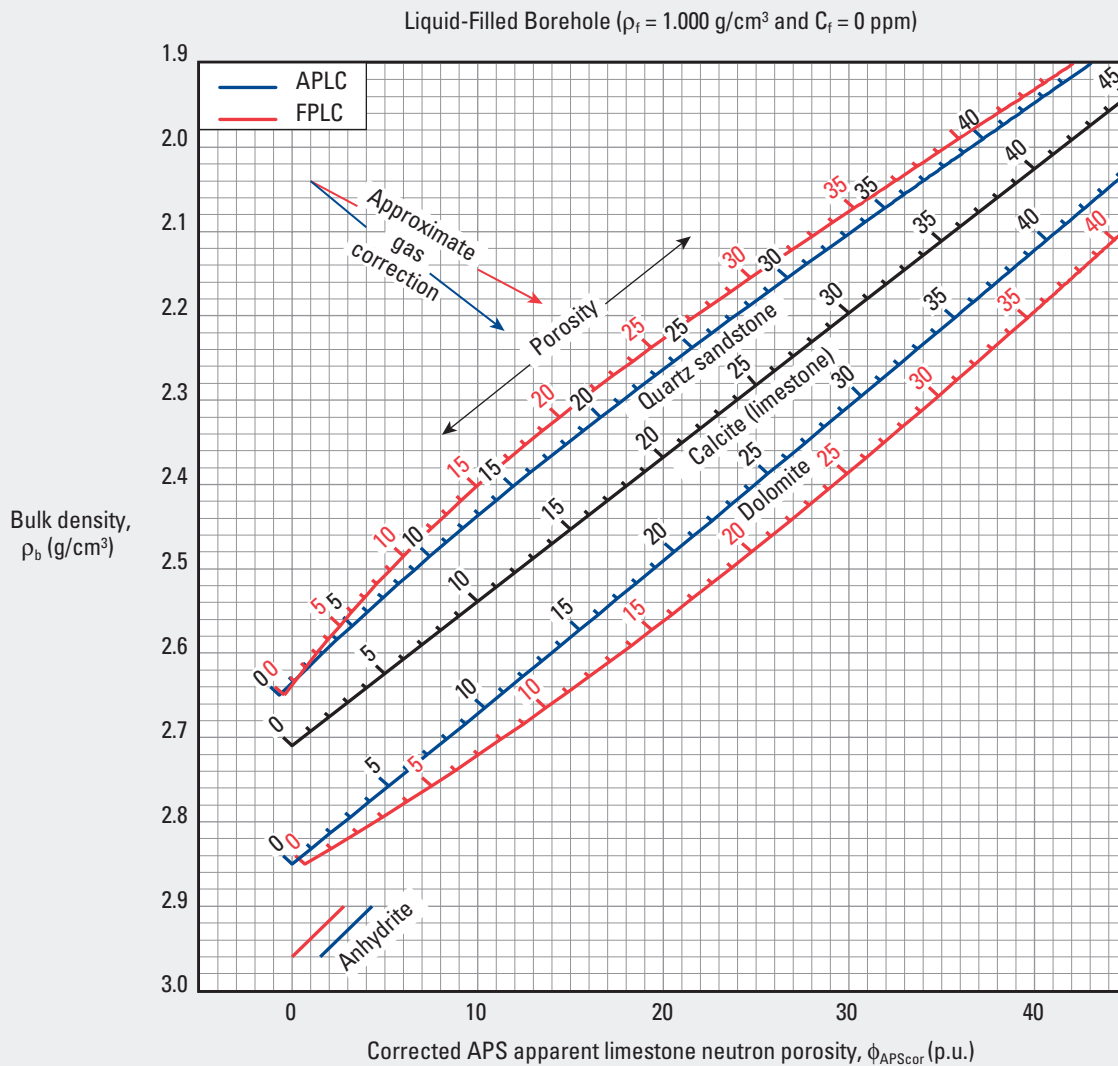
Example

- Given:** Corrected apparent neutron limestone porosity = 16.5 p.u. and bulk density = 2.38 g/cm^3 .
- Find:** Crossplot porosity and lithology.
- Answer:** Crossplot porosity = 20 p.u. The lithology is approximately 55% quartz and 45% limestone.

APS* and Litho-Density* Tools

Porosity and Lithology—Open Hole

Por-13
(former CP-1g)



*Mark of Schlumberger
© Schlumberger

Purpose

This chart is used to determine the lithology and porosity from the Litho-Density bulk density and APS Accelerator Porosity Sonde porosity log curves (APLC or FPLC). This chart applies to boreholes filled with freshwater drilling fluid; Chart Por-14 is used for saltwater fluids.

Description

Enter either the APLC or FPLC porosity on the x-axis and the bulk density on the y-axis. Use the blue matrix curves for APLC porosity values and the red curves for FPLC porosity values. Anhydrite plots on separate curves. The gas correction direction is indicated for formations containing gas. Move parallel to the blue correction line if the APLC porosity is used or to the red correction line if the FPLC porosity is used.

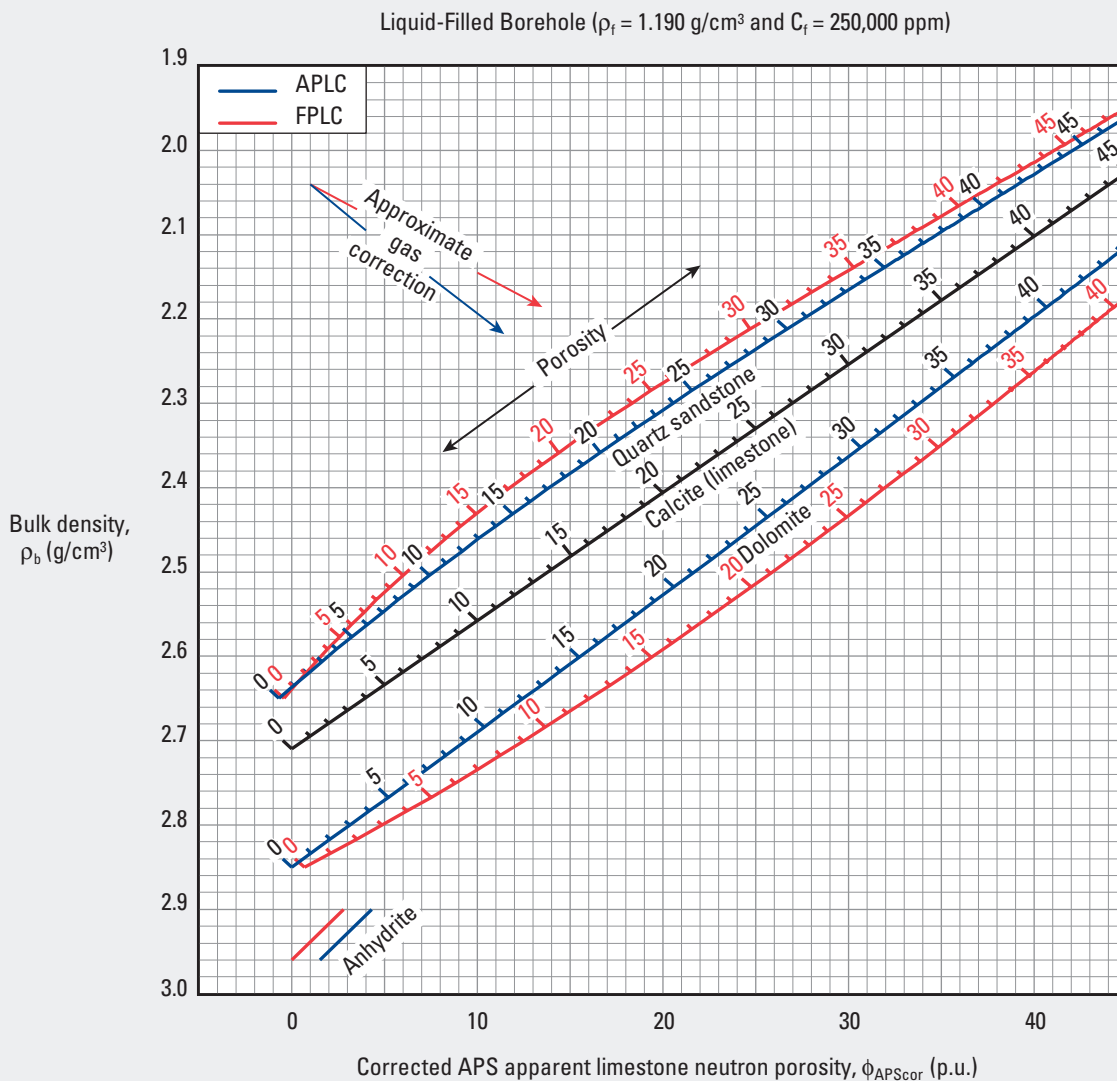
Example

Given: APLC porosity = 8 p.u. and bulk density = 2.2 g/cm³.
Find: Approximate quartz sandstone porosity.
Answer: Enter at 8 p.u. on the x-axis and 2.2 g/cm³ on the y-axis to find the intersection point is in the gas-in-formation correction region. Because the APLC porosity value was used, move parallel to the blue gas correction line until the blue quartz sandstone curve is intersected at approximately 19 p.u.

APS* and Litho-Density* Tools (saltwater formation)

Porosity and Lithology—Open Hole

Por-14
(former CP-1h)



*Mark of Schlumberger
© Schlumberger

Por

Purpose

This chart is used similarly to Chart Por-13 to determine the lithology and porosity from Litho-Density* bulk density and APS* porosity log curves (APLC or FPLC) in saltwater boreholes.

Example

Given: APLC porosity = 8 p.u. and bulk density = 2.2 g/cm^3 .

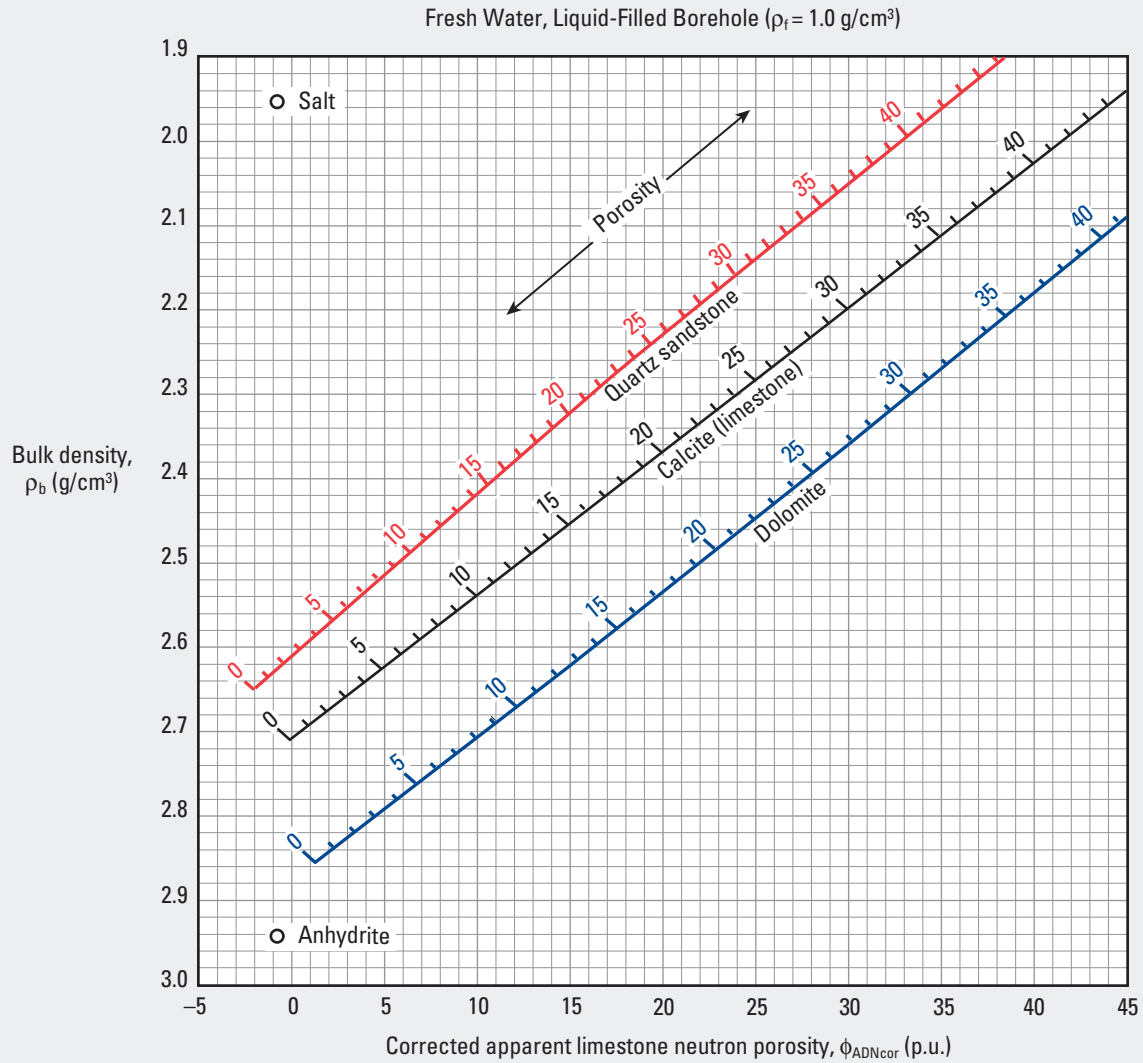
Find: Approximate quartz sandstone porosity.

Answer: Enter 8 p.u. on the x-axis and 2.2 g/cm^3 on the y-axis to find the intersection point is in the gas-in-formation correction region. Because the APLC porosity value was used, move parallel to the blue gas correction line until the blue quartz sandstone curve is intersected at approximately 20 p.u.

adnVISION475* 4.75-in. Azimuthal Density Neutron Tool

Porosity and Lithology—Open Hole

Por-15



*Mark of Schlumberger
© Schlumberger

Purpose

This chart is used to determine the crossplot porosity and lithology from the adnVISION475 4.75-in. density and neutron porosity.

Description

Enter the chart with the adnVISION475 corrected apparent limestone neutron porosity (from Chart Neu-31) and bulk density. The intersection of the two values is the crossplot porosity. The position of the point of intersection between the matrix curves represents the relative percentage of each matrix material.

Example

Given: $\phi_{ADNcor} = 20$ p.u. and $\rho_b = 2.24$ g/cm³.

Find: Crossplot porosity and matrix material.

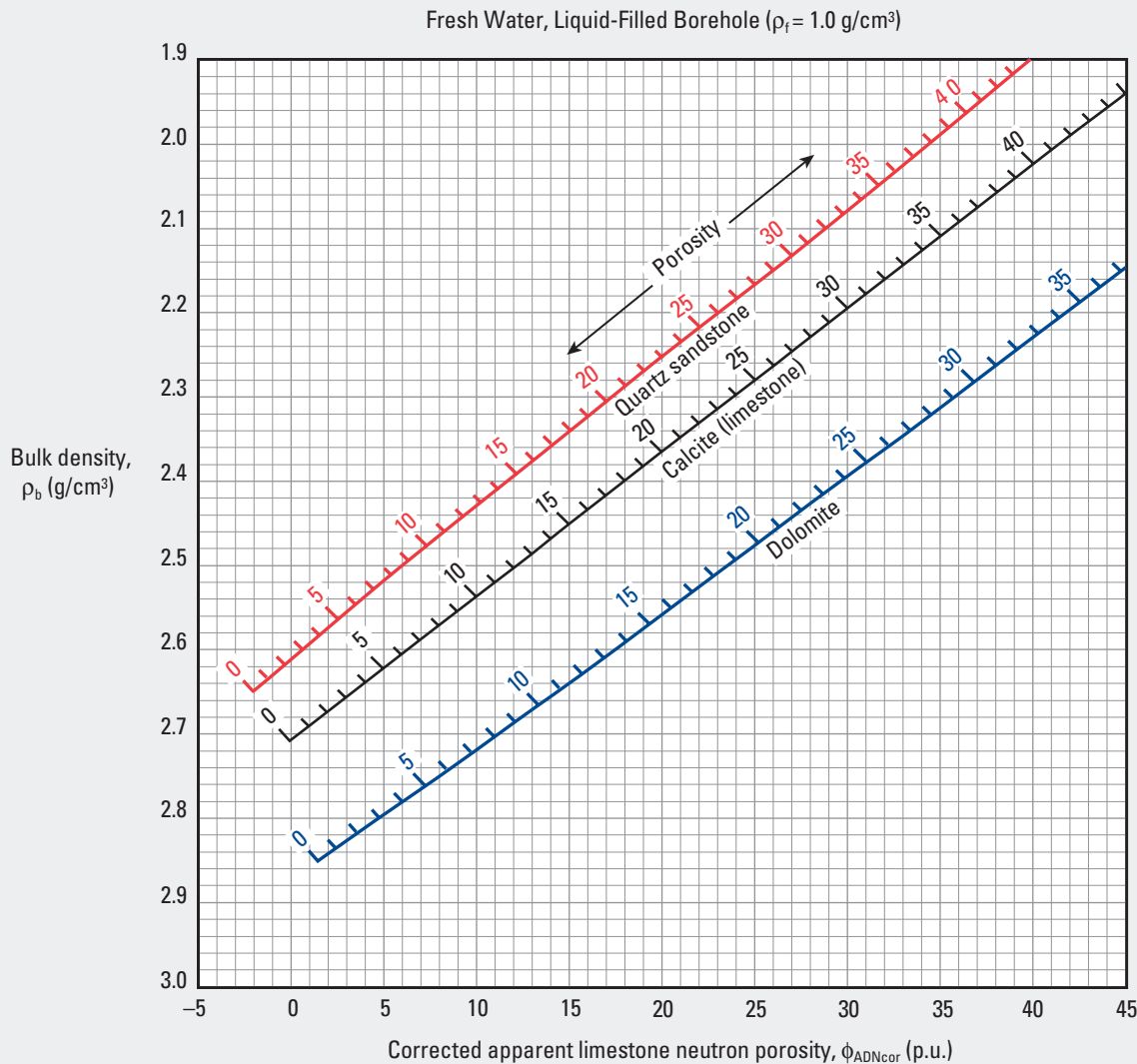
Answer: 25 p.u. in sandstone.

Por

adnVISION675* 6.75-in. Azimuthal Density Neutron Tool

Porosity and Lithology—Open Hole

Por-16



*Mark of Schlumberger
© Schlumberger

Purpose

This chart uses the bulk density and apparent limestone porosity from the adnVISION 6.75-in. Azimuthal Density Neutron tool to determine the lithology of the logged formation and the crossplot porosity.

Description

This chart is applicable for logs obtained in freshwater drilling fluid. Enter the corrected apparent limestone porosity and the bulk density on the x- and y-axis, respectively. Their intersection point determines the lithology and crossplot porosity.

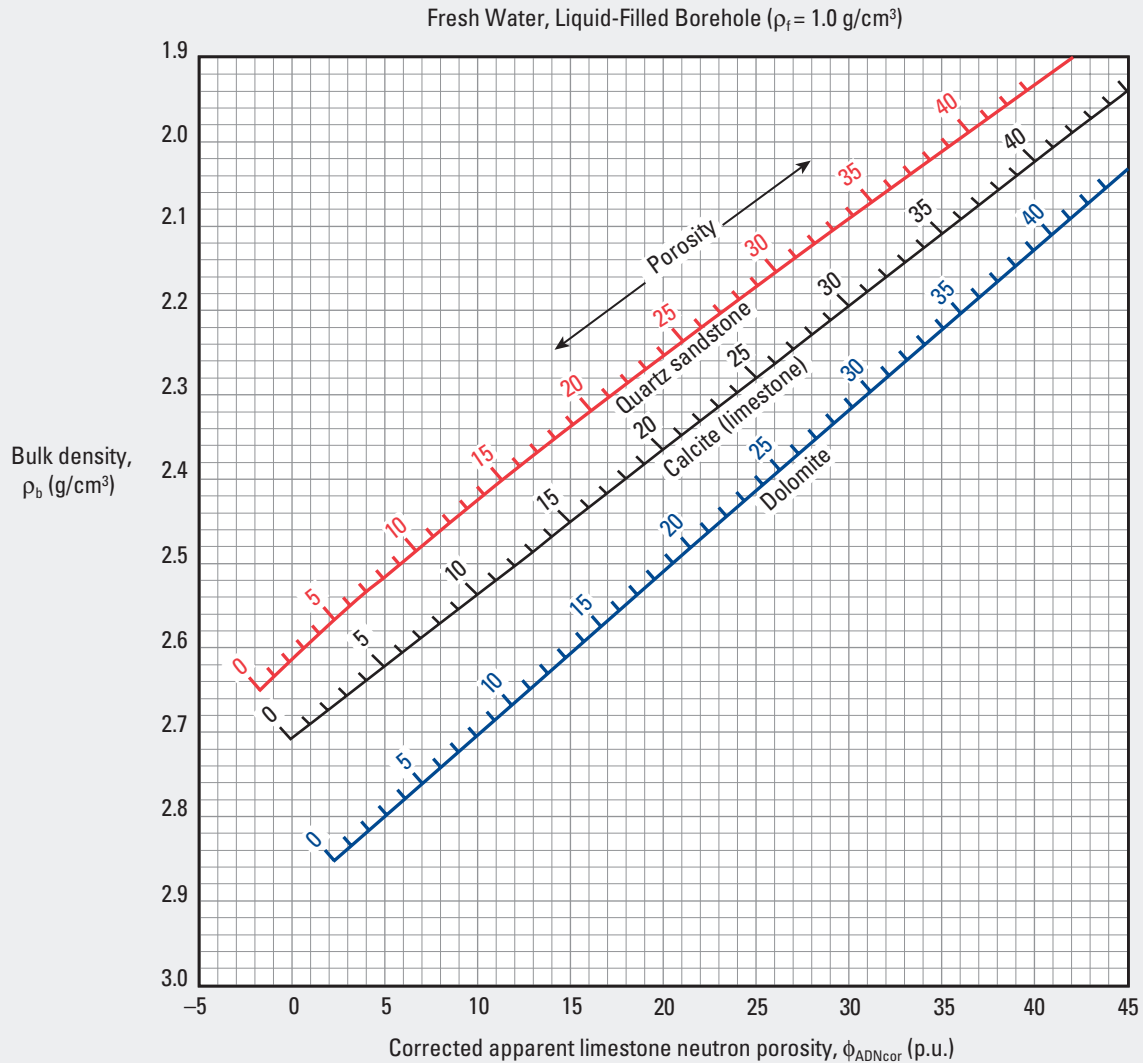
Example

- Given:** Corrected adnVISION675 apparent limestone porosity = 20 p.u. and bulk density = 2.3 g/cm^3 .
- Find:** Porosity and lithology type.
- Answer:** Entering the chart at 20 p.u. on the x-axis and 2.3 g/cm^3 on the y-axis corresponds to a crossplot porosity of 21.5 p.u. and formation comprising approximately 60% quartz sandstone and 40% limestone.

adnVISION825* 8.25-in. Azimuthal Density Neutron Tool

Porosity and Lithology—Open Hole

Por-17



*Mark of Schlumberger
© Schlumberger

Por

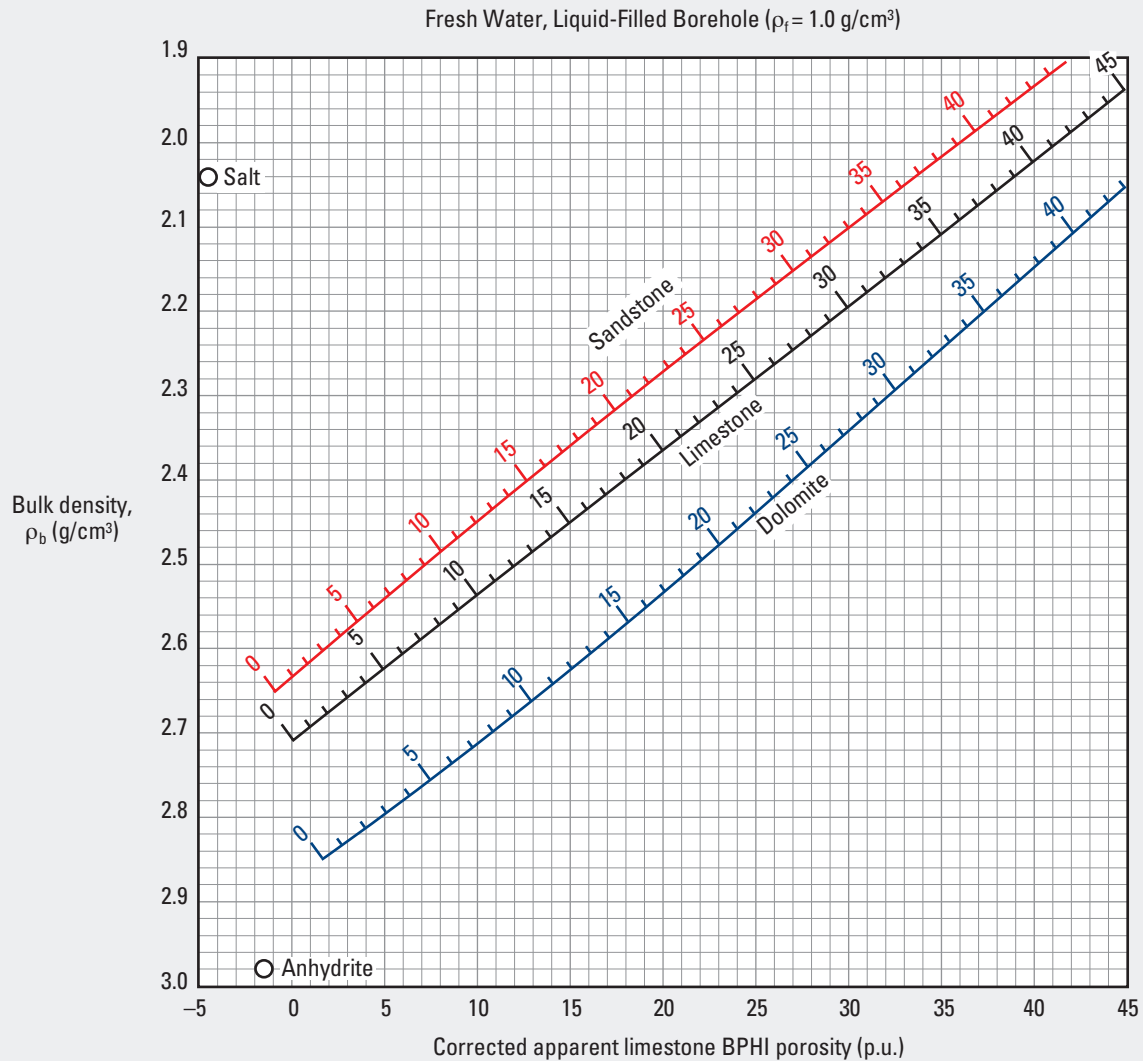
Purpose

This chart is used similarly to Chart Por-15 to determine the lithology and crossplot porosity from adnVISION825 8.25-in. Azimuthal Density Neutron values.

EcoScope* 6.75-in. Integrated LWD Tool

Porosity and Lithology—Open Hole

Por-18



*Mark of Schlumberger
© Schlumberger

Por

Purpose

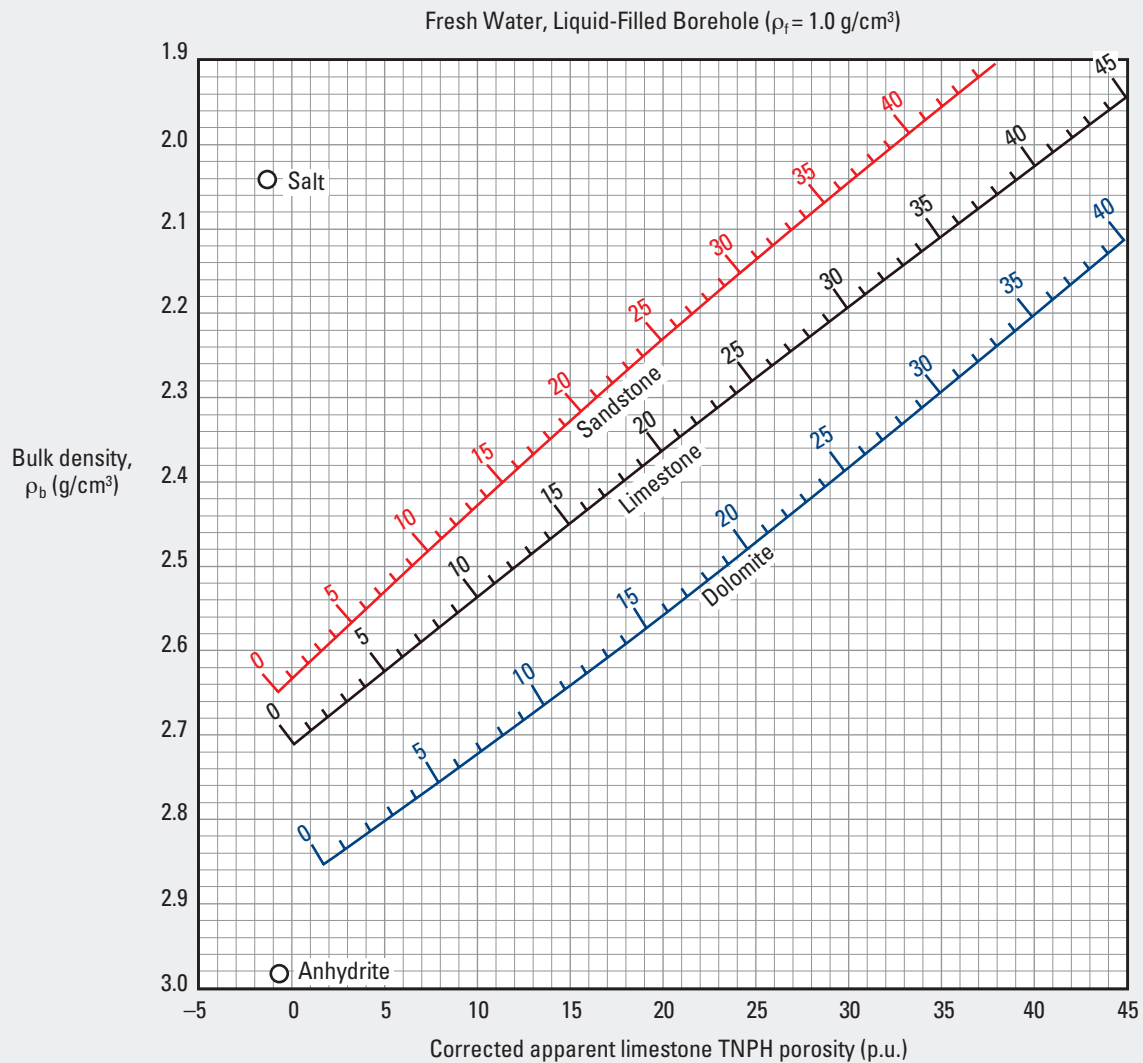
This chart is used similarly to Chart Por-15 to determine the lithology and crossplot porosity from EcoScope 6.75-in. density and best thermal neutron porosity (BPHI) values.

Use this chart only with EcoScope BPHI neutron porosity; use Chart Por-19 with EcoScope thermal neutron porosity (TNPH) measurements.

EcoScope* 6.75-in. Integrated LWD Tool

Porosity and Lithology—Open Hole

Por-19



*Mark of Schlumberger
© Schlumberger

Purpose

This chart is used similarly to Chart Por-15 to determine the lithology and crossplot porosity from EcoScope 6.75-in. density and thermal neutron porosity (TNPH) values.

Use this chart only with EcoScope TNPH neutron porosity; use Chart Por-18 with EcoScope best thermal neutron porosity (BPHI) measurements.

Sonic and Thermal Neutron Crossplot

Porosity and Lithology—Open Hole, Freshwater Invaded

Purpose

This chart is used to determine crossplot porosity and an approximation of lithology for sonic and thermal neutron logs in freshwater drilling fluid.

Description

Enter the corrected neutron porosity (apparent limestone porosity) on the x-axis and the sonic slowness time (Δt) on the y-axis to find their intersection point, which describes the crossplot porosity and lithology composition of the formation. Two sets of curves are drawn on the chart. The blue set of curves represents the crossplot porosity values using the sonic time-average algorithm. The red set of curves represents the field observation algorithm.

Example

Given: Thermal neutron apparent limestone porosity = 20 p.u. and sonic slowness time = 89 $\mu\text{s}/\text{ft}$ in freshwater drilling fluid.

Find: Crossplot porosity and lithology.

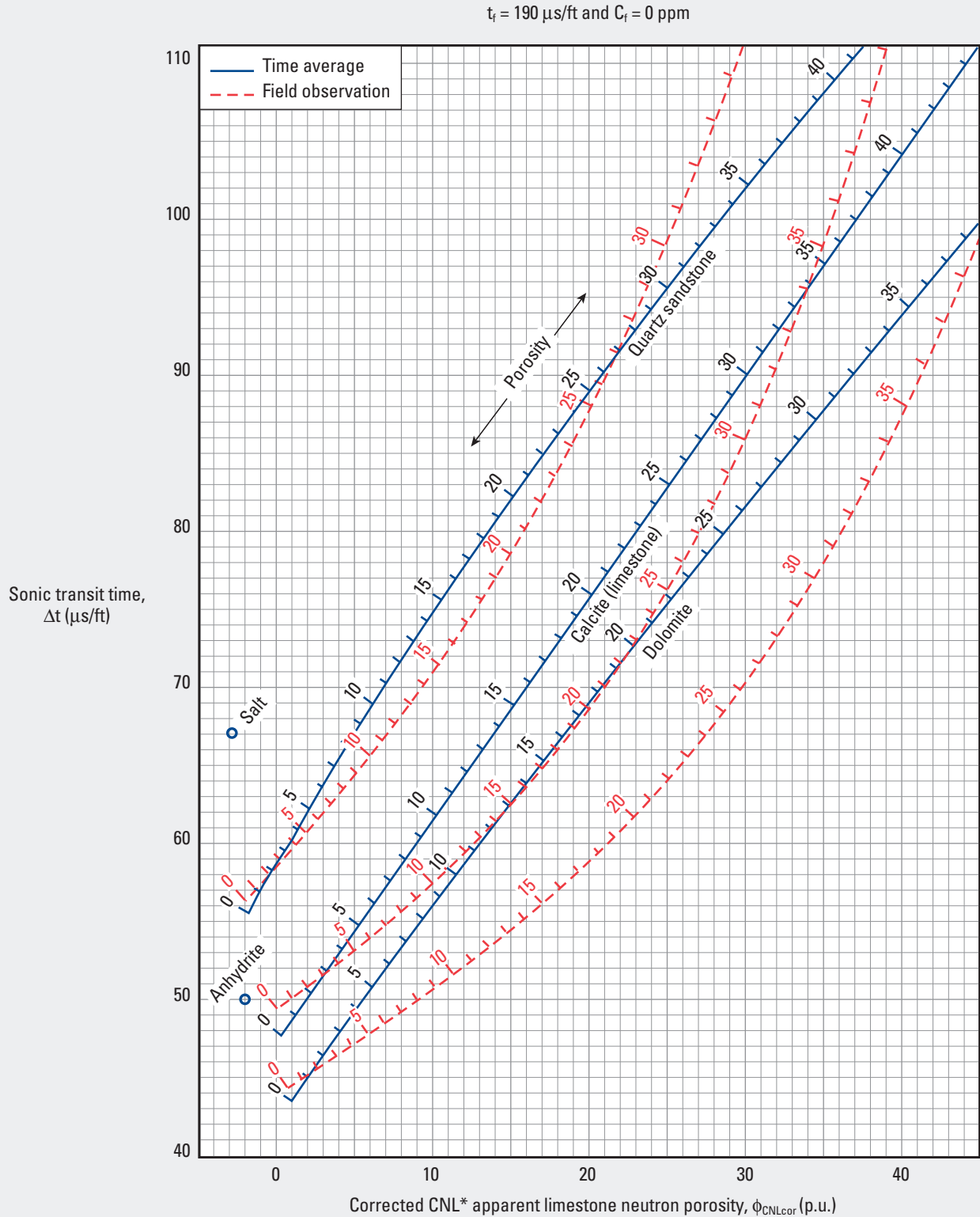
Answer: Enter the neutron porosity on the x-axis and the sonic slowness time on the y-axis. The intersection point is at about 25 p.u. on the field observation line and 24.5 p.u. on the time-average line. The matrix is quartz sandstone.

Sonic and Thermal Neutron Crossplot

Porosity and Lithology—Open Hole, Freshwater Invaded

Por-20

(customary, former CP-2c)



*Mark of Schlumberger
© Schlumberger

Por

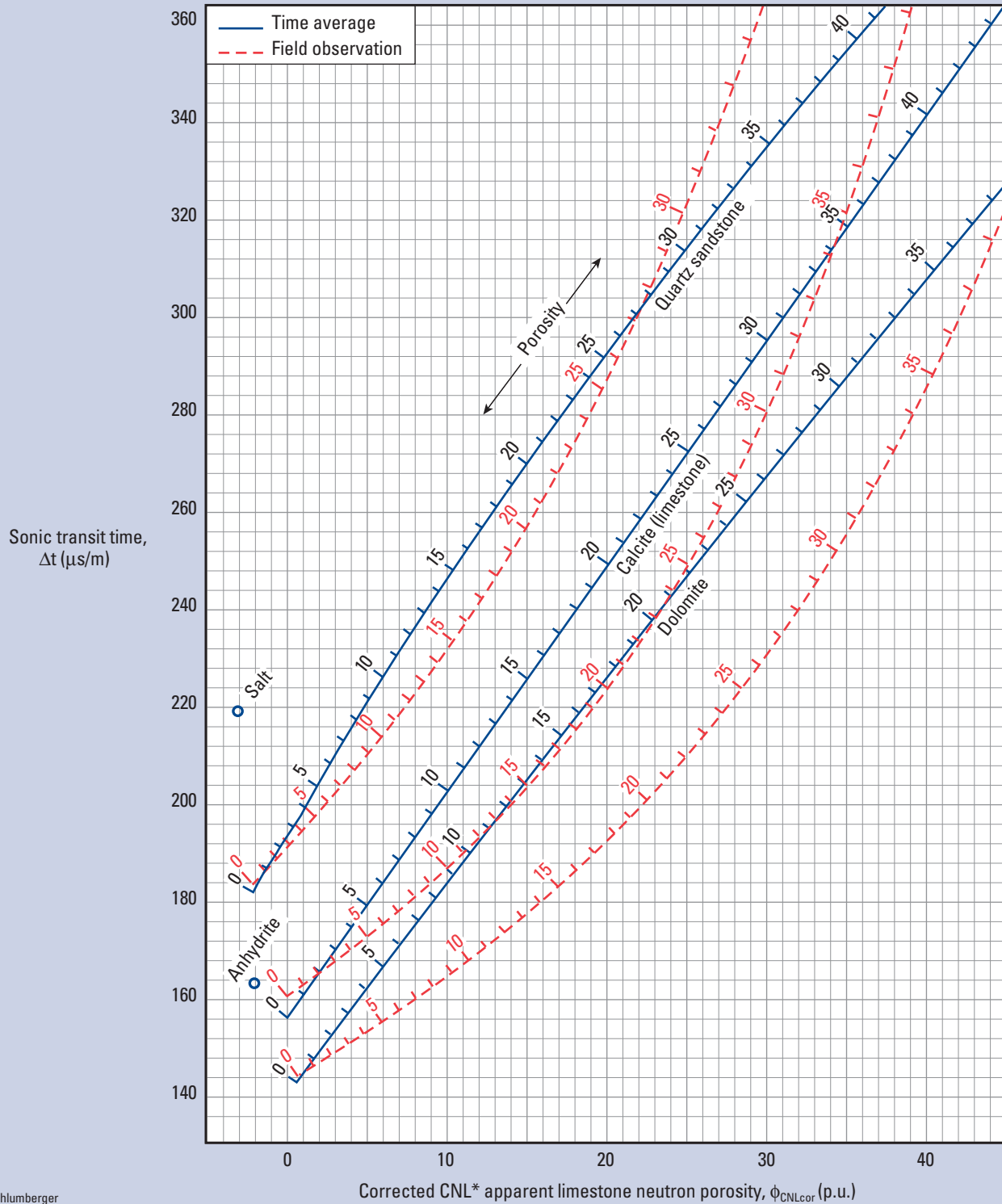
Sonic and Thermal Neutron Crossplot

Porosity and Lithology—Open Hole, Freshwater Invaded

Por-21

(metric, former CP-2cm)

$t_i = 620 \mu\text{s/m}$ and $C_f = 0 \text{ ppm}$



*Mark of Schlumberger
© Schlumberger

Purpose

This chart is used similarly to Chart Por-20 for metric units.

Density and Sonic Crossplot

Porosity and Lithology—Open Hole, Freshwater Invaded

Purpose

This chart is used to determine porosity and lithology for sonic and density logs in freshwater-invaded zones.

Description

Enter the chart with the bulk density on the y-axis and sonic slowness time on the x-axis. The point of intersection indicates the type of formation and its porosity.

Example

Given: Bulk density = 2.3 g/cm^3 and sonic slowness time = $82 \text{ } \mu\text{s/ft}$.

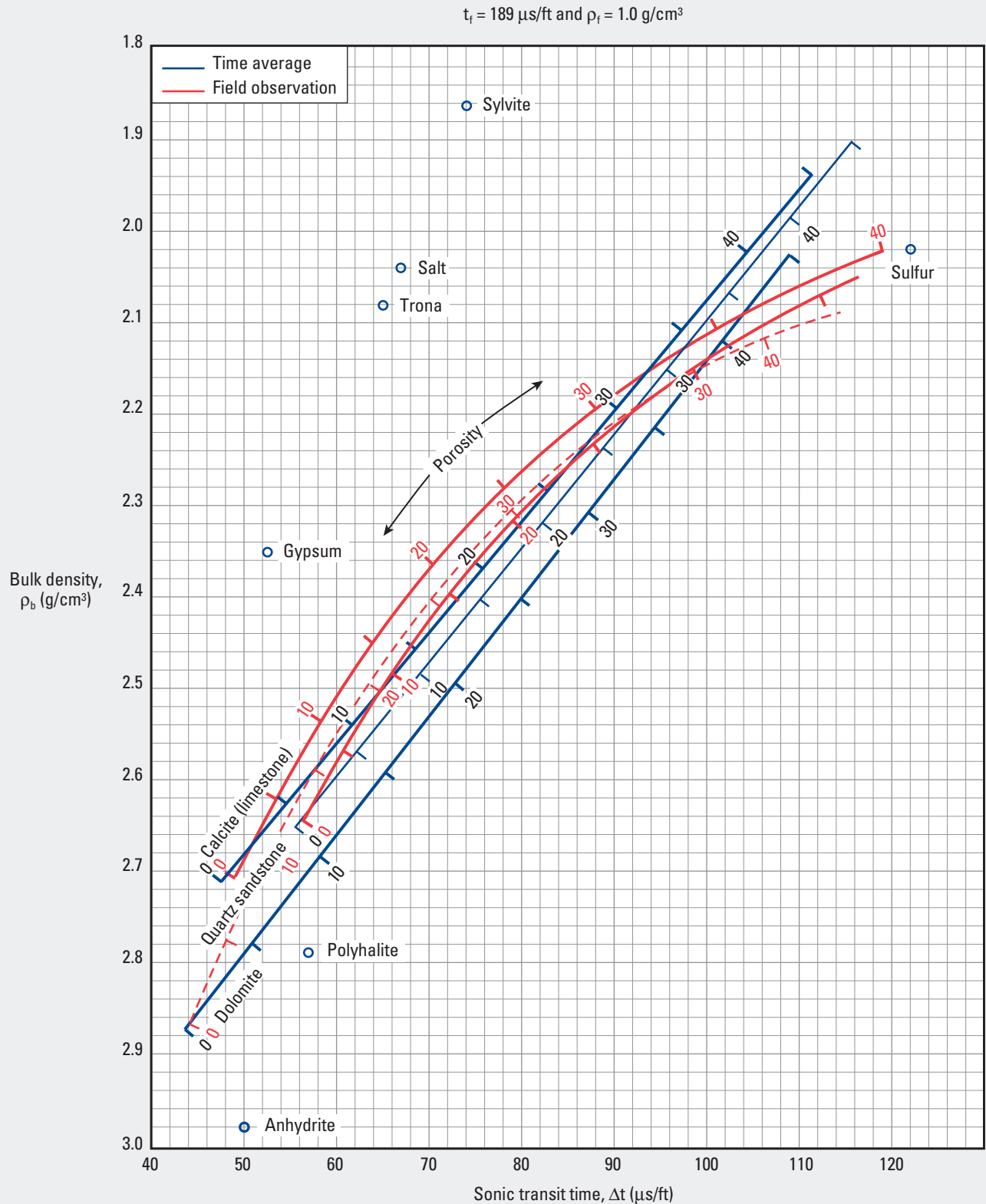
Find: Crossplot porosity and lithology.

Answer: Limestone with a crossplot porosity = 24 p.u.

Density and Sonic Crossplot

Porosity and Lithology—Open Hole, Freshwater Invaded

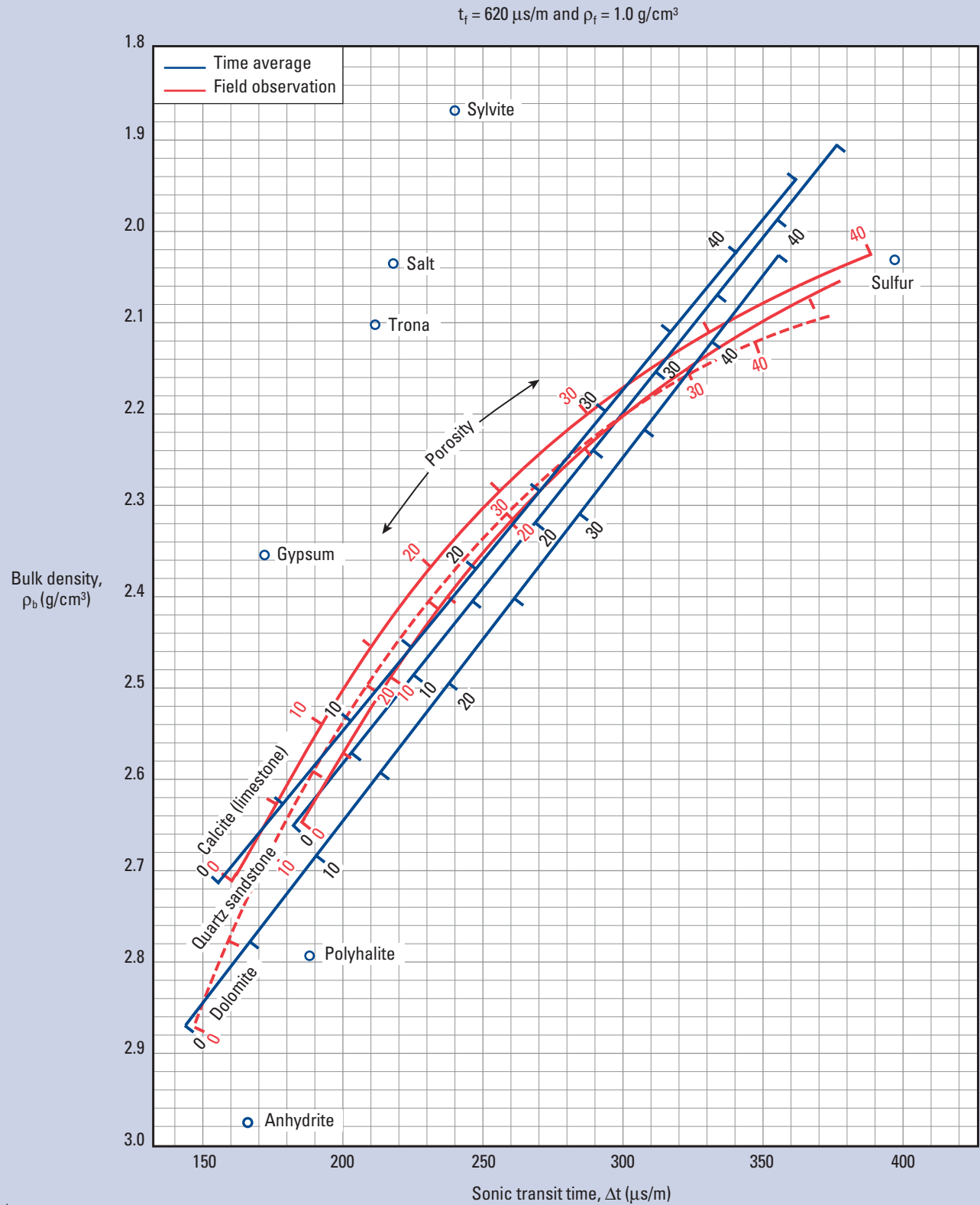
Por-22
(customary, former CP-7)



Density and Sonic Crossplot

Porosity and Lithology—Open Hole, Freshwater Invaded

Por-23
(metric, former CP-7m)



© Schlumberger

Purpose

This chart is used similarly to Chart Por-22 for metric units.

Por

Density and Neutron Tool

Porosity Identification—Gas-Bearing Formation

Purpose

This chart is used to determine the porosity and average water saturation in the flushed zone (S_{xo}) for freshwater invasion and gas composition of $C_{1.1}H_{4.2}$ (natural gas).

Description

Enter the chart with the neutron- and density-derived porosity values (ϕ_N and ϕ_D , respectively). On the basis of the table, use the blue curves for shallow reservoirs and the red curves for deep reservoirs.

Example

Given: $\phi_D = 25$ p.u. and $\phi_N = 10$ p.u. in a low-pressure, shallow (4,000-ft) reservoir.

Find: Porosity and S_{xo} .

Answer: Enter the chart at 25 p.u. on the y-axis and 10 p.u. on the x-axis. The point of intersection identifies (on the blue curves for a shallow reservoir) $\phi = 20$ p.u. and $S_{xo} = 62\%$.

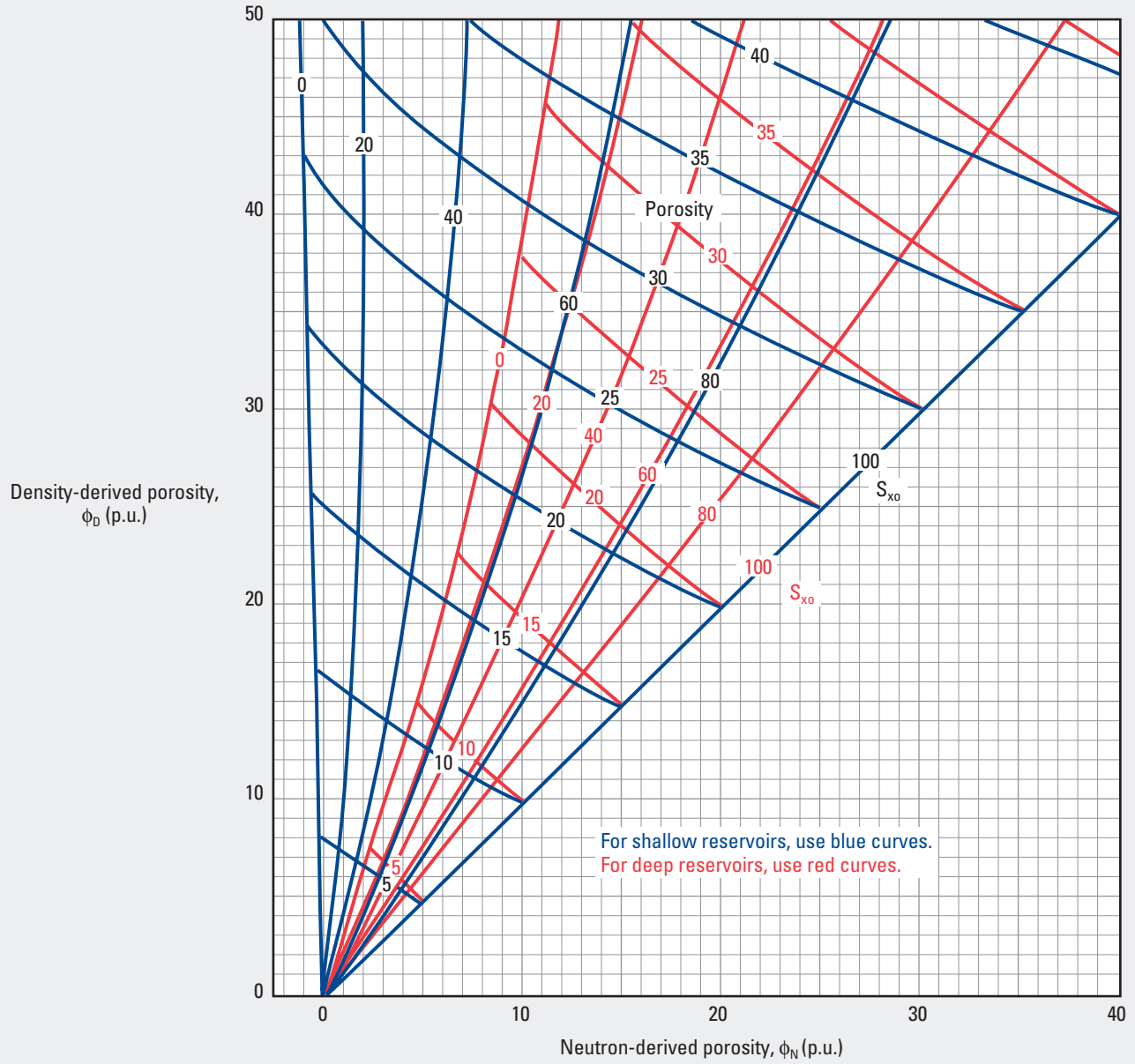
Depth	Pressure	Temperature	ρ_w (g/cm ³)	I_{Hw}	ρ_g (g/cm ³)	I_{Hg}
Shallow reservoir	~2,000 psi [~14,000 kPa]	~120°F [~50°C]	1.00	1.00	0	0
Deep reservoir	~7,000 psi [~48,000 kPa]	~240°F [~120°C]	1.00	1.00	0.25	0.54

ρ_w = density of water, ρ_g = density of gas, I_{Hw} = hydrogen index of water, and I_{Hg} = hydrogen index of gas

Density and Neutron Tool

Porosity Identification—Gas-Bearing Formation

Por-24
(former CP-5)



Density and APS* Epithermal Neutron Tool

Porosity Identification—Gas-Bearing Formation

Purpose

This chart is used to determine the porosity and average water saturation in the flushed zone (S_{xo}) for freshwater invasion and gas composition of CH_4 (methane).

Description

Enter the chart with the APS Accelerator Porosity Sonde neutron- and density-derived porosity values (ϕ_N and ϕ_D , respectively). On the basis of the table, use the blue curves for shallow reservoirs and the red curves for deep reservoirs.

Example

Given: $\phi_D = 15$ p.u. and APS $\phi_N = 8$ p.u. in a normally pressured deep (14,000-ft) reservoir.

Find: Porosity and S_{xo} .

Answer: $\phi = 11$ p.u. and $S_{xo} = 39\%$.

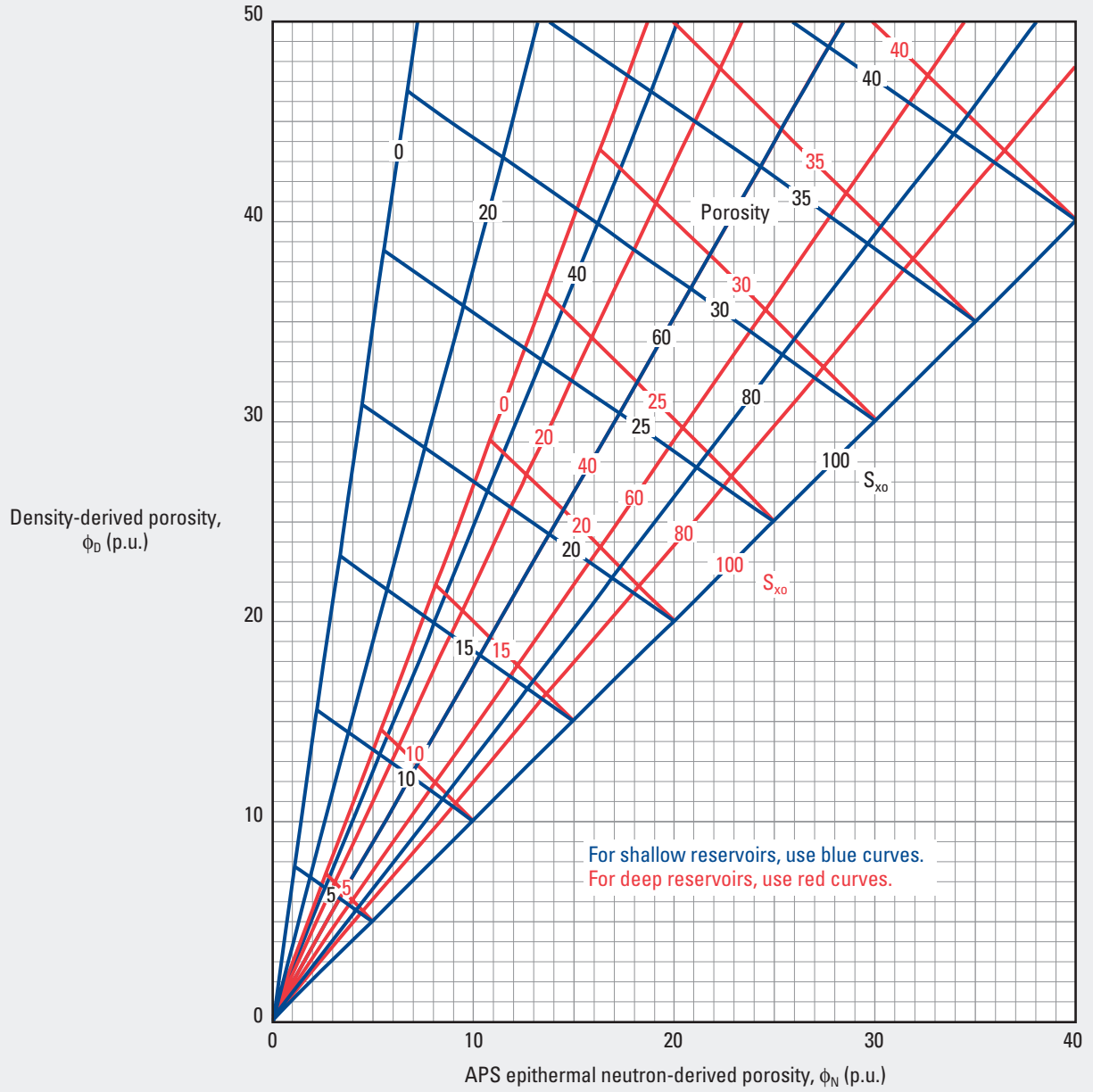
Depth	Pressure	Temperature	ρ_w	I_{Hw}	ρ_g	I_{Hg}
Shallow reservoir	~2,000 psi [~14,000 kPa]	~120°F [~50°C]	1.00	1.00	0.10	0.23
Deep reservoir	~7,000 psi [~48,000 kPa]	~240°F [~120°C]	1.00	1.00	0.25	0.54

ρ_w = density of water, ρ_g = density of gas, I_{Hw} = hydrogen index of water, and I_{Hg} = hydrogen index of gas

Density and APS* Epithermal Neutron Tool

Porosity Identification—Gas-Bearing Formation

Por-25
(former CP-5a)



*Mark of Schlumberger
© Schlumberger

Density, Neutron, and R_{xo} Logs

Porosity Identification in Hydrocarbon-Bearing Formation—Open Hole

Purpose

This nomograph is used to estimate porosity in hydrocarbon-bearing formations by using density, neutron, and resistivity in the flushed zone (R_{xo}) logs. The density and neutron logs must be corrected for environmental effects and lithology before entry to the nomograph. The chart includes an approximate correction for excavation effect, but if hydrocarbon density (ρ_h) is $<0.25 \text{ g/cm}^3$ (gas), the chart may not be accurate in some extreme cases:

- very high values of porosity (>35 p.u.) coupled with medium to high values of hydrocarbon saturation (S_{hr})
- $S_{hr} = 100\%$ for medium to high values of porosity.

Description

Connect the apparent neutron porosity value on the appropriate neutron porosity scale (CNL* Compensated Neutron Log or sidewall neutron porosity [SNP] log) with the corrected apparent density porosity on the density scale with a straight line. The intersection point on the ϕ_1 scale indicates the value of ϕ_1 .

Draw a line from the ϕ_1 value to the origin (lower right corner) of the chart for $\Delta\phi$ versus S_{hr} .

Enter the chart with S_{hr} from ($S_{hr} = 1 - S_{xo}$) and move vertically upward to determine the porosity correction factor ($\Delta\phi$) at the intersection with the line from the ϕ_1 scale.

This correction factor algebraically added to the porosity ϕ_1 gives the corrected porosity.

Example

Given: Corrected CNL apparent neutron porosity = 12 p.u.,
corrected apparent density porosity = 38 p.u., and
 $S_{hr} = 50\%$.

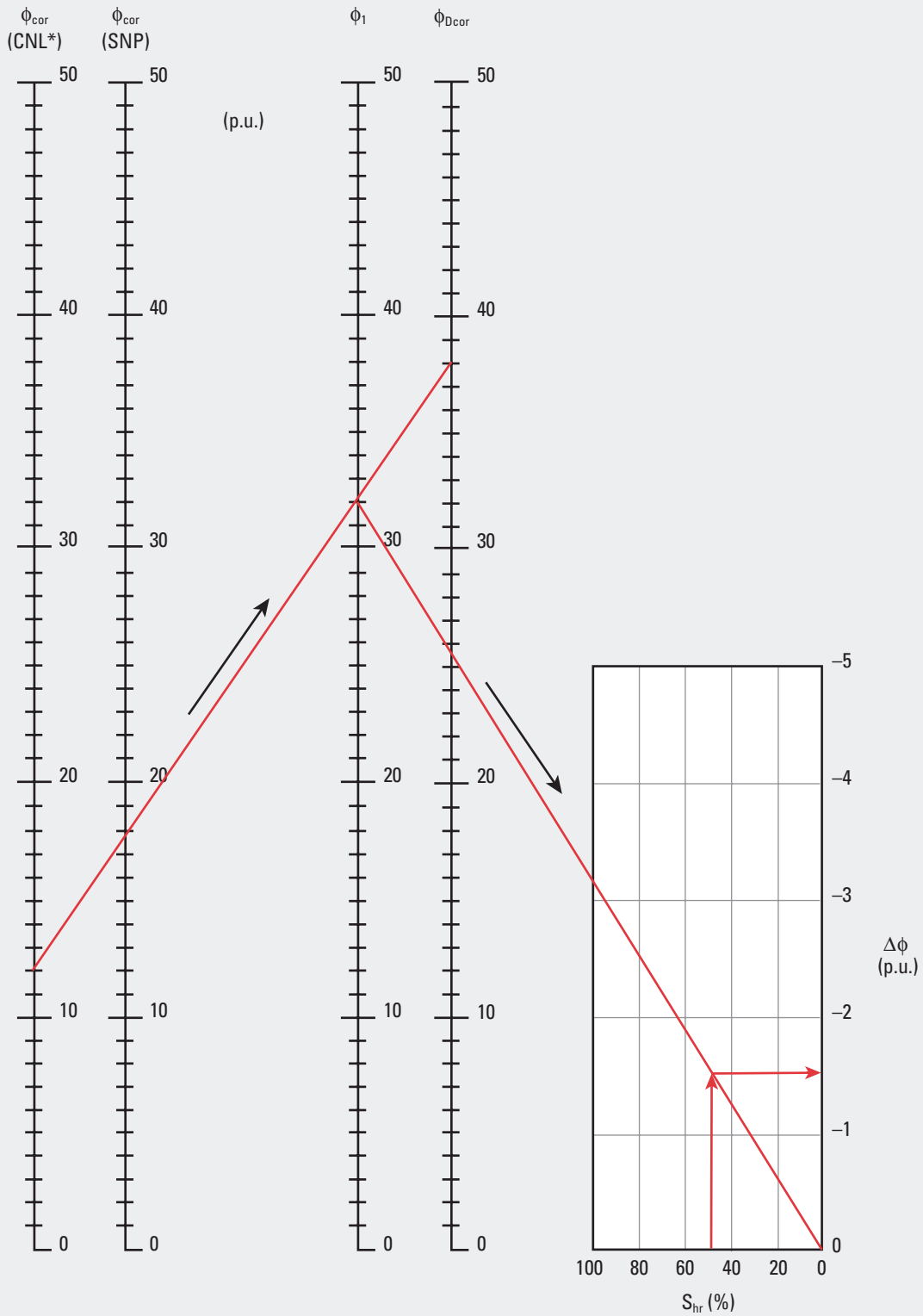
Find: Hydrocarbon-corrected porosity.

Answer: Enter the 12-p.u. ϕ_{cor} value on the CNL scale. A line from this value to 38 p.u. on the ϕ_{Dcor} scale intersects the ϕ_1 scale at 32.2 p.u. The intersection of a line from this value to the graph origin and $S_{hr} = 50\%$ is $\Delta\phi = -1.6$ p.u.
Hydrocarbon-corrected porosity: $32.2 - 1.6 = 30.6$ p.u.

Density, Neutron, and R_{x0} Logs

Porosity Identification in Hydrocarbon-Bearing Formation—Open Hole

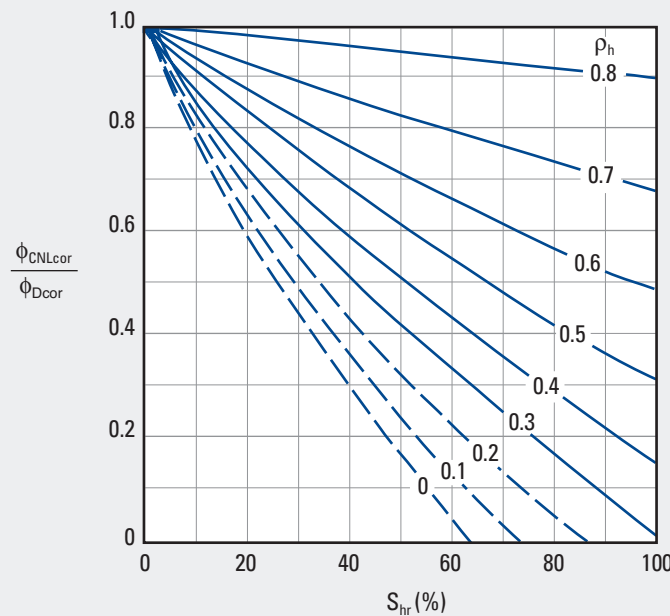
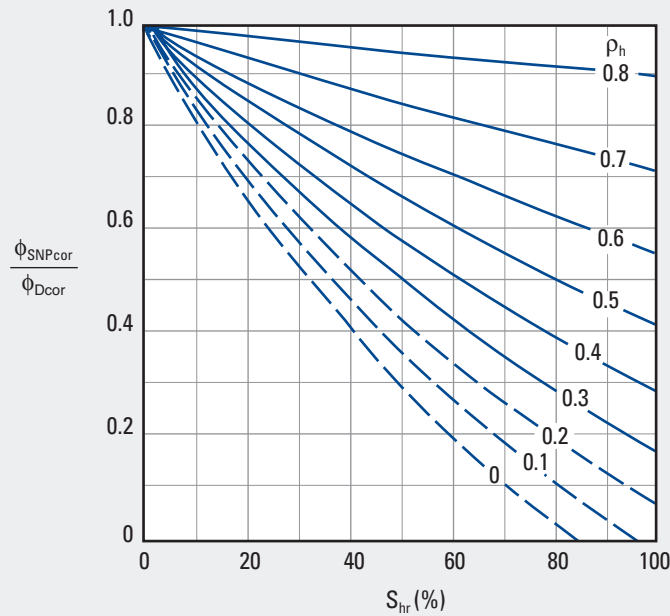
Por-26
(former CP-9)



*Mark of Schlumberger
© Schlumberger

Hydrocarbon Density Estimation

Por-27
(former CP-10)



*Mark of Schlumberger
© Schlumberger

Purpose

This chart is used to estimate the hydrocarbon density (ρ_h) within a formation from corrected neutron and density porosity values.

Description

Enter the ratio of the sidewall neutron porosity (SNP) or CNL* Compensated Neutron Log neutron porosity and density porosity corrected for lithology and environmental effects (ϕ_{SNPcor} or $\phi_{CNLCor} / \phi_{Dcor}$, respectively) on the y-axis and the

hydrocarbon saturation on the x-axis. The intersection point of the two values defines the density of the hydrocarbon.

Example

Given: Corrected CNL porosity = 15 p.u., corrected density porosity = 25 p.u., and $S_{hr} = 30%$ (residual hydrocarbon).

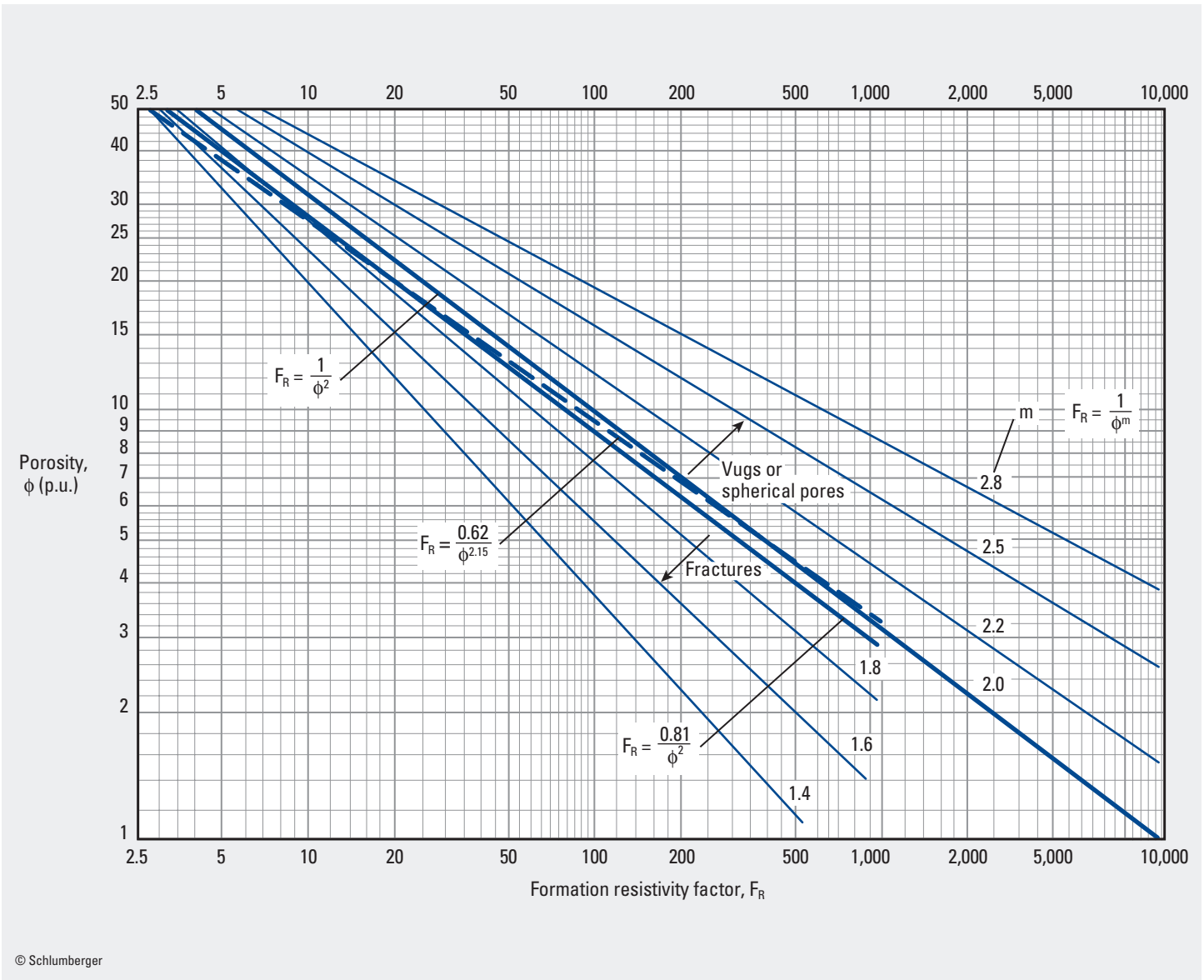
Find: Hydrocarbon density.

Answer: Porosity ratio = $15/25 = 0.6$. $\rho_h = 0.29 \text{ g/cm}^3$.

Porosity Versus Formation Resistivity Factor

Open Hole

SatOH-1
(former Por-1)



© Schlumberger

Purpose

This chart is used for a variety of conversions of the formation resistivity factor (F_R) to porosity.

Description

The most appropriate conversion is best determined by laboratory measurement or experience in the area. In the absence of this knowledge, recommended relationships are the following:

- Soft formations (Humble formula): $F_R = 0.62/\phi^{2.51}$ or $F_R = 0.81/\phi^2$
- Hard formations: $F_R = 1/\phi^m$ with the appropriate cementation factor (m).

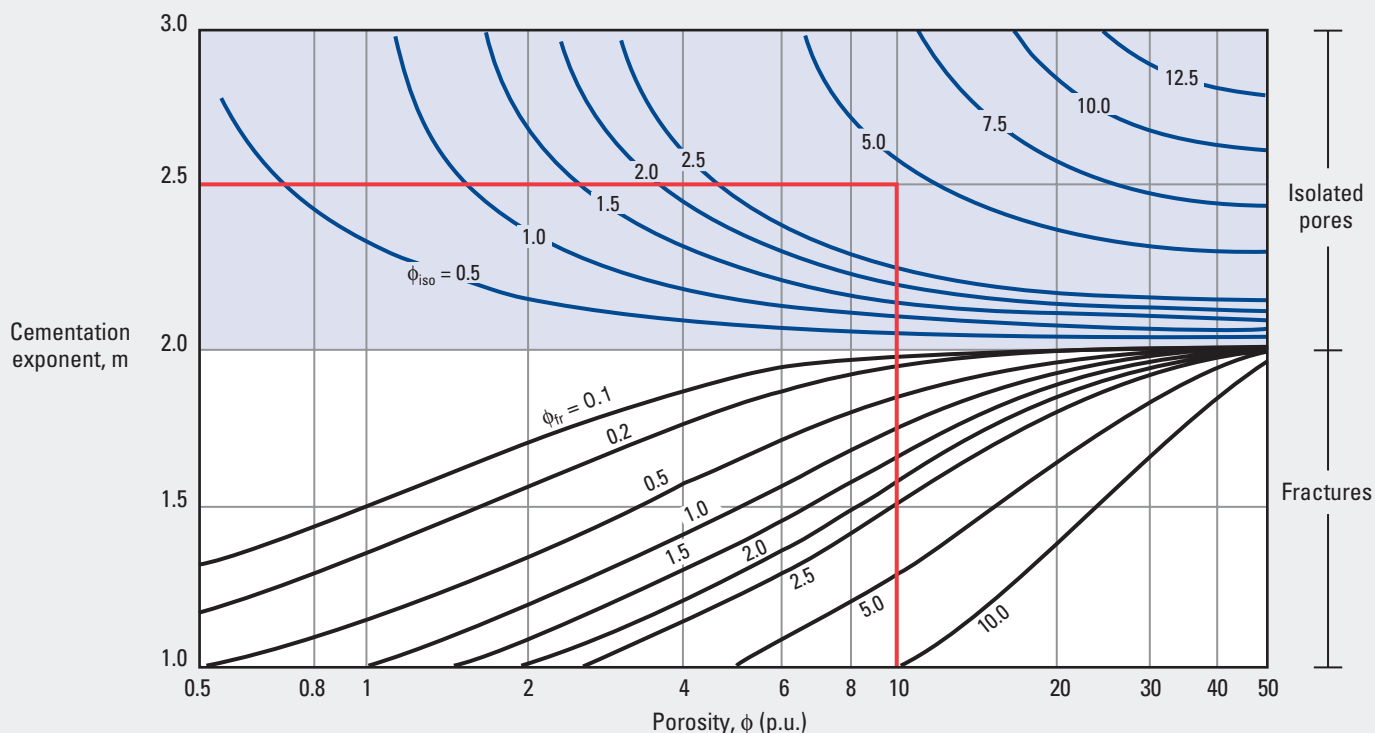
Example

Given:	Soft formation with $\phi = 25$ p.u.	Hard formation ($m = 2$) with $\phi = 8$ p.u.
Find:	F_R .	F_R .
Answer:	$F_R = 13$ (from chart). $F_R = 12.96$ (calculated).	$F_R = 160$ (from chart). $F_R = 156$ (calculated).

SatOH

Spherical and Fracture Porosity

Open Hole

SatOH-2
(former Por-1a)

© Schlumberger

Purpose

This chart is used to identify how much of the measured porosity is isolated (vugs or moldic) or fractured porosity.

Description

This chart is based on a simplified model that assumes no contribution to formation conductivity from vugs and moldic porosity and the cementation exponent (m) of fractures is 1.0.

When the pores of a porous formation have an aspect ratio close to 1 (vugs or moldic porosity), the value of m of the formation is usually greater than 2. Fractured formations typically have a cementation exponent less than 2.

Enter the chart with the porosity (ϕ) on the x-axis and m on the y-axis. The intersection point gives an estimate of either the amount of isolated porosity (ϕ_{iso}) or the amount of porosity resulting from fractures (ϕ_{fr}).

Example

Given: $\phi = 10$ p.u. and cementation exponent = 2.5.

Find: Intergranular (matrix) porosity.

Answer: Entering the chart with 10 p.u. and 2.5 gives an intersection point of $\phi_{iso} =$ approximately 4.5 p.u.
Intergranular porosity = $10 - 4.5 = 5.5$ p.u.

Saturation Determination

Open Hole

Purpose

This nomograph is used to solve the Archie water saturation equation:

$$S_w = \sqrt{\frac{R_o}{R_t}} = \sqrt{\frac{F_R R_w}{R_t}},$$

where

S_w = water saturation

R_o = resistivity of clean-water formation

R_t = true resistivity of the formation

F_R = formation resistivity factor

R_w = formation water resistivity.

It should be used in clean (nonshaly) formations only.

Description

If R_o is known, a straight line from the known R_o value through the measured R_t value indicates the value of S_w . If R_o is unknown, it may be determined by connecting R_w with F_R or porosity (ϕ).

Example

Given: $R_w = 0.05$ ohm-m at formation temperature, $\phi = 20$ p.u. ($F_R = 25$), and $R_t = 10$ ohm-m.

Find: Water saturation.

Answer: Enter the nomograph on the R_w scale at $R_w = 0.05$ ohm-m.

Draw a straight line from 0.05 through the porosity scale at 20 p.u. to intersect the R_o scale.

From the intersection point of $R_o = 1$, draw a straight line through $R_t = 10$ ohm-m to intersect the S_w scale.

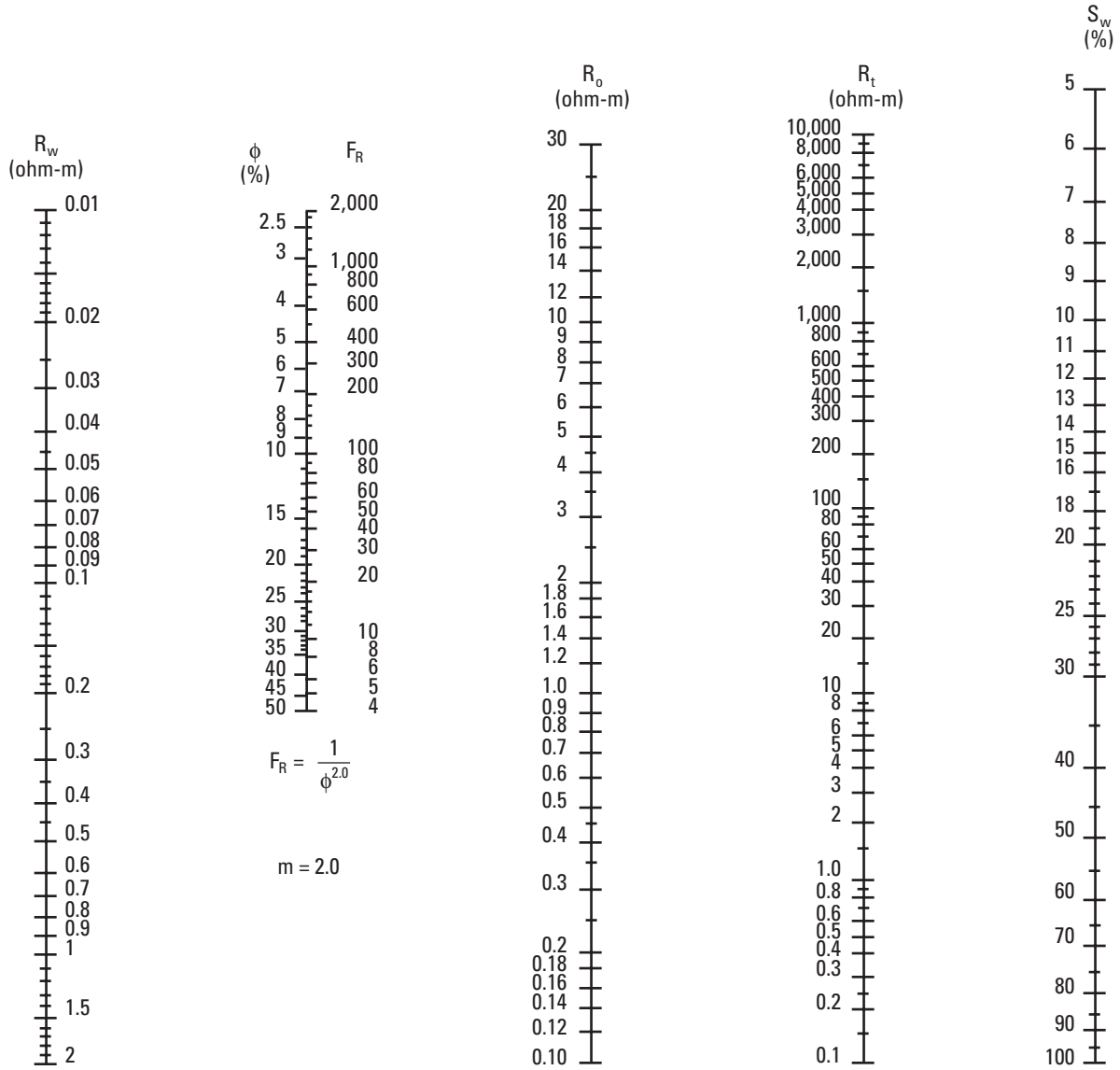
$S_w = 31.5\%$.

Saturation Determination

Open Hole

SatOH-3
(former Sw-1)

Clean Formations, $m = 2$



$$R_o = F_R R_w$$

$$S_w = \sqrt{\frac{R_o}{R_t}}$$

Saturation Determination

Open Hole

Purpose

This chart is used to determine water saturation (S_w) in shaly or clean formations when knowledge of the porosity is unavailable. It may also be used to verify the water saturation determination from another interpretation method. The large chart assumes that the mud filtrate saturation is

$$S_{XO} = \sqrt[5]{S_w}$$

The small chart provides an S_{XO} correction when S_{XO} is known. However, water activity correction is not provided for the SP portion of the chart (see Chart SP-2).

Description

Clean Sands

Enter the large chart with the ratio of the resistivity of the flushed zone to the true formation resistivity (R_{XO}/R_t) on the y-axis and the ratio of the resistivity of the mud filtrate to the resistivity of the formation water (R_{mf}/R_w) on the x-axis to find the water saturation at average residual oil saturation (S_{wa}). If R_{mf}/R_w is unknown, the chart may be entered with the spontaneous potential (SP) value and the formation temperature. If S_{XO} is known, move diagonally upward, parallel to the constant- S_{wa} curves, to the right edge of the chart. Then, move horizontally to the known S_{XO} (or residual oil saturation [ROS], S_{or}) value to obtain the corrected value of S_w .

Example

Given: $R_{XO} = 12$ ohm-m, $R_t = 2$ ohm-m, $R_{mf}/R_w = 20$, and $S_{or} = 20\%$.

Find: S_w (after correction for ROS).

Answer: Enter the large chart at $R_{XO}/R_t = 12/2 = 6$ on the y-axis and $R_{mf}/R_w = 20$ on the x-axis. From the point of intersection (labeled A), move diagonally to the right to intersect the chart edge and directly across to enter the small chart and intersect $S_{or} = 20\%$.

$S_w = 43\%$.

Description

Shaly Sands

Enter the chart with R_{XO}/R_t and the SP in the shaly sand (E_{PSP}). The point of intersection gives the S_{wa} value. Draw a line from the chart's origin (the small circle located at $R_{XO}/R_t = R_{mf}/R_w = 1$) through this point to intersect with the value of static spontaneous potential (E_{SSP}) to obtain a value of R_{XO}/R_t corrected for shaliness. This value of R_{XO}/R_t versus R_{mf}/R_w is plotted to find S_w if R_{mf}/R_w is unknown because the point defined by R_{XO}/R_t and E_{SSP} is a reasonable approximation of S_w . The small chart to the right can be used to further refine S_w if S_{or} is known.

Example

Given: $R_{XO}/R_t = 2.8$, $R_{mf}/R_w = 25$, $E_{PSP} = -75$ mV, $E_{SSP} = -120$ mV, and electrochemical SP coefficient (K_c) = 80 (formation temperature = 150°F).

Find: S_w and corrected value for $S_{or} = 10\%$.

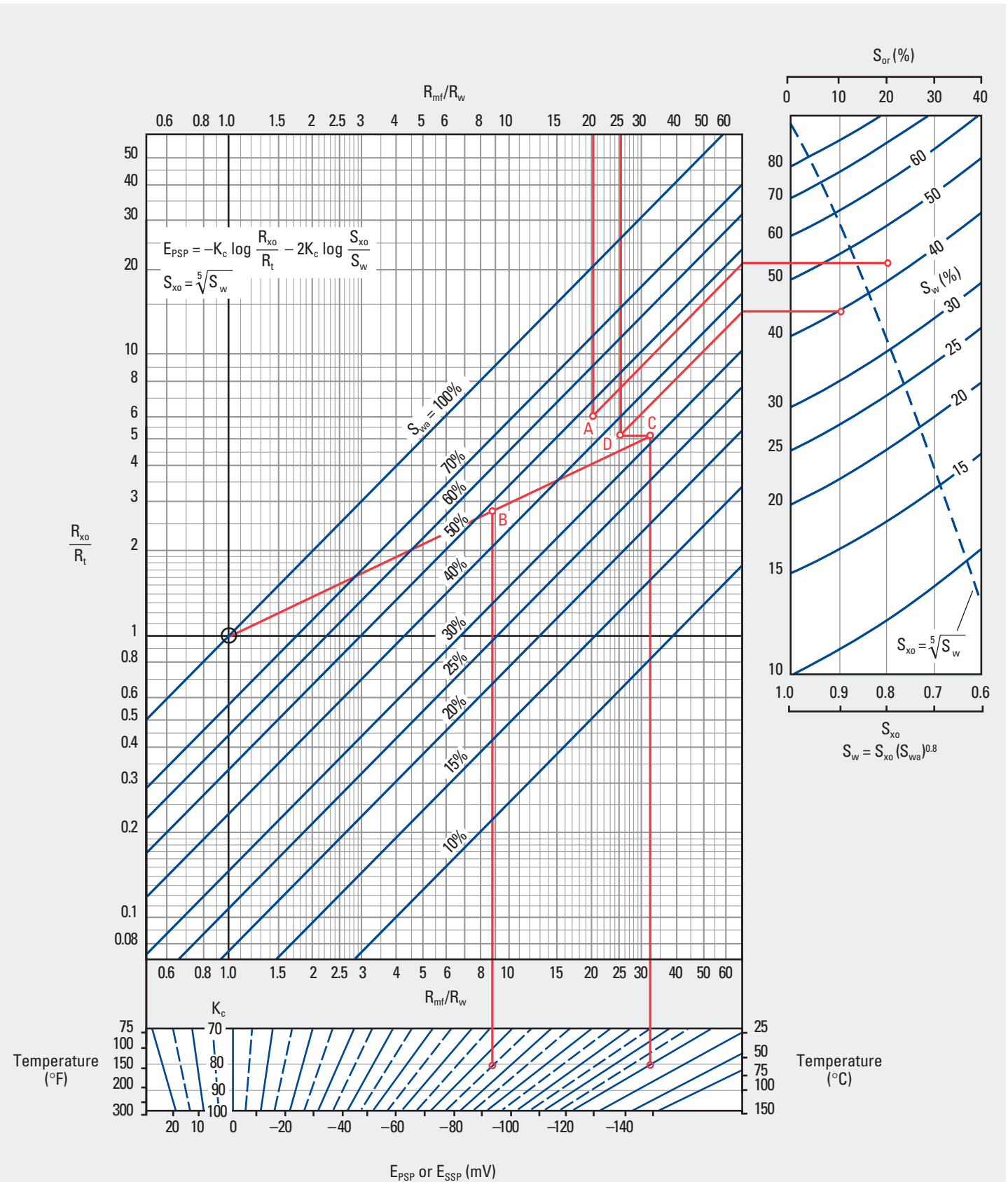
Answer: Enter the large chart at $R_{XO}/R_t = 2.8$ and the intersection of $E_{PSP} = -75$ mV at $K_c = 80$ from the chart below. A line from the origin through the intersection point (labeled B) intersects the -120 -mV value of E_{SSP} at Point C. Move horizontally to the left to intersect $R_{mf}/R_w = 25$ at Point D. Then move diagonally to the right to intersect the right y-axis of the chart. Move horizontally to the small chart to determine $S_{XO} = 0.9\%$, $S_w = 38\%$, and corrected $S_w = 40\%$.

For more information, see Reference 12.

Saturation Determination

Open Hole

SatOH-4
(former Sw-2)

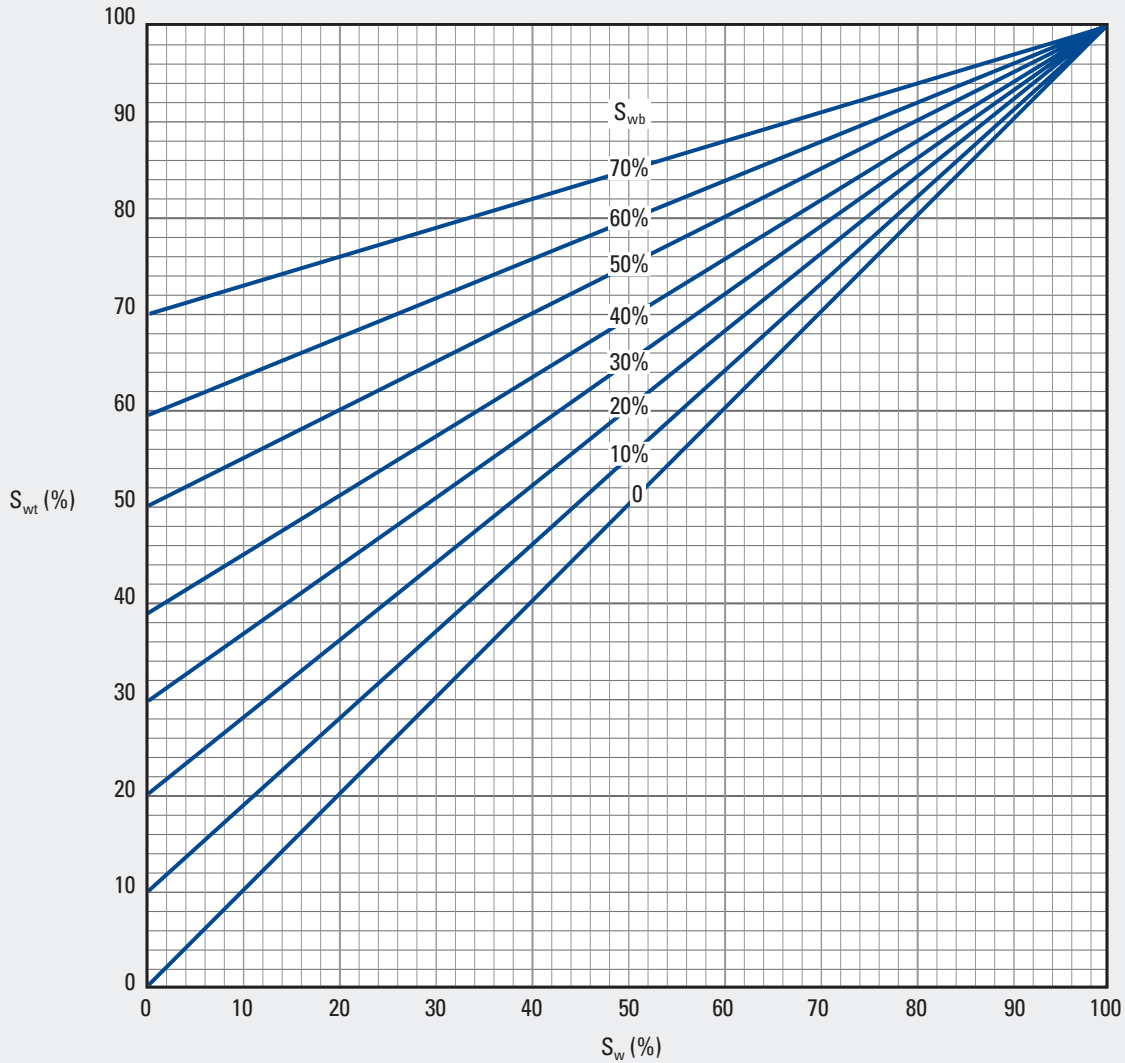


SatOH

Graphical Determination of S_w from S_{wt} and S_{wb}

Open Hole

SatOH-5
(former Sw-14)



© Schlumberger

Purpose

This chart is used to derive a value of water saturation (S_w) corrected for the bound-water volume in shale.

Description

This is a graphical determination of S_w from the total water saturation (S_{wt}) and the saturation of bound water (S_{wb}):

$$S_w = \frac{S_{wt} - S_{wb}}{1 - S_{wb}}$$

Enter the y-axis with S_{wt} and move horizontally to intersect the appropriate S_{wb} curve. Read the value of S_w on the x-axis.

Example

Given: $S_{wt} = 45\%$ and $S_{wb} = 10\%$.

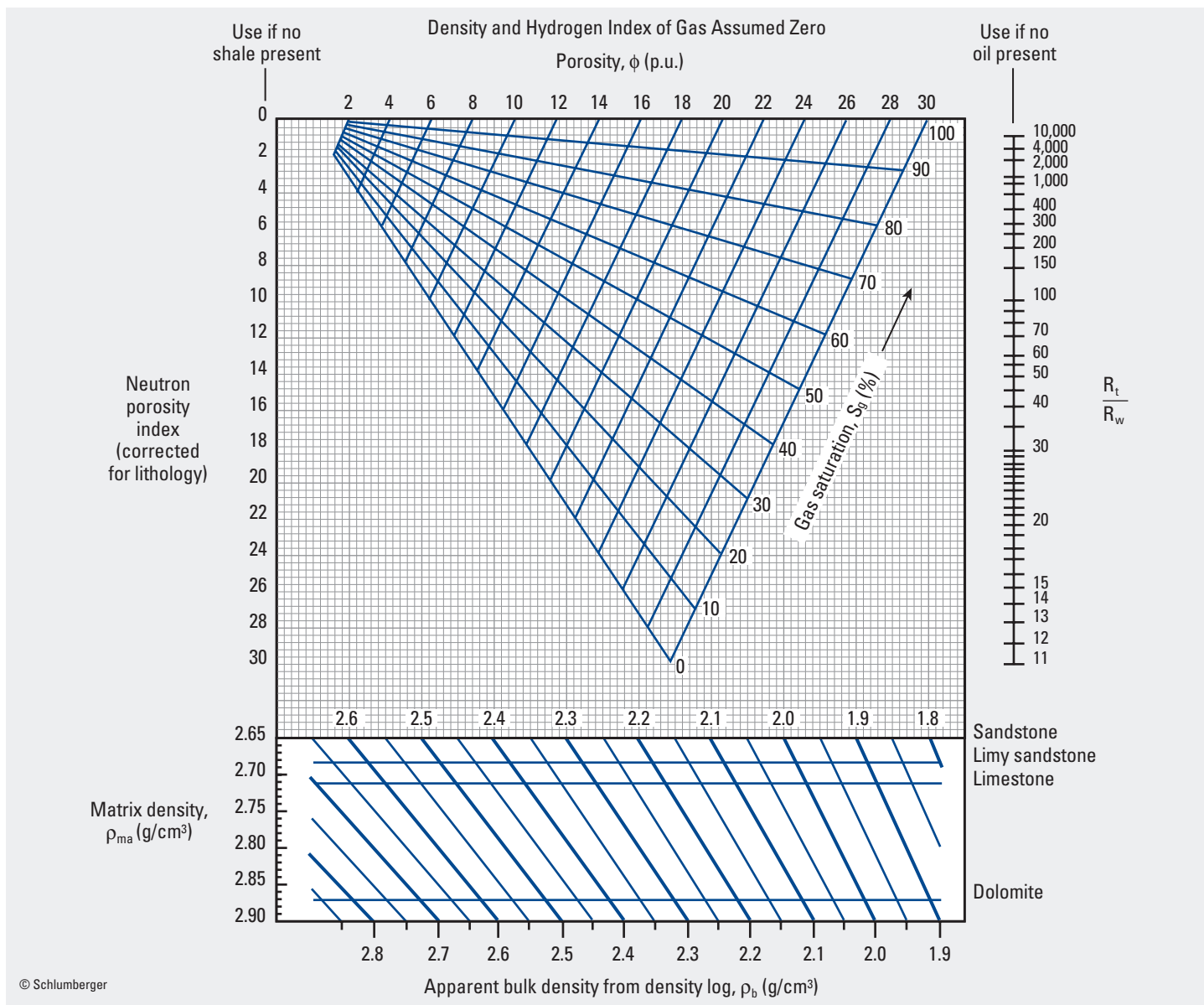
Find: S_w .

Answer: $S_w = 39.5\%$.

Porosity and Gas Saturation in Empty Hole

Open Hole

SatOH-6
(former Sw-11)



© Schlumberger

Purpose

This chart is used to determine porosity (ϕ) and gas saturation (S_g) from the combination of density and neutron or from density and resistivity measurements.

Description

Enter from the point of intersection of the matrix density (ρ_{ma}) and apparent bulk density (ρ_b). Move vertically upward to intersect either neutron porosity (ϕ_N , corrected for lithology) or the ratio of true resistivity to connate water resistivity (R_t/R_w). This point defines the actual porosity and S_g on the curves.

Oil saturation (S_o) can also be determined if all three measurements (density, neutron, and resistivity) are available. Find the values of ϕ and S_g as before, and then find the intersection of R_t/R_w with ϕ to read the value of the total hydrocarbon saturation (S_h) on the saturation scale for use in the following equations:

$$S_o = S_h - S_g$$

$$S_w = 100 - S_h$$

Example

Given: Limy sandstone ($\rho_{ma} = 2.68 \text{ g/cm}^3$), $\rho_b = 2.44 \text{ g/cm}^3$, $\phi_N = 9 \text{ p.u.}$, $R_t = 74 \text{ ohm-m}$, and $R_w = 0.1 \text{ ohm-m}$.

Find: ϕ , S_g , S_h , S_o , and S_w .

Answer: First, find $R_t/R_w = 74/0.1 = 740$.

$\phi = 12 \text{ p.u.}$ and $S_g = 25\%$.

$S_h = 70\%$ (total hydrocarbon saturation).

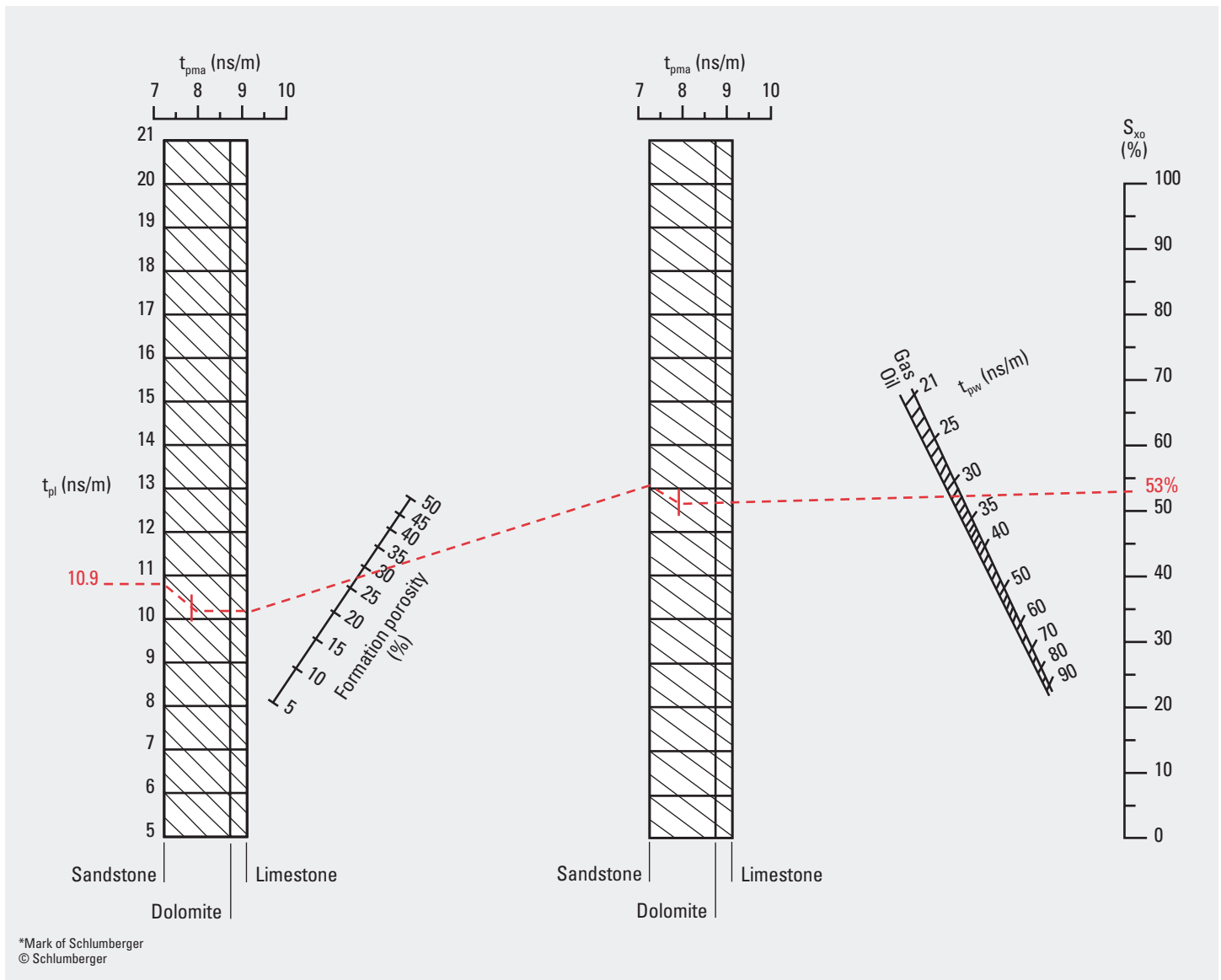
$S_o = 70 - 25 = 45\%$.

$S_w = 100 - 70 = 30\%$.

EPT* Propagation Time

Open Hole

SatOH-7
(former Sxo-1)



Purpose

This nomograph is used to define flushed zone saturation (S_{xo}) in the rock immediately adjacent to the borehole by using the EPT Electromagnetic Propagation Tool time measurement (t_{pi}).

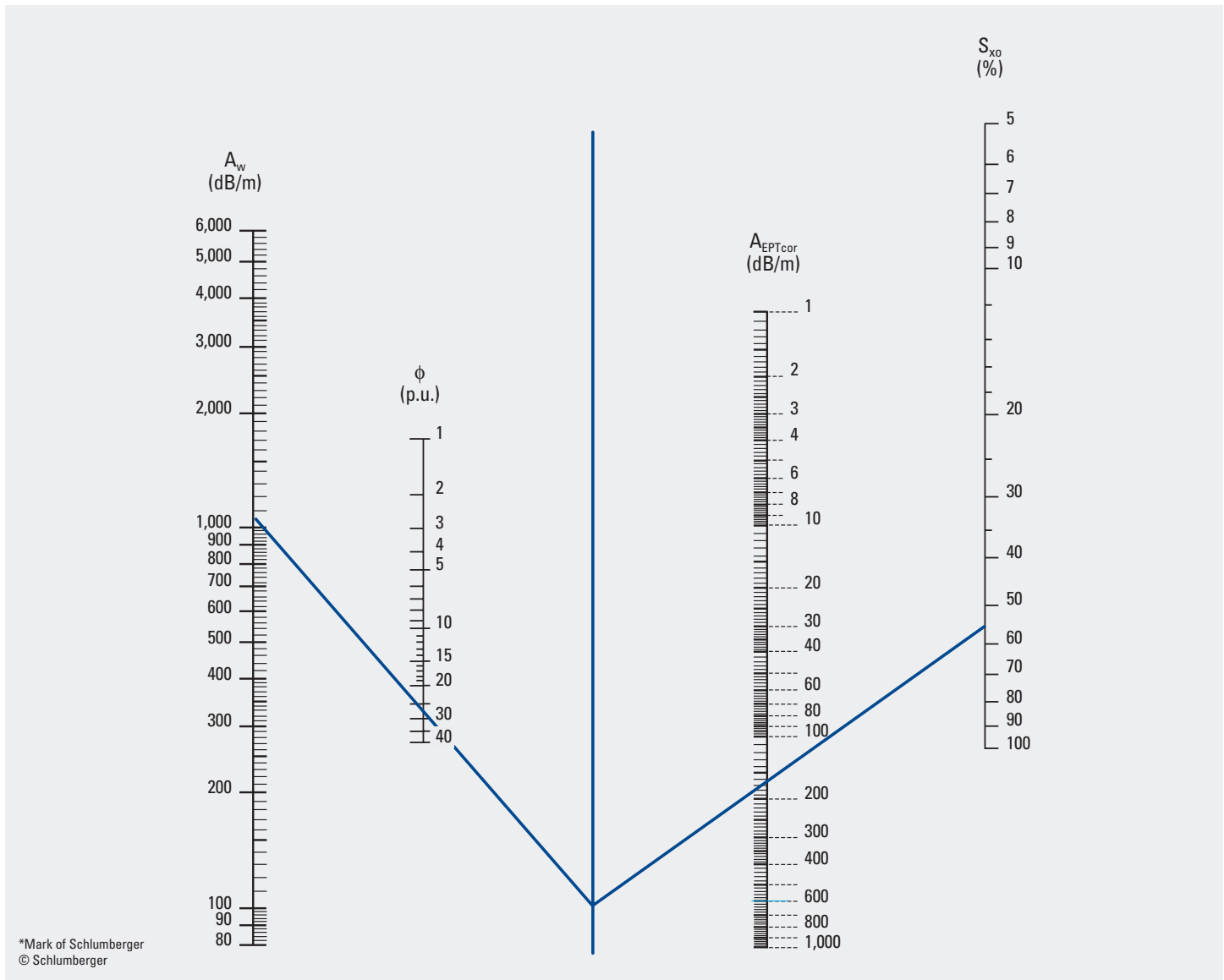
Description

Use of this chart requires knowledge of the reservoir lithology or matrix propagation time (t_{pma}), saturating water propagation time (t_{pw}), porosity (ϕ), and expected hydrocarbon type. Enter the far-left scale with t_{pi} and move parallel to the diagonal lines to intersect the appropriate t_{pma} value. From this point move horizontally to the right

edge of the scale grid. From this point, extend a straight line through the porosity scale to the center scale grid; again, move parallel to the diagonal lines to the appropriate t_{pma} value and then horizontally to the right edge of the grid scale. From this point, extend a straight line through the intersection of t_{pw} and the hydrocarbon type point to intersect the S_{xo} scale. For more information, see Reference 25.

EPT* Attenuation

Open Hole

SatOH-8
(former Sxo-2)**Purpose**

This nomograph is used to determine the flushed zone saturation (S_{xo}) in the rock immediately adjacent to the borehole by using the EPT Electromagnetic Propagation Tool attenuation measurement. It requires knowledge of the saturating fluid (usually mud filtrate) attenuation (A_w), porosity (ϕ), and the EPT EATT attenuation (A_{EPTcor}) corrected for spreading loss.

Description

The value of A_w must first be determined. Chart Gen-16 is used to estimate A_w by using the equivalent water salinity and formation temperature. EPT-D spreading loss is determined from the inset on Chart Gen-16 based on the uncorrected EPT propagation time (t_{pl}) measurement. The spreading loss correction algebraically added to the EPT-D EATT attenuation measurement gives the corrected EPT attenuation (A_{EPTcor}). These values are used with porosity on the nomograph to determine S_{xo} .

Example

Given: EATT = 250 dB/m, t_{pl} = 10.9 ns/m, ϕ = 28 p.u., water salinity = 20,000 ppm, and bottomhole temperature = 150°F.

Find: Spreading loss (from Chart Gen-16 inset) and S_{xo} .

Answer: The spreading loss determined from the inset on Chart Gen-16 is -82 dB/m.

$$A_{EPTcor} = 250 - 82 = 168 \text{ dB/m.}$$

$$A_w \text{ (from Chart Gen-16)} = 1,100 \text{ dB/m.}$$

Enter the far-left scale at $A_w = 1,100$ dB/m and draw a straight line through $\phi = 28$ p.u. on the next scale to intersect the median line. From this intersection point, draw a straight line through $A_{EPTcor} = 168$ dB/m on the next scale to intersect the S_{xo} value on the far-right scale. $S_{xo} = 56$ p.u.

Capture Cross Section Tool

Cased Hole

Purpose

This chart is used to determine water saturation (S_w) from capture cross section, or sigma (Σ), measurements from the TDT* Thermal Decay Time pulsed neutron log.

Description

This chart uses sigma water (Σ_w), matrix capture cross section (Σ_{ma}), and porosity (ϕ) to determine water saturation in clean formations. The chart may be used in shaly formations if sigma shale (Σ_{sh}), the volume fraction of shale in the formation (V_{sh}), and the porosity corrected for shale are known.

Thermal decay time (t and t_{sh} in shale) is also shown on some of the chart scales because it is related to Σ .

Procedure

Clean Formation

The S_w determination for a clean formation requires values known for Σ_{ma} (based on lithology), ϕ , Σ_w from the NaCl salinity (see Chart Gen-12 or Gen-13), and sigma hydrocarbon (Σ_h) (see Chart Gen-14). Enter the value of Σ_{ma} on Scale B and draw a line to Pivot Point B. Enter Σ_{log} on Scale B and draw Line b through the intersection of Line a and the value of ϕ to intersect the sigma of the formation fluid (Σ_f) on Scale C. Draw Line 5 from Σ_f through the intersection of Σ_h and Σ_w to determine the value of S_w on Scale D.

Example: Clean Formation

Given: $\Sigma_{log} = 20$ c.u., $\Sigma_{ma} = 8$ c.u. (sandstone) from TDT tool, $\Sigma_h = 18$ c.u., $\Sigma_w = 80$ c.u. (150,000 ppm or mg/kg), and $\phi = 30$ p.u.

Find: S_w .

Answer: Following the procedure for a clean formation, $S_w = 43\%$.

Procedure

Shaly Formation

The S_w determination in a shaly formation requires additional information: sigma shale (Σ_{sh}) read from the TDT log in adjacent shale, V_{sh} from porosity-log crossplot or gamma ray, shale porosity (ϕ_{sh}) read from a porosity log in adjacent shale, and the porosity corrected for shaliness (ϕ_{shcor}) with the relation for neutron and density logs in liquid-filled formations of $\phi_{shcor} = \phi_{log} - V_{sh}\phi_{sh}$.

Enter the value of Σ_{ma} on Scale B and draw Line 1 to intersect with Pivot Point A. From the value of Σ_{sh} on Scale A, draw Line 2 through the intersection of Line 1 and V_{sh} to determine the shale-corrected Σ_{cor} on Scale B. Draw Line 3 from Σ_{cor} to the value of Σ_{ma} on the scale to the left of Scale C. Enter Σ_{log} on Scale B and draw Line 4 through the intersection of Line 3 and the value of ϕ to determine Σ_f on Scale C. From Σ_f on Scale C, draw Line 5 through the intersection of Σ_h and Σ_w to determine S_w on Scale D.

Example

Given: $\Sigma_{log} = 25$ c.u.
 $\Sigma_{ma} = 8$ c.u.
 $\Sigma_h = 18$ c.u.
 $\Sigma_w = 80$ c.u.
 $\Sigma_{sh} = 45$ c.u.
 $\phi_{log} = 33$ p.u.
 $\phi_{sh} = 45$ p.u.
 $V_{sh} = 0.2$.

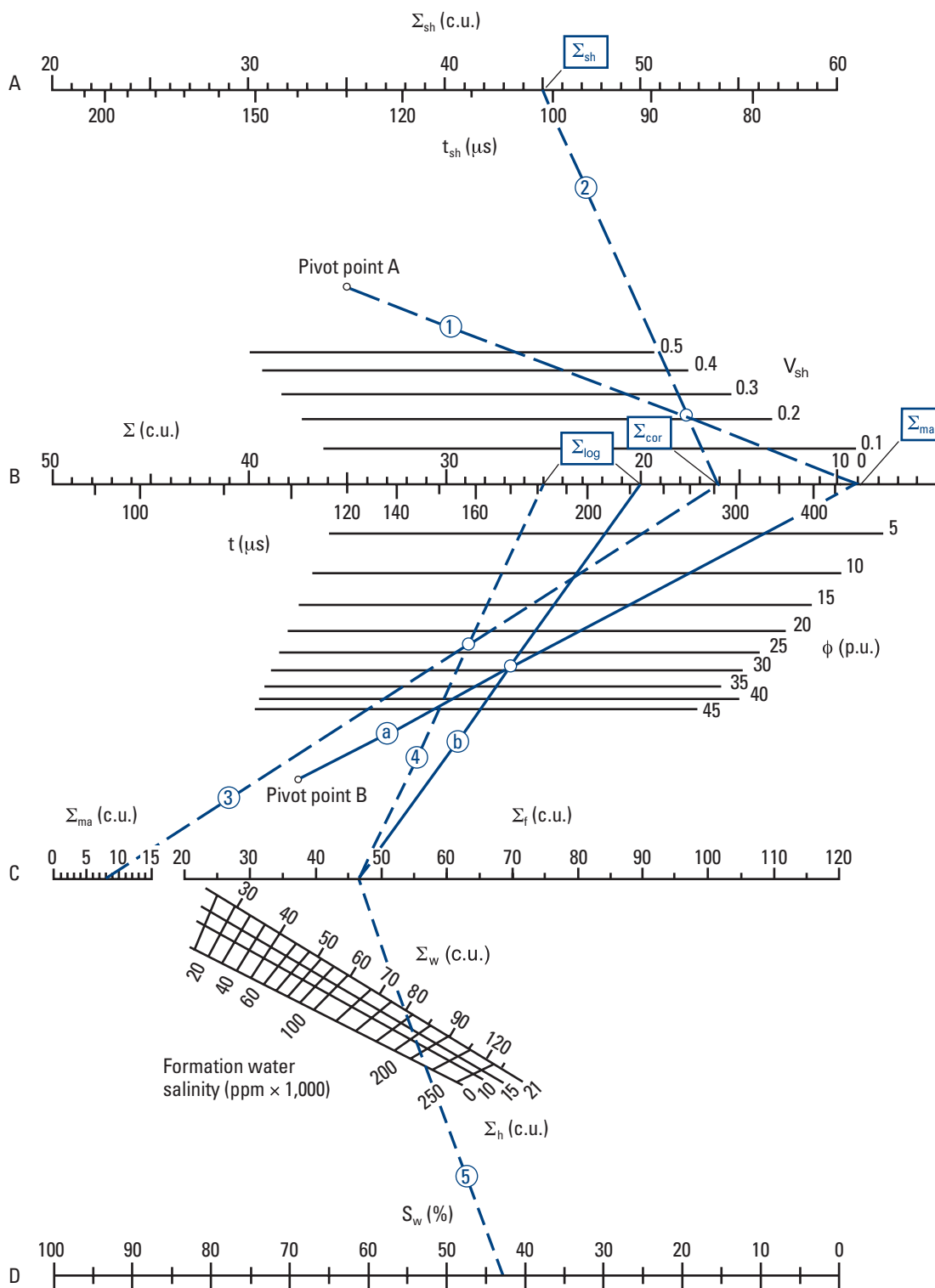
Find: ϕ_{shcor} and S_w .

Answer: First find the porosity corrected for shaliness, $\phi_{shcor} = 33$ p.u. $- (0.2 \times 45$ p.u.) $= 24$ p.u. This value is used for the ϕ point between Scales B and C.
 $S_w = 43\%$.

Capture Cross Section Tool

Cased Hole

SatCH-1
(former Sw-12)



$$S_w = \frac{(\Sigma_{log} - \Sigma_{ma}) - \phi(\Sigma_h - \Sigma_{ma}) - V_{sh}(\Sigma_{sh} - \Sigma_{ma})}{\phi(\Sigma_w - \Sigma_h)}$$

Capture Cross Section Tool

Cased Hole

Purpose

This chart is used to graphically interpret the TDT* Thermal Decay Time log. In one technique, applicable in shaly as well as clean sands, the apparent water capture cross section (Σ_{wa}) is plotted versus bound-water saturation (S_{wb}) on a specially constructed grid to determine the total water saturation (S_{wt}).

Description

To construct the grid, refer to the example chart on this page. Three fluid points must be located: free-water point (Σ_{wf}), hydrocarbon point (Σ_h), and a bound-water point (Σ_{wb}). The free- (or connate formation) water point is located on the left y-axis and can be obtained from measurement of a formation water sample, from Charts Gen-12 and Gen-13 if the water salinity is known, or from the TDT log in a clean water-bearing sand by using the following equation:

$$\Sigma_{wa} = \frac{\Sigma_{log} - \Sigma_{ma}}{\phi} + \Sigma_{ma} \quad (1)$$

The hydrocarbon point is also located on the left y-axis of the grid. It can be determined from Chart Gen-14 based on the known or expected hydrocarbon type.

The bound-water point (S_{wb}) can be obtained from the TDT log in shale intervals also by using the Σ_{wa} equation. It is located on the right y-axis of the grid.

The distance between the free-water and hydrocarbon points is linearly divided into lines of constant water saturation drawn parallel to a straight line connecting the free-water and bound-water points. The $S_{wt} = 0\%$ line originates from the hydrocarbon point, and the $S_{wt} = 100\%$ line originates from the free-water point.

The value of Σ_{wa} from the equation is plotted versus S_{wb} to give S_{wt} . The value of S_{wb} can be estimated from the gamma ray or other bound-water saturation estimator.

Once S_{wt} and S_{wb} are known, the water saturation of the reservoir rock exclusive of shale can be determined using

$$S_w = \frac{S_{wt} - S_{wb}}{1 - S_{wb}} \quad (2)$$

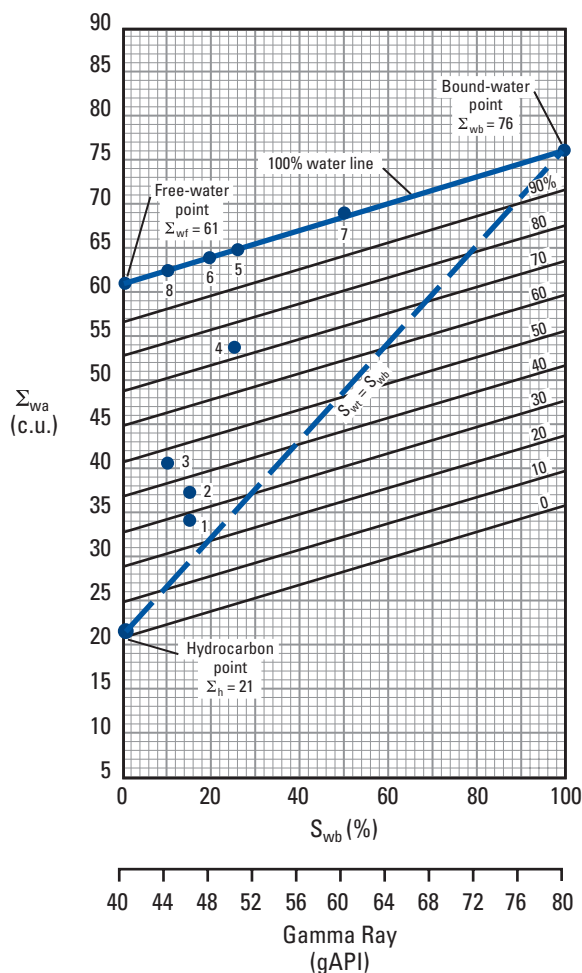
Example

Given: $\Sigma_{wf} = 61$ c.u. and $\Sigma_h = 21$ c.u. (medium-gravity oil with modest GOR from Chart Gen-14), and $\Sigma_{wb} = 76$ c.u. (from TDT log in a shale interval and the preceding Eq. 1).

Find: S_{wt} and S_w for Point 4.

Answer: $\Sigma_{wa} = 54$ c.u. (from Eq. 1) and $S_{wb} = 25\%$ (from gamma ray).

$S_{wt} = 72\%$ and $S_w = 63\%$ (from the preceding S_w equation).



*Mark of Schlumberger
© Schlumberger

The grid can also be used to graphically determine water saturation (S_w) in clean formations by crossplotting Σ_{log} on the y-axis and porosity (ϕ) on the x-axis. The values of Σ_{ma} and S_w need not be known but must be constant over the interval studied. There must be some points from 100% water zones and a good variation in porosity. These water points define the $S_w = 100\%$ line; when extrapolated, this line intersects the zero-porosity axis at Σ_{ma} . The $S_w = 0\%$ line is drawn from Σ_{ma} at $\phi = 0$ p.u. to $\Sigma = \Sigma_h$ at $\phi = 100$ p.u. (or $\Sigma = \frac{1}{2}(\Sigma_{ma} + \Sigma_h)$ at $\phi = 50$ p.u.). The vertical distance from $S_w = 0\%$ to $S_w = 100\%$ is divided linearly to define lines of constant water saturation. The water saturation of any plotted point can thereby be determined.

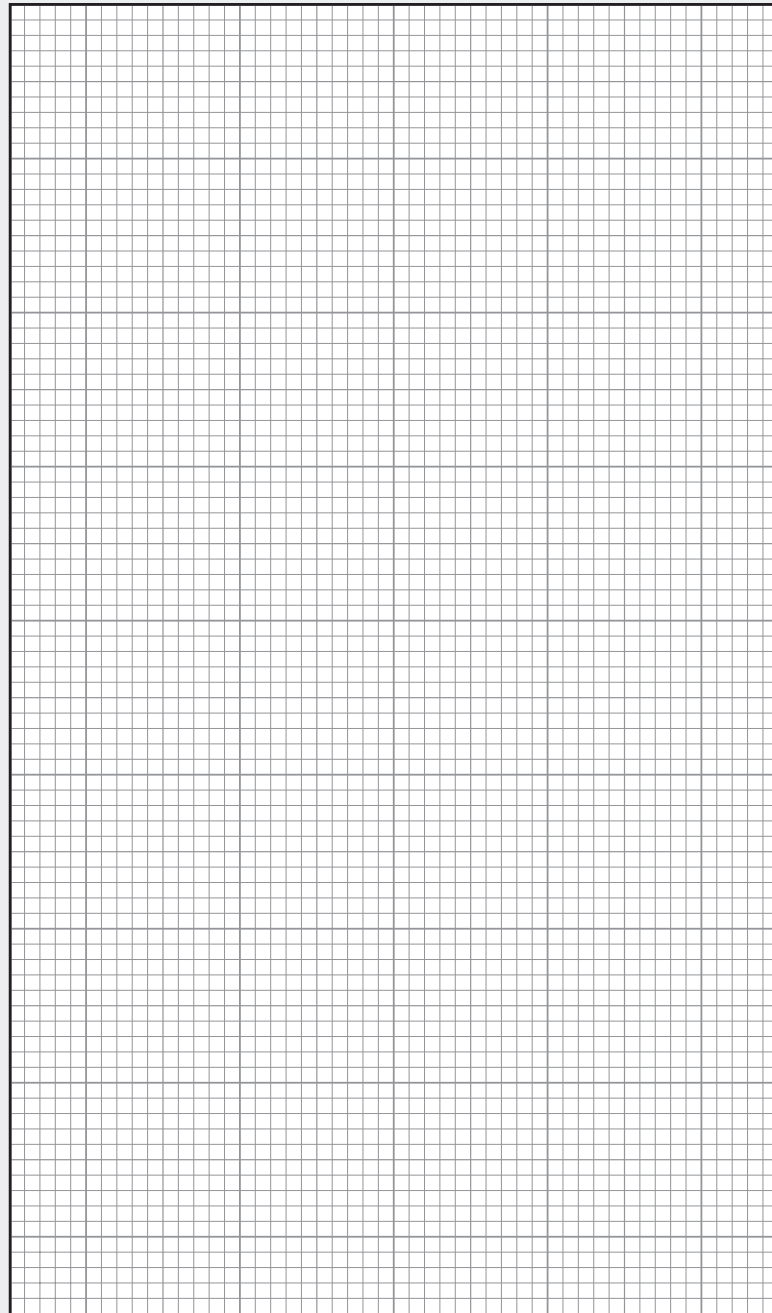
continued on next page

Capture Cross Section Tool

Cased Hole

SatCH-2
(former Sw-17)

Σ_{log}
or
 Σ_{wa}



ϕ or S_{wb}



RSTPro* Reservoir Saturation Tool—1.6875 in. and 2.5 in.

Carbon/Oxygen Ratio—Open Hole

Purpose

Charts SatCH-3 through SatCH-8 are presented for illustrative purposes only. They are used to ensure that the measured near- and far-detector carbon/oxygen (C/O) ratio data are consistent with the interpretation model. These example charts are drawn for specific cased and open holes and tool sizes to provide trapezoids for the determination of oil saturation (S_o) and oil holdup (y_o).

Description

Known formation and borehole data define the expected C/O ratio values, which are determined in water saturation and borehole holdup values ranging from 0 to 1. All log data for formations with porosity (ϕ) greater than 10 p.u. should be within the trapezoidal area bounded by the limits of the S_o and y_o values. If data plot consistently outside the trapezoid, the interpretation model may require revision.

The rectangle within each chart is constructed from four distinct points determined by the intersection of the near- and far-detector C/O ratios:

WW = water/water point

WO = water/oil point

OW = oil/water point

OO = oil/oil point.

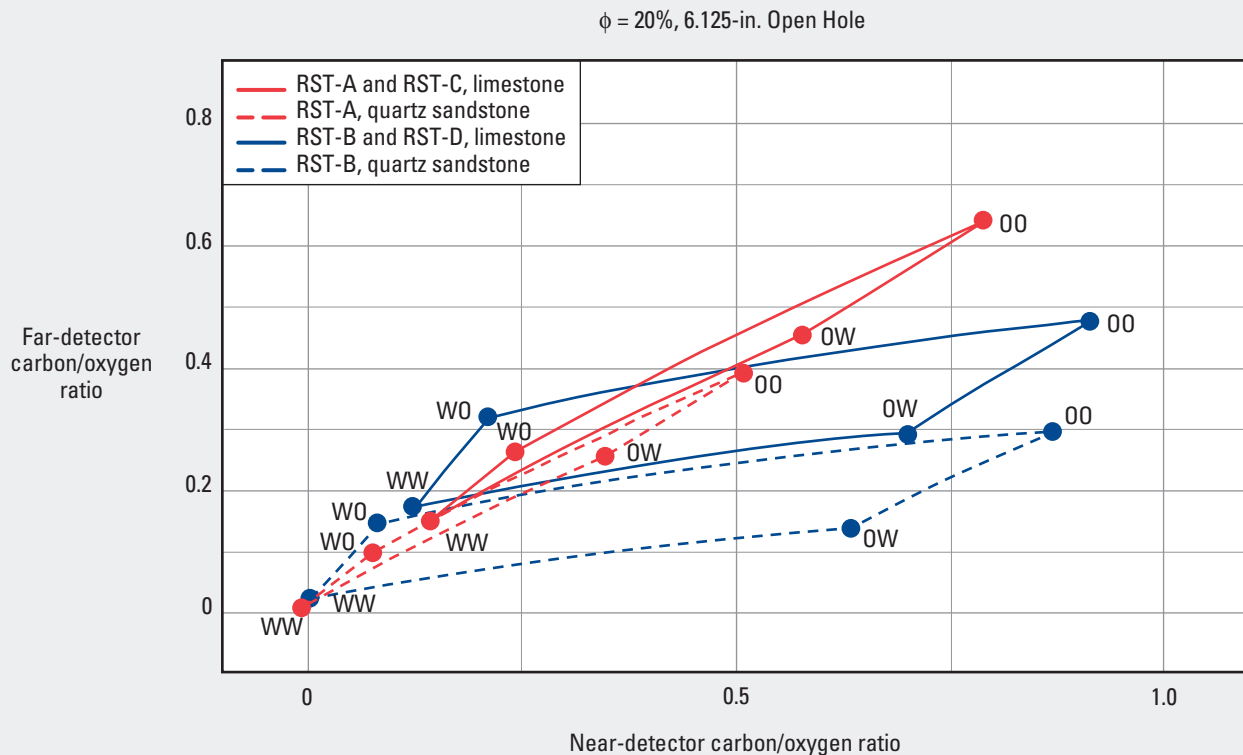
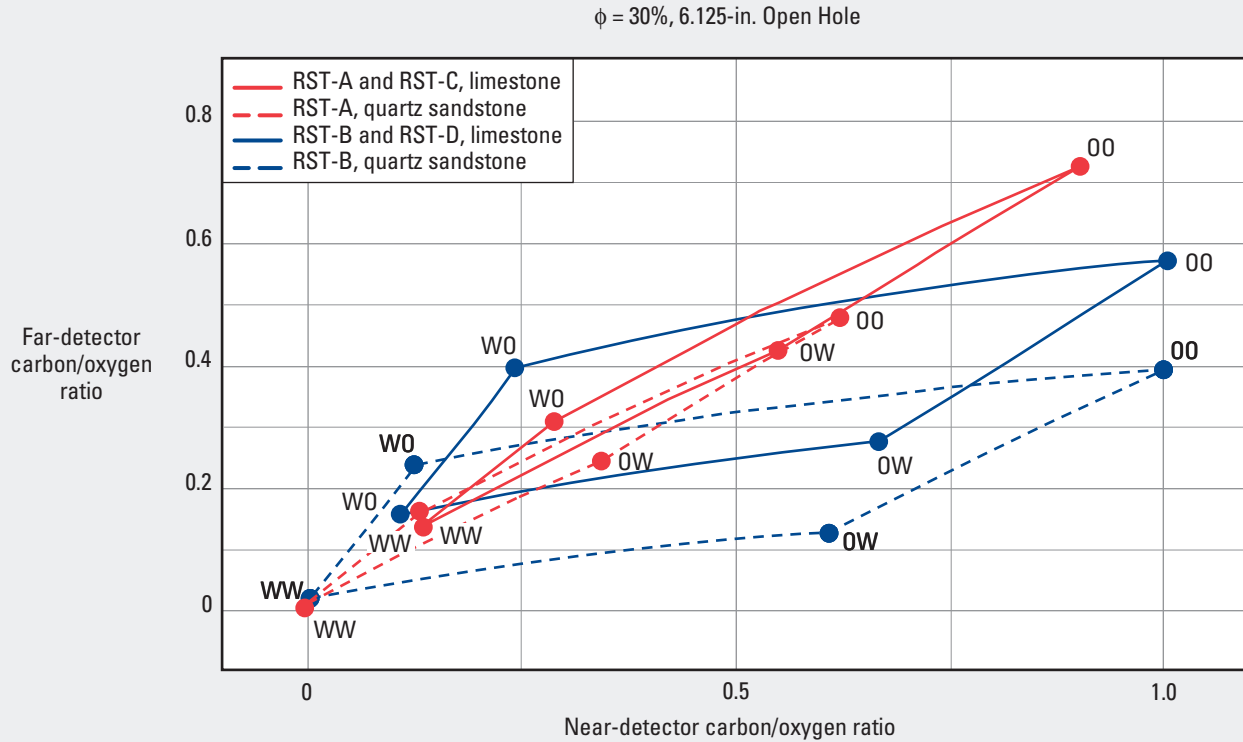
The oil used for both the formation and borehole is #2 diesel fuel with a carbon density value (CDV) of 0.7313-g carbon per cm^3 fuel.

RSTPro Reservoir Saturation Tool processing then determines the water saturation (S_w) of the formation.

RSTPro* Reservoir Saturation Tool—1.6875 in. and 2.5 in. in 6.125-in. Borehole,
 #2 Diesel CDV = 0.7313-g Carbon per cm³

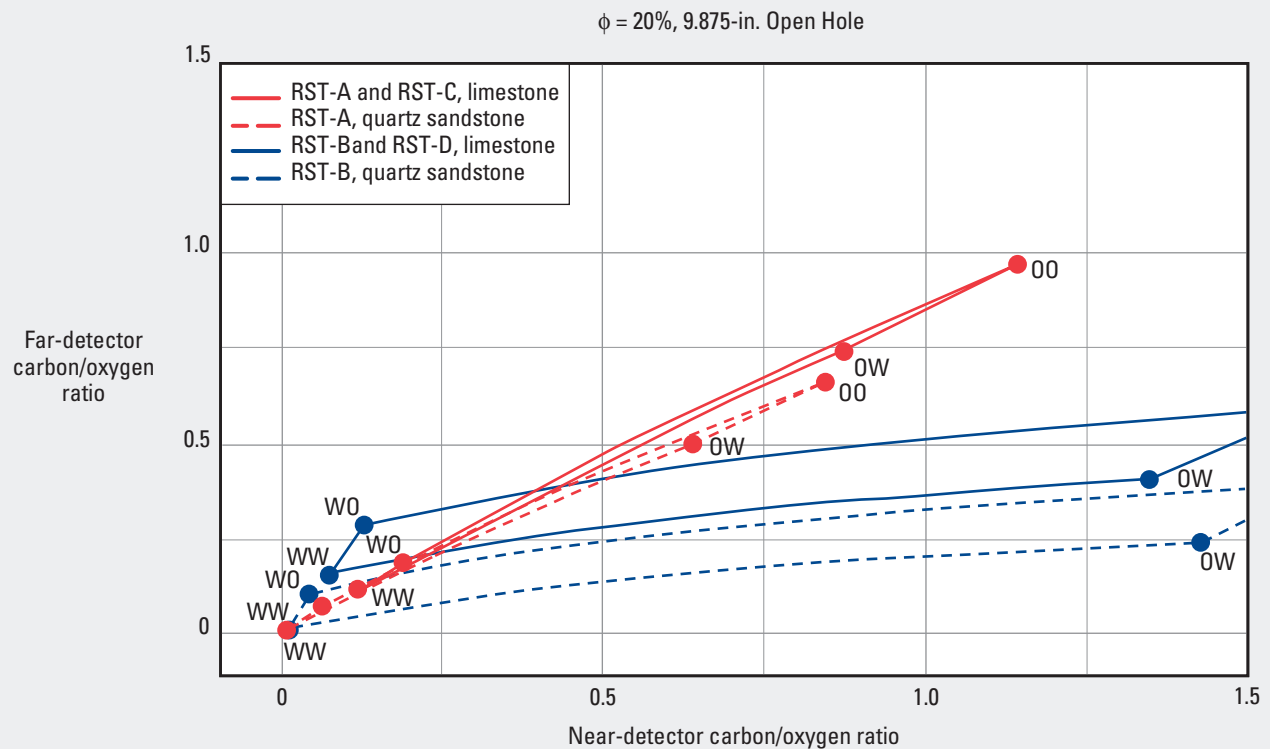
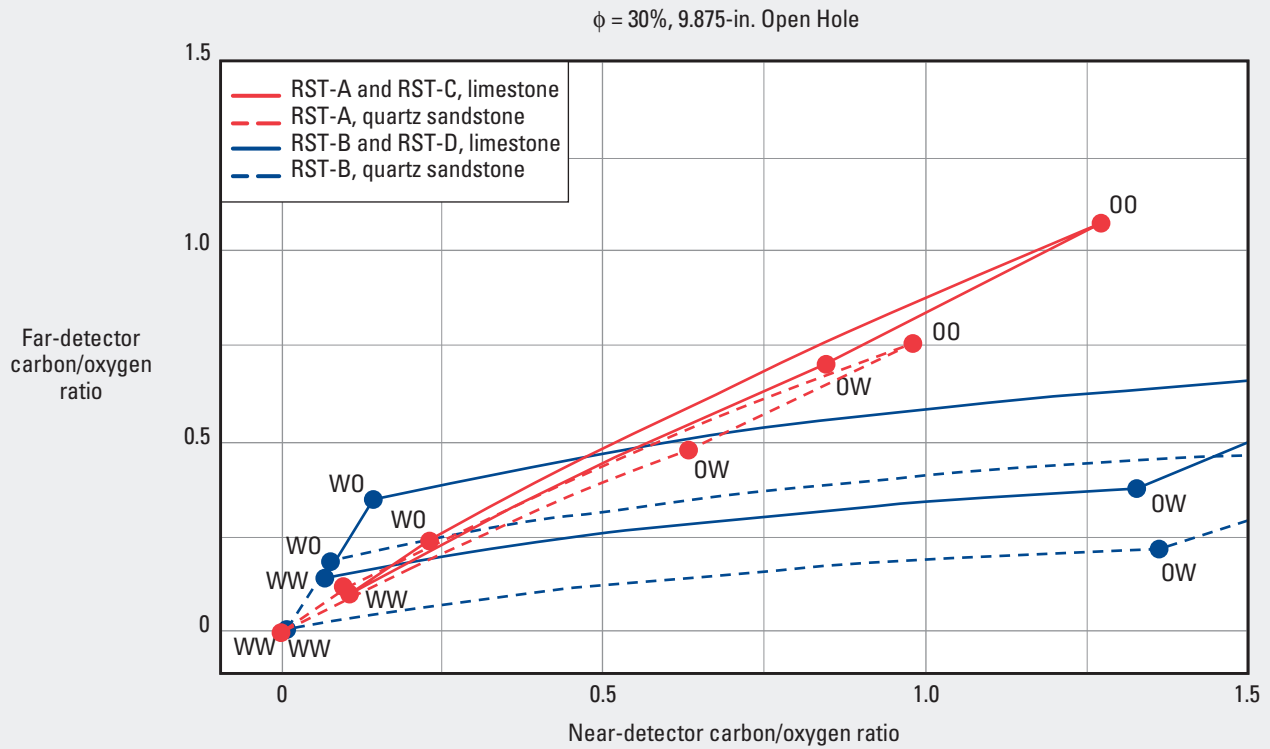
SatCH-3
 (former RST-3)

Carbon/Oxygen Ratio—Open Hole



RSTPro* Reservoir Saturation Tool—1.6875 in. and 2.5 in. in 9.875-in. Borehole,
 #2 Diesel CDV = 0.7313-g Carbon per cm³
 Carbon/Oxygen Ratio—Open Hole

SatCH-4

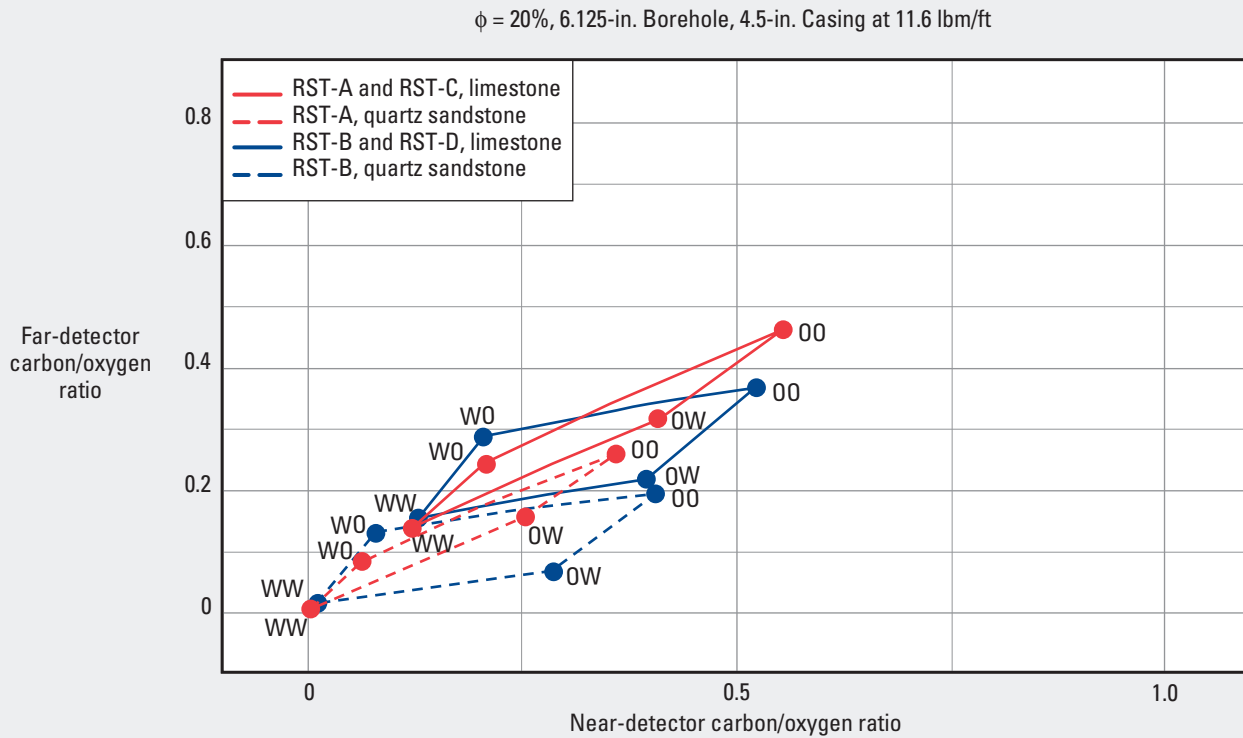
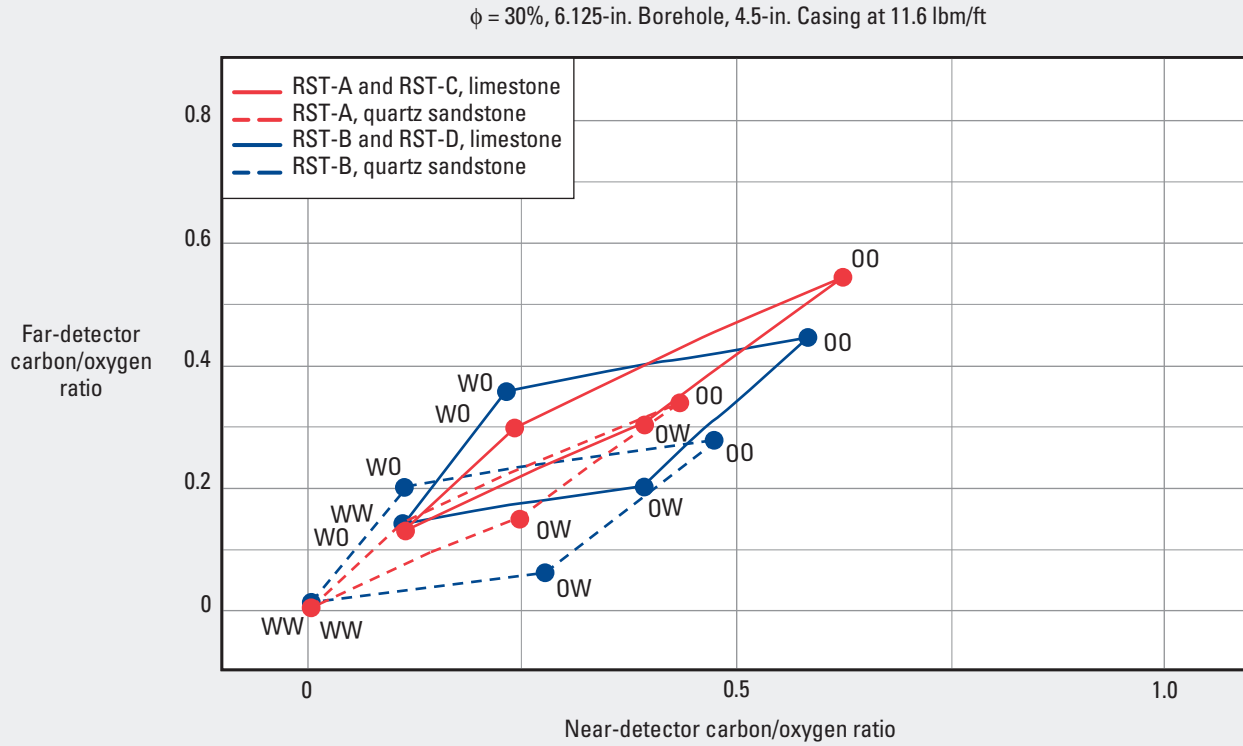


*Mark of Schlumberger
 © Schlumberger

RSTPro* Reservoir Saturation Tool—1.6875 in. and 2.5 in. in 6.125-in. Borehole with 4.5-in. Casing at 11.6 lbf/ft, #2 Diesel CDV = 0.7313-g Carbon per cm³

SatCH-5
(former RST-5)

Carbon/Oxygen Ratio—Cased Hole



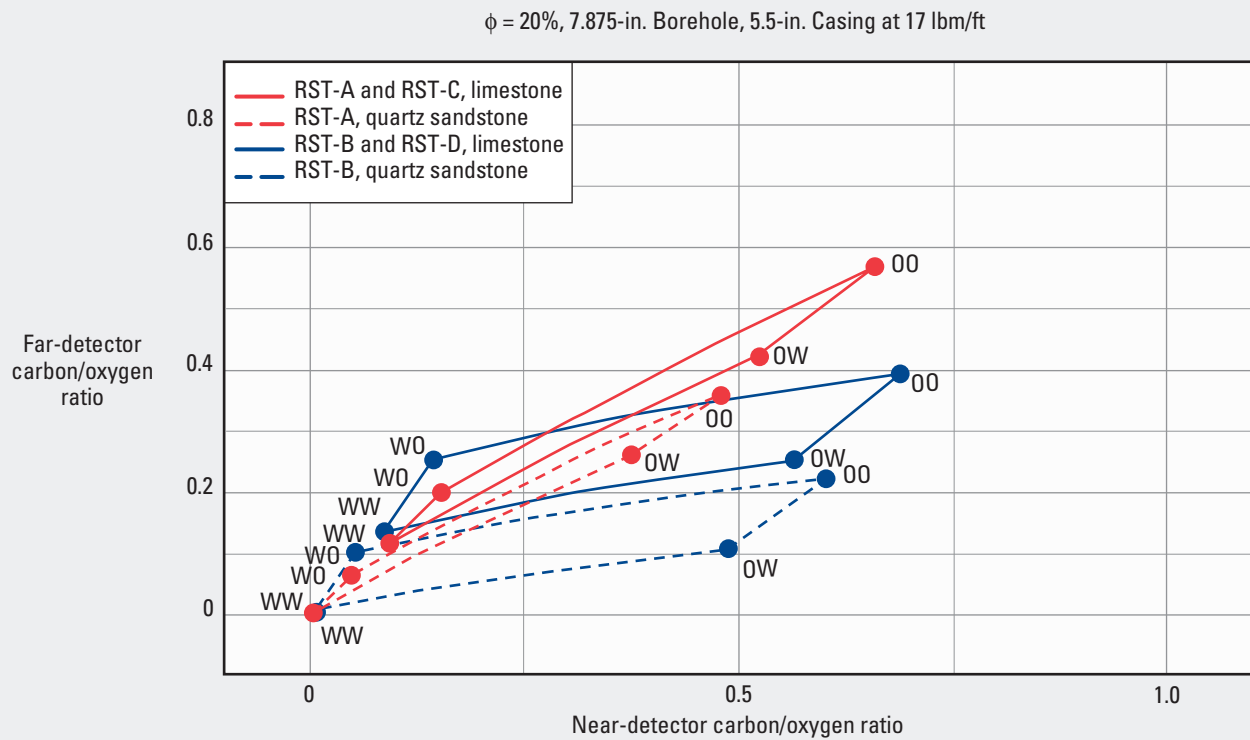
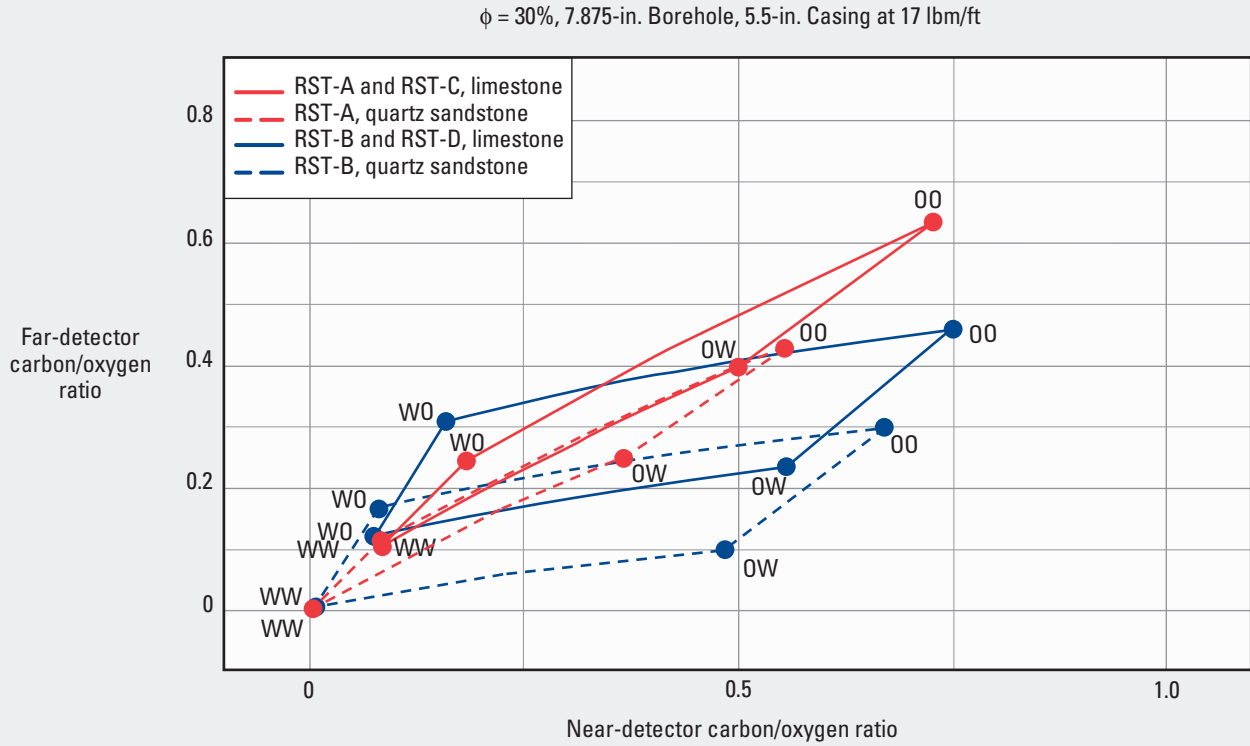
SatCH

*Mark of Schlumberger
© Schlumberger

RSTPro* Reservoir Saturation Tool—1.6875 in. and 2.5 in. in 7.875-in. Borehole with 5.5-in. Casing at 17 lbm/ft, #2 Diesel CDV = 0.7313-g Carbon per cm³

SatCH-6

Carbon/Oxygen Ratio—Cased Hole

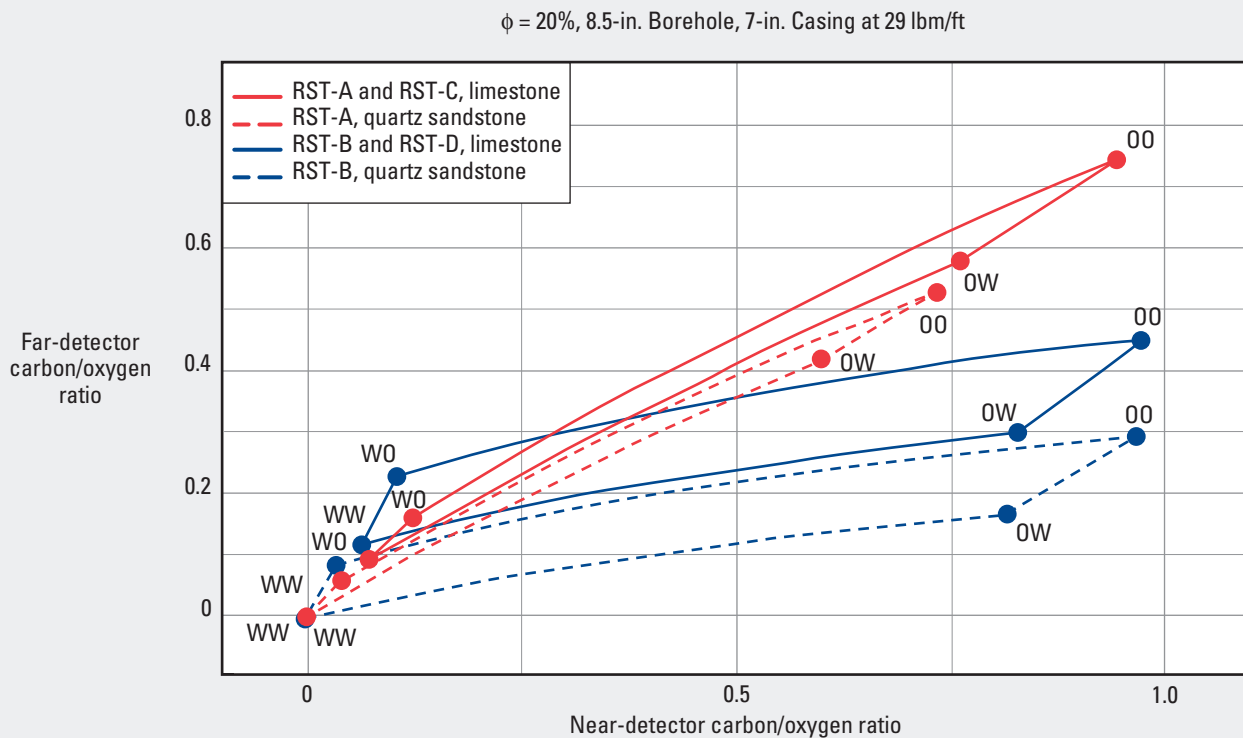
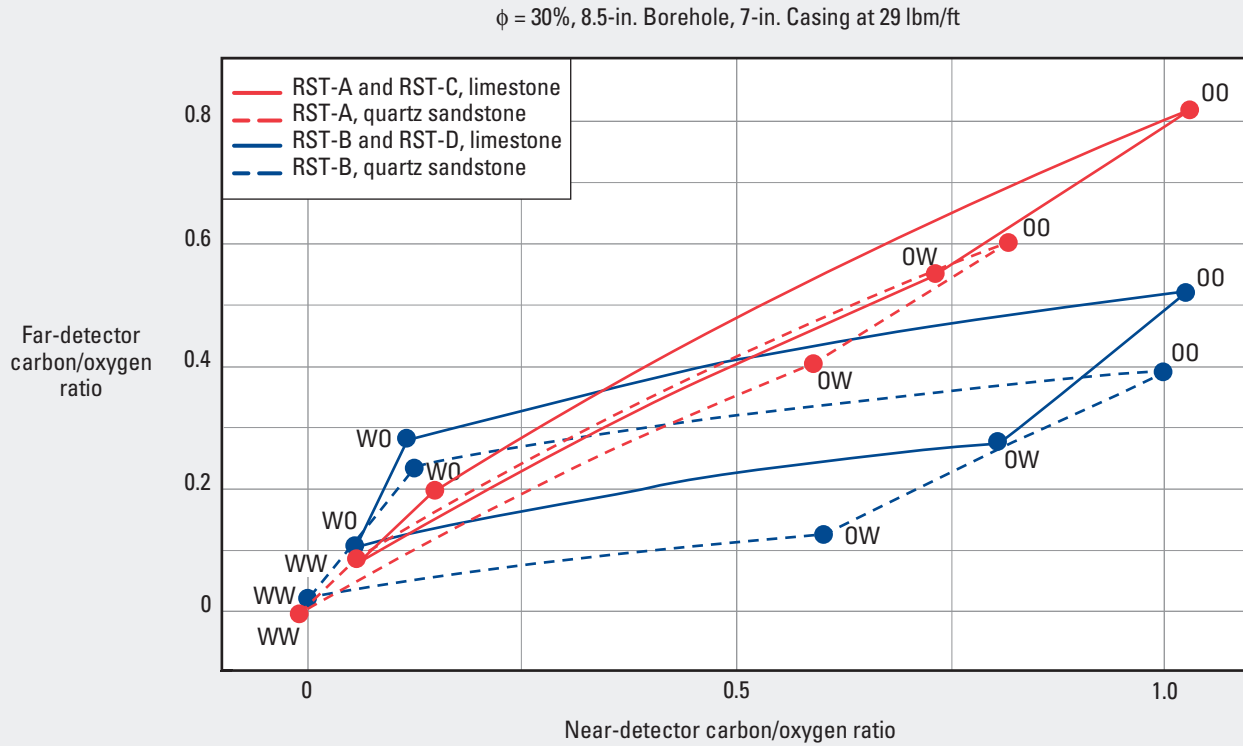


*Mark of Schlumberger
© Schlumberger

RSTPro* Reservoir Saturation Tool—1.6875 in. and 2.5 in. in 8.5-in. Borehole with 7-in. Casing at 29 lbm/ft, #2 Diesel CDV = 0.7313-g Carbon per cm³

SatCH-7
(former RST-1)

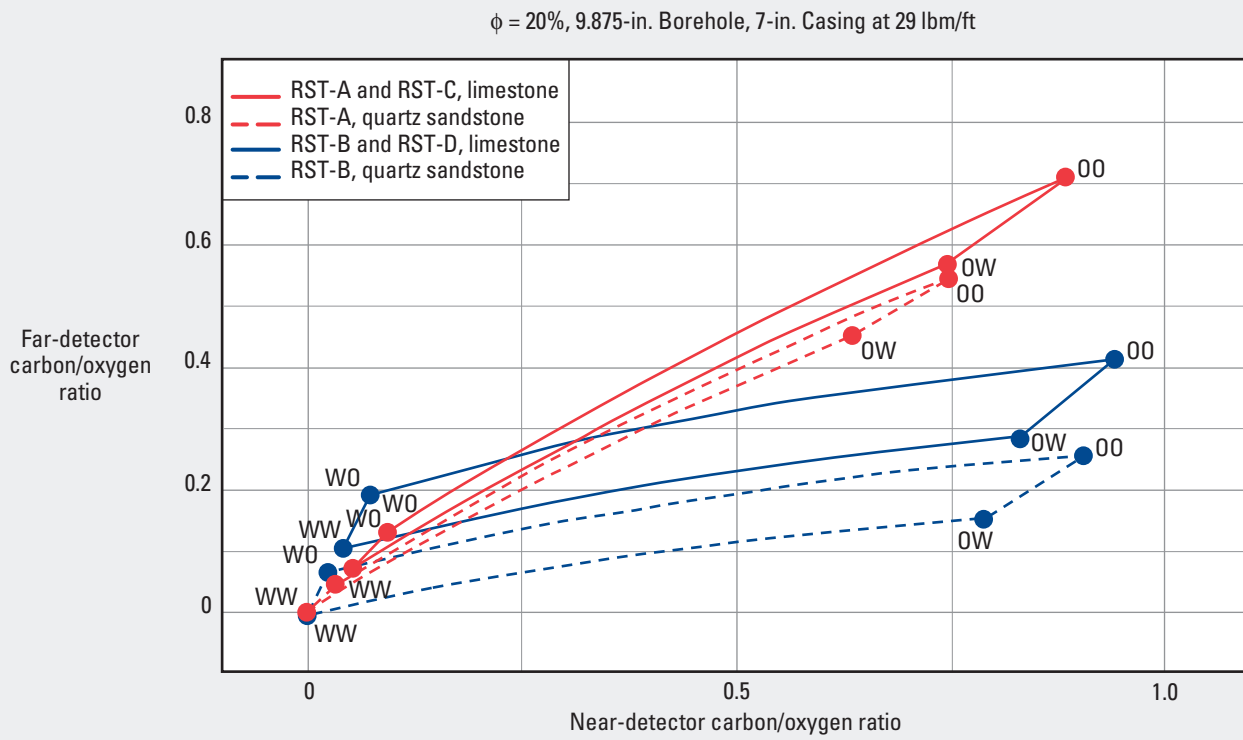
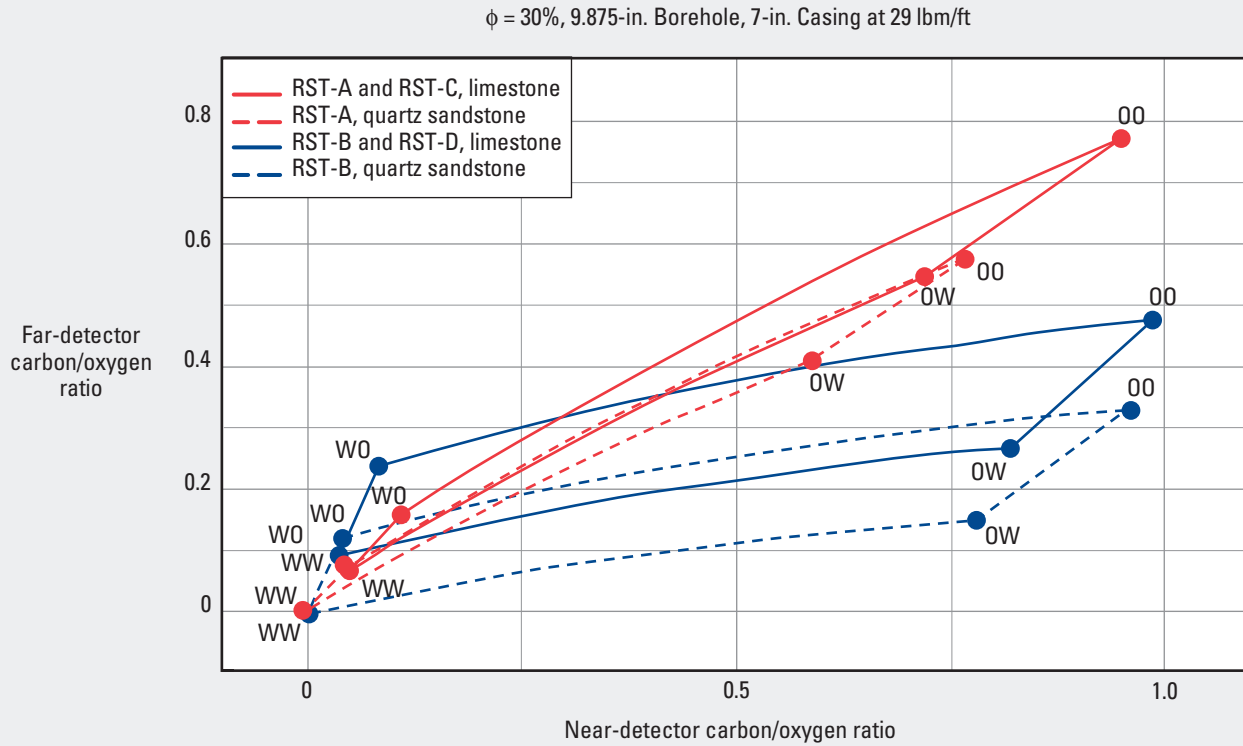
Carbon/Oxygen Ratio—Cased Hole



RSTPro* Reservoir Saturation Tool—1.6875 in. and 2.5 in. in 9.875-in. Borehole with 7-in. Casing at 29 lbm/ft, #2 Diesel CDV = 0.7313-g Carbon per cm³

SatCH-8
(former RST-2)

Carbon/Oxygen Ratio—Cased Hole



*Mark of Schlumberger
© Schlumberger

Permeability from Porosity and Water Saturation

Open Hole

Purpose

Charts Perm-1 and Perm-2 are used to estimate the permeability of shales, shaly sands, or other hydrocarbon-saturated intergranular rocks at irreducible water saturation (S_{wi}).

Description

The charts are based on empirical observations and are similar in form to a general expression proposed by Wyllie and Rose (1950) (see Reference 49):

$$k^{1/2} = \left(\frac{C\phi}{S_{wi}} \right) + C' \quad (1)$$

Chart Perm-1 presents the results of one study for which the observed relation was

$$k^{1/2} = \left(\frac{100\phi^{2.25}}{S_{wi}} \right) \quad (2)$$

Chart Perm-2 presents the results of another study:

$$k^{1/2} = 70\phi_e^2 \left(\frac{1 - S_{wi}}{S_{wi}} \right) \quad (3)$$

The charts are valid only for zones at irreducible water saturation.

Enter porosity (ϕ) and S_{wi} on a chart. Their intersection defines the intrinsic (absolute) rock permeability (k). Medium-gravity oil is assumed. If the saturating hydrocarbon is other than medium-gravity oil, a correction factor (C') based on the fluid densities of water and hydrocarbons (ρ_w and ρ_h , respectively) and elevation above the free-water level (h) should be applied to the S_{wi} value before it is entered on the chart. The chart on this page provides the correction factor based on the capillary pressure:

$$p_c = \frac{h(\rho_w - \rho_h)}{2.3} \quad (4)$$

Charts Perm-1 and Perm-2 can be used to recognize zones at irreducible water saturation, for which the product ϕS_{wi} from levels within the zone is generally constant and plots parallel to the ϕS_{wi} lines.

Example

Given: $\phi = 23$ p.u., $S_{wi} = 30\%$, gas saturation with $\rho_h = 0.3$ g/cm³ and $\rho_w = 1.1$ g/cm³, and $h = 120$ ft.

Find: Correction factor and k .

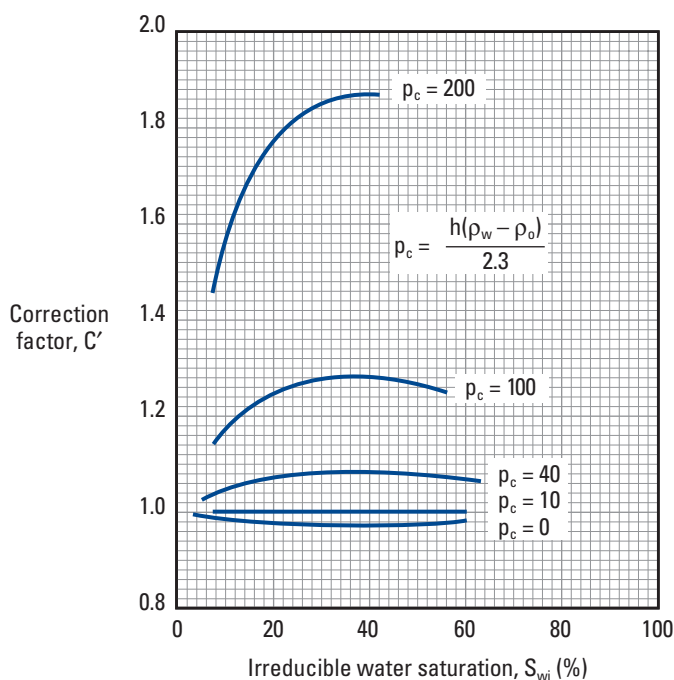
Answer: First, find p_c to determine the correction factor if the zone of interest is not at irreducible water saturation:

$$p_c = \frac{h(\rho_w - \rho_h)}{2.3} = \frac{120(1.1 - 0.3)}{2.3} = 42.$$

Enter the correction factor chart with $S_{wi} = 30\%$ to intersect the curve for $p_c = 40$ (nearest to 42), for which the correction factor is 1.08. The corrected S_{wi} value is $1.08 \times 30\% = 32.4\%$.

Chart Perm-1: $\phi S_{wi} = 0.072\%$ and $k = 130$ mD.

Chart Perm-2: $\phi S_{wi} = 0.072\%$ and $k = 65$ mD.

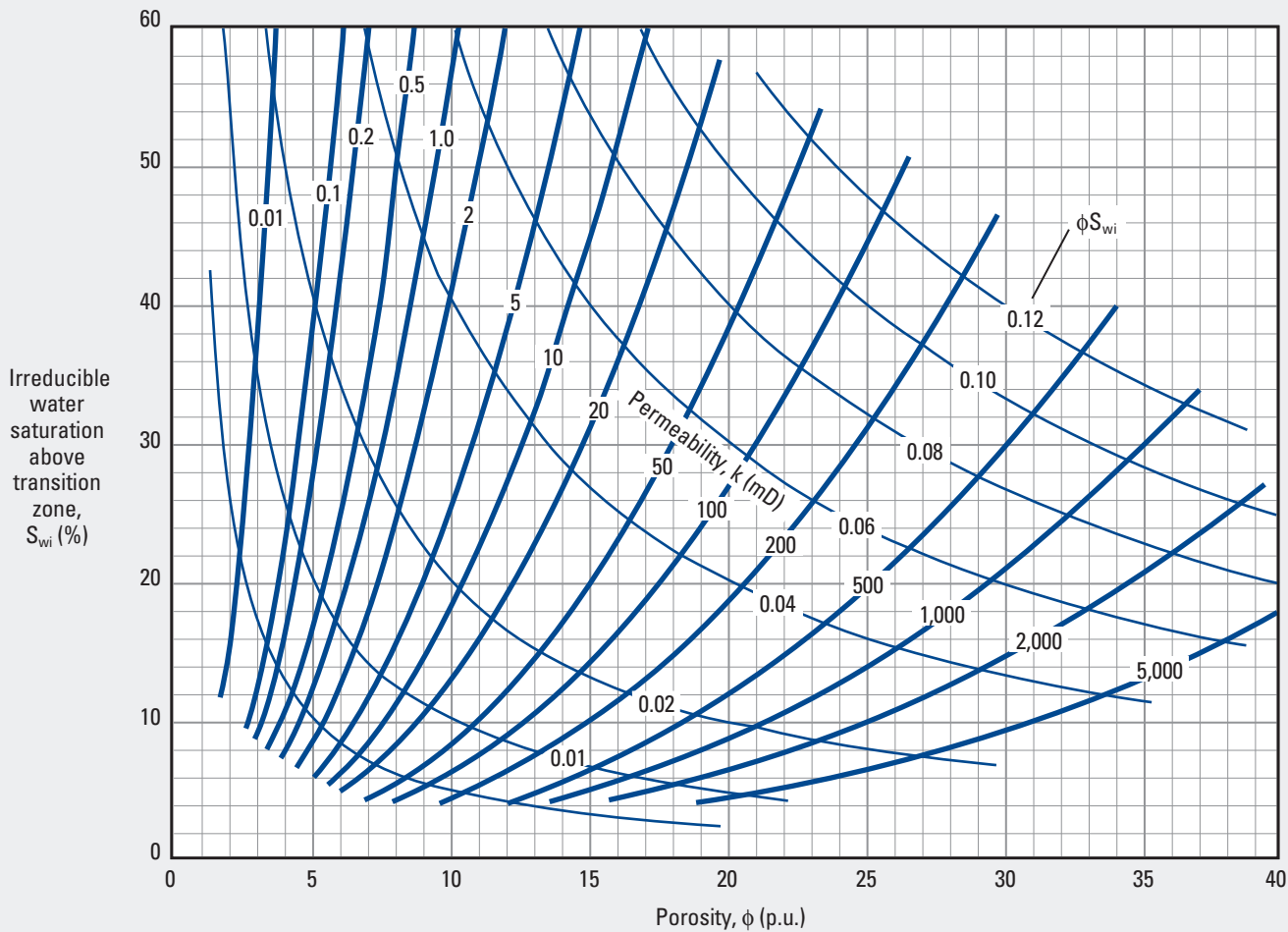


© Schlumberger

Permeability from Porosity and Water Saturation

Open Hole

Perm-1
(former K-3)

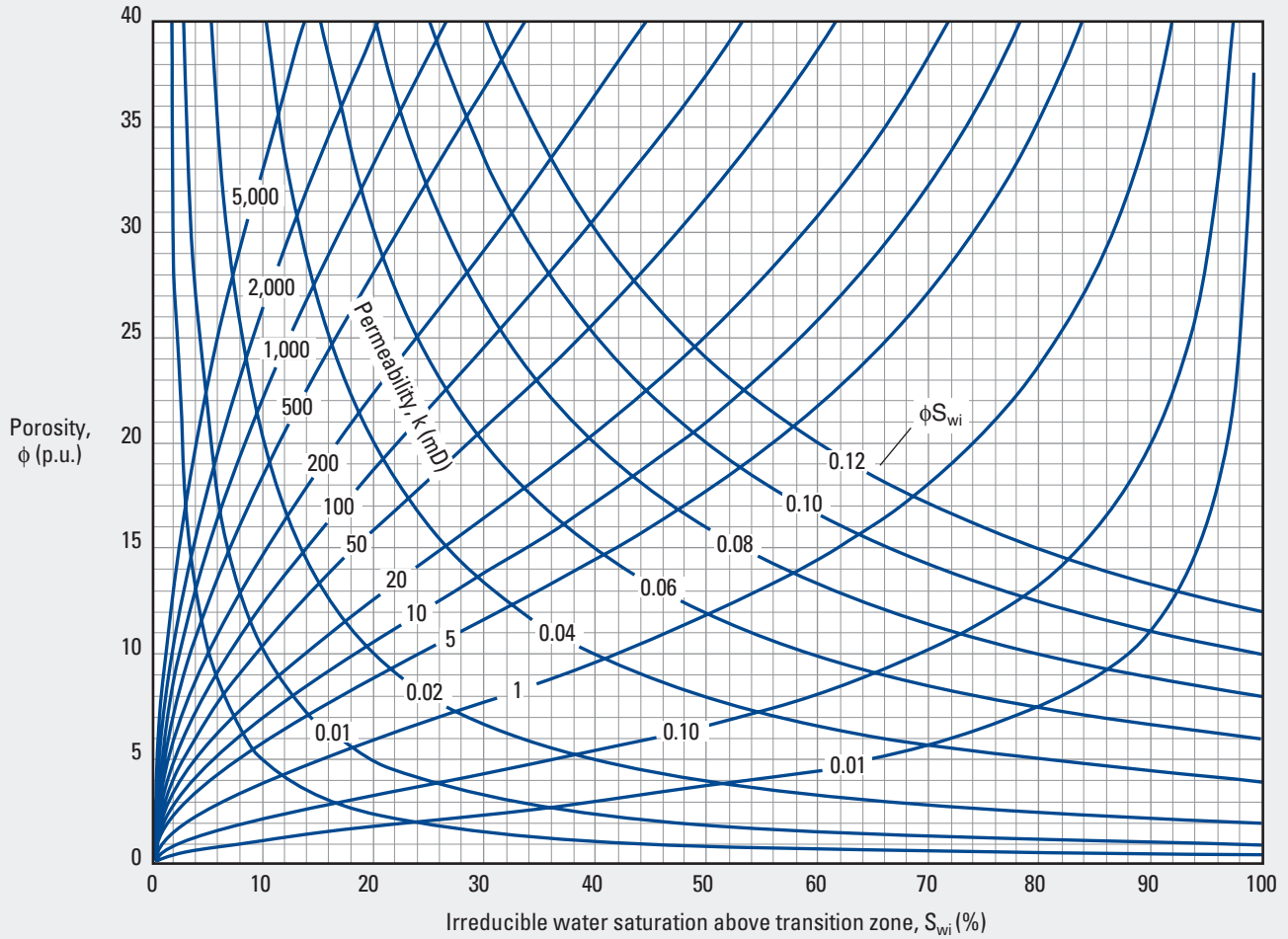


© Schlumberger

Permeability from Porosity and Water Saturation

Open Hole

Perm-2
(former K-4)



© Schlumberger

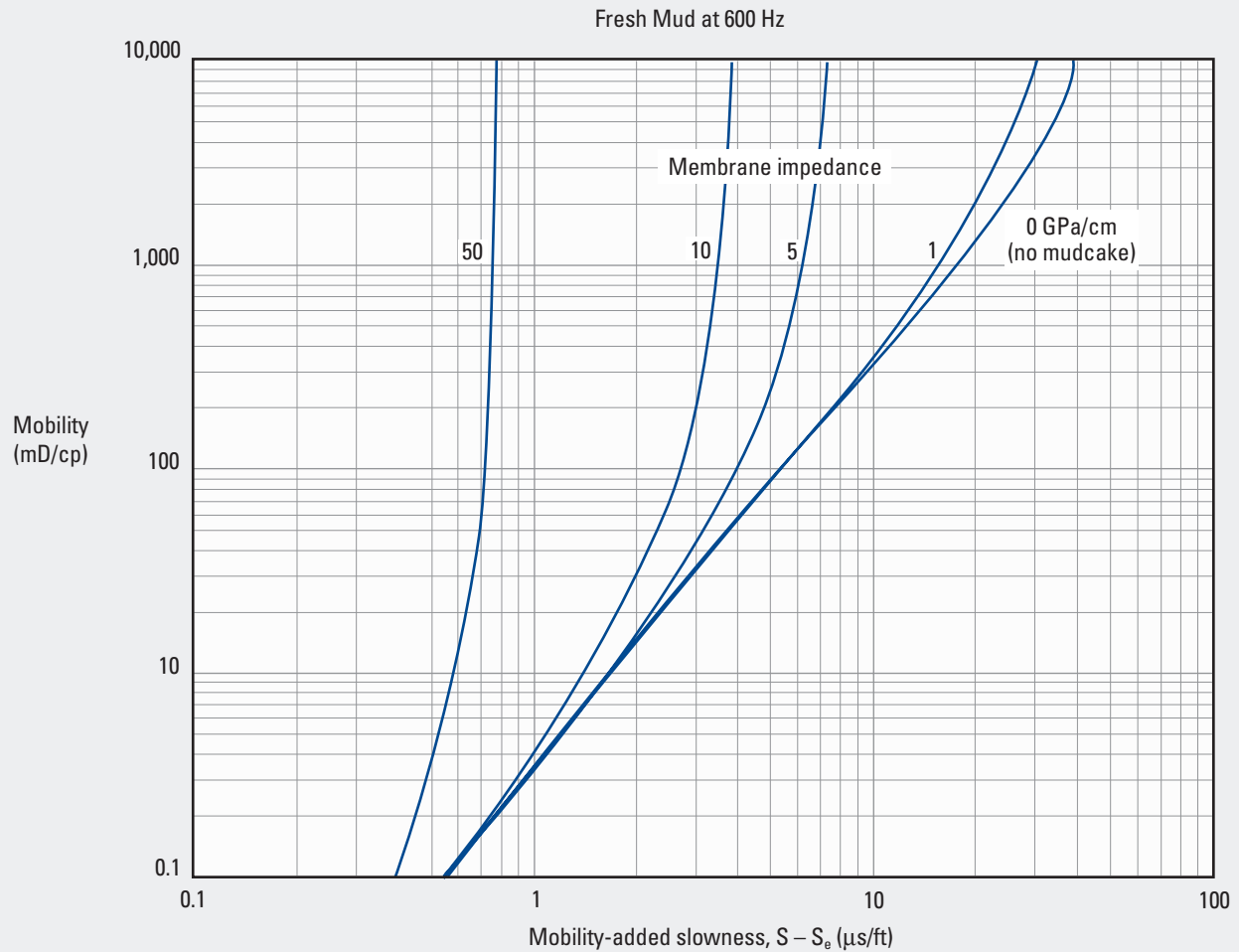
This chart is used similarly to Chart Perm-1 for the relation

$$k^{1/2} = 70\phi_e^2 \left(\frac{1 - S_{wi}}{S_{wi}} \right)$$

Fluid Mobility Effect on Stoneley Slowness

Open Hole

Perm-3



© Schlumberger

Purpose

This chart is used to estimate ease of movement through a formation by a fluid.

Description

The mobility-added slowness, which is the difference between the Stoneley slowness and the calculated elastic Stoneley slowness, is plotted on the x-axis and the mobility of the fluid is on the y-axis. The membrane impedance curves represent the effect that the mudcake has on the determination of the mobility of the fluid in the formation. The membrane impedance is scaled in gigapascal per centimeter.

Cement Bond Log—Casing Strength

Interpretation—Cased Hole

Purpose

This chart is used to determine the decibel attenuation of casing from the measured cement bond log (CBL) amplitude and convert it to the compressive strength of bonded cement (either standard or foamed).

Description

The amplitude of the first casing arrival is recorded by an acoustic signal-measuring device such as a sonic or cement bond tool. This amplitude value is a measure of decibel attenuation that can be translated into a bond index (an indication of the percent of casing cement bonding) and the compressive strength (psi) of the cement at the time of logging.

Enter the chart on the y-axis with the log value of CBL amplitude and move upward parallel to the 45° lines to intersect the appropriate casing size. At that point, move horizontally right to the attenuation scale on the right-hand y-axis. From this point, draw a line through the appropriate casing thickness value to intersect the compressive strength scale. The casing wall thickness is calculated by subtracting the nominal inside diameter (ID) from the outside diameter (OD) listed on the table for threaded nonupset casing and dividing the difference by 2.

Example

- Given:** Log amplitude reading = 3.5 mV in zone of interest and 1.0 mV in a well-bonded section (usually the lowest millivolt value on the log), casing size = 7 in. at 29 lbm/ft, casing thickness = 0.41 in., and neat cement (not foamed).
- Find:** Compressive strength and bond index of the cement at the time of logging.
- Answer:** Enter the 3.5-mV reading on the left y-axis of Chart Cem-1 and proceed to the 7-in. casing line. Move horizontally to intersect the right-hand y-axis at 8.9 dB/ft. Determine the casing thickness as $(7 - 6.184)/2 = 0.816/2 = 0.41$ in. Draw a line from 8.9 dB/ft through the 0.41-in. casing thickness point to the compressive strength scale. Cement compressive strength = 2,100 psi.

To find the bond index, determine the decibel attenuation of the lowest recorded log value by entering 1.0 mV on the left-hand y-axis and proceeding to the 7-in. casing line. Move horizontally to intersect the right-hand y-axis at 12.3 dB/ft.

Divide the precisely determined decibel attenuation for the CBL amplitude in the zone of interest by this value for the lowest millivolt value: $8.9/12.3 = 72\%$ bond index.

A 72% bond index means that 72% of the casing is bonded. This is not a well-bonded zone because a value of 80% bonding over a 10-ft interval is historically considered well bonded. Although the logging scale is a linear millivolts scale, the decibel attenuation scale is logarithmic. The millivolts log scale for the CBL value cannot rescaled in percent of bonding. If it were, the apparent percent bonding would be 65% because most bond log scales are from 0 to 100 mV reading from left to right, over 10 divisions of track 1, or conversely 100% to 0% cement bonding for 0 mV = 100% bonding and 100 mV = 0% bonding.

Cement Bond Log—Casing Strength

Interpretation—Cased Hole

Threaded Nonupset Casing

OD (in.)	Weight per ft [†] (lbm)	Nominal ID (in.)	Drift Diameter [‡] (in.)	OD (in.)	Weight per ft [†] (lbm)	Nominal ID (in.)	Drift Diameter [‡] (in.)	OD (in.)	Weight per ft [†] (lbm)	Nominal ID (in.)	Drift Diameter [‡] (in.)						
4	11.60	3.428	3.303	7	17.00	6.538	6.413	10	33.00	9.384	9.228						
4½	9.50	4.090	3.965		20.00	6.456	6.331	10%	32.75	10.192	10.036						
	11.60	4.000	3.875		22.00	6.398	6.273		40.00	10.054	9.898						
	13.50	3.920	3.795		23.00	6.366	6.241		40.50	10.050	9.894						
4%	16.00	4.082	3.957		24.00	6.336	6.211		45.00	9.960	9.804						
					26.00	6.276	6.151		45.50	9.950	9.794						
5	11.50	4.560	4.435		28.00	6.214	6.089		48.00	9.902	9.746						
					29.00	6.184	6.059		51.00	9.850	9.694						
					30.00	6.154	6.029		54.00	9.784	9.628						
					32.00	6.094	5.969		55.50	9.760	9.604						
				35.00	6.004	5.879	11%		38.00	11.150	10.994						
38.00	5.920	5.795	42.00	11.084	10.928												
40.00	5.836	5.711	47.00	11.000	10.844												
5½	13.00	5.044	4.919	7%	20.00	7.125		7.000		54.00	10.880	10.724					
									24.00	7.025	6.900	60.00	10.772	10.616			
									26.40	6.969	6.844	12	40.00	11.384	11.228		
									29.70	6.875	6.750						
									33.70	6.765	6.640	13	40.00	12.438	12.282		
									39.00	6.625	6.500						
5%	14.00	5.290	5.165	8%	24.00	8.097		7.972	13%	48.00	12.715	12.559					
							28.00						8.017	7.892			
							32.00		7.921	7.796	16	55.00	15.375	15.187			
							36.00		7.825	7.700							
							38.00		7.775	7.650	18%	78.00	17.855	17.667			
40.00	7.725	7.600															
6	15.00	5.524	5.399		9	34.00	8.290	8.165	20	90.00	19.190	19.002					
													43.00	7.651	7.526		
									44.00	7.625	7.500	21½	92.50	20.710	20.522		
									49.00	7.511	7.386					103.00	20.610
				114.00					20.510	20.322							
6%	17.00	6.135	6.010	9%	29.30	9.063	8.907	24½	100.50	23.750	23.562						
												32.30	9.001	8.845			
								36.00	8.921	8.765	113.00	23.650	23.462				
								40.00	8.835	8.679							
								43.50	8.755	8.599							
				47.00	8.681	8.525	9%	32.30	9.001	8.845							
				53.50	8.535	8.379											

[†] Weight per foot in pounds is given for plain pipe (no threads or coupling).

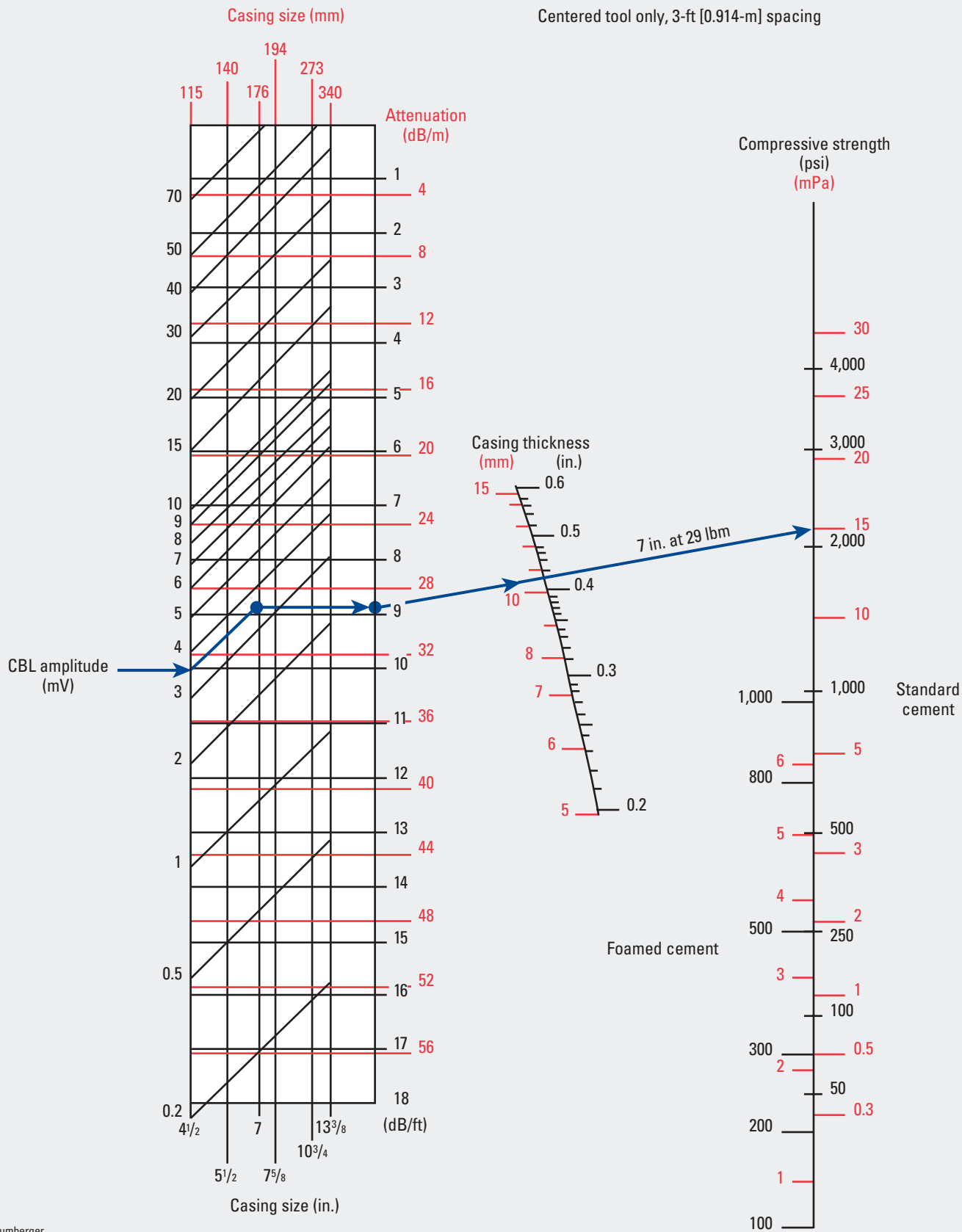
[‡] Drift diameter is the guaranteed minimum inside diameter of any part of the casing. Use drift diameter to determine the largest-diameter equipment that can be safely run inside the casing. Use inside diameter for volume capacity calculations.

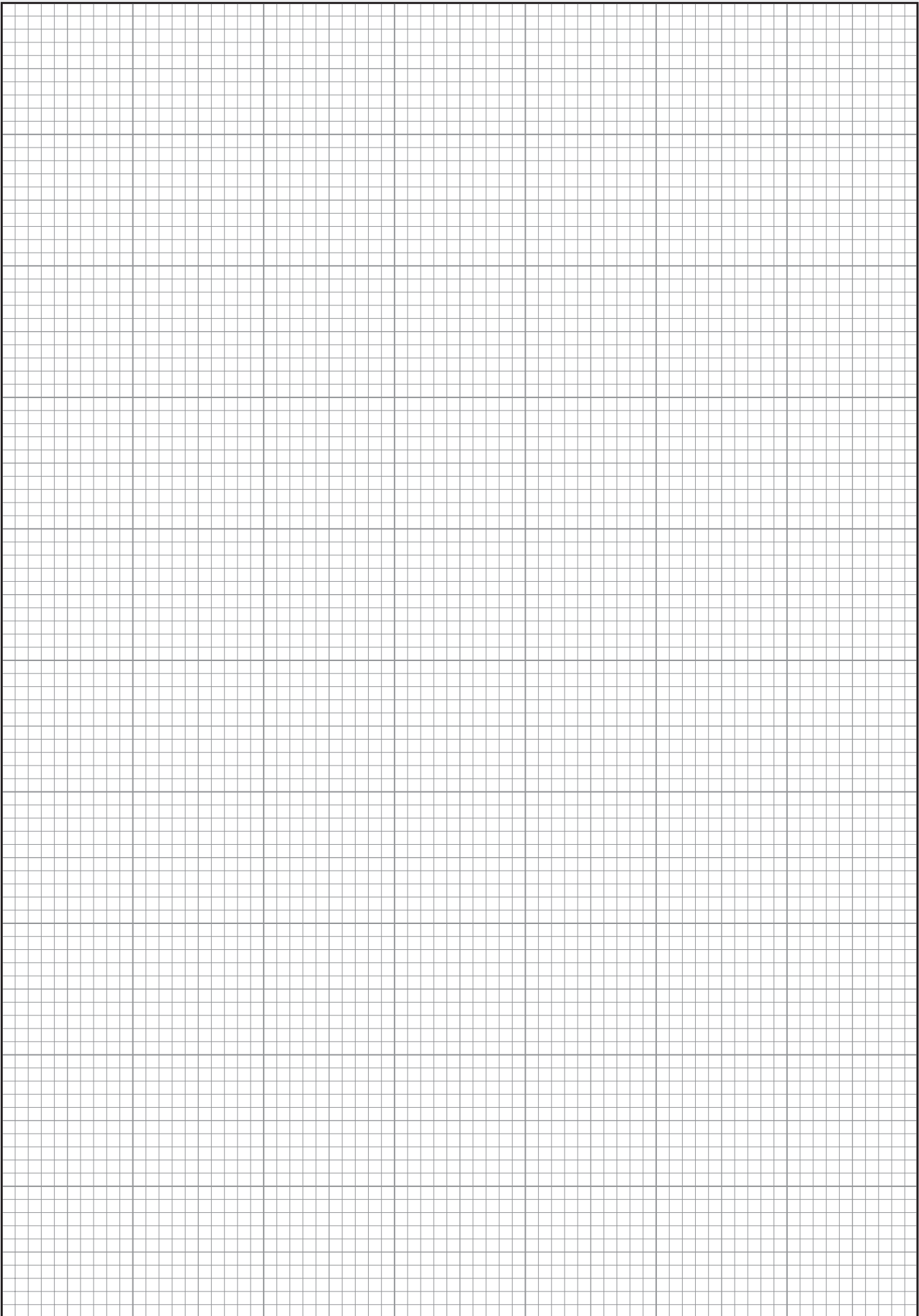
Cement Bond Log—Casing Strength

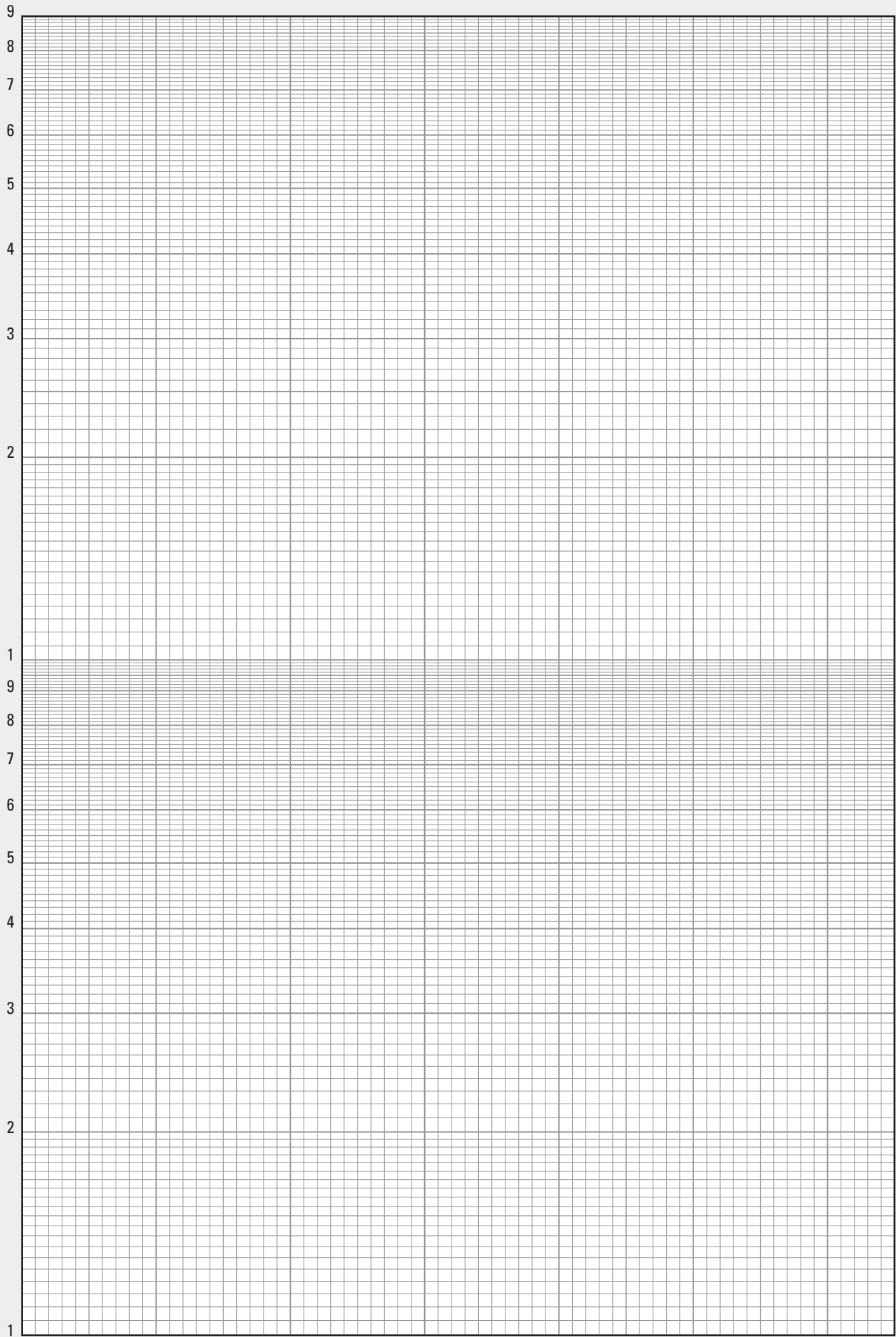
Interpretation—Cased Hole

Cem-1
(former M-1)

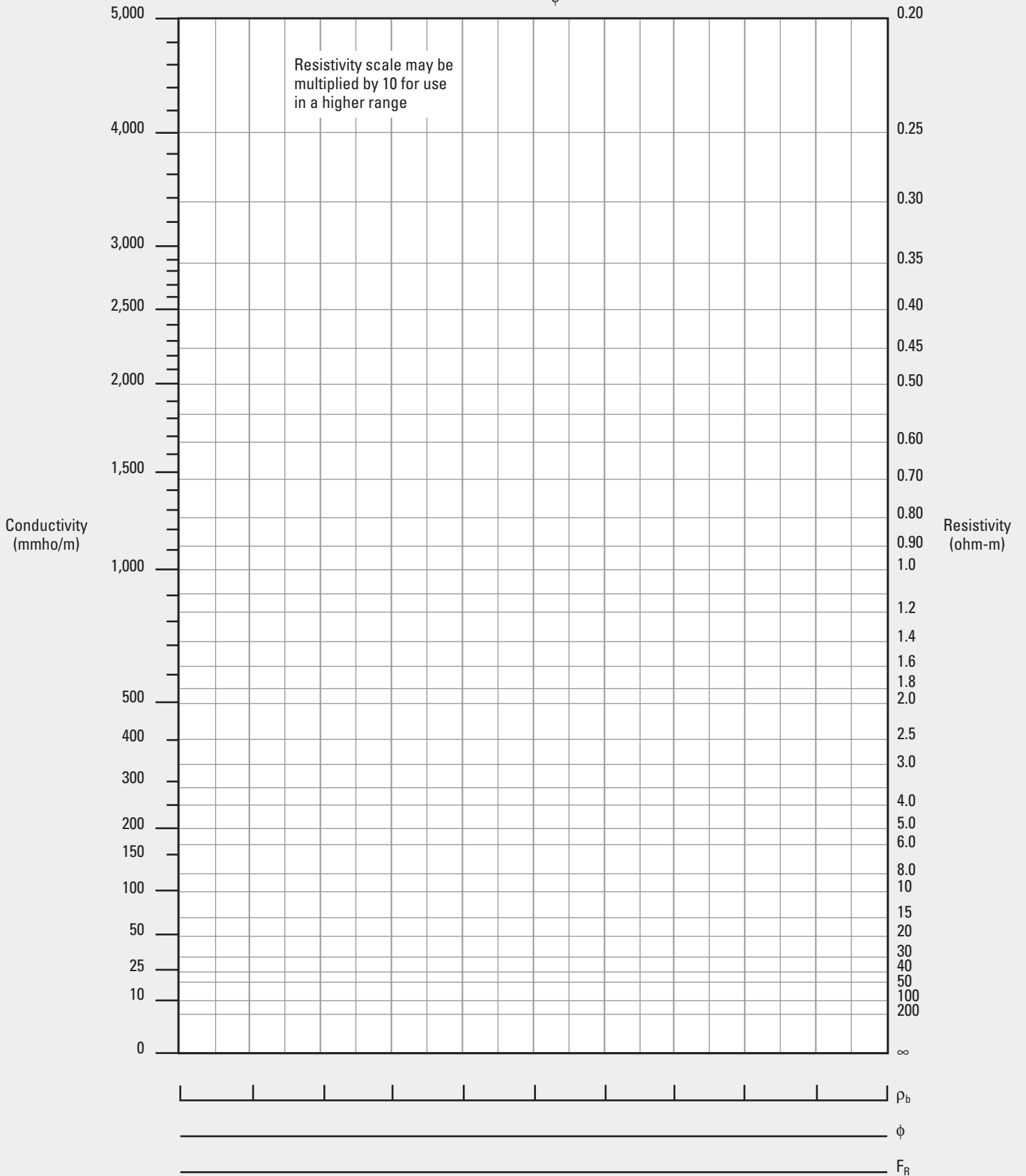
Centered tool only, 3-ft [0.914-m] spacing



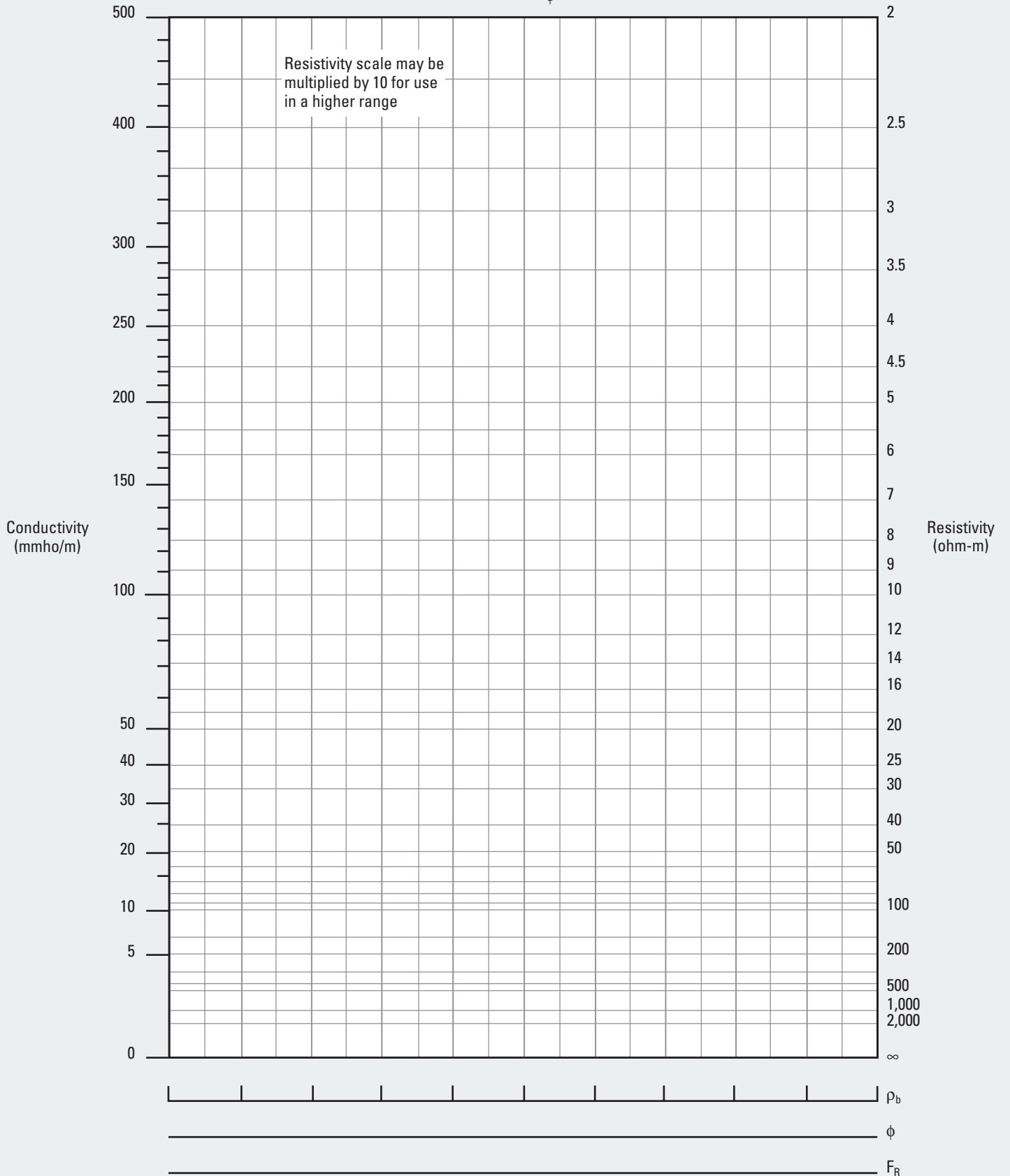




$$\text{For } F_R = \frac{0.62}{\phi^{2.15}}$$



$$\text{For } F_R = \frac{1}{\phi^2}$$



Name	Formula	ρ_{\log} (g/cm ³)	ϕ_{SNP} (p.u.)	ϕ_{CNL} (p.u.)	ϕ_{APS}^{\dagger} (p.u.)	Δt_c (μ s/ft)	Δt_s (μ s/ft)	Pe	U	ϵ (farad/m)	t_p (ns/m)	Gamma Ray (gAPI Units)	Σ (c.u.)
Silicates													
Quartz	SiO ₂	2.64	-1	-2	-1	56.0	88.0	1.8	4.8	4.65	7.2		4.3
β -cristobalite	SiO ₂	2.15	-2	-3				1.8	3.9				3.5
Opal (3.5% H ₂ O)	SiO ₂ (H ₂ O) _{0.1209}	2.13	4	2		58		1.8	3.7				5.0
Garnet [†]	Fe ₃ Al ₂ (SiO ₄) ₃	4.31	3	7				11	48				45
Hornblende [†]	Ca ₂ NaMg ₂ Fe ₂ AlSi ₈ O ₂₂ (OH) ₂	3.20	4	8		43.8	81.5	6.0	19				18
Tourmaline	NaMg ₃ Al ₆ B ₃ Si ₆ O ₂₂ (OH) ₄	3.02	16	22				2.1	6.5				7450
Zircon	ZrSiO ₄	4.50	-1	-3				69	311				6.9
Carbonates													
Calcite	CaCO ₃	2.71	0	0	0	49.0	88.4	5.1	13.8	7.5	9.1		7.1
Dolomite	CaCO ₃ MgCO ₃	2.85	2	1	1	44.0	72	3.1	9.0	6.8	8.7		4.7
Ankerite	Ca(Mg,Fe)(CO ₃) ₂	2.86	0	1				9.3	27				22
Siderite	FeCO ₃	3.89	5	12	3	47		15	57	6.8-7.5	8.8-9.1		52
Oxidates													
Hematite	Fe ₂ O ₃	5.18	4	11		42.9	79.3	21	111				101
Magnetite	Fe ₃ O ₄	5.08	3	9		73		22	113				103
Goethite	FeO(OH)	4.34	50+	60+				19	83				85
Limonite [†]	FeO(OH)(H ₂ O) _{2.05}	3.59	50+	60+		56.9	102.6	13	47	9.9-10.9	10.5-11.0		71
Gibbsite	Al(OH) ₃	2.49	50+	60+				1.1					23
Phosphates													
Hydroxapatite	Ca ₅ (PO ₄) ₃ OH	3.17	5	8		42		5.8	18				9.6
Chlorapatite	Ca ₅ (PO ₄) ₃ Cl	3.18	-1	-1		42		6.1	19				130
Fluorapatite	Ca ₅ (PO ₄) ₃ F	3.21	-1	-2		42		5.8	19				8.5
Carbonapatite	(Ca ₅ (PO ₄) ₃) ₂ CO ₃ H ₂ O	3.13	5	8				5.6	17				9.1
Feldspars—Alkali[†]													
Orthoclase	KAlSi ₃ O ₈	2.52	-2	-3		69		2.9	7.2	4.4-6.0	7.0-8.2	~220	16
Anorthoclase	KAlSi ₃ O ₈	2.59	-2	-2				2.9	7.4	4.4-6.0	7.0-8.2	~220	16
Microcline	KAlSi ₃ O ₈	2.53	-2	-3				2.9	7.2	4.4-6.0	7.0-8.2	~220	16
Feldspars—Plagioclase[†]													
Albite	NaAlSi ₃ O ₈	2.59	-1	-2	-2	49	85	1.7	4.4	4.4-6.0	7.0-8.2		7.5
Anorthite	CaAl ₂ Si ₂ O ₈	2.74	-1	-2		45		3.1	8.6	4.4-6.0	7.0-8.2		7.2
Micas[†]													
Muscovite	KAl ₂ (Si ₃ AlO ₁₀)(OH) ₂	2.82	12	~20	~13	49	149	2.4	6.7	6.2-7.9	8.3-9.4	~270	17
Glauconite	K _{0.7} (Mg,Fe ₂ ,Al) (Si ₄ ,Al ₁₀)O ₂ (OH)	2.86		~38	~15			4.8	14				21
Biotite	K(Mg,Fe) ₃ (AlSi ₃ O ₁₀)(OH) ₂	~2.99	~11	~21	~11	50.8	224	6.3	19	4.8-6.0	7.2-8.1	~275	30
Phlogopite	KMg ₃ (AlSi ₃ O ₁₀)(OH) ₂					50	207						33

[†]APS* Accelerator Porosity Sonde porosity derived from near-to-array ratio (APLC)

*Mean value, which may vary for individual samples

For more information, see Reference 41.

Name	Formula	ρ_{\log} (g/cm ³)	ϕ_{SNP} (p.u.)	ϕ_{CNL} (p.u.)	ϕ_{APS}^{\dagger} (p.u.)	Δt_c (μ s/ft)	Δt_s (μ s/ft)	Pe	U	ϵ (farad/m)	t_p (ns/m)	Gamma Ray (gAPI Units)	Σ (c.u.)
Clays[‡]													
Kaolinite	Al ₂ Si ₄ O ₁₀ (OH) ₈	2.62	34	~37	~34			1.48	3.87	~5.8	~8.0	80–130	14
Chlorite	(Mg,Fe,Al) ₆ (Si,Al) ₄ O ₁₀ (OH) ₈	2.76	37	~52	~35			6.3	17	~5.8	~8.0	180–250	25
Illite	K _{1–1.5} Al ₄ (Si _{7–6.5} ,Al _{1–1.5}) O ₂₀ (OH) ₄	2.77	20	~30	~17			2.33	6.45	~5.8	~8.0	250–300	18
Montmorillonite	(Ca,Na) ₇ (Al,Mg,Fe) ₄ (Si,Al) ₈ O ₂₀ (OH) ₄ (H ₂ O) _n	2.12		~60	~60			2.0	4.0	~5.8	~8.0	150–200	14
Evaporites													
Halite	NaCl	2.04	–2	–3	21	67.0	120	4.7	9.5	5.6–6.3	7.9–8.4		754
Anhydrite	CaSO ₄	2.98	–1	–2	2	50		5.1	15	6.3	8.4		12
Gypsum	CaSO ₄ (H ₂ O) ₂	2.35	50+	60+	60	52		4.0	9.4	4.1	6.8		19
Trona	Na ₂ CO ₃ NaHCO ₃ H ₂ O	2.08	24	35		65		0.71	1.5				16
Tachhydrite	CaCl ₂ (MgCl ₂) ₂ (H ₂ O) ₁₂	1.66	50+	60+		92		3.8	6.4				406
Sylvite	KCl	1.86	–2	–3				8.5	16	4.6–4.8	7.2–7.3	500+	565
Carnalite	KClMgCl ₂ (H ₂ O) ₆	1.57	41	60+				4.1	6.4			~220	369
Langbeinite	K ₂ SO ₄ (MgSO ₄) ₂	2.82	–1	–2				3.6	10			~290	24
Polyhalite	K ₂ SO ₄ Mg SO ₄ (CaSO ₄) ₂ (H ₂ O) ₂	2.79	14	25				4.3	12			~200	24
Kainite	MgSO ₄ KCl(H ₂ O) ₃	2.12	40	60+				3.5	7.4			~245	195
Kieserite	MgSO ₄ (H ₂ O)	2.59	38	43				1.8	4.7				14
Epsomite	MgSO ₄ (H ₂ O) ₇	1.71	50+	60+				1.2	2.0				21
Bischofite	MgCl ₂ (H ₂ O) ₆	1.54	50+	60+		100		2.6	4.0				323
Barite	BaSO ₄	4.09	–1	–2				267	1,090				6.8
Celestite	SrSO ₄	3.79	–1	–1				55	209				7.9
Sulfides													
Pyrite	FeS ₂	4.99	–2	–3		39.2	62.1	17	85				90
Marcasite	FeS ₂	4.87	–2	–3				17	83				88
Pyrrhotite	Fe ₇ S ₈	4.53	–2	–3				21	93				94
Sphalerite	ZnS	3.85	–3	–3				36	138	7.8–8.1	9.3–9.5		25
Chalcopyrite	CuFeS ₂	4.07	–2	–3				27	109				102
Galena	PbS	6.39	–3	–3				1,630	10,400				13
Sulfur	S	2.02	–2	–3		122		5.4	11				20
Coals													
Anthracite	CH _{0.358} N _{0.009} O _{0.022}	1.47	37	38		105		0.16	0.23				8.7
Bituminous	CH _{0.793} N _{0.015} O _{0.078}	1.24	50+	60+		120		0.17	0.21				14
Lignite	CH _{0.849} N _{0.015} O _{0.211}	1.19	47	52		160		0.20	0.24				13

[†]APS* Accelerator Porosity Sonde porosity derived from near-to-array ratio (APLC)

[‡]Mean value, which may vary for individual samples

For more information, see Reference 41.

Nonporous Solids

Material	Δt ($\mu\text{s}/\text{ft}$)	Sound Velocity		Acoustic Impedance (MRayl)
		(ft/s)	(m/s)	
Casing	57.0	17,500	5,334	41.60
Dolomite	43.5	23,000	7,010	20.19
Anhydrite	50.0	20,000	6,096	18.17
Limestone	47.6	21,000	6,400	17.34
Calcite	49.7	20,100	6,126	16.60
Quartz	52.9	18,900	5,760	15.21
Gypsum	52.6	19,000	5,791	13.61
Halite	66.6	15,000	4,572	9.33

Water-Saturated Porous Rock

Material	Porosity (%)	Δt ($\mu\text{s}/\text{ft}$)	Sound Velocity		Acoustic Impedance (MRayl)
			(ft/s)	(m/s)	
Dolomite	5–20	50.0–66.6	20,000–15,000	6,096–4,572	16.95–11.52
Limestone	5–20	54.0–76.9	18,500–13,000	5,639–3,962	14.83–9.43
Sandstone	5–20	62.5–86.9	16,000–11,500	4,877–3,505	12.58–8.20
Sand	20–35	86.9–111.1	11,500–9,000	3,505–2,743	8.20–6.0
Shale		58.8–143.0	17,000–7,000	5,181–2,133	12.0–4.3

Liquids and Gases

Material	Δt ($\mu\text{s}/\text{ft}$)	Sound Velocity		Acoustic Impedance (MRayl)
		(ft/s)	(m/s)	
Water	208	4,800	1,463	1.46
Water + 10% NaCl	192.3	5,200	1,585	1.66
Water + 20% NaCl	181.8	5,500	1,676	1.84
Seawater	199	5,020	1,531	1.57
Kerosene	230	4,340	1,324	1.07
Air at 15 psi, 32°F [0°C]	920	1,088	331	0.0004
Air at 3,000 psi, 212°F [100°C]	780	1,280	390	0.1

Length										
Multiply Number of to Obtain by	Centimeters	Feet	Inches	Kilometers	Nautical Miles	Meters	Mils	Miles	Millimeters	Yards
Centimeters	1	30.48	2.540	10^5	1.853×10^5	100	2.540×10^{-3}	1.609×10^5	0.1	91.44
Feet	3.281×10^{-2}	1	8.333×10^{-2}	3281	6080.27	3.281	8.333×10^{-5}	5280	3.281×10^{-3}	3
Inches	0.3937	12	1	3.937×10^4	7.296×10^4	39.37	0.001	6.336×10^4	3.937×10^{-2}	36
Kilometers	10^{-5}	3.048×10^{-4}	2.540×10^{-5}	1	1.853	0.001	2.540×10^{-8}	1.609	10^{-6}	9.144×10^{-4}
Nautical miles		1.645×10^{-4}		0.5396	1	5.396×10^{-4}		0.8684		4.934×10^{-4}
Meters	0.01	0.3048	2.540×10^{-2}	1000	1853	1		1609	0.001	0.9144
Mils	393.7	1.2×10^4	1000	3.937×10^7		3.937×10^4	1		39.37	3.6×10^4
Miles	6.214×10^{-6}	1.894×10^{-4}	1.578×10^{-5}	0.6214	1.1516	6.214×10^{-4}		1	6.214×10^{-7}	5.682×10^{-4}
Millimeters	10	304.8	25.40	10^5		1000	2.540×10^{-2}		1	914.4
Yards	1.094×10^{-2}	0.3333	2.778×10^{-2}	1094	2027	1.094	2.778×10^{-5}	1760	1.094×10^{-3}	1

Area										
Multiply Number of to Obtain by	Acres	Circular Mils	Square Centimeters	Square Feet	Square Inches	Square Kilometers	Square Meters	Square Miles	Square Millimeters	Square Yards
Acres	1			2.296×10^{-5}		247.1	2.471×10^{-4}	640		2.066×10^{-4}
Circular mils		1	1.973×10^5	1.833×10^8	1.273×10^6		1.973×10^9		1973	
Square centimeters		5.067×10^{-6}	1	929.0	6.452	10^{10}	10^4	2.590×10^{10}	0.01	8361
Square feet	4.356×10^4		1.076×10^{-3}	1	6.944×10^{-3}	1.076×10^7	10.76	2.788×10^7	1.076×10^{-5}	9
Square inches	6,272,640	7.854×10^{-7}	0.1550	144	1	1.550×10^9	1550	4.015×10^9	1.550×10^{-3}	1296
Square kilometers	4.047×10^{-3}		10^{-10}	9.290×10^{-8}	6.452×10^{-10}	1	10^{-6}	2.590	10^{-12}	8.361×10^{-7}
Square meters	4047		0.0001	9.290×10^{-2}	6.452×10^{-4}	10^6	1	2.590×10^6	10^{-6}	0.8361
Square miles	1.562×10^{-3}		3.861×10^{-11}	3.587×10^{-8}		0.3861	3.861×10^{-7}	1	3.861×10^{-13}	3.228×10^{-7}
Square millimeters		5.067×10^{-4}	100	9.290×10^4	645.2	10^{12}	10^6		1	8.361×10^5
Square yards	4840		1.196×10^{-4}	0.1111	7.716×10^{-4}	1.196×10^6	1.196	3.098×10^6	1.196×10^{-6}	1

Length										
Multiply Number of by	Bushels (Dry)	Cubic Centimeters	Cubic Feet	Cubic Inches	Cubic Meters	Cubic Yards	Gallons (Liquid)	Liters	Pints (Liquid)	Quarts (Liquid)
Bushels (dry)	1		0.8036	4.651×10^{-4}	28.38			2.838×10^{-2}		
Cubic centimeters	3.524×10^4	1	2.832×10^4	16.39	10^6	7.646×10^5	3785	1000	473.2	946.4
Cubic feet	1.2445	3.531×10^{-5}	1	5.787×10^{-4}	35.31	27	0.1337	3.531×10^{-2}	1.671×10^{-2}	3.342×10^{-2}
Cubic inches	2150.4	6.102×10^{-2}	1728	1	6.102×10^4	46,656	231	61.02	28.87	57.75
Cubic meters	3.524×10^{-2}	10^{-6}	2.832×10^{-2}	1.639×10^{-5}	1	0.7646	3.785×10^{-3}	0.001	4.732×10^{-4}	9.464×10^{-4}
Cubic yards		1.308×10^{-6}	3.704×10^{-2}	2.143×10^{-5}	1.308	1	4.951×10^{-3}	1.308×10^{-3}	6.189×10^{-4}	1.238×10^{-3}
Gallons (liquid)		2.642×10^{-4}	7.481	4.329×10^{-3}	264.2	202.0	1	0.2642	0.125	0.25
Liters	35.24	0.001	28.32	1.639×10^{-2}	1000	764.6	3.785	1	0.4732	0.9464
Pints (liquid)		2.113×10^{-3}	59.84	3.463×10^{-2}	2113	1616	8	2.113	1	2
Quarts (liquid)		1.057×10^{-3}	29.92	1.732×10^{-2}	1057	807.9	4	1.057	0.5	1

Mass and Weight									
Multiply Number of to Obtain by	Grains	Grams	Kilograms	Milligrams	Ounces [†]	Pounds [†]	Tons (Long)	Tons (Metric)	Tons (Short)
Grains	1	15.43	1.543×10^4	1.543×10^{-2}	437.5	7000			
Grams	6.481×10^{-2}	1	1000	0.001	28.35	453.6	1.016×10^6	10^6	9.072×10^5
Kilograms	6.481×10^{-5}	0.001	1	10^{-6}	2.835×10^{-2}	0.4536	1016	1000	907.2
Milligrams	64.81	1000	10^6	1	2.835×10^4	4.536×10^5	1.016×10^9	10^9	9.072×10^8
Ounces [†]	2.286×10^{-3}	3.527×10^{-2}	35.27	3.527×10^{-5}	1	16	3.584×10^4	3.527×10^4	3.2×10^4
Pounds [†]	1.429×10^{-4}	2.205×10^{-3}	2.205	2.205×10^{-6}	6.250×10^{-2}	1	2240	2205	2000
Tons (long)		9.842×10^{-7}	9.842×10^{-4}	9.842×10^{-10}	2.790×10^{-5}	4.464×10^{-4}	1	0.9842	0.8929
Tons (metric)		10^{-6}	0.001	10^{-9}	2.835×10^{-5}	4.536×10^{-4}	1.016	1	0.9072
Tons (short)		1.102×10^{-6}	1.102×10^{-3}	1.102×10^{-9}	3.125×10^{-5}	0.0005	1.120	1.102	1

[†] Avoirdupois pounds and ounces

Area											
to Obtain	Multiply Number of by	Atmospheres [†]	Bayres or Dynes per Square Centimeter [‡]	Centimeters of Mercury at 0°C [§]	Inches of Mercury at 0°C [§]	Inches of Water at 4°C	Kilograms per Square Meter ^{††}	Pounds per Square Foot	Pounds per Square Inch ^{††}	Tons (short) per Square Foot	Pascals
Atmospheres [†]		1	9.869×10^{-7}	1.316×10^{-2}	3.342×10^{-2}	2.458×10^{-3}	9.678×10^{-5}	4.725×10^{-4}	6.804×10^{-2}	0.9450	9.869×10^{-6}
Bayres or dynes per square centimeter [‡]		1.013×10^6	1	1.333×10^4	3.386×10^4	2.491×10^{-3}	98.07	478.8	6.895×10^4	9.576×10^5	10
Centimeters of mercury at 0°C [§]		76.00	7.501×10^{-5}	1	2.540	0.1868	7.356×10^{-3}	3.591×10^{-2}	5.171	71.83	7.501×10^{-4}
Inches of mercury at 0°C [§]		29.92	2.953×10^{-5}	0.3937	1	7.355×10^{-2}	2.896×10^{-3}	1.414×10^{-2}	2.036	28.28	2.953×10^{-4}
Inches of water at 4°C		406.8	4.015×10^{-4}	5.354	13.60	1	3.937×10^{-2}	0.1922	27.68	384.5	4.015×10^{-3}
Kilograms per square meter ^{††}		1.033×10^4	1.020×10^{-2}	136.0	345.3	25.40	1	4.882	703.1	9765	0.1020
Pounds per square foot		2117	2.089×10^{-3}	27.85	70.73	5.204	0.2048	1	144	2000	2.089×10^{-2}
Pounds per square inch ^{††}		14.70	1.450×10^{-5}	0.1934	0.4912	3.613×10^{-2}	1.422×10^{-3}	6.944×10^{-3}	1	13.89	1.450×10^{-4}
Tons (short) per square foot		1.058	1.044×10^{-5}	1.392×10^{-2}	3.536×10^{-2}	2.601×10^{-3}	1.024×10^{-4}	0.0005	0.072	1	1.044×10^{-5}
Pascals		1.013×10^5	10^{-1}	1.333×10^3	3.386×10^3	2.491×10^{-4}	9.807	47.88	6.895×10^3	9.576×10^4	1

[†] One atmosphere (standard) = 76 cm of mercury at 0°C
[‡] Bar
[§] To convert height h of a column of mercury at $t^\circ\text{C}$ to the equivalent height h_0 at 0°C , use $h_0 = h \{1 - [(m - l) t / 1 + mt]\}$, where $m = 0.0001818$ and $l = 18.4 \times 10^{-6}$ if the scale is engraved on brass; $l = 8.5 \times 10^{-6}$ if on glass. This assumes the scale is correct at 0°C ; for other cases (any liquid) see *International Critical Tables*, Vol. 1, 68.
^{††} 1 gram per square centimeter = 10 kilograms per square meter
^{††} psi = MPa \times 145.038
 psi/ft = $0.433 \times \text{g/cm}^3 = \text{lbf/ft}^3/144 = \text{lbf/gal}/19.27$

Density or Mass per Unit Volume						
to Obtain	Multiply Number of by	Grams per Cubic Centimeter	Kilograms per Cubic Meter	Pounds per Cubic Foot	Pounds per Cubic Inch	Pounds per Gallon
Grams per cubic centimeter		1	0.001	1.602×10^{-2}	27.68	0.1198
Kilograms per cubic meter		1000	1	16.02	2.768×10^4	119.8
Pounds per cubic foot		62.43	6.243×10^{-2}	1	1728	7.479
Pounds per cubic inch		3.613×10^{-2}	3.613×10^{-5}	5.787×10^{-4}	1	4.329×10^{-3}
Pounds per gallon		8.347	8.3×10^{-3}	13.37×10^{-2}	231.0	1

Temperature	
°F	$1.8^\circ\text{C} + 32$
°C	$\frac{5}{9} (\text{°F} - 32)$
°R	$^\circ\text{F} + 459.69$
K	$^\circ\text{C} + 273.16$

Traditional Symbol	Standard SPE and SPWLA [†]	Standard Computer Symbol [†]	Description	Customary Unit or Relation	Standard Reserve Symbol [‡]
a	a	ACT	electrochemical activity	equivalents/liter, moles/liter	
a	K _R	COER	coefficient in F _R – φ relation	F _R = K _R /φ ^m	M _R , a, C
A	A	AWT	atomic weight	amu	
C	C	ECN	conductivity (electrical logging)	millimho per meter (mmho/m)	σ
C _p	B _{cp}	CORCP	sonic compaction correction factor	φ _{SVcor} = B _{cp} φ _{SV}	C _{cp}
D	D	DPH	depth	ft, m	y, H
d	d	DIA	diameter	in.	D
E	E	EMF	electromotive force	mV	V
F	F _R	FACHR	formation resistivity factor	F _R = K _R /φ ^m	
G	G	GMF	geometrical factor (multiplier)		f _G
H	I _H	HYX	hydrogen index		i _H
h	h	THK	bed thickness, individual	ft, m, in.	d, e
I	I	–X	index		i
FFi	I _{ff}	FFX	free fluid index		i _{ff}
SI	I _{sl}	SLX	silt index		I _{slt} , i _{sl} , i _{sit}
	I _φ	PRX	porosity index		i _φ
SPI	I _{φ2}	PRXSE	secondary porosity index		i _{φ2}
J	G _p	GMFP	pseudogeometrical factor		f _{Gp}
K	K _c	COEC	electrochemical SP coefficient	E _c = K _c log(a _w /a _{mf})	M _c , K _{ec}
k	k	PRM	permeability, absolute (fluid flow)	mD	K
L	L	LTH	length, path length	ft, m, in.	s, ℓ
M	M	SAD	slope, sonic interval transit time versus density × 0.01, in M–N plot	M = [(τ _f – τ _{LOG})/(ρ _b – ρ _f)] × 0.01	m _{θD}
m	m	MXP	porosity (cementation) exponent	F _R = K _R /φ ^m	
N	N	SND	slope, neutron porosity versus density, in M–N Plot	N = (φ _{Nf} – φ _N)/(ρ _b – ρ _f)	m _{φND}
n	n	SXP	saturation exponent	S _w ⁿ = F _R R _w /R _t	
P	C	CNC	salinity	g/g, ppm	c, n
p	p	PRS	pressure	psi, kg/cm ² [§] atm	P
P _c	P _c	PRSCP	capillary pressure	psi, kg/cm ² [§] atm	P _c , p _c
Pe			photoelectric cross section		

[†] SPE Letter and Computer Symbols Standard (1986).

[‡] Used only if conflict arises between standard symbols used in the same paper

[§] The unit of kilograms per square centimeter to be replaced in use by the SI metric unit of the pascal

^{||} "DEL" in the operator field and "RAD" in the main-quantity field

^{**} Suggested computer symbol

Traditional Symbol	Standard SPE and SPWLA [†]	Standard Computer Symbol [†]	Description	Customary Unit or Relation	Standard Reserve Symbol [‡]
Q_v			shaliness (CEC per mL water)	meq/mL	
q	$f_{\phi\text{shd}}$	FiMSHD	dispersed-shale volume fraction of intermatrix porosity		ϕ_{imfshd}, q
R	R	RES	resistivity (electrical)	ohm-m	ρ, r
r	r	RAD	radial distance from hole axis	in.	R
S	S	SAT	saturation	fraction or percent of pore volume	ρ, s
T	T	TEM	temperature	$^{\circ}\text{F}, ^{\circ}\text{C}, \text{K}$	θ
BHT, T_{bh}	T_{bh}	TEMBH	bottomhole temperature	$^{\circ}\text{F}, ^{\circ}\text{C}, \text{K}$	θ_{BH}
FT, T_{fm}	T_{f}	TEMF	formation temperature	$^{\circ}\text{F}, ^{\circ}\text{C}, \text{K}$	
t	t	TIM	time	$\mu\text{s}, \text{s}, \text{min}$	t
t	t	TAC	interval transit time		Δt
U			volumetric cross section	barns/cm ³	
v	v	VAC	velocity (acoustic)	ft/s, m/s	V, u
V	V	VOL	volume	cm ³ , ft ³ , etc.	v
V	V	VLF	volume fraction		f_v, F_v
Z	Z	ANM	atomic number		
α	α_{SP}	REDSP	SP reduction factor		
γ	γ	SPG	specific gravity (ρ/ρ_w or ρ_g/ρ_{air})		s, F_s
ϕ	ϕ	POR	porosity	fraction or percentage of bulk volume, p.u.	f, ε
	ϕ_1	PORPR	primary porosity	fraction or percentage of bulk volume, p.u.	f_1, e_1
	ϕ_2	PORSE	secondary porosity	fraction or percentage of bulk volume, p.u.	f_2, e_2
	ϕ_{ig}	PORIG	intergranular porosity	$\phi_{\text{ig}} = (V_b - V_{\text{gr}})/V_b$	$f_{\text{ig}}, \varepsilon_{\text{ig}}$
ϕ_z, ϕ_{im}	ϕ_{im}	PORIM	intermatrix porosity	$\phi_{\text{im}} = (V_b - V_{\text{ma}})/V_b$	$f_{\text{im}}, \varepsilon_{\text{im}}$
Δr	Δr	DELRAD ^{††}	radial distance (increment)	in.	ΔR
Δt	t	TAC	sonic interval transit time	$\mu\text{s}/\text{ft}$	Δt
$\Delta\phi_{\text{Nex}}$		DELPORN ^{††}	excavation effect	p.u.	
λ	K_{ani}	COEANI	coefficient of anisotropy		M_{ani}
ρ	ρ	DEN	density	g/cm ³	D
Σ	Σ	XST XSTMAC	neutron capture cross section macroscopic	c.u., cm ⁻¹	S
τ	τ_{dN}	TIMDN	thermal neutron decay time	μs	t_{dN}

[†] SPE Letter and Computer Symbols Standard (1986).

[‡] Used only if conflict arises between standard symbols used in the same paper

[§] The unit of kilograms per square centimeter is to be replaced in use by the SI metric unit of the pascal.

^{††} "DEL" in the operator field and "RAD" in the main-quantity field

^{†††} Suggested computer symbol

Traditional Subscript	Standard SPE and SPWLA [†]	Standard Computer Subscript [‡]	Explanation	Example	Standard Reserve Subscript [‡]
a	LOG	L	apparent from log reading (or use tool description subscript)	$R_{\text{LOG}}, R_{\text{LL}}$	log
a	a	A	apparent (general)	R_a	ap
abs	cap	C	absorption, capture	Σ_{cap}	
anh	anh	AH	anhydrite		
b	b	B	bulk	ρ_b	B, t
bh	bh	BH	bottomhole	T_{bh}	w, BH
clay	cl	CL	clay	V_{cl}	cla
cor, c	cor	COR	corrected	t_{cor}	
c	c	C	electrochemical	E_c	ec
cp	cp	CP	compaction	B_{cp}	
D	D	D	density log		d
dis	shd	SHD	dispersed shale	V_{shd}	
dol	dol	DL	dolomite	t_{dol}	
e, eq	eq	EV	equivalent	$R_{\text{weq}}, R_{\text{mfeq}}$	EV
f, fluid	f	F	fluid	ρ_f	fl
fm	f	F	formation (rock)	T_f	fm
g, gas	g	G	gas	S_g	G
	gr	GR	grain	ρ_{gr}	
gxo	gxo	GXO	gas in flushed zone	S_{gxo}	GXO
gyp	gyp	GY	gypsum	ρ_{gyp}	
h	h	H	hole	d_h	H
h	h	H	hydrocarbon	ρ_h	H
hr	hr	HR	residual hydrocarbon	S_{hr}	
i	i	I	invaded zone (inner boundary)	d_i	I
ig	ig	IG	intergranular (incl. disp. and str. shale)	ϕ_{ig}	
im, z	im	IM	intermatrix (incl. disp. shale)	ϕ_{im}	
int	int	I	intrinsic (as opposed to log value)	Σ_{int}	
irr	i	IR	irreducible	S_{wi}	ir, i
J	j	J	liquid junction	E_j	τ
k	k	K	electrokinetic	E_k	ek
l		L	log	t_{pl}	log
lam	ℓ	LAM	lamination, laminated	$V_{\text{sh}} \ell$	L
lim	lim	LM	limiting value	ϕ_{lim}	
liq	L	L	liquid	ρ_L	ℓ

[†] SPE Letter and Computer Symbols Standard (1986).

[‡] Used only if conflict arises between standard symbols used in the same paper

Traditional Subscript	Standard SPE and SPWLA [†]	Standard Computer Subscript [†]	Explanation	Example	Standard Reserve Subscript [†]
log	LOG	L	log values	t_{LOG}	log
ls	ls	LS	limestone	t_{ls}	lst
m	m	M	mud	R_{m}	
max	max	MX	maximum	ϕ_{max}	
ma	ma	MA	matrix	t_{ma}	
mc	mc	MC	mudcake	R_{mc}	
mf	mf	MF	mud filtrate	R_{mf}	
mfa	mfa	MFA	mud filtrate, apparent	R_{mfa}	
min	min	MN	minimum value		
ni			noninvaded zone	R_{ni}	
o	o	O	oil (except with resistivity)	S_{o}	N
or	or	OR	residual oil	S_{or}	
o, 0 (zero)	0 (zero)	ZR	100-percent water saturated	F_0	zr
p			propagation	t_{pw}	
PSP	pSP	PSP	pseudostatic SP	E_{pSP}	
pri	1 (one)	PR	primary	ϕ_1	p, pri
r	r	R	relative	$k_{\text{ro}}, k_{\text{rw}}$	R
r	r	R	residual	$S_{\text{or}}, S_{\text{hr}}$	R
s	s	S	adjacent (surrounding) formation	R_{s}	
sd	sd	SD	sand		sa
ss	ss	SS	sandstone		sst
sec	2	SE	secondary	ϕ_2	s, sec
sh	sh	SH	shale	V_{sh}	sha
silt	sl	SL	silt	I_{sl}	slt
SP	SP	SP	spontaneous potential	E_{SP}	sp
SSP	SSP	SSP	static spontaneous potential	E_{SSP}	
str	sh st	SH ST	structural shale	V_{shst}	s
t, ni	t	T	true (as opposed to apparent)	R_{t}	tr
T	t	T	total	C_{t}	T
w	w	W	water, formation water	S_{w}	W
wa	wa	WA	formation water, apparent	R_{wa}	Wap
wf	wf	WF	well flowing conditions	p_{wf}	f
ws	ws	WS	well static conditions	p_{ws}	s
xo	xo	XO	flushed zone	R_{xo}	
z, im	im	IM	intermatrix	ϕ_{im}	

[†] SPE Letter and Computer Symbols Standard (1986).

[†] Used only if conflict arises between standard symbols used in the same paper

Traditional Subscript	Standard SPE and SPWLA [†]	Standard Computer Subscript [†]	Explanation	Example	Standard Reserve Subscript [†]
0 (zero)	0 (zero)	ZR	100 percent water saturated	R ₀	zr
AD		RAD	from CDR attenuation deep	R _{AD}	
D	D	D	from density log	φ _D	d
	GG	GG	from gamma-gamma log	φ _{GG}	gg
IL	I	I	from induction log	R _I	i
ILD	ID	ID	from deep induction log	R _{ID}	id
ILM	IM	IM	from medium induction log	R _{IM}	im
LL	LL (also LL3, LL8, etc.)	LL	from laterolog (also LL3, LL7, LL8, LLD, LLS)	R _{LL}	ll
N	N	N	from normal resistivity log	R _N	n
N	N	N	from neutron log	φ _N	n
PS		RPS	from CDR phase-shift shallow	R _{PS}	
16", 16"N			from 16-in. normal Log	R _{16"}	
1" × 1"			from 1-in. by 1-in. microinverse (MI)	R _{1" × 1"}	
2"			from 2-in. micronormal (MN)	R _{2"}	

[†] SPE Letter and Computer Symbols Standard (1986).

[†] Used only if conflict arises between standard symbols used in the same paper

These unit abbreviations, which are based on those adopted by the Society of Petroleum Engineers (SPE), are appropriate for most publications. However, an accepted industry standard may be used instead. For instance, in the drilling field, ppg may be more common than lbm/gal when referring to pounds per gallon.

In some instances, two abbreviations are given: customary and metric. When using the International System of Units (SI), or metric, abbreviations, use the one designated for metric (e.g., m³/h instead of m³/hr). The use of SI prefix symbols and prefix names with customary unit abbreviations and names, although common, is not preferred (e.g., 1,000 lbf instead of klbf).

Unit abbreviations are followed by a period only when the abbreviation forms a word (for example, in. for inch).

acre	Spell out
acre-foot	acre-ft
ampere	A
ampere-hour	A-hr
angstrom unit (10 ⁻⁸ cm)	Å
atmosphere	atm
atomic mass unit	amu
barrel	bbl
barrels of fluid per day	BFPD
barrels of liquid per day	BLPD
barrels of oil per day	BOPD
barrels of water per day	BWPD
barrels per day	B/D
barrels per minute	bbl/min
billion cubic feet (billion = 10 ⁹)	Bcf
billion cubic feet per day	Bcf/D
billion standard cubic feet per day	Use Bcf/D instead of Bscf/D (see "standard cubic foot")
bits per inch	bpi
bits per second	bps
brake horsepower	bhp
British thermal unit	Btu
capture unit	c.u.
centimeter	cm
centipoise	cp
centistoke	cSt
coulomb	C
counts per second	cps
cubic centimeter	cm ³
cubic foot	ft ³
cubic feet per barrel	ft ³ /bbl
cubic feet per day	ft ³ /D
cubic feet per minute	ft ³ /min
cubic feet per pound	ft ³ /lbm
cubic feet per second	ft ³ /s
cubic inch	in. ³
cubic meter	m ³
cubic millimeter	mm ³
cubic yard	yd ³

curie	Ci
dalton	Da
darcy, darcies	D
day (customary)	D
day (metric)	d
dead-weight ton	DWT
decibel	dB
degree (American Petroleum Institute)	°API
degree Celsius	°C
degree Fahrenheit	°F
degree Kelvin	See "kelvin"
degree Rankine	°R
dots per inch	dpi
electromotive force	emf
electron volt	eV
farad	F
feet per minute	ft/min
feet per second	ft/s
foot	ft
foot-pound	ft-lbf
gallon	gal
gallons per day	gal/D
gallons per minute	gal/min
gigabyte	Gbyte
gigahertz	GHz
gigapascal	GPa
gigawatt	GW
gram	g
hertz	Hz
horsepower	hp
horsepower-hour	hp-hr
hour (customary)	hr
hour (metric)	h
hydraulic horsepower	hhp
inch	in.
inches per second	in./s
joule	J
kelvin	K
kilobyte	kB
kilogram	kg
kilogram-meter	kg-m
kilohertz	kHz
kilojoule	kJ
kilometer	km
kilopascal	kPa
kilopound (force) (1,000 lbf)	klbf
kilovolt	kV
kilowatt	kW
kilowatt-hour	kW-hr
kips per square inch	ksi

lines per inch	lpi	pounds of proppant added	ppa
lines per minute	lpm	pounds per square inch	psi
lines per second	lps	pounds per square inch absolute	psia
liter	L	pounds per square inch gauge	psig
megabyte	MB	pounds per thousand barrels (salt content)	ptb
megagram (metric ton)	Mg	quart	qt
megahertz	MHz	reservoir barrel	res bbl
megajoule	MJ	reservoir barrel per day	RB/D
meter	m	revolutions per minute	rpm
metric ton (tonne)	t or Mg	saturation unit	s.u.
mho per meter	\mathcal{U}/m	second	s
microsecond	μs	shots per foot	spf
mile	Spell out	specific gravity	sg
miles per hour	mph	square	sq
milliamperes	mA	square centimeter	cm ²
millicurie	mCi	square foot	ft ²
millidarcy, millidarcies	mD	square inch	in. ²
milliequivalent	meq	square meter	m ²
milligram	mg	square mile	sq mile
milliliter	mL	square millimeter	mm ²
millimeter	mm	standard	std
millimho	mmho	standard cubic feet per day	Use ft ³ /D instead of scf/D (see "standard cubic foot")
million cubic feet (million = 10 ⁶)	MMcf	standard cubic foot	Use ft ³ or cf as specified on this list. Do not use scf unless the standard conditions at which the measurement was made are specified. The straight volumetric conversion factor is 1 ft ³ = 0.02831685 m ³
million cubic feet per day	MMcf/D		
million electron volts	MeV		
million standard cubic feet per day	Use MMcf/D instead of MMscf/D (see "standard cubic foot")		
milliPascal	mPa		
millisecond	ms		
millisiemens	mS		
millivolt	mV		
mils per year	mil/yr		
minute	min		
mole	mol		
nanosecond	ns		
newton	N		
ohm	ohm		
ohm-centimeter	ohm-cm		
ohm-meter	ohm-m		
ounce	oz		
parts per million	ppm		
pascal	Pa		
picofarad	pF		
pint	pt		
porosity unit	p.u.		
pound (force)	lbf		
pound (mass)	lbm		
pound per cubic foot	lbm/ft ³		
pound per gallon	lbm/gal		
		stock-tank barrel	STB
		stock-tank barrels per day	STB/D
		stoke	St
		teragram	Tg
		thousand cubic feet	Mcf
		thousand cubic feet per day	Mcf/D
		thousand pounds per square inch	kpsi
		thousand standard cubic feet per day	Use Mcf/D instead of Mscf/D (see "standard cubic foot")
		tonne (metric ton)	t
		trillion cubic feet (trillion = 10 ¹²)	Tcf
		trillion cubic feet per day	Tcf/D
		volt	V
		volume percent	vol%
		volume per volume	vol/vol
		watt	W
		weight percent	wt%
		yard	yd
		year (customary)	yr
		year (metric)	a

1. Overton HL and Lipson LB: "A Correlation of the Electrical Properties of Drilling Fluids with Solids Content," *Transactions, AIME* (1958) 213.
2. Desai KP and Moore EJ: "Equivalent NaCl Concentrations from Ionic Concentrations," *The Log Analyst* (May–June 1969).
3. Gondouin M, Tixier MP, and Simard GL: "An Experimental Study on the Influence of the Chemical Composition of Electrolytes on the SP Curve," *JPT* (February 1957).
4. Segesman FF: "New SP Correction Charts," *Geophysics* (December 1962) 27, No. 6, PI.
5. Alger RP, Locke S, Nagel WA, and Sherman H: "The Dual Spacing Neutron Log–CNL," paper SPE 3565, presented at the 46th SPE Annual Meeting, New Orleans, Louisiana, USA (1971).
6. Segesman FF and Liu OYH: "The Excavation Effect," *Transactions of the SPWLA 12th Annual Logging Symposium* (1971).
7. Burke JA, Campbell RL Jr, and Schmidt AW: "The Litho-Porosity Crossplot," *Transactions of the SPWLA 10th Annual Logging Symposium* (1969), paper Y.
8. Clavier C and Rust DH: "MID-PLOT: A New Lithology Technique," *The Log Analyst* (November–December 1976).
9. Tixier MP, Alger RP, Biggs WP, and Carpenter BN: "Dual Induction-Laterolog: A New Tool for Resistivity Analysis," paper 713, presented at the 38th SPE Annual Meeting, New Orleans, Louisiana, USA (1963).
10. Wahl JS, Nelligan WB, Frentrop AH, Johnstone CW, and Schwartz RJ: "The Thermal Neutron Decay Time Log," *SPEJ* (December 1970).
11. Clavier C, Hoyle WR, and Meunier D: "Quantitative Interpretation of Thermal Neutron Decay Time Logs, Part I and II," *JPT* (June 1971).
12. Poupon A, Loy ME, and Tixier MP: "A Contribution to Electrical Log Interpretation in Shaly Sands," *JPT* (June 1954).
13. Tixier MP, Alger RP, and Tanguy DR: "New Developments in Induction and Sonic Logging," paper 1300G, presented at the 34th SPE Annual Meeting, Dallas, Texas, USA (1959).
14. Rodermund CG, Alger RP, and Tittman J: "Logging Empty Holes," *OGJ* (June 1961).
15. Tixier MP: "Evaluation of Permeability from Electric Log Resistivity Gradients," *OGJ* (June 1949).
16. Morris RL and Biggs WP: "Using Log-Derived Values of Water Saturation and Porosity," *Transactions of the SPWLA 8th Annual Logging Symposium* (1967).
17. Timur A: "An Investigation of Permeability, Porosity, and Residual Water Saturation Relationships for Sandstone Reservoirs," *The Log Analyst* (July–August 1968).
18. Wyllie MRJ, Gregory AR, and Gardner GHF: "Elastic Wave Velocities in Heterogeneous and Porous Media," *Geophysics* (January 1956) 21, No. 1.
19. Tixier MP, Alger RP, and Doh CA: "Sonic Logging," *JPT* (May 1959) 11, No. 5.
20. Raymer LL, Hunt ER, and Gardner JS: "An Improved Sonic Transit Time-to-Porosity Transform," *Transactions of the SPWLA 21st Annual Logging Symposium* (1980).
21. Coates GR and Dumanoir JR: "A New Approach to Improved Log-Derived Permeability," *The Log Analyst* (January–February 1974).
22. Raymer LL: "Elevation and Hydrocarbon Density Correction for Log-Derived Permeability Relationships," *The Log Analyst* (May–June 1981).
23. Westaway P, Hertzog R, and Plasic RE: "The Gamma Spectrometer Tool, Inelastic and Capture Gamma Ray Spectroscopy for Reservoir Analysis," paper SPE 9461, presented at the 55th SPE Annual Technical Conference and Exhibition, Dallas, Texas, USA (1980).
24. Quirein JA, Gardner JS, and Watson JT: "Combined Natural Gamma Ray Spectral/Litho-Density Measurements Applied to Complex Lithologies," paper SPE 11143, presented at the 57th SPE Annual Technical Conference and Exhibition, New Orleans, Louisiana, USA (1982).
25. Harton RP, Hazen GA, Rau RN, and Best DL: "Electromagnetic Propagation Logging: Advances in Technique and Interpretation," paper SPE 9267, presented at the 55th SPE Annual Technical Conference and Exhibition, Dallas, Texas, USA (1980).
26. Serra O, Baldwin JL, and Quirein JA: "Theory and Practical Application of Natural Gamma Ray Spectrometry," *Transactions of the SPWLA 21st Annual Logging Symposium* (1980).
27. Gardner JS and Dumanoir JL: "Litho-Density Log Interpretation," *Transactions of the SPWLA 21st Annual Logging Symposium* (1980).
28. Edmondson H and Raymer LL: "Radioactivity Logging Parameters for Common Minerals," *Transactions of the SPWLA 20th Annual Logging Symposium* (1979).
29. Barber TD: "Real-Time Environmental Corrections for the Phasor Dual Induction Tool," *Transactions of the SPWLA 26th Annual Logging Symposium* (1985).
30. Roscoe BA and Grau J: "Response of the Carbon-Oxygen Measurement for an Inelastic Gamma Ray Spectroscopy Tool," paper SPE 14460, presented at the 60th SPE Annual Technical Conference and Exhibition, Las Vegas, Nevada, USA (1985).

31. Freedman R and Grove G: "Interpretation of EPT-G Logs in the Presence of Mudcakes," paper presented at the 63rd SPE Annual Technical Conference and Exhibition, Houston, Texas, USA (1988).
32. Gilchrist WA Jr, Galford JE, Flaum C, Soran PD, and Gardner JS: "Improved Environmental Corrections for Compensated Neutron Logs," paper SPE 15540, presented at the 61st SPE Annual Technical Conference and Exhibition, New Orleans, Louisiana, USA (1986).
33. Tabanou JR, Glowinski R, and Rouault GF: "SP Deconvolution and Quantitative Interpretation in Shaly Sands," *Transactions of the SPWLA 28th Annual Logging Symposium* (1987).
34. Kienitz C, Flaum C, Olesen J-R, and Barber T: "Accurate Logging in Large Boreholes," *Transactions of the SPWLA 27th Annual Logging Symposium* (1986).
35. Galford JE, Flaum C, Gilchrist WA Jr, and Duckett SW: "Enhanced Resolution Processing of Compensated Neutron Logs, paper SPE 15541, presented at the 61st SPE Annual Technical Conference and Exhibition, New Orleans, Louisiana, USA (1986).
36. Lowe TA and Dunlap HF: "Estimation of Mud Filtrate Resistivity in Fresh Water Drilling Muds," *The Log Analyst* (March–April 1986).
37. Clark B, Luling MG, Jundt J, Ross M, and Best D: "A Dual Depth Resistivity for FEWD," *Transactions of the SPWLA 29th Annual Logging Symposium* (1988).
38. Ellis DV, Flaum C, Galford JE, and Scott HD: "The Effect of Formation Absorption on the Thermal Neutron Porosity Measurement," paper presented at the 62nd SPE Annual Technical Conference and Exhibition, Dallas, Texas, USA (1987).
39. Watfa M and Nurmi R: "Calculation of Saturation, Secondary Porosity and Producibility in Complex Middle East Carbonate Reservoirs," *Transactions of the SPWLA 28th Annual Logging Symposium* (1987).
40. Brie A, Johnson DL, and Nurmi RD: "Effect of Spherical Pores on Sonic and Resistivity Measurements," *Transactions of the SPWLA 26th Annual Logging Symposium* (1985).
41. Serra O: *Element Mineral Rock Catalog*, Schlumberger (1990).
42. Grove GP and Minerbo GN: "An Adaptive Borehole Correction Scheme for Array Induction Tools," *Transactions of the SPWLA 32nd Annual Logging Symposium*, Midland, Texas, USA, June 16–19, 1991, paper F.
43. Barber T and Rosthal R: "Using a Multiarray Induction Tool to Achieve Logs with Minimum Environmental Effects," paper SPE 22725, presented at SPE Annual Technical Conference and Exhibition, Dallas, Texas, USA, October 6–9, 1991.
44. Moran JH: "Induction Method and Apparatus for Investigating Earth Formations Utilizing Two Quadrature Phase Components of a Detected Signal," US Patent No. 3,147,429 (September 1, 1964).
45. Barber TD: "Phasor Processing of Induction Logs Including Shoulder and Skin Effect Correction," US Patent No. 4,513,376 (September 11, 1984).
46. Barber T et al.: "Interpretation of Multiarray Induction Logs in Invaded Formations at High Relative Dip Angles," *The Log Analyst* 40, no. 3 (May–June 1990): 202–217.
47. Anderson BI and Barber TD: *Induction Logging*, Sugar Land, Texas, USA: Schlumberger Wireline & Testing, 1995 (SMP-7056).
48. Gerritsma CJ, Oosting PH, and Trappeniers NJ: "Proton Spin-Lattice Relaxation and Self Diffusion in Methanes, II," *Physica* 51 (1971), 381–394.
49. Wyllie MRJ and Rose WD: "Some Theoretical Considerations Related to the Quantitative Evaluation of the Physical Characteristics of Reservoir Rock from Electrical Log Data," *JPT* 2 (1950), 189.

